Stanford Geothermal Program
Interdisciplinary Research in
Engineering and Earth Sciences
STANFORD UNIVERSITY
Stanford, California

SGP-TR-69

DRILLSTEM TEST DATA ANALYSIS CONSIDERING INERTIAL AND FRICTIONAL WELLBORE EFFECTS

By

Miguel-Angel Saldana-Cortez

November 1983

Financial support was provided through the Stanford Geothermal Program under Department of Energy Contract No. DE-AT-03-80SF11459 and by the Department of Petroleum Engineering, Stanford University.

ABSTRACT

A mathematical formulation of the flow phenomena during a slug test, a drillstem test, or a closed-chamber test is derived in the present study. This formulation considers gravitational, inertial, and frictional effects on the fluid column changing in length inside the wellbore. This formulation is based on a transient momentum balance equation for the wellbore fluid column coupled with the diffusivity equation for the reservoir through conditions including wellbore storage and skin effect. Two solution methods for the resulting linear and non-linear mathematical problems obtained under several sets of assumptions are presented to determine the behavior of: (a) bottomhole pressure, (b) wellbore liquid level, (c) rate of change in pressure, (d) flow rate, (e) rate of change of flow rate, and (f) reservoir pressures.

Solutions currently available for these types of tests are discussed from the proposed new results as special cases of the present, more general formulation. New type curves and limiting criteria for their proper application are provided in this study to perform drillstem test data analysis by type-curve matching techniques.

The solution method for linear problems is the Laplace transformation and is applied to evaluate the effect of friction considering laminar flow in the wellbore. The solution method for non-linear problems consists of a comprehensive finite-difference scheme that allows evaluation of: (a) the effect of friction for any flow regime in the wellbore, and, (b) the effect of the slug size or cushion size in the pipe. This numerical method can also be used to simulate pressure buildup during a shut-in period of a drillstem test, or of a closed-chamber test. These solutions open the possibility of performing integral drillstem test data analysis considering one cycle of flowing and shut-in periods.

Analysis of results presented in this study provide useful criteria for estimating the relative importance of inertial and frictional wellbore effects on the transient relationship between bottomhole pressure and wellbore liquid level for practical conditions found in slug, drillstem, and closed-chamber testing. This knowledge improves understanding of the flow phenomena involved, and leads to a correct application of pressure buildup theory to drillstem test and closed-chamber test data analysis.

TABLE OF CONTENTS

PAGE

PAGE

LIST OF TABLES

LIST OF FIGURES

FIGURE PAGE

FIGURE PAGE

FIGURE PAGE

FIGURE PAGE

FIGURE PAGE

FIGURE PAGE

FIGURE PAGE

FIGURE PAGE

SECTION 1
INTRODUCTION

Transient well test data analysis is frequently used to determine physical properties that are required for evaluating reserves and forecasting the production behavior from oil, gas, geothermal, and groundwater reservoirs. Basically, a transient well test consists of deliberately changing the flow conditions in a wellbore and observing the response from the reservoir. Well test data are analyzed by matching the response recorded during a test with a solution provided by a mathematical, numerical, or physical model.

Well test data analysis is based on the assumption that flow phenomena in the tested reservoir are closely represented by the selected model. Reservoir properties are inferred from those properties assigned to the model to obtain a behavior similar to that exhibited by the reservoir during the test.

The many ways in which wellbore flow conditions can be perturbed define a large number of well test types. However, availability of appropriate model solutions determines if a particular well test can be analyzed to obtain an estimation of reservoir properties.

As mentioned in the literature review on well test analysis techniques presented in Section 2, Matthews and Russell (1967) and Earlougher (1977) have described transient well tests that had found practical application by 1967 and 1977, respectively. A quick scan through the table of contents of these two references indicates that many model solutions were presented or improved but few additional practical well test types evolved during that decade, although new analysis methods did arise. Earlougher (1977) includes a description of new solutions for analysis of flow in a drillstem test that were developed during that period of time. These new solutions consider a

test in which the flow of a fluid from a reservoir depends on the changing length of a liquid column in the wellbore. A mathematical description of the corresponding flow phenomena requires specification of wellbore conditions different from constant flow rate or constant bottomhole pressure, which are the boundary conditions most frequently considered in conventional well test analysis solutions.

In the present study, attention is mainly focussed on three transient well tests that involve liquid level changes in the wellbore. These are: (1) slug tests, (2) drillstem tests, and (3) closed-chamber tests. In these tests, fluid from the reservoir flows into the wellbore, or viceversa, in response to a perturbation of the wellbore fluid column in initial hydrostatic equilibrium with a uniform reservoir pressure. In practice, this perturbation is caused by performing or simulating a sudden removal (or addition) of a finite amount of liquid from (or to) the initial static liquid column in a wellbore. The amount of removed liquid is called a "slug", and the amount of liquid remaining in the wellbore at the start of the test is called the "cushion".

Practical experience in drillstem testing indicates that the liquid column in a wellbore can be subjected to rapid changes in length. Then, according to Newton's Laws of Motion, inertia of the fluid column can be important in the flow phenomena for some systems. Friction energy losses during the movement of liquid along the wellbore pipe are also present in a dynamical relationship between liquid column length and bottomhole pressure.

Slug test solutions available in 1977 assume hydrostatic equilibrium in the wellbore at all times during the test. This assumption is equivalent to neglecting inertial and frictional effects in the wellbore. A slug test solution including inertial effects on the liquid column in a wellbore was published recently (Shinohara and Ramey, 1979.b). That solution neglects friction losses. Moreover, that test solution assumes a slug size and a reservoir thickness negligible in comparison to the length of the wellbore liquid column in hydrostatic equilibrium with the initial reservoir pressure.

A physical and mathematical description of the flow phenomena during a slug test, drillstem test, or closed-chamber test is formulated in Section 3 of the present study. This formulation is based on a wellbore equation which considers more terms representing inertial and frictional effects than approximations presented previously.

Two methods for solving linear and non-linear mathematical problems resulting from various sets of assumptions are presented in Section 4. These methods provide evaluation of the behavior of bottomhole pressure, wellbore liquid level, rate of change of bottomhole pressure, flow rate and rate of change of flow rate, and pressure response in the reservoir.

In Section 5, available solutions are unified and extended by discussing additional results obtained with the method proposed for drillstem tests described by linear mathematical problems. This method is also used to evaluate other linear effects assumed negligible by previous authors. New type curves and appropriate criteria for practical application are also proposed in that section.

A numerical method, implemented by a computer program, for solving drillstem test problems with mathematically non-linear effects in the wellbore is calibrated in Section 6 to reproduce many previous solutions for linear problems. This method is then applied to evaluate non-linear wellbore inertial effects caused by the slug size, and non-linear frictional effects of the moving liquid column. This computer program allows specification of length of flow and shut-in periods to simulate a complete drillstem test, or a closed-chamber test.

Practical considerations on the application of the methods and solutions presented in this study to some field cases reported in the literature is discussed in Section 7. A summary of conclusions and recomendations obtained from the present study is provided in Section 8.

A brief review of literature concerning the subject: well tests is given in the following section.

SECTION 2
LITERATURE REVIEW

This literature review concentrates mainly on theoretical improvements for analyzing flow phenomena during a slug test, drillstem test, or closed-chamber test. In order to relate these improvements to the development of conventional transient well test analysis techniques, some major theoretical contributions in conventional analysis are also included in cronological order.

A list of authors of the publications presented in this literature review is given in Table 2.1.

In 1856, Darcy found experimentally that there is a range of conditions in which the flow rate of water through a vertical pipe filled with sand is directly proportional to the pressure difference between the pipe inlet and outlet. The constant of proportionality, corrected for gravity, pipe cross-sectional area, and fluid viscosity, is called permeability and is a property of a porous medium, The relationship describing this observation is called Darcy's Law of Flow through Porous Media and is analogous to other physical laws like Fourier's Law of Heat Conduction, Fick's Law of Mass Diffusion, Newton's Law of Viscosity, and Ohm's Law for Electrical Current. Since then, Darcy's Law has been generalized and applied to describe the multiphase flow of oil, gas, and water through reservoir rocks.

The analogy between the flow of a fluid and the conduction of heat results in the possibility of applying solutions found for one field to the other field of study. An important heat conduction solution is the instantaneous point source solution discussed by Kelvin (1884). It is possible to superimpose instantaneous point source solutions with respect to space to generate instantaneous line and volume source

TABLE 21.- LITERATURE REVIEW SUMMARY

Darcy (1856)
Kelvin (1884)
Carslaw (1921)
Theis (1935)
Muskat (1937)
Jaeger (1940, 1941)
Carslaw and Jaeger (1946)
van Everdingen and Burst (1949)
Miller, Dyes, and Hutchinson (1950)
Rorner (1951)
van Everdingen (1953)
Burst (1953)
Blackwell (1954)
Ferris and Knowles (1954)
Gladfelter, Tracy, and Wilsey (1955)
Hawkins (1956)
Jaeger (1956)
Carslaw and Jaeger (1959)
Brons and Killer (1961)
Horan and Finklea(1962)
Bredehoeft, Cooper, Papadopulos, and Bennett (1965)
Cooper, Bredehoeft, Papadopulos, and Bennett(1965)
Bredehoeft, Cooper, and Papadopulos (1966)
Bredehoeft (1967)
Matthews and Russell (1967)
Papadopulos and Cooper (1967)
Cooper, Bredehoeft, and Papadopulos (1967)
Brill, Bourgoyne, and Dixon (1969)
Ramey (1970)
Agarwal, Al-Hussainy, and Ramey (1970)
Uattenbarger and Ramey (1970)
van Poollen and Weber (1970)
McKinley (1971)
Ramey and Agarwal (1972)
Kohlhaas (1972)
Papadopulos, Bredehoeft, and Cooper (1973)
Earlougher and Kersch (1974)
Fenske (1974)
Ramey, Agarwal, and Martin (1975)
van der Kamp (1976)
Bourwer and Rice (1976)
Sinha, Sigmon, and Montgomery (1976)
Alexander (1977)
Earlougher (1977)
Fenske (1977)
Cooley and Cunningham (1979)
Uraiet and Raghavan (1979)
Ehlig-Economides and Ramey (1979)
Barelli (1979)
Shlnohara and Ramey (1979.a, 1979.b)
Stright (1979)
Raghavan (1979)
Agarwal (1980)
Soliman (1981)
Raghavan, Reynolds, and Heng (1982)
Lee (1982)

solutions, and with respect to time to generate continuous and changing source solutions.

Carslaw (1921) published a book on the mathematical theory of heat conduction in solids with solutions obtained by using source solutions and by applying operational calculus to a large number of practical problems.

Theis (1935) presented an analysis method for transient tests in groundwater wells produced at a constant flow rate. This method is based on a log-log type curve of a continuous line source solution. Theis (1935) also proposed a pressure buildup graph which employs the logarithm of the ratio of flowing plus shut-in times to shut-in time. This graph is now called a Horner plot in petroleum engineering.

Muskat (1937) published a comprehensive book on the flow of a fluid through porous media and included many useful solutions and analysis methods applicable to groudwater, oil, and gas reservoir conditions.

In two separate publications, Jaeger (1940, 1941) utilized the Laplace transformation to solve radial heat conduction problems in cylindrical solids with a general inner boundary condition at the wellbore.

In 1946, Carslaw and Jaeger combined their solutions in a book on conduction of heat in solids.

In 1949, van Everdingen and Hurst used the Laplace transformation to obtain dimensionless pressure solutions for radial fluid flow from an aquifer to an oil or gas reservoir or from a reservoir to a wellbore under a variety of boundary conditions. One boundary condition considered includes the effect of wellbore storage.

Miller, Dyes, and Hutchinson (1950) proposed a method for pressure buildup analysis consisting of drawing a straight line through well test data points of bottomhole pressure vs the logarithm of shut-in time. This method assumes a well producing at constant flow rate in steady or pseudo-steady state from a reservoir prior to being shut-in.

Horner (1951) proposed a pressure buildup analysis technique consisting of drawing a straight line through well test data of bottomhole pressure vs logarithm of the ratio of flowing time plus shut-in time divided by shut-in time. This method is based on superposition in time of two continuous line sources of the same strength but with different sign in a reservoir acting as infinite in lateral extension. Horner (1951) also considered the effects of flow rate change and of a linear flow barrier.

In two separate publications, van Everdingen (1953) and Hurst (1953) introduced the concept of skin effect into the description of radial flow in order to represent a zone around the wellbore with damaged permeability resulting from drilling and production practices.

In 1954, Blackwell applied the Laplace transformation to obtain assymptotic solutions for determining thermal conductivities of solids by using a constant heat source in a borehole with a finite radius and a skin resistance.

Also in 1954, Ferris and Knowles proposed a testing procedure, called a slug test, and a corresponding data analysis method based on an instantaneous line source solution.

Gladfelter, Tracy, and Wilsey (1955) introduced a method for correcting pressure buildup data dominated by wellbore storage effects.

Hawkins (1956) presented an equation relating the skin effect to the permeabilities and radii of the damaged and undamaged reservoir zones around a wellbore.

Jaeger (1956) solved by Laplace transformation two heat conduction problems in an infinite-acting medium. The first problem is analogous to a slug test. The second problem is similar to the one solved by Blackwell (1954) and is analogous to a drawdown test at constant production rate (also analogous to an injectivity test at constant injection rate). These solutions include a constant thermal resistance analogous to a skin effect.

A revised edition of the book by Carslaw and Jaeger was published in 1959.

In 1961, Brons and Miller interpreted a damaged well as an undamaged well with smaller radius called effective wellbore radius, and introduced shape factors for non-circular drainage radii.

Moran and Finklea (1962) presented pressure solutions considering spherical flow for application in data analysis from wireline formation tests.

In 1965, Bredehoeft, Cooper, Papadopulos, and Bennett reported oscillations of up to 16 ft of the level in a groundwater well in Florida in response to the Good Friday Earthquake in Alaska on March 27, 1964. Also in 1965, in another publication, Cooper, Bredehoeft, Papadopulos, and Bennett presented a theory describing a wellbore liquid level response to seismic waves. This theory is based on a momentum balance equation which includes the effect of inertia on the water column and assumes negligible friction losses and a small level variation. According to this theory, such response is analogous to the classical mechanical system of a spring with a mass submerged in a viscous fluid. The wellbore fluid column corresponding to the mass, and the reservoir to the spring. Those authors superimposed line source solutions with respect to time to represent harmonic fluctuations in pressure and coupled those solutions with the wellbore equation and obtained a differential equation describing the motion of the liquid level.

Approximately one year later, Bredehoeft, Cooper, and Papadopulos (1966) presented a modified theory introducing wellbore storage into the problem description, and found wellbore fluid level solutions for a specific case by using a resistance-capacitance electric analog.

Bredehoeft (1967) utilized the previous wellbore equation to describe the wellbore liquid level response to earth tides.

Also in 1967, Matthews and Russell published a monograph showing the state of the art in analysis techniques in petroleum engineering for

pressure buildup and flow tests in wells.

In the same year, Papadopulos and Cooper (1967) presented a pressure solution for an undamaged well of large diameter produced at constant flow rate. This solution is analogous to the one presented by Jaeger (1956), but assumes a skin effect of zero.

Cooper, Bredehoeft, and Papadopulos (1967) presented a solution for the liquid level response during a slug test considering wellbore storage and an undamaged well. Those authors proposed a type curve for analysis of liquid level variation during a slug test. An analogous solution including skin effect was obtained by Jaeger (1956).

In 1969, Brill, Bourgoyne, and Dixon published a finite-difference approximation for drillstem test data interpretation by history matching.

In 1970, Ramey proposed the use of log-log type curves to analyze short-time pressure data for a well produced at constant flow rate including wellbore storage and skin effect. The theoretical basis for these type curves were provided in the same year by Agarwal, Al-Hussainy, and Ramey (1970) from a solution analogous to the one obtained by Jaeger (1956). Wattenbarger and Ramey (1970) calculated by a finite-difference approximation the effect of a large damaged region around the wellbore, and presented a type curve.

Also in 1970, van Poollen and Weber used the slug test type curve presented by Cooper, et al. (1967) to analyze drillstem test bottomhole flowing pressures.

McKinley (1971) published a type curve for pressure buildup analysis considering afterflow wellbore storage effects.

In 1972, Ramey and Agarwal presented a comprehensive derivation and discussion of dimensionless bottomhole pressure solutions for transient well test analysis including wellbore storage and skin effect. In an appendix, those authors considered a drillstem flow problem and arrived to a problem analogous to one previously solved by Jaeger (1956).

The same year, Kohlhaas (1972) converted the slug test type curve proposed by Cooper, et al. (1967) for drillstem test flowing pressure analysis.

Slug test type curves available in 1972 did not include the skin effect. This may have been one of the reasons for the publication by Papadopulos, Bredehoeft, and Cooper (1973) of extended type curves to show apparently unexpected large values of wellbore storage constant required to match field data.

In 1974, Earlougher and Kersch proposed use of the effective wellbore radius concept developed by Brons and Miller (1961) to generate constant production rate type curves for dimensionless pressure vs the ratio of dimensionless time and dimensionless wellbore storage constant, using dimensionless wellbore storage constant multiplied by the exponential of twice the skin factor as a correlation parameter.

Fenske (1974) presented an extension of the solution used by Theis (1935) considering wellbore storage in the active and in an observation undamaged well.

Ramey, Agarwal, and Martin (1975) applied the approach used by Earlougher and Kersch (1974) to generate two log-log and one semi-log type curves for the slug test solutions previously presented by Ramey and Agarwal (1972). These type curves suggest an explanation for the apparently large values of wellbore storage constant observed in practice as being associated with wellbore damage. That is, there was often a combined effect of wellbore storage and a positive skin effect. These solutions do not consider critical flow, a condition that Ramey et al. (1975) speculated to be one of the causes responsible for the paradoxical relationship between an apparent constant flow rate and a bottomhole pressure increasing with time, a situation frequently observed in drillstem test data.

In 1976, van der Kamp proposed an approximate method for determining reservoir transmissivity by means of slug test data analysis for systems exhibiting an oscillatory liquid level response. This theory is based on the wellbore equation previously presented by Cooper,

et al. (1965). This method is applicable to data recorded after the first oscillation of the liquid level.

Bouwer and Rice (1976) presented an expression for evaluation of reservoir transmissivity from a slug test in a partially-penetrating well. This expression was obtained assuming a logarithmic reservoir pressure distribution from a changing pseudo-wellbore radius evaluated by a resistance-conductance electric analog.

Sinha, Sigmon, and Montgomery (1976) described applications of the available log-log and semi-log type curves to a number of drillstem test data sets. Those authors concluded that use of the appropriate type curve in conjunction with the method proposed by Horner (1951) helps to eliminate misinterpretation of data and gives a greater degree of confidence in the analysis. Also, those authors recommended that type curves for the flow period of a drillstem test should be used whenever applicable.

In 1977, Alexander proposed a theory for closed-chamber tests analysis. This theory is the result of several studies published by that author since 1973.

Also in 1977, Earlougher published a monograph on pressure transient analysis methods updating the monograph presented by Matthews and Russell a decade before.

Fenske (1977) proposed type curves for pressure buildup in radial flow systems with wellbore storage in an active well and in an undamaged observation well. That author concluded that as production time becomes very short relative to shut-in time, these buildup type curves approach the slug test type curves presented by Cooper, et al. (1967).

Cooley and Cunningham (1979) developed a finite element model to solve a theory considering total energy losses for the flow of a fluid in a reservoir and in the completion interval of a wellbore.

Uraiet and Raghavan (1979) and Eligh-Economides and Ramey (1979) analyzed pressure buildup for wells produced at a constant bottomhole

pressure, These two publications concluded that the last flow rate before the well is shut-in should be used for pressure buildup analysis. The first reference concluded that the actual production time should also be used in the analysis. However, the second reference demonstrated that the time to be used should be obtained by dividing the cummulative production by the last established flow rate before the shut-in, as recommended by Horner (1951).

Barelli (1979) obtained slug test type curves for linear flow systems by using the Laplace transformation and numerical inversion of the transformed pressure solution.

Shinohara and Ramey (1979.a) considered the condition of critical flow during a drillstem test. Modified slug test type curves were presented by those authors using dimensionless maximum wellbore flow rate as a parameter.

In another publication, Shinohara and Ramey (19'79.b) proposed a theory for slug test data analysis considering wellbore storage, skin effect, and inertial effects on the wellbore liquid column. This theory is based on a wellbore momentum balance equation similar to the one presented by Cooper, et al. (1965). Shinohara and Ramey (1979.b) obtained solutions for dimensionless bottomhole pressure and for dimensionless liquid level. Those authors found that there is a range of practical conditions in which these solutions are related by direct hydrostatic calculations, as assumed in all the slug test solutions mentioned previouly. However, those authors also concluded that erroneous interpretations are obtained for some conditions, found in practice but outside that range, if wellbore inertial effects are not considered in the analysis.

Stright (1979) studied the effect of pressure dependent rock and fluid properties on drillstem test analysis for a naturally-fractured reservoir with negligible matrix porosity. Type curves were obtained by finite differences approximation with the ratio of net confining pressure and apparent fracture healing pressure as an additional parameter. That author reached the conclusion that permeability,

porosity, and compressibility of the fractures can be estimated by using a combination of type curve matching, conventional semi-log buildup analysis, and numerical simulation history matching.

In 1980, Raghavan discussed the applicability of drawdown type curves for pressure buildup data analysis and presented buildup type curves for fractured and unfractured wells with producing time as a parameter.

Agarwal (1980) presented a novel and simple approach to allow the use of existing log-log drawdown type curves for analyzing pressure buildup data by plotting the increase in pressure vs the ratio of the product of production time and shut-in time divided by the sum of these two times.

Soliman (1981) proposed a technique for slug test or variable flow rate analysis that is based on superposition of infinitesimal steps, but uses numerical methods to evaluate the resulting integral. That author recommends the technique to analyze buildup tests preceeded by a changing rate.

Raghavan, Reynolds, and Meng (1982) presented a type curve for estimating dimensionless flowing time for vertically-fractured wells.

In 1982, Lee published a text book giving an excellent description of the fundamental concepts for constant flow rate and constant bottomhole pressure well test analysis, and the use of the superposition principle. However, a parallel description of the flow phenomena during a drillstem test is not included in that important text book.

This brief literature review reveals the evolution of well test data analysis methods that have been accepted as conventional in their application. Also, this review shows that another analysis method has been developing and has become a conventional method for some tests that are currently considered difficult to analyze: slug tests, drillstem tests, and closed-chamber tests.

SECTION 3
PROBLEM DESCRIPTION AND FORMULATION

A physical and mathematical description of the flow phenomena during a slug test, drillstem test, or closed-chamber test is presented in this section. An equation describing the dynamical relationship between wellbore liquid level and bottomhole pressure is derived for a common wellbore geometry. This wellbore equation is obtained by performing a momentum balance on the liquid in a wellbore and includes gravitational, inertial, and frictional effects not considered in previous solutions. This equation plus appropriate initial conditions constitute a mathematical wellbore problem. Flow in the reservoir is assumed to be described by the diffusivity equation plus appropriate initial and external boundary conditions to formulate a mathematical reservoir problem.

A description of the flow phenomena in these types of tests is obtained by coupling the wellbore and reservoir problems through application of continuity conditions including wellbore storage and skin effect.

3.1 Physical Description

The flow period of a drillstem test and a slug test involves similar flow phenomena (Ramey, Agarwal, and Martin, 1975). The flow period of a closed-chamber test is also related to the previous two tests (Shinohara and Ramey, 1979.b). In a slug test, a finite amount of liquid is instantaneously removed from (or added to) the static liquid column in a wellbore open to the atmosphere.

In this study, a static liquid column in a well'bore is defined as that column in hydrostatic equilibrium with a bottom'hole pressure equal to a uniform pressure in a reservoir at the start of the flow test, i. e., a static liquid column corresponds to conditions of no-flow in the wellbore and in the reservoir.

The finite amount of liquid removed from (or added to) a static wellbore liquid column is called a slug. In order to distinguish a test for a removed slug from a test for an added slug, these two tests are referred to as: (a) production slug test, and (b) injection slug test, respectively.

An injection slug test proposed by Ferris and Knowles (1954) can be performed by quickly dumping the water content of a barrel into a groundwater well. A production slug test, presented by van der Kamp (1976), is simulated by pulling up a float partially submerged in the static water column. Another technique to simulate a production slug test consists of injecting gas into a well in order to lower the liquid level below the static liquid column level and start the test by suddenly releasing the gas pressure after waiting for initial static equilibrium between gas pressure, liquid column, and reservoir pressure (Bredehoeft, 1981). A related technique has been applied to put into production hot-water geothermal wells when wellbore conditions allow a thermal shock (Ortiz, 1981).

A schematic diagram of the initial condition in a production slug test is presented in Fig. 3.1. L is the length of a static liquid column and is measured from the level of the top of the formation. A static liquid column in a wellbore has been defined in hydrostatic equilibrium with the initial reservoir pressure, then:

$$\left[L + \frac{h}{2} \right] \rho g = p_i - p_a \qquad \cdots (3.1)$$

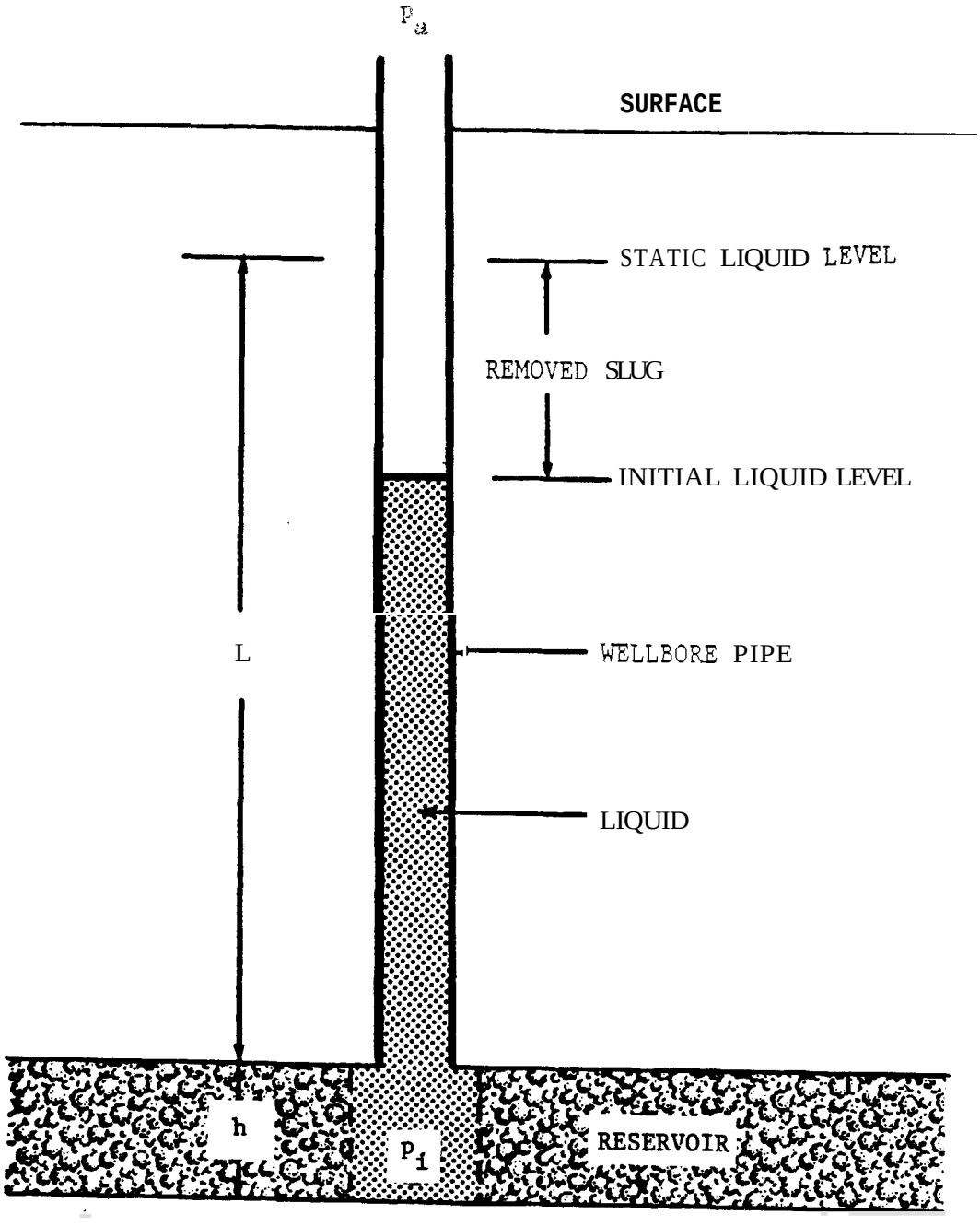

FIG. 31 PRODUCTION SLUG TEST AT INITIAL OONDITIONS

where :

g = gravity acceleration vector, $[LT^{-2}]$

h = reservoir thickness, [L]

L = length of the static liquid column in a wellbore, measured from the top of the formation, [L]

p_a = atmospheric pressure, $[ML^{-1}T^{-2}]$

p_i = initial reservoir pressure at the mid-level of the formation, $[ML^{-1}T^{-2}]$

ρ = average density of the fluid in the wellbore, $[ML^{-3}]$

Throughout this study, independent variables and function arguments are shown inside parenthesis (). Square brackets [] and braces {} are used to associate terms and factors.

According to the information usually available for field data analysis, a known pressure p_i defines length L, or viceversa, by application of Eq. 3.1.

At the beginning of a production slug test, fluid from the reservoir flows into the wellbore to restore the static liquid column. If no fluid is obtained at the surface, the volume of liquid produced from the reservoir at the end of the test will be equal to the volume of the slug instantaneously removed from the static liquid column to start the test. A typical liquid level response in a groundwater well during a production slug test is shown in Fig. 3.2. Reservoir properties and wellbore geometry control this response. For this case, the water level oscillates about its static position. Such system is said to be underdamped.

Initial conditions for an injection slug test are shown in Fig. 3.3. At the beginning of an injection slug test, fluid from the wellbore flows into the reservoir to restore the static liquid column. At the end of this test, the volume of liquid injected into the reservoir will be equal to the volume of the slug instantaneously added into the static liquid column to start the test.

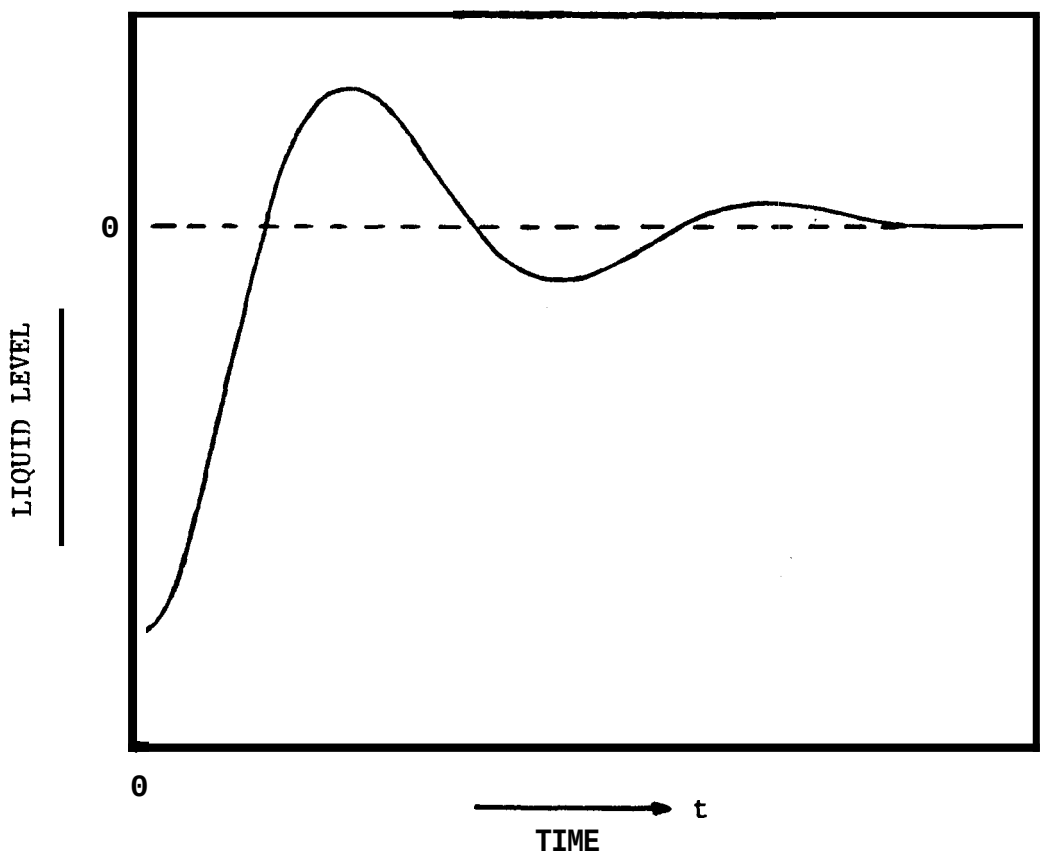

FIG. 3.2. TYPICAL LIQUID LEVEL RESPONSE DURING A PRODUCTION SLUG TEST IN AN UNDERDAMPED GROUNDWATER SYSTEM

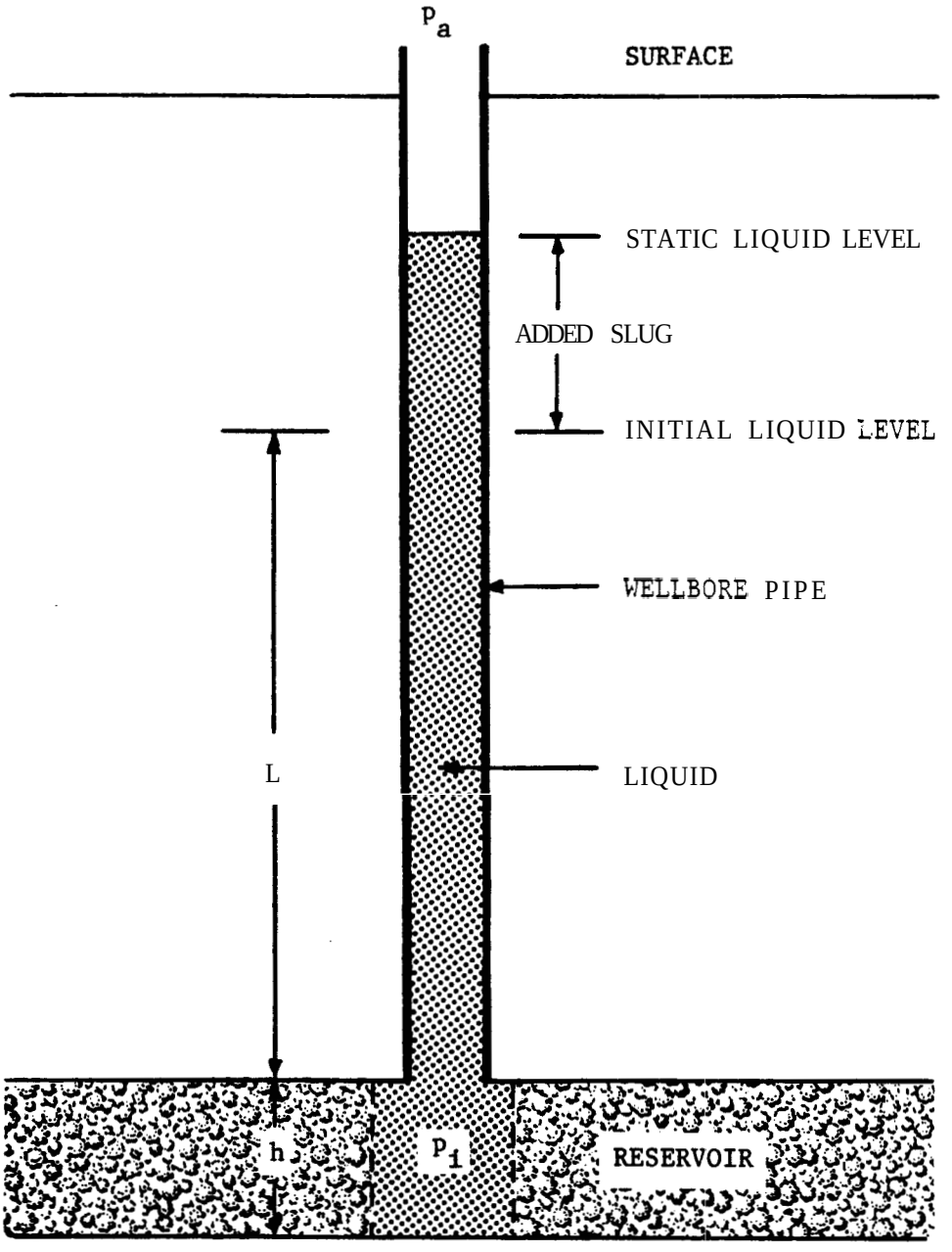

FIG. 3.3. INJECTION SLUG TEST AT INITIAL CONDITIONS

A drillstem test is a temporary well completion and consists of one or several alternated flow and shut-in periods (Earlougher, 1977). A schematic diagram of the initial conditions in a flow period of a drillstem test is presented in Fig. *3.4*. The well is open to the atmosphere. Bottomhole packers have been set to isolate the formation from the drilling mud column. Wellbore pipe is empty except for a liquid cushion. The drillstem tester valve has just been opened to allow flow from the reservoir.

In the case shown in Fig. *3.4*, the length of the static liquid column, L, is larger than the length of the cushion. This implies that initial reservoir pressure, p_i, is higher than hydrostatic cushion pressure, p_c, plus atmospheric pressure, p_a. For this case, fluid from the reservoir will flow into the wellbore in a fashion similar to an equivalent production slug test. On the other hand, if the cushion length is larger than the static liquid column length, fluid from the cushion will flow into the reservoir in a fashion similar to an equivalent injection slug test. Sometimes a drillstem test is operated with a cushion pressure, p_c, nearly equal to formation pressure, p_i. This is called a balanced column test. A typical bottomhole pressure trace recorded during a drillstem test with two flow and shut-in periods, and with no flow at the surface is illustrated in Fig. 3.5. If the initial liquid level is inside the drillcollars, an abrupt change in slope of bottomhole flowing pressure will be noticed. Those cases are not considered in this study. Another situation out of the scope of the present study is that of a drillstem test with a bottomhole choke or other flow restriction that may cause critical flow and impede pressure transmission through that choke.

A situation in which the initial reservoir pressure is higher than the hydrostatic pressure of a liquid column with length equal to the reservoir depth is presented in Fig. *3.6*. This is the case of flowing oil wells and most artesian water wells. During a drillstem test in a well of this type, the liquid level in the wellbore may reach the surface at some time after the start of the test. At that moment, the flow phenomena is abruptly changed because fluid suddenly stops accumulating in the wellbore pipe. Such a well will continue producing

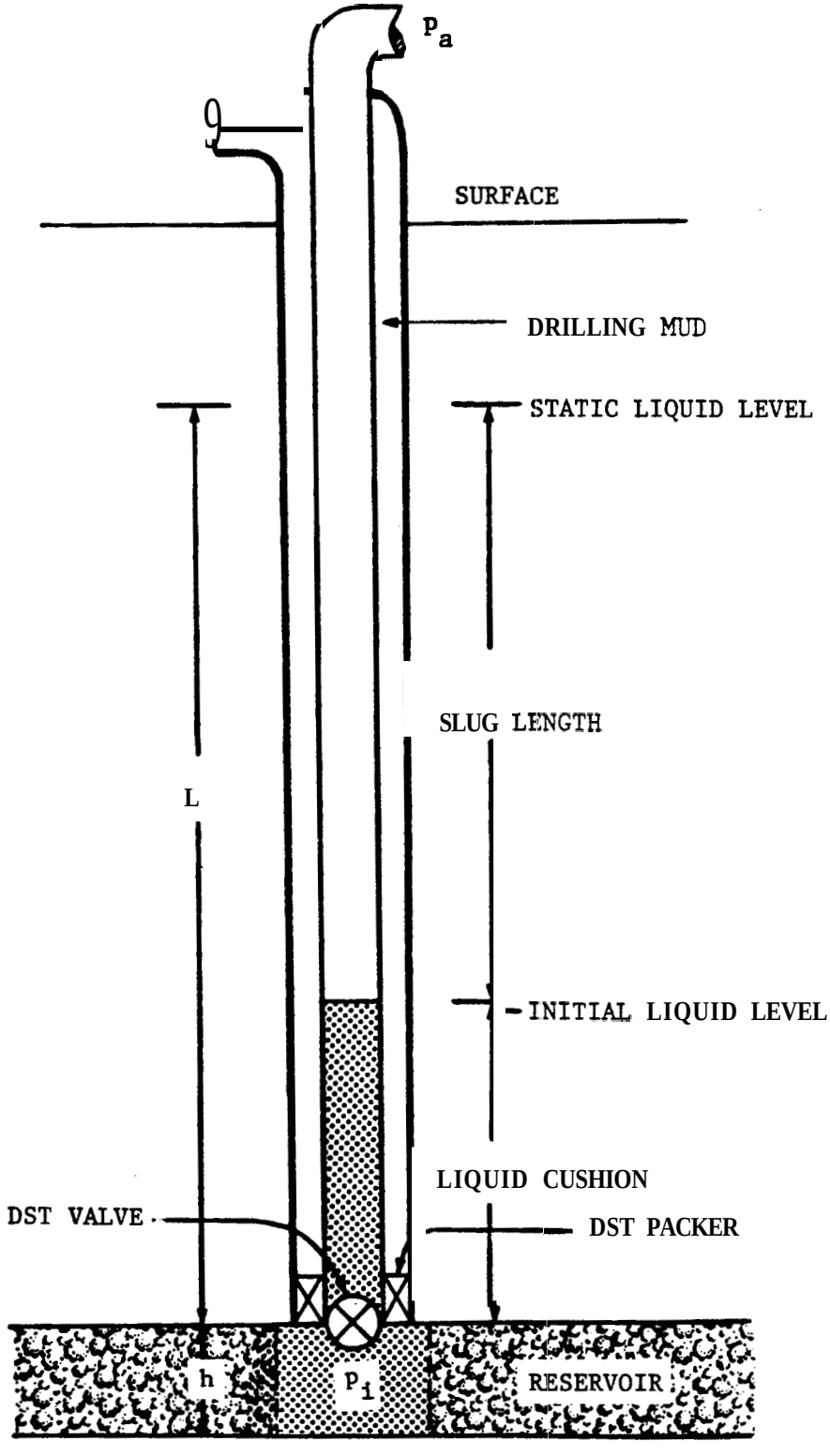

FIG. *3.4.* DRILLSTEM TEST FLOW **PERIOD** AT **INITIAL** CONDITIONS

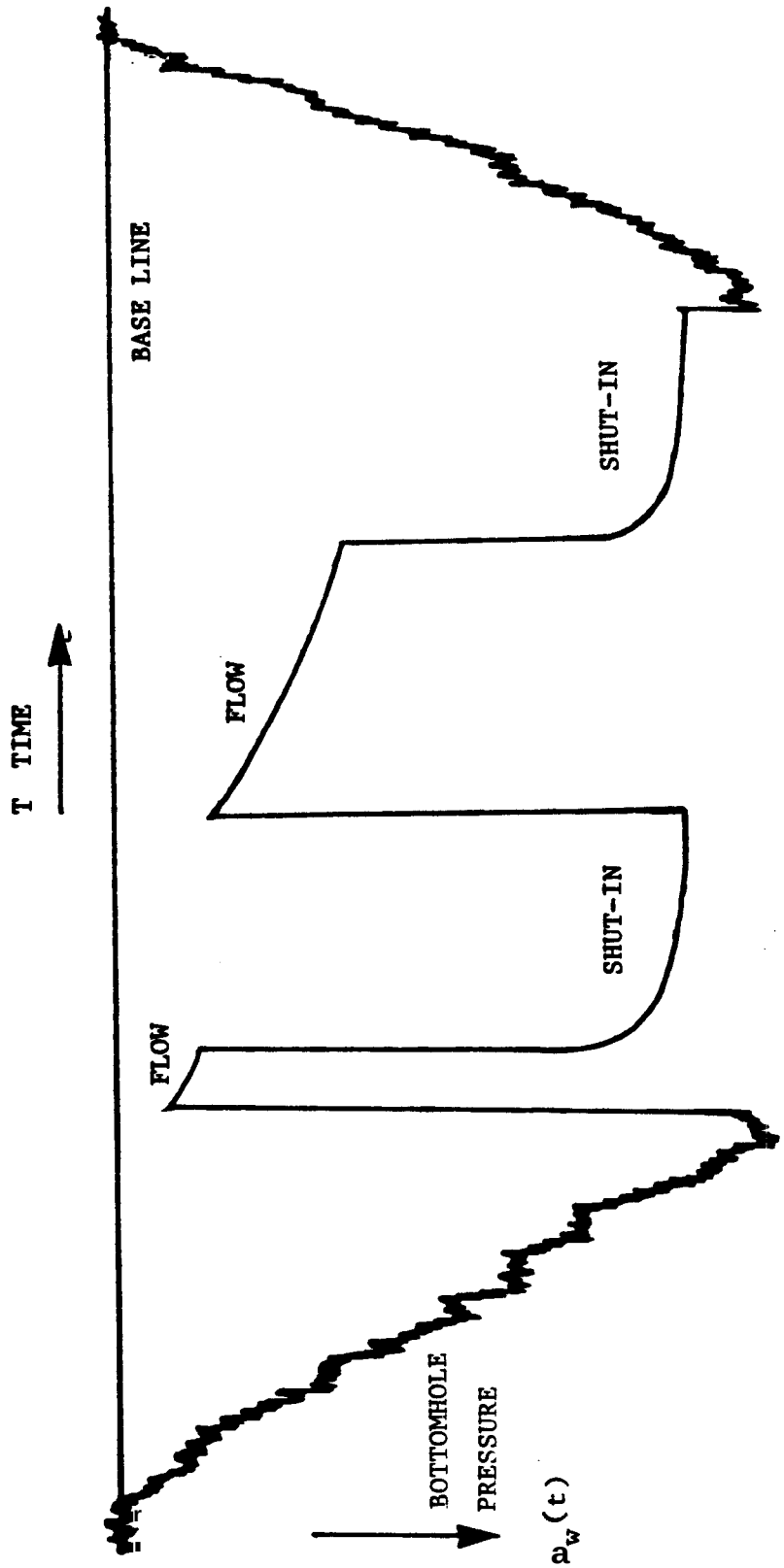

FIG. 3.5. TYPICAL BOTTOMHOLE PRESSURE TRACE DURING A DRILLSTEM TEST

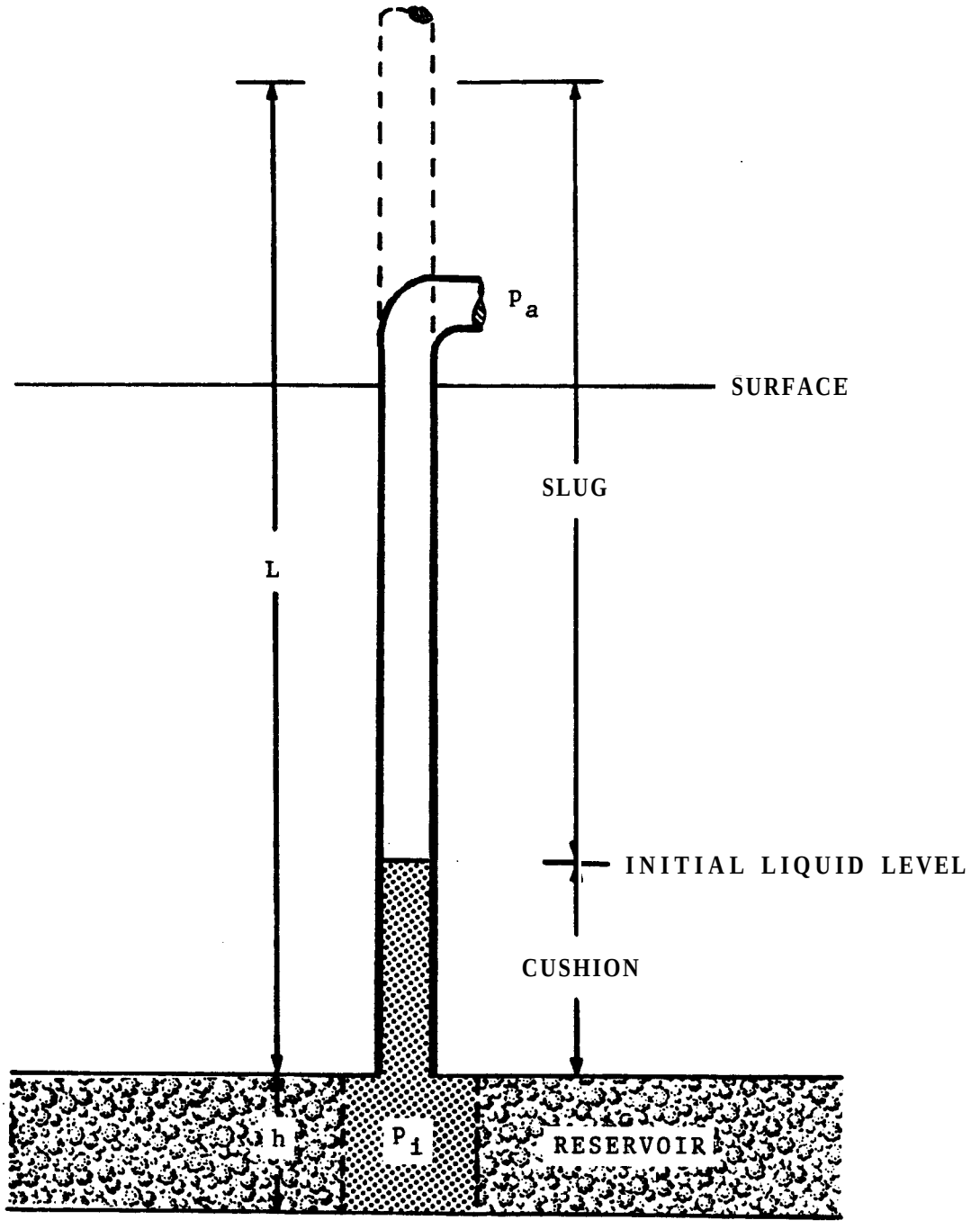

FIG. 3.6. SLUG TEST AT INITIAL OONDITIONS FOR A FLOWING WELL

fluids at the surface as long as the bottomhole pressure remains high enough to support a liquid column up to the surface.

Another case of Figs. 3.3 or 3.4 is worth mentioning. When the static liquid level, L, is near the surface, removal of a slug can lead to ejection of liquid at the surface due to inertial effects on the liquid column in the wellbore.

A closed-chamber test is similar to a drillstem test except for a valve at the wellhead that is shut-in at the start of the test. This valve and the changing liquid level form a chamber inside the wellbore pipe, as shown in Fig. 3.7. Flow phenomena in a closed-chamber test is affected by the changing gas pressure in the chamber in addition to the physical factors governing the flow behavior in a drillstem test. Therefore, if the chamber is not opened during the test, the liquid level in the wellbore will not reach the static level at L because the gas pressure in the chamber will be higher than atmospheric. Instead, the liquid level will stabilize at a lower position at long testing times. This lower level will correspond to hydrostatic equilibrium conditions between reservoir pressure, liquid column length, and final closed-chamber gas pressure. A typical bottomhole pressure trace recorded during a closed-chamber test with two flow periods is illustrated in Fig. 3.8.

3.2 Wellbore Problem

A schematic representation of the wellbore-reservoir system under consideration is shown in Fig. 3.9 at initial conditions for the case of a production slug test. According to the definition given to L, Eq. 3.1, initial reservoir pressure at the mid-level of the formation can support a static liquid column with length L above the top of the formation. Then, fluid from the reservoir will flow into the wellbore and the liquid level will rise inside the pipe in response to these initial conditions.

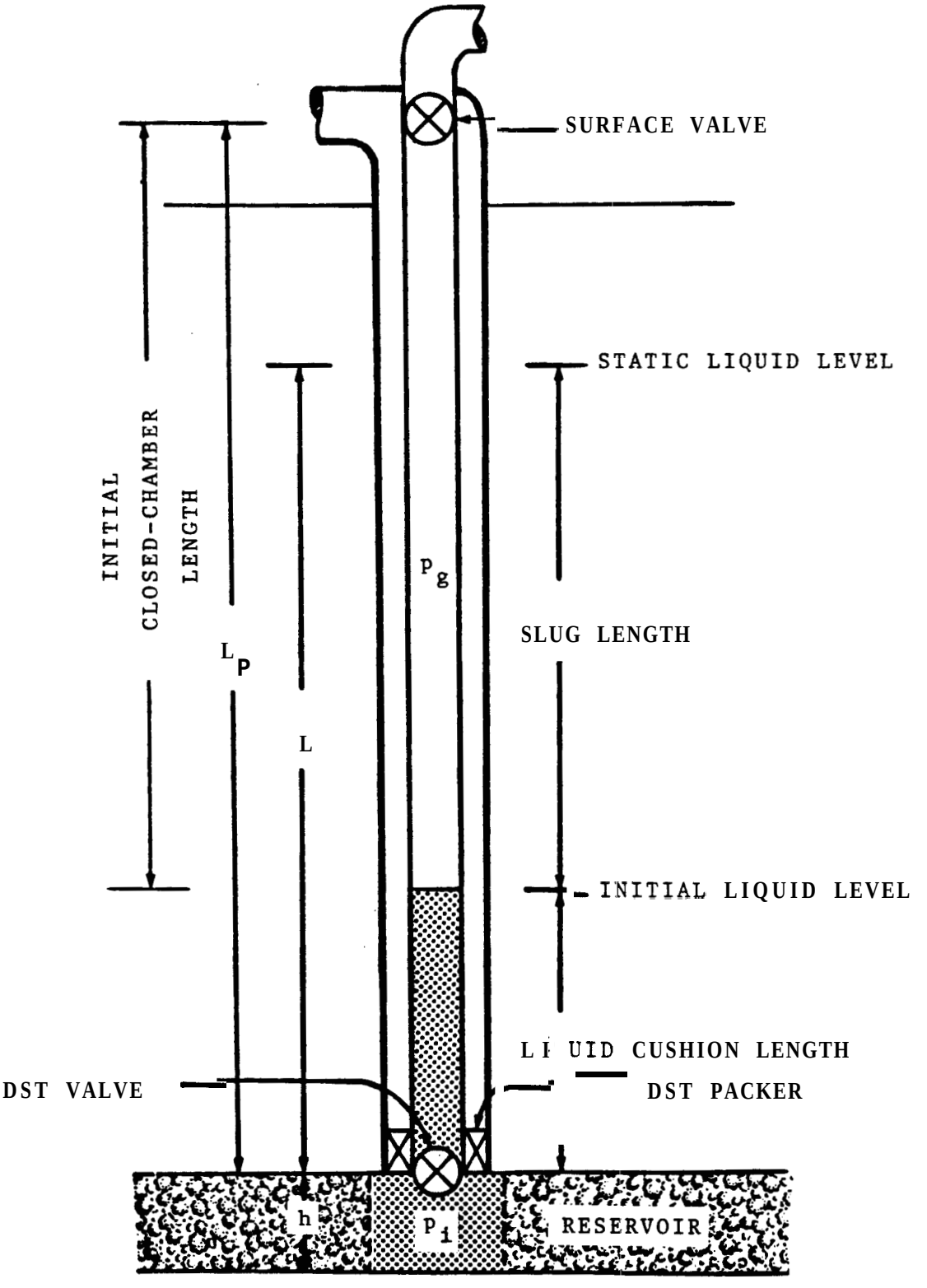

FIG. 3.7. CLOSED-CHAMBER TEST AT INITIAL CONDITIONS

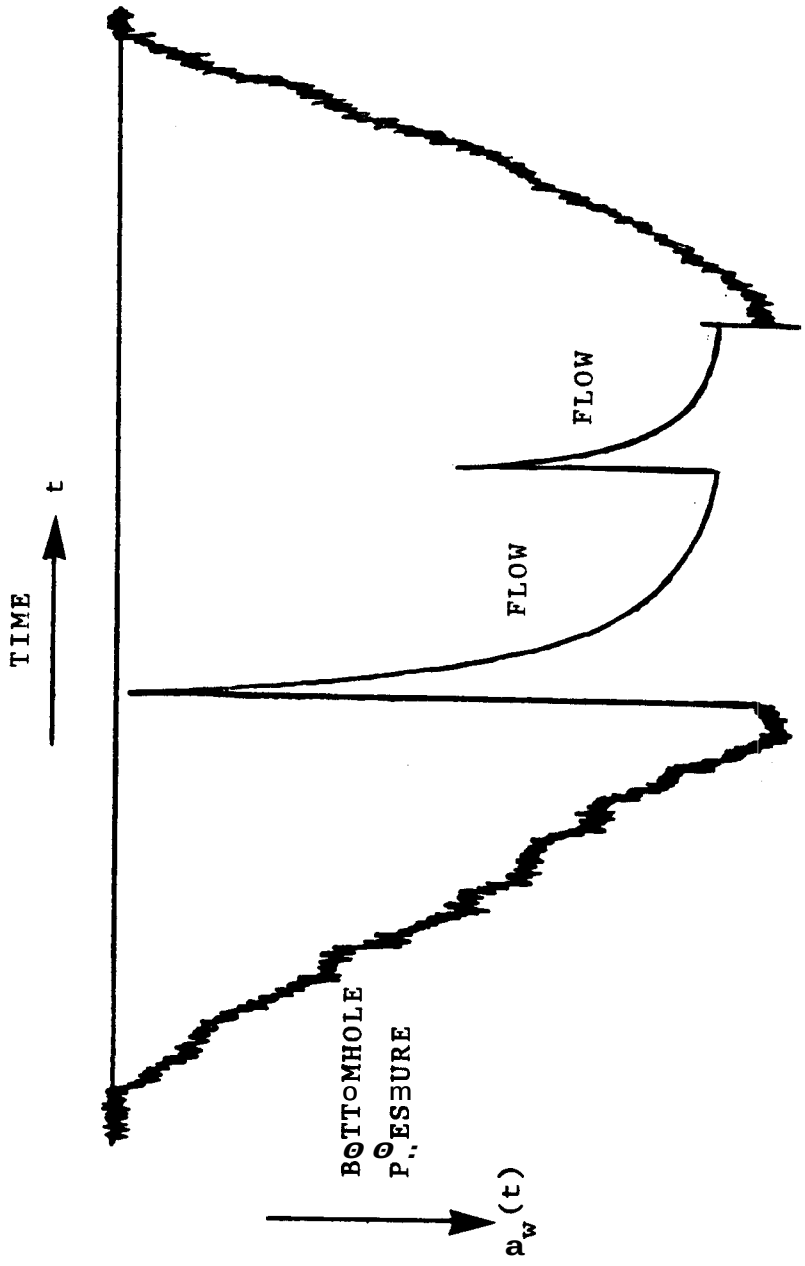

FIG. 3.8. TYPICAL BOTTOMHOLE PRESSURE TRACE DURING A CLOSED-CHAMBER TEST

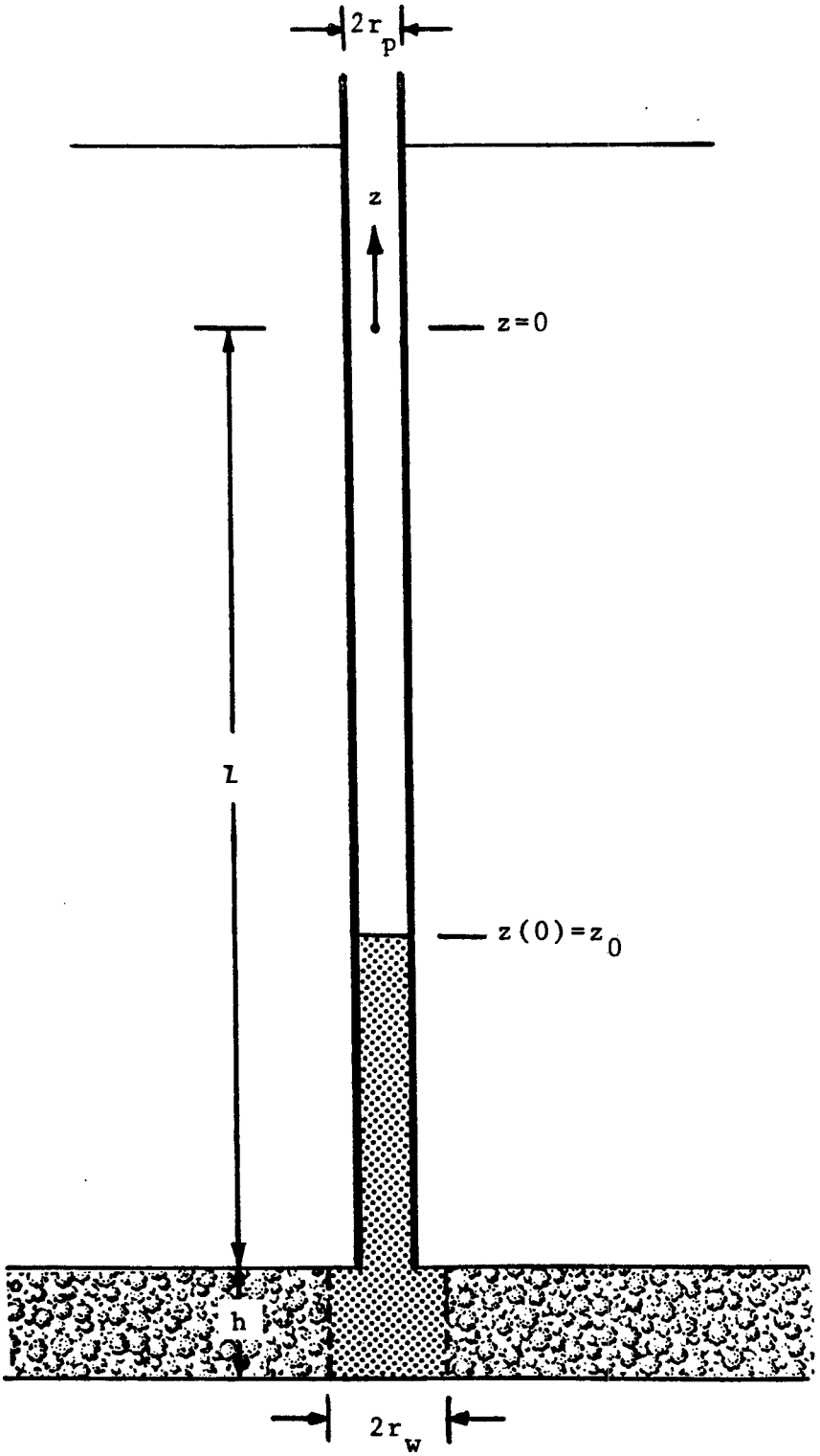

FIG. 3.9. SLUG TEST AT INITIAL CONDITIONS SHOWING THE Z-COORDINATE USED TO DESCRIBE WELLBORE LIQUID LEVEL BEHAVIOR

The behavior of the changing height of liquid in the wellbore is conveniently described by using the z-coordinate also shown in Fig. 3.9. This z-coordinate is measured positive upward from a distance L above the top of the formation. Therefore, the length of the wellbore liquid column, measured from the top of the formation, at any time t is given by $L+z(t)$. For example, the length of the liquid cushion in Fig. 3.9 is $L+z_0$, where z_0 is negative and equal to the value of z at the start of the test, $t=0$. As a second example, the length of the liquid column after an infinite testing time will be equal to L. This is because the liquid level will reach the static liquid level eventually, and z is equal to zero at the static liquid level. This statement applies strictly to an infinite reservoir. However, it is an excellent approximation because the volume of fluid in a wellbore is negligible in comparison with the volume of fluid in a reservoir of economical interest.

3.2.1 Wellbore Equations

In order to derive a mathematical relationship between the changing wellbore liquid level and the changing bottomhole pressure under transient flow conditions, the wellbore is represented by two stationary control volumes. An upper control volume consists of the wellbore section from the top of the reservoir to the surface. A lower control volume consists of the wellbore section in front of the formation. The entire wellbore is composed by coupling these two control volumes through continuity conditions.

Newton's Law of Inertia states that in the absence of external influences, matter tends to remain at rest if it is already at rest, or tends to remain moving in a straight line with uniform velocity if it is already moving at that velocity. The external influences that can set matter into motion or change direction and/or velocity of moving matter are called forces.

Newton's Second Law of Motion states that when a mass m is moved from rest to a given velocity, or when the direction and/or the magnitude of its velocity v are changed, the force F required to perform that change is equal to the rate of change of momentum mv. That is:

$$\frac{d}{dt} [m v] = F \qquad \ldots (3.2)$$

where:

F = force vector, $[MLT^{-2}]$

m = mass, [M]

t = time, [T]

v = velocity vector, $[LT^{-1}]$

Newton's Second Law of Motion applied to a control volume with volume V and external surface area S, yields (Eskinazi, 1962):

$$\frac{\partial}{\partial t} \int_V \rho v \, dV + \int_S \rho v \, |v| \, dS = F \qquad \ldots (3.3)$$

where:

$|v|$ = magnitude of the component of v in the vector direction normal to S, $[LT^{-1}]$

The first term on the left-hand side of Eq. 3.3 represents the rate of change of momentum of the fluid in the control volume due to local variations of the fluid velocity and/or density with time. The second term on the left-hand side represents the net momentum rate crossing the external surface of the control volume due to fluid flow. On the right-hand side, F is the resultant of all external forces on the fluid inside the control volume that causes the instantaneous rate of change of momentum given by the left-hand side. This force F is opposed by an equal reaction force maintaining the control volume in the position in which it is instantaneously analyzed (Eskinazi, 1962).

Equation 3.3 is applied in Appendix A to formulate the following non-homogeneous, non-linear, second-order ordinary differential equation for a wellbore:

$$A_w z'' + B_w z' + C_w z + D_w = E_w p_w \quad \ldots (3.4)$$

where :

$$A_w = L + z + \frac{3}{8} h \left[\frac{r_p}{r_w} \right]^2 \quad \ldots (3.4.a)$$

$$B_w = [L + z] \frac{f}{4} \left| \frac{1}{r_p} z' \right| + \frac{3}{4} \left[\frac{r_p}{r_w} \right]^4 z' \quad \ldots (3.4.b)$$

$$C_w = g \quad \ldots (3.4.c)$$

$$D_w = [L + \tfrac{h}{2}] g + \frac{p_g}{\rho} \quad \ldots (3.4.d)$$

$$E_w = \frac{1}{\rho} \quad \ldots (3.4.e)$$

with:

p_g = gas pressure on the liquid level, $[ML^{-1}T^{-2}]$

p_w = bottomhole pressure at the mid-level of the formation, $[ML^{-1}T^{-2}]$

$z(t)$ = liquid level in the wellbore, measured positive upward from a length L above the top of the formation, $[L]$

$z'(t)$ = velocity of the wellbore fluid column, $[LT^{-1}]$

$z''(t)$ = acceleration of the wellbore fluid column, $[LT^{-2}]$

Equation *3.4* considers the following effects on the flow phenomena inside a wellbore:

(1) inertial effect of a liquid column with length changing with time,

(2) frictional effect of a liquid column moving inside a pipe,

(3) gravitational effect on a liquid column changing in length and including the liquid in the wellbore section in front of the reservoir thickness, and

(4) effect of pipe radius different than wellbore radius.

Equation *3.4* or any of its special forms for particular applications are referred to as wellbore equations throughout this study. Definition of coefficients A_w, B_w, C D_w, and E_w corresponding to particular wellbore equations will be provided in the appropriate place.

Assumptions implicit in wellbore Eq. *3.4* are the following:

(1) fluid velocity vector is vertical and uniform across any pipe cross-section,

(2) average density of the fluid in the wellbore is constant,

(3) pipe frictional resistance in unsteady flow is equal to the frictional resistance in steady flow at the same velocity, and the

(4) fluid column is accelerated by flow from the reservoir uniformly along the wellbore section in front of the formation.

The previous assumptions are listed in the same order as were required in the derivation of the wellbore equation presented in Appendix A. In this derivation, the adoption of each of the previous four assumptions was delayed in an effort to avoid them.

The approach utilized in the present study to derive the wellbore Eq. 3.4 is parallel to the one proposed by Cooper, et al. (1965). However, those authors adopted additional assumptions throughout their derivation, and obtained a simplified equation that is a particular case of wellbore Eq. 3.4. As mentioned in Section 2, the wellbore equation proposed by Cooper, et al. (1965) was used later and simplified further by other authors. Therefore, wellbore Eq. 3.4 can be utilized to analyze the effect of some of the simplifying assumptions adopted in solutions currently available in the literature.

Slug Test Wellbore Equation - During a slug test, the well is open to the atmosphere, and gas pressure, $p_g(t)$, on the wellbore liquid level can be assumed contant and equal to atmospheric pressure, p_a. Then, substituting the definition of L, given by Eq. 3.1, into Eq. 3.4, and simplifying:

$$A_w z'' + B_w z' + C_w z + D_w = E_w [p_i - p_w] \quad \ldots (3.5)$$

where:

$$A_w = L + z + \frac{3}{8} h \left[\frac{\bar{p}}{r_w} \right]^2 \quad \ldots (3.5.a)$$

$$B_w = [L + z] \frac{f}{4} \left| \frac{1}{r_p} z' \right| + \frac{3}{4} \left[\frac{r_p}{r_w} \right]^4 z' \quad \ldots (3.5.b)$$

$$C_w = g \quad \ldots (3.5.c)$$

$$D_w = 0 \quad \ldots \quad (3.5.d)$$

$$E_w = -\frac{1}{\rho} \quad \ldots \quad (3.5.e)$$

Drillstem Test Wellbore Equation - During the flow period of a drillstem test, the well is also open to the atmosphere and, since $p_g(t)=p_a$, wellbore Eq. 3.5 is applicable until the moment, t_s, at which the well is shut-in at the bottom by closing the drillstem test valve. After the well is shut-in the space below the test valve is filled with liquid and no wellbore equation is required if momentum changes and storage by compression are assumed negligible. If a flowing well is not shut-in during a drillstem test, Eq. 3.5 describes the flow phenomena only until the moment at which liquid is produced at the surface.

Closed-Chamber Test Wellbore Equation - For a closed-chamber test, $p_g(t)$ can not be simplified as in a slug test or drillstem test, but can be described by applying the equation of state for a real gas, as used by Shinohara and Ramey (1979.b):

$$p_g(t)\, V_g(t) = Z_g(t)\, n_g\, R\, T_g \quad \ldots \quad (3.6)$$

where :

n_g = number of moles of gas in the closed-chamber, [mole]
p_g = gas pressure, $[ML^{-1}T^{-2}]$
R = universal gas constant, $[ML^2T^{-2}mole^{-1}degree^{-1}]$
T_g = average absolute temperature in the chamber, [degree]
V_g = gas chamber instantaneous volume, $[L^3]$
Z_g = gas deviation factor at the average temperature in the wellbore (Standing, 1952)

Assuming isothermal conditions and also that no gas is liberated from the produced liquid, and since $V_g(t)=\pi r_p^2\{L_p-[L+z(t)]\}$, where L_p is the length of the pipe from the wellhead to the top of the formation, as shown in Fig. 3.7, the following expression can be obtained by applying **Eq.** 3.6 at two conditions:

$$p_g(t) = \frac{L - L_p + z(0)}{L - L_p + z(t)} \frac{Z_g}{Z_g(0)} p_g(0) \qquad \ldots (3.7)$$

where:

$p_g(0)$ = initial gas pressure in the closed-chamber, $[ML^{-1}T^{-1}]$

$Z_g(0)$ = gas deviation factor at $p_g(0)$

Substituting this equation and the definition of L, given by **Eq.** 3.1, into wellbore **Eq.** 3.4:

$$A_w z'' + B_w z' + C_w z + D_w = E_w [\, p_i - p_w \,] \qquad \ldots (3.8)$$

where:

$$A_w = L + z + \frac{3}{8} h \left[\frac{r_p}{r_w} \right]^2 \qquad \ldots (3.8.a)$$

$$B_w = [\, L + z \,] \frac{f}{4} \left| \frac{1}{r_p} z' \right| + \frac{3}{4} \left[\frac{r_p}{r_w} \right]^4 z' \qquad \ldots (3.8.b)$$

$$C_w = g \qquad \ldots (3.8.c)$$

$$D_w = \frac{L - L_p + z(0)}{L - L_p + z(t)} \frac{Z_g}{Z_g(0)} \frac{p_g(0)}{\rho} - \frac{p_a}{\rho} \quad \ldots \text{(3.8.d)}$$

$$E_w = -\frac{1}{P} \quad \ldots \text{(3.8.e)}$$

3.2.2 Wellbore Initial Conditions

Wellbore Eqs. 3.5 and 3.8 are second-order, ordinary differential equations for liquid level $z(t)$. In order to formulate an initial value mathematical problem, $z(t)$ and its first derivative, liquid column velocity, $z'(t)$, must be specified at the start of the test, $t=0$. These initial values can be defined constant as follows:

$$z(0) = z_0 \quad \ldots \text{(3.9)}$$

and:

$$z'(0) = v_0 \quad \ldots \text{(3.10)}$$

Equations 3.9 and 3.10 do not specify initial conditions because they involve unknown constant initial values for liquid level and liquid column velocity, respectively.

For a slug test, drillstem test, or closed-chamber test, the fluid column in a wellbore can be considered static at initial conditions

(Shinohara and Ramey, 1979.b). Then, an adequate liquid column velocity initial condition is:

$$v_0 = 0 \quad \ldots (3.11)$$

From observation of Fig. 3.9, the initial condition for the liquid level z_0 in a production test can be any negative value in the range of $-L<z_0<0$. On the other hand, in an injection test, the liquid level initial condition can be any positive value, $z_0>0$, with an upper bound only restricted by the length of pipe above the static liquid level and by the initial reservoir pressure.

In order to avoid specification of particular values of z_0 and obtain a solution for each z_0, the problem is normalized by z_0 in Section **3.6.** This approach was also used by Shinohara and Ramey (1979.b). Mathematically, this is equivalent to specifying any possible initial level z_0. Since the solutions obtained using this approach are scaled by z_0, qualitative analysis is possible. However, the actual initial wellbore liquid level must be known, or determined, in order to obtain quantitative information. In other words, the specification of the liquid level initial condition is delayed until the application of the dimensionless solutions presented in this study. Therefore, these solutions are applicable to production slug tests, injection slug tests, drillstem tests, and closed-closed-chamber tests, under the corresponding constraints.

From Fig. 3.10, the length of the cushion, measured from the level of the top of the formation, L_c, is given by:

$$L_C = L + z_0 \quad \ldots (3.12)$$

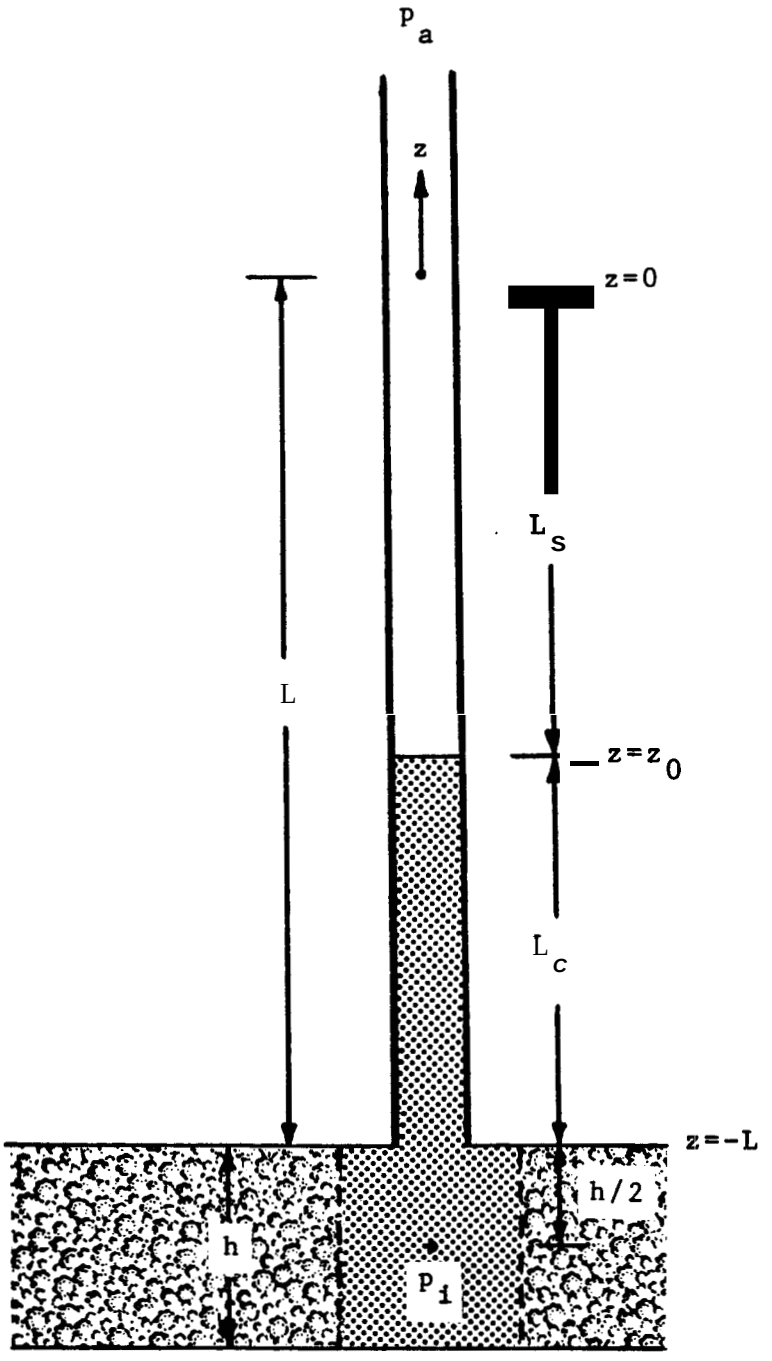

FIG. 3.10. SLUG TEST AT INITIAL CONDITIONS SHOWING DEFINITION OF SLUG LENGTH AND CUSHION LENGTH

Also from Fig. 3.10, the length of the slug, L_s, is given by:

$$L_s = - z_0 \qquad \ldots (3.13)$$

Note that L_s is negative for an injection slug test.

When L_c, h, ρ, and p_i are known, z_0 can be evaluated from the following relationship obtained by substituting Eq. 3.1 into Eq. 3.12:

$$z_0 = L_c - \frac{p_i - p_a}{\rho g} + \frac{h}{2} \qquad \ldots (3.14)$$

If the position of the static liquid level in a wellbore is known and the length of the slug, L_s, is controlled, z_0 can be directly evaluated from Eq. 3.13. Other appropriate expressions for calculating z_0 from slug test, drillstem test, or closed-chamber test data will be given later in this study.

3.3 Reservoir Problem

In many underground reservoirs, the relatively large distance between wells with respect to formation thickness, structural configuration, and wellbore radii determines a geometry for flow of fluids through the porous medium that closely resembles radial flow in the vicinity of the wells. Since most of the pressure drop occurs in the vicinity of a flowing wellbore, the flow through the reservoir during a drillstem test is assumed to be described by the radial diffusivity equation. This equation, plus initial and boundary conditions appropriate for this type of test define a reservoir problem.

3.3.1 Reservoir Equation

The diffusivity equation for radial flow can be written as:

$$\frac{1}{r}\frac{\partial}{\partial r}\left[r \frac{\partial p}{\partial r} \right] = \frac{\phi \mu c_t}{k} \frac{\partial p}{\partial t} \qquad \ldots (3.15)$$

where:

c_t = total compressibility of the system, $[M^{-1}LT^{23}$

k = reservoir permeability, $\{L^2\}$

p = reservoir pressure, $[ML^{-1}T^{-2}]$

r = radial coordinate, $\{L]$

ϕ = reservoir porosity

μ = fluid viscosity at reservoir conditions, $[ML^{-1}T^{-1}]$

This equation results from the application of the Law of Conservation of Mass to a porous elementary control volume, Darcy's Law for Flow through Porous Media, and an Equation of State for a Slightly Compressible Fluid (Matthews and Russell, 1967).

Reservoir Eq. 3.15 implies the following assumptions:

(1) radial horizontal flow,

(2) homogeneous porous medium,

(3) isotropic porous medium,

(4) constant reservoir porosity,

(5) constant reservoir permeability,

(6) flow of a single fluid,

(7) constant fluid viscosity, and

(8) small pressure gradients in the reservoir.

Although this list of assumptions may appear excessively restrictive, the radial diffusivity equation has been found applicable to many practical conditions and constitutes a milestone for modern transient well test analysis techniques (Ramey, 1982).

3.3.2 Reservoir Initial Condition

Pressure distribution in the reservoir is assumed uniform at the initial conditions of a drillstem test. Then:

$$p(r,0) = p_i \quad , r \geq r_w \qquad \ldots (3.16)$$

This is an initial reservoir condition normally achieved by allowing a period of time in which the reservoir is not perturbed before the start of the flow test. Since a drillstem test is commonly performed during the drilling process of a well, this initial condition is also applicable to a flow period of a drillstem test conducted under the following precautions:

(1) packers are properly set on casing or cap rock. This prevents mud in the annular space from filtering through a permeable zone, by-passing the packers, and transmitting pressure from the mud column into the tested zone.

(2) Mud fluid losses are kept small. This can be achieved by controlling drilling mud density to obtain a small positive pressure difference between bottomhole mud column pressure and fluid pressure in the tested zone.

(3) Over-pressurization (supercharge) due to mud filtrate invasion is released and reservoir pressure is allow to stabilize. This can be achieved by performing a short flow period and a conveniently long subsequent shut-in period before the flow period used for pressure analysis.

3.3.3 Reservoir Outer Boundary Condition

The reservoir outer boundary is assumed to be located far from the wellbore, at a distance at which the flow phenomena observed during a drillstem test is not appreciably affected by the conditions there. Under this assumption, the flow phenomena in an actual finite reservoir during the range of times of interest are similar to those of a sufficiently large reservoir. This can be written mathematically in the following form:

$$\lim_{r \to \infty} p(r,t) = p_i \quad , t>0 \qquad \ldots \text{(3.17)}$$

This reservoir boundary condition is not a result of the relatively small volume of fluids flowing into the wellbore in comparison with the volume of fluids within the reservoir. However, this characteristic causes a practical recovery of the liquid level to the static liquid level for long testing times in a well that does not flow at the surface.

3.4 Coupling Conditions

Wellbore Eqs. *3.5* and *3.8* relate wellbore liquid level $z(t)$ with bottomhole pressure $p_w(t)$. Reservoir Eq. 3.15 applies from the sandface into the reservoir. Coupling conditions between wellbore and reservoir are described in this section to complete a formulation of a drillstem test. Wellbore storage and skin effect can be used as coupling conditions as proposed by Ramey and Agarwal. (1972).

3.4.1 Wellbore Storage

The wellbore storage concept was introduced by van Everdingen and Hurst in 1949. For a drillstem test, the liquid level rate of change in the wellbore, $z'(t)$, reflects the flow rate from the reservoir. According to Darcy's Law, this flow rate depends on the pressure gradient at the sandface. Then, applying Darcy's Law at the cylindrical sandface, $r=r_w$:

$$q(t) = \pi r_p^2 z' = \frac{2akh}{\mu} \left[r \frac{\partial p}{\partial r} \right]_{r=r_w} \quad \ldots (3.18)$$

where:

$q(t)$ = instantaneous flow rate, (+) for flow from the reservoir into the wellbore, (-) for flow from the wellbore into the reservoir, $[L^3T^{-1}]$

Ramey, Agarwal and Martin (1975) defined a wellbore storage constant due to liquid level change as follows:

$$C = \frac{ar_p^2}{\rho g} \quad \ldots (3.19)$$

where:

C = wellbore storage constant for liquid level change, $[M^{-1}L^4T^2]$

The wellbore storage coupling condition may be obtained by substituting Eq. 3.19 into Eq. 3.18:

$$z'(t) = \frac{2\pi kh}{\mu} \frac{1}{\rho g C} \left[r \frac{\partial p}{\partial r} \right]_{r=r_w} \quad \ldots (3.20)$$

3.4.2 Skin Effect Condition

The well drilling process and well stimulation techniques may cause an alteration to the reservoir effective permeability in a region near the wellbore. Hurst (1953) and van Everdingen (1953) proposed a mathematical concept to describe that wellbore damage. This concept is called the infinitesimal skin effect. Those authors considered a homogeneous reservoir and assumed that the additional pressure drop due to a damaged zone occurs exactly at the sandface. Also, since transient flow conditions around the bottom of a wellbore closely resemble a succession of steady-state conditions, those authors introduced the following steady-state pressure drop at the sandface, proportional to the instantaneous flow rate:

$$p(r_w,t) - p_w(t) = \left[s \frac{\mu}{2\pi kh} \right] q(t) \qquad \ldots (3.21)$$

where the group of parameters inside the brackets is a proportionality factor, and s is referred to *as* the skin effect or skin.

Equation 3.21 relates bottomhole pressure and sandface pressure. The skin effect coupling condition is obtained by substituting Eq. 3.18 into Eq. 3.21:

$$p_w = \left\{ p - s \left[r \frac{\partial p}{\partial r} \right] \right\}_{r=r_w} \qquad \ldots (3.22)$$

3.5 Problem Statement

Simultaneous solution of the equations and conditions previously derived in Section 3.4 constitute the following mathematical initial value problem describing the flow phenomena during a slug test or drillstem test including gravitational, inertial, and frictional effects on the wellbore fluid column:

Wellbore Equation

$$A_w z'' + B_w z' + C_w z + D_w = E_w [p_i - p_w] \quad , t>0 \qquad \ldots (3.5)$$

where :

$$A_w = L + z + \frac{3}{8} h [\frac{r_p}{r_w}]^2 \qquad \ldots (3.5.a)$$

$$B_w = [L + z] \frac{f}{4} \left| \frac{1}{r_p} z' \right| + \frac{3}{4} [\frac{r_p}{r_w}]^4 z' \qquad \ldots (3.5.b)$$

$$C_w = g \qquad \ldots (3.5.c)$$

$$D_w = 0 \qquad \ldots (3.5.d)$$

$$E_w = -\frac{1}{P} \qquad \ldots \text{(3.5.e)}$$

For the flow period of a closed-chamber test, the previous wellbore equation is applicable with the following modification:

$$D_w = \frac{L - L_p + z(0)}{L - L_p + z(t)} \frac{Z_g}{Z_g(0)} \frac{p_g(0)}{\rho} - \frac{p_a}{\rho} \qquad \ldots \textbf{(3.8.d)}$$

Reservoir Equation

$$\frac{1}{r}\frac{\partial}{\partial r}\left[r \frac{\partial p}{\partial r} \right] = \frac{\phi \mu c_t}{k} \frac{\partial p}{\partial t} \quad , r \geq r_w, \; t \geq 0 \qquad \ldots \text{(3.15)}$$

Wellbore Storage Condition

$$z' = \frac{2\pi kh}{\mu} \frac{1}{\rho g C} \left[r \frac{\partial p}{\partial r} \right]_{r=r_w} \quad , t \geq 0 \qquad \ldots \text{(3.20)}$$

Skin Effect Condition

$$p_w = \left\{ p - s \left[r \frac{\partial p}{\partial r} \right] \right\}_{r=r} \quad , t \geq 0 \qquad \ldots \text{(3.22)}$$

Reservoir Outer Boundary Condition

$$\lim_{r \to \infty} p(r,t) = p_i \quad , \; t>0 \qquad \ldots (3.17)$$

Initial Wellbore Liquid Level Condition

$$z(0) = z_0 \qquad \ldots (3.9)$$

Initial Wellbore Liquid Column Velocity Condition

$$z'(0) = 0 \qquad \ldots (3.11)$$

Initial Reservoir Condition

$$p(r,0) = p_i \quad , \; r>r_w \qquad \ldots (3.16)$$

3.6 Dimensionless Problem Statement

In order to avoid specifying a particular initial liquid level z_0 in the problem statement presented in Section 3.5, dependent variables $z(t)$, $p_w(t)$, and $p(r,t)$ are normalized by z_0 as follows (Shinohara and Ramey, 1979.b):

Dimensionless Liquid Level

$$z_D = \frac{z}{-z_0} = \frac{\rho g z}{p_i - [\, p_c + p_a \,]} \qquad \ldots (3.23)$$

Dimensionless Bottomhole Pressure

$$p_{wD} = \frac{p_i - p_w}{-\rho g z_0} = \frac{p_i - p_w}{p_i - [\, p_c + p_a \,]} \qquad \ldots (3.24)$$

A useful relationship obtained from this definition is the following:

$$1 - p_{wD} = \frac{p_w - [\, p_c + p_a \,]}{p_i - [\, p_c + p_a \,]} \qquad \ldots (3.25)$$

Dimensionless Reservoir Pressure

$$p_D = \frac{p_i - p}{-\rho g z_0} = \frac{p_i - p}{p_i - [\, p_c + p_a \,]} \qquad \ldots (3.26)$$

The far-right equivalent definitions in the previous three equations are obtained by observing from Fig. 3.10 that the cushion hydrostatic pressure at the mid-level of the formation, p_c, is given by:

$$p_c = \rho g \left[\, L + z_0 + \frac{h}{2} \,\right] \qquad \ldots (3.27)$$

and substituting Eq. 3.1 into Eq. 3.27, as follows:

$$-\rho g z_0 = p_i - [\, p_c + p_a \,] \qquad \ldots (3.28)$$

Independent variable r is normalized as usual by dividing by wellbore radius, r_w:

Dimensionless Radius

$$r_D = \frac{r}{r_w} \qquad \ldots (3.29)$$

Independent variable t is normalized by the inverse of the diffusivity constant and the square of the wellbore radius, $k/[\phi\mu c_t r_w^2]$:

Dimensionless Time

$$t_D = \frac{kt}{\phi\mu c_t r_w^2} \qquad \ldots (3.30)$$

Characteristic lengths of the system, L, h, r_p, and r_w, are normalized by z_0, as follows:

Dimensionless Static Liquid Column Length

$$L_D = \frac{L}{-z_0} \qquad \ldots (3.31)$$

Dimensionless Reservoir Thickness

$$h_D = \frac{h}{-z_0} \qquad \ldots (3.32)$$

Dimensionless Pipe Radius with respect to Slug Size

$$r_{pDz} = \frac{r_p}{-z_0} \qquad \ldots (3.33)$$

Dimensionless Wellbore Radius with respect to Slug Size

$$r_{wDz} = \frac{r_w}{-z_0} \qquad \ldots (3.34)$$

Flow rate and the rate of change of flow rate are important functions that can be obtained from the following dimensionless groups, derived from the definition of z_D and t_D, Eqs. *3.23* and *3.30*, respectively:

Dimensionless Liquid Column Velocity

$$z'_D = \frac{1}{-z_0} \left[\frac{\phi \mu c_t r_w^2}{k} \right] z' \qquad \ldots (3.35)$$

Dimensionless Liquid Column Acceleration

$$z_D'' = \frac{1}{-z_0} \left[\frac{\phi \mu c_t r_w^2}{k} \right]^2 z'' \qquad \ldots (3.36)$$

Flow rate behavior, q(t), during a drillstem test can be evaluated from solutions for z_D' and the following equation obtained from Eq. 3.35:

$$q(t) = \pi r_p^2 z' = -z_0 \pi r_p^2 \left[\frac{k}{\phi \mu c_t r_w^2} \right] z_D' \qquad \ldots (3.37)$$

Similarly, rate of change of flow rate, dq/dt, during a drillstem test can be obtained from solutions for z_D'' using Eq. 3.36 in the following form:

$$\frac{dq}{dt}(t) = \pi r_p^2 z'' = -z_0 \pi r_p^2 \left[\frac{k}{\phi \mu c_t r_w^2} \right]^2 z_D'' \qquad \ldots (3.38)$$

Application of these definitions to the problem statement presented in Section 3.5 results in the following dimensionless formulation of the flow phenomena during a slug test or a drillstem test including gravitational, inertial, and frictional effects on the wellbore fluid column:

Wellbore Equation

$$A_w z_D'' + B_w z_D' + C_w z_D + D_w = E_w p_{wD} \quad , 0 < t_D < t_{Ds} \qquad \ldots (3.39)$$

where:

$$A_w = \alpha 2 \left\{ 1 + \frac{z_D}{L_D} + \frac{3}{8} \frac{\mu}{L_D} \left[\frac{r_{pDz}}{r_{wDz}}, 2 \right] \right\} \quad \ldots \text{(3.39.a)}$$

$$B_w = \alpha^2 \left\{ \left[1 + \frac{z_D}{L_D} \right] \frac{f}{4} \left| \frac{1}{r_{pDz}} z'_D \right| + \frac{3}{4} \frac{1}{L_D} \left[\frac{r_{pDz}}{r_{wDz}} \right]^4 z'_D \right\} \quad \ldots \text{(3.39.b)}$$

$$C_w = 1 \quad \ldots \text{(3.39.c)}$$

$$D_w = 0 \quad \ldots \text{(3.39.d)}$$

$$E_w = -1 \quad \ldots \text{(3.39.e)}$$

This wellbore equation is also applicable to the flow period of a closed-chamber test, except for the following modification:

$$D_w = - \frac{L_D - L_{pD} - 1}{L_D - L_{pD} + z_D} \frac{Z}{Z_g(0)} p_{gD}(0) - p_{aD} \quad \ldots \text{(3.39.d')}$$

Reservoir Eauation

$$\frac{1}{r_D}\frac{\partial}{\partial r_D}\left[r_D \frac{\partial p_D}{\partial r_D} \right] = \frac{\partial p_D}{\partial t_D} \quad , r_D \geq 1,\ t_D > 0 \qquad \ldots (3.40)$$

Wellbore Storage Condition

$$z_D' = -\frac{1}{C_D}\left[r_D \frac{\partial p_D}{\partial r_D} \right]_{r_D=1} \quad , t_D > 0 \qquad \ldots (3.41)$$

Skin Effect Condition

$$p_{wD} = \left\{ p_D - s \left[r_D \frac{\partial p_D}{\partial r_D} \right] \right\}_{r_D = 1} \quad , t_D > 0 \qquad \ldots (3.42)$$

Reservoir Outer Boundary Condition

$$\lim_{r_D \to \infty} p_D(r_D, t_D) = 0 \quad , t_D > 0 \qquad \ldots (3.43)$$

Initial Wellbore Liquid Level Condition

$$z_D(0) = -1 \qquad \ldots (3.44)$$

Initial Wellbore Liquid Column Velocity Condition

$$z_D'(0) = 0 \qquad \ldots (3.45)$$

Initial Reservoir Condition

$$p_D(r_D,0) = 0 \quad , r_D > 1 \qquad \ldots (3.46)$$

In Eq. 3.41, C_D is the dimensionless wellbore storage constant defined by Ramey (1970) and is equal to the $\overline{C}$ defined by van Everdingen and Hurst (1949):

$$C_D = \frac{C}{2\pi\phi c_t h r_w^2} \qquad \ldots (3.47)$$

where C is given by Eq. 3.19.

The following dimensionless parameters have also been defined and introduced in the problem statement for closed-chamber tests:

Dimensionless Pipe Length

$$L_{pD} = \frac{L_p}{-z_0} \qquad \ldots (3.48)$$

Dimensionless Closed-Chamber Gas Pressure

$$p_{gD} = \frac{p_g}{-\rho g z_0} = \frac{p_g}{p_i - [\, p_c + p_a \,]} \qquad \ldots \quad (3.49)$$

Dimensionless Atmospheric Pressure

$$p_{aD} = \frac{p_a}{-\rho g z_0} = \frac{p_a}{p_i - [\, p_c + p_a \,]} \qquad \ldots \quad (3.50)$$

In addition, the following dimensionless group of reservoir, wellbore, and fluid properties appears in this problem statement:

Dimensionless Initial Deacceleratine Factor

$$\alpha = \sqrt{\frac{L}{g}} \left[\frac{k}{\phi \mu c_t r_w^2} \right] = \sqrt{\frac{1}{g} \left[\frac{p_i - p_a}{\rho g} - \frac{h}{2} \right]} \left[\frac{k}{\phi \mu c_t r_w^2} \right] \qquad (3.51)$$

This parameter is slightly different than the group defined as *a* by Shinohara and Ramey (*1979.* b) because of a different definition of L. Dimensionless initial deaccelerating factor, initial deaccelerating factor, or just deaccelerating factor are descriptive names proposed and used throughout this study for the group of parameters given in Eq. 3.51. This proposal is based on an analysis of the effect of *a* on the solutions for dimensionless liquid column velocity, z_D' and acceleration, z_D'', presented later in this study.

The effect of the initial deaccelerating factor can be visualized at this stage by considering the wellbore equation used by Shinohara and Ramey (1979.b), which can be written as:

$$A_w z''_D + B_w z'_D + C_w z_D + D_w = E_w p_{wD} \quad \ldots (3.52)$$

with:

$$A_w = a^2 \quad \ldots (3.52.a)$$

$$B_w = 0 \quad \ldots (3.52.b)$$

$$C_w = 1 \quad \ldots (3.52.c)$$

$$D_w = 0 \quad \ldots (3.52.d)$$

$$E_w = -1 \quad \ldots (3.52.e)$$

Although this is a simplified special case of wellbore Eq. 3.39 derived in the present study, Eq. 3.52 can be used to gain some insight into the effect of the deaccelerating factor.

Consider a drillstem test at initial conditions or at an infinitesimal period of time after the start of the test. Substituting initial conditions given by Eqs. *3.44 - 3.46* into Eq. *3.52:*

$$a^2 z_D'' = 1 \quad , t_D = 0+\varepsilon, \ \varepsilon \to 0 \qquad \ldots (3.53)$$

The arithmetic operation performed by ***a*** in a wellbore equation defines it as a factor. Eq. *3.53* shows that the initial value of the dimensionless liquid level acceleration z_D'' is inversely proportional to α^2. This equation also indicates that the value of ***a*** affects the initial value of z_D''. Each of these effects is reflected in the full name proposed to ***a,*** dimensionless initial deaccelerating factor.

According to the definition of ***a*** and z_D', Eqs. *3.51* and *3.26,* respectively, Eq. *3.53* specifies the following initial liquid column acceleration, as related to gravity acceleration:

$$\frac{z''}{z_0} = -\frac{g}{L} \quad , t=0+\varepsilon, \ \varepsilon \to 0 \qquad \ldots (3.54)$$

Solution methods for the problem stated in this section are presented in the following section.

SECTION 4
SOLUTION METHODS

Two solution methods for slug tests, drillstem 'tests, or closed-chamber tests are presented in this section. These methods give the following dimensionless solutions: (a) bottomhole pressure, $p_{wD}(t_D)$, (b) rate of change of bottomhole pressure, $p_{wD}'(t_D)$, (c) wellbore liquid level, $z_D(t_D)$, (d) liquid column velocity, $z_D'(t_D)$, (e) liquid column acceleration, $z_D''(t_D)$, and (f) reservoir pressures, $p_D(r_D,t_D)$.

The first solution method was obtained by applying the Laplace transformation to a generalized, linear mathematical problem. The complexity of the resulting transformed solutions prevented analytical inversion from Lapace space. A numerical algorithm proposed by Stehfest (1970) was used to perform inversion into real space.

The second solution method is an approximation by finite-difference of a generalized linear or non-linear mathematical problem resulting in systems of simultaneous algebraic equations solved with the Thomas Algorithm (Aziz and Settari, 1979).

4.1 Laplace Transformation for Linear Problems

In the mathematical description of a slug test, drillstem test, or closed-chamber test, Eq. 3.39 - 3.46, all but one of the equations are mathematically linear. According to the definition of coefficients A_w, B_w, and D_w, Eqs. 3.39.a, 3.39,b, and 3.39.d', respectively, wellbore Eq. 3.39 derived in the present study is non-linear.

The non-linearity introduced by the wellbore equation into the problem description has been overcome by previous investigators by

adopting assumptions leading to simplified linear wellbore equations.

In this part of the study, previous solutions are unified and extended by using a semi-analytical method. This method, described in Appendix B, considers a generalized linear wellbore equation resulting from simplifying assumptions discussed and eliminated later in this study.

This solution method considers any definition for wellbore equation coefficients A_w, B_w, C_w, D_w, and E_w as long as the definition results in a wellbore equation that is mathematically linear.

In Appendix B, a generalized linear problem is transformed into Laplace space (Churchill, 1972). The resulting transformed problem is solved analytically and expressions are obtained for Laplace-transformed dimensionless bottomhole pressure and its rate of change and wellbore liquid level and its first and second time derivatives. These transformed solutions can be expressed conveniently as follows:

Transformed Dimensionless Liquid Level

$$\overline{z_D}(u) = -\frac{1}{u}\left\{\frac{\sqrt{u}K_1(\sqrt{u})[A_w u+B_w+D_w/u-E_w C_D s]-E_w C_D K_0(\sqrt{u})}{\sqrt{u}K_1(\sqrt{u})[A_w u+B_w+C_w/u-E_w C_D s]-E_w C_D K_0(\sqrt{u})}\right\} \quad \ldots (4.1)$$

Transformed Dimensionless Bottomhole Pressure

$$\overline{p_{wD}}(u) = \frac{C_D\,[\,u\,\overline{z_D}(u)+1\,]}{\sqrt{u}\,K_1(\sqrt{u})}\,[\,K_0(\sqrt{u})+s\sqrt{u}\,K_1(\sqrt{u})\,] \quad \ldots (4.2)$$

Transformed Dimensionless Rate of Change of Bottomhole Pressure

$$\overline{p_{wD}'}(u) = u\,\overline{p_{wD}}(u) \quad \ldots (4.3)$$

Transformed Dimensionless Liquid Column Velocity

For A_w and/or $B_w \neq 0$:

$$\overline{z'_D}(u) = \frac{- C_w \overline{z_D}(u) - D_w / u + E_w \overline{p_{wD}}(u)}{A_w + B_w} \quad \ldots (4.4)$$

For A_w and $B_w = 0$:

$$\overline{z'_D}(u) = u \overline{z_D}(u) + 1 \quad \ldots (4.5)$$

Transformed Dimensionless Liquid Column Acceleration

For $A_w \neq 0$:

$$\overline{z''_D}(u) = \frac{- B_w \overline{z'_D}(u) - C_w \overline{z_D}(u) - D_w / u + E_w \overline{p_{wD}}(u)}{A_w} \quad \ldots (4.6)$$

For $A_w = 0$:

$$\overline{z''_D}(u) = u \overline{z'_D}(u) \quad \ldots (4.7)$$

Transformed Dimensionless Reservoir Pressures

$$\overline{p_D}(r_D, u) = \frac{C_D [\, u \overline{z_D}(u) + 1 \,]}{\sqrt{u}\, K_1(\sqrt{u})} K_0(r_D \sqrt{u}) \quad \ldots (4.8)$$

where :

K_0 = modified Bessel function of the second kind of order zero

K_1 = modified Bessel function of the second kind of order unity

u = Laplace transformation variable

Throughout this study, a super bar on a dependent variable indicates the corresponding transformed variable in Laplace space.

The previously transformed solutions are expressed in terms of $\overline{z_D}$, which is given by Eq. 4.1,

A brief discussion of results obtained by applying the Stehfest numerical algorithm to two simple oscillatory functions is presented in Appendix C.

The Stehfest algorithm involves calculating an even number, N, of coefficients V_i, as follows:

$$V_i = [-1]^{[N/2+i]} \sum_{k=\frac{i+1}{2}}^{\min(i,N/2)} \frac{k^{N/2}[2k]!}{[N/2-k]![k]![k-1]![i-k]![2k-i]!} \quad \ldots (4.9)$$

The coefficients, V_i, are used in the following; summation:

$$g(T) \simeq g_a = \frac{\ln(2)}{T} \sum_{i=1}^{N} V_i \, \overline{g}(U_i) \quad \ldots (4.10)$$

where :

$$U_i = i \frac{\ln(2)}{T} \quad \ldots (4.11)$$

With this algorithm, an approximate value, g_a, of the unknown function g is calculated for a stipulated value T of the independent variable t, if the transformed function $\overline{g}(u)$ is a known mathematical expression that can be evaluated for the required arguments, U_i.

Application of Stehfest inversion algorithm to the transformed generalized linear problem solutions given by Eqs. 4.1 - 4.8 also requires known values of coefficients A_w, B_w, C_w, D_w, and E_w, and of parameters C_D and s. When t_D is set equal to a desired value T, this algorithm provides an approximate value for $p_{wD}(T)$, $p_{wD}'(T)$, $z_D(T)$, $z_D'(T)$, $z_D''(T)$, and $p_D(r_D,T)$. These results are independent of previous calculations for other values of t_D.

Graphs and tables of p_{wD}, p_{wD}', z_D, z_D', z_D'', aind p_D vs t_D can be generated by applying this inversion algorithm for desired values of t_D. A computer program was written to perform these calculations. This program is presented in Appendix E.

4.2 Finite Differences for Non-Linear Problems

The problem statement given by Eqs. 3.39 - 3.46 describes flow phenomena during a slug test, a drillstem test, or a closed-chamber test. This problem is mathematically non-linear because of the definitions of wellbore equation coefficients A_w, B_w, and D_w, Eqs. 3.39.a, 3.39.b, and 3.39.d', respectively. Solutions for this problem and for special simplified cases can be obtained by using the finite-difference approximation derived in Appendix D.

In this approximation, the problem statement is posed as an implicit scheme with respect to time. A convenient change of variable is applied to the diffusivity equation. Then, the second-order partial derivative of p_D with respect to r_D is approximated by a three-point central difference form. The first-order partial derivative of p_D with respect to t_D is approximated by a two-point backward difference form. The gradient of p_D with respect to r_D at the sandface, r_D=l, is

approximated by a three-point backward difference form. Also, all ordinary derivatives with respect to t_D are approximated by three-point backward difference forms.

An equation to determine the size of a reservoir sufficiently large to be considered as infinite-acting for any value of C_D is derived in Appendix D. This method results in a tridiagonal system of algebraic equations that must be generated and solved at each time step for linear problems. However, for non-,linear problems, coefficients A_w^{k+1}, B_w^{k+1}, and D_w^{k+1} must be estimated and solutions obtained by iterative successive approximations of these coefficients for calculated values of z_D^{k+1} and $z_D'^{k+1}$.

A computer program was written to perform the calculations required by this finite difference approximation. This program is presented in Appendix F. Several options for this program allow application to problems with different wellbore equations. This computer program provides results for the behavior of p_{wD}, z_D, p_{wD}', z_D', z_D'', and p_D at radii logarithmically distributed in the reservoir. Knowledge of the reservoir pressure distribution at the end of each time step also allows an option to simulate a shut-in period after a flow period during a drillstem test or during a closed-chamber test.

Results from this computer program are presented in Section 6. First, the program is validated by reproducing previous solutions for linear problems, including the semi-analytical solutions presented in Section 5. Then, the non-linear effects of cushion size and of pipe friction are evaluated to reach useful criteria for estimating conditions under which these effects are either negligible or dominant on the flow phenomena. New type curves for integral analysis of flow and shut-in drillstem test data are presented for practical applications. Solutions for closed-chamber tests are also given in Section 6.

Solutions for slug tests and drillstem tests described by linear mathematical problems are presented in the following section.

SECTION 5
EVALUATION AND DISCUSSION OF LINEAR PROBLEMS SOLUTIONS

In this section, the semi-analytical solution method for slug test and drillstem test linear problems presented in Section *4.1* is applied to evaluate effects assumed negligible by previous authors. Solutions for p_{wD} and z_D currently available in the literature are analyzed using a systematic approach in Section 5.1. These solutions are also extended by evaluating the corresponding p_{wD}', z_D', and z_D''. In Section 5.2, a slug test or drillstem linear problem, obtained by considering laminar flow friction in the wellbore, is formulated and solved to study the effect of this particular case of friction in conjunction with inertial wellbore effects. Solutions including inertial linear effects of the reservoir thickness/static column length ratio [h/L] and of the pipe/wellbore radii ratio [r_p/r_w] are presented in Section 5.3.

5.1 Discussion of Previous Solutions

Available solutions for slug-test linear problems are discussed in this section. These solutions are analyzed from results for p_{wD}', z_D', and z_D'', in addition to p_{wD} and z_D, obtained in the present study. These additional results provide insight into flow phenomena, and allow analysis of the assumptions adopted previously.

5.1.1 Negligible Gravity, Inertia, and Friction

Reservoir response to an initial perturbation in wellbore pressure or liquid level, without considering an effect of the wellbore fluid column, is described by using an analogy of the instantaneous line

source presented by Kelvin (1884). In this solution, the reservoir response is assumed to be independent of hydrostatic pressure, inertia, and friction of the changing wellbore liquid column.

The instantaneous line source solution can be expressed in terms of dimensionless groups defined in this study as follows:

$$p_D(r_D,t_D) = \frac{1}{2}\frac{C_D}{t_D} e^{-\frac{r_D^2}{4t_D}} \quad \ldots (5.1)$$

Then, assuming hydrostatic equilibrium inside the wellbore at all times, and measuring the response at $r_D = 1$:

$$-z_D = p_{wD} = \frac{1}{2}\frac{C_D}{t_D} e^{-\frac{1}{4t_D}} \quad \ldots (5.2)$$

Instantaneous line source solutions evaluated from Eq. 5.2 for different values of C_D are shown as solid lines in Cartesian graphs in Figs. 5.1.a - 5.1.c, in a semi-log graph in Fig. 5.1.d, and in log-log graphs in Fig. 5.1.e. The small circles in these figures correspond to an approximation proposed by Ferris and Knowles (1954) and discussed later in this section. In order to have a reference for qualitative analysis of the solutions, the format used in these graphs is followed consistently throughout this study. Since oscillating solutions are expected to occur for some of the conditions discussed in this study, a special presentation of two adjacent log-log graphs was designed to help in visualizing the nature of those solutions. In those graphs, the upper log-log plot shows the positive values of the solution, and the lower log-log plot shows the negative values of the corresponding solution. The value of zero, about which some solutions oscillate, can not be included in a log-log graph, but can be imagined as between the upper and lower log-log graphs presented in this study.

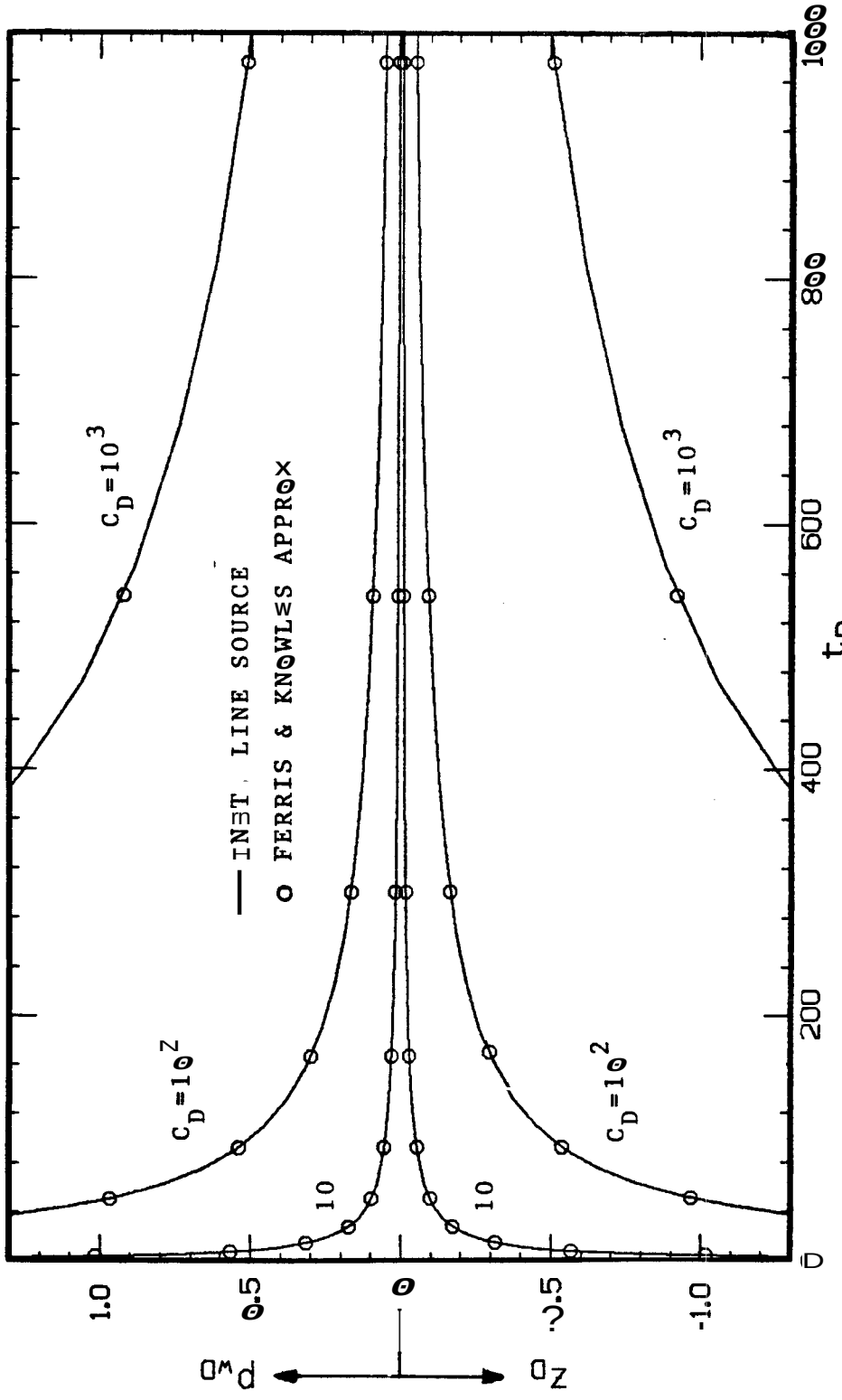

FIG. 5.1.a. CARTESIAN GRAPH OF SLUG TEST SOLUTIONS FOR P_{wD} AND z_D VS t_D NEGLECTING GRAVITATIONAL, INERTIAL, AND FRICTIONAL WELLBORE EFFECTS FOR PRACTICAL VALUES OF C_D AND $t_D < 10^3$

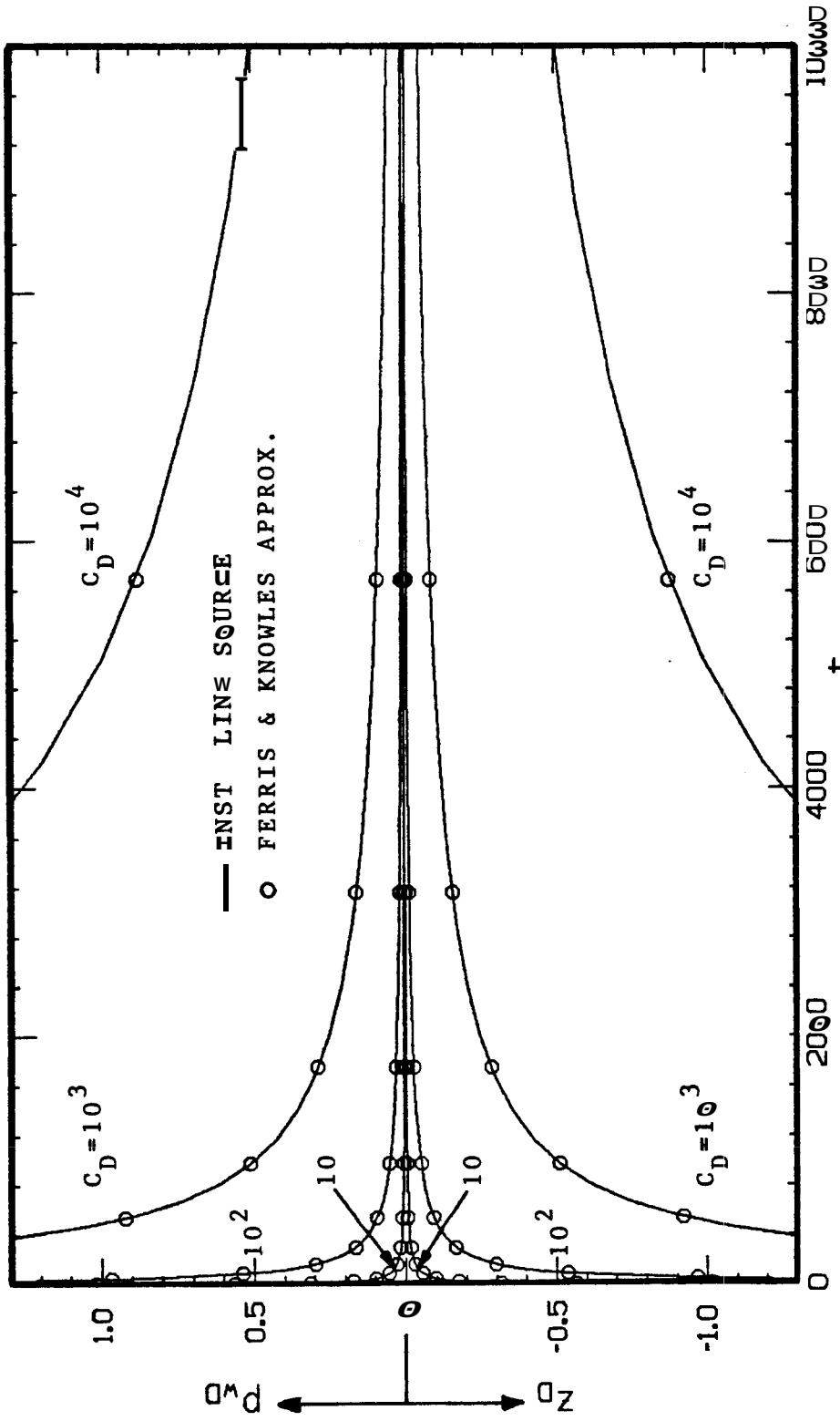

FIG. 5.1.b. CARTESIAN GRAPH OF SLUG TEST SOLUTIONS FOR P_{wD} AND z_D VS t_D NEGLECTING GRAVITATIONAL, INERTIAL, AND FRICTIONAL WELLBORE EFFECTS FOR PRACTICAL VALUES OF C_D AND $t_D<1.6$

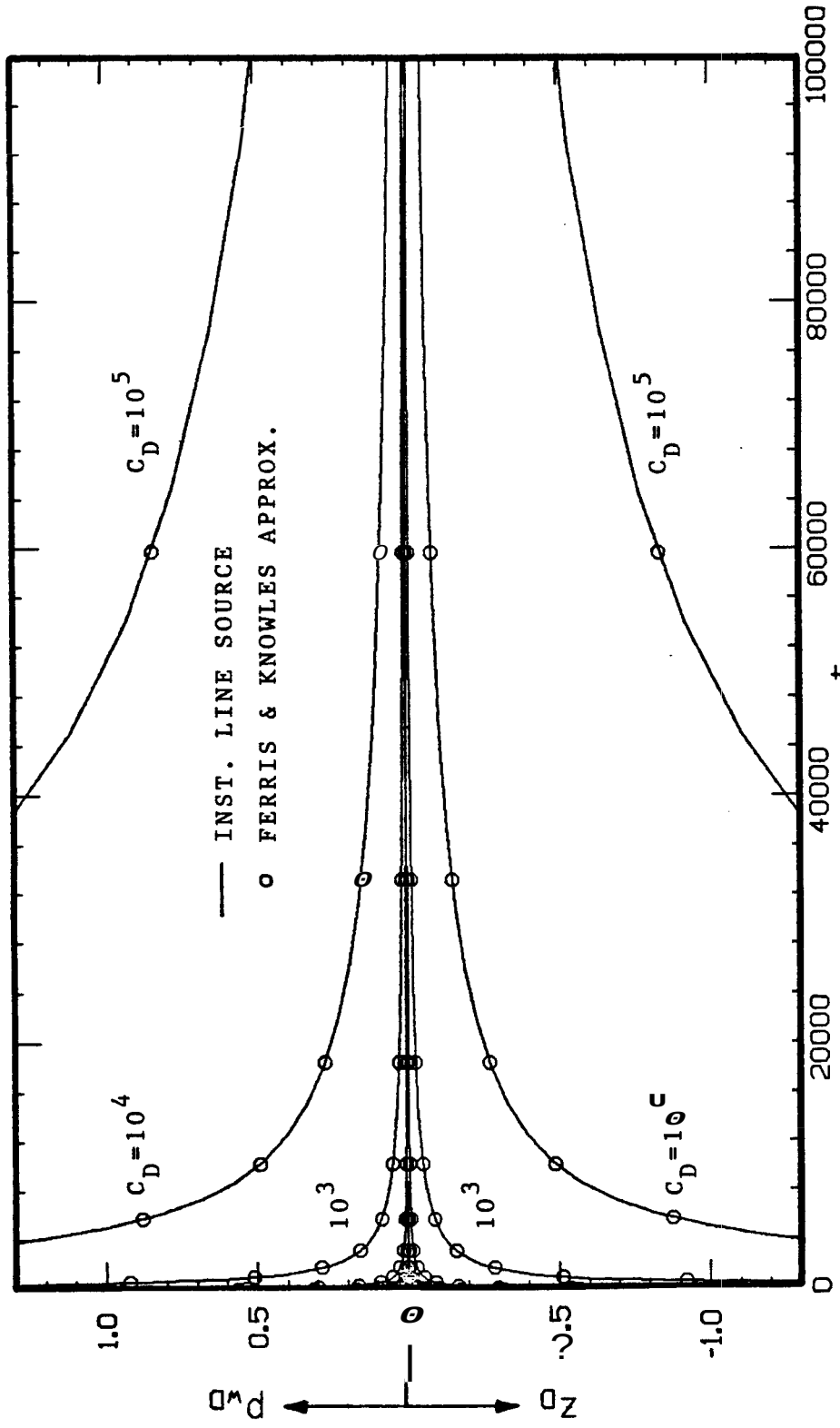

FIG. 5.1.c. CARTESIAN GRAPH OF SLUG TEST SOLUTIONS FOR P_{wD} AND z_D VS t_D NEGLECTING GRAVITATIONAL, INERTIAL, AND FRICTIONAL WELLBORE EFFECTS FOR PRACTICAL VALUES OF C_D AND $t_D<10^5$

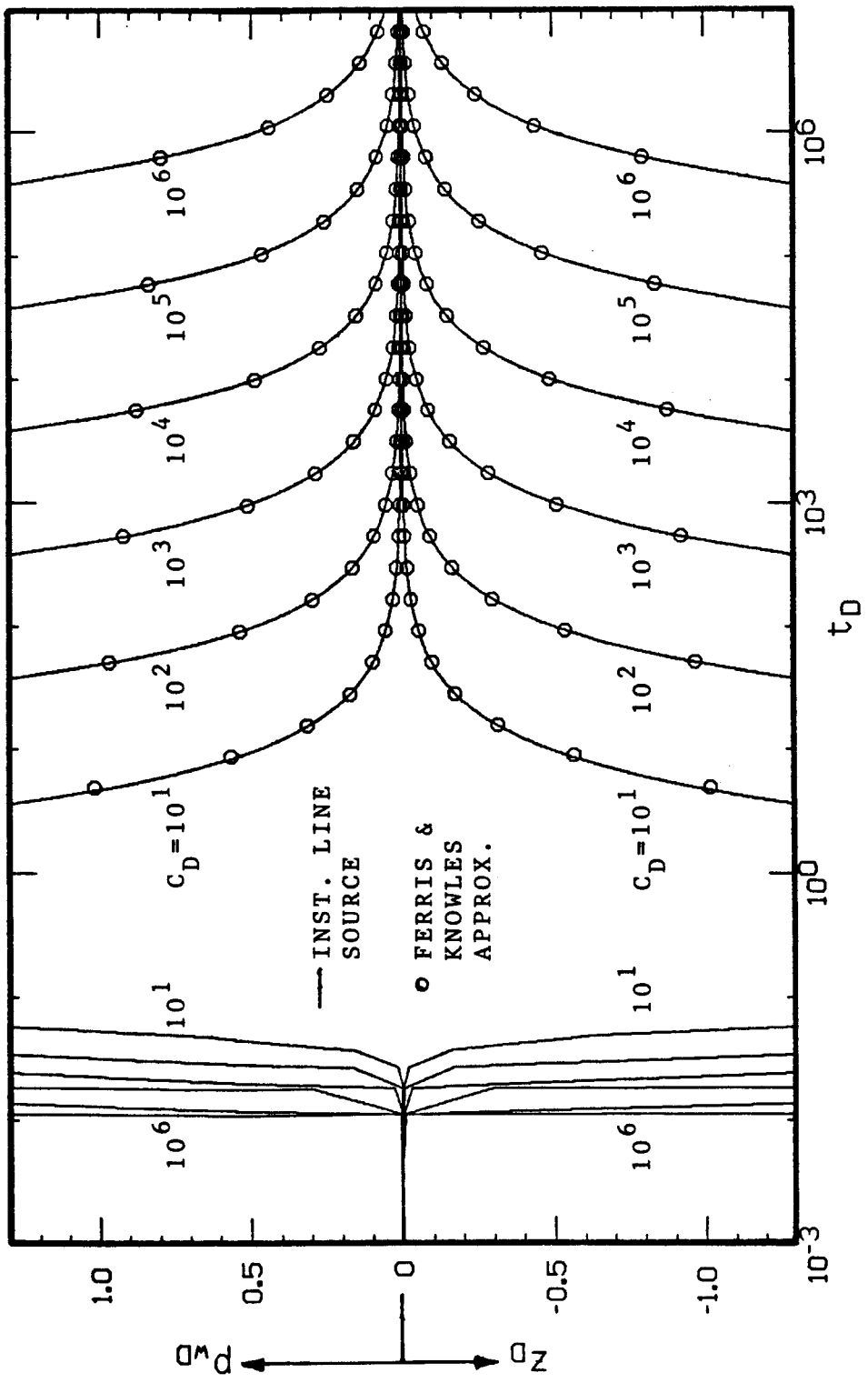

FIG. 5.1.d. SEMI-LOG GRAPH OF SLUG TEST SOLUTIONS FOR p_{wD} AND z_D VS t_D NEGLECTING GRAVITATIONAL, INERTIAL, AND FRICTIONAL WELLBORE EFFECTS FOR PRACTICAL VALUES OF C_D

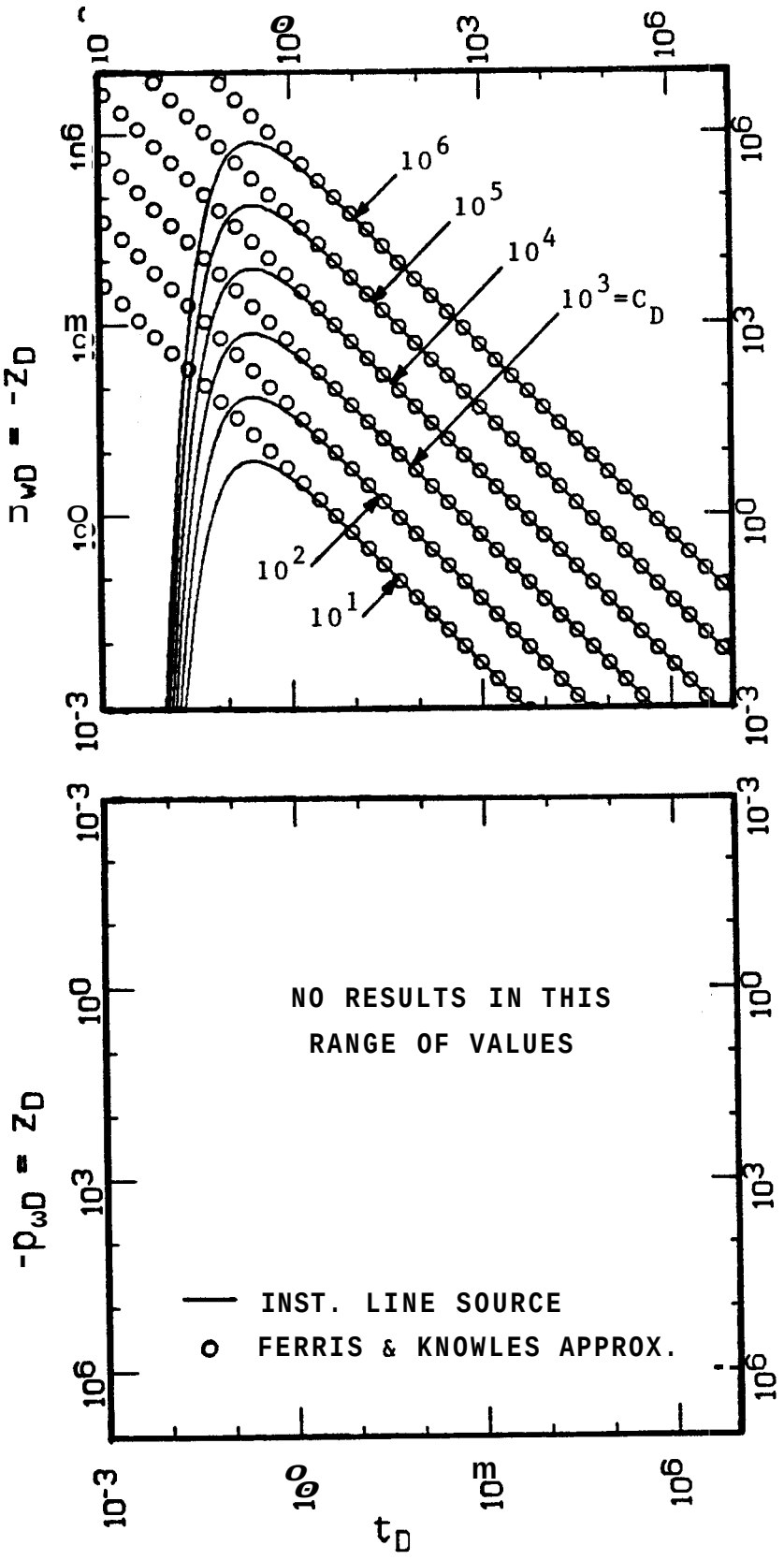

FIG. 5.1.e. LOG–LOG **GRAPH OF SLUG TEST SOLUTIONS FOR** p_{wD} **AND** z_D **VS** t_D **NEGLECTING GRAVITATIONAL, INERTIAL, AND FRICTIONAL, WELLBORE EFFECTS FOR PRACTICAL VALUES OF** C_D

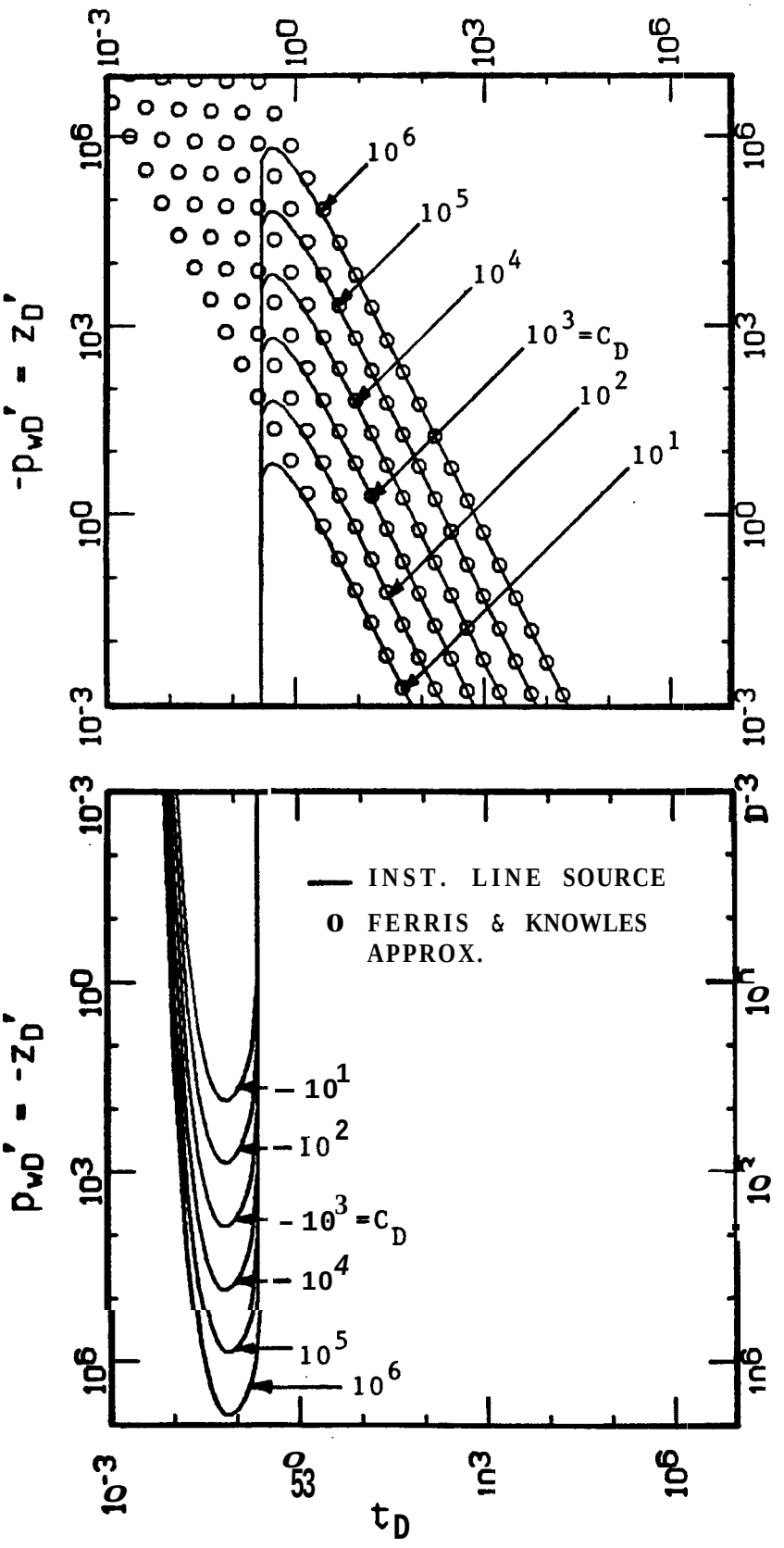

FIG. 5.1.f. LOG-LOG GRAPH OF SLUG TEST SOLUTIONS FOR p_{wD}' AND z_D' VS t_D NEGLECTING GRAVITATIONAL, INERTIAL, AND FRICTIONAL WELLBORE EFFECTS FOR PRACTICAL VALUES OF C_D

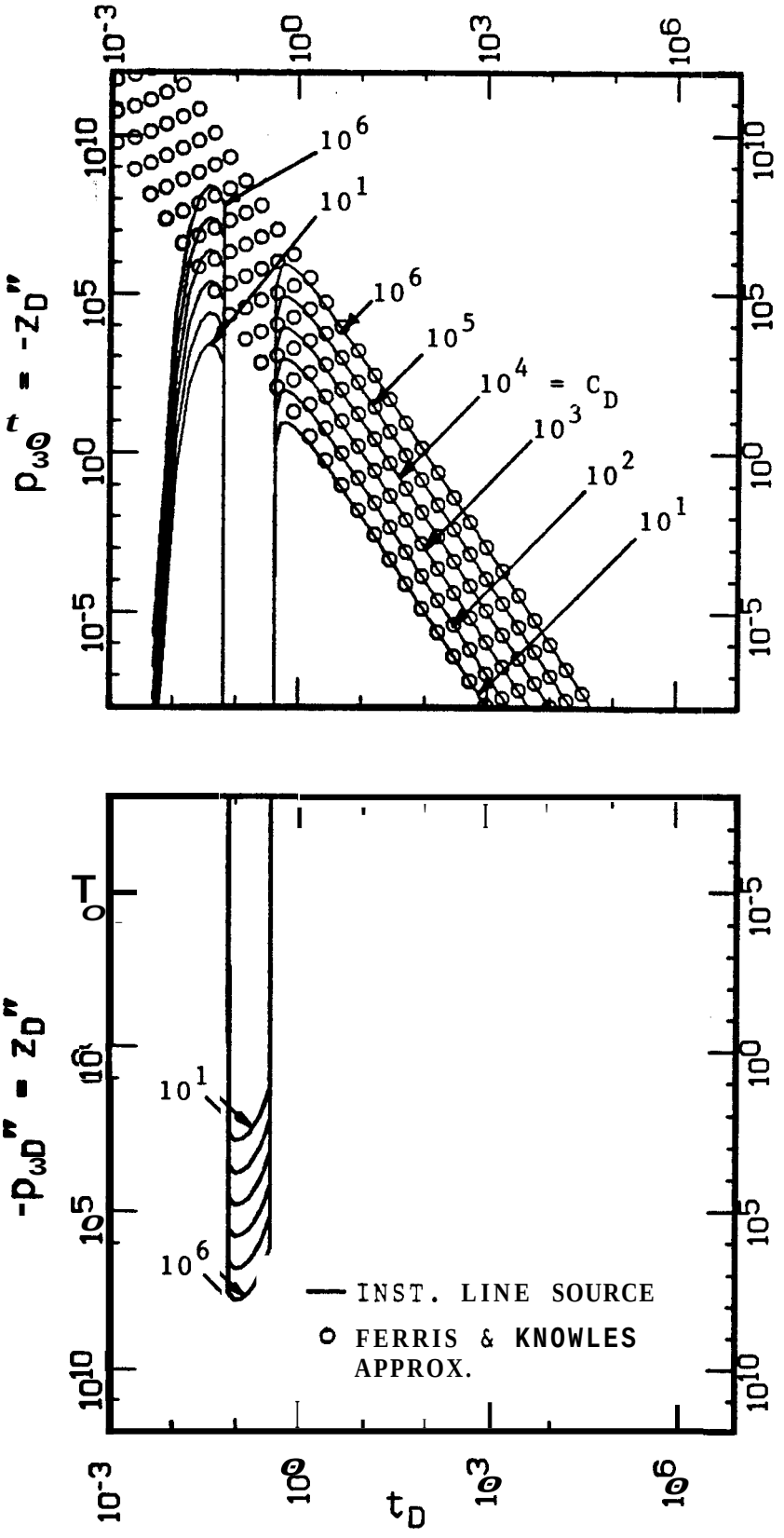

FIG. 5.1.g. LOG-LOG GRAPH OF SLUG TEST SOLUTIONS FOR p_{wD}'' AND z_D'' VS t_D NEGLECTING GRAVITATIONAL, INERTIAL, AND FRICTIONAL WELLBORE EFFECTS FOR PRACTICAL VALUES OF C_D

Solutions for dimensionless level velocity, z_D', and dimensionless level acceleration, z_D'', can be obtained for the instantaneous line source solution by successive derivatives of Eq. 5.2. with respect to t_D, resulting in:

$$z_D' = - p_{wD}' = \frac{1}{2} \frac{C_D}{t_D^2} e^{\frac{1}{4 t_D}} \left[1 - \frac{1}{4t_D} \right] \quad \ldots (5.3)$$

and:

$$- z_D'' = p_{wD}'' = - \frac{C_D}{t_D^3} e^{- \frac{1}{4t_D}} \left[1 - \frac{1}{2t_D} + \frac{1}{32 t_D^2} \right] \quad \ldots (5.4)$$

Solutions for z_D' and z_D'' evaluated from these equations for typical values of C_D are presented as log-log graphs in Figs. 5.1.f and 5.1.g, respectively.

The instantaneous line source solution results shown in Fig. 5.1.d indicate that p_{wD} is initially zero and increases at early times, reaches a maximum and then decreases with time. The maximum value of p_{wD} for a given C_D and the corresponding t_D can be obtained by equating Eq. 5.3 to zero, solving for t_D, and substituting t_D into Eq. 5.2. This results in a maximum $p_{wD}=2C_D/e$ at $t_D=1/4$. Under the assumption of hydrostatic equilibrium in the wellbore, z_D is symmetric to p_{wD}, and has a minimum value $z_D=-2C_D/e$ at $t_D=1/4$.

Instantaneous line source solution results in Fig. 5.1.f show that z_D' decreases at early times, reaches a minimum and increases abruptly. Then, z_D' reaches a maximum and starts decreasing linearly with time. The value of t_D at which z_D' is minimum and maximum are obtained by equating Eq. 5.4 to zero, resulting $4t_D=1\pm\sqrt{2}/2$. The minimum and maximum values of z_D' for a given C_D can be obtained by substituting these two values of t_D into Eq. 5.3, resulting $z_D' \simeq 0.633C_D$ and $z_D' \simeq -7.408C_D$, respectively.

Instantaneous line source solution results in Fig. 5.1.g indicate that z_D'' starts from zero, reaches a negative maximum and becomes positive in the range $1-\sqrt{2}/2<4t_D<1+\sqrt{2}/2$. After this oscillation, z_D'' reaches a negative maximum and tends to zero linearly as time increases.

An approach suggested by Ferris and Knowles (1954) to analyze slug test data consists of considering that for a given value of $k/(\phi\mu c_t r_w^2)$, the exponent of e in Eq. 5.2 approaches zero as t becomes large. Then, after a sufficiently large value of t_D:

$$- z_D = p_{wD} = \frac{1}{2}\frac{C_D}{t_D} \qquad \ldots (5.5)$$

According to Eq. 5.5, a Cartesian graph of p_{wD} or $-z_D$ vs t_D^{-1} should give a straight line with slope equal to $C_D/2$ and passing through the origin. This approximation was used by Ferris and Knowles (1954) to propose an analysis method to determine reservoir properties kh/μ from the slope of a straight line joining slug test data and passing through the origin of a Cartesian plot of z vs t^{-1}. Analogously, Eq. 5.5 shows that a graph of $[p_i-p_w]$ vs t^{-1} can also be used for slug test analysis following an approach parallel to the one proposed by Ferris and Knowles (1954).

The basis for this slug test data analysis method is shown in the following expression obtained by substituting the definition of z_D, t_D, and C_D, Eq. 3.23, 3.30, and 3.47, respectively, into Eq. 5.5:

$$z = -\frac{\pi r_p^2[-z_0]}{4\pi\rho g}\frac{\mu}{kh}\frac{1}{t} \qquad \ldots (5.6)$$

Interpretation of Eq. 5.5 shows that a graph of $[p_i-p_w]$ vs t^{-1} can be used for the same purpose because substituting the definition of p_{wD}, t_D, and C_D, Eqs. 3.24, 3.30, and 3.47, respectively, into Eq. 5.5:

$$p_i - p_w = \frac{\pi r_p^2 [-z_0]}{4\pi} \frac{\mu}{kh} \frac{1}{t} \quad \ldots (5.7)$$

Knowledge of the volume of the slug added, $-\pi r_p^2[-z_0]$, or removed, $\pi r_p^2[-z_0]$, to start the test is required in both cases in order to evaluate kh/μ using Eqs. 5.6 or 5.7.

Approximate expressions for z_D' and z_D'', corresponding to Eqs. 5.3 and 5.4, can be obtained by successive derivation of Eq. 5.5 with respect to t_D:

$$z_D' = - p_{wD}' = \frac{1}{2} \frac{C_D}{t_D^2} \quad \ldots (5.8)$$

and:

$$- z_D'' = p_{wD} = \frac{C_D}{t_D^3} \quad \ldots (5.9)$$

Results of p_{wD}, z_D, p_{wD}', z_D', p_{wD}'', and z_D'' for practical values of C_D obtained by using approximations given by Eqs. 5.5, 5.8, and 5.9, respectively, are also shown in Figs. 5.1.a - 5.1.g as small circles for comparison with the instantaneous line source solution and its derivatives, Eqs. 5.2 - 5.4. The value of t_D after which these solutions are equivalent may be obtained from inspection of those figures, and is approximately equal to $t_D=10$.

Cartesian graphs and a semi-log graph of z_D and p_{wD} vs t_D/C_D obtained from the instantaneous line source solution, Eq. 5.2, and the approximation proposed by Ferris and Knowles (1954), Eq. 5.5, are presented in Figs. 5.2.a - 5.2.d. No apparent difference between these two solutions is observed in the range of practical testing time, $10^{-2} < t_D/C_D < 10^{-3}$, for expected values of p_{wD} and z_D.

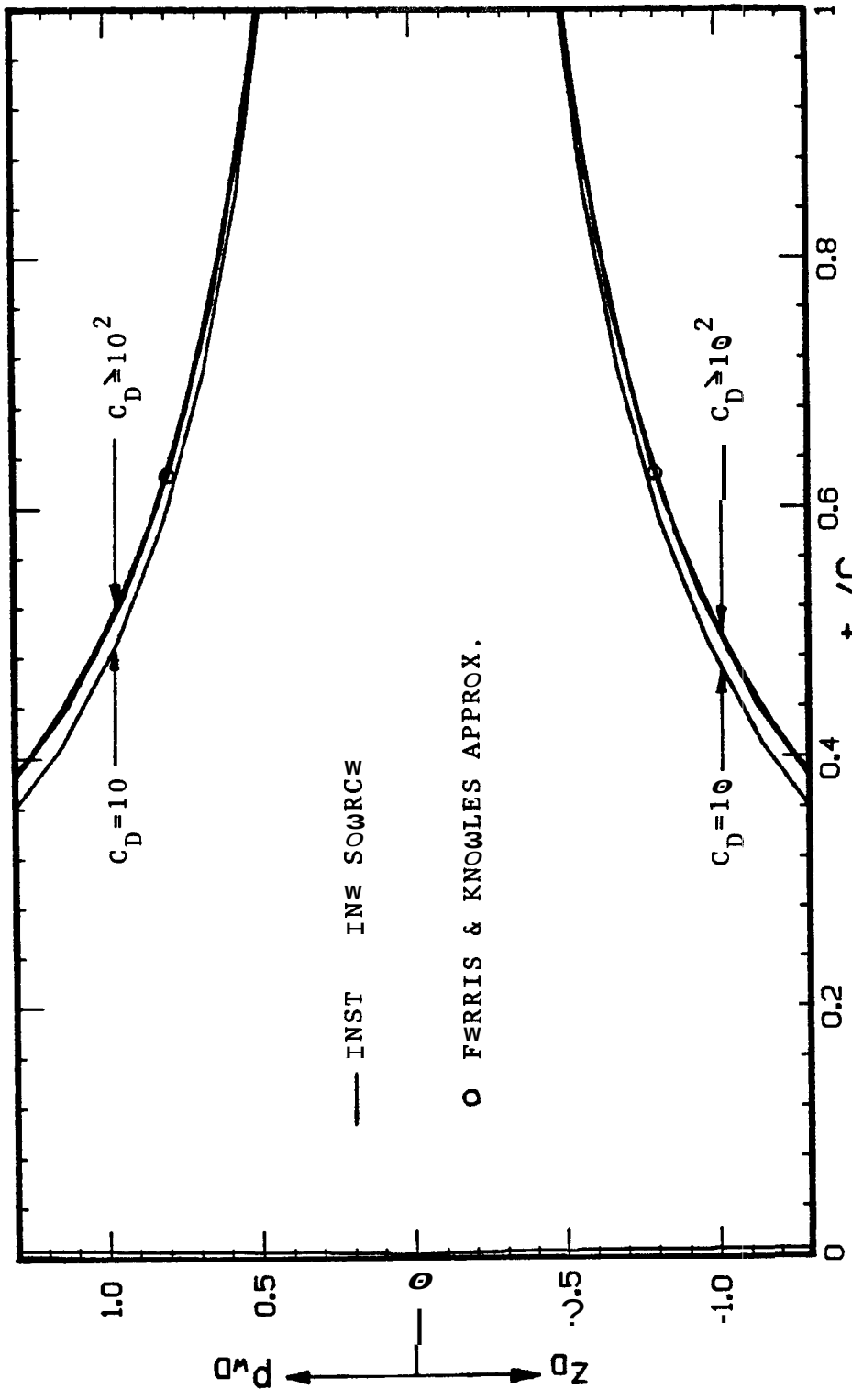

FIG. 5.2.a. CARTESIAN GRAPH OF SLUG TEST SOLUTIONS FOR P_{wD} AND z_D VS t_D/C_D NEGLECTING GRAVITATIONAL, INERTIAL, AND FRICTIONAL WELLBORE EFFECTS FOR PRACTICAL VALUES OF C_D AND $t_D/C_D<1$

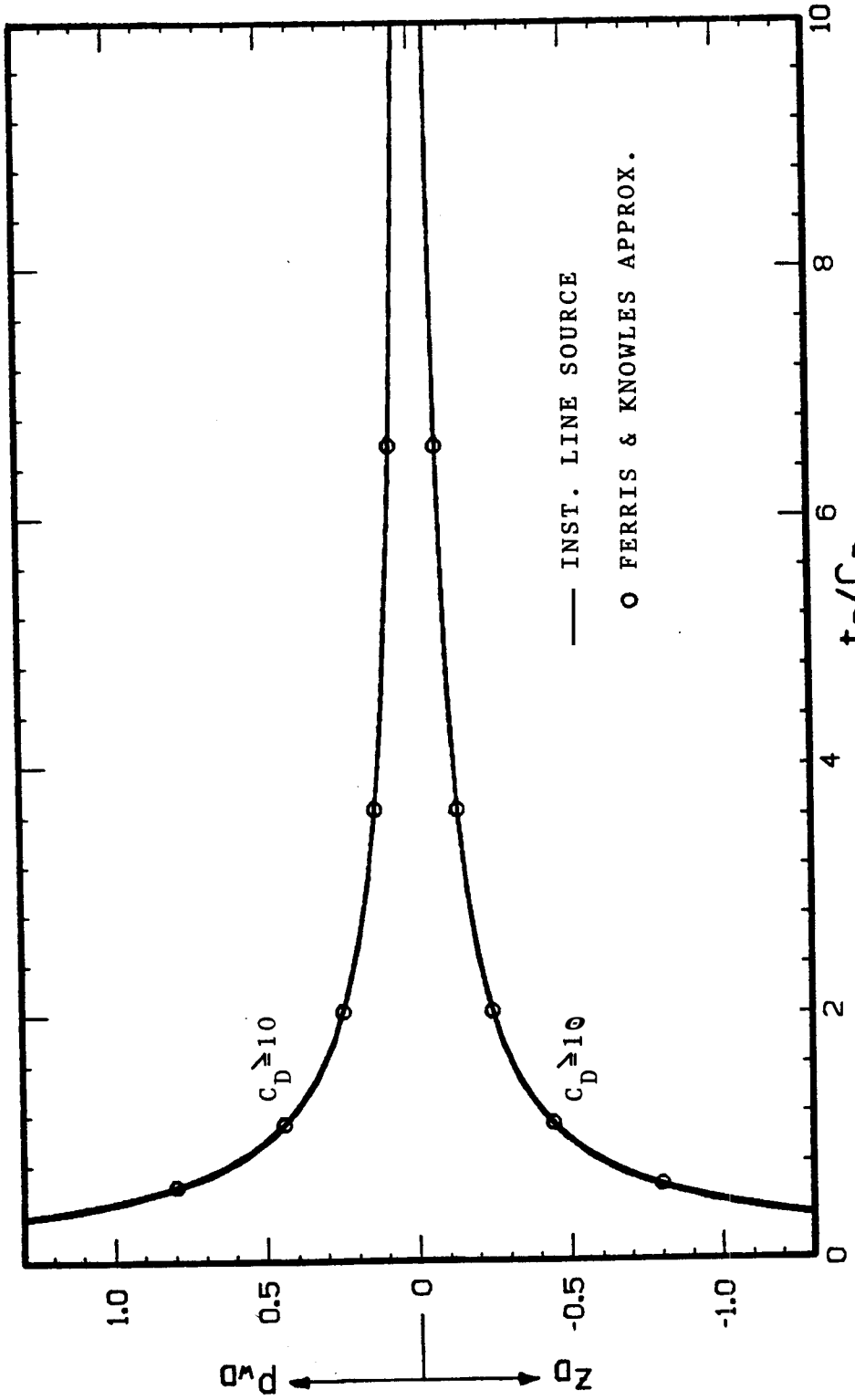

FIG. 5.2.b. CARTESIAN GRAPH OF SLUG TEST SOLUTIONS OF P_{wD} AND z_D VS t_D/C_D NEGLECTING GRAVITATIONAL, INERTIAL, AND FRICTIONAL WELLBORE EFFECTS FOR PRACTICAL VALUES OF C_D AND $t_D/C_D \leq 10$

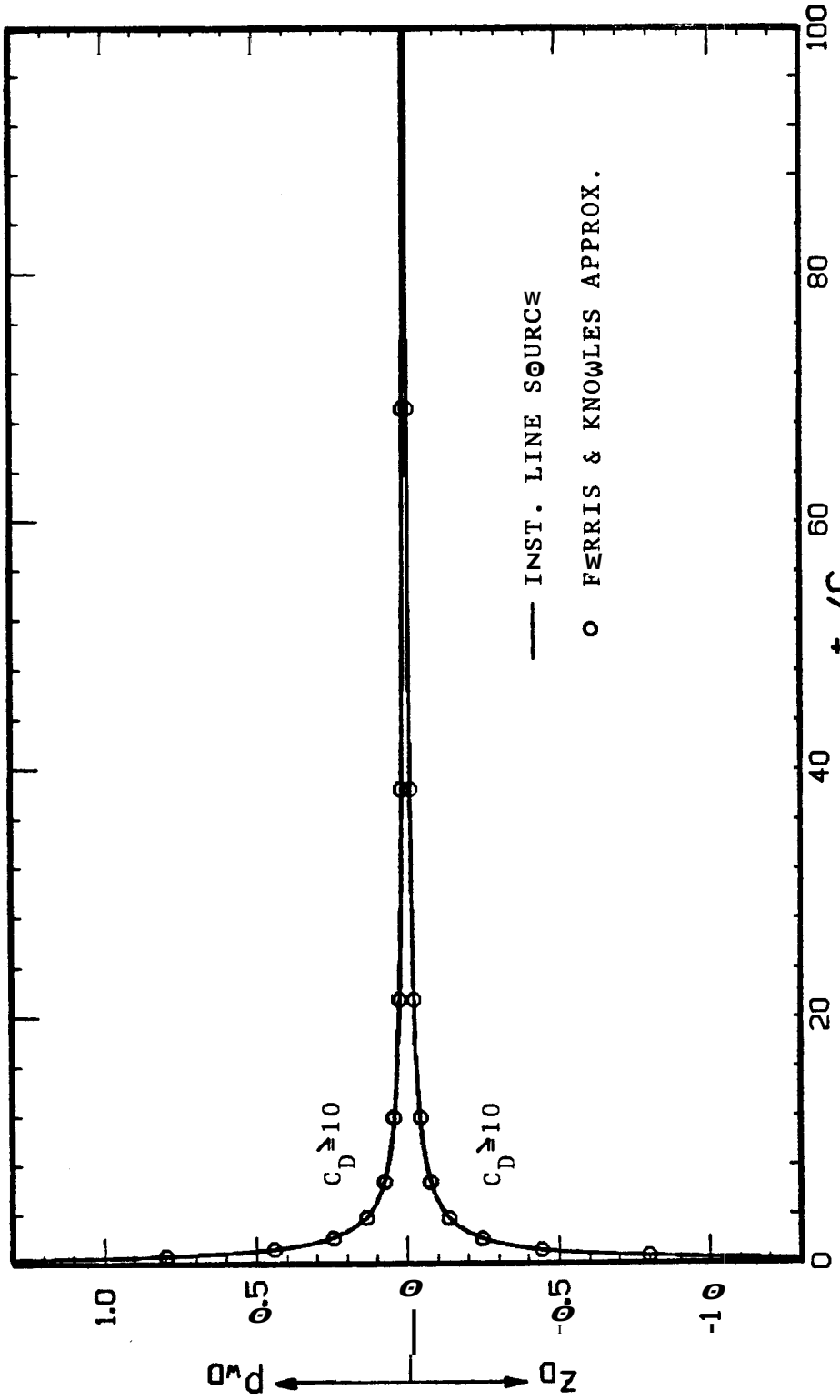

FIG. 5.2.c. CARTESIAN GRAPH OF SLUG TEST SOLUTIONS OF p_{wD} AND z_D VS t_D/C_D NEGLECTING GRAVITATIONAL, INERTIAL, AND FRICTIONAL WELLBORE EFFECTS FOR PRACTICAL VALUES OF C_D AND t_D/C_D<100

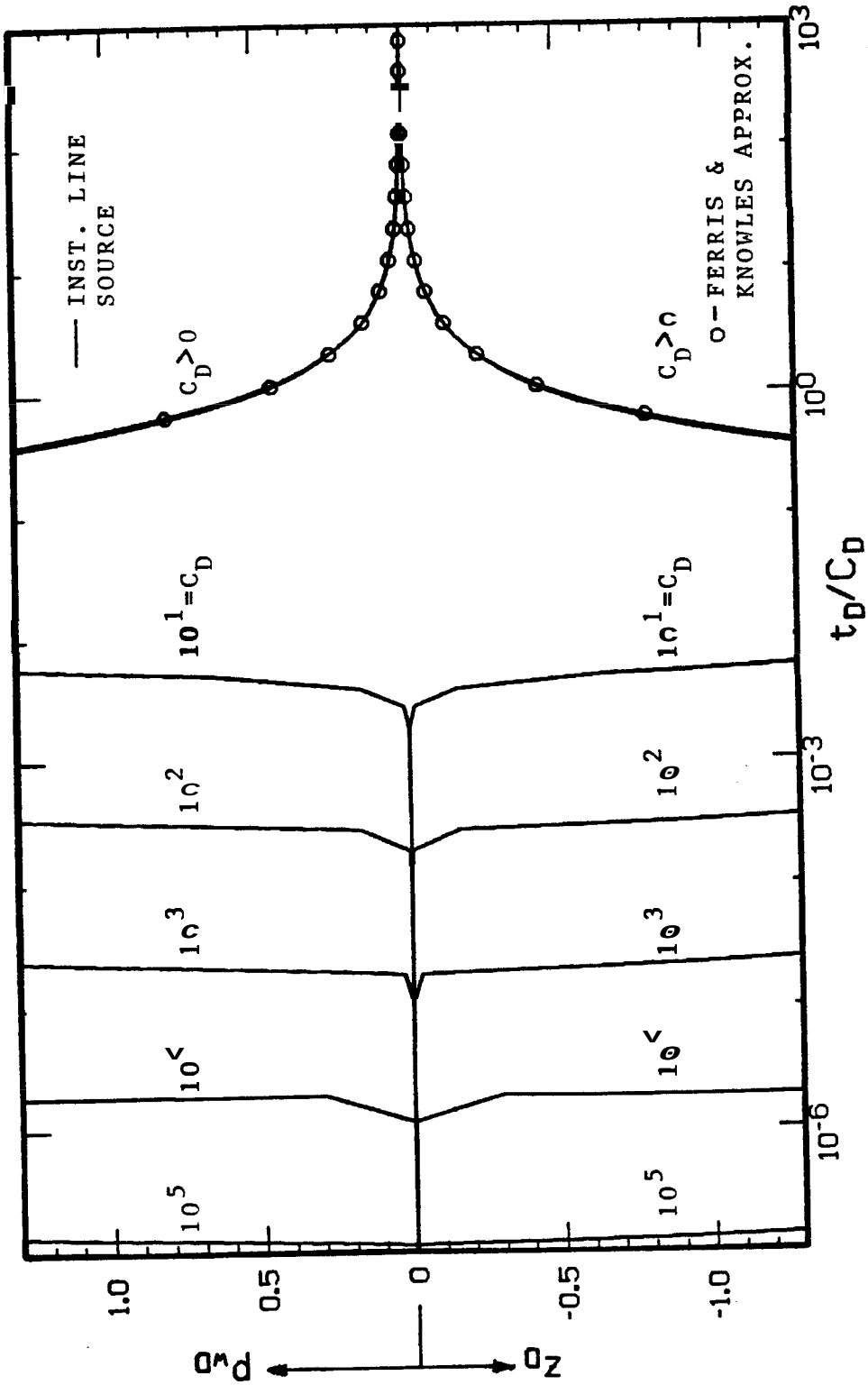

FIG. 5.2.d. SEMI-LOG TYPE CURVE FOR SLUG TEST ANALYSIS OF P_{wD} OR z_D VS t_D/C_D NEGLECTING GRAVITATIONAL, INERTIAL, AND FRICTIONAL WELLBORE EFFECTS FOR PRACTICAL VALUES OF C_D

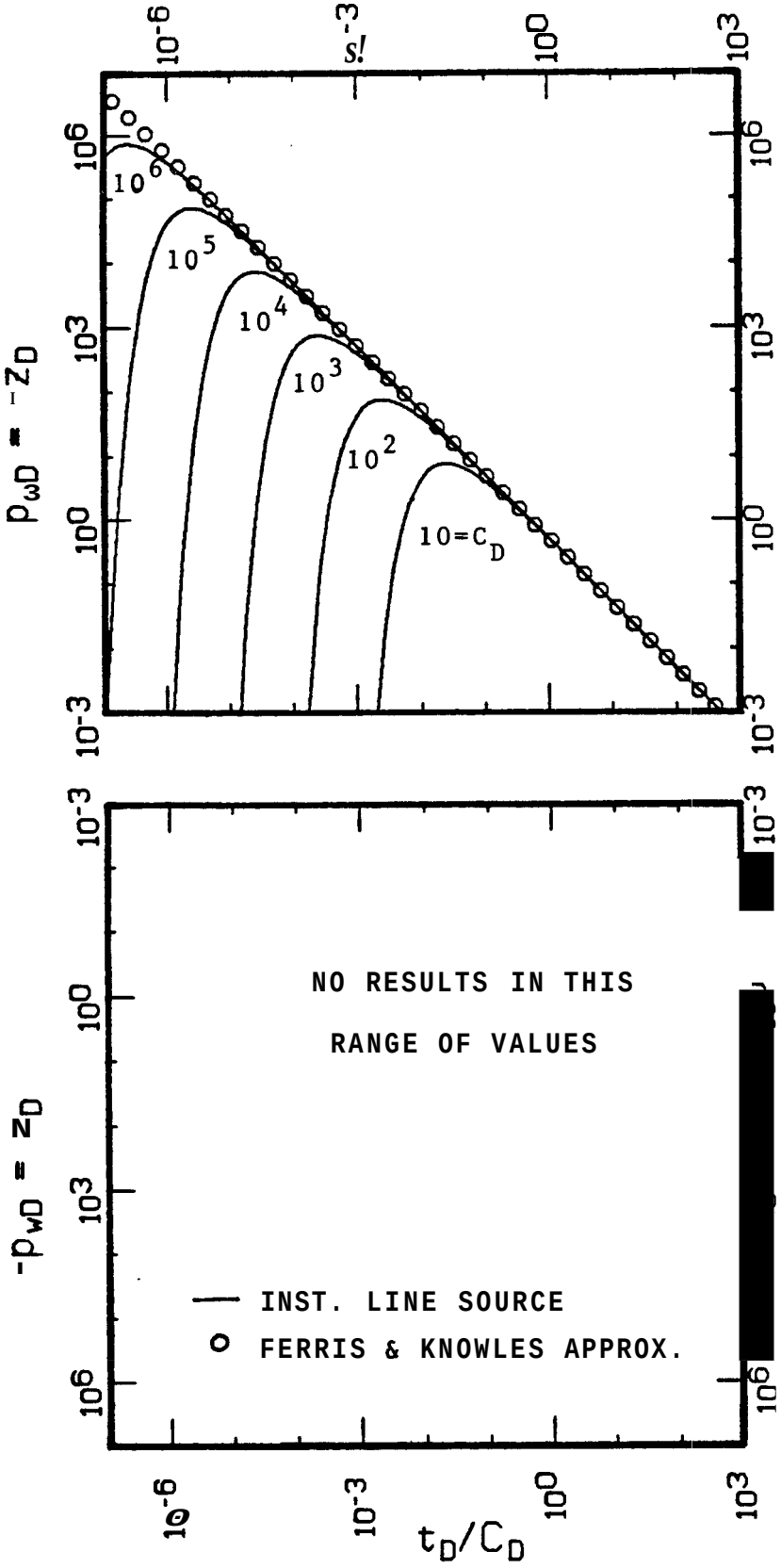

FIG. 5.2.e. LOG-LOG TYPE CURVE FOR SLUG TEST ANALYSIS OF p_{wD} OR z_D VS t_D/C_D NEGLECTING GRAVITATIONAL, INERTIAL, AND FRICTIONAL WELLBORE EFFECTS FOR PRACTICAL VALUES OF C_D

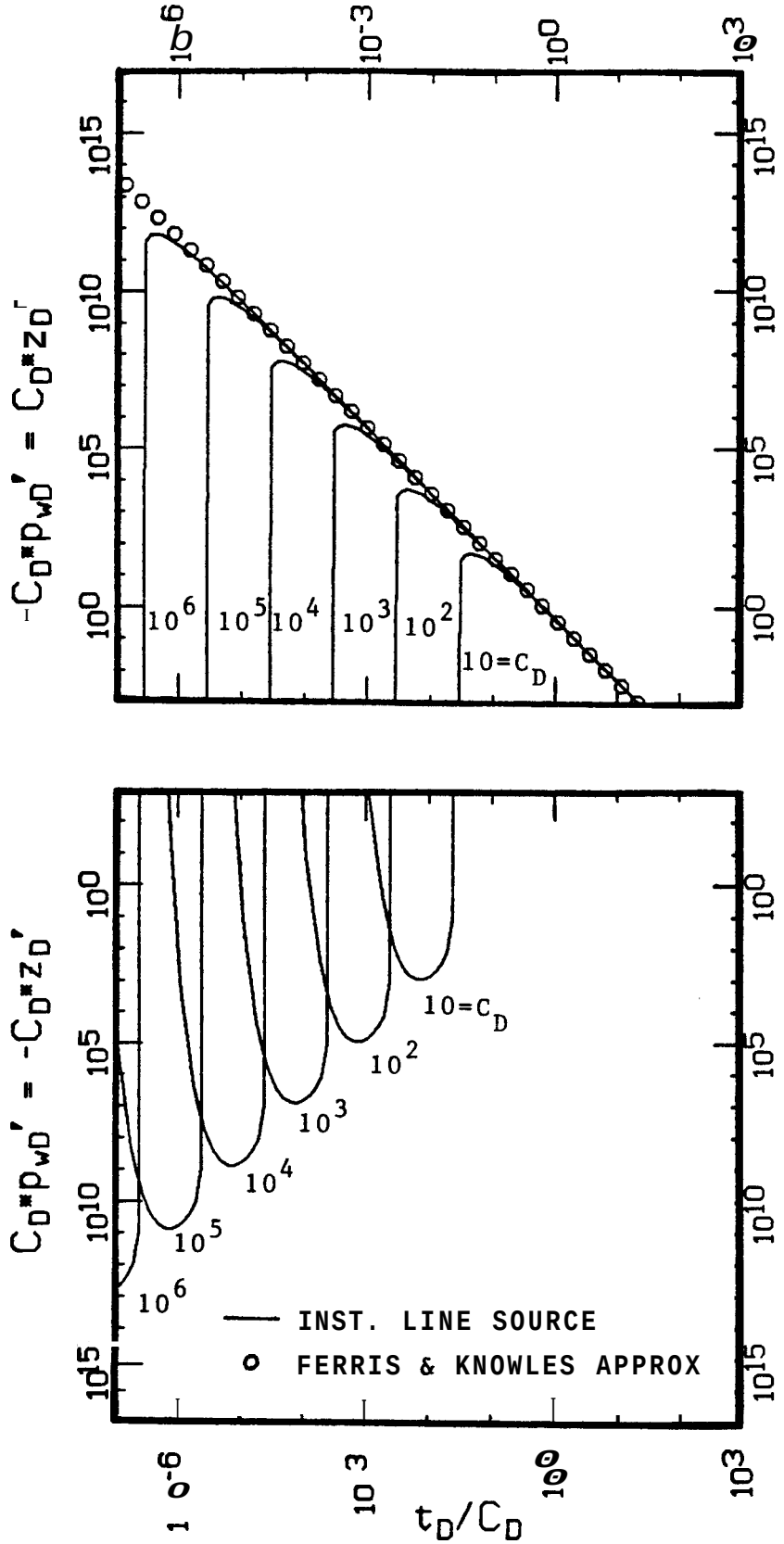

FIG. 5.2.f. LOG-LOG TYPE CURVE FOR SLUG TEST ANALYSIS OF p_{wD}' OR z_D' VS t_D/C_D NEGLECTING GRAVITATIONAL, INERTIAL, AND FRICTIONAL WELLBORE EFFECTS FOR PRACTICAL VALUES OF C_D

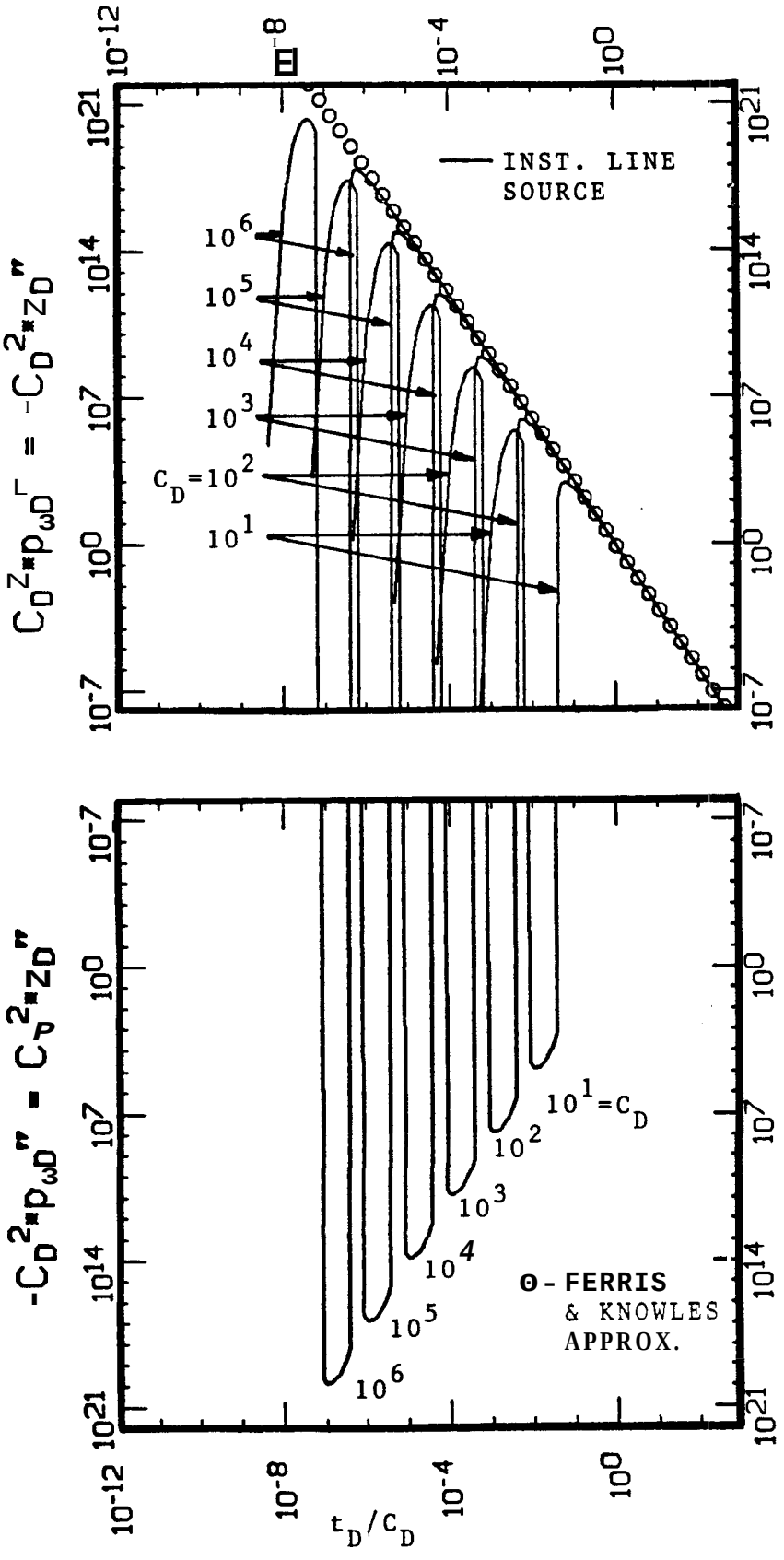

FIG. 5.2.g. LOG-LOG TYPE CURVE FOR SLUG TEST ANALYSIS OF p_{wD}'' OR z_D'' VS t_D/C_D NEGLECTING GRAVITATIONAL, INERTIAL, AND FRICTIONAL WELLBORE EFFECTS FOR PRACTICAL VALUES OF C_D

Inspection of approximations given by Eqs. 5.5, 5.8, and 5.9 shows that these solutions forecast linear behaviors in appropriate graphs. In order to cover the range of times of practical interest and to analyze early-time behavior, log-log graphs are a useful presentation of solutions and field data.

Solutions neglecting gravitational, inertial, and frictional wellbore effects can be correlated in log-log graphs; with abscissae axes obtained in the following form:

Taking decimal logarithms on both sides of Eq. 5.5 and rearranging terms:

$$\log(-z_D) = \log(p_{wD}) = -\log\left(\frac{t_D}{C_D}\right) - \log(2) \quad \ldots (5.10)$$

Then a log-log graph of $-z_D$ or p_{wD} vs t_D/C_D obtained from Eq. 5.5 results in a unique straight line with slope equal to minus unity and ordinate at $t_D/C_D=1$ of $-\log(2)$. This graph is presented and compared with the instantaneous line source solution in Fig. 5.2.e. In the range of practical testing times, $10^{-2}<t_D/C_D<10^{3}$, the instantaneous line source solution results deviate from the correlation for values of $C_D<10^{3}$ at early times. This is to be expected, because for those values of C_D, $10^{-2}C_D$ is smaller than the value of $t_D=10$ previously determined in Figs. 5.1.a - 5.1.g.

Multiplying both sides of Eq. 5.8 by C_D, and taking decimal logarithms:

$$\log(C_D z'_D) = \log(-C_D p'_{wD}) = -2\log\left(\frac{t_D}{C_D}\right) - \log(2) \quad \ldots (5.11)$$

Then, a log-log graph of $C_D z_D'$ or $C_D p_{wD}'$ vs t_D/C_D obtained from Eq. 5.8 results in a unique straight line with slope –2 and ordinate at $t_D/C_D=1$ of $-\log(2)$. This graph is presented and compared with the instantaneous line source solution in Fig. 5.2.f.

Multiplying Eq. 5.9 by C_D^2 and taking decimal logarithms:

$$\log(- C_D^2 z_D'') = \log(C_D^2 p_{wD}'') = - 3 \log (\frac{t_D}{C_D}) \quad \cdots (5.12)$$

A log-log graph of $-C_D^2 z_D''$ or $C_D^2 p_{wD}''$ vs t_D/C_D obtained from Eq. 5.9 results in a unique straight line with slope of –3. This graph is presented and compared with the instantaneous line source solution in Fig. 5.2.g.

Correlations shown in Figs. 5.2.f and 5.2.g also exhibit deviations at early times for $C_D<10^3$ in the practical range $10^{-2}<t_D/C_D<10^3$, because $10^{-2}C_D<10$.

According to the definition of C_D, z_D', and z_D'', given by Eqs. 3.47, 3.35, and 3.36, respectively, flow rate $q(t)$ and its rate of change, $q'(t)$, during a slug test, drillstem test, or closed-chamber test can be obtained from the following relationships:

$$C_D z_D' = \frac{1}{2\pi\rho g} \frac{\mu}{kh} \frac{1}{-z_0} q \quad \cdots (5.13)$$

and:

$$C_D^2 z_D'' = [\frac{1}{2\pi\rho g} \frac{\mu}{kh}]^2 \frac{\pi r_p^2}{-z_0} q' \quad \cdots (5.14)$$

Solutions considering the weight of the wellbore fluid column are discussed in the following section.

5.1.2 Negligible Inertia and Friction

In this type of solution, the effect of the hydrostatic weight of the wellbore liquid column on the reservoir response to an initial perturbation in liquid level or pressure is considered. This effect is called the gravitational effect of the wellbore liquid column throughout the present study.

In 1966, Bredehoeft, Cooper, and Papadopulos obtained slug test solutions including wellbore liquid column gravitational effects by using a resistance-capacitance electric analog. In a later publication, Cooper, Bredehoeft, and Papadopulos (1967) presented an analytical slug test solution including wellbore liquid level gravitational effects for an undamaged well (s=0). As mentioned by Cooper et al. (1967), this solution is analogous to a heat conduction solution presented by Carslaw and Jaeger (1959). Moreover, Cooper et al. (1967) correlated their results in the form of a semi-log type curve that can be decribed in terms of the variables used in the present study as a semi-log graph of $-z_D$ vs t_D/C_D for different values of C_D.

In 1970, van Poollen and Weber applied this type curve to drillstem test flowing pressure analysis by assuming a hydrostatic relationship between the liquid level column length and bottomhole pressure. Kohlhaas (1972) stated the slug test problem in terms of pressures, and obtained a type curve of p_{wD} vs t_D/C_D for different values of C_D analogous to the semi-log type curve presented by Cooper, Bredehoeft, and Papadopulos (1967).

In 1972, Ramey and Agarwal formulated a slug test problem in terms of pressures taking into consideration a skin effect, and reaching the following Laplace transformed solution for p_{wD}:

$$\overline{p_{wD}}(u) = \frac{C_D \left[K_0(\sqrt{u}) + s \sqrt{u} K_1(\sqrt{u}) \right]}{\sqrt{u} K_1(\sqrt{u}) + C_D u \left[K_0(\sqrt{u}) + s \sqrt{u} K_1(\sqrt{u}) \right]} \quad \ldots (5.15)$$

This is a special case of the transformed solutions obtained in the present study for p_{wD}, given by Eq. 4.2, and corresponds to the following wellbore equation:

$$z_D = - p_{wD} \quad \ldots (5.16)$$

According to the definition of z_D and p_{wD}, Eqs. 3.23 and 3.24, respectively, and using the definition of L given implicitly in Eq. 3.1, it can be shown that Eq. 5.16 is equivalent to:

$$p_w(t) = p_a + \rho g \left[L + z(t) + \frac{h}{2} \right] \quad \ldots (5.17)$$

From Eq. 5.17, it can be concluded that bottomhole pressure at a given time is considered equal to atmospheric pressure plus the hydrostatic pressure of the liquid column in a wellbore.

Equation 5.16 can be obtained by simplifying the wellbore **Eq. 3.39** derived **in** the present study, as follows:

$$A_w z_D'' + B_w z_D' + C_w z_D + D_w = E_w p_{wD} \quad \ldots (5.18)$$

with:

$$A_w = 0 \quad \ldots (5.18.a)$$

$$B_w = 0 \quad \ldots (5.18.b)$$

$$C_w = 1 \quad \ldots (5.18.c)$$

$$D_w = 0 \quad \ldots (5.18.d)$$

$$E_w = -1 \quad \ldots (5.18.e)$$

Therefore, the value of zero for coefficient A_w indicates that the acceleration term, $A_w z_D''$, in the wellbore equation is assumed negligible in this type of solution. Moreover, the value of zero for B_w shows that the velocity term $B_w z_D'$ is also assumed negligible in comparison to z_D and p_{wD}. These implicit assumptions may be described by stating

that this type of solution neglects inertial and frictional effects on the wellbore fluid column.

As mentioned by Ramey and Agarwal (1972), an analogous heat conduction problem was solved by Jaeger (1956), obtaining the following inversion integral for the transformed solution given by Eq. 5.15:

$$-z_D = p_{wD} = \frac{4\,C_D}{\pi^2} \int_0^\infty \frac{e^{-\sigma^2 t_D}}{\sigma\,[\,J^2(\sigma) + Y^2(\sigma)\,]}\,da \qquad \ldots (5.19)$$

where:

$$J(\sigma) = \sigma\,C_D\,J_0(\sigma) - [\,1 - C_D\,s\,\sigma^2\,]\,J_1(\sigma) \qquad \ldots (5.20)$$

$$Y(\sigma) = \sigma\,C_D\,Y_0(a) - [\,1 - C_D\,s\,\sigma^2\,]\,Y_1(\sigma) \qquad \ldots (5.21)$$

$J_0(\sigma)$ and $J_1(\sigma)$ are Bessel functions of the first kind and zero and unity order, respectively. $Y_0(\sigma)$ and $Y_1(\sigma)$ are Bessel functions of the second kind and zero and unity order, respectively.

Analytical solutions for p_{wD}', z_D', p_{wD}'', and z_D'' can be obtained from the inversion integral given by Eq. 5.19, because that integral is continuous and uniformly convergent. Then, the derivative of that integral exists, and the order of differentiation with respect to t_D and integration with respect to σ can be interchanged (Churchill, 1972). Therefore:

$$z_D' = -p_{wD}' = \frac{4\,C_D}{\pi^2} \int_0^\infty \frac{a\,e^{-a^2 t_D}}{[\,J^2(\sigma) + Y^2(\sigma)\,]}\,da \qquad \ldots (5.22)$$

and:

$$\bar{z}_D - \bar{p}_{wD} = \frac{4\,C_D}{\pi^2} \int_0^\infty \frac{\sigma^3\, e^{-\sigma^2 t_D}}{[\,J^2(\sigma) + Y^2(\sigma)\,]}\, d\sigma \qquad \cdots \quad (5.23)$$

The solution method for linear problems presented in Section 4.1 can be used to reproduce this type of solution. This may be done by assigning the values given by Eqs. 5.18.a - 5.18.e to coefficients A_w - E_w in wellbore Eq. 5.18. One of the options of the computer program presented in Appendix E permits one to reproduce and extend these solutions, in which gravitational effects are considered, but inertial and frictional wellbore effects are assumed negligible.

Results for practical values of t_D and C_D for s=0 are presented in Figs. 5.3.a - 5.3.g. The behavior of p_{wD} from unity to zero represents bottomhole pressure recovery from $[p_c+p_a]$ to p_i. The behavior of z_D from minus unity to zero corresponds to the recovery of liquid level from its initial position at $[L+z_0]$ to the static liquid level at L, where z = 0. Figs. 5.3.a - 5.3.c are Cartesian graphs and Fig. 5.3.d is a semi-log graph of p_{wD} and z_D vs t_D/C_D. The Cartesian graphs show a behavior of pressure recovery and liquid level recovery nearly linear at early times, depending on the value of C_D. The larger the C_D, the larger the range of t_D/C_D showing an almost linear behavior. From Fig. 5.3.a, in the range $0<t_D/C_D<1$, the behavior of p_{wD} and z_D is essentially linear for $C_D>10^3$. But, from Fig. 5.3.b, in the range of $0<t_D/C_D<10$, the linear behavior of p_{wD} and z_D is not apparent for $101<C_D<10^6$. This indicates that the duration of data recording can result in apparent linear recovery responses for systems with a relatively large value of C_D. Fig. 5.3.e presents the same results in a log-log graph.

Figure 5.3.f shows the corresponding log-log graphs for $C_D p_{wD}'$ and $C_D z_D'$ vs t_D/C_D. At early practical times, these solutions decline slowly and almost linearly from maximum values that vary between 0.2 and 2. The larger the value of C_D, the smaller the corresponding initial

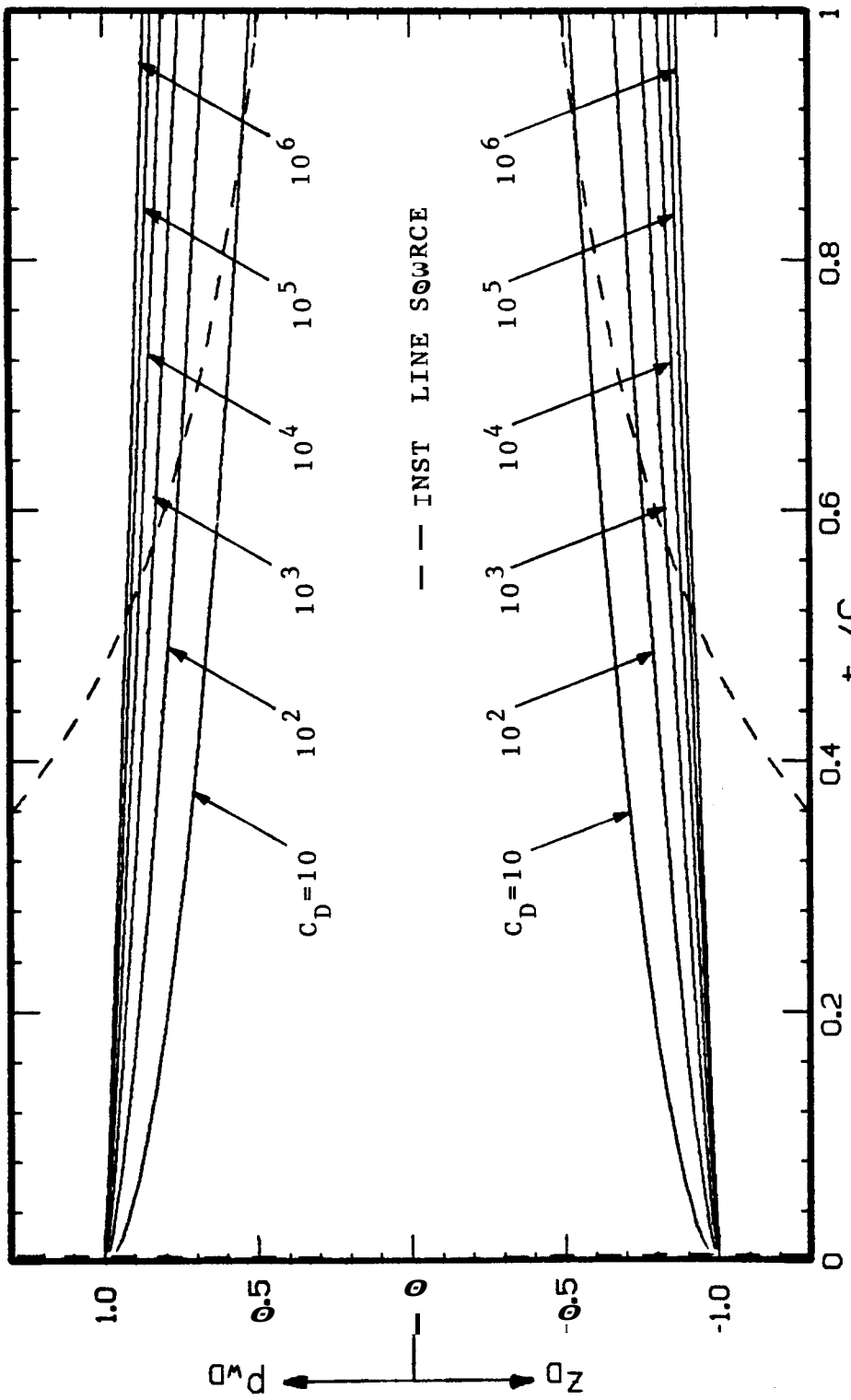

FIG. 5.3.9. CARTESIAN GRAPH OF SLUG TEST SOLUTIONS FOR P_{wD} AND z_D VS t_D/C_D INCLUDING GRAVITATIONAL WELLBORE EFFECTS FOR PRACTICAL VALUES OF C_D, s=0 AND $t_D/C_D<1$

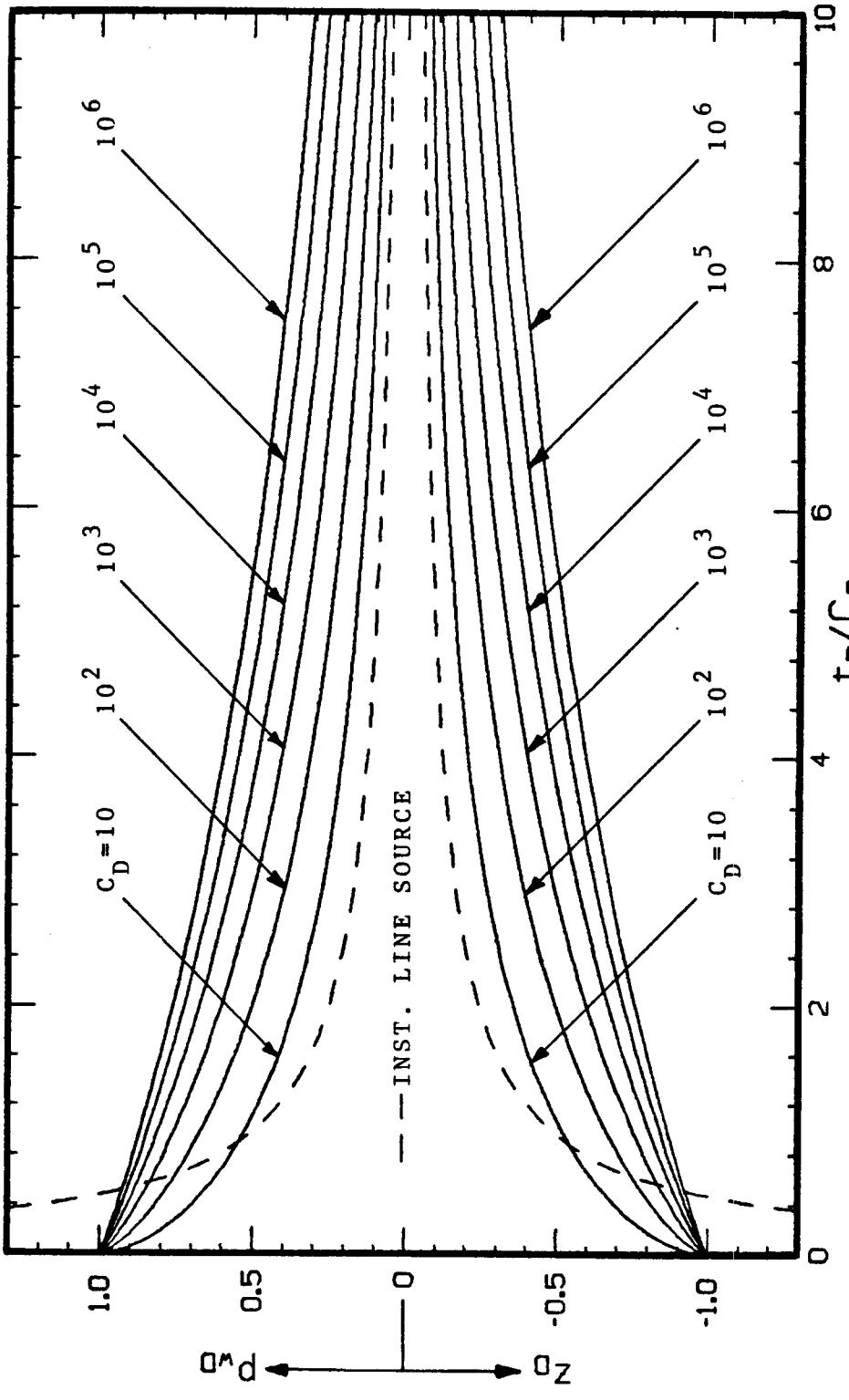

FIG. 5.3.b. CARTESIAN GRAPH OF SLUG TEST SOLUTIONS FOR P_{wD} AND z_D VS t_D/C_D INCLUDING GRAVITATIONAL WELLBORE EFFECTS FOR PRACTICAL VALUES OF C_D, s=0 AND $t_D/C_D<10$

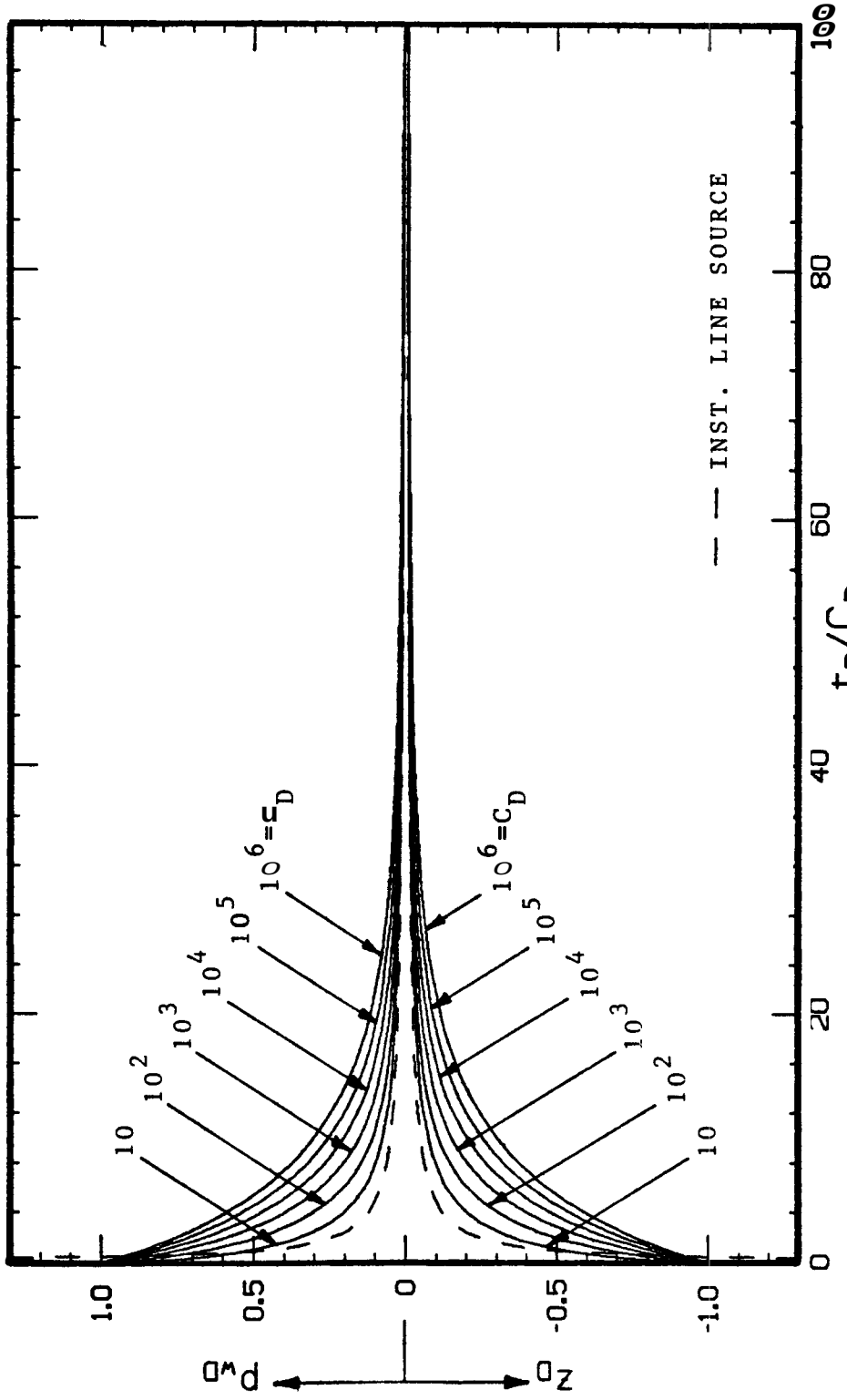

FIG. 5.3.c. CARTESIAN GRAPH OF SLUG TEST SOLUTIONS FOR P_{wD} AND z_D VS t_D/C_D INCLUDING GRAVITATIONAL WELLBORE EFFECTS FOR PRACTICAL VALUES OF C_D, s=0 AND $t_D/C_D \leq 100$

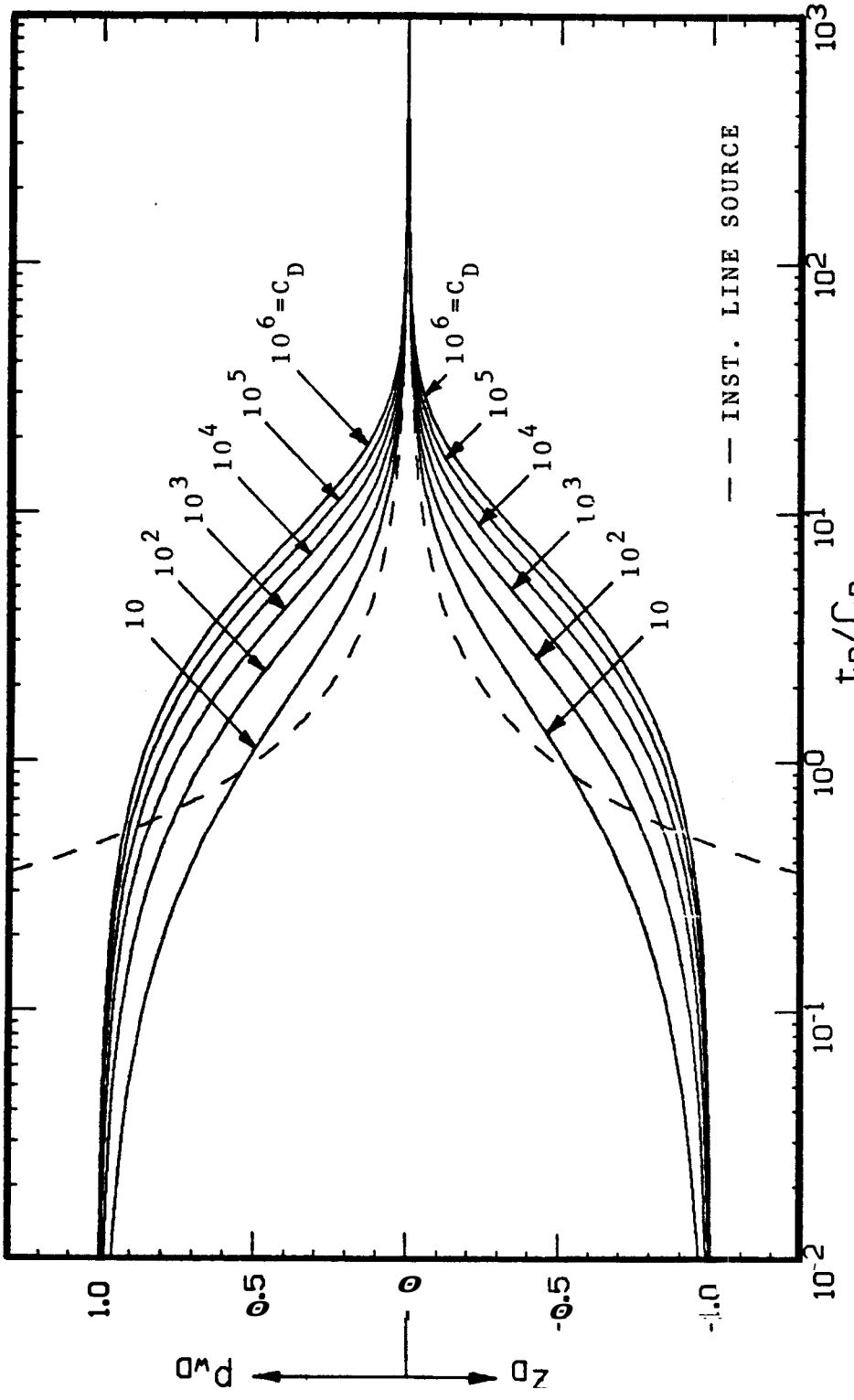

FIG. 5.3.d. SEMI-LOG GRAPH OF SLUG TEST SOLUTIONS FOR p_{wD} AND z_D VS t_D/C_D INCLUDING GRAVITATIONAL WELLBORE EFFECTS FOR PRACTICAL VALUES OF C_D AND s=0

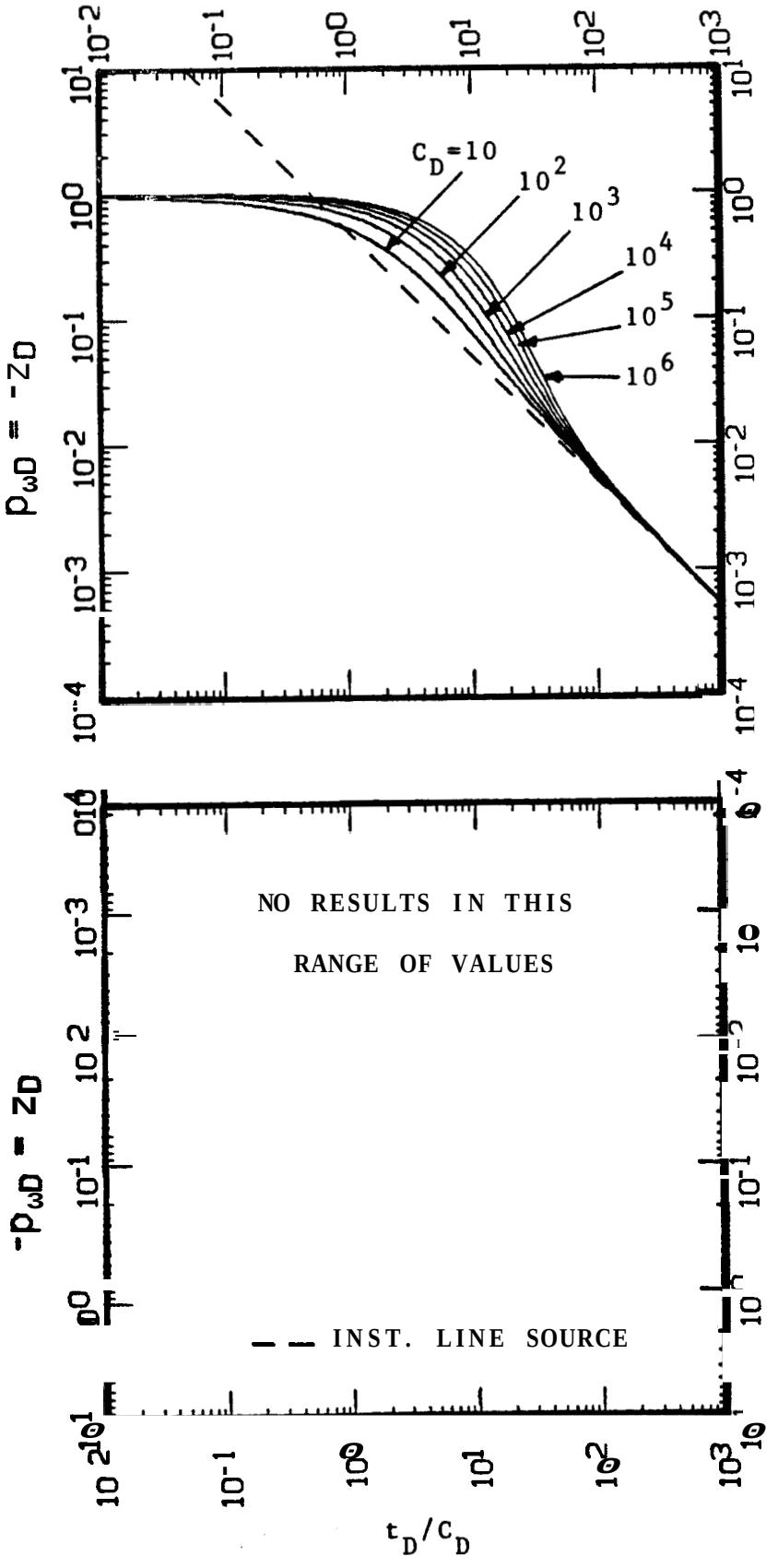

FIG. 5.3.e. **LUG-LUG GRAPH** OF SLUG TEST SOLUTIONS FOR p_{wD} *AND* z_D VS t_D/C_D INCLUDING GRAVITATIONAL WELLBORE EFFECTS FOR PRACTICAL VALUES OF C_D AND s=0

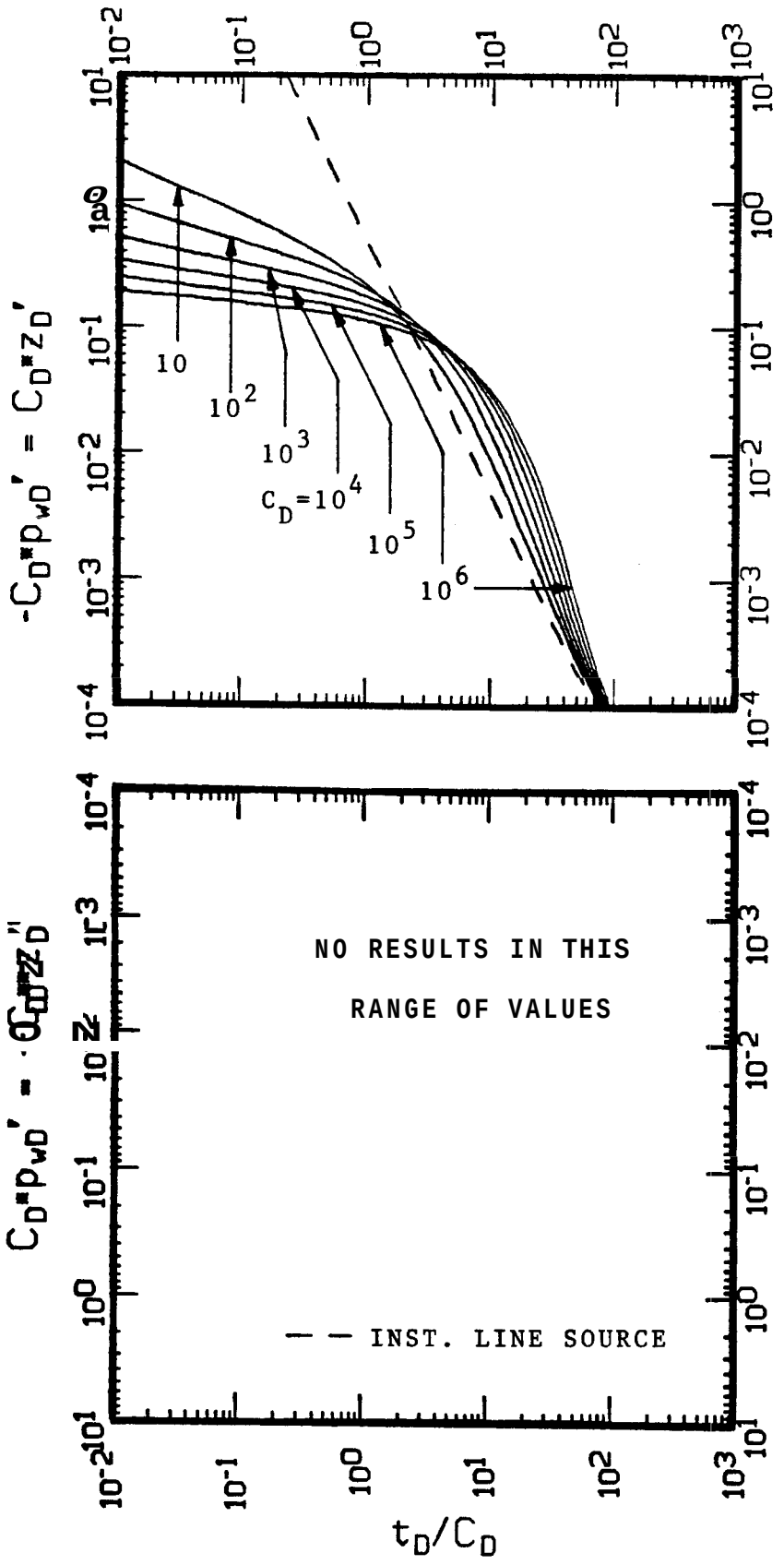

FIG. 5.3.f. LOG-LOG GRAPH OF SLUG TEST SOLUTIONS FOR p_{wD}' AND z_D' VS t_D/C_D INCLUDING GRAVITATIONAL WELLBORE EFFECTS FOR PRACTICAL VALUES OF C_D AND s=0

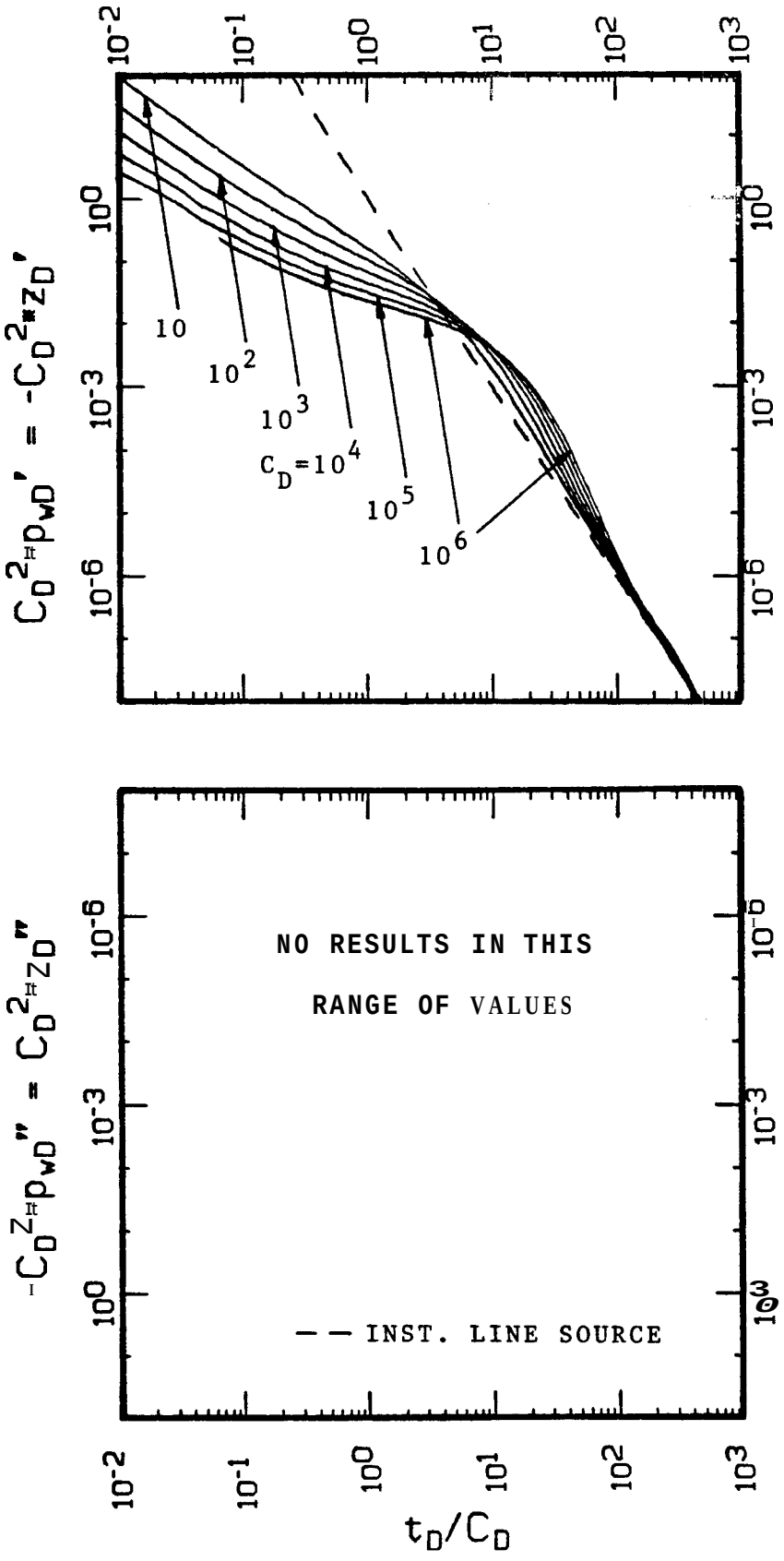

FIG. 5.3.g. LOG-LOG GRAPH OF SLUG TEST SOLUTIONS FOR p_{wD}'' AND z_D'' VS t_D/C_D INCLUDING GRAVITATIONAL WELLBORE EFFECTS FOR PRACTICAL VALUES OF C_D AND $s=0$

maximum value. At late times, these solutions cross the instantaneous line source solution and approach it after an abrupt drop. For a system with large C_D, these solutions decline slower at early times and the abrupt decline occurs later. Since, according to Eq. 5.13, $q(t)$ is proportional to $C_D z_D'$, a system with a larger C_D will sustain a smaller but nearly constant flow rate, longer.

Solutions for $C_D^2 p_{wD}''$ and $C_D 2 z_D''$ vs t_D/C_D are shown in the log-log graph of Fig. 5.3.g. These solutions show a decline at early practical times. After crossing the line source solution, these solutions also approach the line source solution at later times for large values of C_D.

Papadopulos, Bredehoeft and Cooper (1973) extended the type curve presented by Cooper, Bredehoeft, and Papadopulos (1967) to include solutions required to match slug test data showing unexpected large values of C_D.

In 1975, Ramey, Agarwal, and Martin applied to drillstem test flow analysis an approach parallel to the one suggested by Earlougher and Kersch (1974) for conventional well test analysis. Ramey, Agarwal, and Martin (1975) prepared three type curves for slug test or drillstem test analysis obtained from the solution previously presented by Ramey and Agarwal (1972). These type curves are based on a correlation of p_{wD} vs t_D/C_D with $C_D e^{2s}$ as a parameter. As mentioned by those authors, this correlation is excellent for values of $C_D e^{2s} > 10^2$. For smaller values of $C_D e^{2s}$, deviations are observed depending on the particular combination of C_D and s. For $C_D e^{2s} < 10^2$, the smaller the value of s, the smaller the deviation from the correlation.

This correlation is based on the assumption that the flow behavior in a damaged system with a steady-state pressure drop caused by a skin effect at the sandface is similar to the behavior in an equivalent undamaged system with an appropriate wellbore radius (Brons and Miller, 1961).

This assumption results in an effective wellbore radius, r_{we}, dependent on s and on the actual wellbore radius r_w, given by:

$$r_{we} = r_w e^{-s} \quad \ldots (5.24)$$

Using this effective wellbore radius instead of r_w in the problem formulation results in an analogous problem solution. The only difference is that s is equal to zero in Eq. 5.19, because it is implicitly considered in r_{we}. Since r_{we} would appear in both t_D and C_D, r_{we} cancels in the ratio t_D/C_D. However, when r_{we} does not cancel in a dimensionless group, a solution in terms of r_w requires explicit expecification of s. By example, C_D in terms of r_{we} is equivalent to $C_D e^{2s}$ in terms of r_w.

Results for p_{wD}, z_D, $C_D p_{wD}'$, $C_D z_D'$, $C_D^2 p_{wD}''$, and $C_D^2 z_D''$ vs t_D/C_D provided by the semi-analytical solution method for linear problems presented in this study are shown in Figs. 5.4.a - 5.4.h. Solutions for p_{wD} and z_D are given in Figs. 5.4.a - 5.4.c as cartesian graphs, in Fig. 5.4.d as a semi-log type curve, and in Figs. 5.4.e and 5.4.f as log-log type curves for different values of $C_D e^{2s}$. Type curves for p_{wD} more detailed than Figs. 5.4.d - 5.4.f were presented by Ramey, Agarwal, and Martin (1975).

Cartesian graphs for different ranges of t_D/C_D, given in Figs. 5.4.a - 5.4.b, show apparent linear behavior for large values of C_D. From Fig. 5.4.a, systems with $C_D e^{2s} > 103$ exhibit nearly linear behavior in the range $0 < t_D/C_D < 1$. From Fig. 5.4.b, systems with $C_D e^{2s} > 109$ show linear behavior for $0 < t_D/C_D < 10$. Fig. 5.4.c indicate no apparent linear behavior sustained in the range of $0 < t_D/C_D < 100$

Figs. 5.4.g and 5.4.h are new type curves providing the corresponding solutions for $z_D' = -p_{wD}'$ and $z_D'' = -p_{wD}''$, respectively. Under the assumptions intrinsic in this kind of solution, type curves for z_D' in Fig. 5.4.g describe the flow rate behavior during a slug test

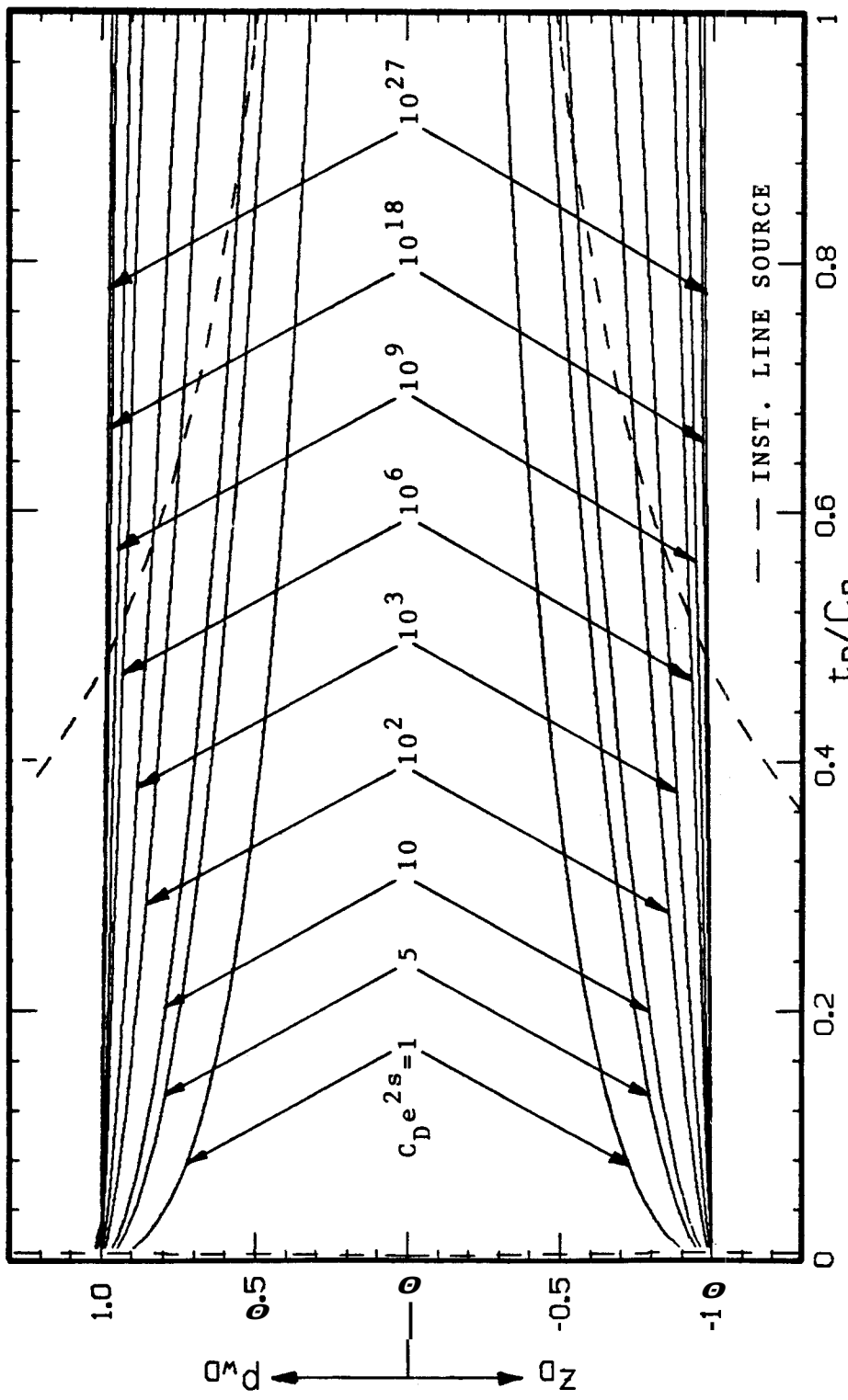

FIG. 5.4.a. CARTESIAN GRAPH OF SLUG TEST SOLUTIONS FOR p_{wD} OR z_D VS t_D/C_D INCLUDING GRAVITATIONAL WELLBORE EFFECTS FOR PRACTICAL VALUES OF C_De^{2s} WITH $t_D/C_D<1$

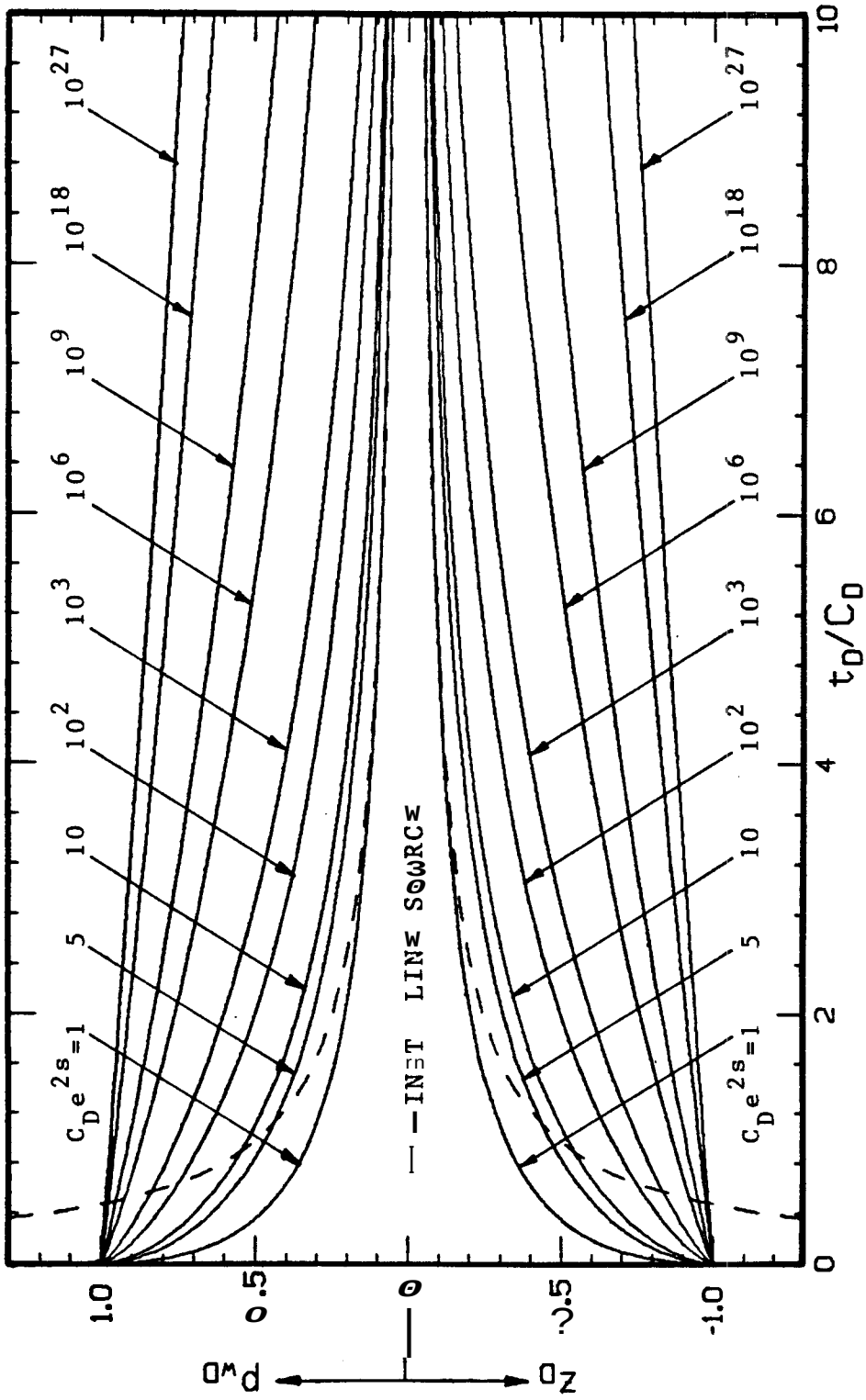

FIG. 5.4.b. CARTESIAN GRAPH OF SLUG TEST SOLUTIONS FOR p_{wD} OR z_D VS t_D/C_D INCLUDING GRAVITATIONAL WELLBORE EFFECTS FOR PRACTICAL VALUES OF C_De^{2s} WITH $t_D/C_D<10$

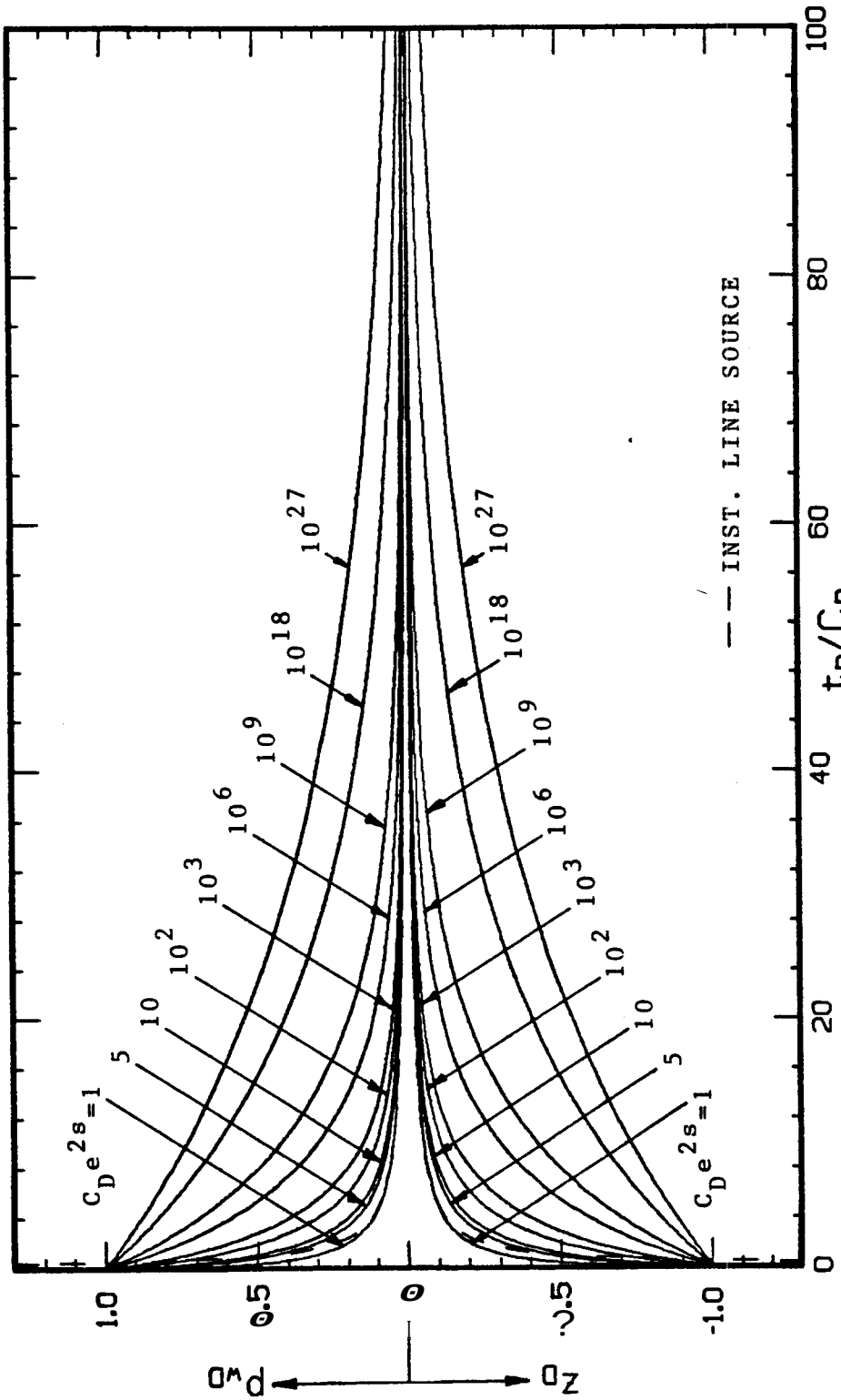

FIG. 5.4.c. CARTESIAN GRAPH OF SLUG TEST SOLUTIONS FOR P_{wD} OR z_D VS t_D/C_D INCLUDING GRAVITATIONAL WELLBORE EFFECTS FOR PRACTICAL VALUES OF C_De^{2s} WITH $t_D/C_D<100$

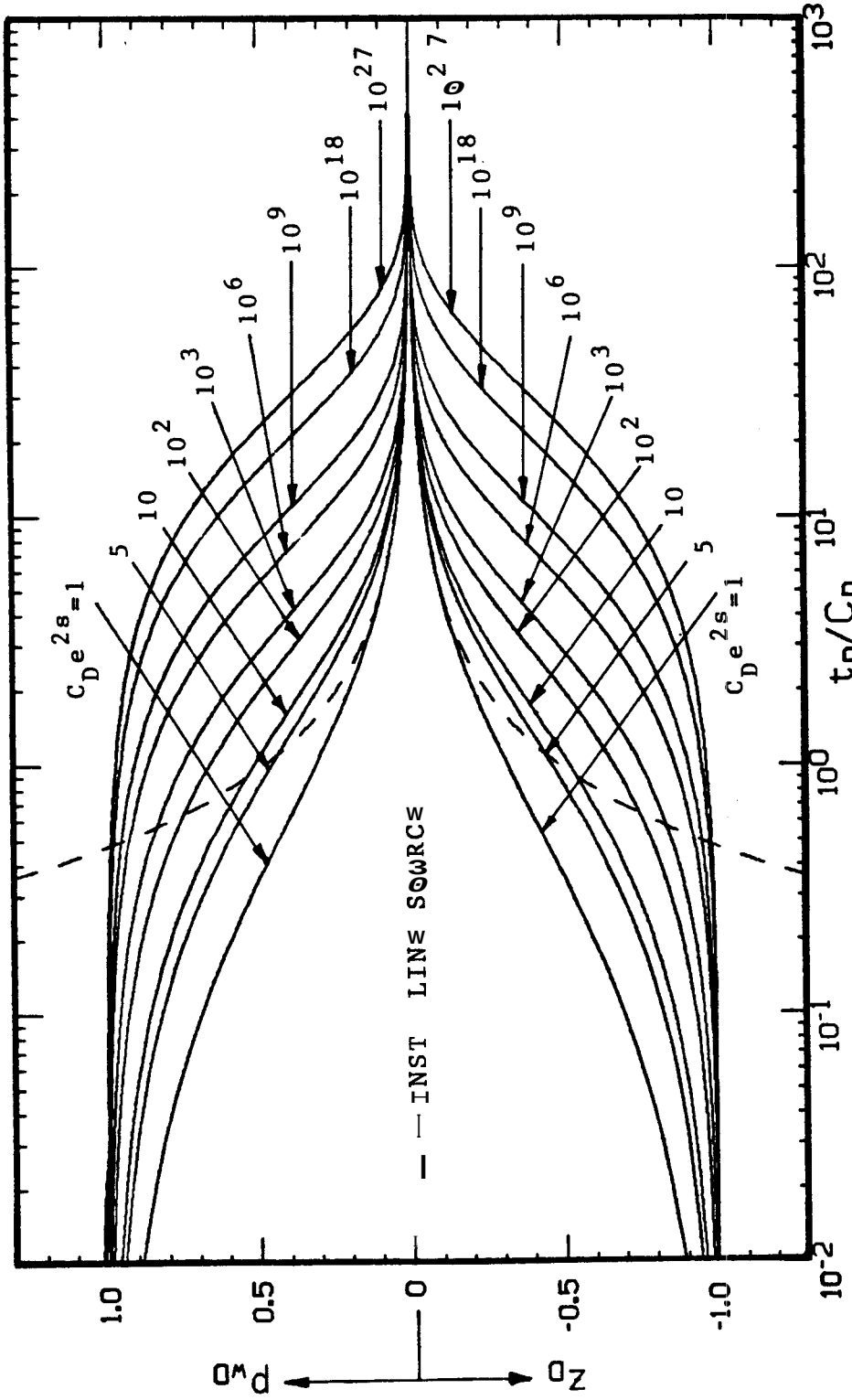

FIG. 5.4.d. SEMI-LOG TYPE CURVE FOR SLUG TEST ANALYSIS OF P_{wD} OR z_D VS t_D/C_D INCLUDING GRAVITATIONAL WELLBORE EFFECTS FOR PRACTICAL VALUES OF C_De^{2s}

(After Ramey, et al., 1975)

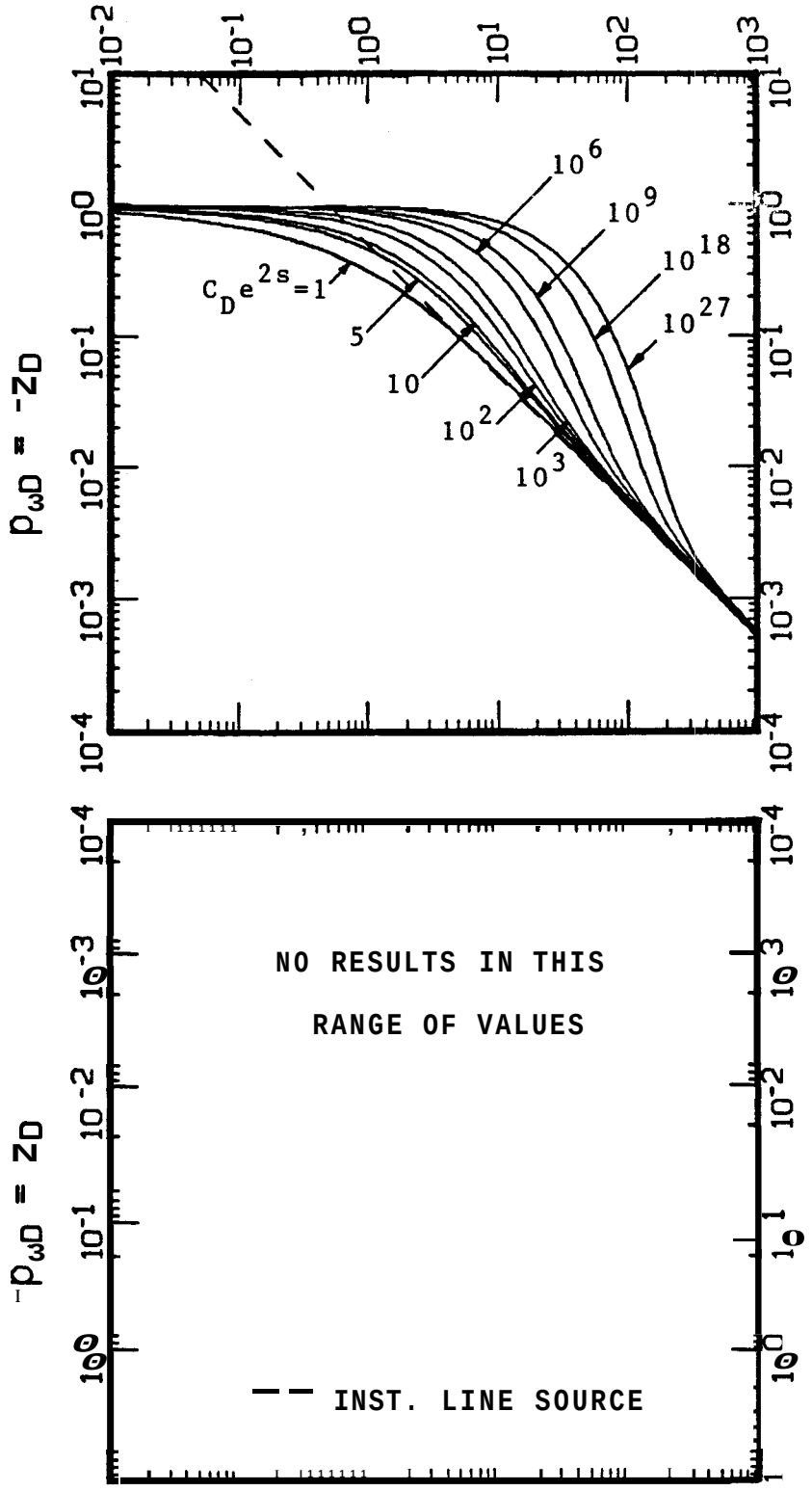
$p_{\omega D} = -z_D$
$C_D e^{2s} = 1$
5
10
10^2
10^3
10^6
10^9
10^{18}
10^{27}
$p_{\omega D} = z_D$
NO RESULTS IN THIS
RANGE OF VALUES
INST. LINE SOURCE

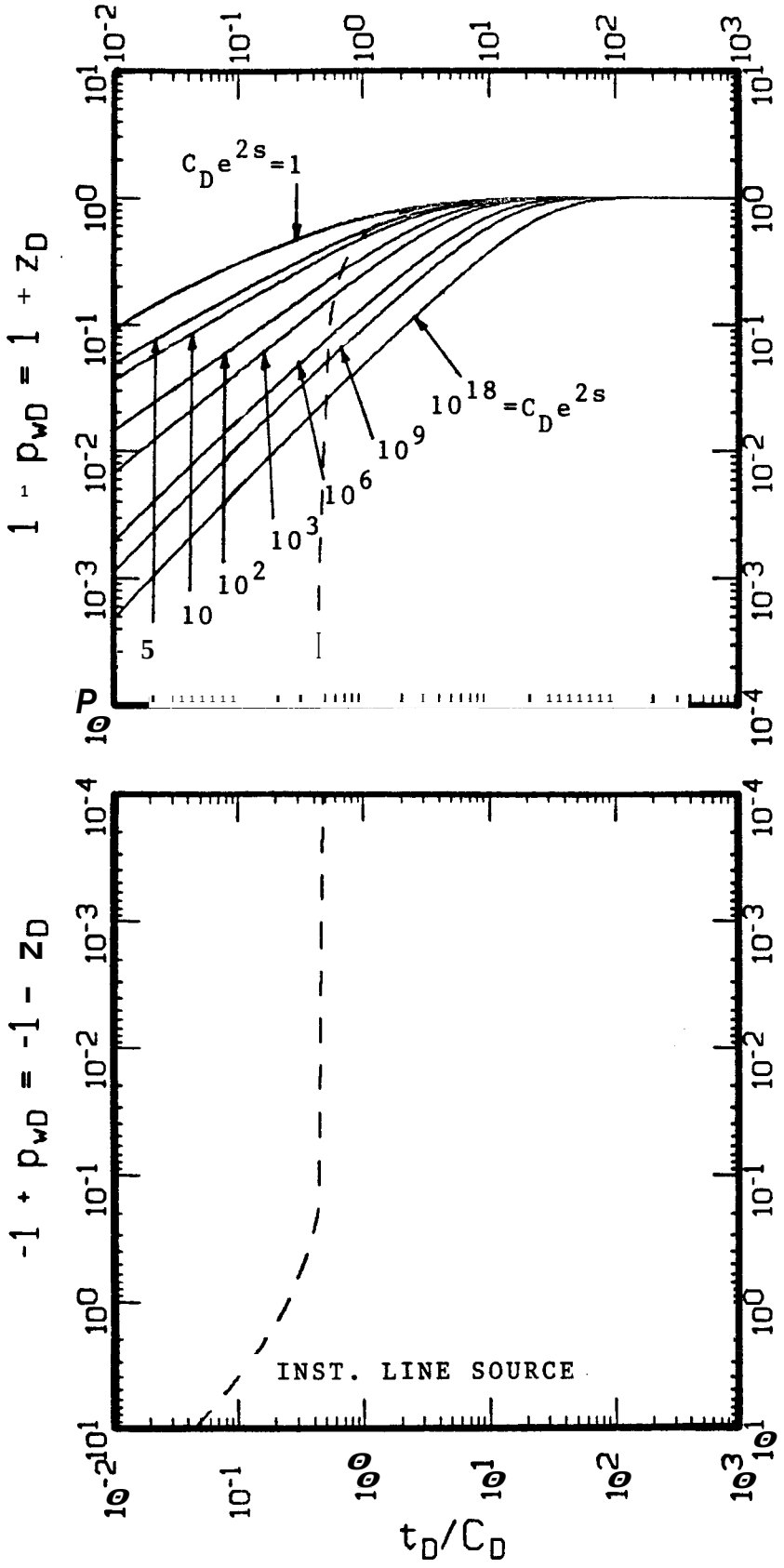

FIG. 5.4.f - LOG-LOG TYPE CURVE FOR SLUG TEST ANALYSIS OF $1-p_{wD}$ OR z_D-1 VS t_D/C_D INCLUDING GRAVITATIONAL WELLBORE EFFECTS FOR PRACTICAL VALUES OF $C_D e^{2s}$ (After Ramey, et al., 1975)

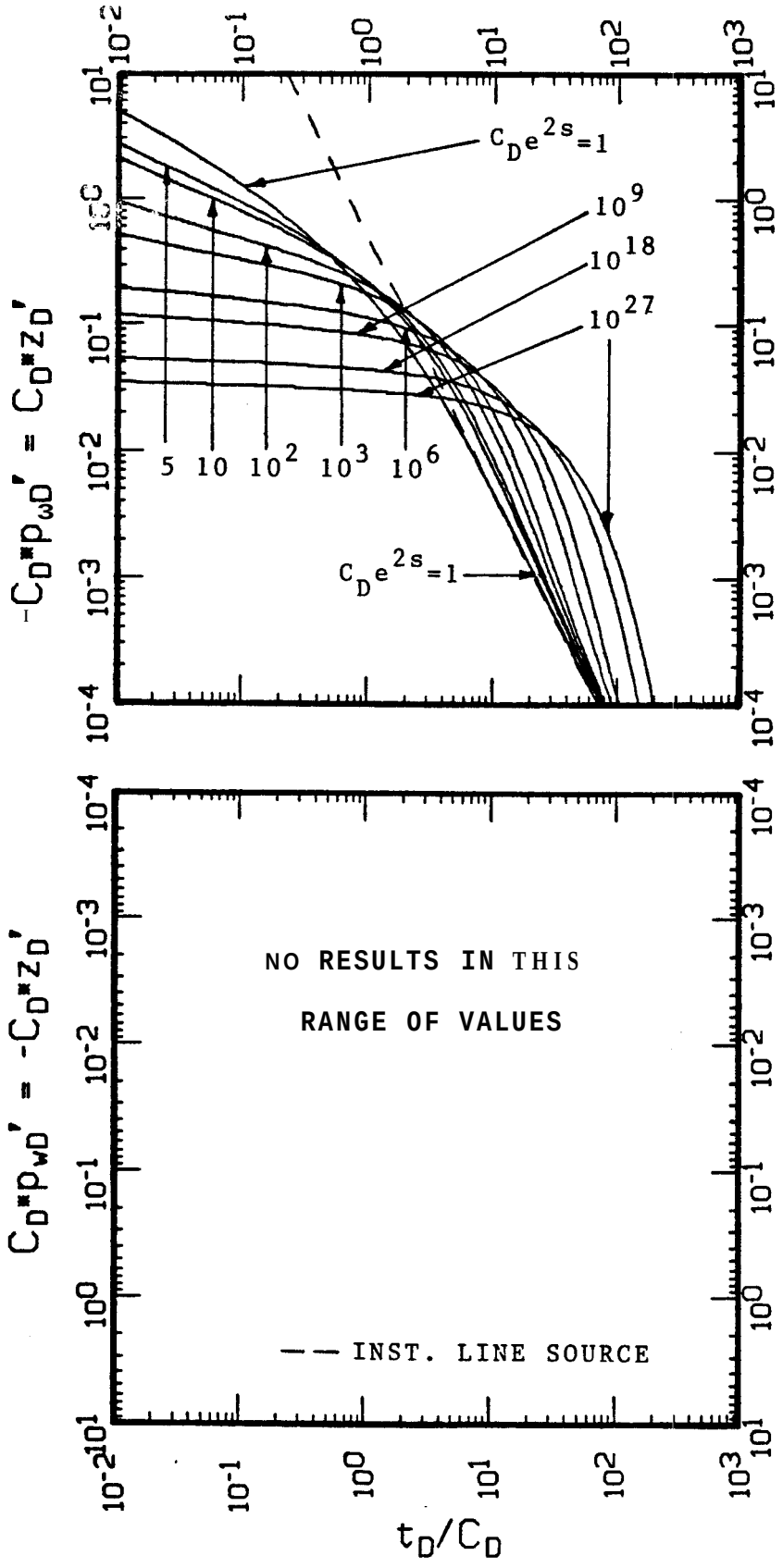

FIG. 5.4.g. LOG-LOG **TYPE** CURVE **FOR** SLUG TEST ANALYSIS **OF** p_{wD}' OR z_D' VS t_D/C_D INCLUDING GRAVITATIONAL WELLBORE **EFFECTS FOR** PRACTICAL VALUES **OF** $C_D e^{2s}$

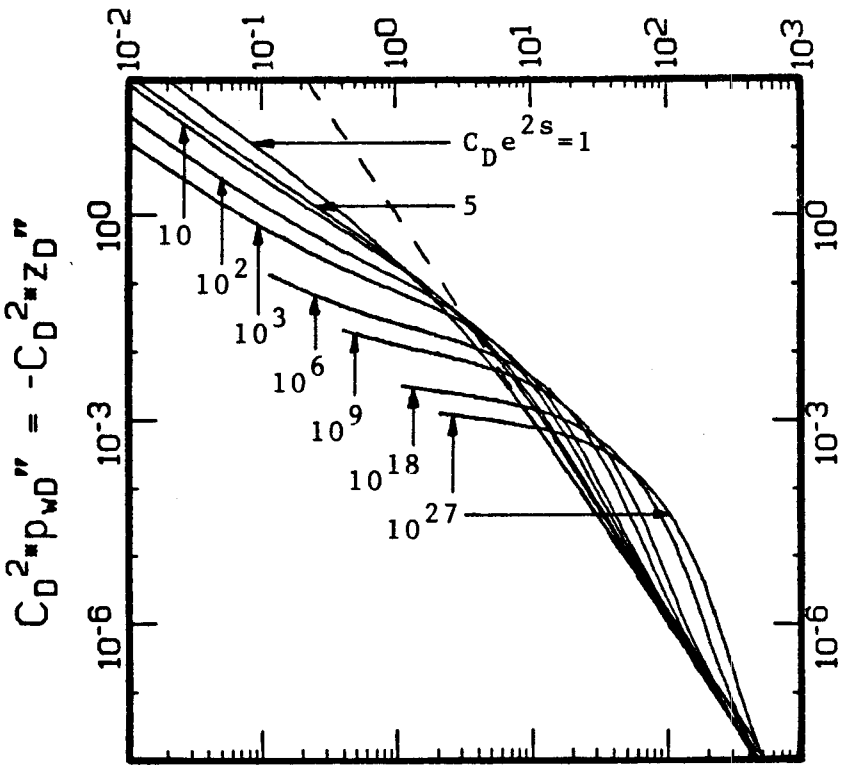
$C_D^2 * p_{wD}'' = -C_D^{2} * z_D''$
$C_D e^{2s} = 1$
5
10
10^2
10^3
10^6
10^9
10^{18}
10^{27}

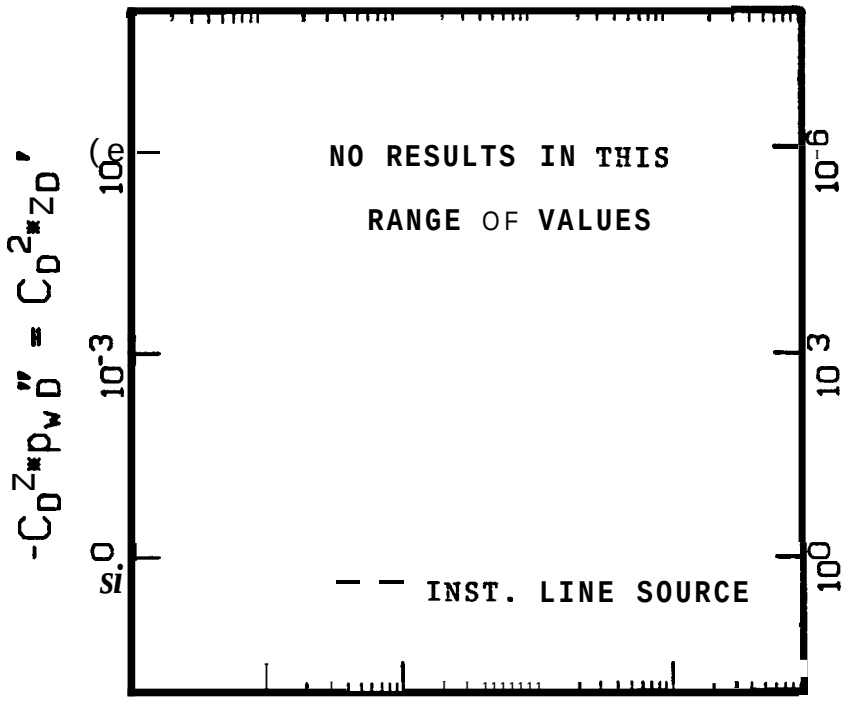
$-C_D^2 * p_{wD}'' = C_D^2 * z_D'$
NO RESULTS IN THIS
RANGE OF VALUES
INST. LINE SOURCE

or a drillstem test. Type curves shown in Fig. 5.4.h correspond to the behavior of the rate of change of the flow rate during these tests.

Solutions including gravitational and inertial wellbore effects are discussed in the following section.

5.1.3 Negligible Friction - Effect of *a*

A simplified wellbore equation was derived by Cooper, Bredehoeft, Papadopulos, and Bennett (1965) to describe the response of a water level in a groundwater well to seismic waves. That equation considered inertial effects on the movement of the wellbore liquid column. Frictional effects in the wellbore were assumed negligible. Also, the range of variation of the liquid level about the static liquid level was supposed to be small in comparison to the length of the column of water in static equilibrium with the aquifer pressure.

In 1966, Bredehoeft, Cooper, and Papadopulos considered the wellbore equation presented by Cooper et al. (1965) in a resistance-conductance electric analog to study effects of inertia, in both the aquifer and wellbore, for problems involving rapid acceleration of the liquid.

Ten years later, van der Kamp (1976) also used the wellbore equation proposed by Cooper et al. (1965) and obtained an approximate solution method to analyze slug test data showing an underdamped response. The term "underdamped" was used to differentiate previous studies which neglect inertia as "fully-damped".

Recently, Shinohara and Ramey (1979.b) derived solutions for p_{wD} and z_D including the effect of inertia of the wellbore fluid column on flow phenomena during a slug test, drillstem test, or closed-chamber test. The following wellbore equation used by Shinohara and Ramey (1979.b) is also similar to the one presented by Cooper, et al. (1965):

$$a^2 z_D'' + z_D = - p_{wD} \quad \ldots (5.25)$$

This is a special case of wellbore Eq. 3.39 derived in the present study, simplified as follows:

$$A_w z_D'' + B_w z_D' + C_w z_D + D_w = E_w p_{wD} \quad \ldots (5.26)$$

with:

$$A_w = a^2 \quad \ldots (5.26.a)$$

$$B_w = 0 \quad \ldots (5.26.b)$$

$$C_w = 1 \quad \ldots (5.26.c)$$

$$D_w = 0 \quad \ldots (5.26.d)$$

$$E_w = -1 \quad \ldots (5.26.e)$$

where, according to the definition of a, given by Eq. 3.51:

$$\alpha^2 = \frac{L}{g}\left[\frac{k}{\phi\mu c_t r_w^2}\right]^2 = \frac{1}{g}\left[\frac{p_i - p_a}{\rho g} - \frac{h}{2}\right]\left[\frac{k}{\phi\mu c_t r_w^2}\right]^2 \quad \ldots (5.27)$$

Comparison of Eq. 5.26 and wellbore Eq. 3.39 reveals the following assumptions, as declared by Shinohara and Ramey (1979.b):

(1) slug size negligible with respect to static liquid column length, $-z_0 \ll L$,

(2) negligible wellbore frictional losses, $f \simeq 0$,

(3) reservoir thickness negligible with respect to liquid column length, $h \ll L$, and

(4) negligible inertial and frictional wellbore effects of pipe radius different than wellbore radius.

Shinohara and Ramey (1979.b) obtained the following Laplace transformed solutions:

$$\overline{z_D}(u) = \frac{\{[\alpha^2 u + C_D s]\sqrt{u}K_1(\sqrt{u}) + C_D K_0(\sqrt{u})\}z_D(0) + [\alpha^2\sqrt{u}K_1(\sqrt{u})]z_D'(0)}{[\alpha^2 u^2 + C_D su + 1]\sqrt{u}K_1(\sqrt{u}) + C_D uK_0(\sqrt{u})} \quad \ldots (5.28)$$

$$\overline{p_{wD}}(u) = \frac{C_D\,[s\sqrt{u}K_1(\sqrt{u}) + K_0(\sqrt{u})][-z_D(0) + \alpha^2 uz_D'(0)]}{[\alpha^2 u^2 + C_D su + 1]\sqrt{u}K_1(\sqrt{u}) + C_D uK_0(\sqrt{u})} \quad \ldots (5.29)$$

$$\overline{p_D}(r_D, u) = \frac{C_D K_0(r_D\sqrt{u})[-z_D(0) + \alpha^2 uz_D'(0)]}{[\alpha^2 u^2 + C_D su + 1]\sqrt{u}K_1(\sqrt{u}) + C_D uK_0(\sqrt{u})} \quad \ldots (5.30)$$

For a test starting from static conditions, $z_D(0)=-1$ and $z_D'(0)=0$, these transformed solutions are equivalent to the solutions obtained in the present study, given by Eqs. 4.1, 4.2, and 4.8, for the simplified wellbore equation given by Eq. 5.26.

From analysis of their results, Shinohara and Ramey (1979.b) concluded that inertia of the wellbore liquid column can cause a lack of symmetry between p_{wD} and z_D. Then, the assumption that p_{wD} and z_D are related through simple hydrostatic head calculations can give erroneous estimations of the properties for some systems.

Results presented by Shinohara and Ramey can be complemented with the transformed solutions for p_{wD}', z_D', and z_D'' derived in the present study, and given by Eqs. 4.3 - 4.7.

Comparison of results obtained in this study for a system with $s=0$, $C_D=103$, and values of $104<\alpha 2<10^8$ with the results presented by Shinohara (1980) show differences for values of t_D near 2. Shinohara (1980) obtained inconsistent solutions for p_{wD} and z_D for values of t_D near 2. Since the solutions in Laplace space were the same, these differences may be attributed to less accurate Bessel function approximations used by Shinohara (1980), and not to a problem in the application of the Stehfest algorithm. In this study, Bessel functions were evaluated by using double-precision subroutines available from the Center for Information Technology at Stanford University. On the other hand, Shinohara (1980) used approximations published by Abramowitz and Stegun (1972).

The values of $10^4<\alpha^2<10^8$ were selected to illustrate damped, critically-damped, and underdamped conditions, corresponding to the three kinds of behavior possible during a test for a given system with specific s and C_D.

Results are presented in Figs 5.5.a - 5.5.i. For $s=0$ and $C_D=10^3$, systems with $a^2<10^5$ show negligible wellbore inertial effects, for all practical purposes, and such tests can be analyzed from solutions with $\alpha^2=0$, which corresponds to the type curves presented by Ramey, Agarwal, and Martin (1975). For $\alpha^2=10^6$, the behavior of the solutions for p_{wD}

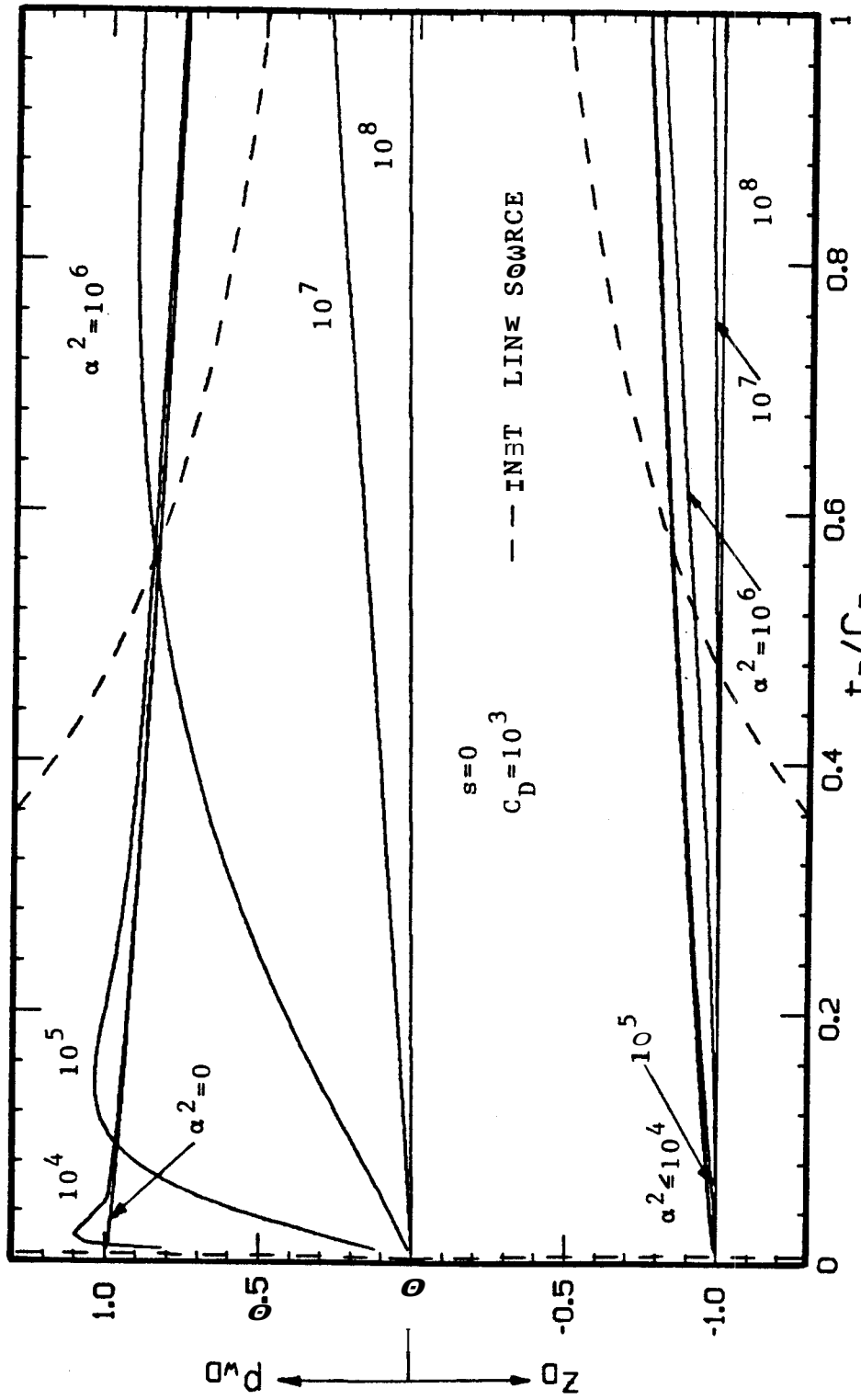

FIG. 3.5.a. CARTESIAN GRAPH OF SLUG TEST SOLUTIONS FOR P_{wD} AND z_D VS t_D/C_D INCLUDING GRAVITATIONAL AND INERTIAL WELLBORE EFFECTS FOR DIFFERENT VALUES OF α^2 FOR A SYSTEM WITH s=0, $C_D=10^3$, AND $t_D/C_D\leq1$ (After Shinohara and Ramey, 1979.b)

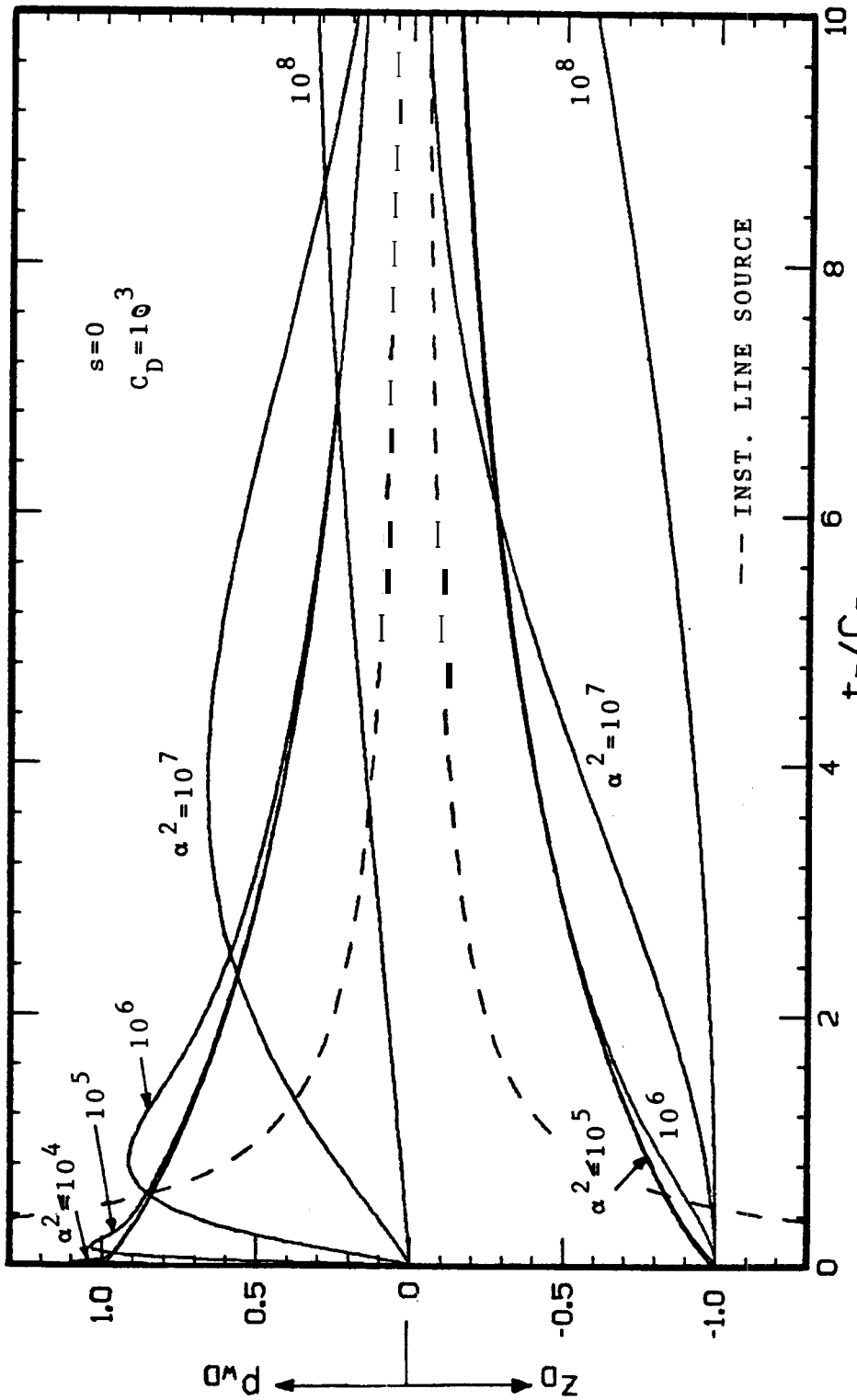

FIG. 5.5.b. CARTESIAN GRAPH OF SLUG TEST SOLUTIONS FOR p_{wD} AND z_D VS t_D/C_D INCLUDING GRAVITATIONAL AND INERTIAL WELLBORE EFFECTS FOR DIFFERENT VALUES OF α^2 F SYSTEM WITH s=0, $C_D=10^3$, AND $t_D/C_D<10$ (After Shinohara and Ramey, 1979.b)

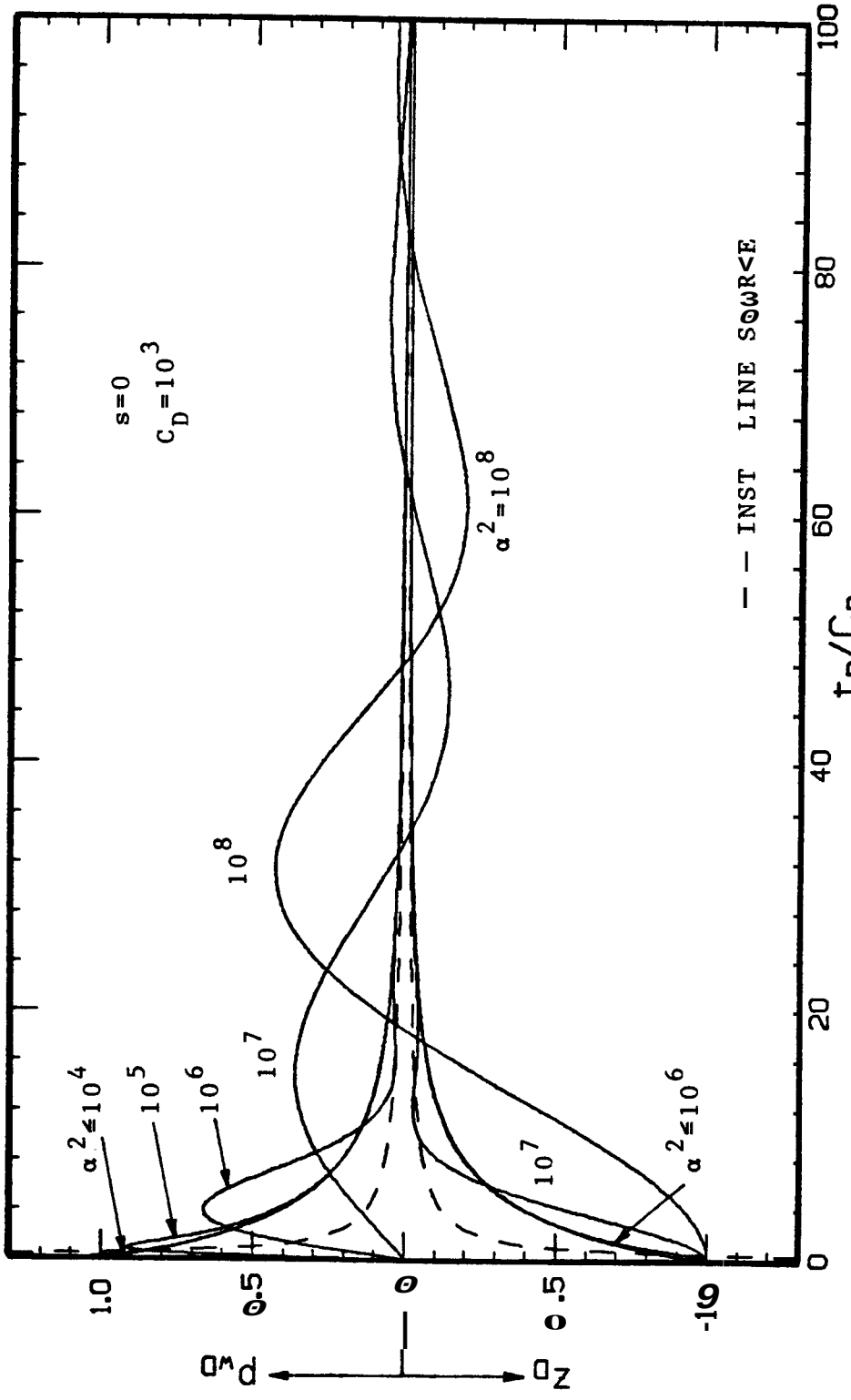

FIG. 5.5.c. CARTESIAN GRAPH OF SLUG TEST SOLUTIONS FOR P_{wD} AND z_D VS t_D/C_D INCLUDING GRAVITATIONAL AND INERTIAL WELLBORE EFFECTS FOR DIFFERENT VALUES OF α^2 FOR A SYSTEM WITH s=0, $C_D=10^3$, AND $t_D/C_D<100$ (After Shinohara and Ramey, 1979.b)

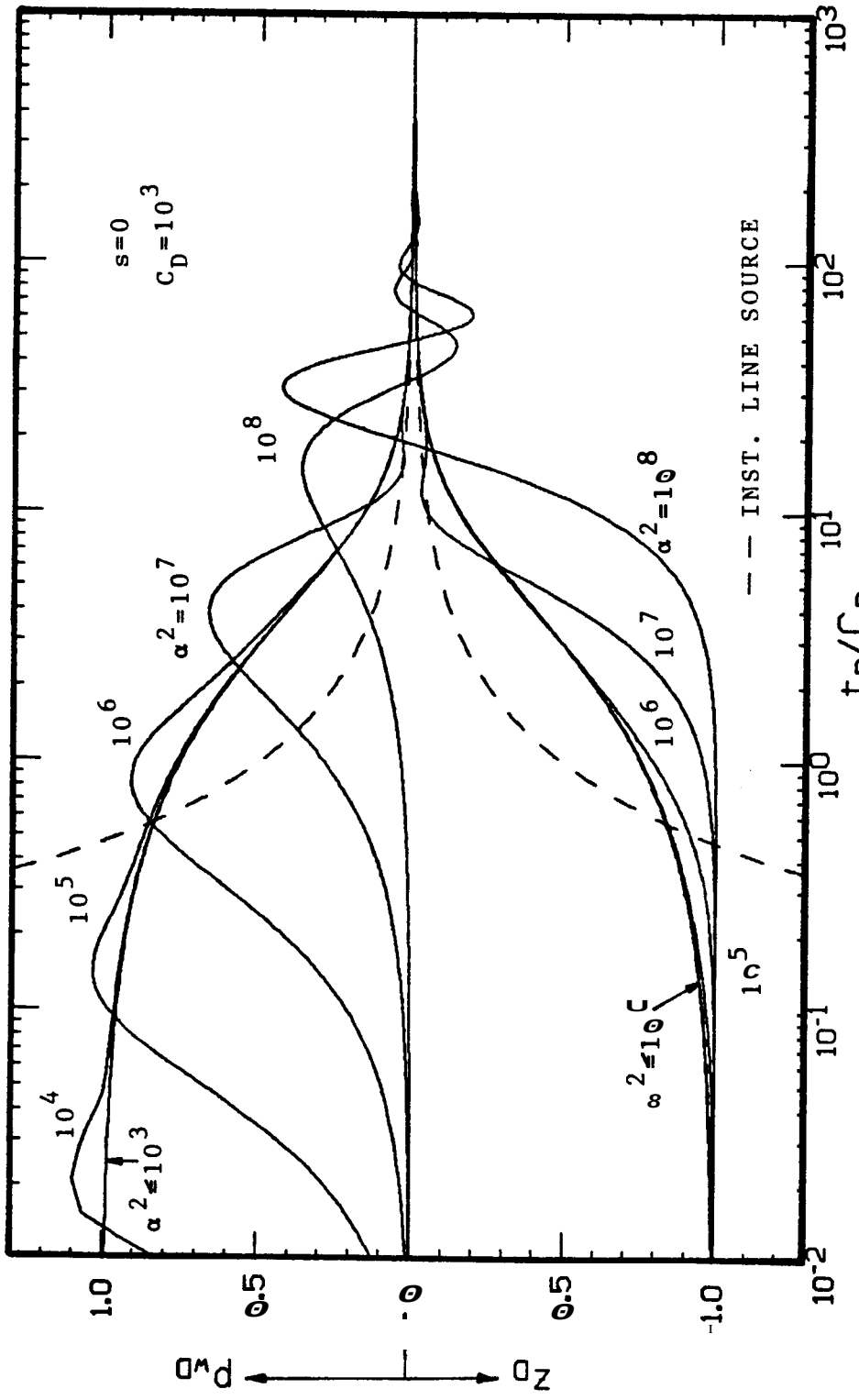

FIG. 5.5.d. SEMI-LOG GRAPH OF SLUG TEST SOLUTIONS FOR p_{wD} AND z_D VS t_D/C_D INCLUDING GRAVITATIONAL AND INERTIAL WELLBORE EFFECTS FOR DIFFERENT VALUES OF α^2 FOR A SYSTEM WITH s=0 AND $C_D=10^3$ (After Shinohara and Ramey, 1979.b)

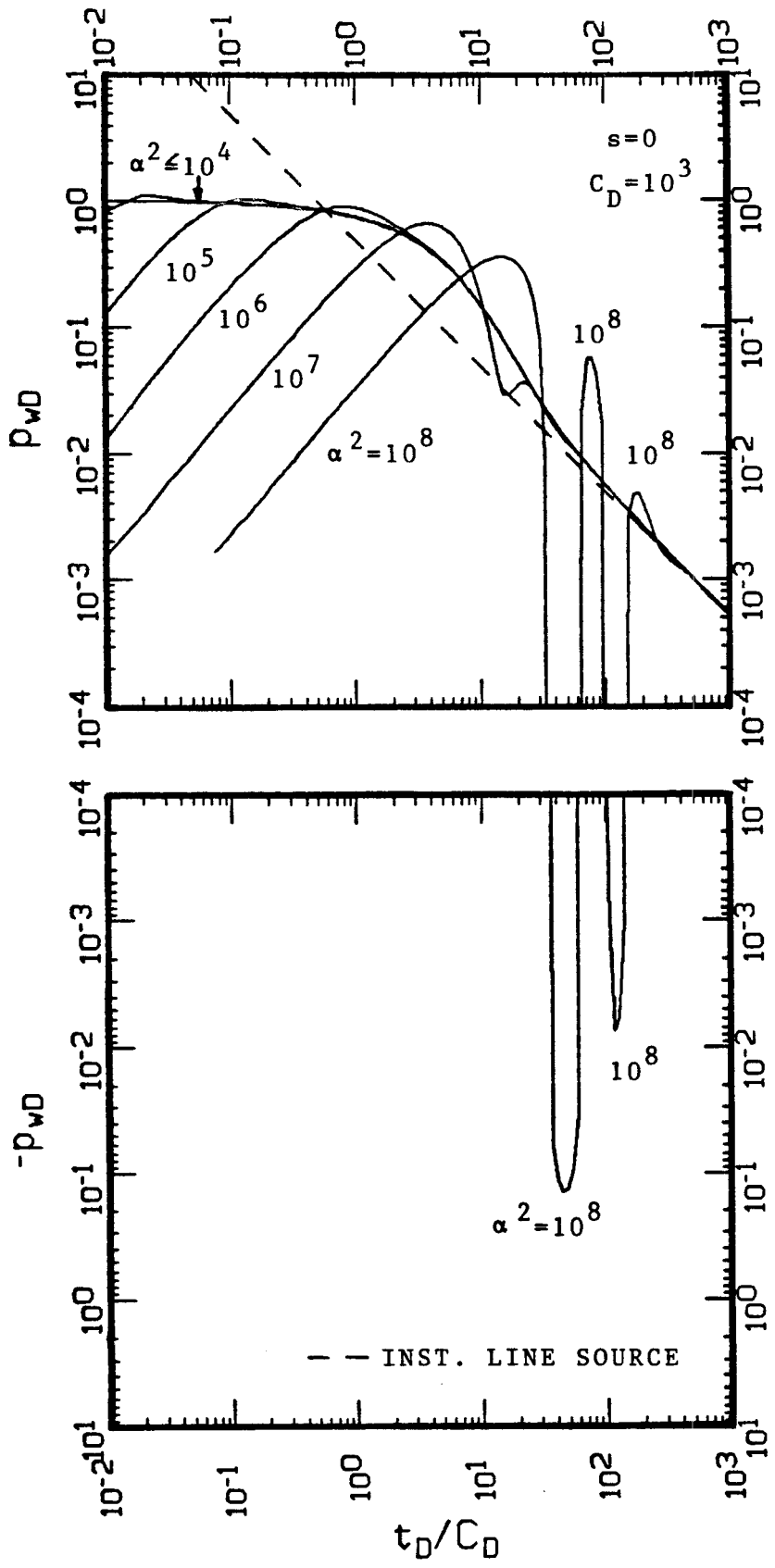

FIG. 5.5.e. LOG-LOG GRAPH OF SLUG TEST SOLUTIONS **FOR** p_{wD} VS t_D/C_D INCLUDING GRAVITATIONAL AND INERTIAL WELLBORE **EFFECTS FOR** DIFFERENT VALUES OF α^2 **FOR A SYSTEM WITH** $s=0$ AND $C_D=10^3$

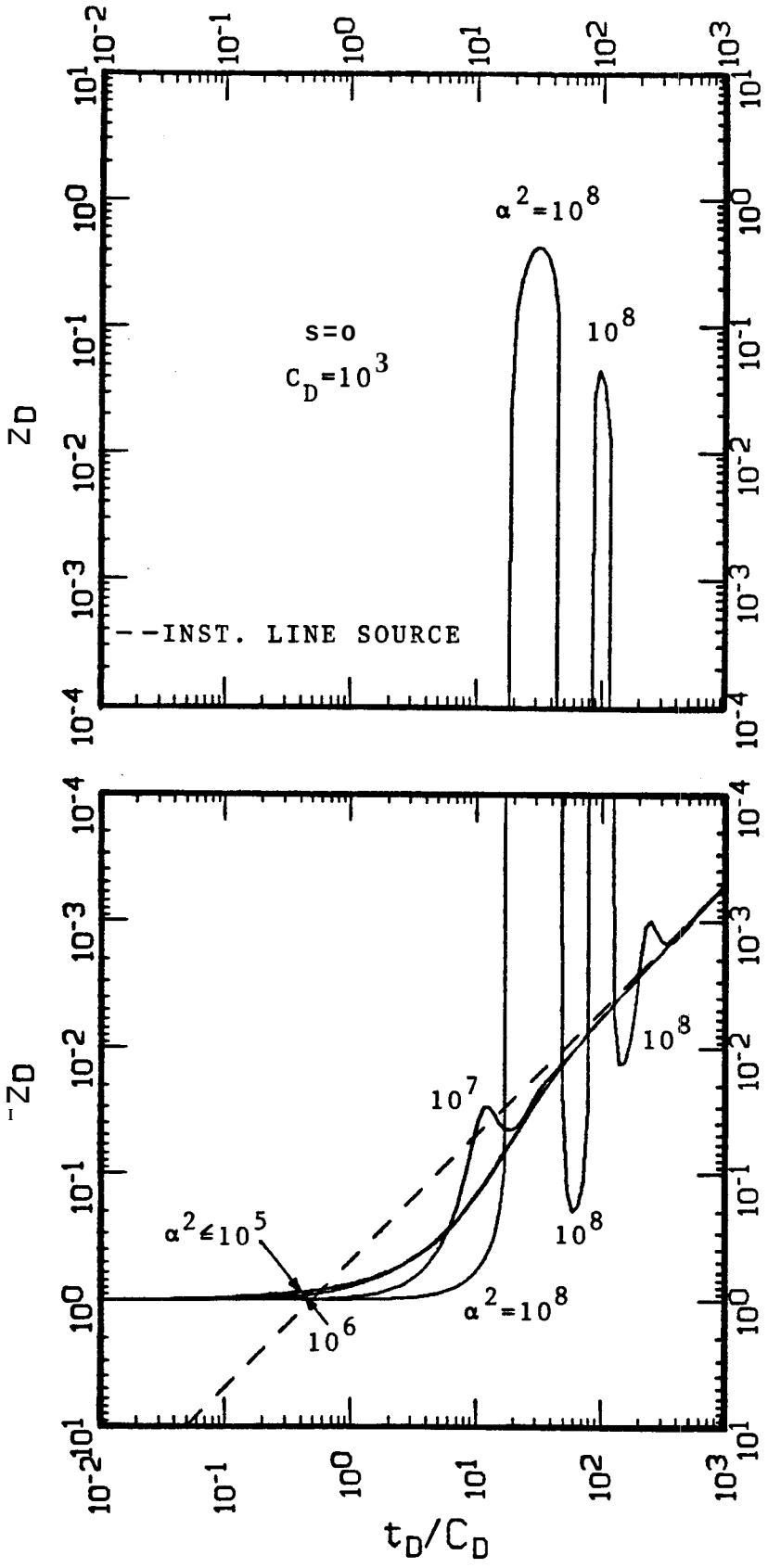

FIG. 5.5.f. LOG-LOG GRAPH OF SLUG TEST SOLUTIONS FOR z_D VS t_D/C_D INCLUDING GRAVITATIONAL *AND* INERTIAL WELLBORE EFFECTS FOR DIFFERENT VALUES OF α^2 FOR A SYSTEM WITH s=0 AND C_D=103

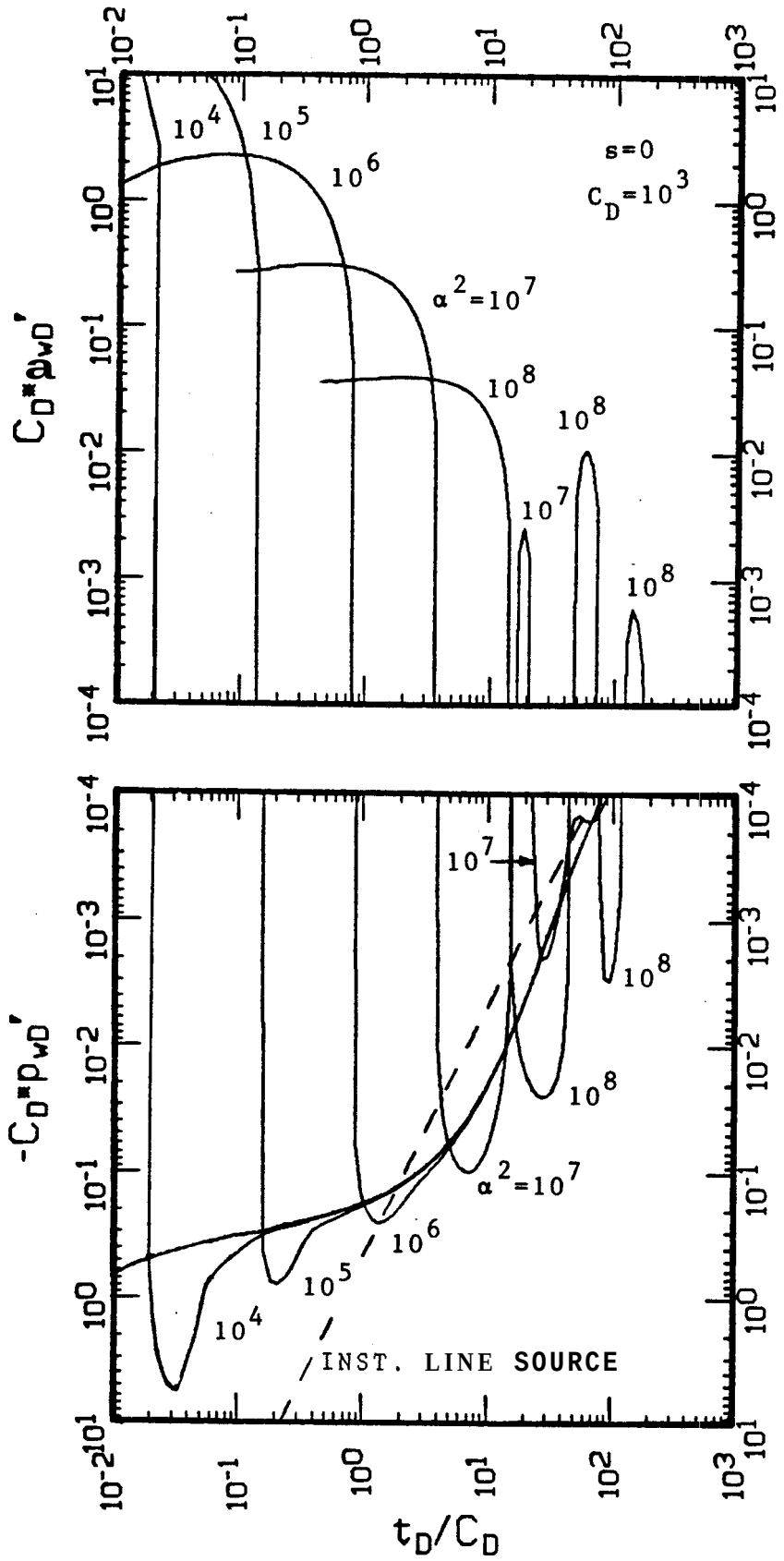

FIG. 5.5.g. LOG-LOG GRAPH OF SLUG TEST SOLUTIONS FOR p_{wD}' VS t_D/C_D INCLUDING GRAVITATIONAL *AND* INERTIAL WELLBORE EFFECTS FOR DIFFERENT VALUES OF α^2 FOR A SYSTEM WITH $s=0$ AND $C_D=10^3$

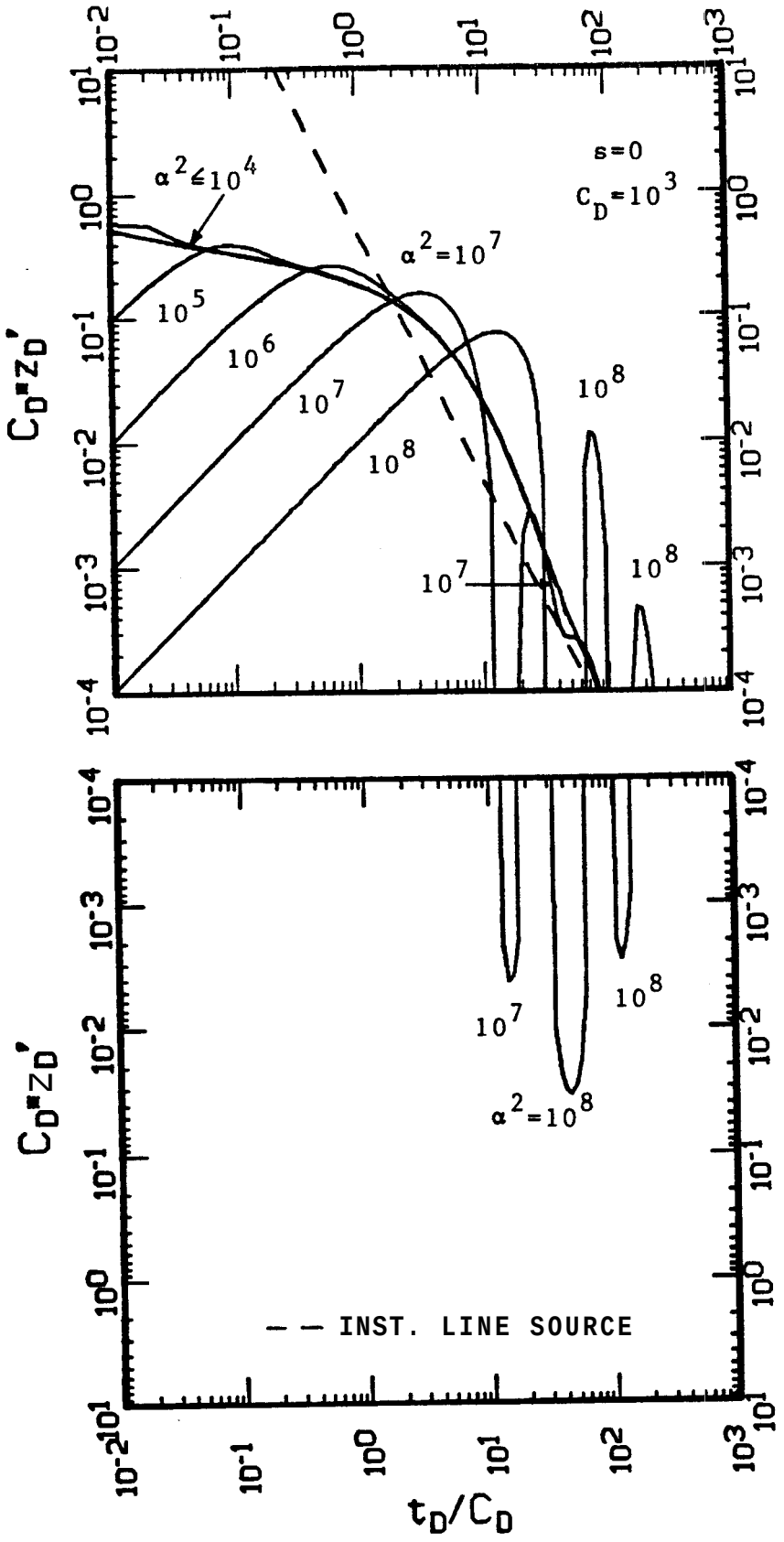

FIG. 5.5.h. LOG-LOG GRAPH OF SLUG TEST SOLUTIONS FOR z_D' VS t_D/C_D INCLUDING GRAVITATIONAL AND INERTIAL WELLBORE EFFECTS FOR DIFFERENT VALUES OF α^2 FOR A SYSTEM WITH s=0 AND $C_D=10^3$

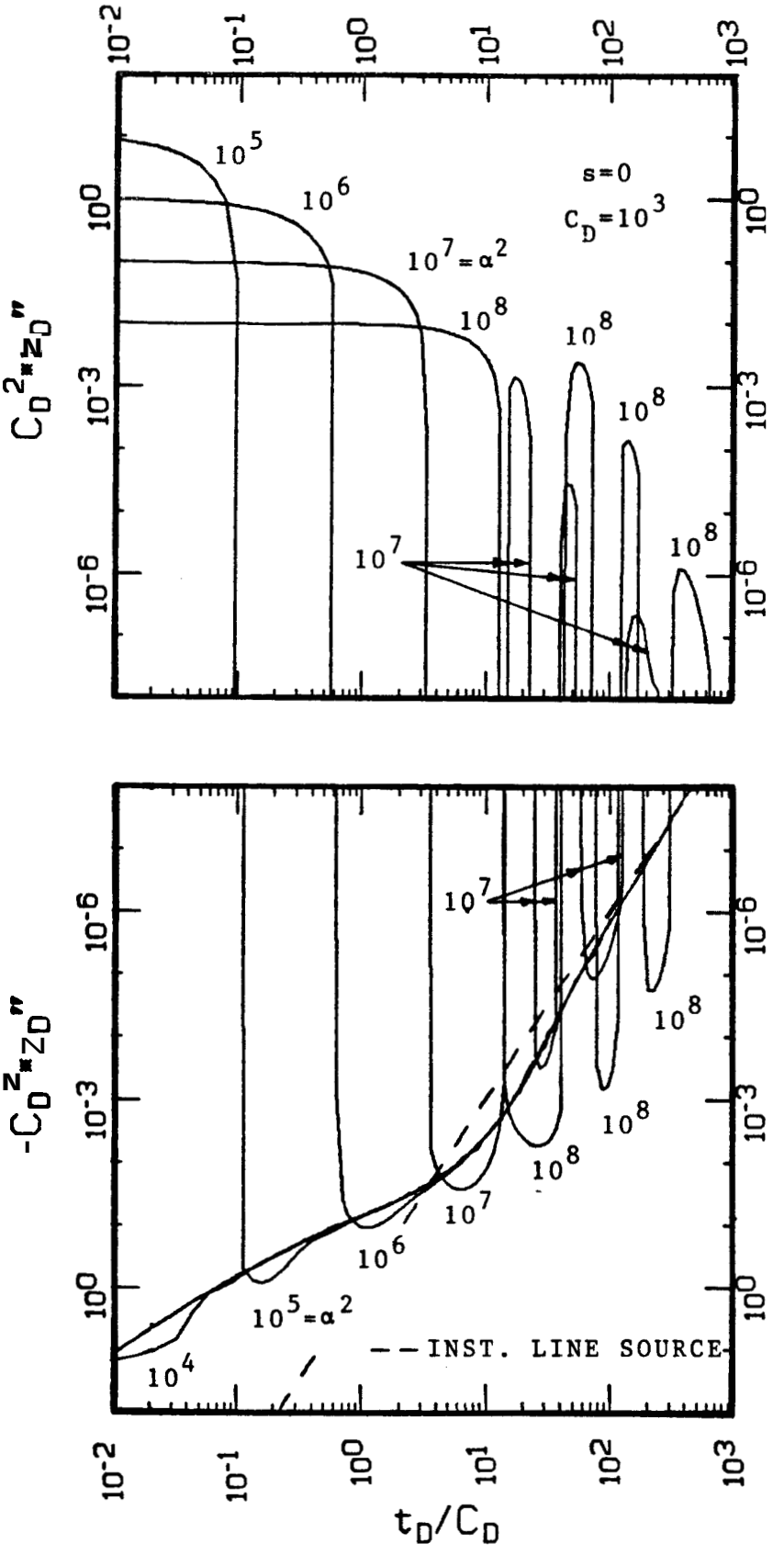

FIG. 5.5.1. LOG-LOG GRAPH OF SLUG TEST SOLUTIONS FOR z_D'' VS t_D/C_D INCLUDING GRAVITATIONAL *AND* INERTIAL WELLBORE EFFECTS FOR DIFFERENT VALUES OF α^2 FOR A SYSTEM WITH s=0 AND C_D=103

and z_D neglecting and including wellbore inertial effects agree only in the second half of the range of interest of t_D. Systems with $\alpha^2 \geq 10^7$ exhibit pressure and liquid level oscillations, and completely differ from the solution for negligible wellbore inertial effects, $\alpha^2=0$.

Figure 5.5.g shows the rate of change of p_{wD}, p_{wD}', and its oscillatory behavior for systems with $\alpha^2 \geq 10^7$. Figure 5.5.h illustrates the behavior of the corresponding flow rate during a slug test or drillstem test. This figure shows that flow rate increases linearly at early times, reaches a maximum value and then either follows the solution for negligible wellbore inertial effects or oscillates about it. Comparison of Figs. 5.5.g and 5.5.h leads to the conclusion that the rate of change in presure and the flow rate are not similar at early times but, at later times, systems with values of $\alpha^2 \leq 10^6$ follow the solution for $\alpha^2=0$.

Figure 5.5.i presents the behavior of z_D'' and shows that the value of α^2 controls both magnitude and duration of a constant initial acceleration. The larger the value of α, the smaller the initial value of z_D''. These effects of α are reflected in the name proposed for this parameter, dimensionless initial deaccelerating factor.

Observation of the solutions including inertia but neglecting friction, shown in Figs. 5.5.a - 5.5.i, indicate four distict features in the behavior of p_{wD}: (1) an early pressure drop from initial reservoir pressure ($p_{wD}=0$) towards hydrostatic cushion pressure plus atmospheric pressure ($p_{wD}=1$), (2) an overshoot in pressure drop ($p_{wD}>1$), (3) a later pressure recovery from hydrostatic cushion pressure ($p_{wD}=1$) towards initial reservoir pressure ($p_{wD}=0$), and (4) convergent oscillations of p_{wD} with alternating sign about the initial reservoir pressure ($p_{wD}=0$).

For small values of α^2, these solutions show a large overshoot in pressure drop at early times, follow the solution for no inertia ($\alpha^2=0$) during the pressure recovery, and do not exhibit oscillations at late times. On the other hand, for large values of α^2, no overshoot is observed, oscillations may occur, and these solutions follow the case

with no inertia ($\alpha^2=0$) only at late times.

The values of α^2 for which these features are apparent depend on C_D and to a lesser degree on s, as detemined by Shinohara (1980). Results presented by Shinohara (1980) for the conditions under which wellbore inertial effects are negligible are shown as solid lines in Fig. 5.6.a. In this figure, α_I is the value of a below which the behavior of p_{wD} is essentially the same as the behavior of p_{wD} for a system with no inertia ($\alpha^2=0$). Those results were analyzed in the present study and the following approximation was found to reflect the strong dependency of α_I on C_D and the weak effect of s on α_I, by stating that wellbore inertial effects are negligible for:

$$a^2 < \alpha_I^2 = \frac{C_D^2}{10} e^{60\frac{4s}{}} \quad \ldots (5.31)$$

This approximation for α_I results in parallel straight lines with slope of 2 and intercept at $C_D=1$ of $0.029[s]-1$, as shown with special symbols in Fig. 5.6.a for different values of C_D with s as parameter. Considering the difficulty of determining the values of α_I by visual inspection of solutions obtained for different values of a for given combinations of s and C_D, the previous approximation is acceptable for all values of C_D when $s>5$ and also for values of $C_D>10^3$ when $s>0$.

Similarly, from analysis of results presented by Shinohara (1980), shown in Fig. 5.6.b as solids lines, the following approximation is proposed to estimate conditions under which a system will exhibit oscillations of p_{wD} or z_D:

$$a^2 > \alpha_O^2 = 20\, C_D^2\, e^{60\frac{4s}{}} \quad \ldots (5.32)$$

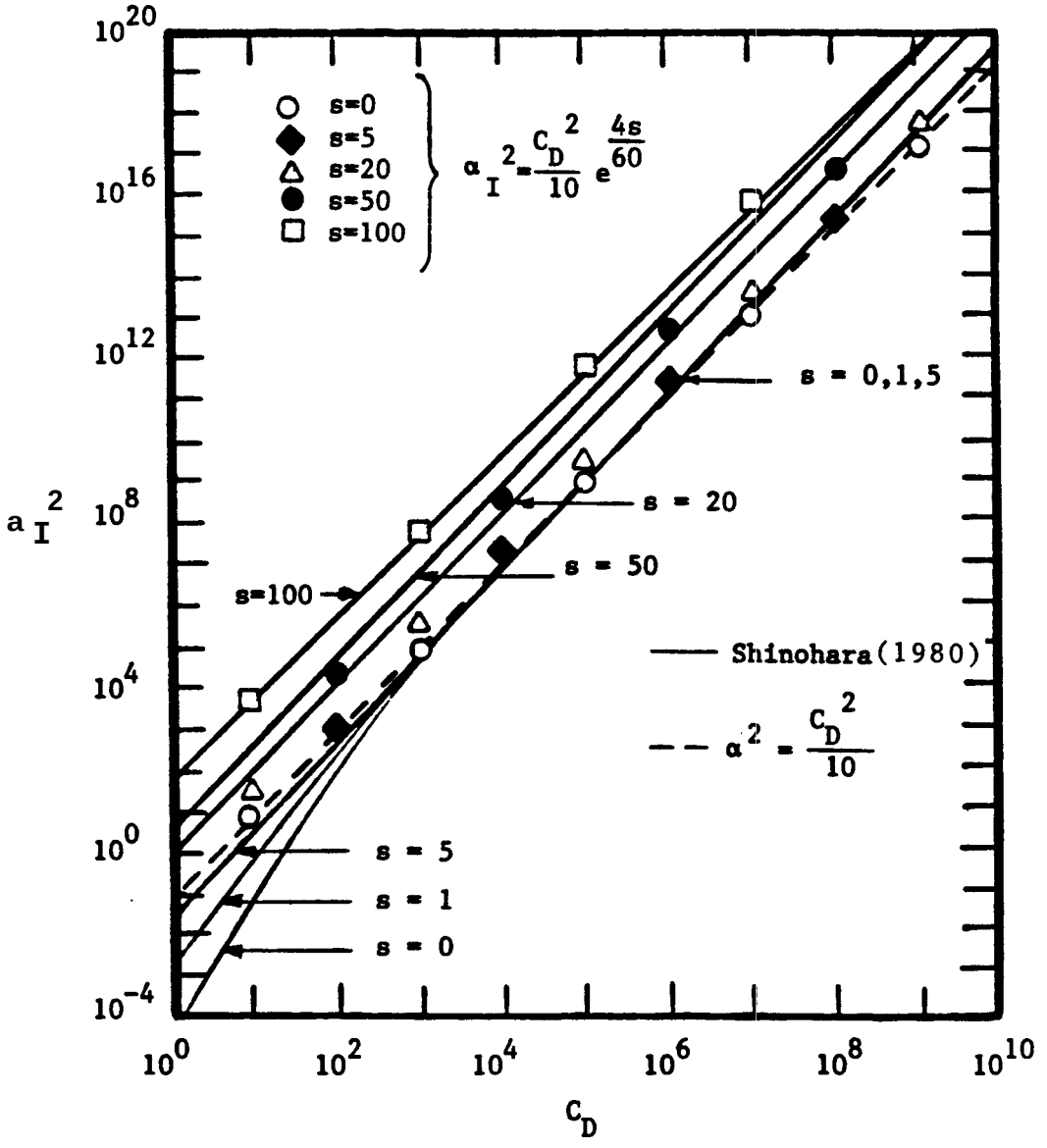

FIG. 5.6.a. LOG-LOG GRAPH OF α_I^2, VALUE OF α^2 BELOW WHICH INERTIAL WELLBORE EFFECTS ARE NEGLIGIBLE ON SLUG TEST SOLUTIONS, VS C_D FOR DIFFERENT VALUES OF s

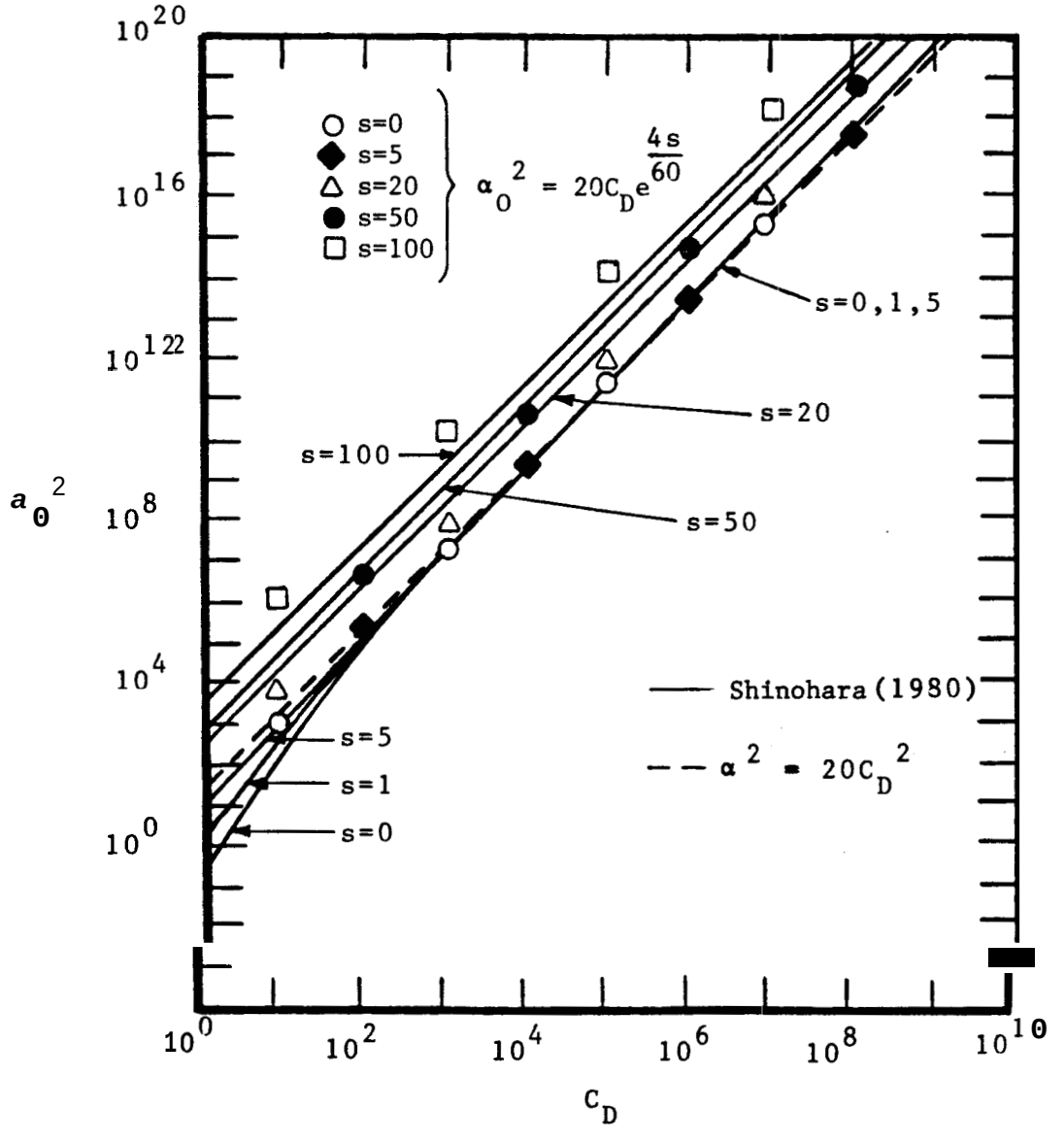

PIG. 5.6.b. LOG-LOG GRAPH OF α_0^2, VALUE OF α^2 ABOVE WHICH SLUG TEST SOLUTIONS EXHIBIT OSCILLATIONS, VS C_D FOR DIFFERENT VALUES OF s

where α_O is the value of a above which the behavior of p_{wD} and z_D will exhibit oscillations about the eventual final value of zero. The previous approximation results in parallel straight lines with slope of 2 and intercept at C_D=1 of 0.029[s]+1.3, as shown with special symbols in Fig. 5.6.b for different values of C_D with s as parameter.

Results presented by Shinohara and Ramey (1979.b) indicate that for a given value of *a*, the larger the value of C_D, the earlier the pressure drop, the greater the pressure drop overshoot, and the later the pressure recovery. Also, the larger the value of s, the earlier the pressure drop and the later the pressure recovery, but the lower the pressure drop overshoot. That is, except for the difference in the pressure overshoot, C_D and s affect the test response in the same direction. However, the effect of s on α_I and α_O is relatively small in comparison to the effect of C_D. As shown in Fig. 5.6.a and Fig. 5.6.b, the effect of s on α_I and α_O can be considered negligible in the range of values of $0 \leq s \leq 5$ for $C_D \geq 10^3$.

From these approximations, and according to the definition of a and C_D, given by Eqs. 3.47 and 3.50, inertial wellbore effects can be considered negligible from Eq. 5.31, for:

$$a^2 < \alpha_I^2 = \frac{C_D^2}{10} \quad , \text{for } 0 \leq s \leq 5,\ C_D \geq 10^3 \qquad \ldots (5.33)$$

or:

$$\sqrt{\frac{L}{g}} \left[\frac{\rho g}{r_P^2}\right] \left[\frac{kh}{\mu}\right] < \frac{1}{2\sqrt{10}} \quad , \text{for } 0 \leq s \leq 5,\ C_D \geq 10^3 \qquad \ldots (5.34)$$

and, from Eq. 5.32, inertial wellbore effects can cause oscillations for:

$$\alpha^2 > \alpha_0^2 \simeq 20\, C_D^2 \quad , \; 0<s<5, \; C_D>10^3 \qquad \ldots (5.35)$$

or:

$$\sqrt{\frac{L}{g}}\sqrt{\left[\frac{\rho g}{r_p^2}\right]\left[\frac{kh}{\mu}\right]} < \sqrt{5} \quad , \; 0<s<5, \; C_D>10^3 \qquad \ldots (5.36)$$

Shinohara (1980) presented approximate type curves for p_{wD} and z_D vs t_D/C_D with $\alpha^2 e^{4s}$ as a correlation parameter for different values of $C_D e^{2s}$. As pointed out by that author, selecting a particular type curve for a practical application is difficult and not unique because of the similar shapes of the type curves for different values of $C_D e^{2s}$. The following alternate approach based on Eqs. 5.30.a and 5.31.a is proposed to obtain a single type curve for slug test analysis considering gravitational and inertial effects.

Figures 5.7.a - 5.7.c are Cartesian graphs of p_{wD} vs t_D/C_D for practical values of C_D and corresponding values of $a^2=0$, $a^2 = C_D^2/10$, $a^2 = C_D^2$, $a^2 = 20\, C_D^2$. These figures show that bottomhole pressure drop from initial reservoir pressure to cushion pressure, which corresponds to the early-time behavior of p_{wD} from 0 to 1, can not be considered to happen instantaneously for relatively large values of dimensionless deaccelerating factor, a. These values of a depend on the range of time of analysis. From Fig. 5.7.a, values of $C_D^2/10<\alpha^2<C_D^2$ will exhibit a measurable delay for the pressure drop to occur in the range $0<t_D/C_D<1$. More practical ranges for times of interest in drillstem test analysis are shown in Figs. 5.7.b and 5.7.c. These figures indicate that only systems with $a^2>20C_D^2$ will show an appreciable delay.

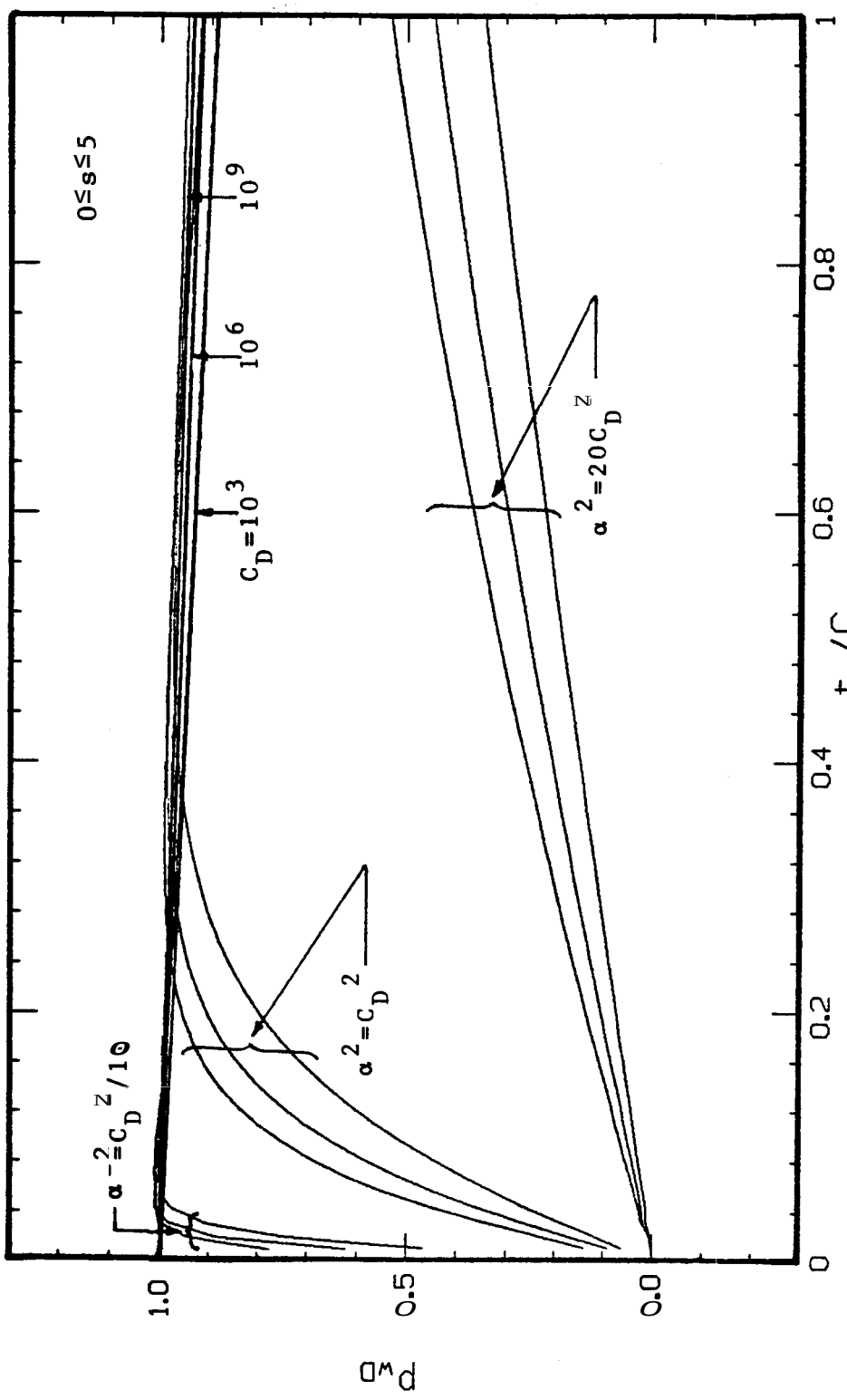

FIG. 5.7.a. CARTESIAN GRAPH OF SLUG TEST SOLUTIONS FOR p_{wD} VS t_D/C_D INCLUDING GRAVITATIONAL AND INERTIAL WELLBORE EFFECTS FOR $C_D > 10^3$, $0 < s < 5$, AND $\varepsilon_3/C_D < 1$

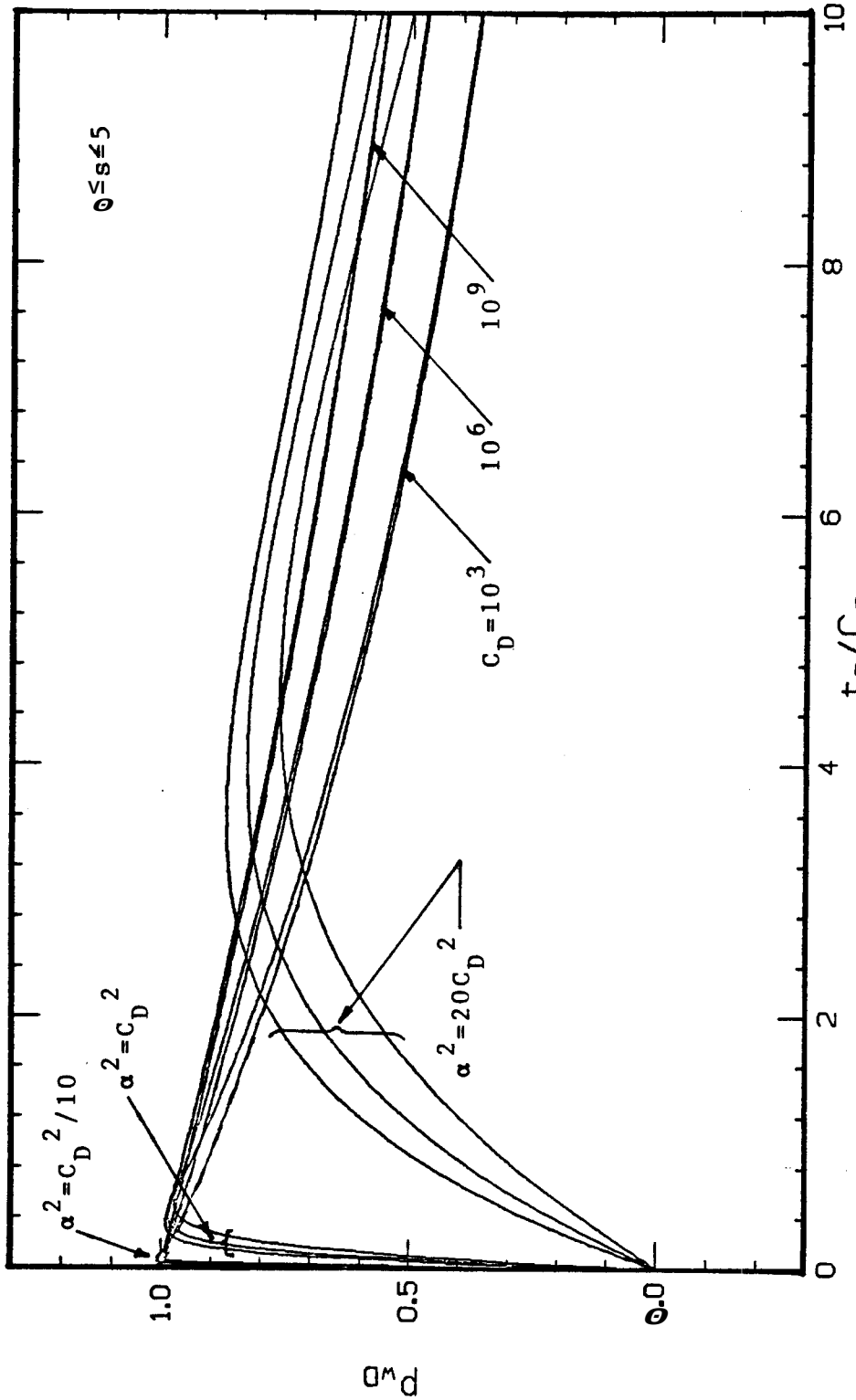

FIG. 5.7.b. CARTESIAN GRAPH OF SLUG TEST SOLUTIONS FOR p_{wD} VS t_D/C_D INCLUDING GRAVITATIONAL AND INERTIAL WELLBORE EFFECTS FOR $C_D > 10^3$, $0 < s < 5$, AND $t_D/C_D < 10$

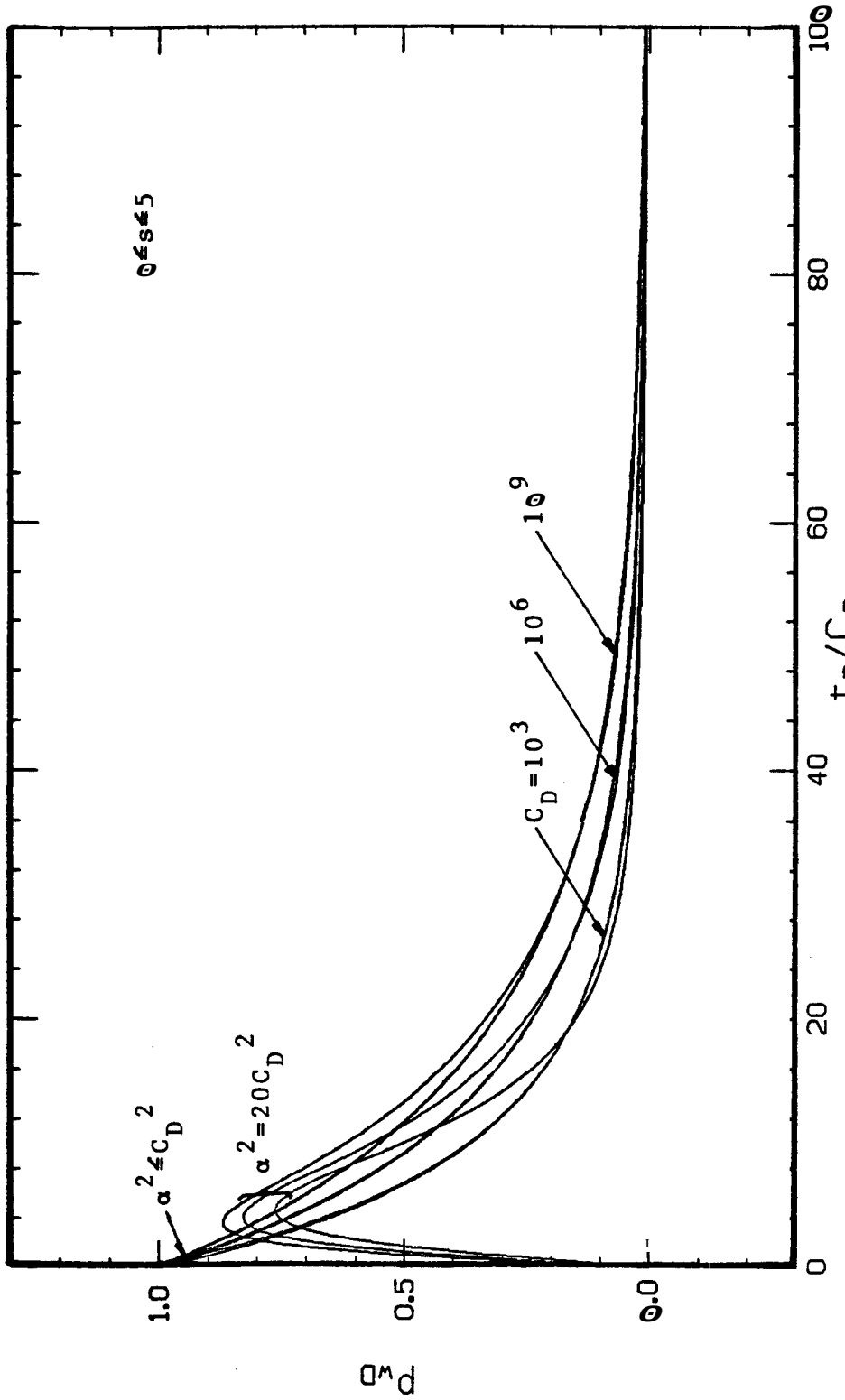

FIG. 5.7.c. CARTESIAN GRAPH OF SLUG TEST SOLUTIONS FOR p_{wD} VS t_D/C_D INCLUDING GRAVITATIONAL AND INERTIAL WELLBORE EFFECTS FOR $C_D \geq 10^3$, $0 \leq s \leq 5$, AND $t_D/C_D \leq 100$

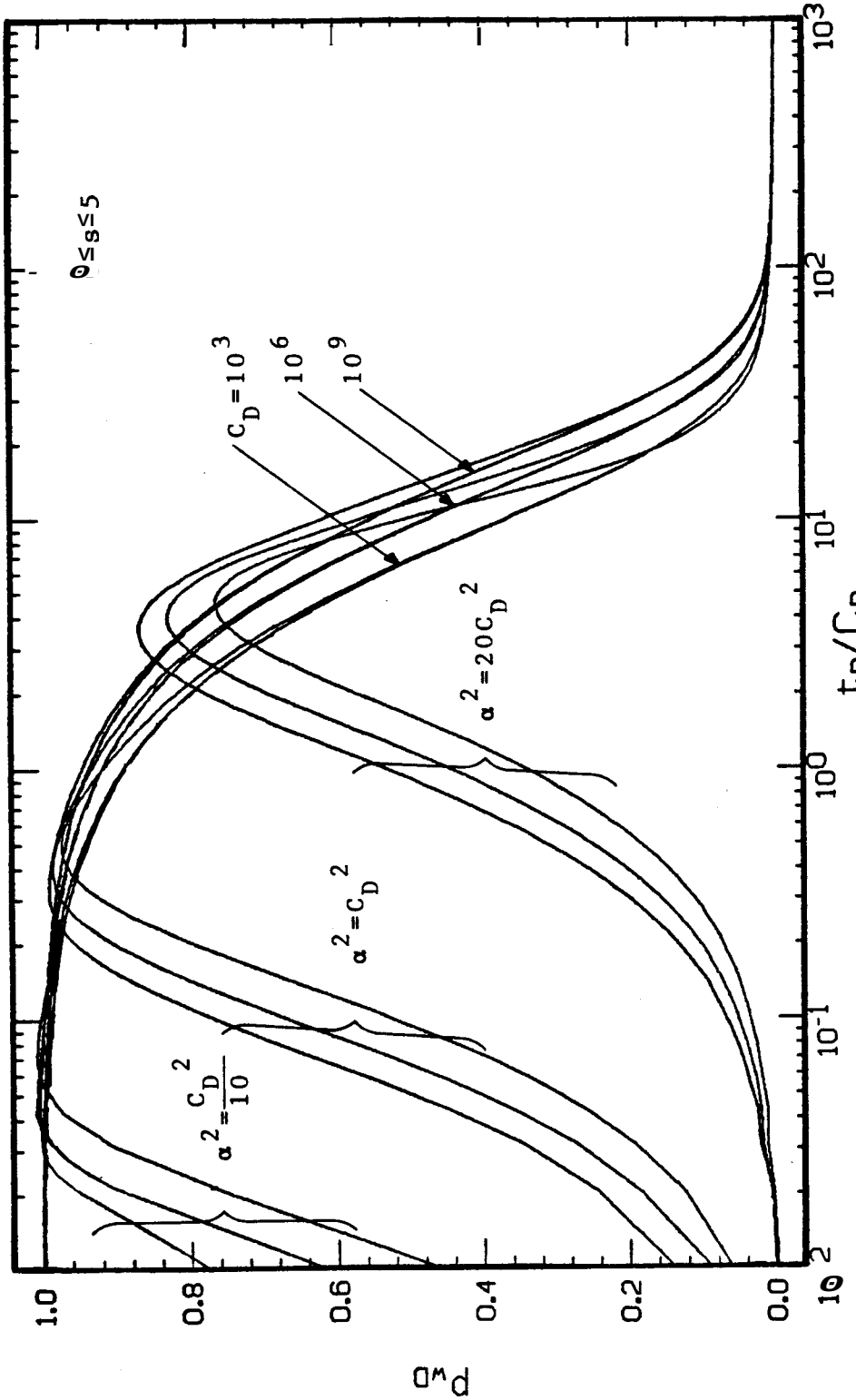

FIG. 5.7.d. SEMI-LOG TYPE CURVE FOR SLUG TEST ANALYSIS OF P_{wD} VS t_D/C_D INCLUDING GRAVITATIONAL AND INERTIAL WELLBORE EFFECTS FOR PRACTICAL VALUES OF C_D

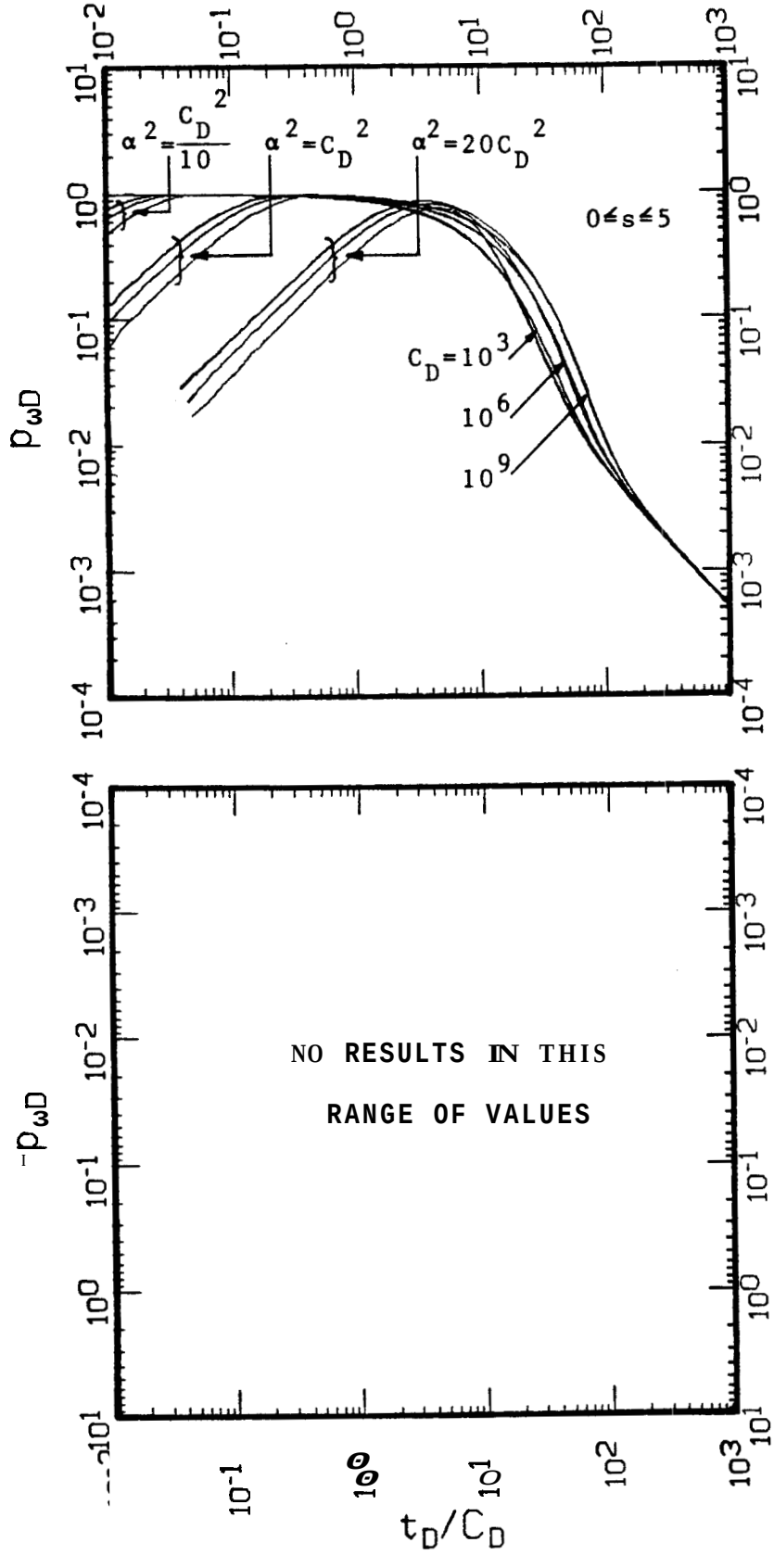

FIG. 5.7.e, LOG-LOG TYPE CURVE FOR SLUG TEST ANALYSIS OF p_{wD} VS t_D/C_D INCLUDING GRAVITATIONAL AND INERTIAL WELLBORE EFFECTS FOR PRACTICAL VALUES OF C_D

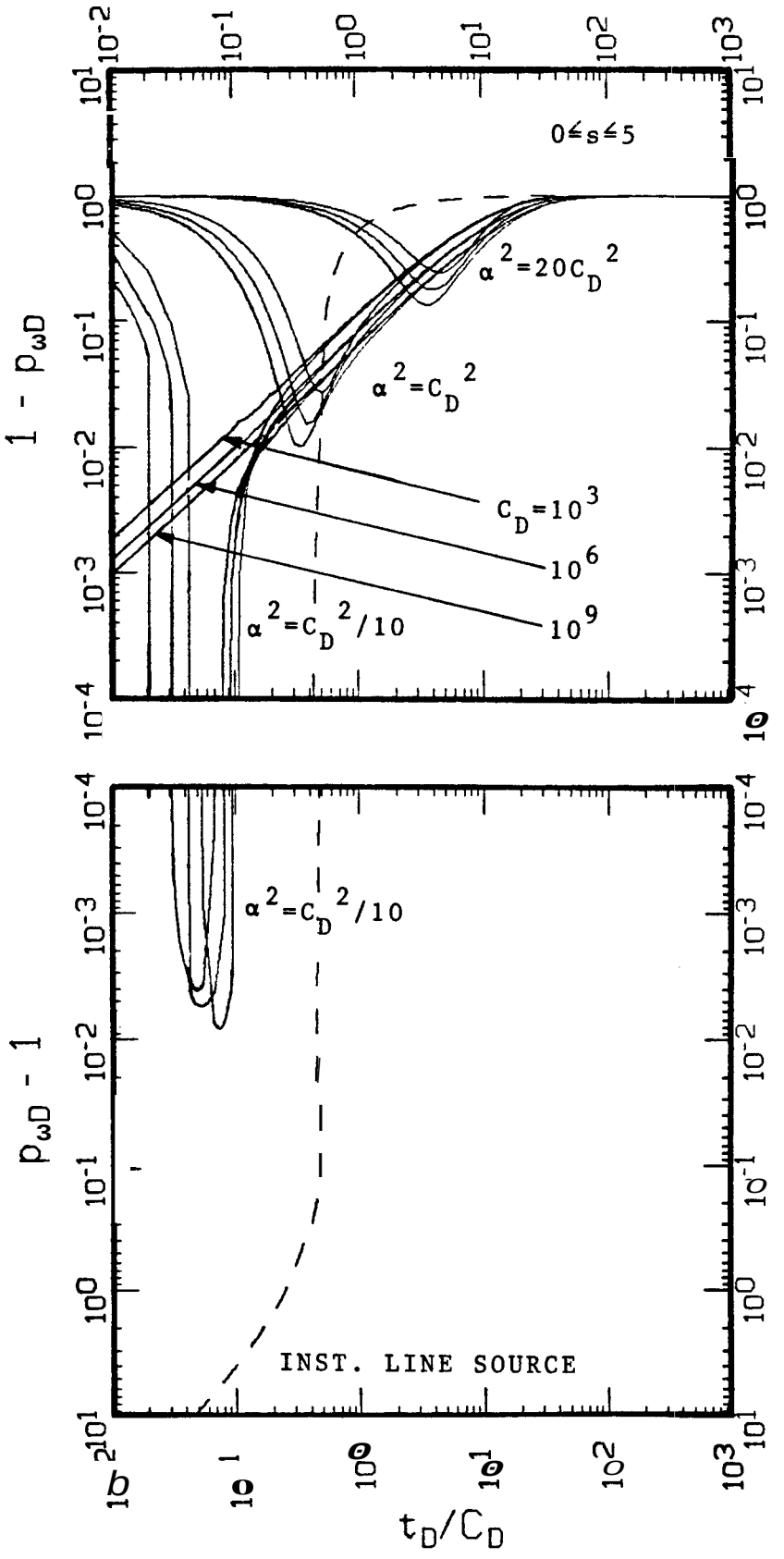

FIG. 5.7.f. LOG-LOG TYPE CURVE FOR SLUG TEST ANALYSIS OF $1-p_{wD}$ VS t_D/C_D INCLUDING GRAVITATIONAL AND INERTIAL WELLBORE EFFECTS FOR PRACTICAL VALUES OF C_D

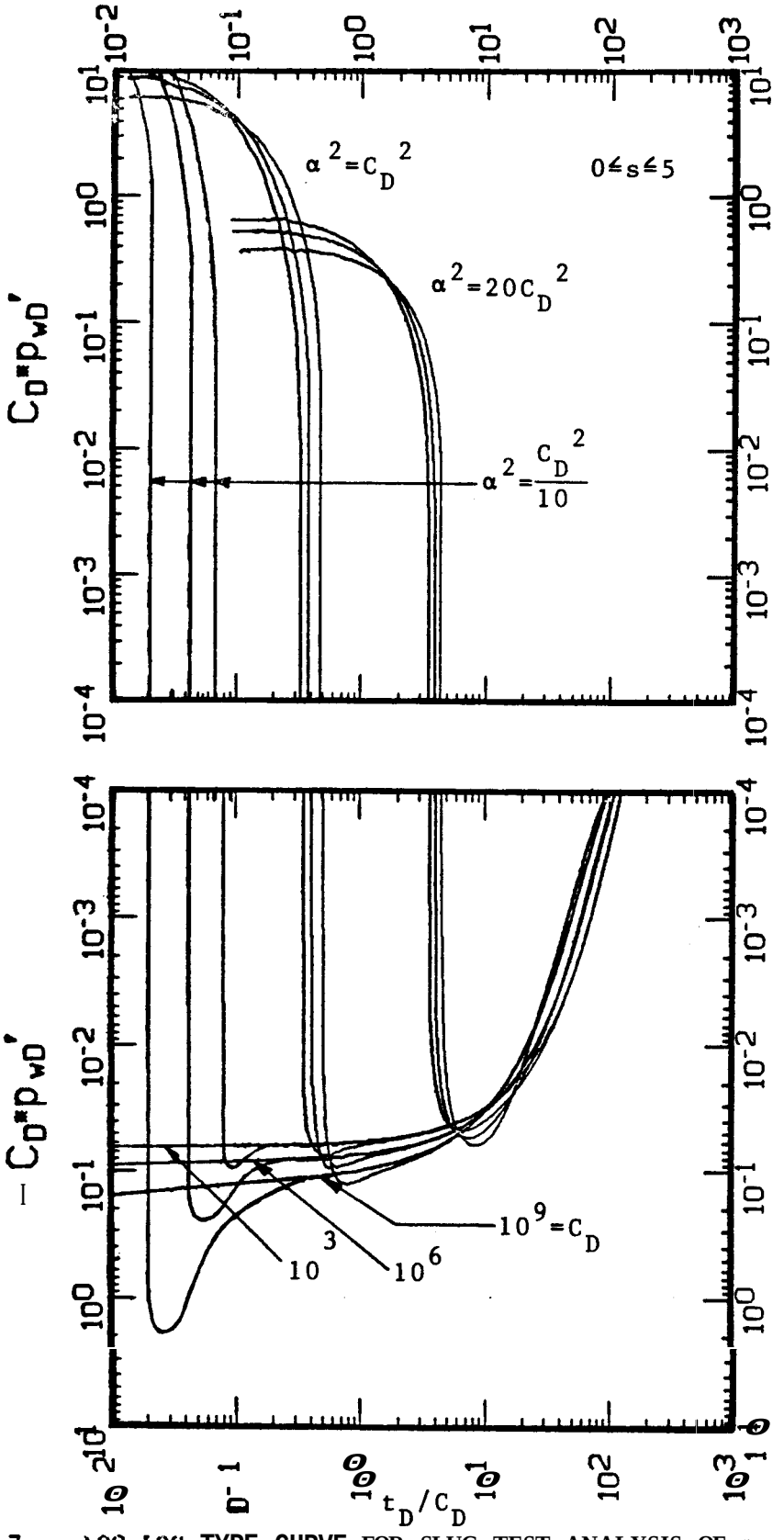

FIG. 5.7.g. LOG-LOG TYPE CURVE FOR SLUG TEST ANALYSIS OF p_{wD}' VS t_D/C_D INCLUDING GRAVITATIONAL AND INERTIAL WELLBORE EFFECTS FOR PRACTICAL VALUES OF C_D

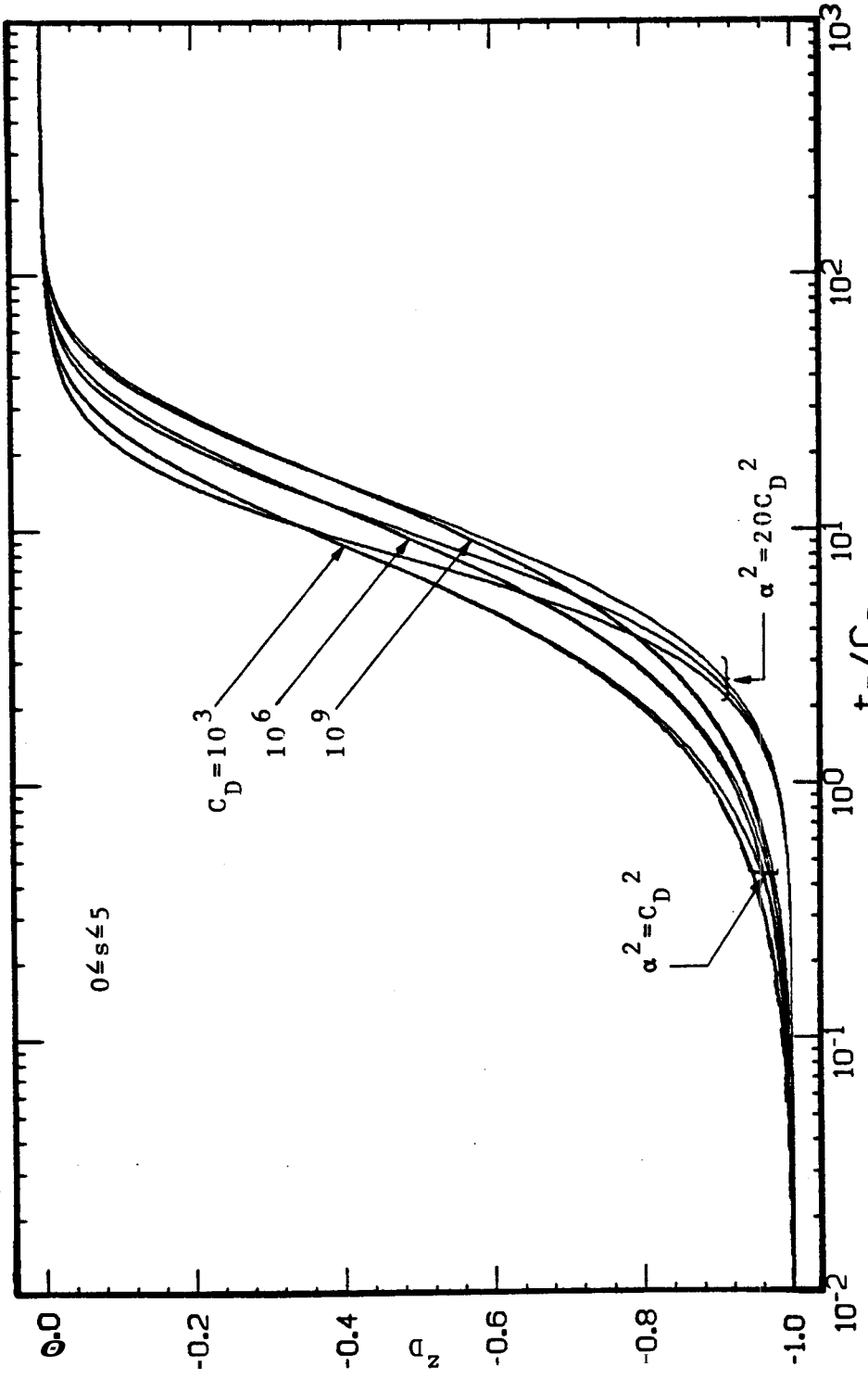

FIG. 5.7.h. SEMI-LOG TYPE CURVE FOR SLUG TEST ANALYSIS OF z_D VS t_D/C_D INCLUDING GRAVITATIONAL AND INERTIAL WELLBORE EFFECTS FOR PRACTICAL VALUES OF C_D

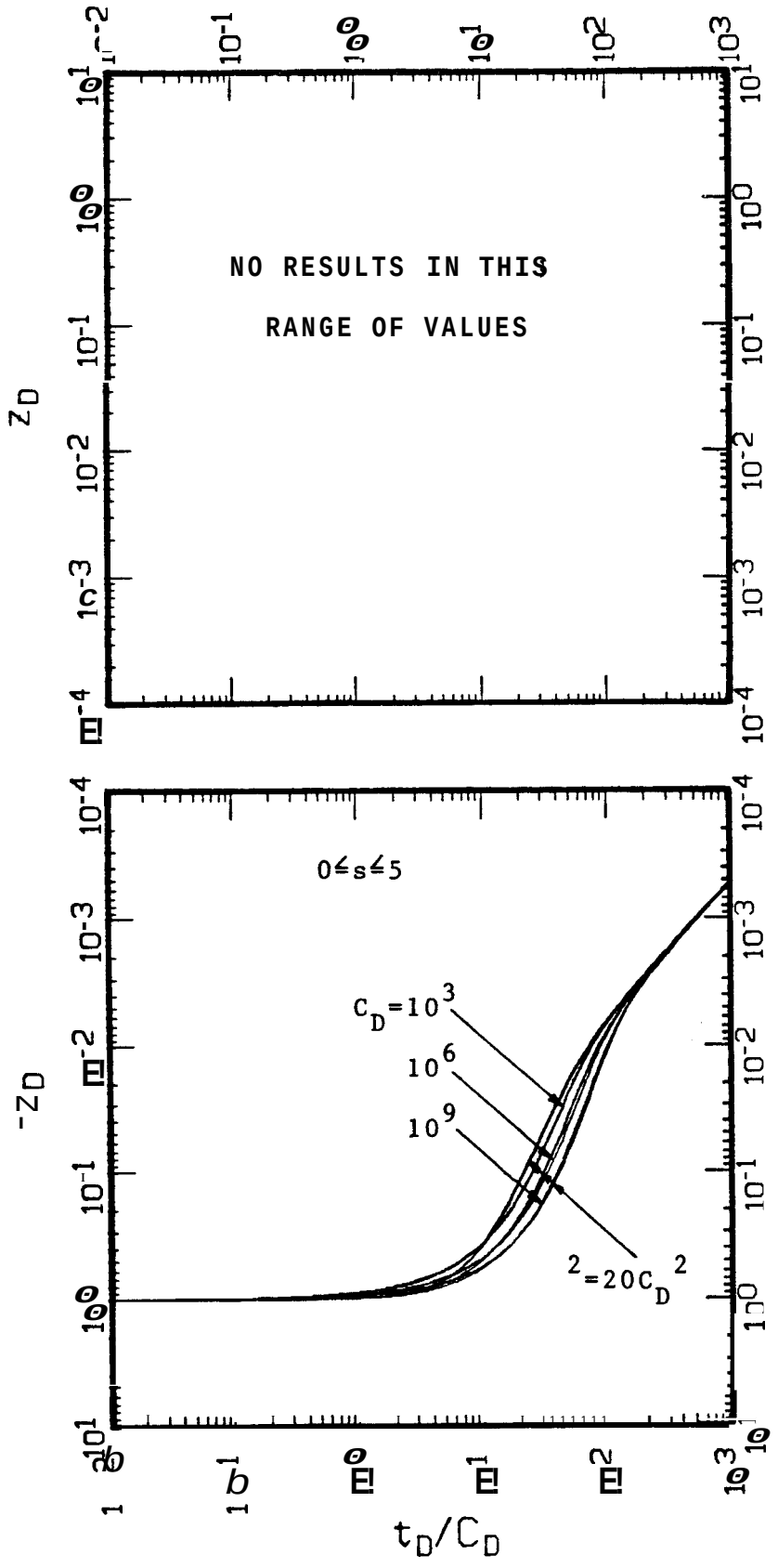

FIG. 5.7.1. LOG-LOG TYPE CURVE FOR SLUG TEST ANALYSIS OF z_D VS t_D/C_D INCLUDING GRAVITATIONAL AND INERTIAL WELLBORE EFFECTS FOR PRACTICAL VALUES OF C_D

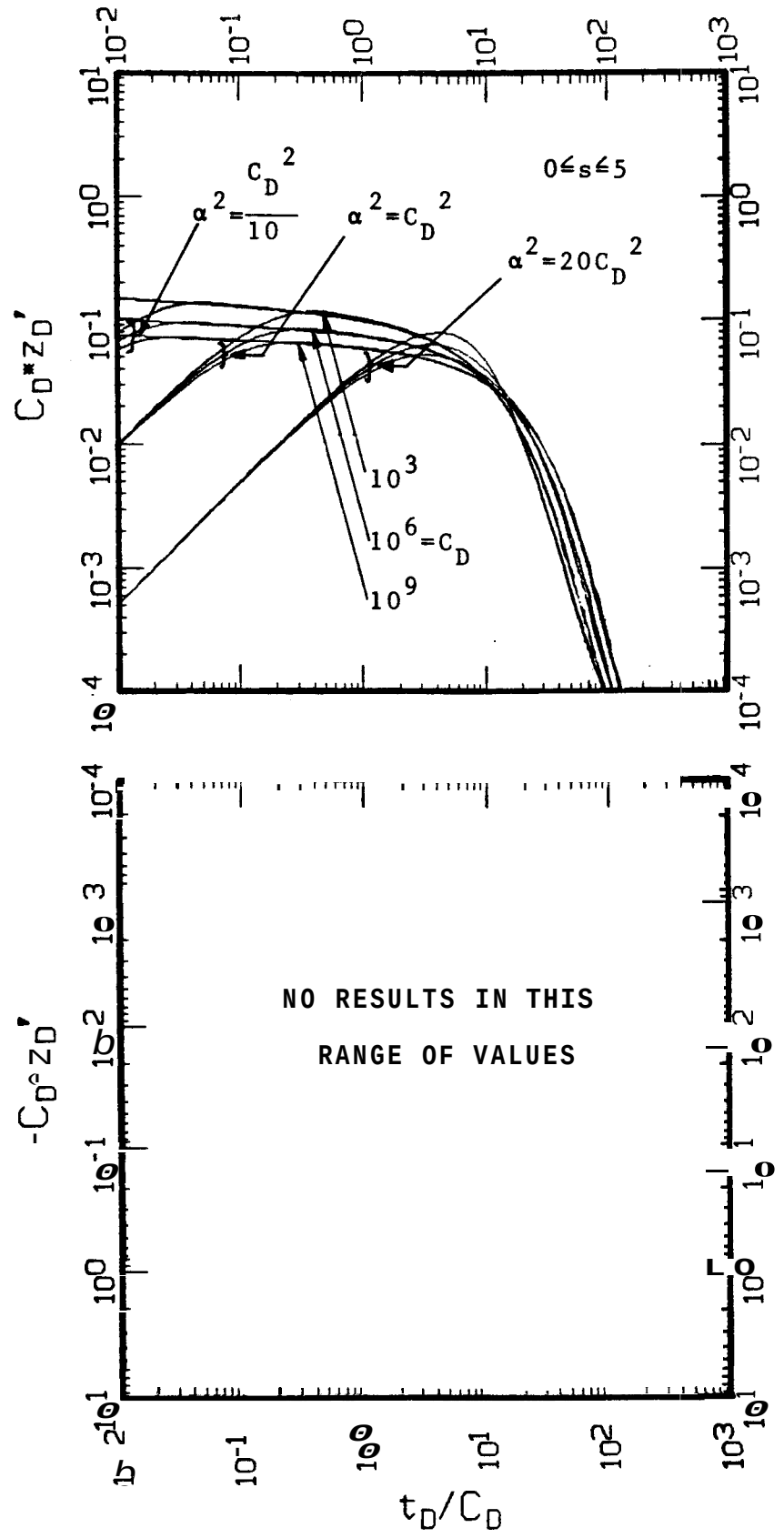

FIG. 5.7.j. LOG-LOG TYPE CURVE FOR SLUG TEST ANALYSIS OF $z_D{}'$ VS t_D/C_D INCLUDING GRAVITATIONAL AND INERTIAL WELLBORE EFFECTS FOR PRACTICAL VALUES OF C_D

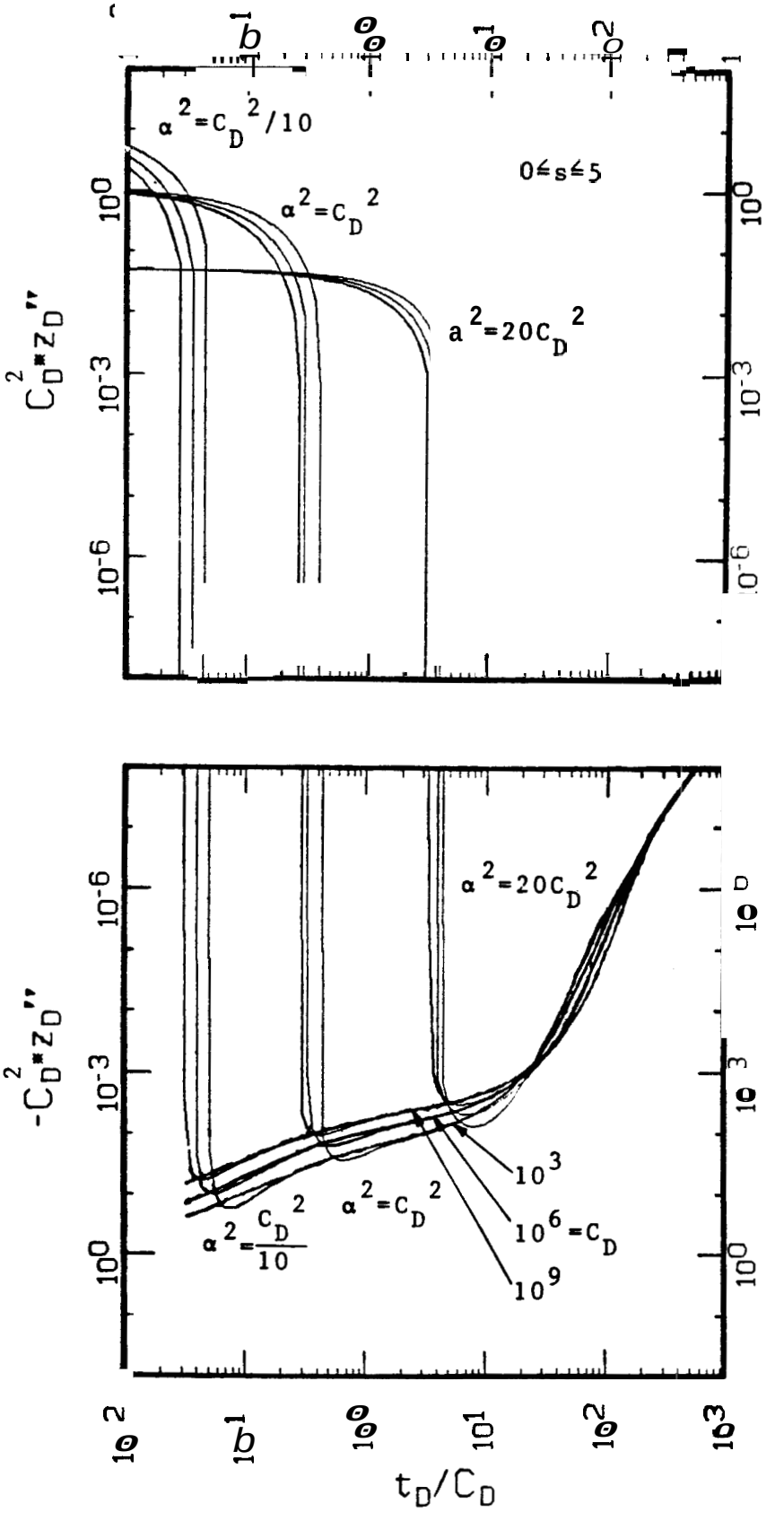

PIG. 5.7.k. LOG-LOG TYPE CURVE FOR SLUG TEST ANALYSIS OF z_D^* VS t_D/C_D INCLUDING GRAVITATIONAL AND INERTIAL WELLBORE EFFECTS FOR PRACTICAL VALUES OF C_D

Figure 5.7.d is a semi-log type curve for p_{wD}. Figs. 5.7.e and 5.7.f are log-log type curves of p_{wD} and $[1-p_{wD}]$ vs t_D/C_D, respectively. Fig. 5.7.g shows the behavior of $C_D p_{wD}'$. Figs. 5.7.h - 5.7.i are the corresponding type curves for z_D. And Figs. 5.7.j and 5.7.k correspond to the solutions for $C_D z_D'$ and $C_D{}^2 z_D''$ vs t_D/C_D, respectively.

Although these type curves were generated for s=5, they can be used for other values of $0<s<5$, because they correspond to the average behavior shown in Figs. 5.6.a and 5.6.b.

This concludes the review of previous solutions. New solutions will be presented and discussed in the following sections of this study.

5.2 Solutions for Laminar Friction

A special case of wellbore Eq. 3.39, in which frictional effects are taken into account, is obtained in this section by assuming friction losses for laminar flow. The resulting problem is linear and can be solved with the semi-analytical method using Laplace transformation presented in Section 4.1. These solutions depend cn a group of parameters called dimensionless laminar friction factor and denoted by β in this study. The effect of β on the flow phenomena during a slug test or drillstem test is analyzed in this section.

5.2.1 Special Wellbore Equation

Consider the following simplification of wellbore Eq. 3.39 derived in the present study:

$$A_w z_D'' + B_w z_D' + C_w z_D + D_w = E_w p_{wD} \quad \ldots (5.37)$$

with:

$$A_w = a^2 \quad \ldots \quad (5.37.a)$$

$$B_w = \alpha^2 \frac{f}{4} \left| \frac{1}{r_{pDz}} z_D' \right| \quad \ldots \quad (5.37.b)$$

$$C_w = 1 \quad \ldots \quad (5.37.c)$$

$$D_w = 0 \quad \ldots \quad (5.37.d)$$

$$E_w = -1 \quad \ldots \quad (5.37.e)$$

Comparison of the definition of the coefficients in this equation and those of wellbore Eq. 3.39 indicates that the following assumptions have been adopted to obtain Eq. 5.37:

(1) negligible slug size in comparison to static liquid column length, and

(2) negligible reservoir thickness with respect to static column length.

Although the wellbore liquid column velocity term, $B_w z_D'$, in Eq. 5.37 is apparently non-linear, it can be simplified by noting that for the laminar flow regime in the wellbore pipe (Moody, 1944):

$$f = \frac{64}{Re} \quad \ldots (5.38)$$

where Re is Reynold's number, which can be expressed for the problem under consideration as follows:

$$Re = \frac{2\, r_p\, \rho}{\mu_p} \mid z' \quad \ldots (5.39)$$

where:

μ_p = average fluid viscosity in the wellbore pipe, $[ML^{-1}T^{-1}]$

Substituting the definition of r_{pDz} and z_D', given by Eqs. 3.33 and 3.35, respectively, into Eq. 5.39:

$$Re = \frac{2\,\rho}{\mu_p} \left[\frac{k}{\phi\, \mu\, c_t\, r_w^2} \right] z_0^2 \mid r_{pDz}\, z_D' \quad \ldots (5.40)$$

Substituting Eqs. 5.38 and 5.40 into Eq. 5.37:

$$\alpha^2 z_D'' + \alpha^2 \frac{^{o} \mid \overline{r_{pDz}}\, z_D' \mid}{\frac{\rho}{\mu_p} \left[\frac{k}{\phi \mu c_t r_w^2} \right] z_0^2 \mid r_{pDz} z_D' \mid} z_D' + z_D = - p_{wD} \quad \ldots (5.41)$$

Simplifying:

$$A_w\, z_D'' + B_w\, z_D' + C_w\, z_D + D_w = E_w\, p_{wD} \qquad \ldots (5.42)$$

with:

$$A_w = a^2 \qquad \ldots (5.42.a)$$

$$B_w = \alpha^2\, \beta \qquad \ldots (5.42.b)$$

$$C_w = 1 \qquad \ldots (5.42.c)$$

$$D_w = 0 \qquad \ldots (5.42.d)$$

$$E_w = -1 \qquad \ldots (5.42.e)$$

where the following dimensionless group of parameters characterizes the effect of laminar kinematic viscous friction as a liquid column moves inside a wellbore pipe:

Dimensionless Wellbore Friction Factor

$$\beta = \frac{8}{\frac{\rho}{\mu_p}\left[\frac{k}{\phi\mu c_t r_w^2}\right] r_p^2} \qquad \ldots (5.43)$$

5.2.2 Effect of B for Laminar Flow Regime

Wellbore Eq. 5.42 considering laminar friction losses is mathematically linear. A slug test or drillstem test flow problem based on this equation can be solved by using the Laplace transformation method proposed in Section 4.1.

An option in the computer program presented in Appendix E allows evaluation of solutions for p_{wD}, z_D, p_{wD}', z_D', z_D'', and $p_D(r_D)$ vs t_D with s, C_D, α, and β as input parameters.

Figures 5.8.a - 5.8.f, 5.9.a - 5.9.f, and 5.10.a - 5.10.f are graphs of the results for system with s=0, $C_D=10^3$ for different values of B for a damped case, $\alpha^2=10^4$, a critically damped case, $\alpha^2=10^6$, and an underdamped case, $\alpha^2=10^8$, respectively.

Figures 5.8.a, 5.9.a, and 5.10.a show that dimeinsionless bottomhole pressure p_{wD} decreases as laminar friction factor β increases above a characteristic value. The larger the value of β, the lower and flatter the behavior of p_{wD}. This behavior corresponds to higher bottomhole pressures, sustained longer during the test, as can be seen in the solutions for $C_D p_{wD}'$ presented in Figs. 5.8.d, 5.9.d, and 5.10.d. On the other hand, Figs. 5.8.c, 5.9.c, and 5.10.c illustrate the effect of β on the solutions for dimensionless liquid level z_D. The larger the value of B, the later the response of wellbore liquid level.

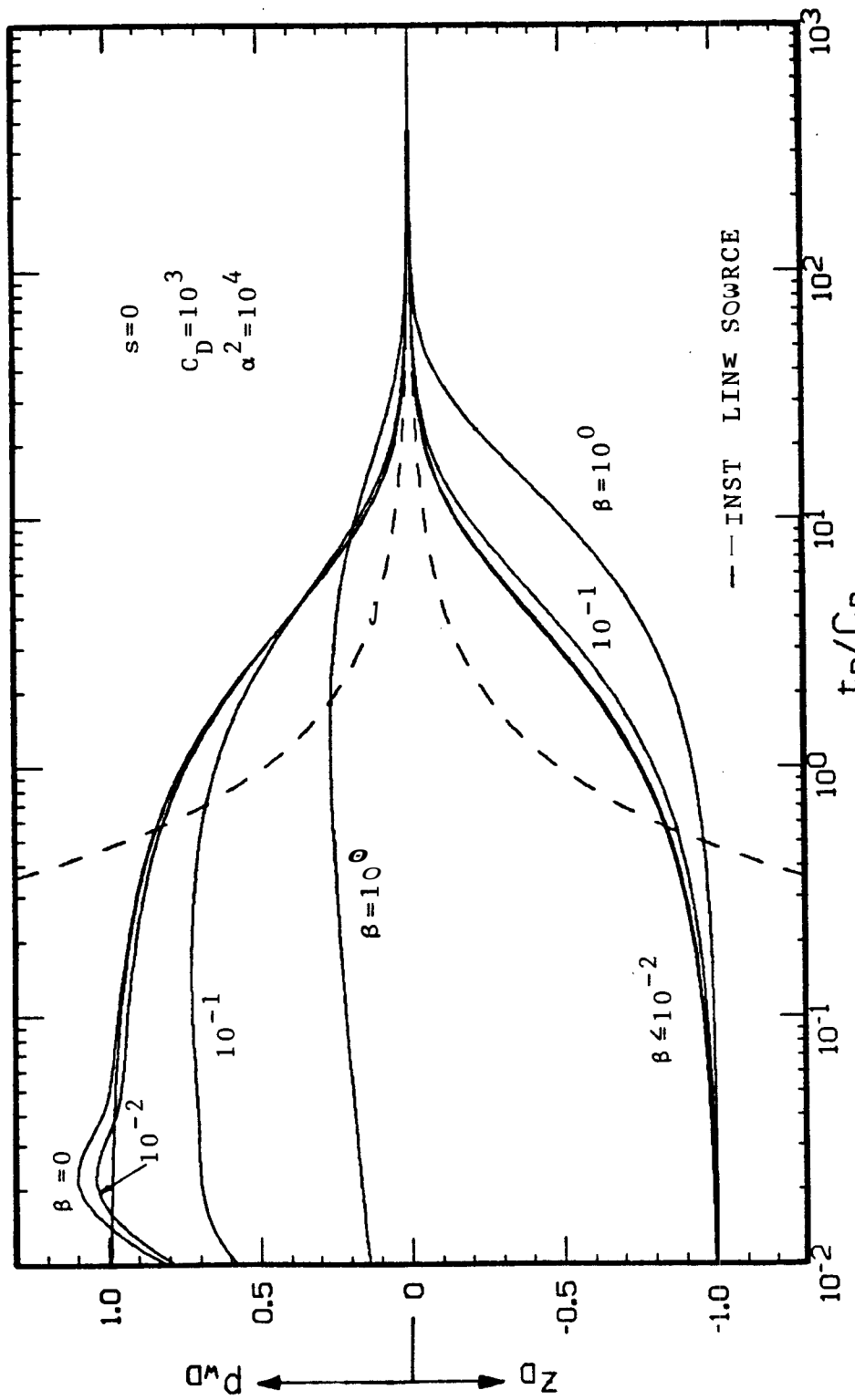

FIG. 5.8.a. SEMI-LOG GRAPH OF SLUG TEST SOLUTIONS FOR P_{wD} AND z_D VS t_D/C_D INCLUDING GRAVITATIONAL, INERTIAL, AND LAMINAR FRICTIONAL WELLBORE EFFECTS FOR DIFFERENT VALUES OF β IN A SYSTEM WITH s=0, $C_D=10^3$, AND $\alpha^2=10^4$

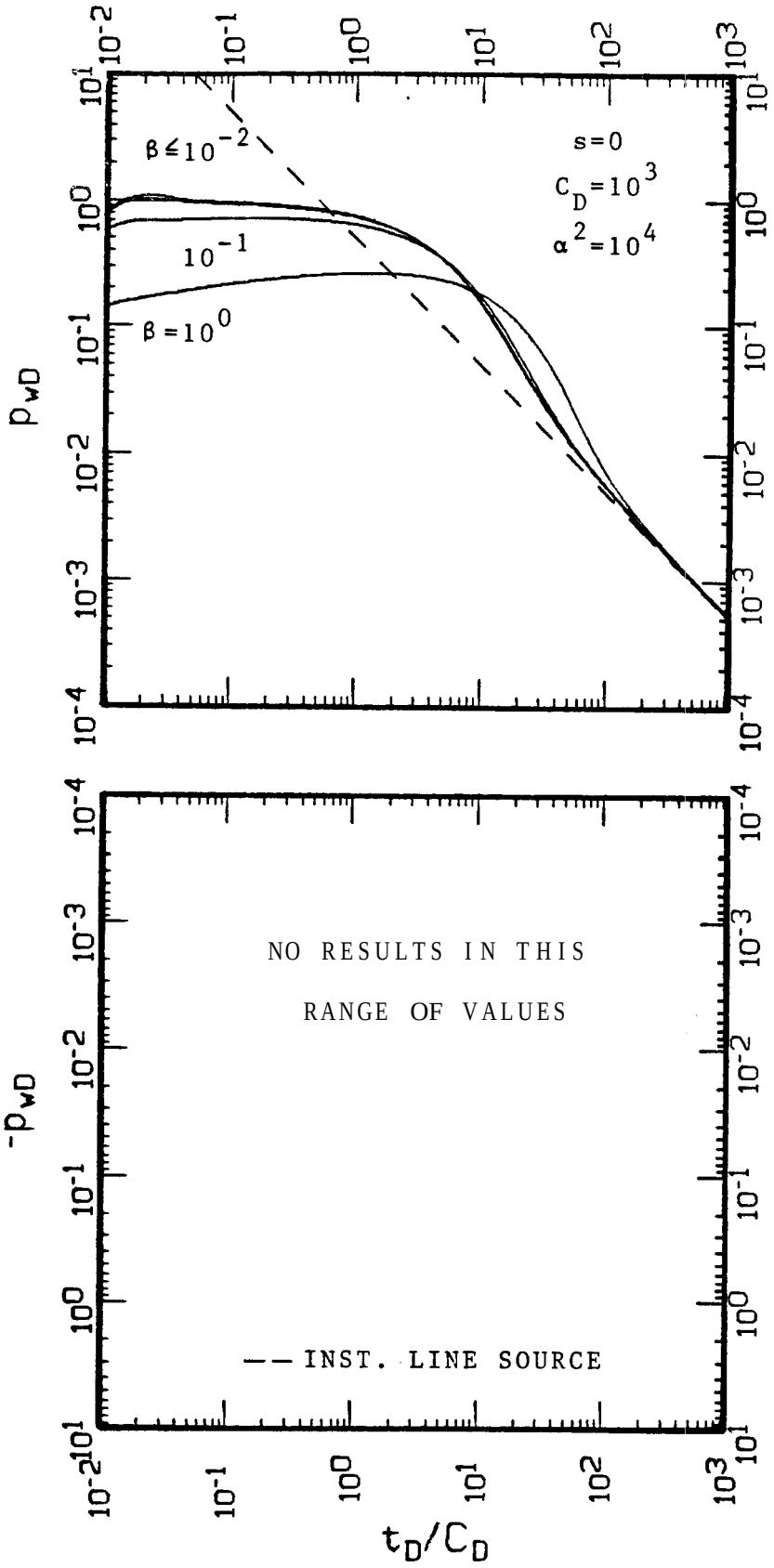

FIG. 5.8.b. LOG–LOG **GRAPH** OF SLUG TEST SOLUTIONS FOR p_{wD} VS t_D/C_D INCLUDING GRAVITATIONAL, INERTIAL, **AND** LAMINAR FRICTIONAL WELLBORE EFFECTS FOR DIFFERENT VALUES OF β IN A SYSTEM WITH s=0, $C_D=10^3$, AND $\alpha^2=10^4$

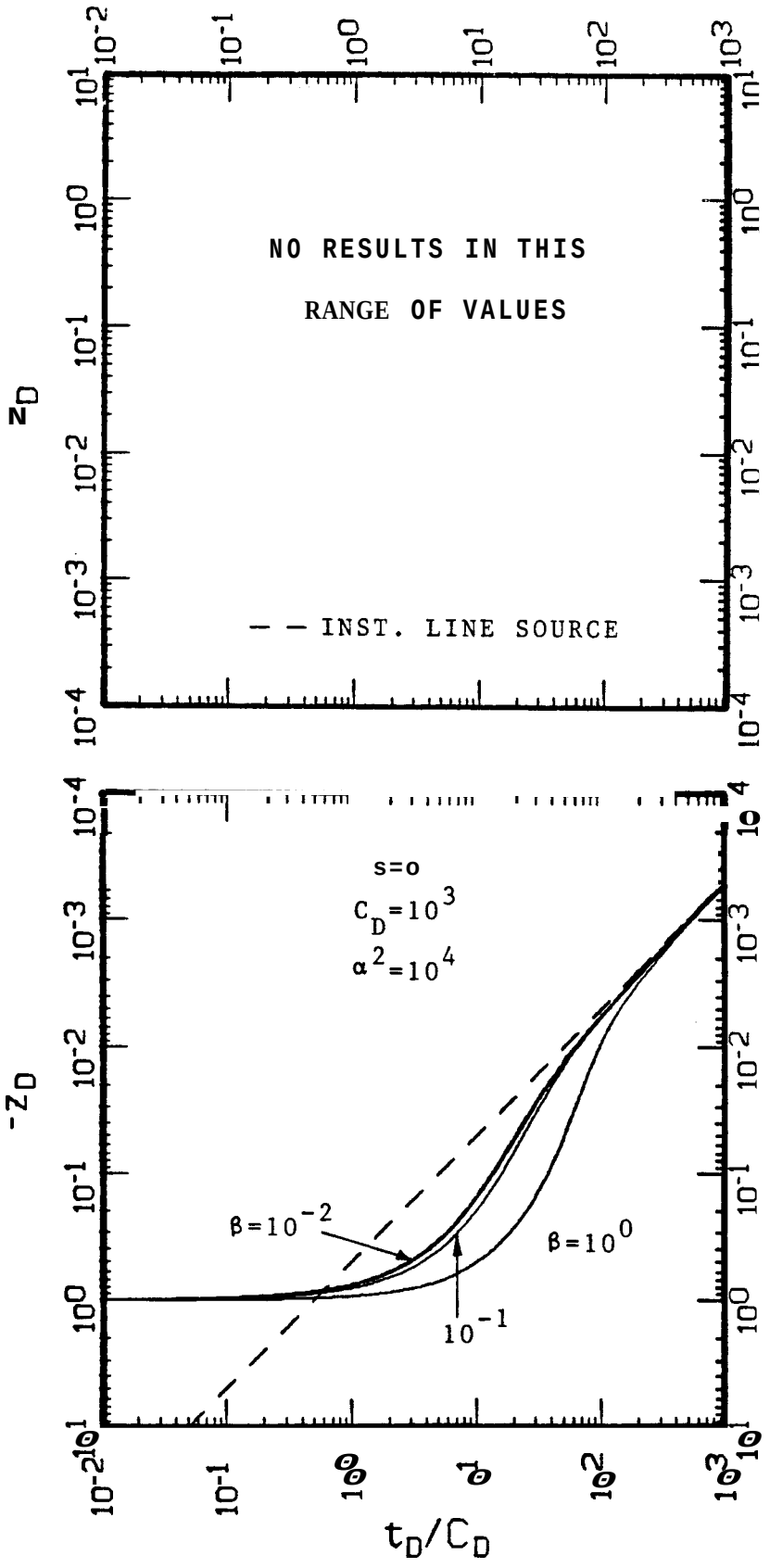

FIG. 5.8.c. LOG-LOG GRAPH OF SLUG TEST SOLUTIONS FOR z_D VS t_D/C_D INCLUDING GRAVITATIONAL, INERTIAL, AND LAMINAR FRICTIONAL, WELLBORE EFFECTS FOR DIFFERENT VALUES OF β IN A SYSTEM WITH $s=0$, $C_D=10^3$, AND $a^2=10^4$

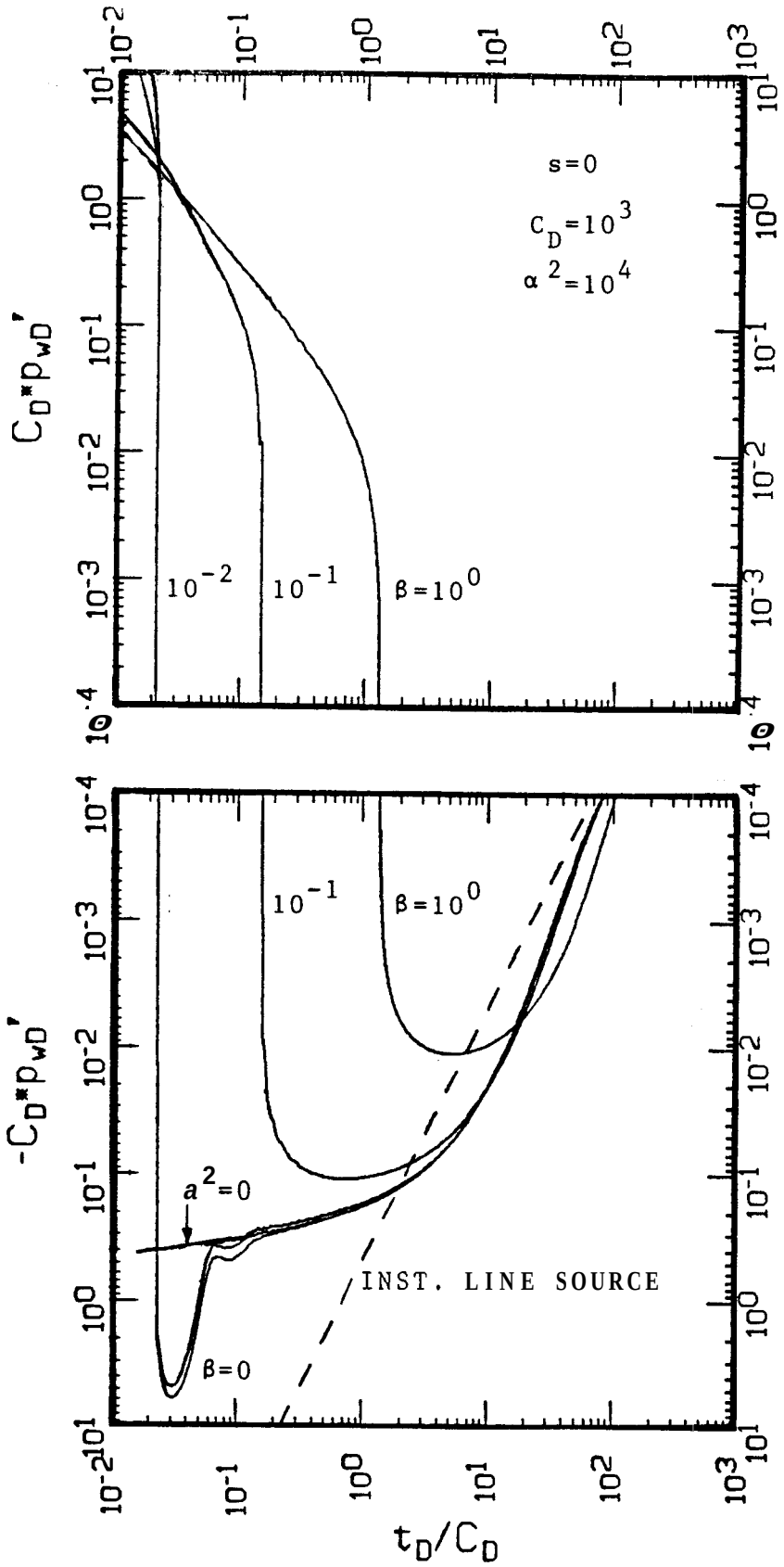

FIG. 5.8.d. **LOG-LOG** GRAPH OF SLUG TEST SOLUTIONS FOR p_{wD}' VS t_D/C_D INCLUDING GRAVITATIONAL, INERTIAL, AND LAMINAR FRICTIONAL WELLBORE EFFECTS FOR DIFFERENT VALUES OF β IN A **SYSTEM WITH** $s=0$, $C_D=10^3$, **AND** $\alpha^2=10^4$

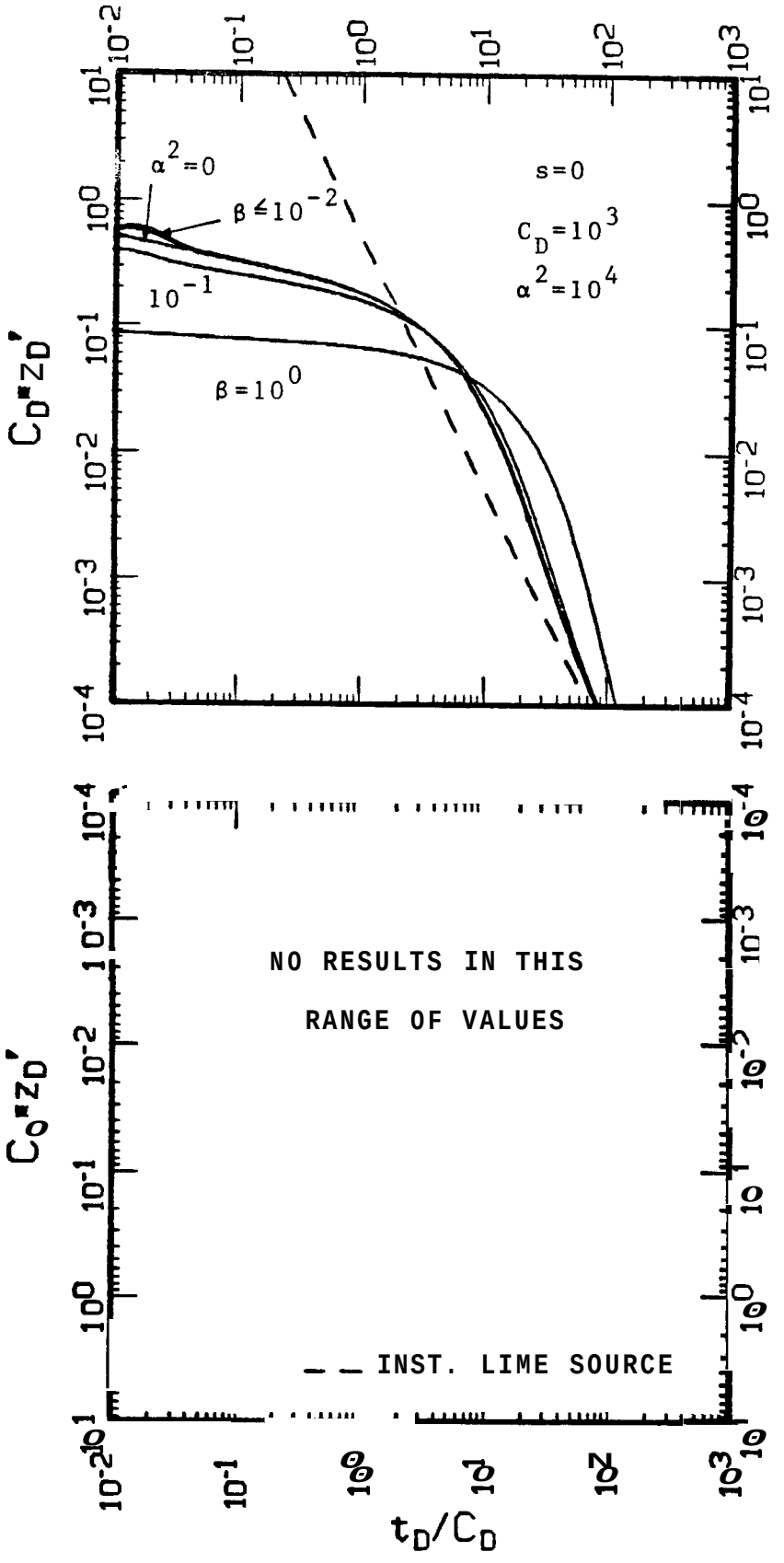

FIG. 5.8.e. LOG-LOG GRAPH OF SLUG TEST SOLUTIONS FOR z_D' VS t_D/C_D INCLUDING GRAVITATIONAL, INERTIAL, AND LAMINAR FRICTIONAL WELLBORE EFFECTS FOR DIFFERENT VALUES OF β IN A SYSTEM WITH s=0, $C_D=10^3$, AND $\alpha^2=10^4$

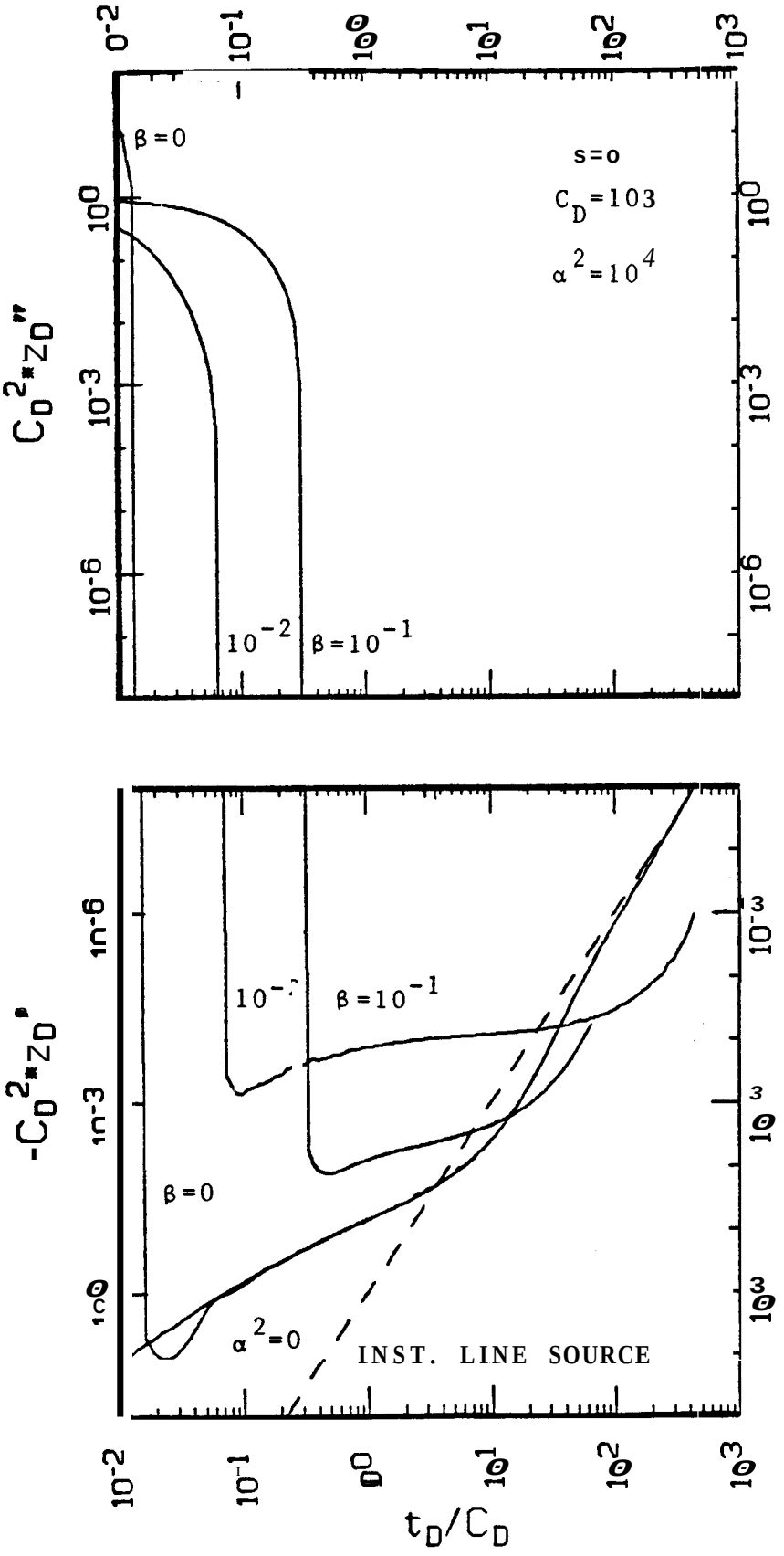

FIG. 5.8.f. LOG-LOG GRAPH OF SLUG TEST SOLUTIONS FOR z_D'' VS t_D/C_D INCLUDING GRAVITATIONAL, INERTIAL, AND LAMINAR FRICTIONAL WELLBORE EFFECTS FOR DIFFERENT VALUES OF β IN A SYSTEM WITH s=0, $C_D=10^3$, AND $\alpha^2=10^4$

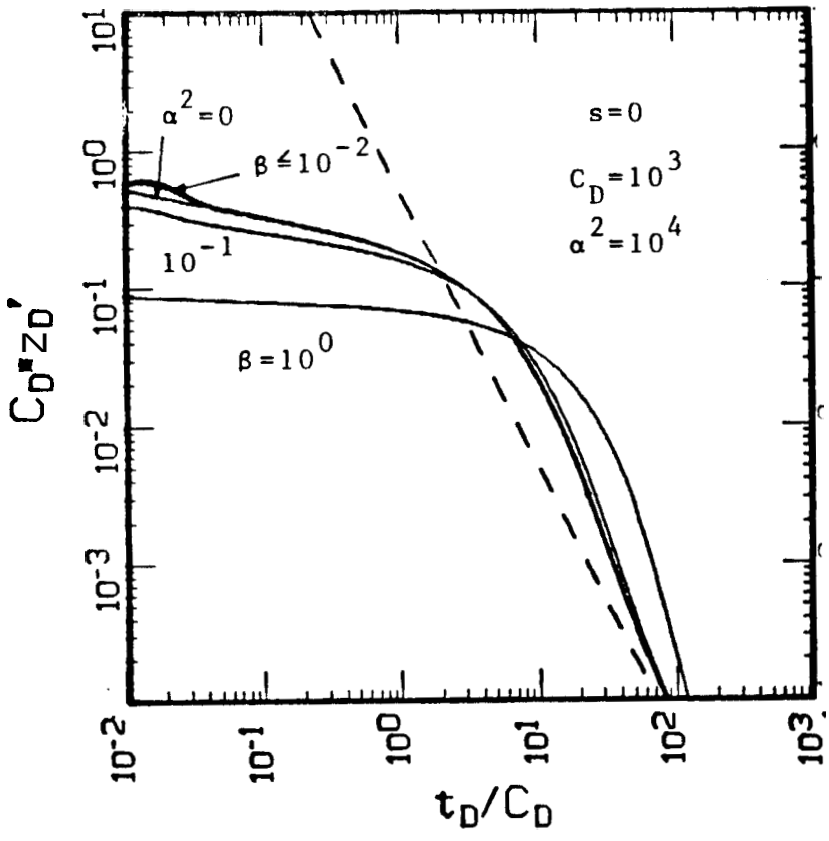

Fig. 15.- Solutions for $C_D z_D'$ versus t_D/C_D for systems with $s=0$, $C_D=10^3$, $\alpha^2=10^4$ but different values of β, including inertial and frictional wellbore effects.

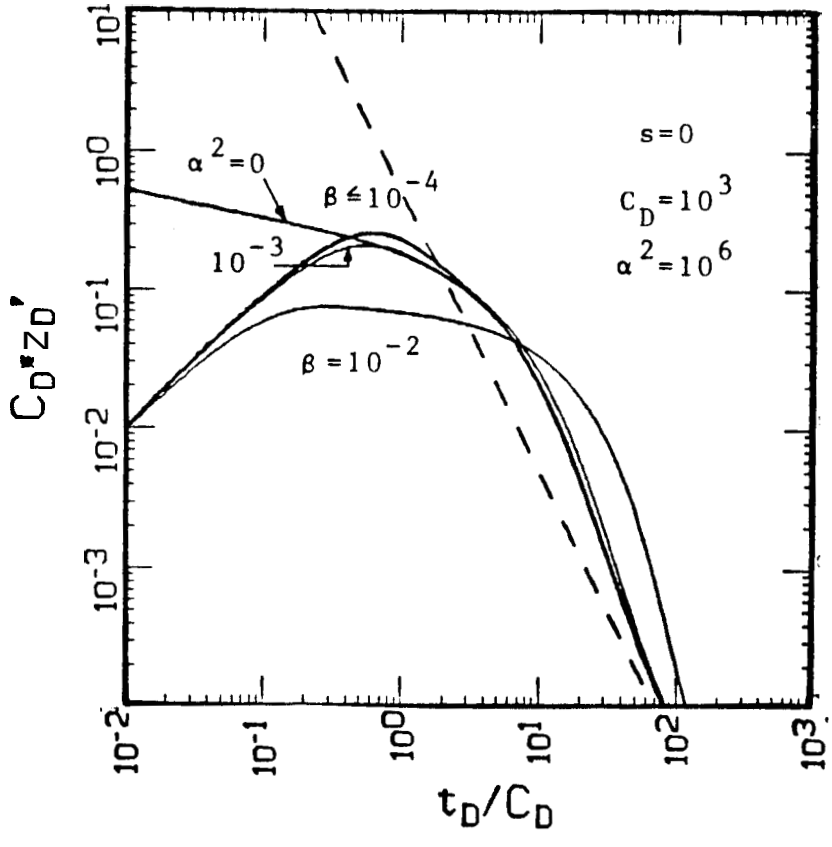

Fig. 16.- Solutions for $C_D z_D'$ versus t_D/C_D for systems with $s=0$, $C_D=10^3$, $\alpha^2=10^6$ but different values of β, including inertial and frictional wellbore effects.

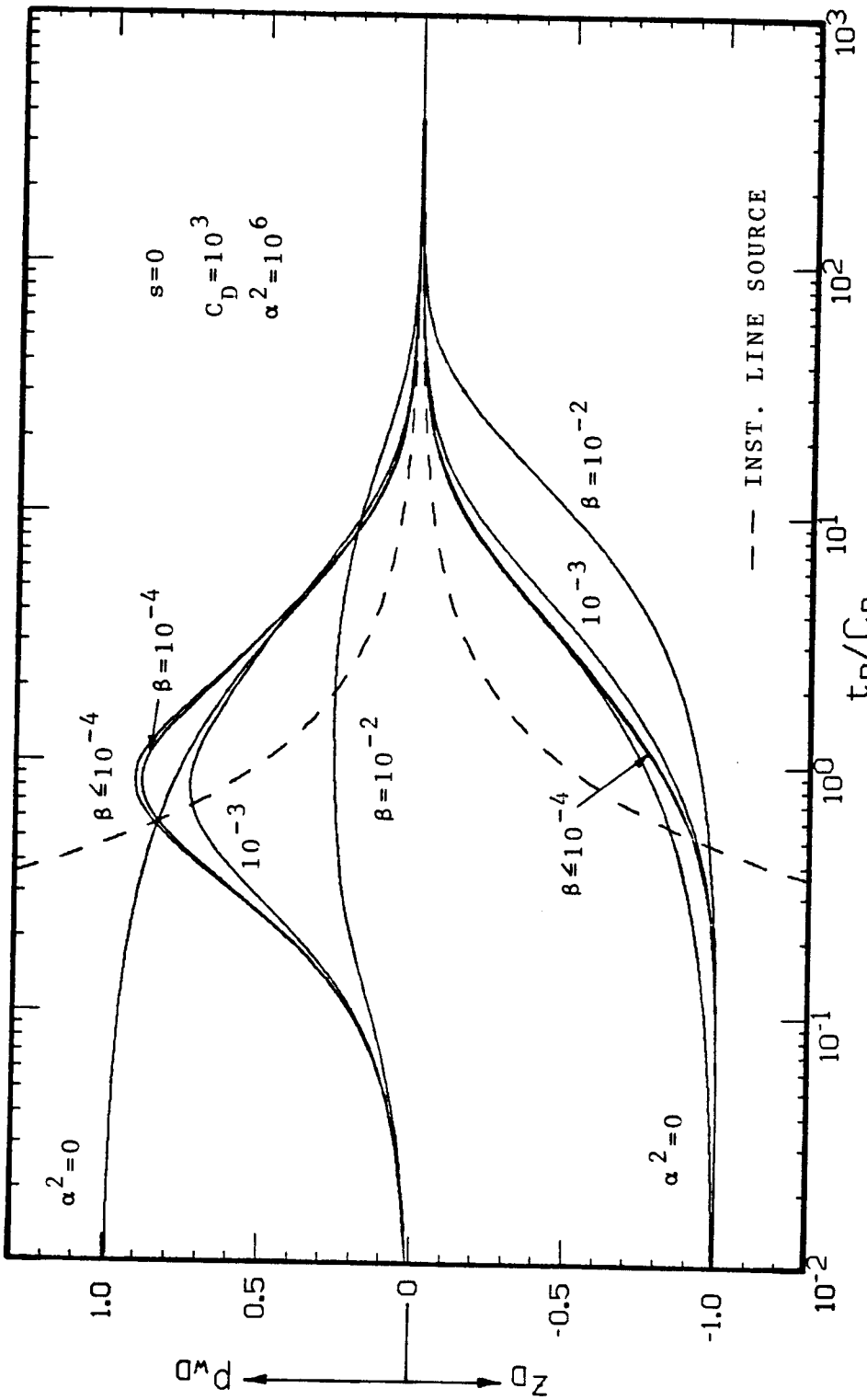

FIG. 5.9.a. SEMI-LOG GRAPH OF SLUG TEST SOLUTIONS FOR p_{wD} AND z_D VS t_D/C_D INCLUDING GRAVITATIONAL, INERTIAL, AND LAMINAR FRICTIONAL WELLBORE EFFECTS FOR DIFFERENT VALUES OF β IN A SYSTEM WITH s=0, $C_D=10^3$, AND $\alpha^2=10^6$

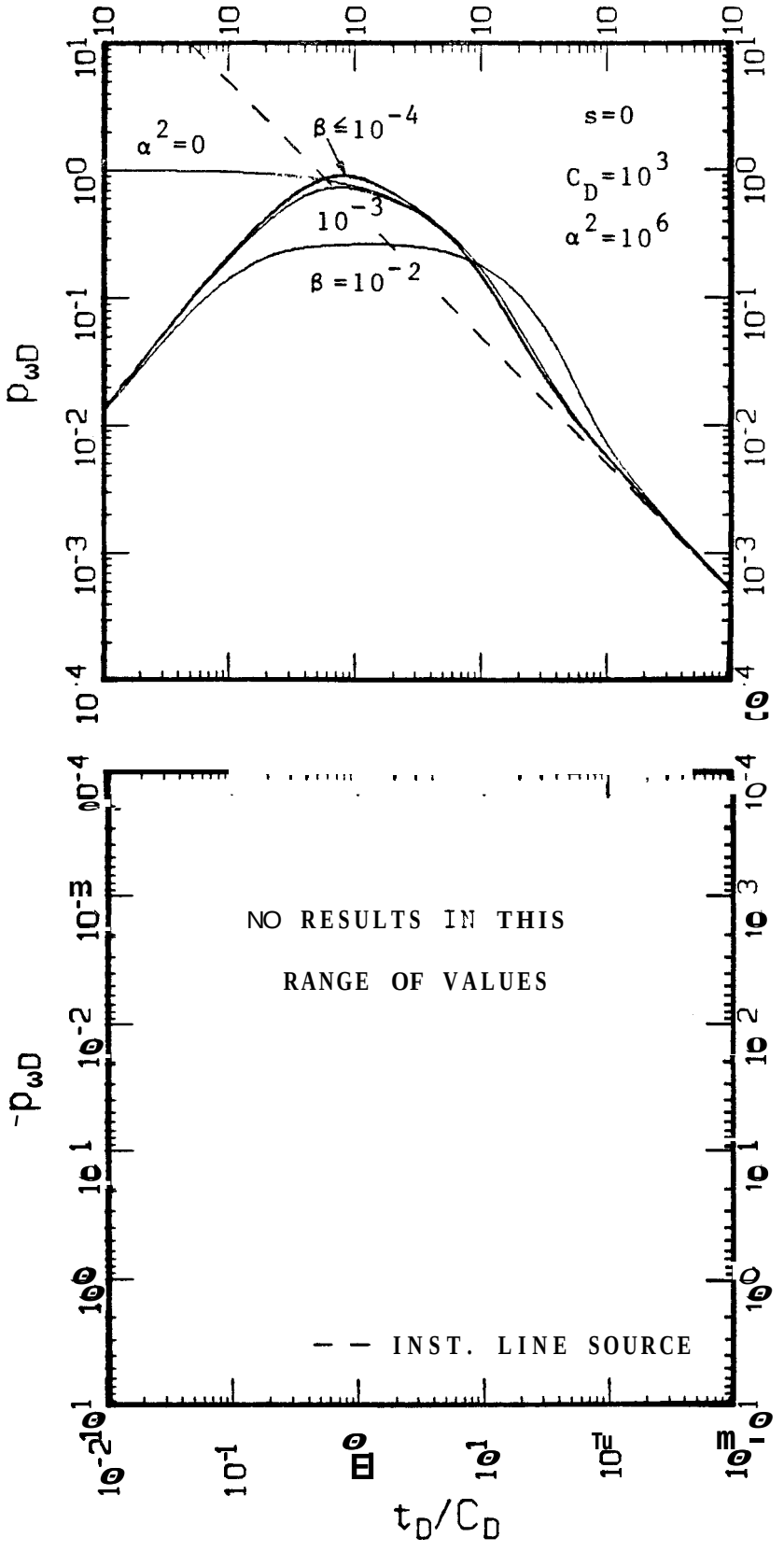

FIG. 5.9.b. LOG-LOG GRAPH OF SLUG TEST SOLUTIONS FOR p_{wD} VS t_D/C_D INCLUDING GRAVITATIONAL, INERTIAL, AND LAMINAR FRICTIONAL WELLBORE EFFECTS FOR DIFFERENT VALUES OF β IN A SYSTEM WITH s=0, $C_D=10^3$, AND $\alpha^2=10^6$

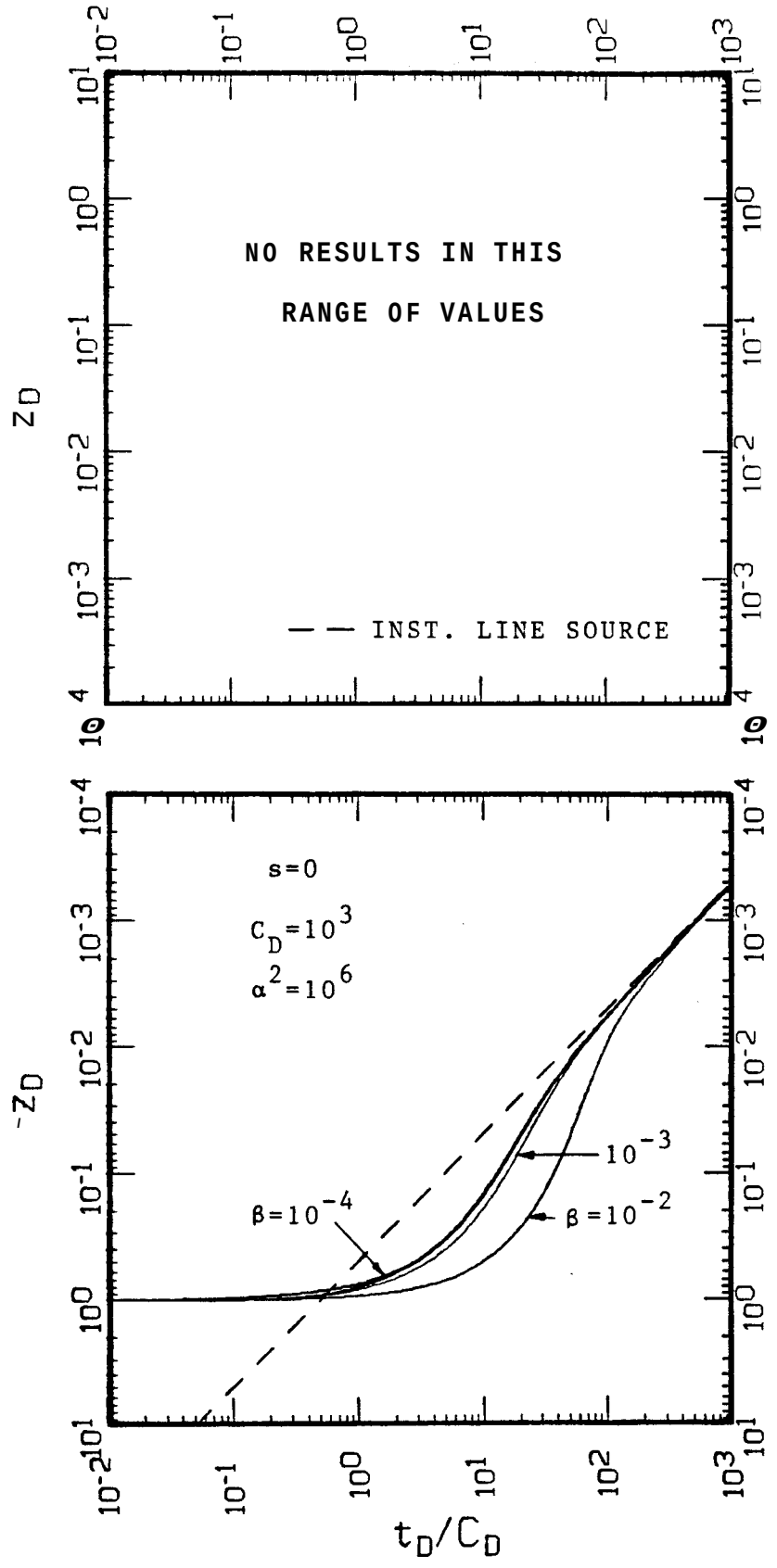

FIG. 5.9.c. LOG-LOG GRAPH OF SLUG TEST SOLUTIONS FOR z_D VS t_D/C_D INCLUDING GRAVITATIONAL, INERTIAL, AND LAMINAR FRICTIONAL WELLBORE EFFECTS FOR DIFFERENT VALUES OF β IN A SYSTEM WITH s=0, $C_D=10^3$, AND $\alpha^2=10^6$

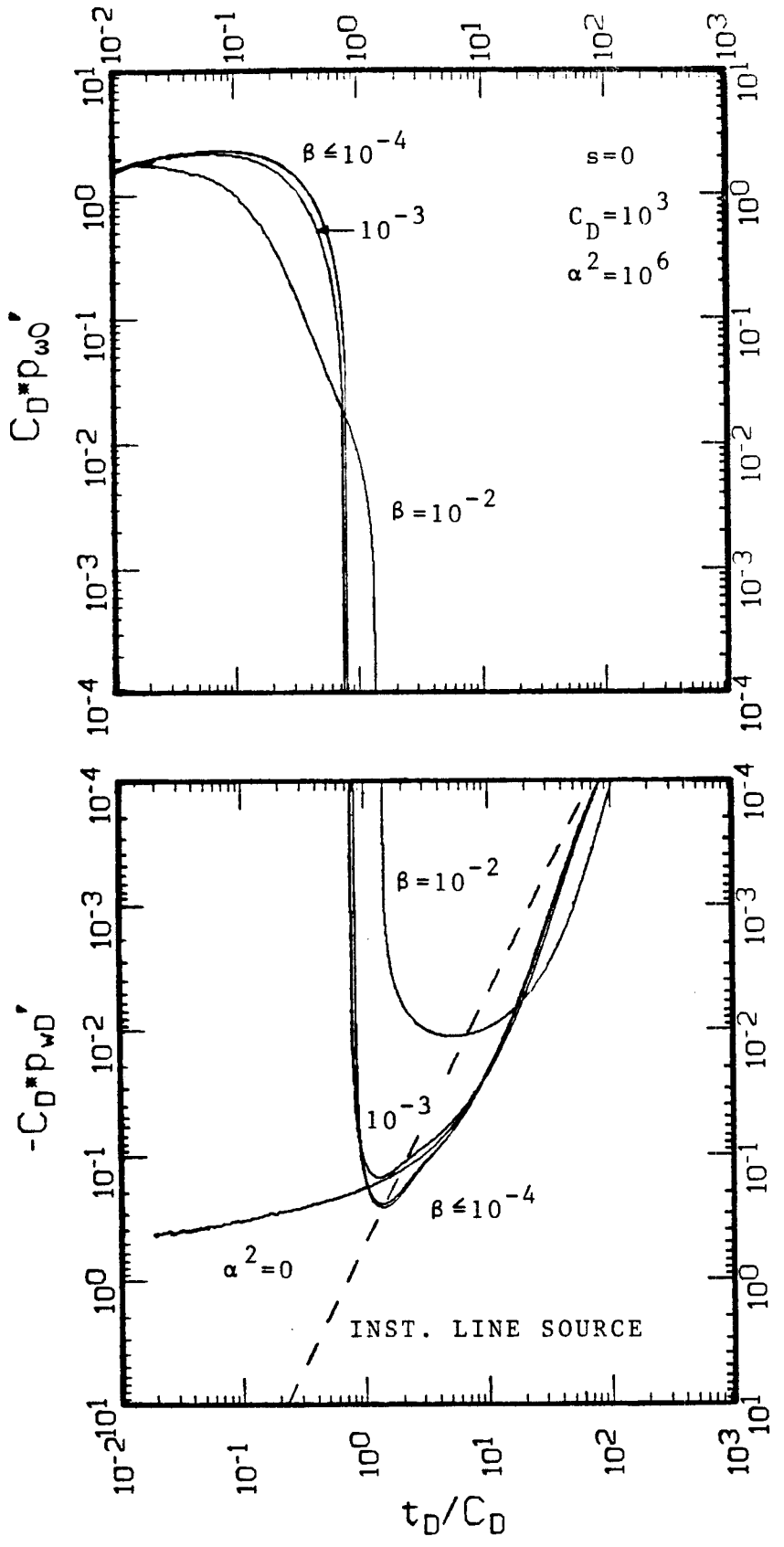

FIG. 5.9.d. LOG-LOG GRAPH OF SLUG TEST SOLUTIONS FOR p_{wD}' VS t_D/C_D INCLUDING GRAVITATIONAL, INERTIAL, AND LAMINAR FRICTIONAL WELLBORE EFFECTS FOR DIFFERENT VALUES OF β IN A SYSTEM WITH s=0, $C_D=10^3$, AND $\alpha^2=10^6$

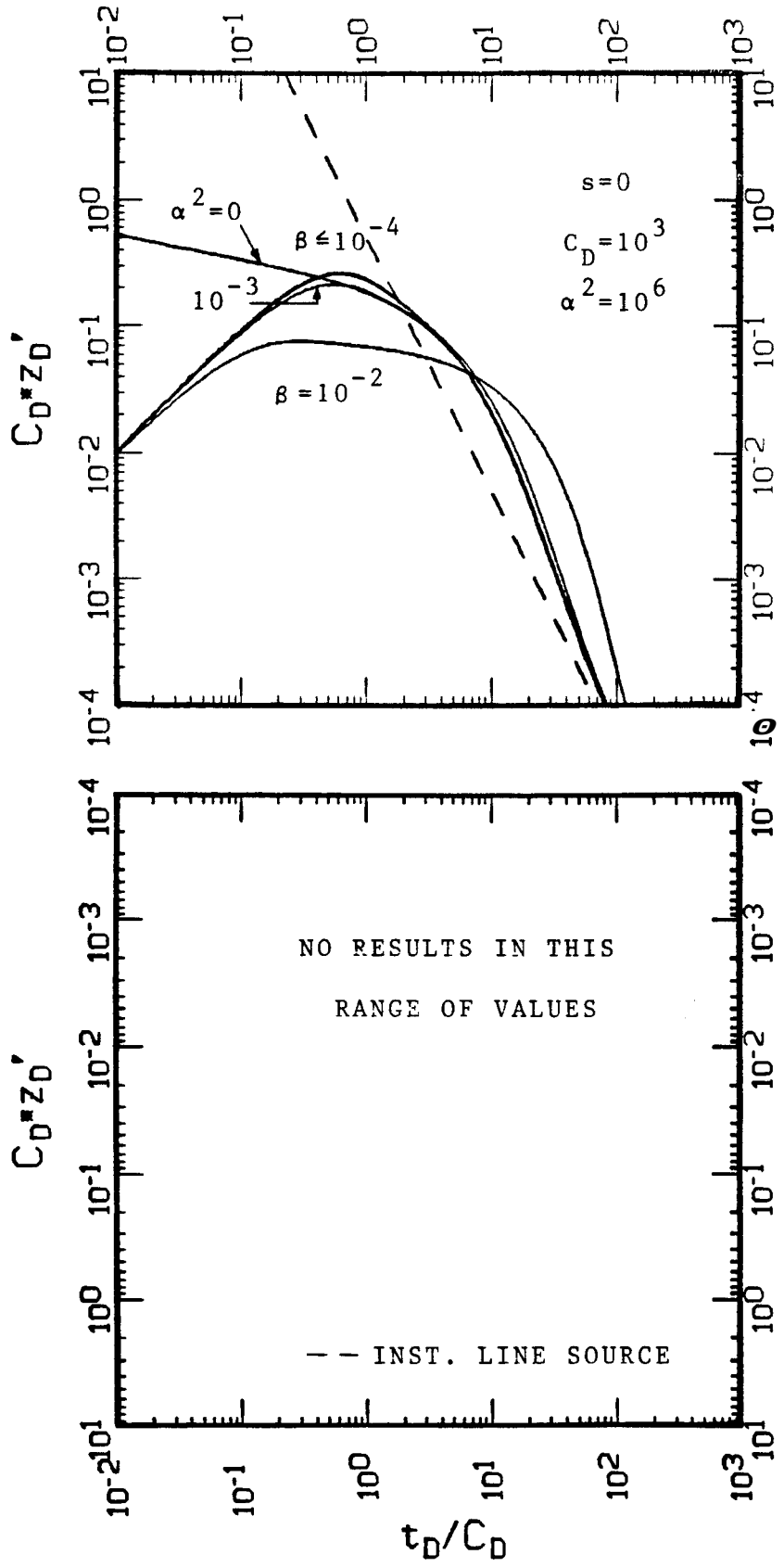

FIG. 5.9.e. LOG-LOG GRAPH OF SLUG TEST SOLUTIONS FOR z_D' VS t_D/C_D INCLUDING GRAVITATIONAL, INERTIAL, AND LAMINAR FRICTIONAL WELLBORE EFFECTS FOR DIFFEREYT VALUES OF β IN A SYSTEM WITH $s=0$, $C_D=10^3$, AND $\alpha^2=10^6$

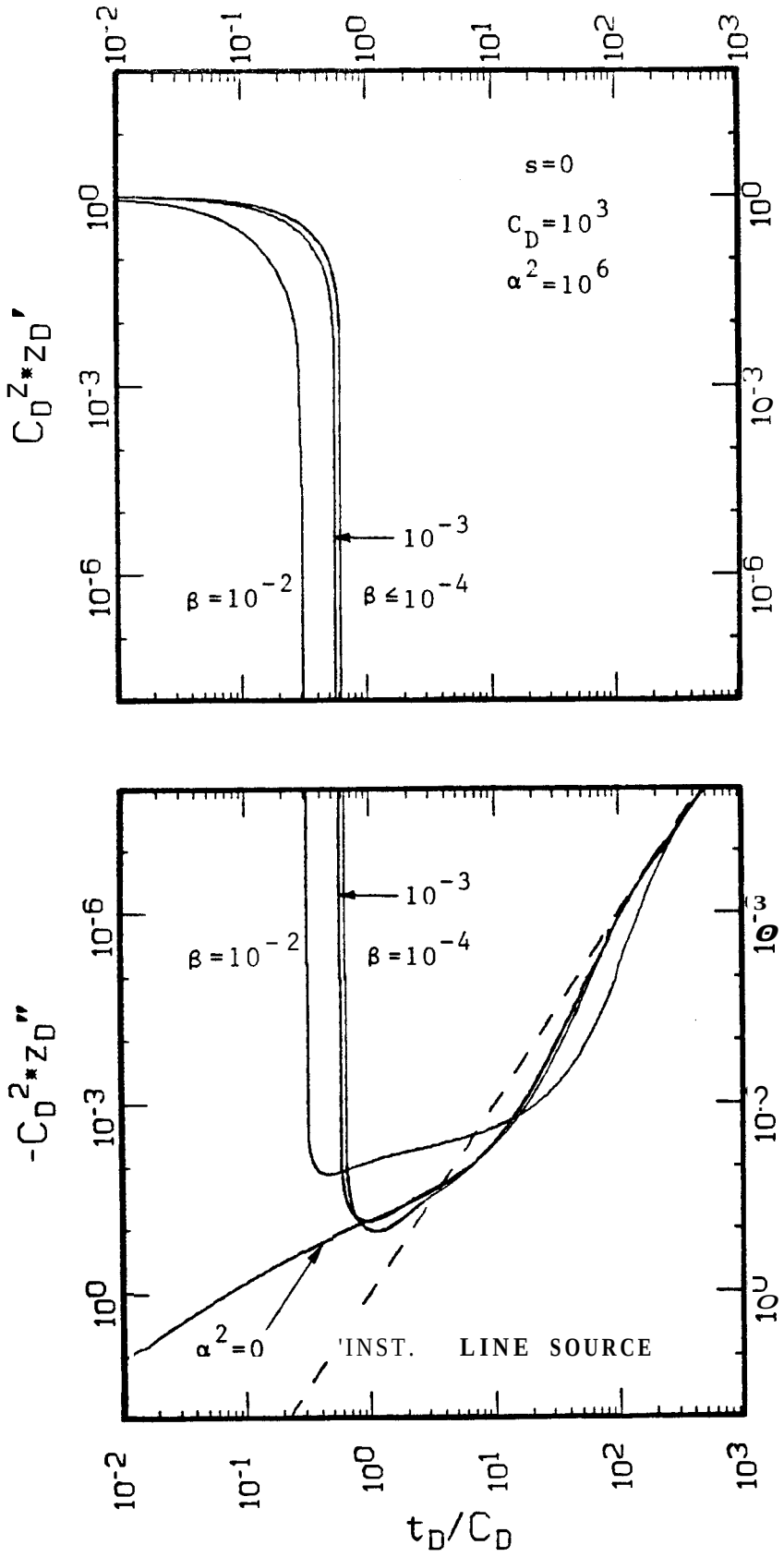

FIG. 5.9.f. LOG-LOG GRAPH OF SLUG TEST SOLUTIONS FOR z_D'' VS t_D/C_D INCLUDING GRAVITATIONAL, INERTIAL, AND LAMINAR FRICTIONAL WELLBORE EFFECTS FOR DIFFERENT VALUES OF β IN A SYSTEM WITH $s=0$, $C_D=10^3$, AND $\alpha^2=106$

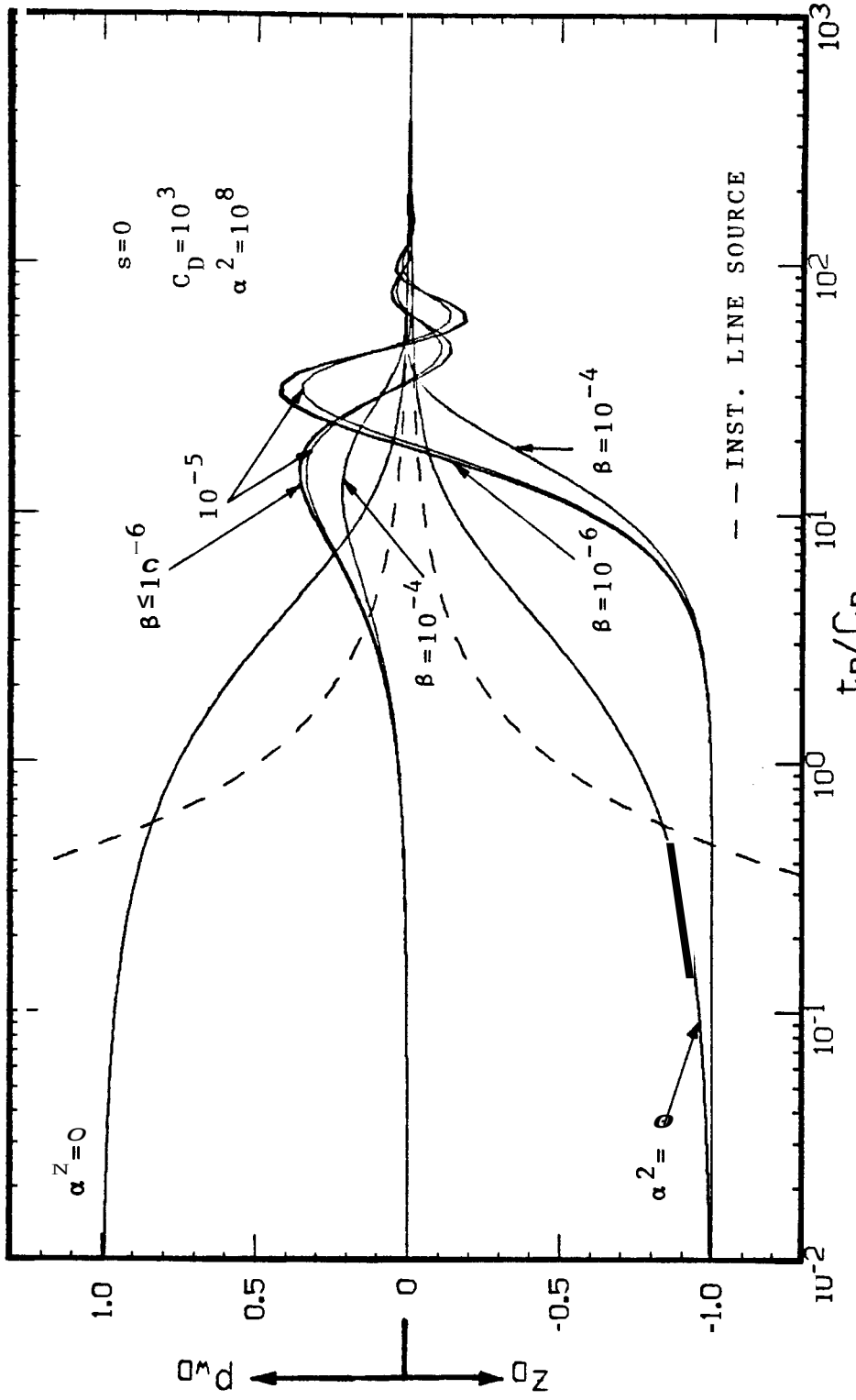

FIG. 5.10.a. SEMI-LOG GRAPH OF SLUG TEST SOLUTIONS FOR p_{wD} AND z_D VS t_D/C_D INCLUDING GRAVITATIONAL, INERTIAL, AND LAMINAR FRICTIONAL WELLBORE EFFECTS FOR DIFFERENT VALUES OF β IN A SYSTEM WITH s=0, $C_D=10^3$, AND $\alpha^2=10^8$

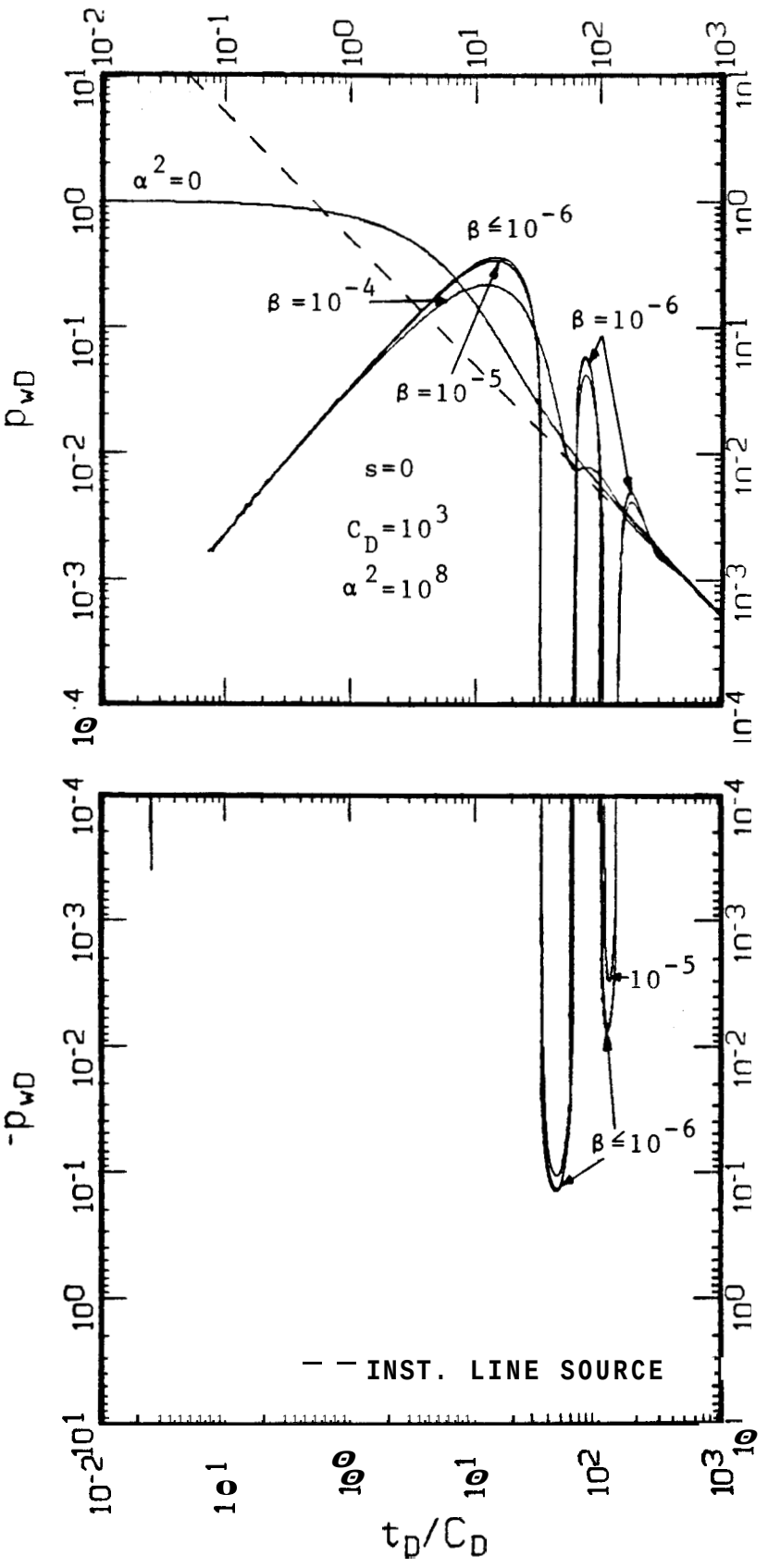

FIG. 5.10.b. LOG-LOG GRAPH OF SLUG TEST SOLUTIONS FOR p_{wD} VS t_D/C_D INCLUDING GRAVITATIONAL, INERTIAL, AND LAMINAR FRICTIONAL WELLBORE EFFECTS FOR DIFFERENT VALUES OF β IN A SYSTEM WITH s=0, $C_D=10^3$, AND $\alpha^2=10^8$

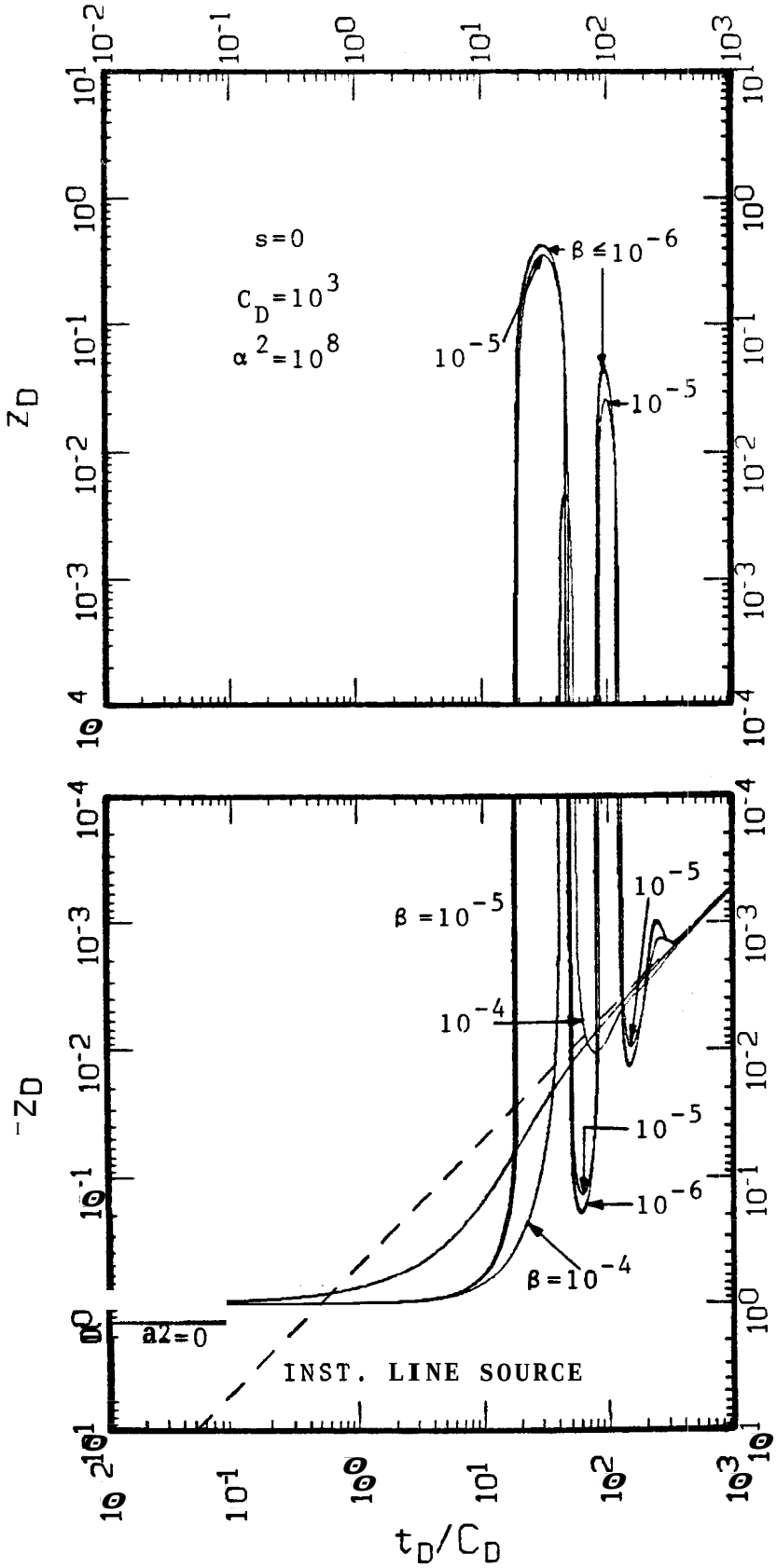

FIG. 5.10.c. LOG-LOG GRAPH OF SLUG TEST SOLUTIONS FOR z_D F'S t_D/C_D INCLUDING GRAVITATIONAL$_a$ INERTIAL$_s$ AND LAMINAR FRICTIOEIAL WELLBORE EFFECTS FOR DIFFERENT VALUES OF β IN A SYSTEM WITH s=0, $C_D=10^3$, AND $\alpha^2=10^8$

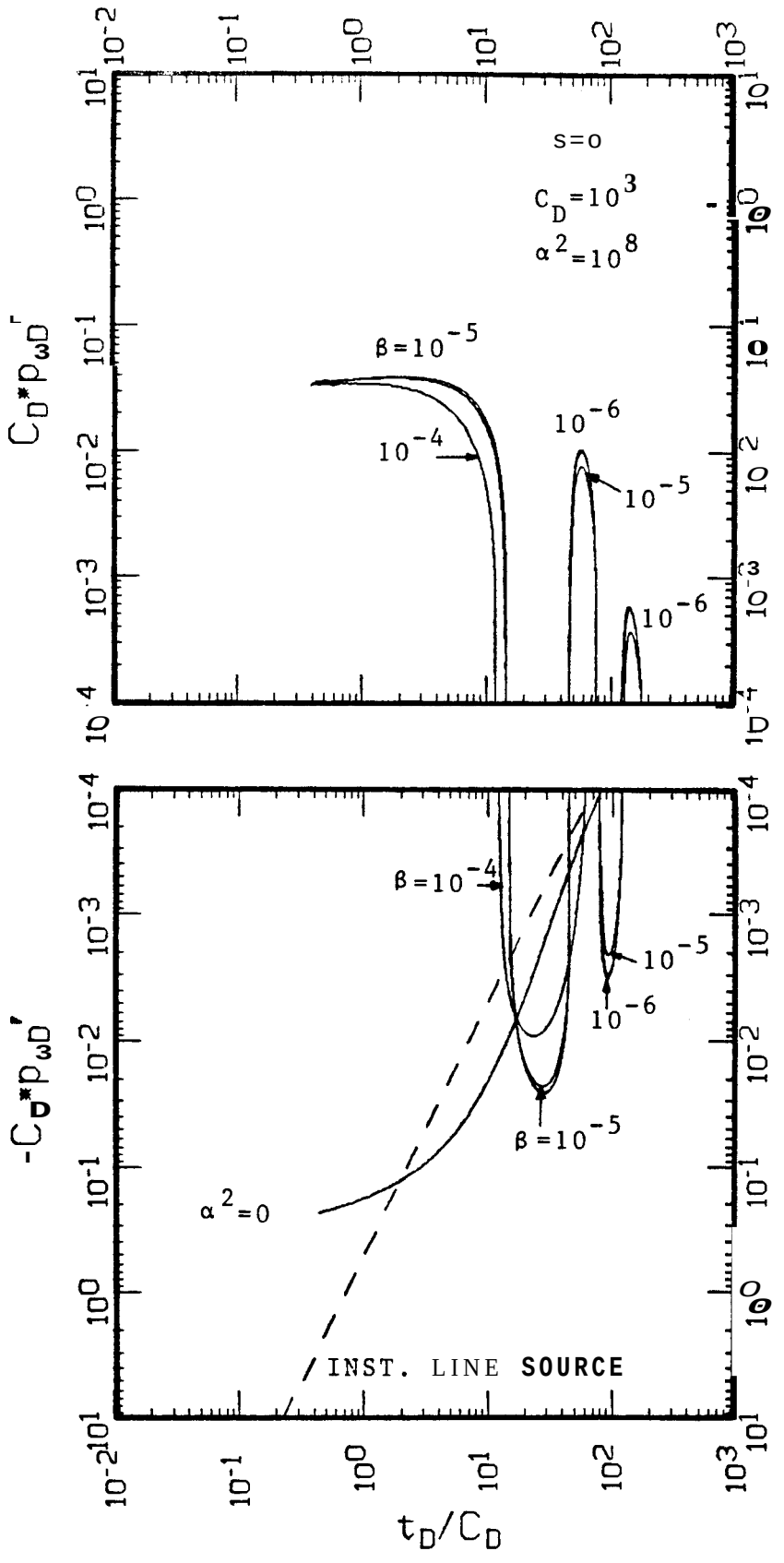

FIG. 5.10.d. LOG-LOG GRAPH OF SLUG TEST SOLUTIONS FOR p_{wD}' VS t_D/C_I INCLUDING GRAVITATIONAL, INERTIAL, AND IAMINAR FRICTIONAL WELLBORE EFFECTS FOR DIFFERENT VALUES OF β IN A SYSTEM WITH s=0, $C_D=10^3$, AND $\alpha^2=10^8$

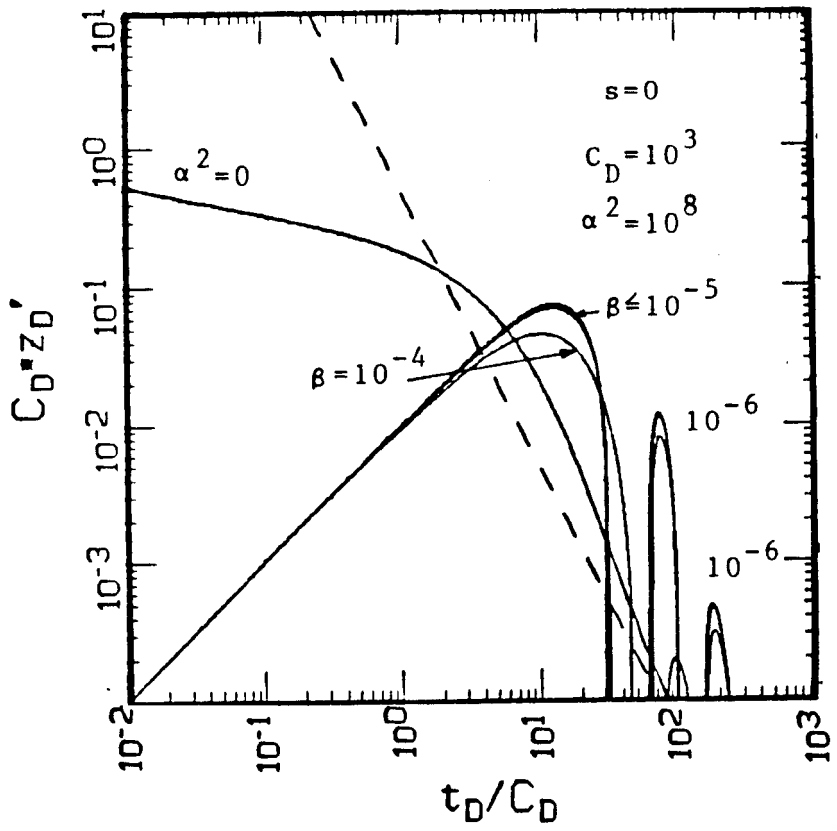

Fig. 17 .- Solutions for $C_D z_D'$ versus t_D/C_D for systems with s=0, $C_D=10^3$, $\alpha^2=10^8$ but different values **of** β, including inertial and frictional wellbore effects.

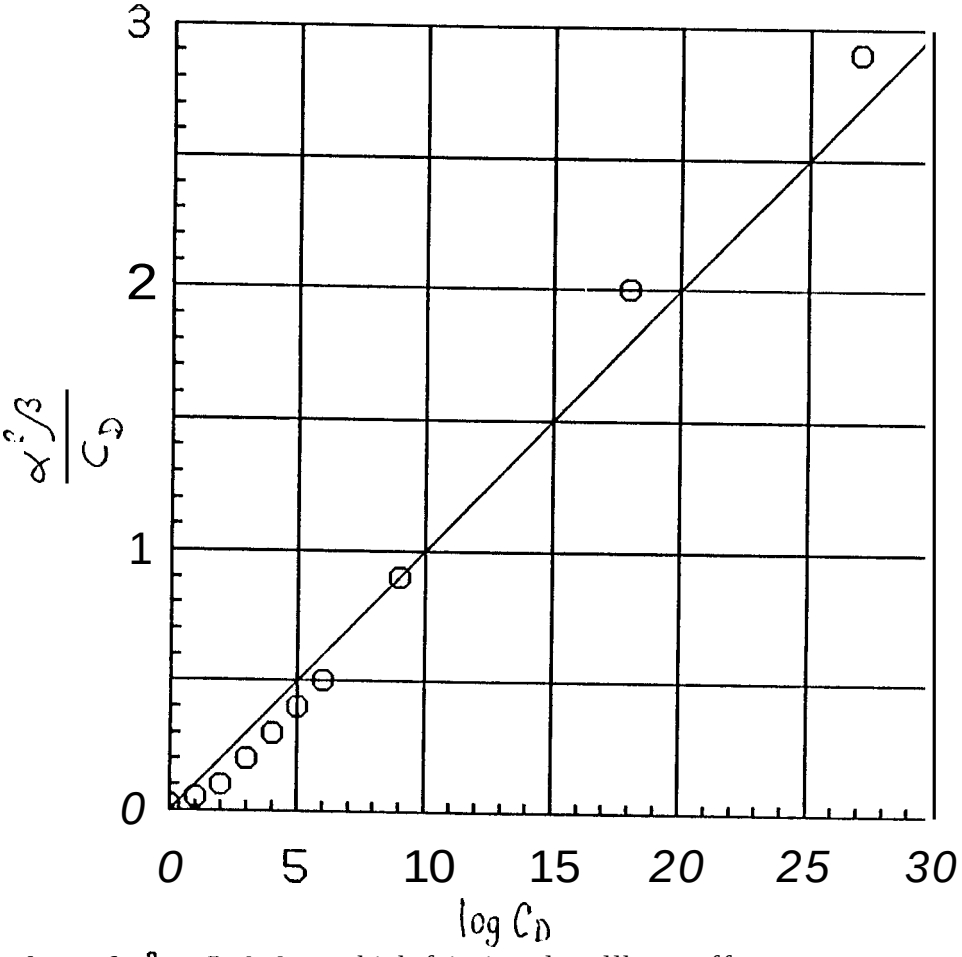

Fig. 18 .- Values **of** $\alpha^2\beta/C_D$ below which frictional wellbore effects can be considered negligible **for** systems with $s=0$ and different values **of** C_D.

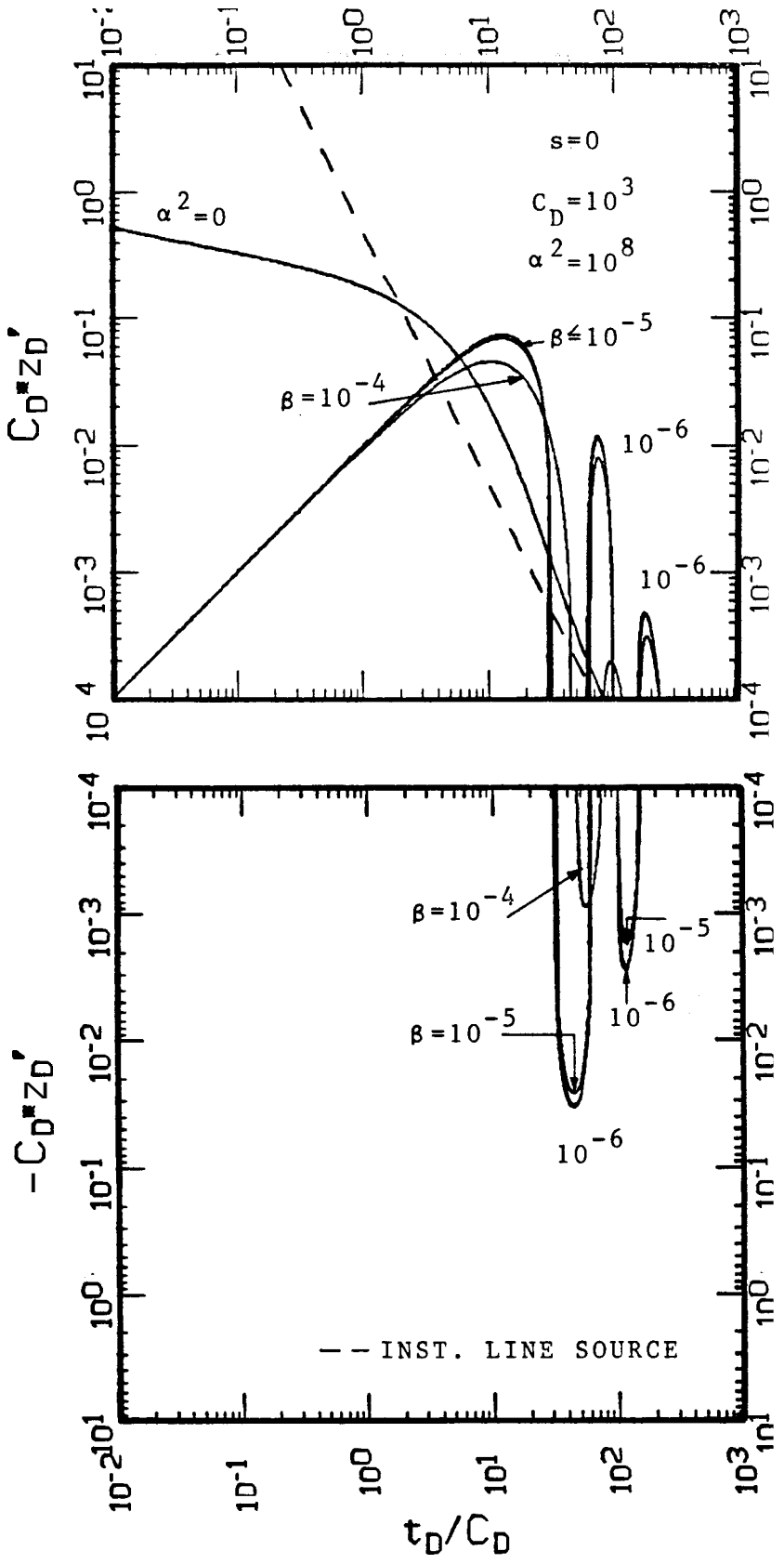

FIG. 5.10.e. LOG-LOG GRAPH OF SLUG TEST SOLUTIONS FOR z_D' VS t_D/C_D INCLUDING GRAVITATIONAL, INERTIAL, AND LAMINAR FRICTIONAL WELLBORE EFFECTS FOR DIFFERENT VALUES OF β IN A SYSTEM WITH s=0, $C_D=10^3$, AND $\alpha^2=10^8$

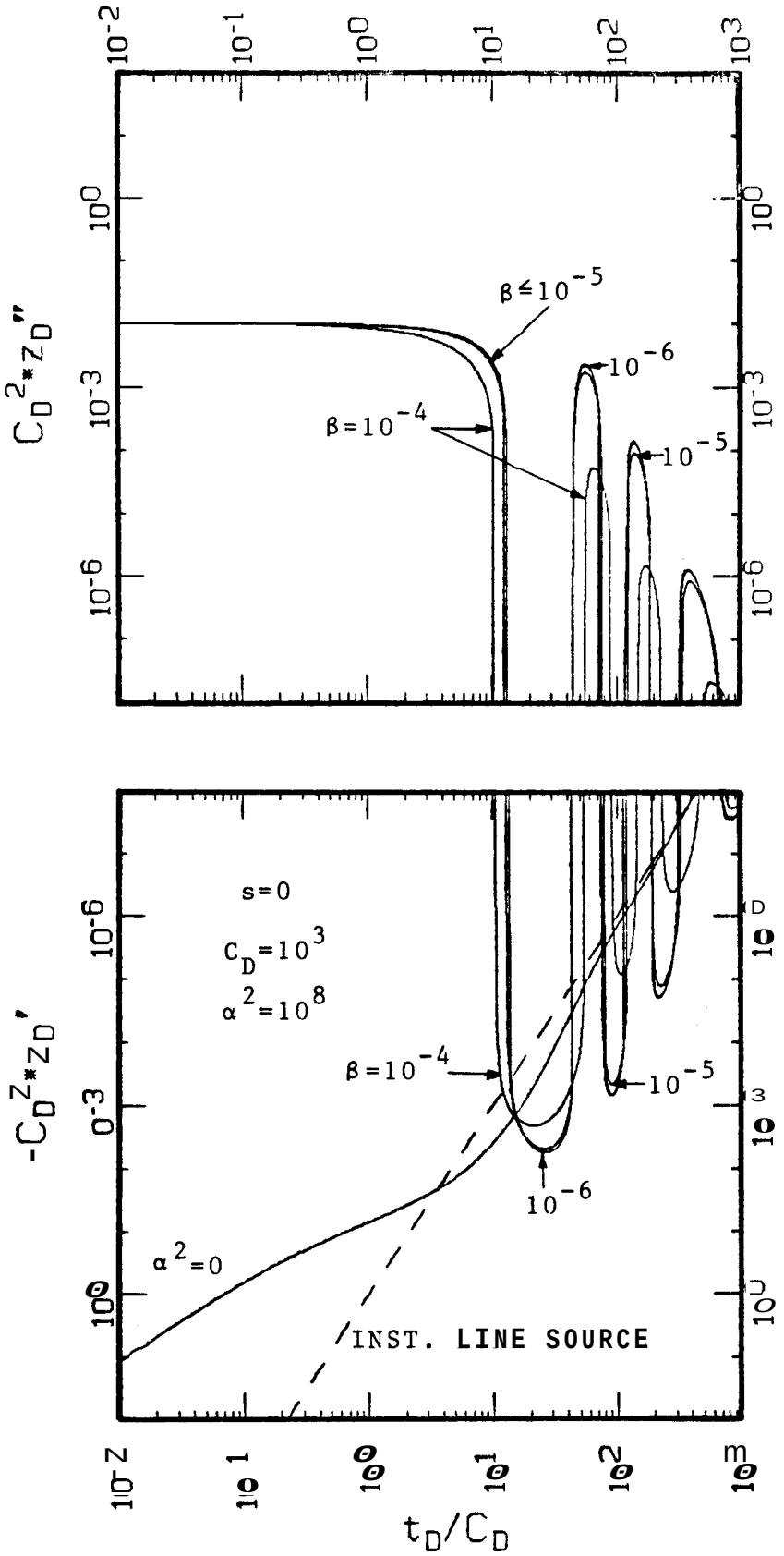

FIG. 5.10.f. LOG-LOG GRAPH OF SLUG TEST SOLUTIONS FOR z_D'' VS t_D/C_D INCLUDING GRAVITATIONAL, INERTIAL, AND LAMINAR FRICTIONAL WELLBORE EFFECTS FOR DIFFERENT VALUES OF β IN A SYSTEM WITH s=0, $C_D=10^3$, AND $\alpha^2=10^8$

Observation of the solutions for $C_D z_D'$, shown in Figs. 5.8.e, 5.9.e, and 5.10.e, indicates that for a given value of deaccelerating factor a, the larger the value of wellbore friction factor β, the smaller and flatter the behavior of $C_D z_D'$, which corresponds to lower flow rates sustained during longer periods of time. A quantitative indication of the flatness of the solutions for $C_D z_D'$ is indicated by the low values of the solutions for $C_D^2 z_D''$ presented in Figs. 5.8.f, 5.9.f, and 5.10.f. All these figures show that for this system case with s=0 and C_D=103 the solutions for z_D, z_D', and z_D'' including laminar friction agree with those neglecting friction (β=0) for values of $\alpha^2\beta < 10^2$. This observation and solutions previously reviewed in Section 5.1 can be used to deduce criteria for estimating conditions under which laminar frictional wellbore effects are negligible.

Figure 5.4.f shows solutions with no inertia (α^2=0) for $C_D z_D'$ for $1 < C_D e^{2s} < 10^{27}$. At early times, these solutions vary between 100 and 10^{-1} for most practical conditions. The larger the value of $C_D e^{2s}$, the smaller and more stable the value of $C_D z_D'$. Also, as shown in Fig. 5.5.h, at early times, solutions including wellbore inertial effects slightly overshoot solutions for $C_D z_D'$ with no inertia. Moreover, Shinohara and Ramey (1979.b) determined that the larger the value of s, the earlier the pressure response and the smaller and flatter the pressure overshoot. Therefore, it can be expected that typical field conditions will exhibit an approximate maximum flow rate implicit in the value of $C_D z'_{Dmax} \approx 10^{-1}$.

This approximation can be combined with the observation that laminar friction effects are negligible for $\alpha^2\beta < 10^2$ when C_D=10^3 and s=0 to calculate the approximate maximum value of the liquid column velocity term in Eq. 5.42 required for laminar friction effects to be negligible:

$$B_w z'_{Dmax} = \alpha^2 \beta z'_{Dmax} < 10^2 z'_{Dmax} \approx \frac{10^2}{10 C_D} \approx \frac{10}{C_D} = 10^{-2} \quad \ldots \quad (5.44)$$

This equation approximates the maximum value that the liquid column velocity term in wellbore Eq. *5.42* can attain. Since z_D and p_{wD} vary between 0 and *1*, it is reasonable to expect negligible frictional effects if the maximum value of the liquid column velocity term is *1%*. This result leads to hypothesize that wellbore laminar friction effects are negligible for a system with:

$$\alpha^2 \beta < \frac{C_D}{10} \qquad \ldots (5.45)$$

or, according to the definition of α, β, and C_D, given by Eqs. *3.51*, *5.43*, and *3.47:*

$$\frac{L k h}{r_p^4} \frac{\mu_p}{\mu} < \frac{1}{160} \qquad \ldots (5.46)$$

Results for other practical values of s, C_D, and a show that this criterion for estimating conditions under which laminar friction effects are negligible is appropriate for practical wellbore–reservoir systems.

Inspection of the chart for f vs Re presented by Moody *(1944)* indicates that at high velocities, the laminar friction assumption leads to values of f smaller than those for other flow regimes. A higher value of f implies a higher value of the liquid column velocity term, as indicated by Eq. **3.39.b.** This implies that the criterion developed in this section gives low friction losses for systems in which the flow is turbulent for some intermediate period of time. However, the relative simplicity and linearity of the problem is useful for understanding the wellbore frictional effects on the flow phenomena during a slug test or a drillstem test. Also, this solution is utilized in Section *6.1* to validate a numerical solution method including wellbore frictional effects corresponding to changing flow regimes.

5.3 Solutions considering other Linear Inertial Effects

According to the definition of coefficient A_w, Eq. 3.39.a, in wellbore Eq. 3.39 derived in the present study, reservoir thickness/static wellbore column length ratio and pipe/wellbore radii ratio are combined in a linear term that affects dimensionless liquid column acceleration, z_D''. The effect of these ratios is analyzed in this section.

5.3.1 Special Wellbore Equation

The following simplified linear equation is obtained by neglecting only the non-linear terms in wellbore Eq. 3.39, and assuming laminar friction as described in Section 5.2:

$$A_w z_D'' + B_w z_D' + C_w z_D + D_w = E_w p_{wD} \quad \ldots (5.47)$$

where:

$$A_w = \alpha^2 \left\{ 1 + \frac{3}{8} \frac{h_D}{L_D} \left[\frac{r_{pDz}}{r_{wDz}} \right]^2 \right\} \quad \ldots (5.47.a)$$

$$B_w = \alpha^2 \beta \quad \ldots (5.47.b)$$

$$C_w = 1 \quad \ldots (5.47.c)$$

$$D_w = 0 \quad \ldots \text{(5.47.d)}$$

$$E_w = -1 \quad \ldots \text{(5.47.e)}$$

Wellbore Eq. 5.47 is mathematically linear and can be solved with the semi-analytical method using Laplace transformation described in Section 4.1. An option in the computer program presented in Appendix E performs the calculations required by this method to evaluate p_{wD}, z_D, p_{wD}, z_D', z_D'', and $p_D(r_D)$ vs t_D for supplied values of parameters s, C_D, α, β, h_D, L_D, r_{pDz}, and r_{wDz}.

5.3.2 Effect of h/L

Definition of coefficient A_w given by Eq. 5.47.a indicates that dimensionless reservoir thickness, h_D, and dimensionless static wellbore liquid column length, L_D, appear as a ratio. According to the definition of h_D and L_D, Eqs. 3.32 and 3.31, respectively, their ratio can be simplified to $h_D/L_D=h/L$. Moreover, the effect of h_D and L_D can be analyzed simultaneously, because these parameters appear only once in the problem statement considered in this section, constituted by Eqs. 5.47 and 3.40 - 3.46.

Figure 5.11 illustrates the solutions obtained for a system with $s=0$, $C_D=10^3$, $\alpha=106$, $\beta=0$, and $r_{pDz}/r_{wDz}=1$, for different values of h/L. These solutions show that for values of $h/L<1/10$, the effect of this ratio is negligible on the flow phenomena. Therefore, it can be concluded that the effects of h/L is negligible for most practical applications found in oil wells because usually $h<L/10$. However, a small effect of h/L can be expected for shallow water wells completed in thick aquifers. The combined effect of h/L and r_p/r_w is discussed further after analyzing the separate effect of r_p/r_w.

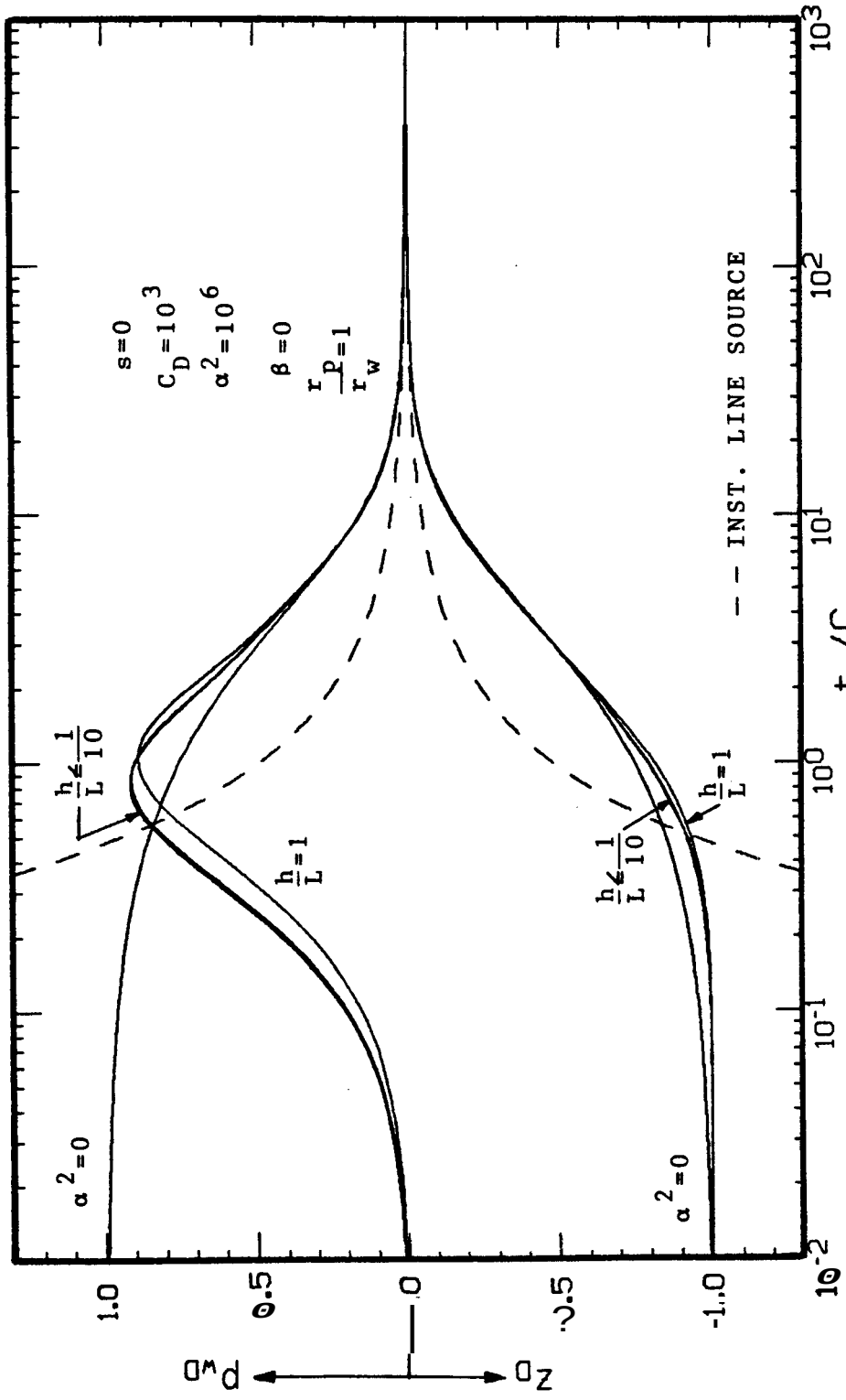

FIG. 5.11. SEMI-LOG GRAPH OF SLUG TEST SOLUTIONS FOR P_{wD} AND z_D VS t_D/C_D INCLUDING GRAVITATIONAL AND INERTIAL WELLBORE EFFECTS FOR DIFFERENT VALUES OF h/L IN A SYSTEM WITH s=0, $C_D=10^3$, $\alpha^2=10^6$, β=0, AND $r_p/r_w=1$

5.3.3 Effect of r_p/r_w

The coefficient A_w given by Eq. 5.47.a contains the ratio of dimensionless pipe radius with respect to slug size, and dimensionless wellbore radius with respect to slug size. According to Eqs. 3.33 and 3.34, this ratio can be simplified as $r_{pDz}/r_{wDz}=r_p/r_w$ to study the effect on slug test flow phenomena.

Figure 5.12 presents solutions obtained by applying the method for linear problems to a system with $s=0$, $C_D=10^3$, $\alpha^2=10^6$, $\beta=0$, and $h_D/L_D=1/10$, for different values of r_p/r_w. These solutions show negligible effects for $r_p/r_w<1$, which is the most common case. Only for systems with a pipe radius larger than twice the wellbore radius, i. e., $r_p/r_w>2$, some deviations are observed from the unaffected solution.

5.3.4 Combined Linear Effects

As described in sections 5.3.2 and 5.3.3, the inertial linear effects of h_D/L_D and r_{pDz}/r_{wDz} are small in comparison to other terms in wellbore Eq. 3.39.

Observation of solutions for $C_D{}^2 z_D{}''$ shown in Fig. 5.5.i indicates that dimensionless liquid column acceleration is maximum and constant at early times of a slug test. Moreover, Fig. 5.7.k shows that this maximum value is $z_{Dmax}{}''=\alpha^{-2}$ for a given system. Therefore, at early times, the liquid column acceleration term in wellbore Eq. 5.47 is maximum and equal to:

$$A_w\, z''_{Dmax} = 1 + \frac{3}{8}\frac{h_D}{L_D}\left[\frac{r_{pDz}}{r_{wDz}}\right]^2 \qquad \ldots (5.48)$$

From this expression, it can be said that the linear effects of h_D, L_D, r_{pDz}, and r_{wDz} are negligible for small values of the term which

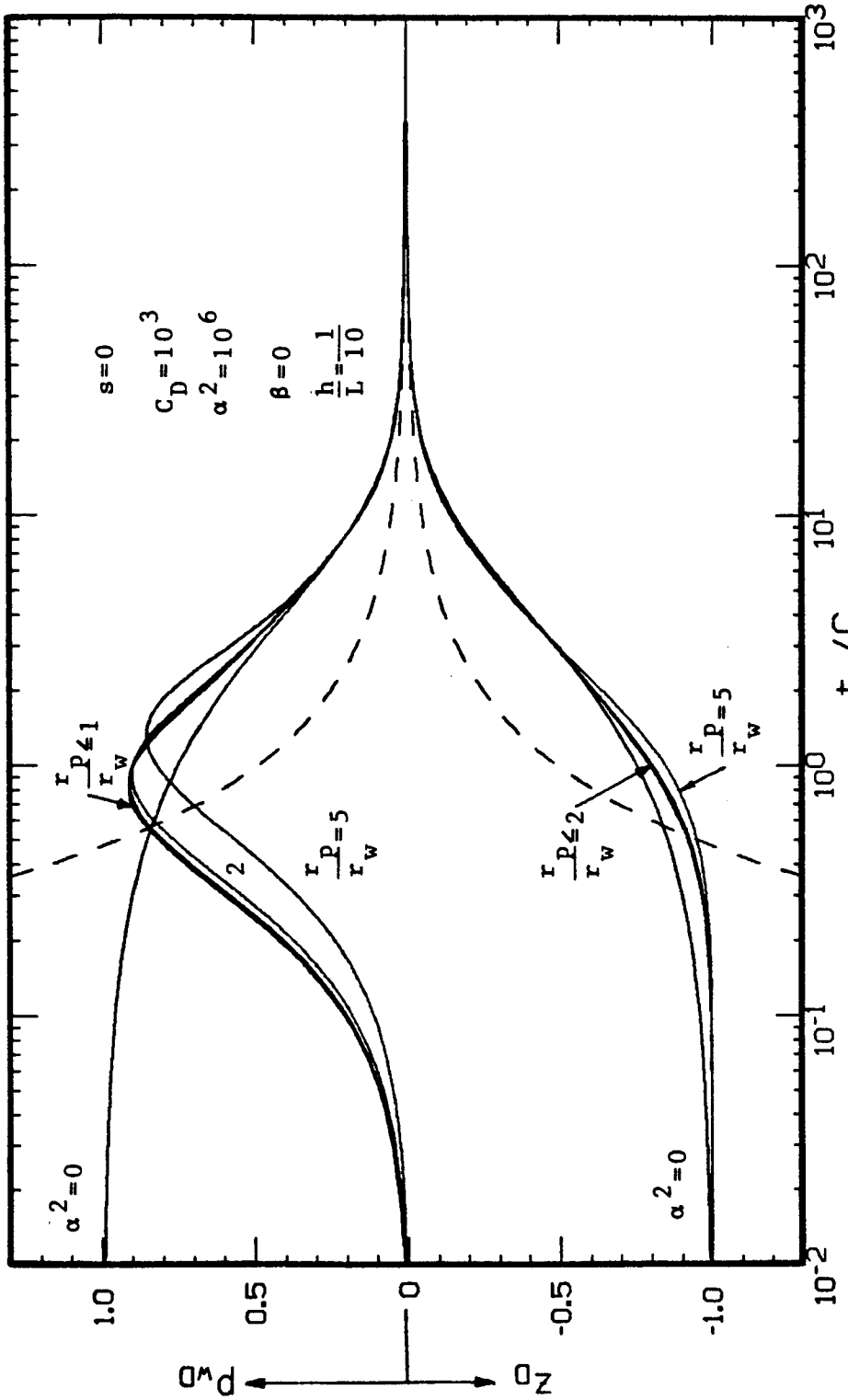

FIG. 5.12. SEMI-LOG GRAPH OF SLUG TEST SOLUTIONS FOR p_{wD} AND z_D VS t_D/C_D INCLUDING GRAVITATIONAL AND INERTIAL WELLBORE EFFECTS FOR DIFFERENT VALUES OF r_p/r_w IN A SYSTEM WITH s=0, $C_D=10^3$, $\alpha^2=10^6$, β=0, AND h/L=1/10

contains those parameters, as compared to unity. Taking this small value as 5%:

$$\frac{3}{8}\frac{h_D}{L_D}\left[\frac{r_{pDz}}{r_{wDz}}\right]^2 < \frac{5}{100} \qquad \ldots (5.49)$$

or, according to the definition of those parameters, the combined linear effect of h, L, r_p, and r_w is negligible for:

$$\frac{h}{L}\left[\frac{r_p}{r_w}\right]^2 < \frac{2}{15} \qquad \ldots (5.50)$$

Figures 5.13. 5.14, and 5.15 show results for some example systems. These results are analyzed qualitatively in Table 5.1. These examples were designed to obtain distinguishable effects to check the criteria developed in this section. No effort was made to use sets of dimensionless parameters for practical situations.

Solutions obtained for slug test, drillstem tests, and closed-chamber tests described by non-linear mathematical problems are presented in the following section.

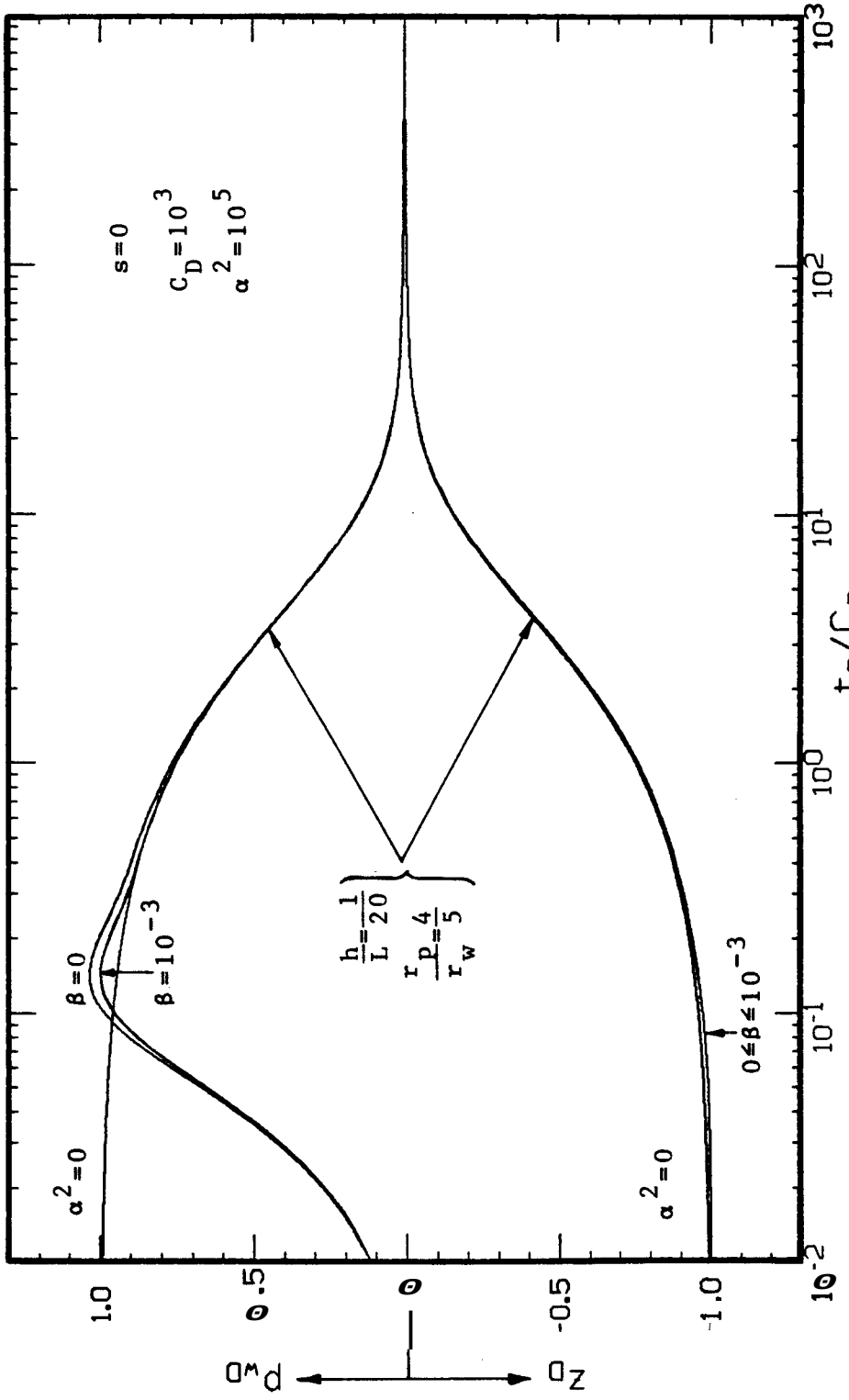

FIG. 5.13. SEMI-LOG GRAPH OF SLUG TEST SOLUTIONS FOR P_{wD} AND z_D VS t_D/C_D INCLUDING GRAVITATIONAL, INERTIAL, AND LAMINAR FRICTIONAL WELLBORE EFFECTS IN A SYSTEM WITH s=0, $C_D=10^3$, $\alpha^2=10^5$, $\beta=10^{-3}$, h/L=1/20, AND $r_p/r_w=C/5$

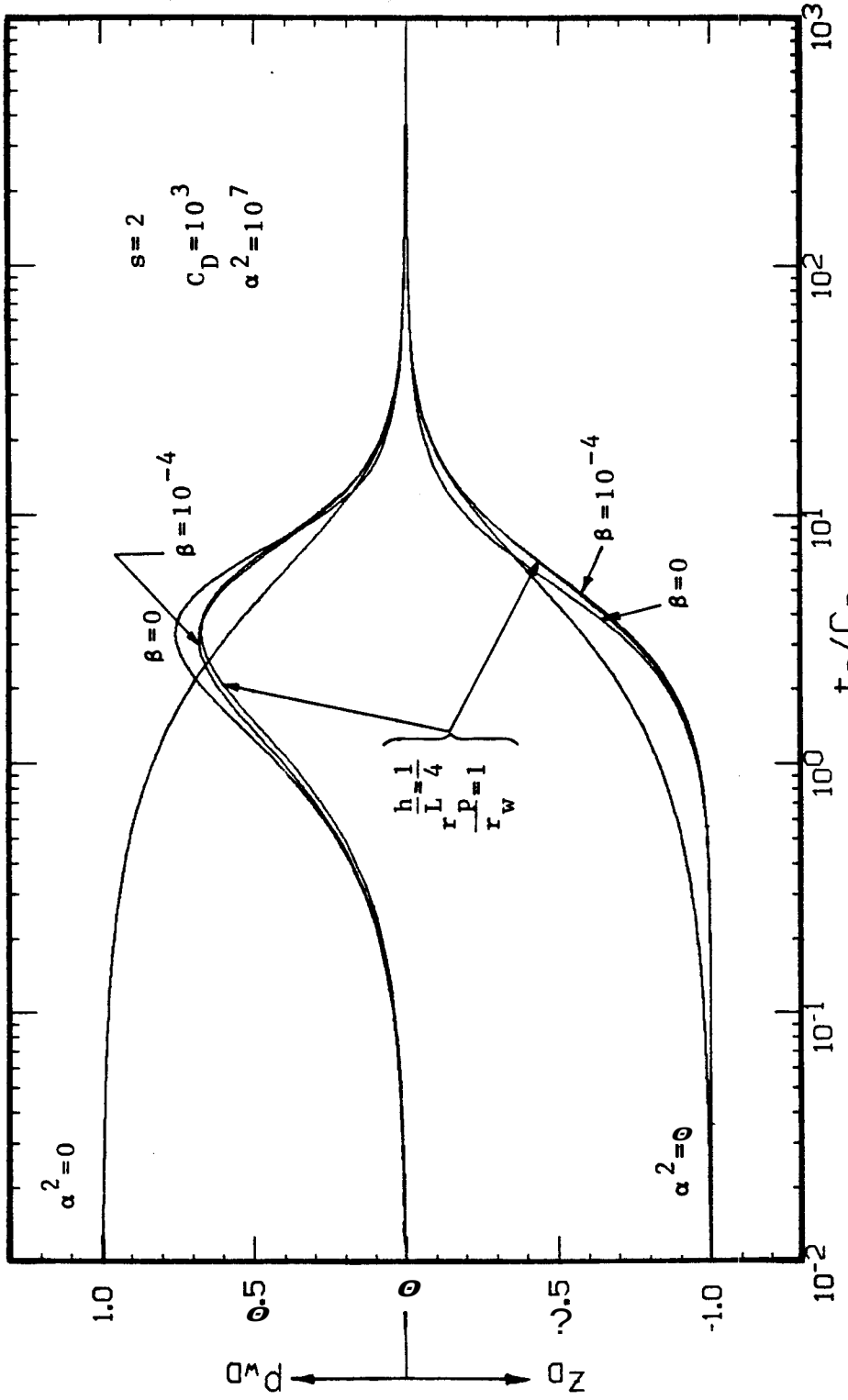

FIG. 5.14. SEMI-LOG GRAPH OF SLUG TEST SOLUTIONS FOR p_{wD} AND z_D VS t_D/C_D INCLUDING GRAVITATIONAL, INERTIAL, AND LAMINAR FRICTIONAL WELLBORE EFFECTS IN A SYSTEM WITH s=2, $C_D=10^3$, $\alpha^2=10^7$, $\beta=10^{-4}$, h/L=1/4, AND $r_p/r_w=1$

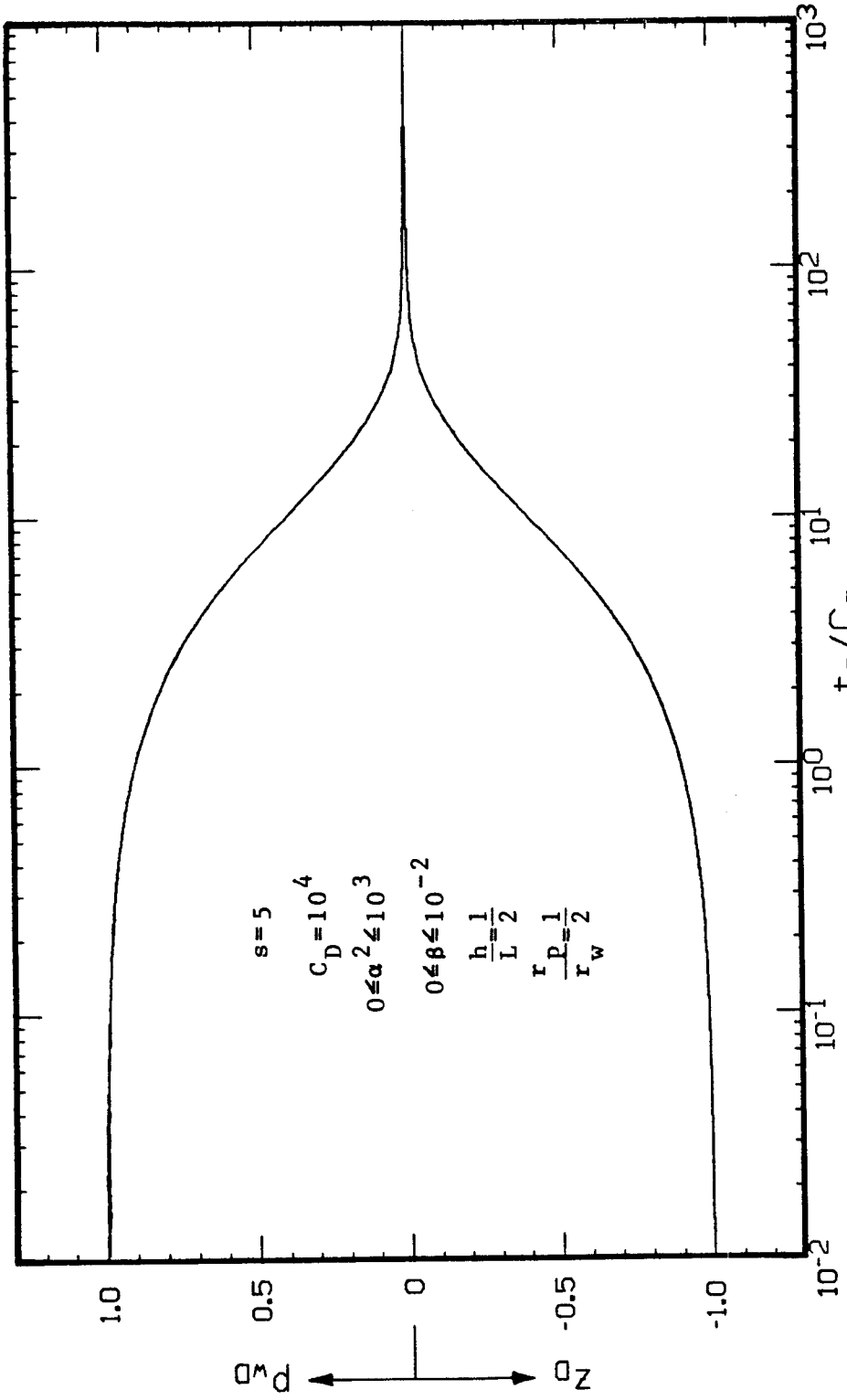

FIG. 5.15. SEMI-LOG GRAPH OF SLUG TEST SOLUTIONS FOR P_{wD} AND z_D" VS t_D/C_D INCLUDING GRAVITATIONAL, INERTIAL, AND LAMINAR FRICTIONAL WELLBORE EFFECTS IN A SYSTEM WITH s=5, $C_D=10^4$, $\alpha^2=10^3$, $\beta=10^{-2}$, h/L=1/2, AND $r_p/r_w=1/2$

TABLE 5.1. QUALITATIVE ANALYSIS OF LINEAR SLUG TEST EFFECTS FOR RESULTS SHOWN IN FIGS. 5.13 - 5.15.

FIG.	DATA						EFFECTS						
							INERTIAL		FRICTIONAL				COMBINED h/L & r_p/r_w
	s	C_D	α^2	β	h/L	r_p/r_w	$C_D^2/10$	EQ. 5.33	$\alpha^2\beta$	$C_D/10$	EQ. 5.35	$\frac{3}{8}\frac{h}{L}[\frac{r_p}{r_w}]^2$	EQ. 5.49
5.13	0	10^3	10^5	10^{-3}	1/20	1/5	10^5	S	10^2	10^2	S	3/250	N
5.14	2	10^3	10^7	10^{-4}	1/4	1	10^5	L	10^3	10^2	L	1/8	L
5.15	5	10^4	10^4	10^{-2}	1/2	1/2	10^7	N	10^1	10^3	N	3/64	S

N = NEGLIGIBLE
S = SMALL
L = LARGE

SECTION 6
EVALUATION AND DISCUSSION OF NON-LINEAR PROBLEM SOLUTIONS

In this section, the numerical method described in Section 4.2, and implemented by the computer program presented in Appendix F, is used to evaluate solutions including non-linear wellbore effects not previously considered in the literature. First, the computer program was validated by reproducing available solutions for linear problems. The non-linear effect of the cushion size, which is directly related to the slug size, was evaluated and analyzed in Section 6.2. The complete wellbore equation, Eq. 3.39, was used to evaluate the non-linear effect of liquid friction caused by a changing flow rate during a drillstem test, or during a closed-chamber test. Flow phenomena in a reservoir after the well is shut-in can also be evaluated by this numerical method to obtain pressure buildup solutions that permit the possibility of performing integral analysis of both the flowing and the shut-in periods of a drillstem test, or of a closed-chamber test.

6.1. Computer Program Validation

A numerical solution should be validated before application. Validation should be performed to assure a correct formulation and a minimal effect of truncation and round-off errors. The computer program presented in Appendix F was tested against a number of linear problems for which a solution was known from the application of the semi-analytical method presented in Section 4.1.

Figures 6.1 - 6.3 show comparisons of results from numerical and semi-analytical solutions for systems with $s=0$, and $C_D=10^3$ for different values of β, and for values of $\alpha^2=10^4$, 10^6, and 10^8, respectively.

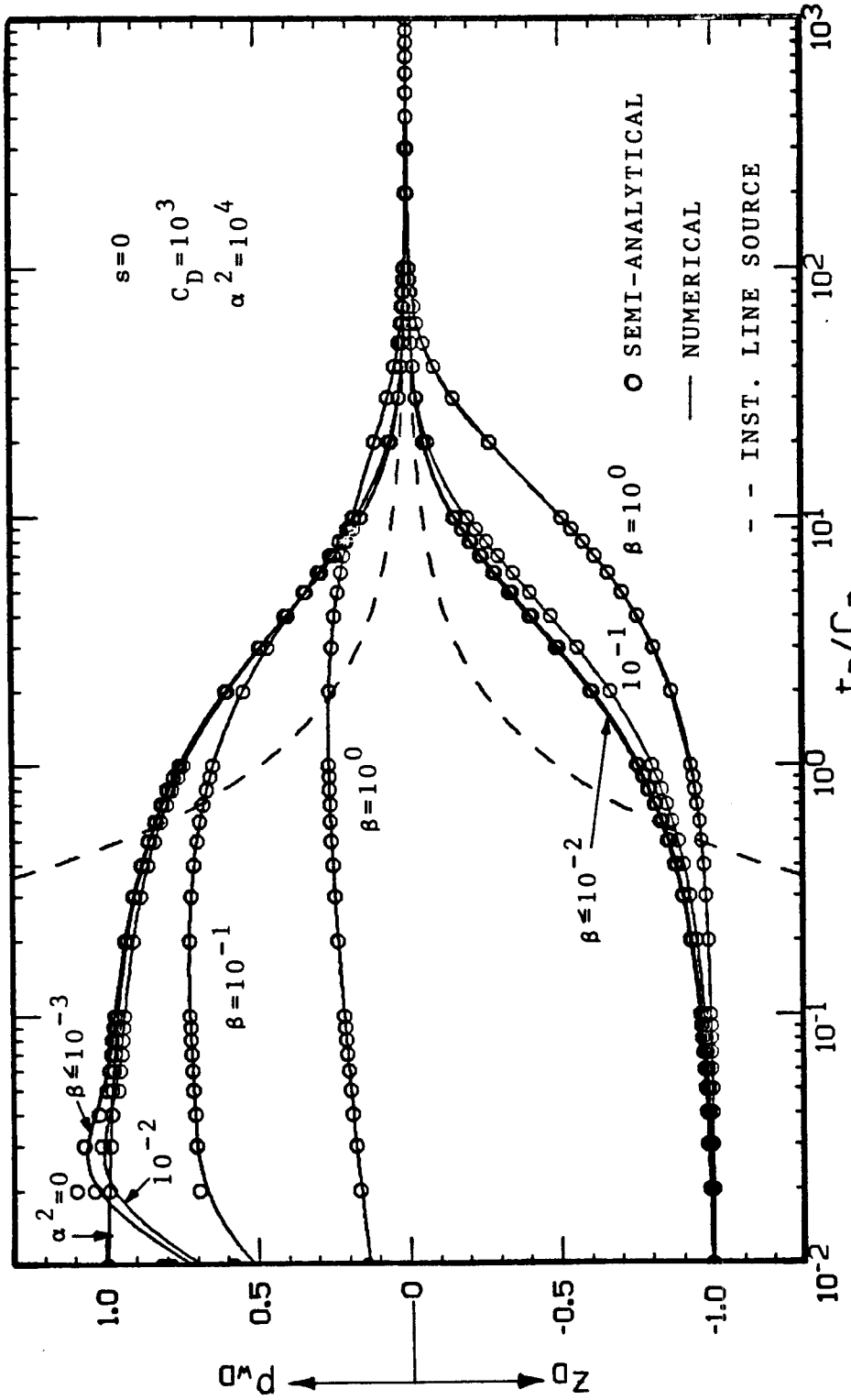

FIG. 6.1. COMPARISON OF SEMI-ANALYTICAL AND NUMERICAL SOLUTIONS FOR P_{wD} AND z_D VS t_D/C_D INCLUDING GRAVITATIONAL, INERTIAL, AND LAMINAR FRICTIONAL WELLBORE EFFECTS FOR A SYSTEM WITH s=0, $C_D=10^3$, AND $\alpha^2=10^4$

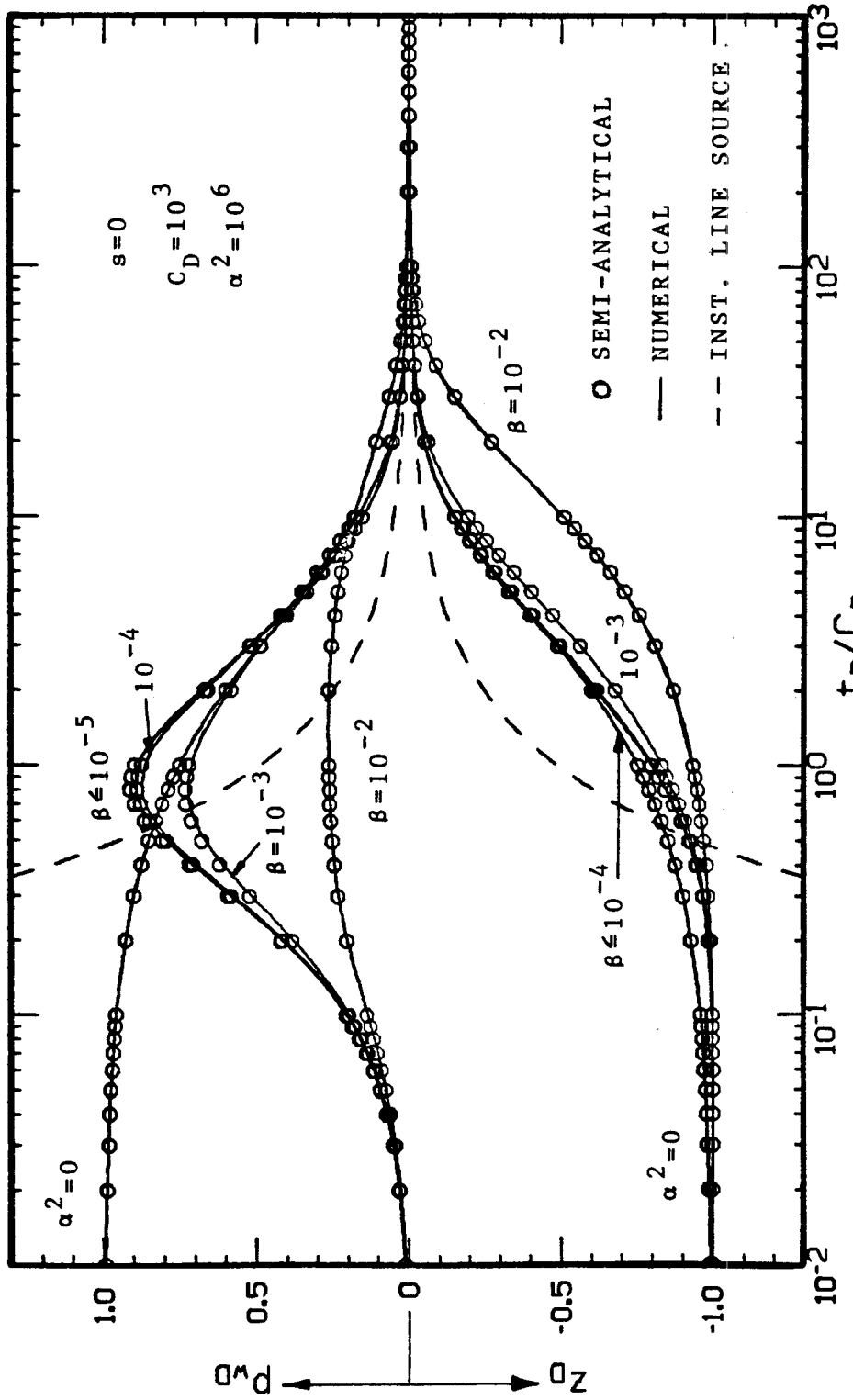

FIG. 6.2. COMPARISON OF SEMI-ANALYTICAL AND NUMERICAL SOLUTIONS FOR p_{wD} AND z_D VS t_D/C_D INCLUDING GRAVITATIONAL, INERTIAL, AND LAMINAR FRICTIONAL WELLBORE EFFECTS FOR A SYSTEM WITH s=0, $C_D=10^3$, AND $\alpha^2=10^6$

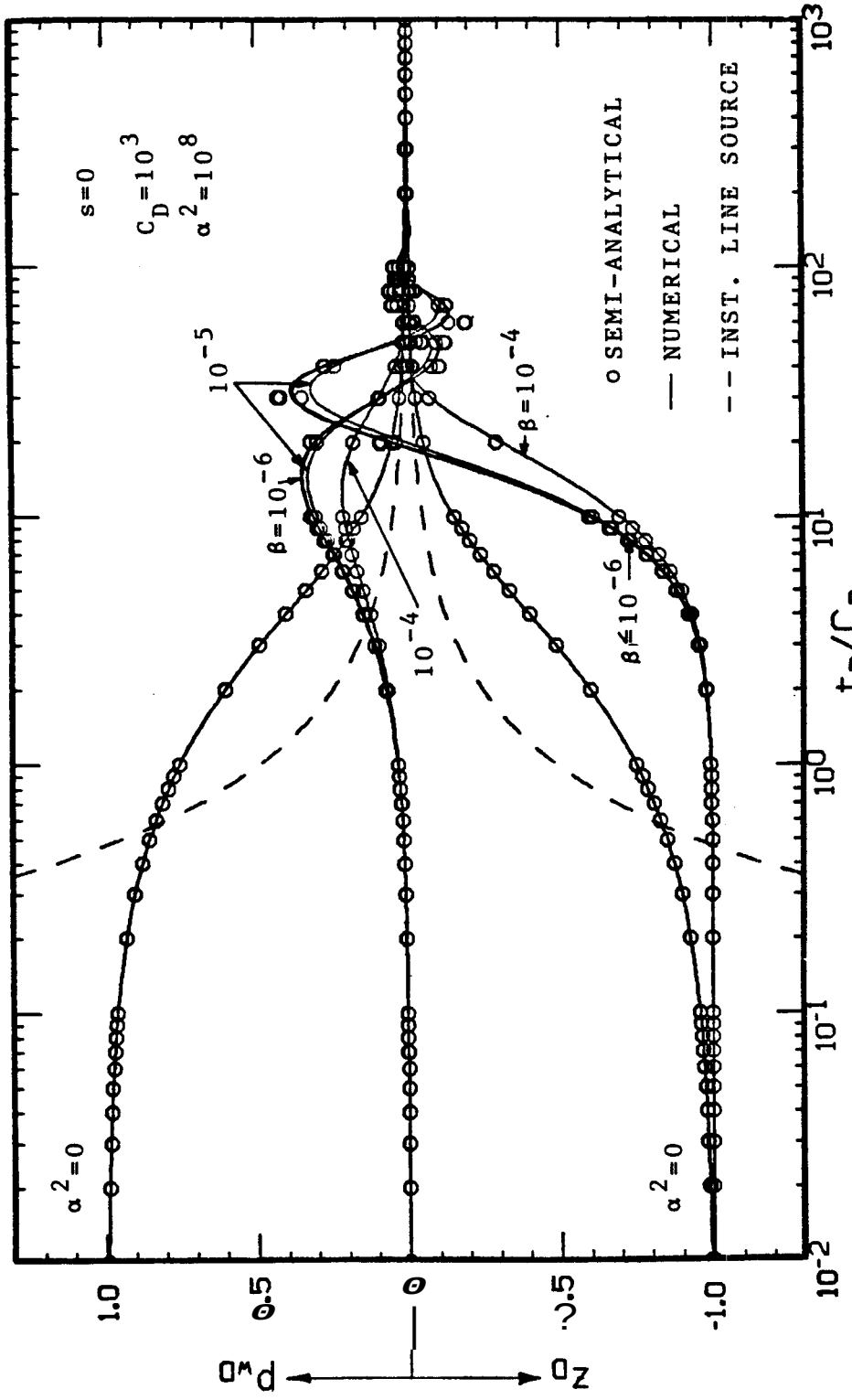

FIG. 6.3. COMPARISON OF SEMI-ANALYTICAL AND NUMERICAL SOLUTIONS FOR p_{wD} AND z_D" VS t_D/C_D INCLUDING GRAVITATIONAL, INERTIAL, AND LAMINAR FRICTIONAL WELLBORE EFFECTS FOR A SYSTEM WITH s=0, $C_D=10^3$, AND $\alpha^2=10^8$

The numerical solutions shown in Figs. 6.1 - 6.3 were obtained by using an algorithm that increases the time step size by multiplying by a constant factor of $f_t=1.05$. The solution requires approximately 40 time steps per logarithmic cycle of time, except for the initial cycle, for which the algorithm requires approximately 10 time steps. Thus, all simulations were started at least one logarithmic cycle before the earliest time shown in the results presented in this study.

The number of nodes used to discretize a reservoir and obtain the results shown in this study was J=51. The radius of the outer boundary of a reservoir was evaluated by an expression derived in Appendix D, $r_{De}=2\sqrt{1000C_D}$. The validity of the approximation was tested by printing the dimensionless reservoir pressure at the outer boundary, p_{wD_J}, and it was observed that p_{wD_J} was smaller than 10^{-3} during all simulated tests. The values of $f_t=1.05$, J=51, and $r_{De}=2\sqrt{1000C_D}$ were used to generate all of the solutions presented in this study.

6.2 Effect of Cushion Size

A momentum balance wellbore equation including inertial effects was proposed by Cooper, Bredehoeft, Papadopulos, and Bennett (1965) to explain observations of liquid level oscillations in response to seismic waves. Those authors assumed that liquid level variations z(t) were small when compared to the static liquid level length, L. As a consequence, those authors reached the conclusion that the aquifer-wellbore response was analogous to the response of the classical mechanical system of a spring supporting a mass submerged in a viscous fluid.

As described in the literature review, other authors have used a similar wellbore equation, or special cases of it, to include the effect of inertia on the analysis of slug test data. Therefore, the assumption that the slug length, $L_s=-z_0$, is negligible in comparison to L is also implicit in the slug test solutions considering wellbore inertia currently available in the literature.

As mentioned in Section 3, a flow period of a drillstem test contains all the elements of a slug test. However, a drillstem test is usually conducted early in the development of a reservoir, when an accurate estimation of the initial reservoir pressure is not available. A common practice is to start the flow period of a drillstem test with a liquid cushion, normally water, above the drillstem test valve with the purpose of avoiding an extreme drop in pressure and shock on the formation. The length of the cushion is decided mainly by experience and often is only of the order of a few hundred feet. Since initial reservoir pressure is related to hydrostatic geo-pressure gradient, the cushion length, $L_c=L+z_0$, is generally small compared to L for most drillstem conditions found in practice. This situation corresponds to a large slug size, $-z_0$, of the order of L. Moreover, this initial condition can also result in large variations of z(t).

6.2.1 Special Wellbore Equation

The effect of the cushion size, or its complement, the slug size, can be analyzed by considering the following simplification of wellbore Eq. 3.39 derived in the present study:

$$A_w z''_D + B_w z'_D + C_w z_D + D_w = E_w p_{wD} \qquad \ldots (6.1)$$

with:

$$A_w = a^2 \left[1 + \frac{z_D}{L_D} \right] \qquad \ldots (6.1.a)$$

$$B_w = 0 \qquad \ldots (6.1.b)$$

$$C_w = 1 \qquad \ldots (6.1.c)$$

$$D_w = 0 \qquad \ldots (6.1.d)$$

$$E_w = -1 \qquad \ldots (6.1.e)$$

According to the definition of coefficient A_w, Eq. 6.1.a, this wellbore equation is non-linear. The definition of coefficient B_w, Eq. 6.1.b, indicates that frictional effects are considered negligible to isolate the inertial effect of the cushion size.

The numerical method for non-linear problems described in Section 4.2 can be used to solve the problem stated by Eqs. 6.1 and 3.40 - 3.46. An option in the computer program presented in Appendix F allows evaluation of the behavior of p_{wD}, z_D, $C_D p_{wD}'$, $C_D z_D'$, $C_D^2 z_D''$, and $p_D(r_D)$ with s, C_D, α^2, and L_D as input data.

6.2.2 Effect of L_D

Wellbore Eq. 6.1 includes one more term than the wellbore equation considered by Shinohara and Ramey (1979.b), Eq. 5.25. This additional term is $[\alpha^2 z_D/L_D]z_D''$. Since z_D varies from -1 to 0, the relative importance of this additional term with respect to the term $\alpha^2 z_D''$ is defined by the magnitude of $L_D = L/-z_0$.

Figure 6.4 shows the values of L_D considered in this study for a production slug test. Figure 6.5 is useful to relate values of L_D with the relative magnitude of the slug size or cushion size with respect to the static liquid column length, L. The larger the absolute value of L_D, the smaller the slug size and the larger the cus'hion size.

Figures 6.6 - 6.8 present results for p_{wD} and z_D for systems with s=0, C_D=103, for values of L_D shown in Fig. 6.4, and for values of α^2=104, 10^6, and 108, respectively. The time axis in Fig. 6.6 has been shifted to the left one logarithmic cycle to show the effects of the cushion size. These figures indicate that for large slug sizes (small cushion sizes) the initial pressure drops are shifted to earlier times as L_T approaches 1. This corresponds to a condition with no cushion, which implies an initial infinite acceleration because z_D=-1, p_{wD}=0, and A_w=0 at initial conditions. In this case, wellbore Eq. 6.1 simplifies to $A_w z_D''$=1. Also, these figures show that the approximation of negligible slug size is closely met for conditions given by:

$$L_D > 20 \qquad \ldots (6.2)$$

or, in terms of real variables:

$$-z_0 < \frac{L}{20} \qquad \ldots (6.3)$$

Figures 6.6 and 6.7, which correspond to systems with practically negligible inertial effects because a2<α_I^2=C_D2/10=105, indicate that the early pressure drop shifts towards earlier times for smaller cushion sizes, reducing the inertial effects. However, Fig. 6.8 for α^2=108 shows large oscillations of p_{wD} and z_D, with larger oscillations for z_D than for p_{wD}, as the cushion size decreases. This indicates that for a2>α_0^2=20C_D^2=2[107], a small cushion size increases the inertial effects. These two different effects of the cushion size lead one to

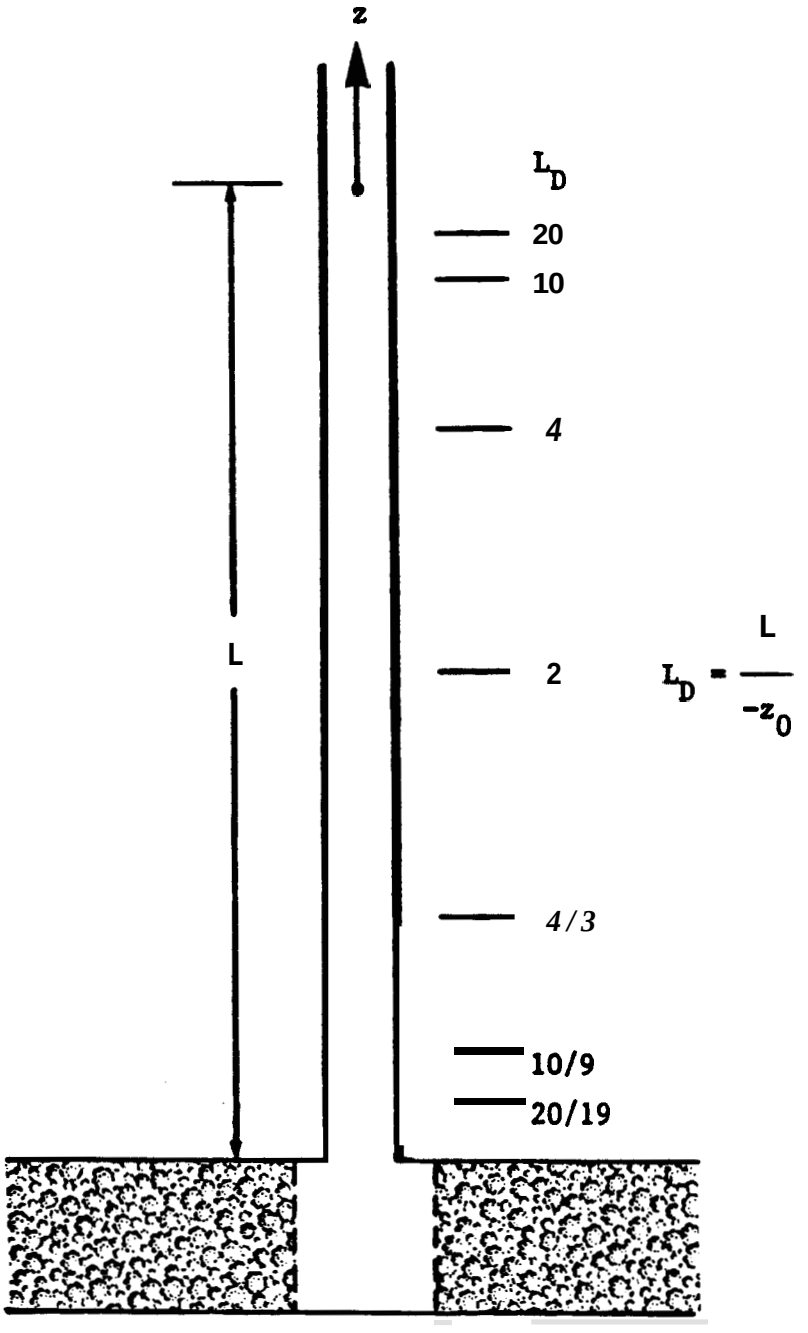

FIG. 6.4. SCHEMATIC DIAGRAM SHOWING VALUES OF L_D USED TO ANALYZE THE EFFECT OF THE CUSHION SIZE ON THE FLOW PHENOMENA WRING A DRILLSTEM TEST

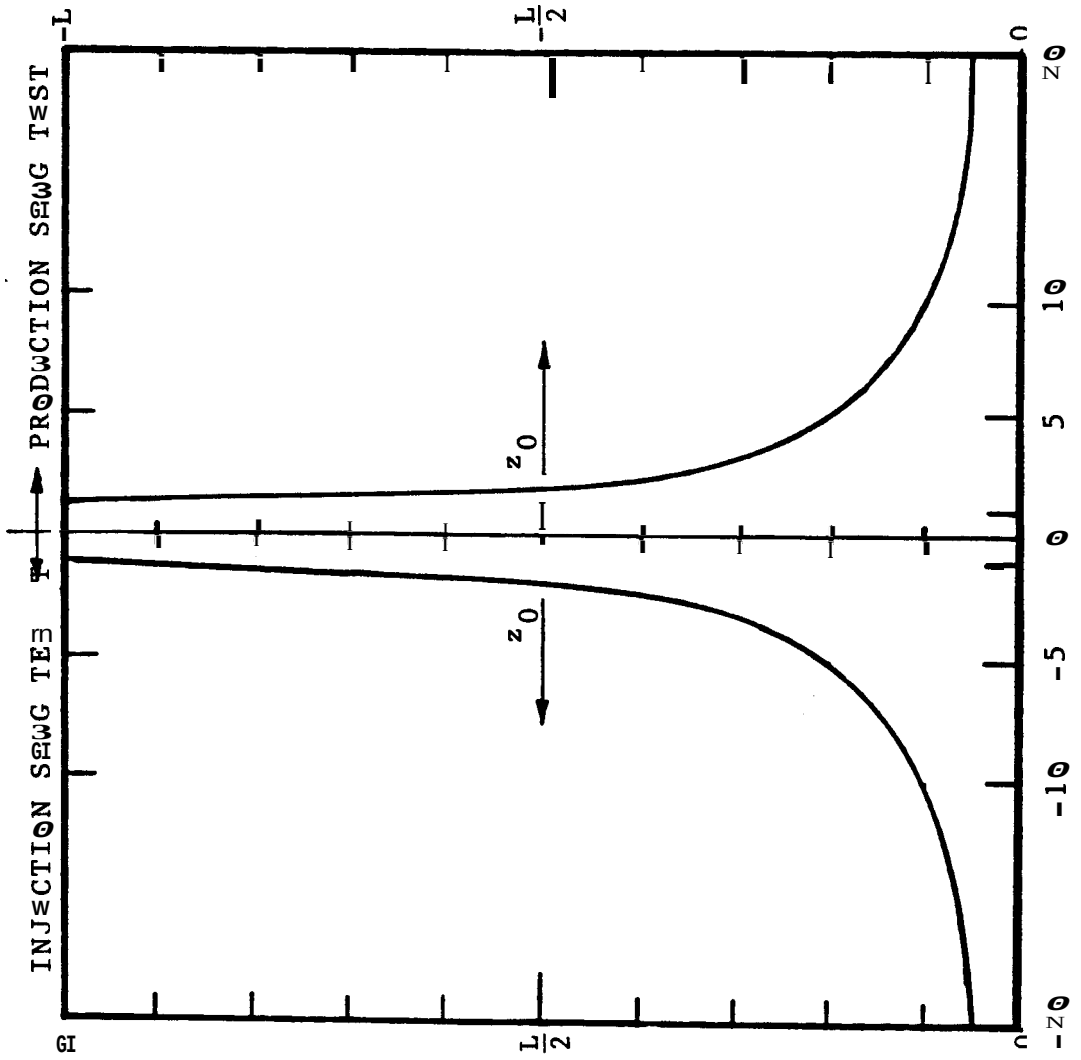

FIG. 6.5. GRAPHICAL REPRESENTATION OF THE RELATIONSHIP BETWEEN L_D AND THE CUSHION AND SLUG SIZE FOR PRODUCTION AND INJECTION SLUG TESTS

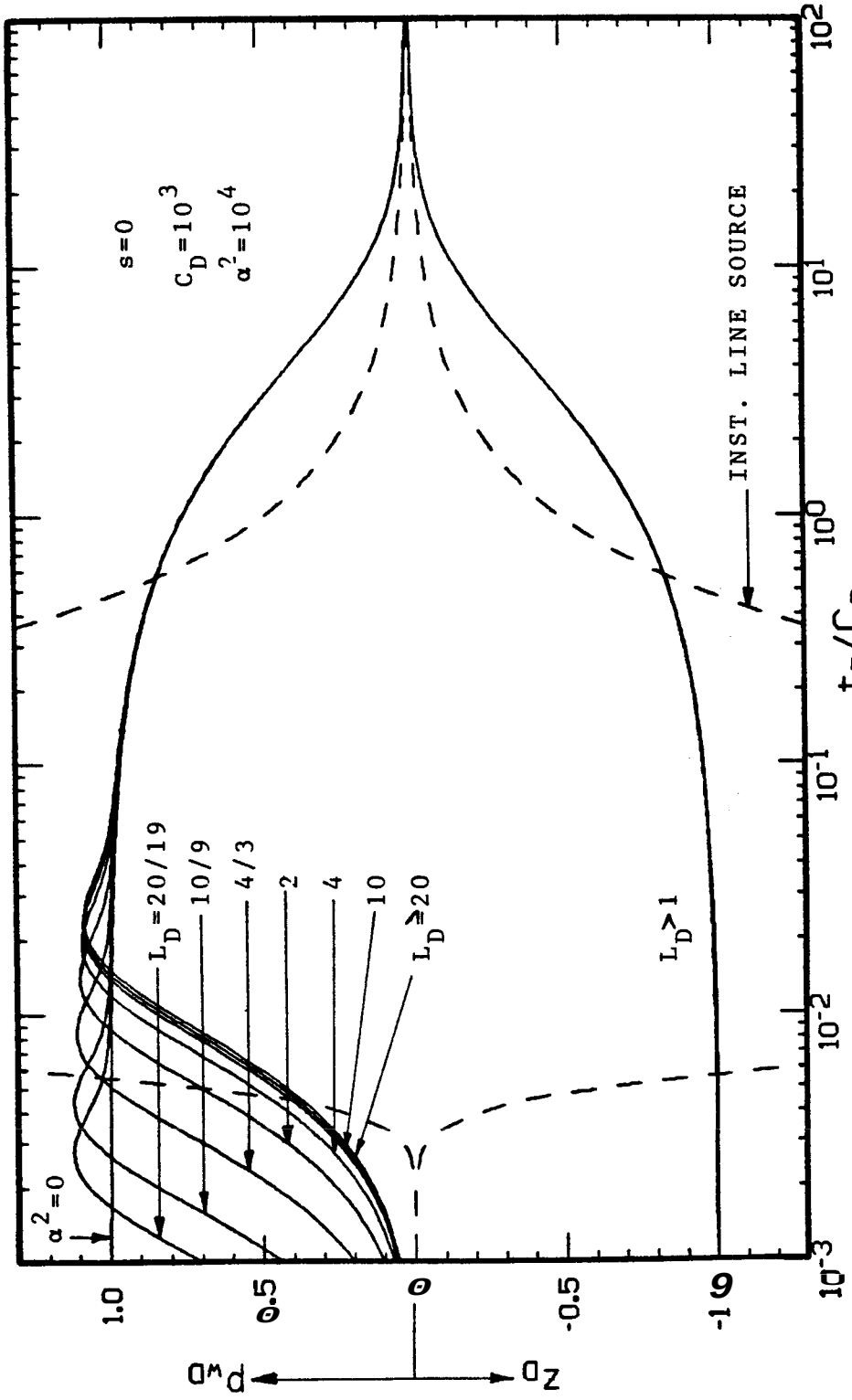

FIG. 6.6. EFFECT OF CUSHION SIZE ON FLOW PHENOMENA DURING A DRILLSTEM TEST FOR A SYSTEM WITH s=0, $C_D=10^3$, AND $\alpha^2=10^4$

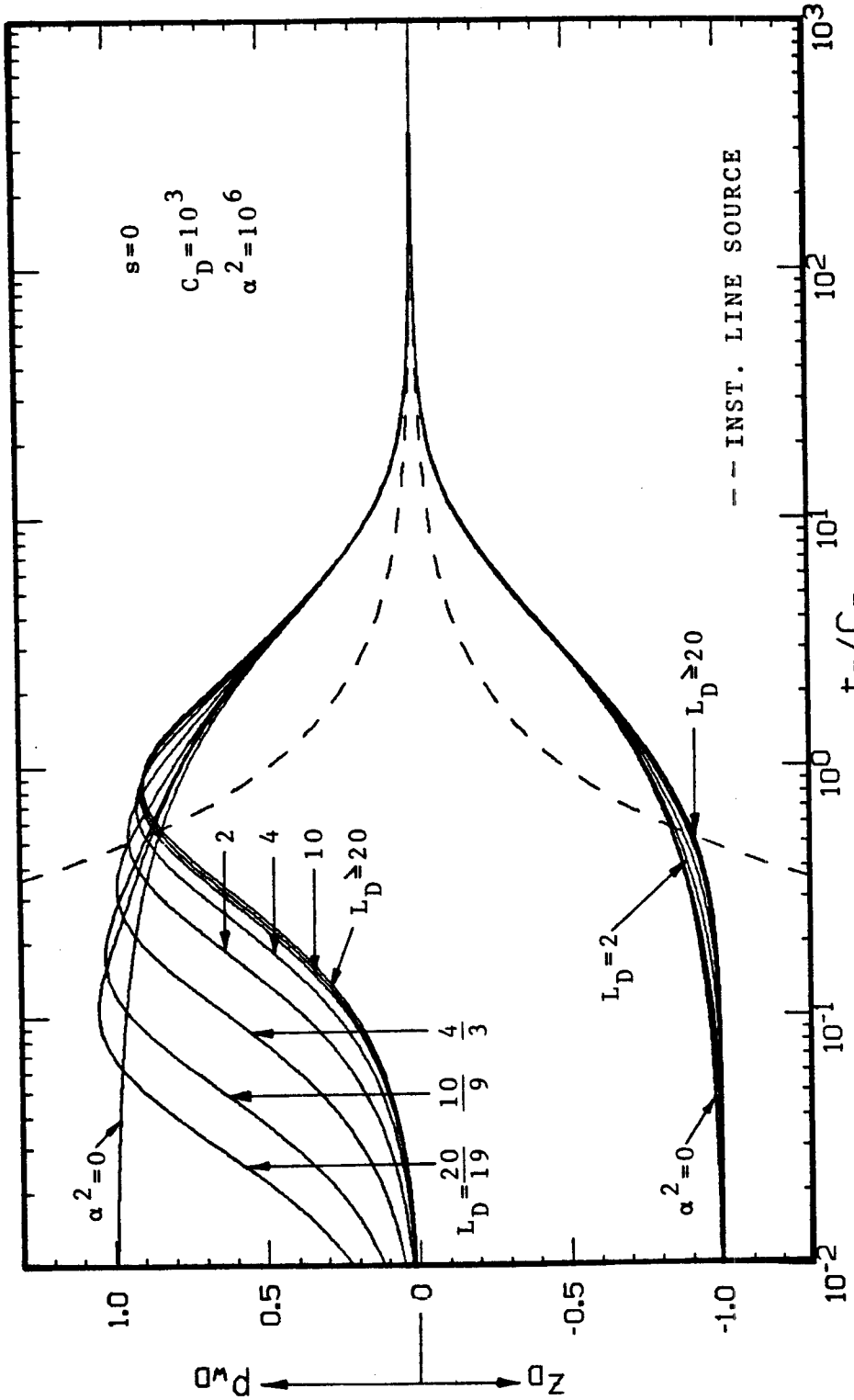

FIG. 6.7. EFFECT OF CUSHION SIZE ON FLOW PHENOMENA DURING A DRILLSTEM TEST FOR A SYSTEM WITH s=0, $C_D=10^3$, AND $\alpha^2=10^6$

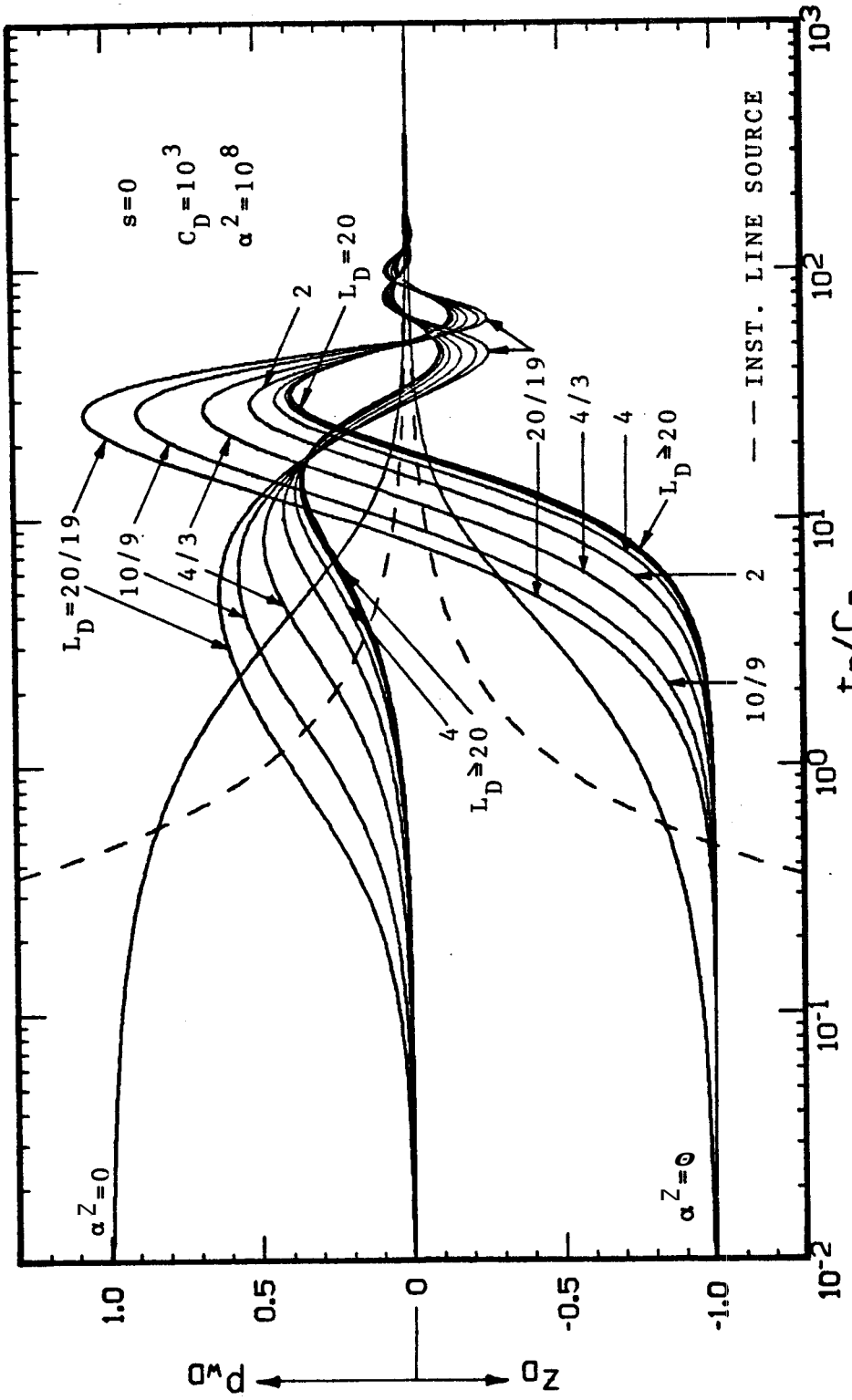

FIG. 6.8. EFFECT OF CUSHION SIZE ON FLOW PHENOMENA DURING A DRILLSTEM TEST FOR A SYSTEM WITH s=0, $C_D=10^3$, AND $\alpha^2=10^8$

conclude that the mass of liquid in the wellbore can not be considered constant for the case of a small cushion, especially for underdamped systems. Hence, for a small cushion length, $L+z_0$, with respect to L, the analogy between the response of a reservoir–wellbore system and the response of the classical mechanical system of a spring with a mass submerged in a viscous fluid is valid only if the mass is considered a function of the displacement.

For the case of an injection slug test, z_0 is positive and L_D is negative. The computer program in Appendix F can also be used to solve this problem. For this type of test, the solutions for p_{wD} and z_D at early times shift towards later times as L_D increases in the range $0>L_D>-20$, increasing the inertial effect. However, this range of values of L_D is not of much importance in slug test or drillstem test practice.

6.3 Solutions including Friction

The effect of friction as the fluid moves along the vertical wellbore pipe was studied in Section 5.2 for the particular case of laminar flow friction. When other flow regimes are considered, wellbore Eq. 3.39 is non–linear but can be solved by using the numerical method described in Section 4.2.

6.3.1 Special Wellbore Equation

In order to isolate the non–linear effect of friction for pipe flow changing in regime, the following simplified wellbore equation is considered in this section:

$$A_w z''_D + B_w z'_D + C_w z_D + D_w = E_w p_{wD} \qquad \ldots (6.4)$$

with:

$$A_w = a^2 \quad \ldots (6.4.a)$$

$$B_w = \alpha 2 \frac{f}{4} \left| \frac{1}{r_{pDz}} z'_D \right| \quad \ldots (6.4.b)$$

$$C_w = 1 \quad \ldots (6.4.c)$$

$$D_w = 0 \quad \ldots (6.4.d)$$

$$E_w = -1 \quad \ldots (6.4.e)$$

In this wellbore equation, slug size and reservoir thickness are assumed negligible in comparison to the static liquid column length to isolate the effect of friction.

For flow of a liquid in a smooth pipe, the Moody friction factor, f, depends on Reynold's number, Re, and flow regime for laminar and critical flow, but also depends on relative roughness, e_D, for transition and turbulent flow, as follows:

For $Re \leq 2000$, Laminar Flow Regime:

$$f = \frac{64}{Re} \qquad \ldots (6.5)$$

For $2000 < Re \leq 4000$, Critical Flow Regime:

$$f = \frac{0.5}{Re^{0.3}} \qquad \ldots (6.6)$$

For $4000 < Re \leq \left[\frac{2000}{e_D} \right]^{1.16}$, Transition Flow Regime:

$$f = \left\{ 1.14 - 2 \log \left[e_D + \frac{9.34}{Re \sqrt{f}} \right] \right\}^{-2} \qquad \ldots (6.7)$$

For $Re > \left[\frac{2000}{e_D} \right]^{1.16}$, Turbulent Flow Regime:

$$f = \left[1.14 - 2 \log(e_D) \right]^{-2} \qquad \ldots (6.8)$$

These equations for evaluating f have been implemented by a subroutine of the computer program presented in Appendix F. For the transition flow regime, Eq. 6.7 requires iterative calculation of f.

The definition of Reynold's number for the system under consideration is given by Eqs. 5.39 and 5.40. Equation 5.40 can be expressed as:

$$Re = \frac{16}{\beta} \left| \frac{1}{r_{pDz}} z'_D \right| \qquad \ldots (6.9)$$

where β was defined in Eq. 5.43, as follows:

$$\beta = \frac{8}{\frac{\rho}{\mu_p}\left[\frac{k}{\phi\mu c_t r_w^2}\right] r_p^2} \qquad \ldots (5.46)$$

Solutions for this problem are presented in the following section.

6.3.2 Effect of β, e_D, and r_{pDz} for changing Flow Regimes

An option in the computer program presented in Appendix F allows one to evaluate a numerical solution for the problem statement given by **Eqs.** 6.4 and 3.40 - 3.46. This option requires input values of s, and C_D to evaluate the skin factor and wellbore storage effects, a value of α^2 to include inertial effects, and a value of β and r_{pDz} to calculate the Reynold's number and determine the flow regime to compute the correct Moody friction factor. Also, a value of relative roughness e_r is required to perform calculations for either the transition or turbulent flow regimes.

Figures 6.9 - 6.11 are semi-log graphs of the results of this program for p_{wD} and z_D including gravitational, inertial, and frictional effects for systems with s=0, $C_D=10^3$, for different combinations of values of β, r_{pDz}, and e_D, and for values of $\alpha^2=10^4$, 10^6, and 10^8, respectively. The different flow regimes for each case are also indicated in these figures. The value of the parameters used to generate these figures was chosen to have a noticeable effect. Since there are several reservoir properties, fluid characteristics, and wellbore dimensions that appear in more than one of the dimensionless parameters involved in the description of this problem, the solutions obtained may not correspond to a real system. More discussion of the possible values of a dimensionless parameter in a given combination set of data is given in Section 7, where some practical considerations are presented.

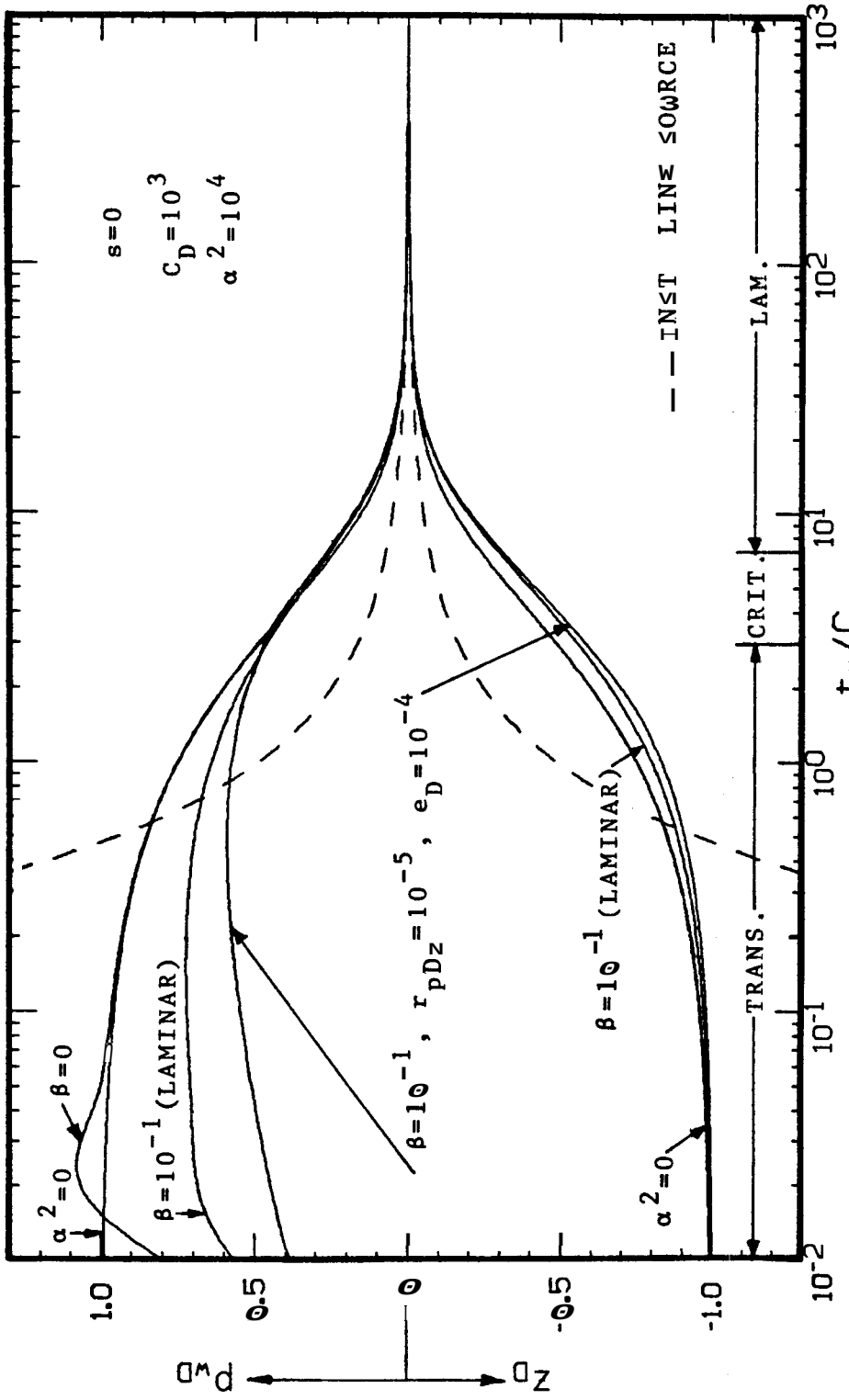

FIG. 6.9. SEMI-LOG GRAPH OF SLUG TEST SOLUTIONS FOR P_{wD} AND z_D VS t_D/C_D INCLUDING GRAVITATIONAL, INERTIAL, AND FRICTIONAL WELLBORE EFFECTS FOR A SYSTEM WITH s=0, $C_D=10^3$, $\alpha^2=10^4$, $\beta=10^{-1}$, $e_D=10^{-4}$, $r_{pDz}=10^{-5}$

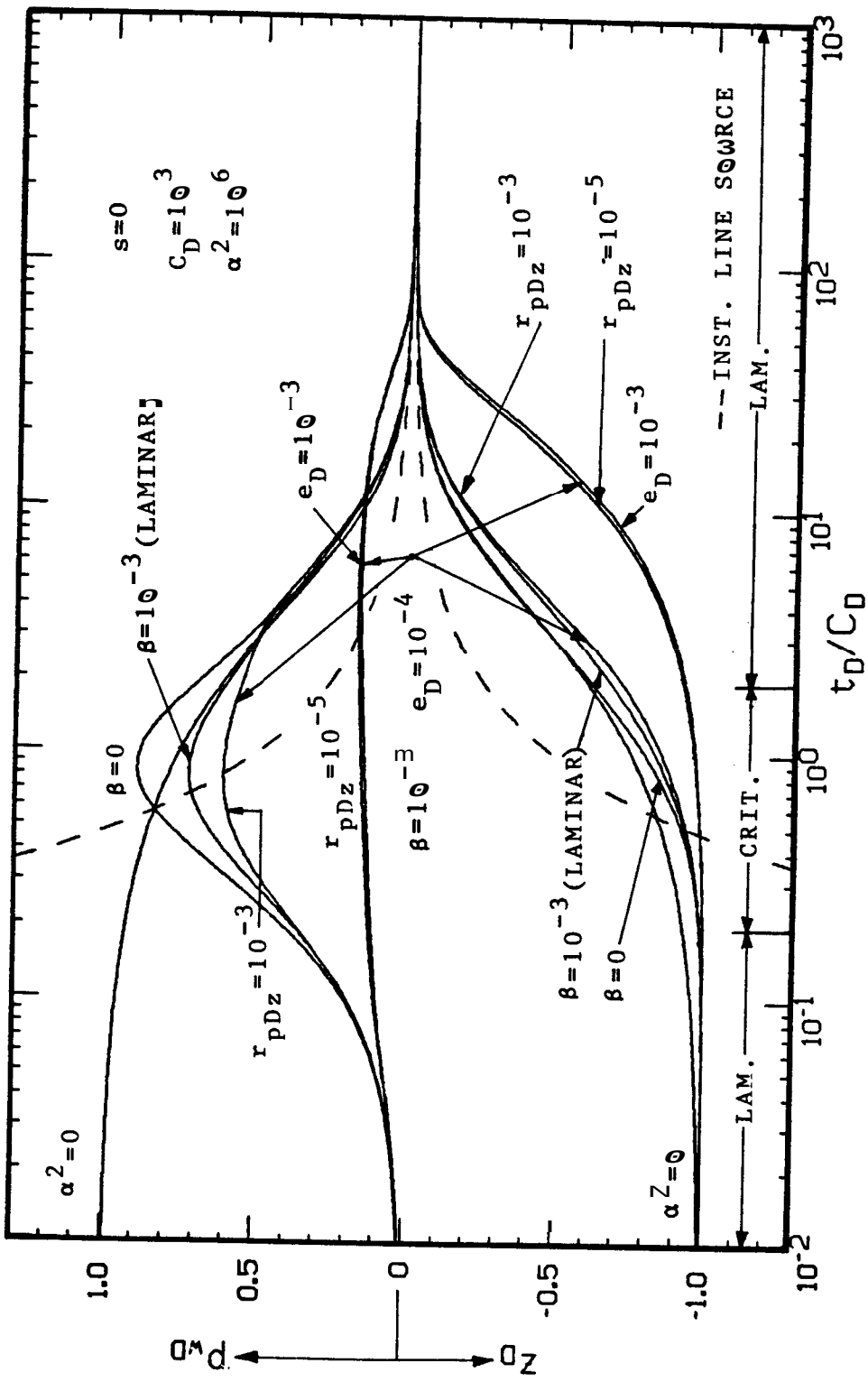

FIG. 6.10. SEMI-LOG GRAPH OF SLUG TEST SOLUTIONS FOR P_{wD} AND z_D VS t_D/C_D INCLUDING GRAVITATIONAL, INERTIAL, AND FRICTIONAL WELLBORE EFFECTS FOR A SYSTEM WITH $s=0$, $C_D=10^3$, $\alpha^2=10^6$, $\beta=10^{-3}$, $e_D=10^{-4}$, $r_{pDz}=10^{-5}$

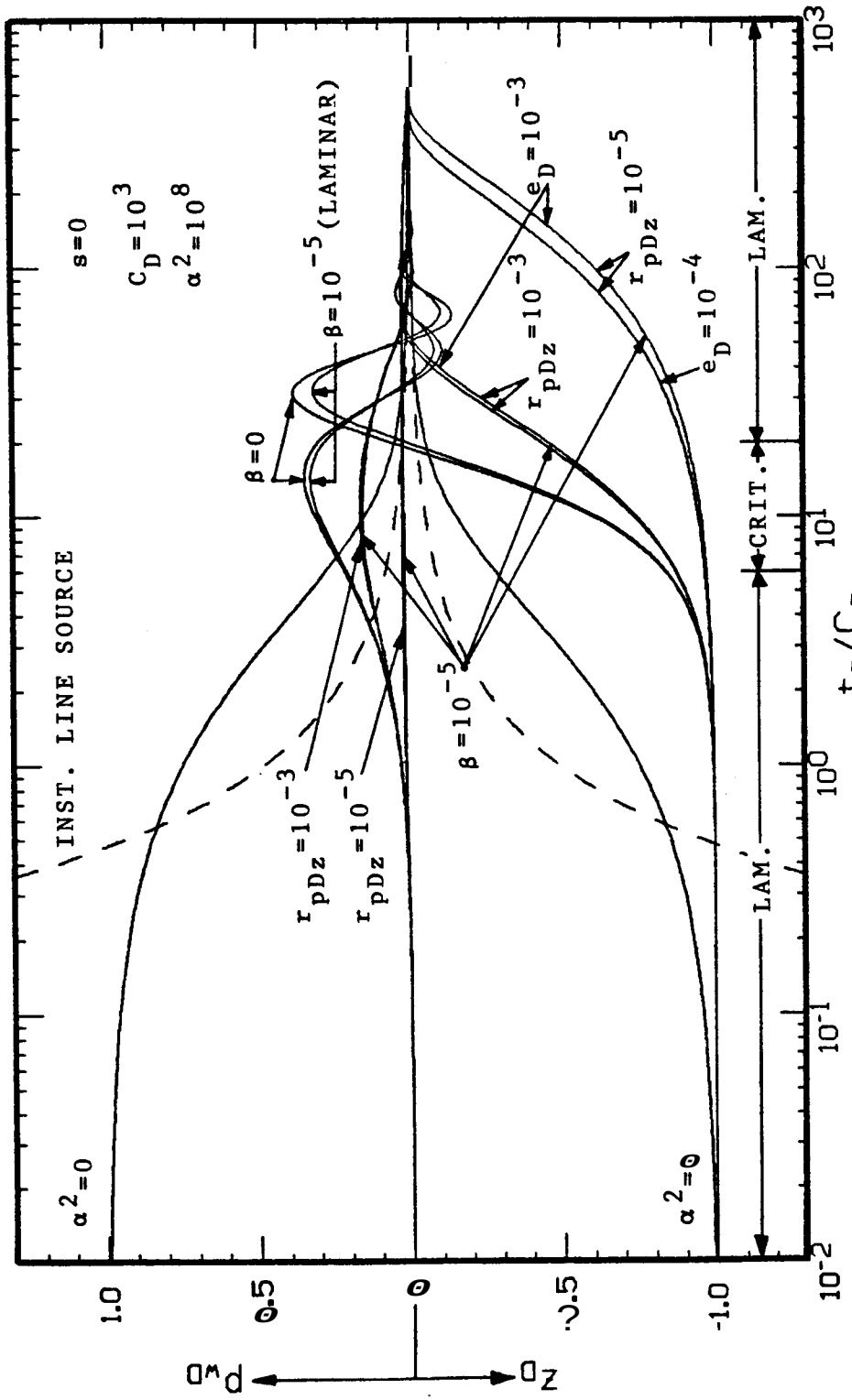

FIG. 6.11. SEMI-LOG GRAPH OF SLUG TEST SOLUTIONS FOR P_{wD} AND z_D VS t_D/C_D INCLUDING GRAVITATIONAL, INERTIAL, AND FRICTIONAL WELLBORE EFFECTS FOR A SYSTEM WITH s=0, $C_D=10^3$, $\alpha^2=10^8$, $\beta=10^{-5}$, $e_D=10^{-4}$, $r_{pDz}=10^{-5}$

Inspection of Figs. 6.9 - 6.11 indicates that, for small values of dimensionless pipe radius, r_{pDz}, solutions including wellbore frictional effects for changing flow regimes may show larger effects than for the case with laminar friction. Moreover, relative roughness, e_D, has only a small effect on the frictional effects for the cases shown in these figures, because transition and turbulent flow regimes occur only during a small period of time for these tests.

6.4 Drillstem Test Flow Period Solutions

Under the assumptions described in previous sections to formulate and solve a slug test problem, the similarity between the flow period of a drillstem test and a slug test allows application of the solutions previously presented in this study to both problems. In this section, a more general problem is solved.

6.4.1 Wellbore Equation

This problem considers the complete wellbore equation, Eq. 3.39, derived in this study to represent a well open to the atmosphere during this type of test:

$$A_w z''_D + B_w z'_D + C_w z_D + D_w = E \; p_{wD} \quad \ldots (3.39)$$

where:

$$A_w = \alpha^2 \left\{ 1 + \frac{\bar{D}}{L_D} + \frac{\bar{\rho}}{8} \frac{\bar{D}}{L_D} \left[\frac{r_{pDz}}{r_{wDz}} \right]^2 \right\} \quad \ldots (3.39.a)$$

$$B_w = \alpha^2 \left\{ \left[1 + \frac{\bar{D}}{L_D} \right] \frac{\bar{\rho}}{4} \left| \frac{\bar{\rho}}{r_{pDz}} z'_D \right| + \frac{3}{4} \frac{1}{L_D} \left[\frac{r_{pDz}}{r_{wDz}} \right]^4 z'_D \right\} \quad \ldots (3.39.b)$$

$$C_W = 1 \quad \ldots \quad (3.39.c)$$

$$D_W = 0 \quad \ldots \quad (3.39.d)$$

$$E_W = -1 \quad \ldots \quad (3.39.e)$$

6.4.2 Combined Effect of Gravity, Inertia, and Friction

The numerical method derived in Appendix D can be used to solve the previous wellbore equation coupled with Eqs. 3.40 - 3.46. An option in the computer program presented in Appendix F allow calculation of p_{wD}, z_D, p_{wD}', z_D', and z_D'' from input data for s, C_D, a^2, β, e_D, r_{pDz}, r_{wDz}, L_D, and h_D. According to Eqs. 3.39.a and 3.39.b, these calculations require iteration on z_D, and z_D'.

Figures 6.12.a - 6.14.b show results for p_{wD} and z_D vs t_D/C_D including gravitational, inertial, and frictional effects, and cushion size, r_p/r_w, and h/L wellbore effects for systems with $s=0$, $C_D=103$, for different combinations of β, e_D, r_{pDz}, r_{wDz}, h_D, and L_D, for values of $\alpha^2 = 10^4$, 10^6, and 10^8, respectively. Again, these combinations were selected for convenience in observing distinct effects for each set of data, and they may not represent practical conditions.

For $a^2=10^4$, Fig. 6.12.a shows a very small effect when L_D changes from 20 to 20/19, i. e., from a small slug to a large one. However, the same change in a solution for $\alpha^2=10^6$, shown in Fig. 6.13.a., gives pressure behaviors that agree only at late times. The effect of the same change is even larger for a larger value of a, as shown in 6.14.a for $\alpha^2=10^8$.

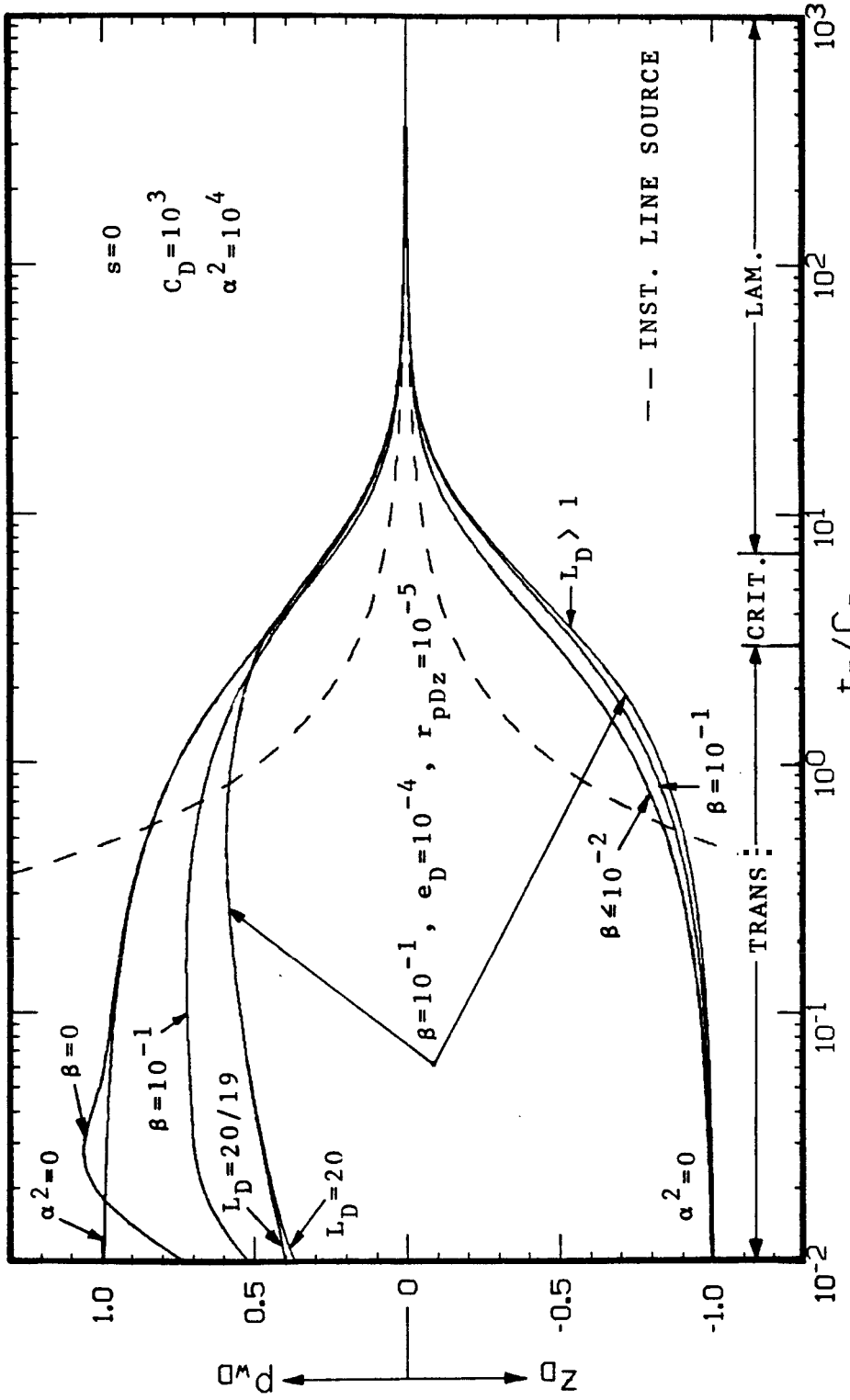

FIG. 6.12.a. SEMI-LOG GRAPH OF SLUG TEST SOLUTIONS FOR p_{wD} AND z_D VS t_D/C_D
INCLUDING GRAVITATIONAL, INERTIAL, AND FRICTIONAL WELLBORE EFFECTS
FOR A SYSTEM WITH s=0, $C_D=10^3$, $\alpha^2=10^4$, $\beta=10^{-1}$, $e_D=10^{-4}$, $r_{pDz}=10^{-5}$,
AND L_D=20 AND 20/19

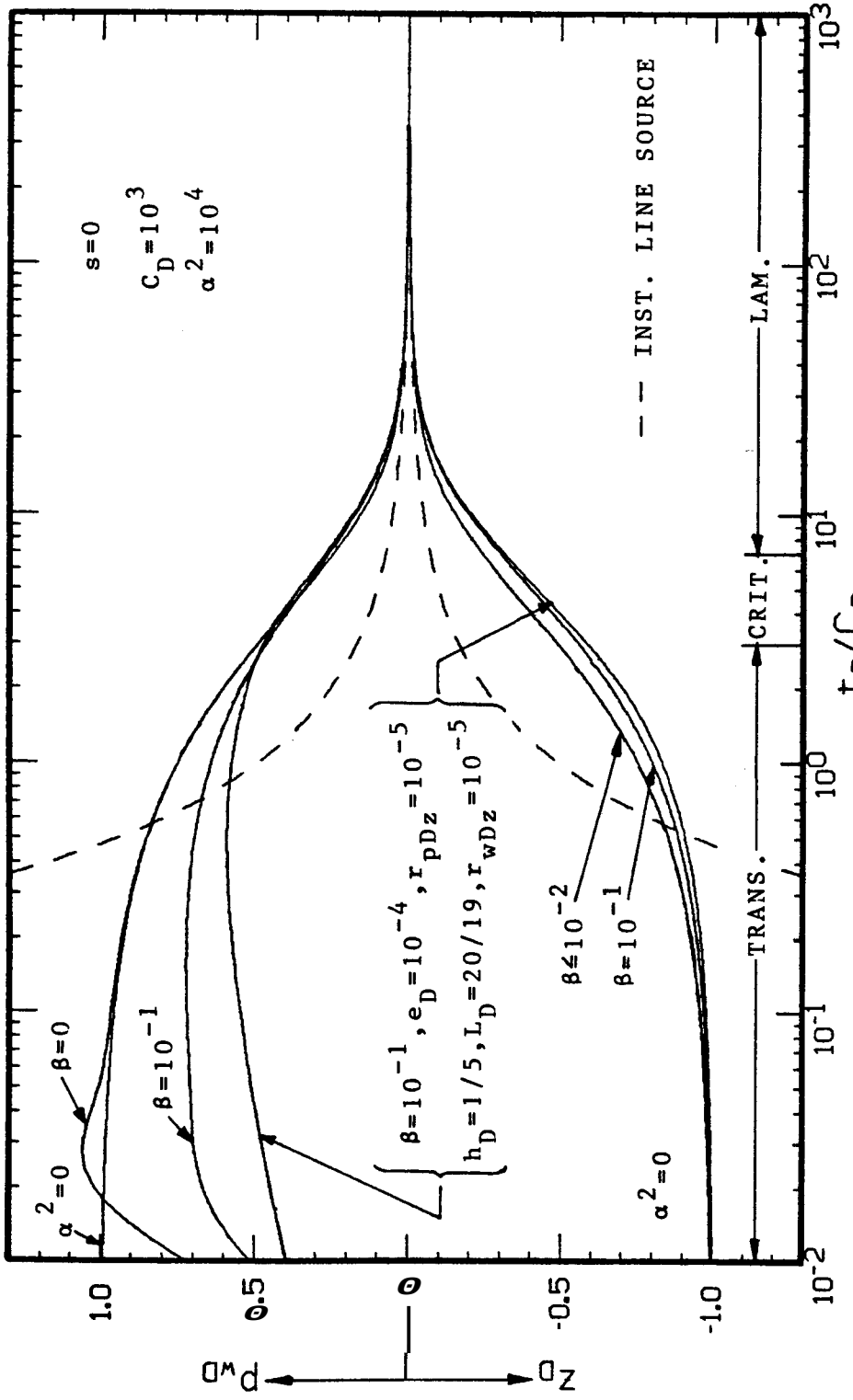

FIG. 6.12.b. SEMI-LOG GRAPH OF SLUG TEST SOLUTIONS FOR p_{wD} AND z_D VS t_D/C_D INCLUDING GRAVITATIONAL, INERTIAL, AND FRICTIONAL WELLBORE EFFECTS FOR A SYSTEM WITH s=0, $C_D=10^3$, $\alpha^2=10^4$, $\beta=10^{-1}$, $e_D=10^{-4}$, $r_{pDz}=10^{-5}$, $L_D=20/19$, $h_D=2/10$, AND $r_{wDz}=10^{-5}$

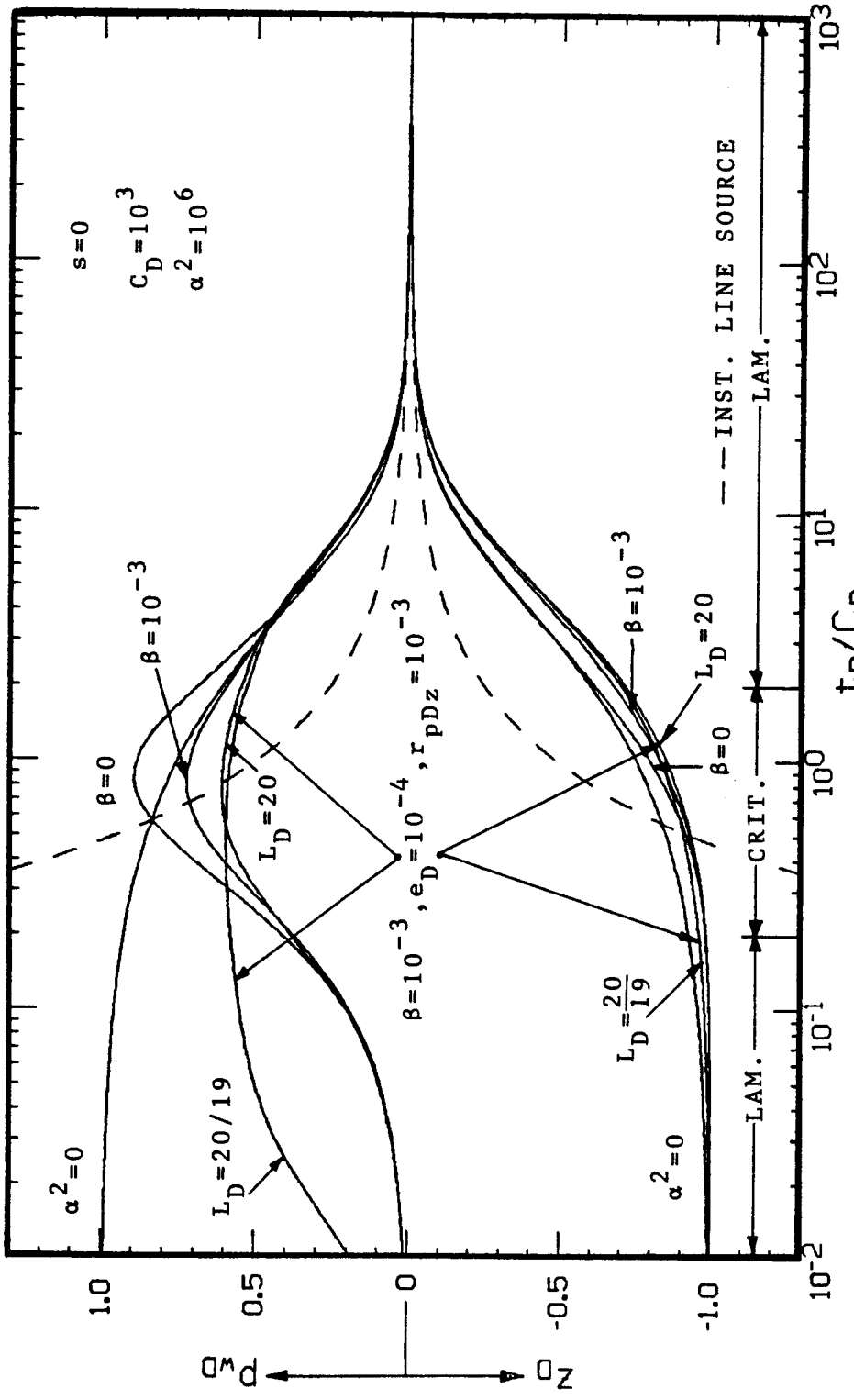

FIG. 6.13.a. SEMI-LOG GRAPH OF SLUG TEST SOLUTIONS FOR p_{wD} AND z_D VS t_D/C_D INCLUDING GRAVITATIONAL, INERTIAL, AND FRICTIONAL WELLBORE EFFECTS FOR A SYSTEM WITH s=0, $C_D=10^3$, $\alpha^2=10^6$, $\beta=10^{-3}$, $e_D=10^{-4}$, $r_{pDz}=10^{-3}$, AND $L_D=20$ AND 20/19

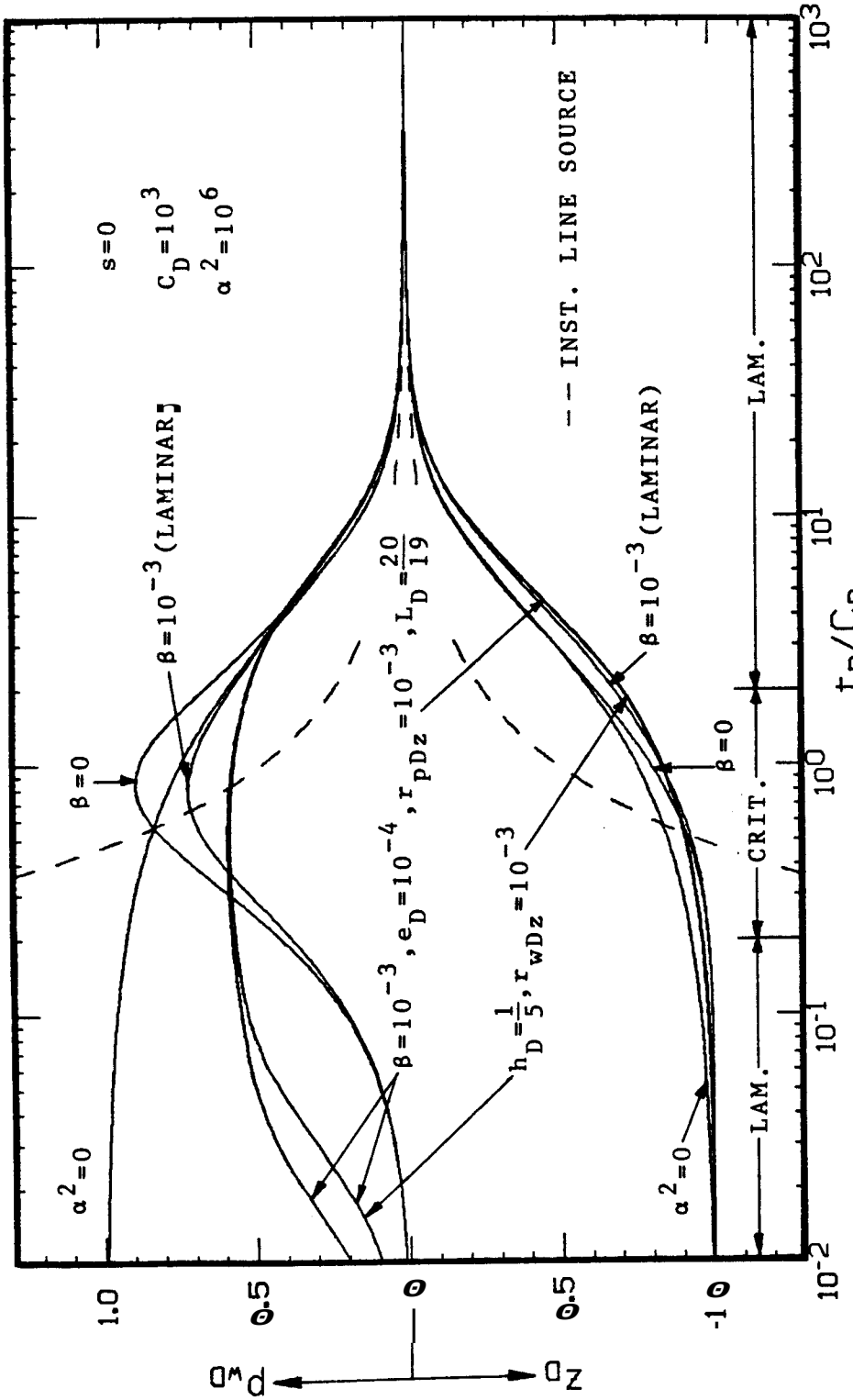

FIG. 6.13.b. SEMI-LOG GRAPH OF SLUG TEST SOLUTIONS FOR p_{wD} AND z_D VS t_D/C_D INCLUDING GRAVITATIONAL, INERTIAL, AND FRICTIONAL WELLBORE EFFECTS FOR A SYSTEM WITH s=0, $C_D=10^3$, $\alpha^2=10^6$, $\beta=10^{-3}$, $e_D=10^{-4}$, $r_{pDz}=10^{-3}$, $L_D=20/19$, $h_D=2/10$, AND $r_{wDz}=10^{-3}$

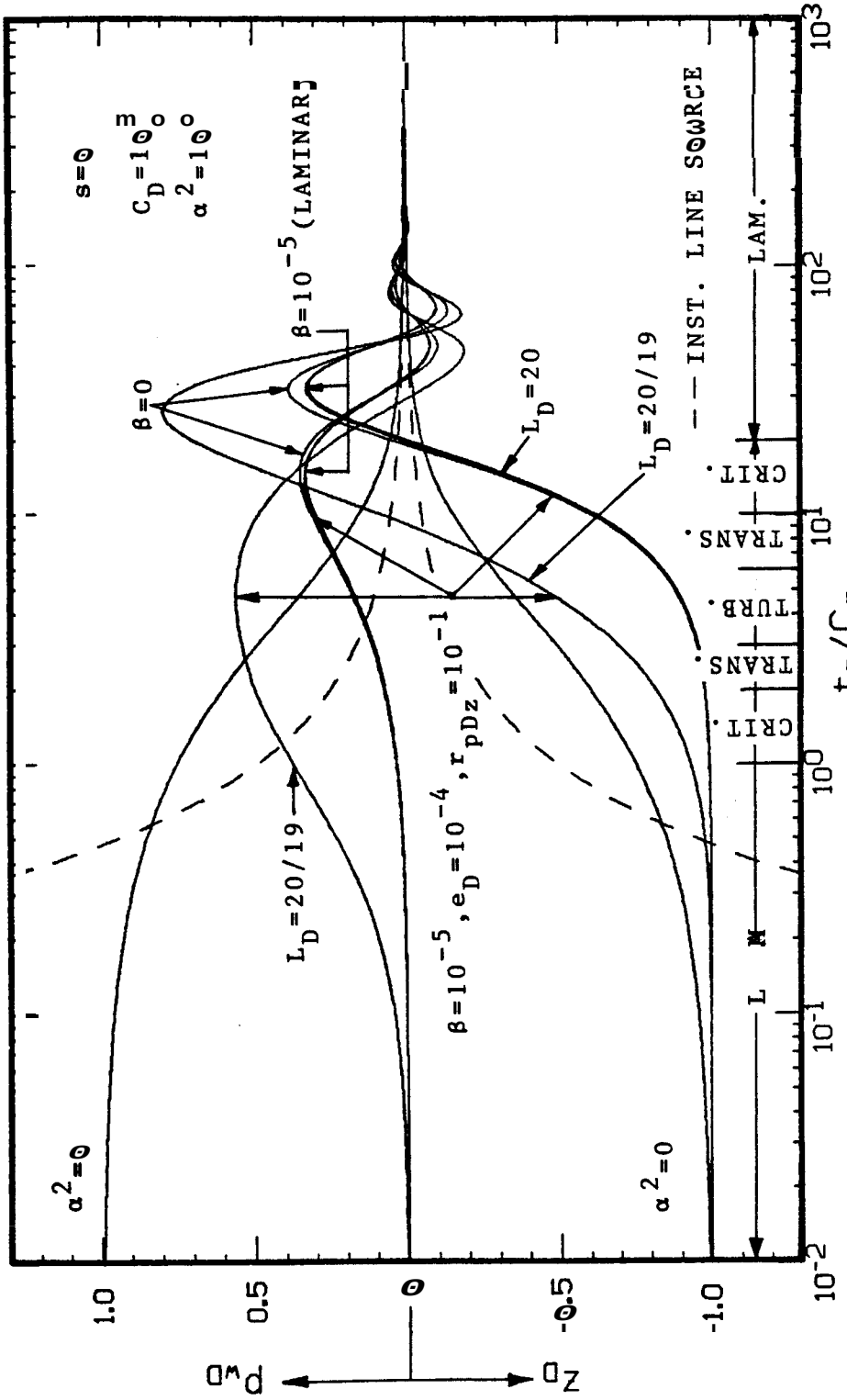

FIG. 6.14.a. SEMI-LOG GRAPH OF SLUG TEST SOLUTIONS FOR p_{wD} AND z_D VS t_D/C_D INCLUDING GRAVITATIONAL, INERTIAL, AND FRICTIONAL WELLBORE EFFECT< FOR A SYSTEM WITH s=0, $C_D=10^3$, $\alpha^2=10^8$, $\beta=10^{-5}$, $e_D=10^{-4}$, $r_{pDz}=10^{-1}$ AND $L_D=20$ AND 20/19

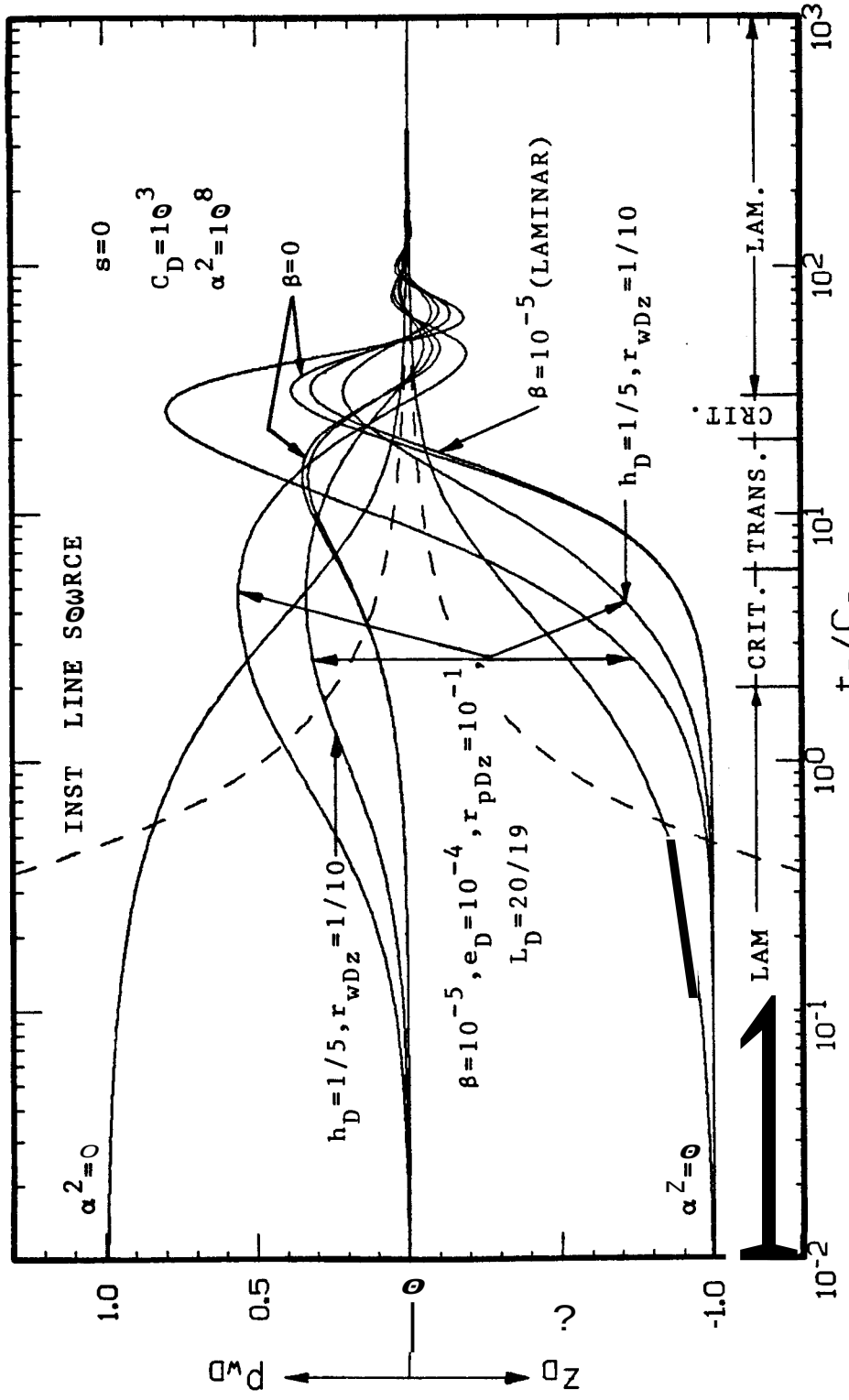

FIG. 6.14.2a. SEMI-LOG GRAPH OF SLUG TEST SOLUTIONS FOR p_{wD} AND z_D VS t_D/C_D INCLUDING GRAVITATIONAL, INERTIAL, AND FRICTIONAL WELLBORE EFFECTS FOR A SYSTEM WITH s=0, $C_D=10^3$, $\alpha^2=10^8$, $\beta=10^{-5}$, $e_D=10^{-4}$, $r_{pDz}=10^{-1}$, $L_D=20/19$, $h_D=2/10$, AND $r_{wDz}=10^{-1}$

For a small cushion size, a relatively large reservoir thickness also results in a negligible effect for $\alpha^2=10^4$, as shown in Fig. 6.12.b, a moderate effect for an intermediate value of a, as shown in Fig. 6.13.b for $a^2=10^6$, and a large effect for $a^2=10^8$, as shown in Fig. 6.14.b.

These observations reflect the conditions defined by the dimensionless initial deaccelerating factor, a, and discussed in Section 5.1.3. Damped conditions for $a^2<C_D^2/10$, underdamped conditions for $a^2>20C_D^2$, and critically-damped conditions for the intermediate range of $C_D2/10<\alpha2<20C_D^2$.

6.5 Drillstem Test Shut-In Period Solutions

The initial value problem statement given by Eqs. 3.39 - 3.46 describes the flow phenomena during a slug test or drillstem test until the moment at which the well is shut-in at the bottom or until the moment at which fluid is produced at the surface.

In this section, the computer program presented in Appendix F is used to evaluate the behavior of p_{wD}, z_D, p_{wD}', z_D', and z_D'' during a drillstem test consisting of a flowing period followed by a shut-in period. This option in the program is specified by a pressure or a time at which the well is shut-in after a drillstem test flow period. As described in Appendix D, this is simulated by instantaneously substituting the wellbore equation in the problem statement by a no-flow inner reservoir condition. This solution implies the assumption of negligible wellbore storage below the drillstem test valve after the valve is closed. If the volume of liquid in that section of the wellbore is large, a small but finite wellbore storage effect can be expected due to the compressibility of the liquid. The presence of gas at the bottom of the wellbore or in the reservoir in a region close to the wellbore may cause a larger wellbore storage. However, typical drillstem test data often does not exhibit large wellbore storage effects during a shut-in period.

Figure 6.15 shows results from the application of the computer program presented in Appendix F to the set of data used to generate Fig. 6.13.b, but considering a shut-in time at t_D/C_D=5. This figure shows the corresponding pressure buildup and stabilization of the liquid level.

6.5.1 Type Curves

The combined results for a flow period and a subsequent shut-in period can be utilized to perform integral analysis of drillstem test data by use of new type curves presented in this section.

Figures 6.16.a, 6.17.a, and 6.18.a are Cartesian graphs displaying results evaluated by the computer program presented in Appendix F for cases in which the well is shut-in at flowing bottomhole pressure recoveries of 25%, 50%, and 75% of the reservoir pressure, respectively. These dimensionless pressure solutions closely resemble typical pressure traces observed in drillstem test field data, showing an almost linear pressure recovery during the flowing period, and an abrupt pressure buildup at the start of the shut-in period. Figures 6.16.b, 6.17.b, and 6.18.b show the same results in the form of new semi-log type curves for integral drillstem test pressure analysis considering all of the flowing and shut-in data. Those figures are semi-log graphs of p_{wD} vs t_D/C_D with C_De^{2s} as a correlation parameter, obtained by applying the effective wellbore radius concept (Brons and Miller, 1961). The corresponding log-log type curves are presented in Figs. 6.16.c, 6.17.c, and 6.18.c. These log-log type curves give a detailed description of the pressure buildup during the shut-in period. On the other hand, the type curves shown in Figs. 6.16.d, 6.17.d, and 6.18.d for $1-p_{wD}$ vs t_D/C_D with C_De^{2s} as a parameter, show a better definition of the pressure recovery during the flow period.

Similar type curves for other flowing pressure recoveries can be generated by using the computer program presented in Appendix F.

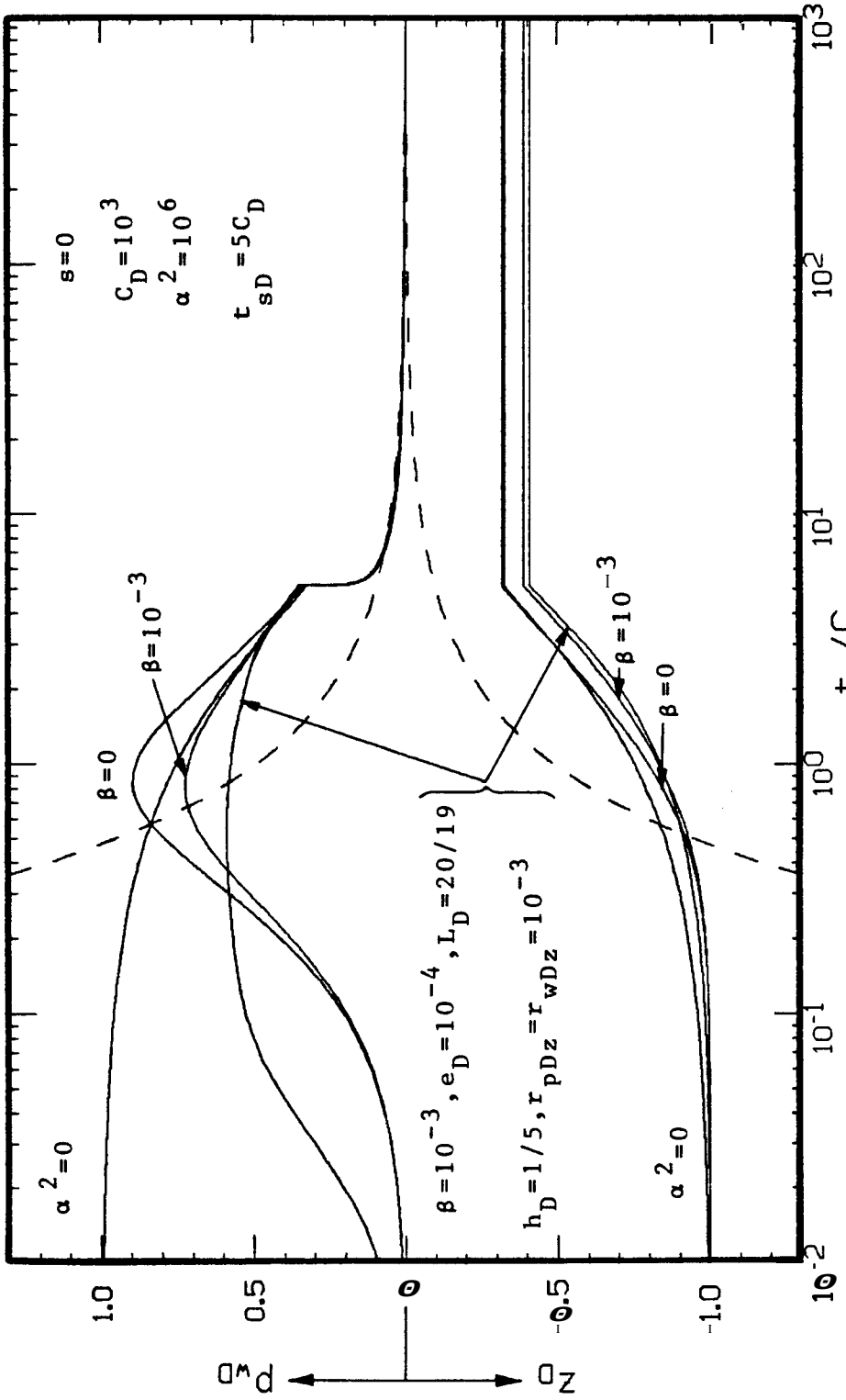

FIG. 6.15. SEMI-LOG GRAPH OF DRILLSTEM TEST FLOW AND SHUT-IN SOLUTIONS FOR P_{wD} VS t_D/C_D INCLUDING GRAVITATIONAL, INERTIAL, AND FRICTIONAL WELLBORE EFFECTS FOR A SYSTEM WITH s=0, $C_D=10^3$, $\alpha^2=10^6$, $\beta=10^{-3}$, $e_D=10^{-4}$, $r_{pDz}=10^{-3}$, $L_D=20/19$, $h_D=1/5$, $r_{wDz}=10^{-3}$ AND $t_{sD}=5C_D$

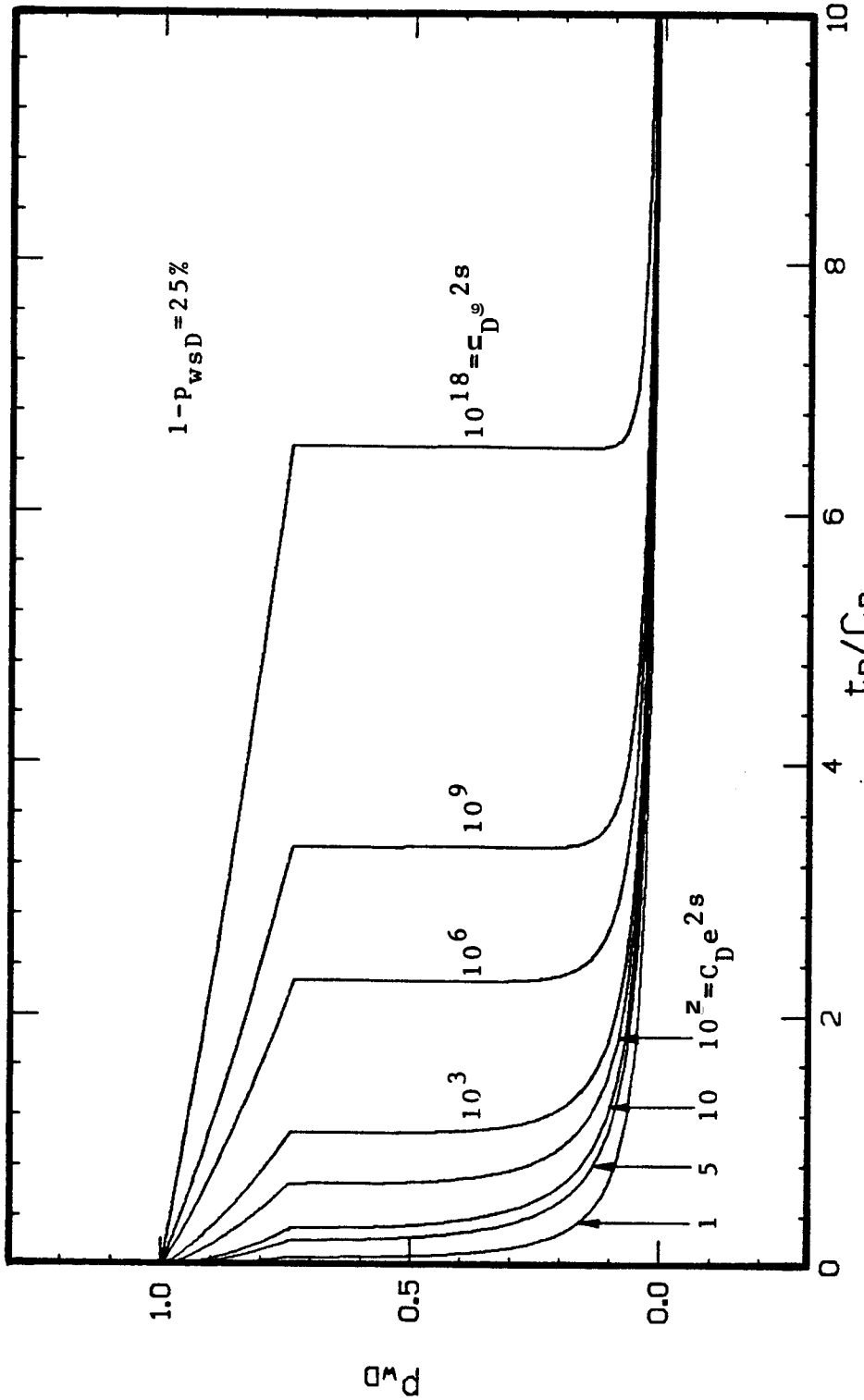

FIG. 6.16.a. CARTESIAN GRAPH OF DRILLSTEM TEST FLOW AND SHUT-IN SOLUTIONS FOR p_{wD} VS t_D/C_D NEGLECTING INERTIAL AND FRICTIONAL WELLBORE EFFECTS FOR PRACTICAL VALUES OF $C_D e^{2s}$ AND $[1-p_{wsD}] = 25\%$

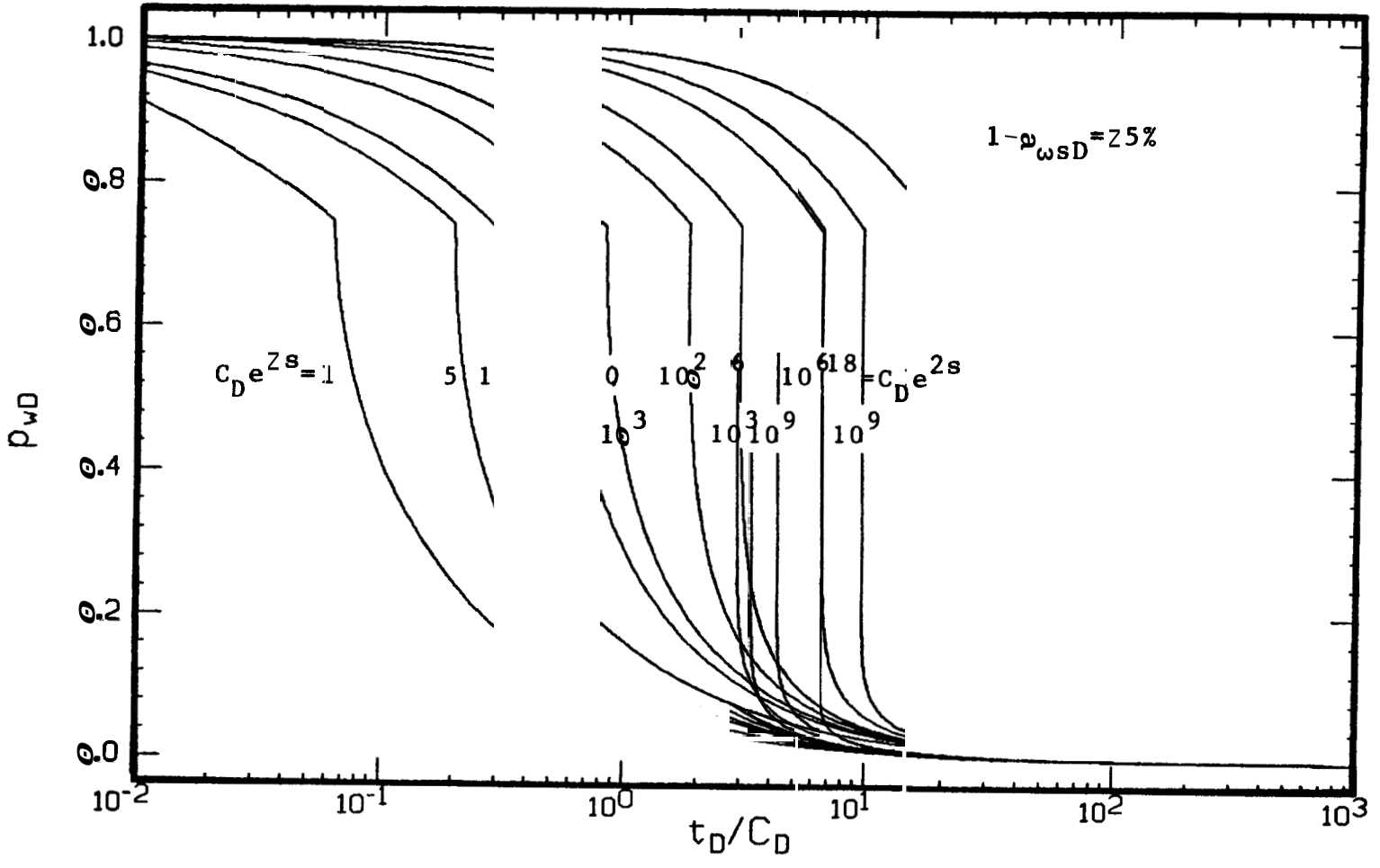

FIG. 6.16.b. SEMI-LOG TYPE CURVE FOR DRILLSTEM TEST FLOW AND SHUT-IN ANALYSIS OF $p_{\omega D}$ VS t_D/C_D NEGLECTING INERTIAL AND FRICTIONAL WELLBORE EFFECTS FOR PRACTICAL VALUES OF $C_D e^{2s}$ AND $[1-p_{\omega sD}] = 25\%$

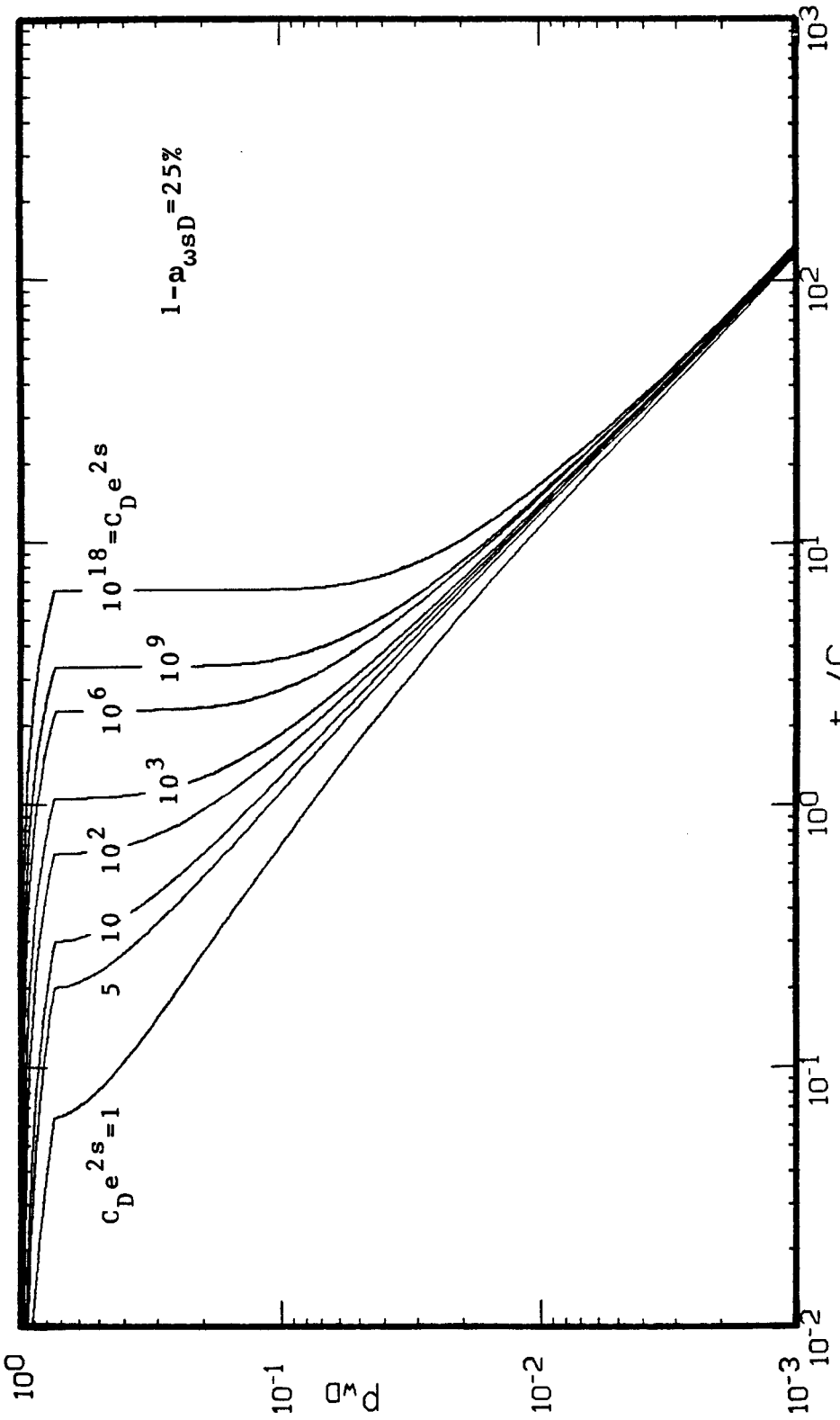

FIG. 6.16.c. LOG-LOG TYPE CURVE FOR DRILLSTEM TEST FLOW AND SHUT-IN ANALYSIS OF p_{wD} VS t_D/C_D NEGLECTING INERTIAL AND FRICTIONAL WELLBORE EFFECTS FOR PRACTICAL VALUES OF C_De^{2s} AND $[1-p_{wsD}] = 25\%$

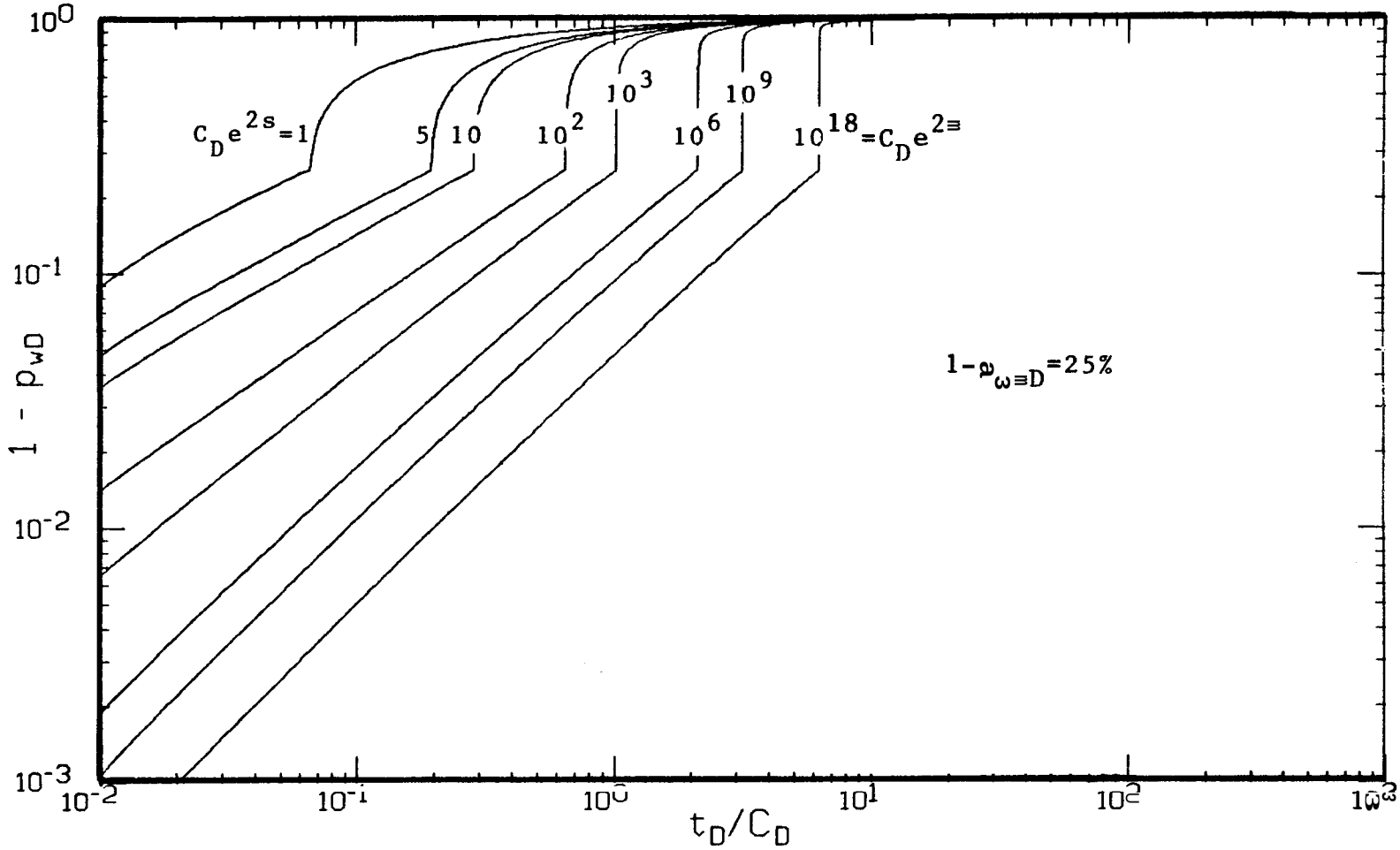

FIG. 6.16.d. LOG-LOG TYPE CURVE FOR DRILLSTEM TEST FLOW AND SHUT-IN ANALYSIS OF $[1-p_{wD}]$ VS t_D/C_D NEGLECTING INERTIAL AND FRICTIONAL WELLBORE EFFECTS FOR PRACTICAL VALUES OF $C_D e^{2s}$ AND $[1-p_{wsD}]$ = 25%

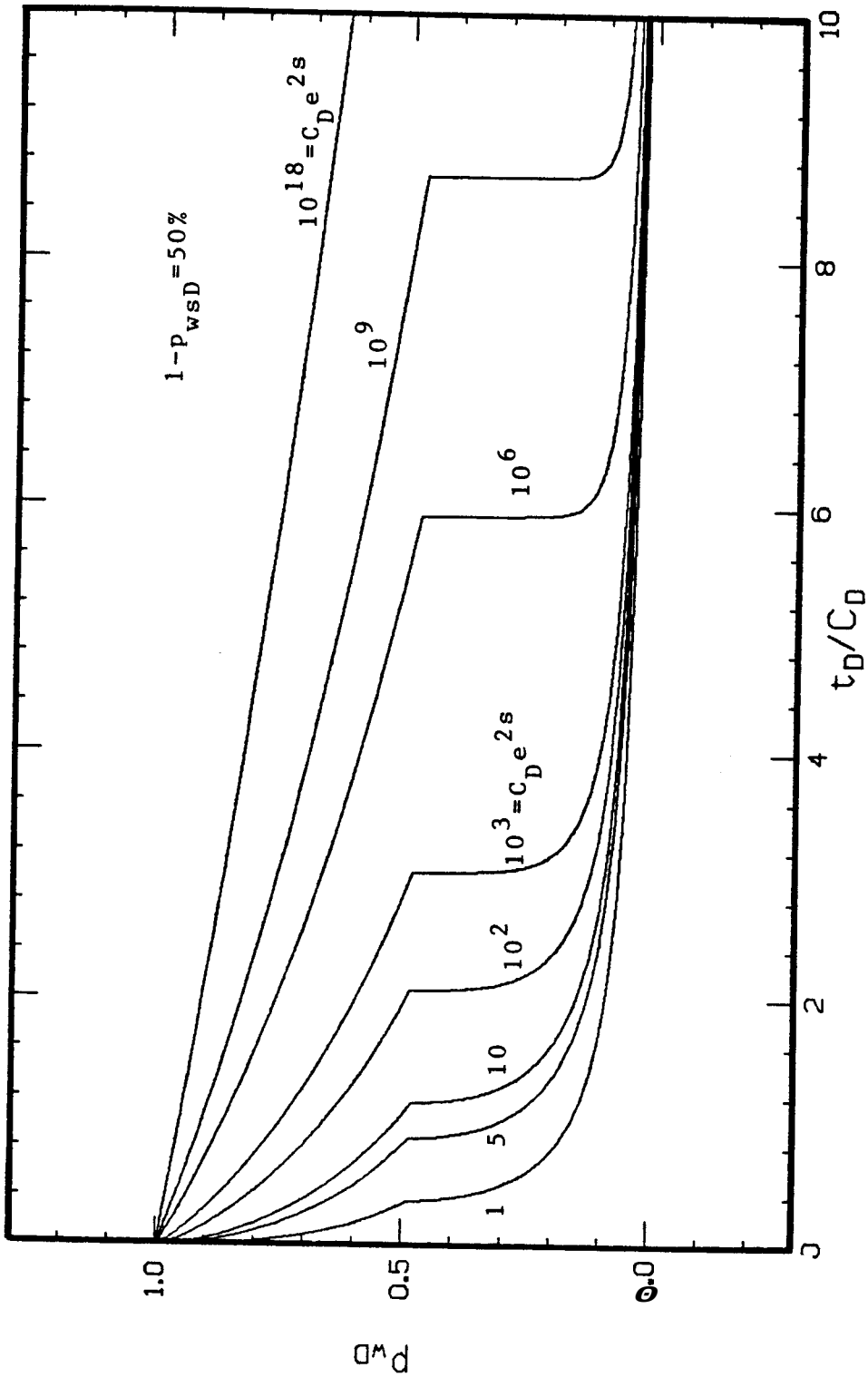

FIG. 6.17.a. CARTESIAN GRAPH OF DRILLSTEM TEST FLOW AND SHUT-IN SOLUTIONS FOR P_{wD} VS t_D/C_D NEGLECTING INERTIAL AND FRICTIONAL WELLBORE EFFECTS FOR PRACTICAL VALUES OF C_De^{2s} AND $[1-p_{wsD}] = 50\%$

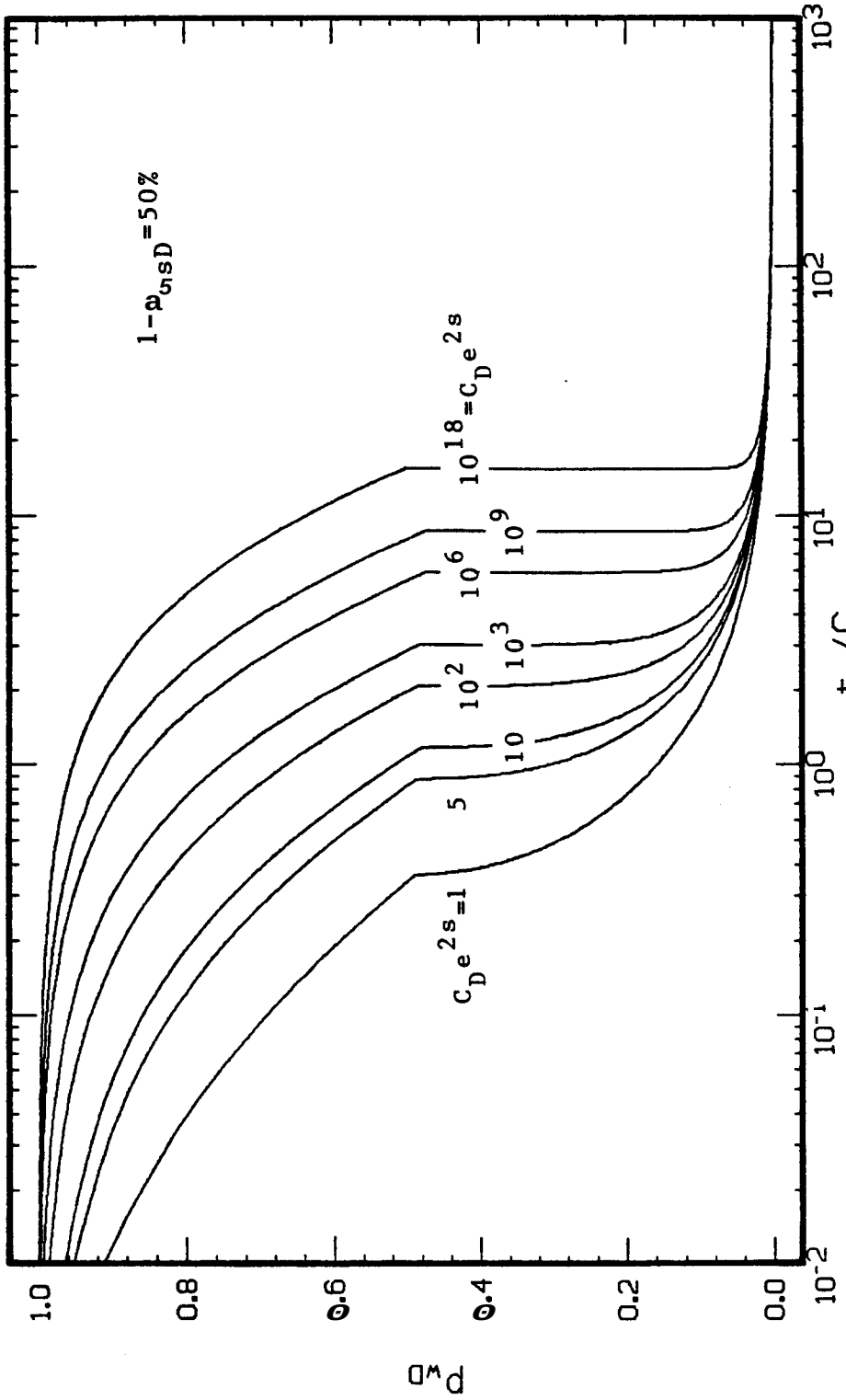

FIG. 6.17.b. SEMI-LOG TYPE CURVE FOR DRILLSTEM TEST FLOW AND SHUT-IN ANALYSIS OF P_{wD} VS t_D/C_D NEGLECTING INERTIAL AND FRICTIONAL WELLBORE EFFECTS FOR PRACTICAL VALUES OF C_De^{2s} AND $[1-P_{wsD}] = 50\%$

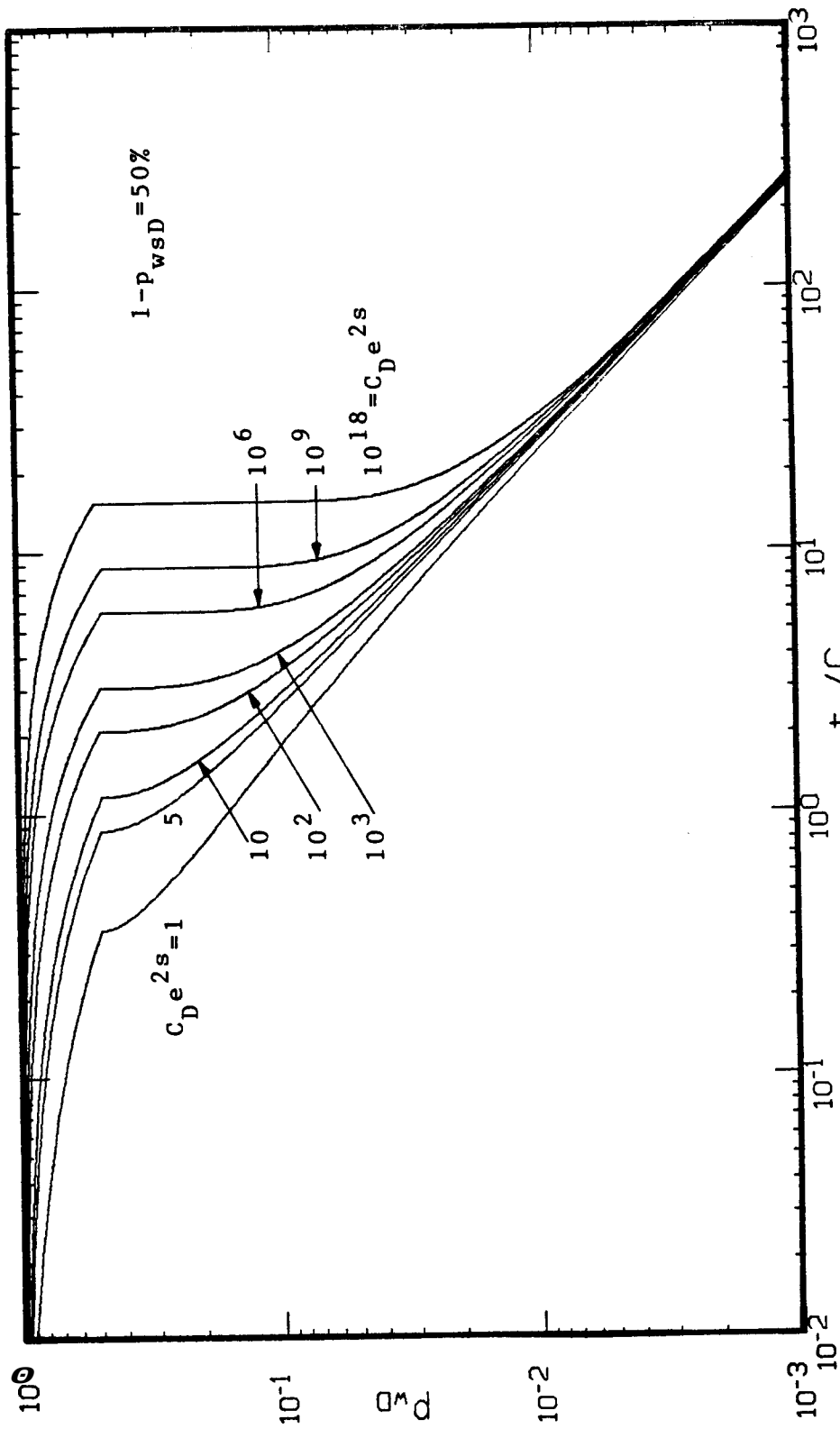

FIG. 6.17.c. LOG-LOG TYPE CURVE FOR DRILLSTEM TEST FLOW AND SHUT-IN ANALYSIS OF P_{wD} VS t_D/C_D NEGLECTING INERTIAL AND FRICTIONAL WELLBORE EFFECTS FOR PRACTICAL VALUES OF C_De^{2s} AND $[1-P_{wsD}] = 50\%$

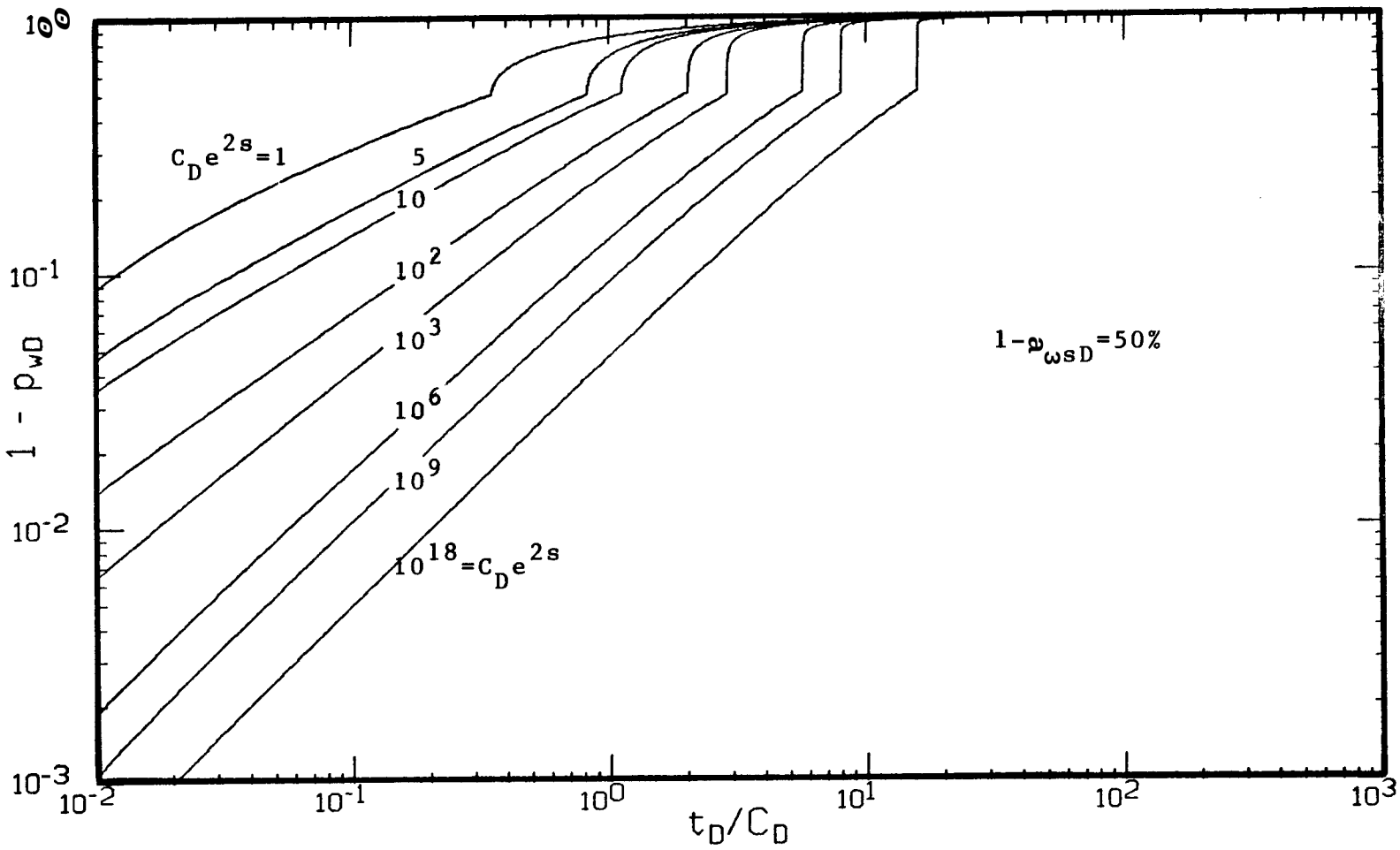

FIG. 6.17.d. LOG-LOG TYPE CURVE FOR DRILLSTEM TEST FLOW AND SHUT-IN ANALYSIS OF $[1-p_{wD}]$ VS t_D/C_D NEGLECTING INERTIAL AND FRICTIONAL WELLBORE EFFECTS FOR PRACTICAL VALUES OF $C_D e^{2s}$ AND $[1-p_{wsD}]$ = 50%

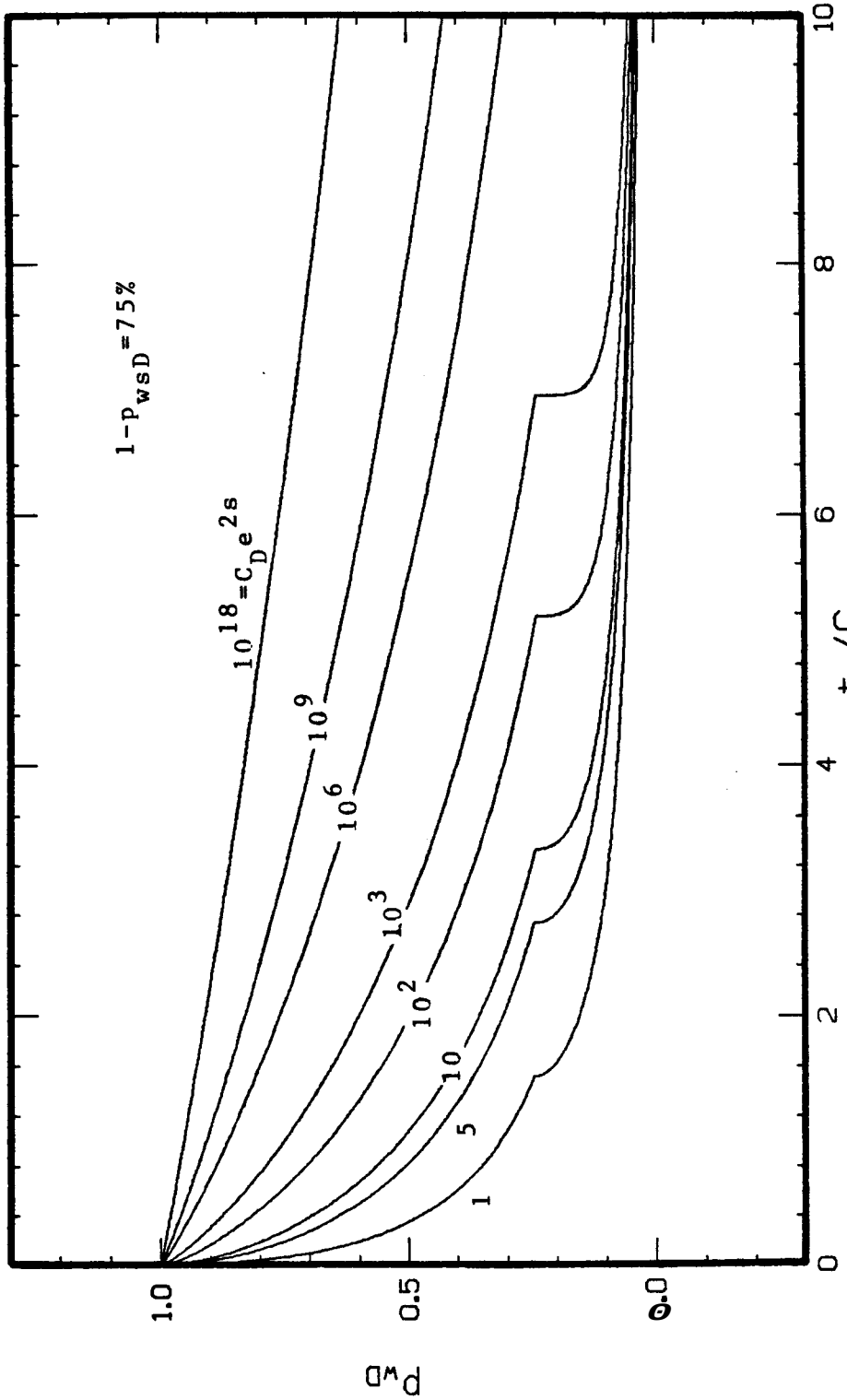

FIG. 6.18.a. CARTESIAN GRAPH OF DRILLSTEM TEST FLOW AND SHUT-IN SOLUTIONS FOR P_{wD} VS t_D/C_D NEGLECTING INERTIAL AND FRICTIONAL WELLBORE EFFECTS FOR PRACTICAL VALUES OF C_De^{2s} AND $[1-P_{wsD}]$ = 75%

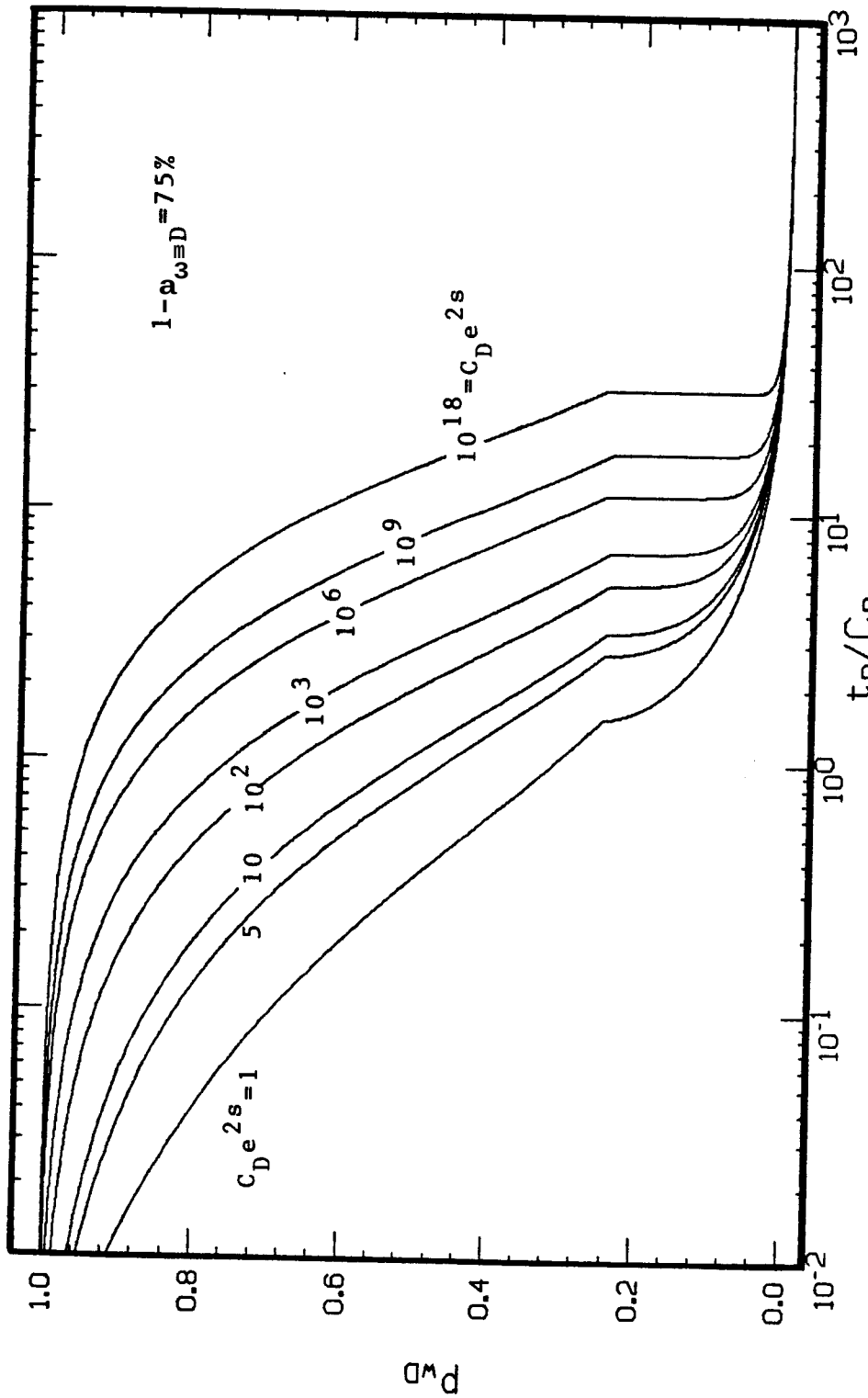

FIG. 6.18.b. SEMI-LOG TYPE CURVE FOR DRILLSTEM TEST FLOW AND SHUT-IN ANALYSIS OF P_{wD} VS t_D/C_D NEGLECTING INERTIAL AND FRICTIONAL WELLBORE EFFECTS FOR PRACTICAL VALUES OF C_De^{2s} AND $[1-p_{wsD}] = 75\%$

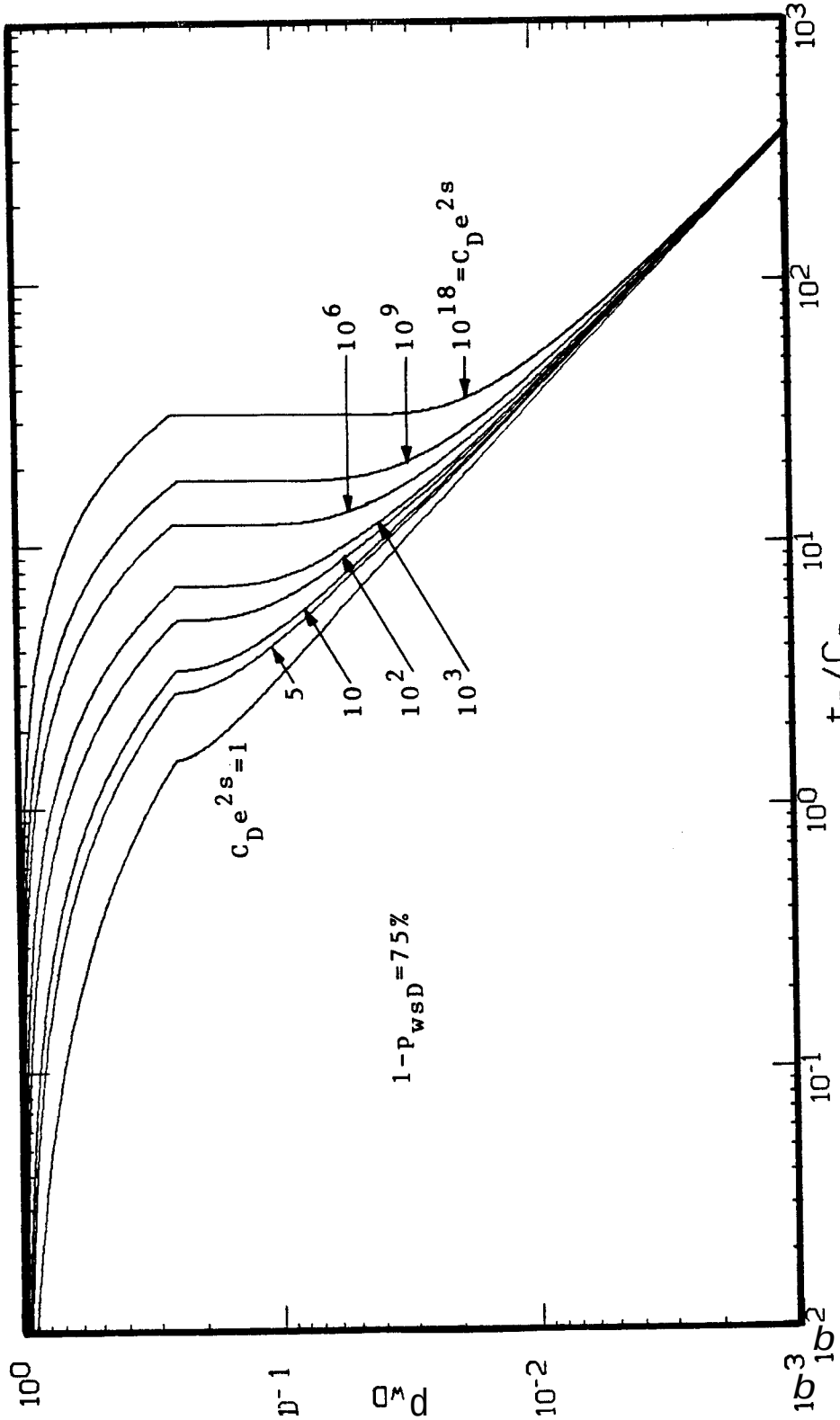

FIG. 6.18.c. LOG-LOG TYPE CURVE FOR DRILLSTEM TEST FLOW AND SHUT-IN ANALYSIS OF P_{wD} VS t_D/C_D NEGLECTING INERTIAL AND FRICTIONAL WELLBORE EFFECTS FOR PRACTICAL VALUES OF C_De^{2s} AND $[1-P_{wsD}] = 75\%$

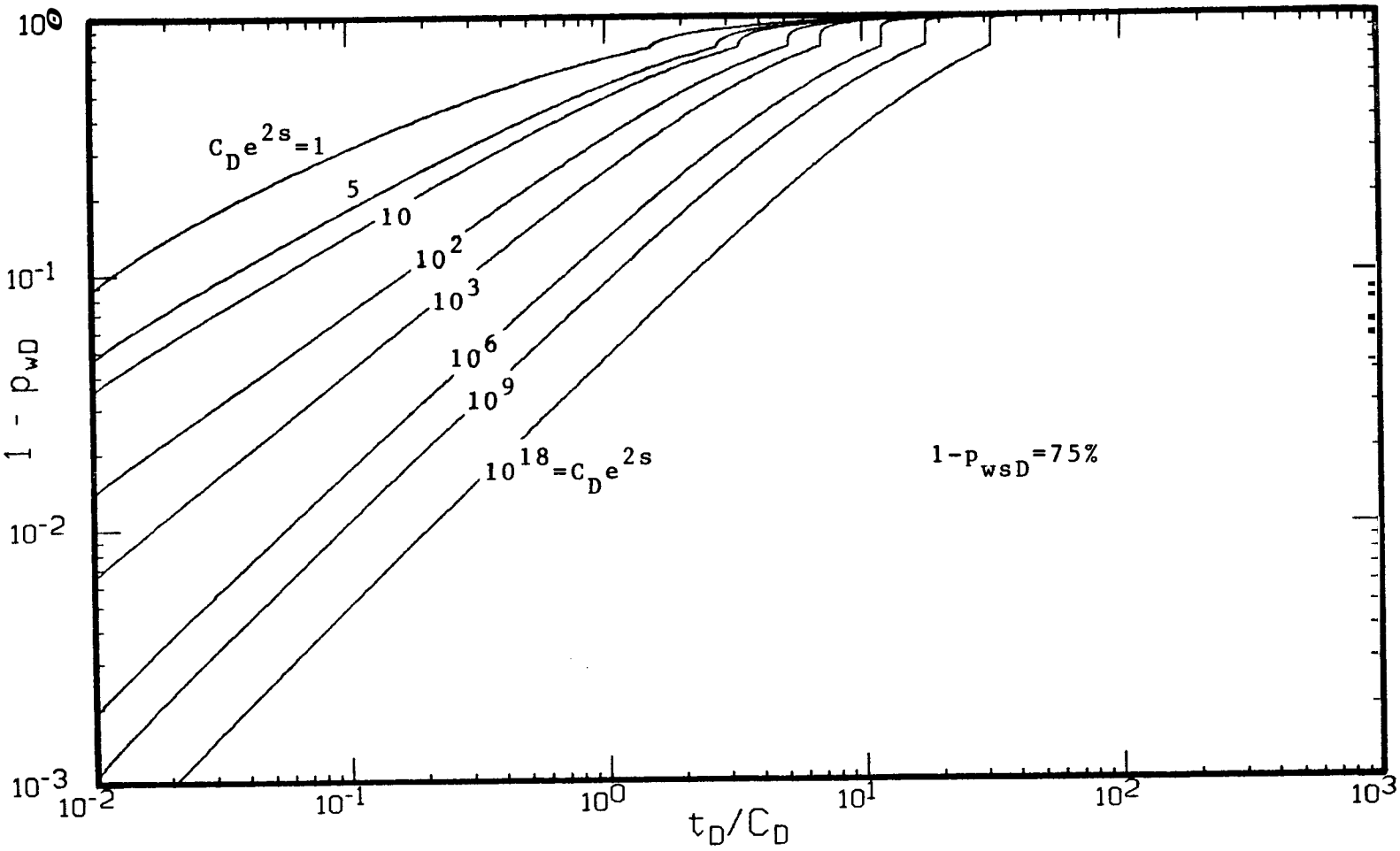

FIG. 6.18.d. LOG-LOG TYPE CURVE FOR DRILLSTEM TEST FLOW AND SHUT-IN ANALYSIS OF $[1-p_{wD}]$ VS t_D/C_D NEGLECTING INERTIAL AND FRICTIONAL WELLBORE EFFECTS FOR PRACTICAL VALUES OF C_De^{2s} AND $[1-p_{wsD}]$ = 75%

These type curves were obtained by considering wellbore Eq. 5.16:

$$z_D = - p_{wD} \quad \ldots \quad (5.16)$$

Therefore, the solutions for the flow period are similar to the ones presented by Ramey, Agarwal, and Martin (1975). These solutions include gravitational effects and assume negligible inertial and frictional wellbore effects. Under these assumptions, the behavior of the dimensionless liquid level, z_D, is symmetrical to the behavior of dimensionless bottomhole pressure, p_{wD}, during the flow period, i. e., $z_D = -p_{wD}$. However, the liquid level z_D remains constant after the start of the shut-in period.

These new type curves open the possibility of performing integral analysis of data usually available from a pressure trace recorded during a drillstem test. This is a significant improvement in interpretation of drillstem tests because the current practice is to analyze only the buildup pressure data recorded during the shut-in period. In most cases, pressure recovery data recorded during the flow period is used exclusively for monitoring the proper operation of the drillstem test tool and estimating flow rate.

The following is a description of one of several techniques in which the proposed type curves can be utilized for estimating reservoir properties:

1. Normalize the drillstem test pressure data, p_w, recorded during a cycle of flowing and shut-in periods, by using the definition of p_{wD}, as follows:

$$p_{wD} = \frac{p_i - p_w}{p_i - [\, p_c + p_a \,]} \qquad \ldots (3.24)$$

where initial reservoir pressure, p_i, can be obtained by extrapolating the pressure buildup data as usual (Matthews and Russell, 1967). Hydrostatic cushion pressure, p, and atmospheric pressure, p_a, can be calculated from data normally available, as described in Section 3.

2. Plot all normalized drillstem test pressure data vs time on transparent paper using the same scales as in the appropriate type curves. Dimensionless pressure data should vary between 1 and 0 and exhibit a discontinuity corresponding to the moment at which the well was shut-in.

3. Compute the following dimensionless maximum flowing bottomhole pressure:

$$[\, 1 - p_{wsD} \,1 = \frac{p_{ws} - p_c}{p_i - [\, p_c - p_a \,1} \qquad \ldots (6.10)$$

where p_{ws} is the bottomhole pressure at the moment at which the well was shut-in.

4. Slide the transparent paper horizontally on the corresponding type curves given in this study, or on similar type curves containing solutions for the calculated value of $[1-p_{wsD}]$.

5. Find the best match between the normalized flowing and shut-in pressure data and a line on the type curve. Read a match point in the data, t_m, and in the type curve, $[t_D/C_D]_m$. Such a point may be the point at the shut-in discontinuity.

6. Record the value of C_De^{2s} of the line matched in the type curve, $[C_De^{2s}]_m$.

7. Use the match point information in the following equation, obtained from the definition of t_D and C_D, to calculate reservoir transmissivity:

$$\frac{k\,h}{\mu} = \frac{1}{2}\,\frac{r_p^{\,2}}{\rho g}\,\left[\frac{t_D}{C_D}\right]_m\,\frac{1}{t_m} \qquad \ldots (6.11)$$

8. Obtain reservoir storativity or skin factor, according to the available information, as follows:

(a) when s is known:

$$\phi\, c_t\, h = \frac{1}{2}\,\frac{r_p^{\,2}}{\rho g\, r_w^{\,2}}\,e^{2s}\,\left[\frac{1}{C_De^{2s}}\right]_m \quad , \text{ and} \qquad \ldots (6.12)$$

(b) when reservoir storativity is known:

$$s = \frac{1}{2}\ln\left(\frac{2\rho g}{r_p^{\,2}}\,\phi c_t\, h r_w^{\,2}\,[C_De^{2s}]_m\right). \qquad \ldots (6.13)$$

9. Estimate the production potential of the well. There are several ways of reporting flow potential that are in used in the oil industry currently. All of them can be obtained from this analysis technique. In fact, the actual flow rate at any time during a drillstem test can be calculated from the information obtained in this analysis and the type curve shown in Fig. 5.4.g, according to Eq. 3.37 expressed as follows:

$$q(t) = \pi r_p^2 \frac{p_i - [p_c + p_a]}{\rho g} \left[\frac{k}{\phi \mu c_t^2 r_w}\right] z'_D \quad \ldots \quad (6.14)$$

6.6 Closed-Chamber Test Solutions

The numerical solution presented in this study was extended to include the non-linear effects of a changing gas pressure on the liquid level during a closed-chamber test.

6.6.1 Wellbore Equation

As derived in Section 3, the following form of wellbore Eq. 3.39 can be used to describe the flow phenomena during a closed-chamber test:

$$A_w z''_D + B_w z'_D + C_w z_D + D_w = E_w p_{wD} \quad \ldots \quad (3.39)$$

$$A_w = \alpha 2 \left\{ 1 + \frac{z_\mu}{L_D} + \frac{3}{8} \frac{h\mu}{L_D} \left[\frac{r_{pDz}}{r_{wDz}} \right]^2 \right\} \quad \ldots \quad (3.39.a)$$

$$B_w = \alpha^2 \left\{ \left[1 + L_D^{z_D} \right] \frac{f}{4} \left| \frac{1}{r_{pDz}} z'_D \right| + \frac{3}{4} \frac{1}{L_D} \left[\frac{r_{pDz}}{r_{wDz}} \right]^4 z'_D \right\} \quad \ldots (3.39.b)$$

$$C_w = 1 \quad \ldots (3.39.c)$$

$$D_w - \frac{L_D - L_{pD} - 1}{L_D - L_{pD} + z_D} \frac{Z_g}{Z_g(0)} P_{gD}(0) - P_{aD} \quad \ldots (3.39.d')$$

$$E_w = - 1 \quad \ldots (3.39.e)$$

The effect of the increasing gas pressure in a closed-chamber as liquid enters the wellbore is non-linear, as stated in the definition of wellbore coefficient D_w, given by Eq. 3.39.d'. At the start of a closed-chamber test, z_D is equal to -1, and this equation reduces to $D_w = p_{gD}(0) - p_{aD}$. Therefore, for the special case in which the initial gas pressure is atmospheric, $D_w = 0$ at initial conditions. If a closed-chamber test is conducted for a long enough period of time, flow of fluids may eventually stop due to static equilibrium between gas pressure plus liquid column and reservoir pressure.

According to the application of the real gas law to obtain the expression for gas pressure, p_g, given in Eq. 3.7 and according to the definition of dimensionless closed-chamber gas pressure, given in Eq. 3.49:

$$p_{gD} = \frac{L_D - L_{pD} - 1}{L_D - L_{pD} + z_D} \frac{Z_g}{Z_g(0)} P_{gD}(0) \quad \ldots (6.15)$$

Therefore, the wellbore coefficient D_w is related to the behavior of the dimensionless gas pressure in the closed-chamber. The behavior of p_{gD} is also calculated by the computer program presented in Appendix F.

6.6.2. Effect of L_{pD}, $p_{gD}(0)$, and p_{aD}

The effect of L_{pD}, $p_{gD}(0)$, and p_{aD} are considered in this section under the assumption of ideal gas behavior, under which $Z_g=1$.

Figure 6.19.a shows results for p_{wD} obtained for a closed-chamber test in a system with $s=0$, $C_D=10^3$, $\alpha^2=106$, $\beta=10^{-3}$, $e_D=10^{-4}$, $L_D=2$, $h_D=1/10$, $r_{pDz}=5[10-5]$, $r_{wDz}=10^{-4}$, $L_{pD}=2$, $p_{gD}(0)=1/10$, and $p_{aD}=1/100$. Also, Fig. 6.19.a shows the corresponding drillstem test results under different assumptions for reference purposes. The effect of the increasing gas pressure is reflected by a higher bottomhole pressure (lower p_{wD}) and the stabilization of the wellbore liquid level at a level ($z_D=-0.31$) lower than that corresponding to a drillstem test ($z_D=0$). Fig. 6.19.b illustrates the behavior of dimensionless closed-chamber gas pressure, p_{gD}, for the same test.

The effect of a larger initial closed-chamber at the same conditions is shown in Figs. 6.20.a and 6.20.b. Bottomhole pressure is lower (higher p_{wD}) throughout the test and the liquid level stabilizes at a higher level, $z_D=-0.16$.

The effect of a higher initial gas pressure, $p_{gD}(0)$, on a closed-chamber test similar to the one shown in Fig. 6.19.a is presented in Figs. 6.21.a and 6.21.b. Bottomhole pressure is higher (lower p_{wD}) throughout the test and liquid level stabilizes at a lower level, $z_D=-0.70$.

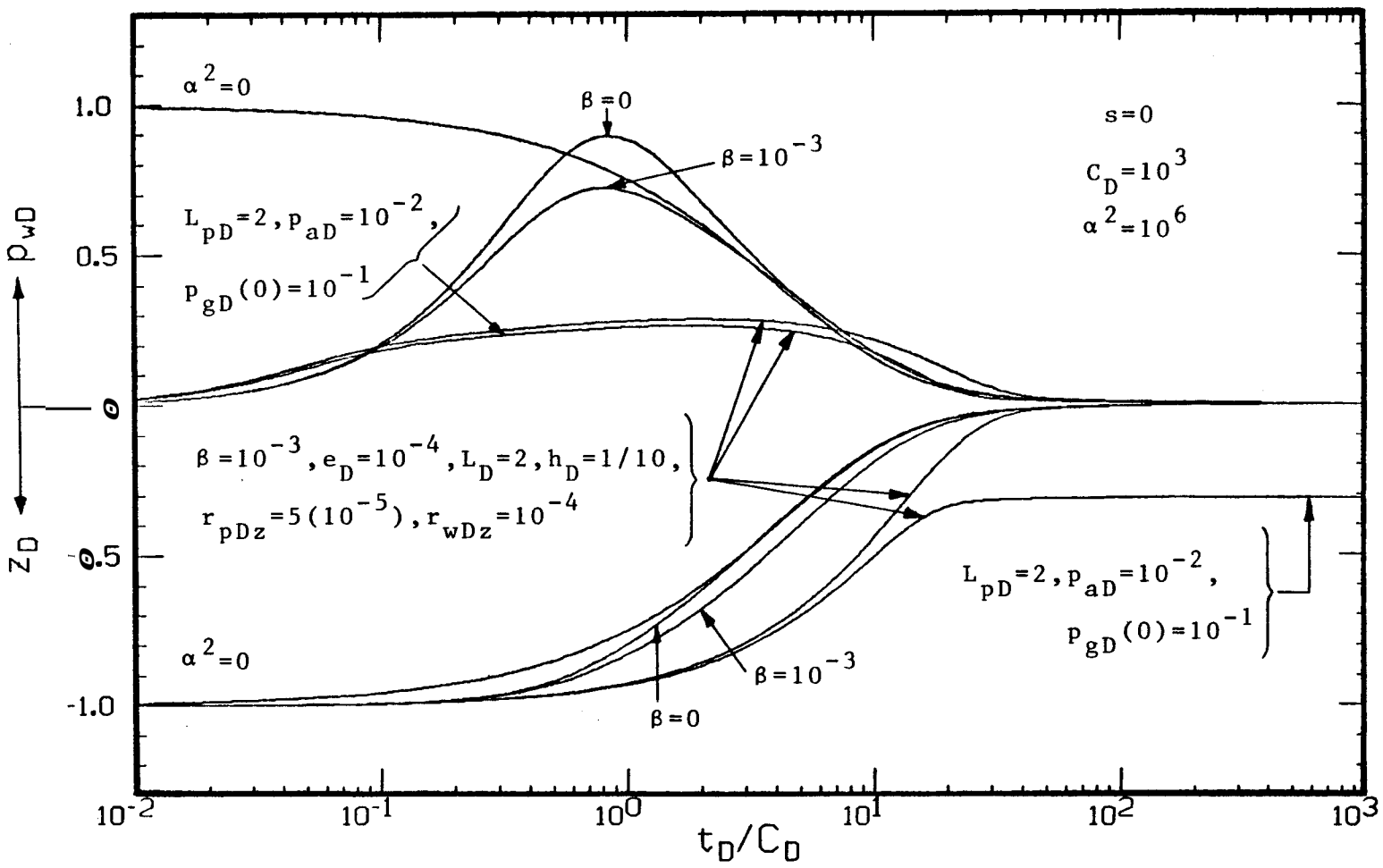

FIG. 6.19.a. SEMI-LOG GRAPH OF CLOSED-CHAMBER TEST SOLUTION FOR p_{wD} VS t_D/C_D IN A SYSTEM WITH s=0, $C_D=10^3$, $\alpha^2=10^6$, $\beta=10^{-3}$, $e_D=10^{-4}$, $L_D=2$, $h_D=1/10$, $r_{pDz}=5[10^{-5}]$, $r_{wDz}=10^{-4}$, $L_{pD}=2$, $p_{gD}(0)=1/10$, AND $p_{aD}=10^{-2}$

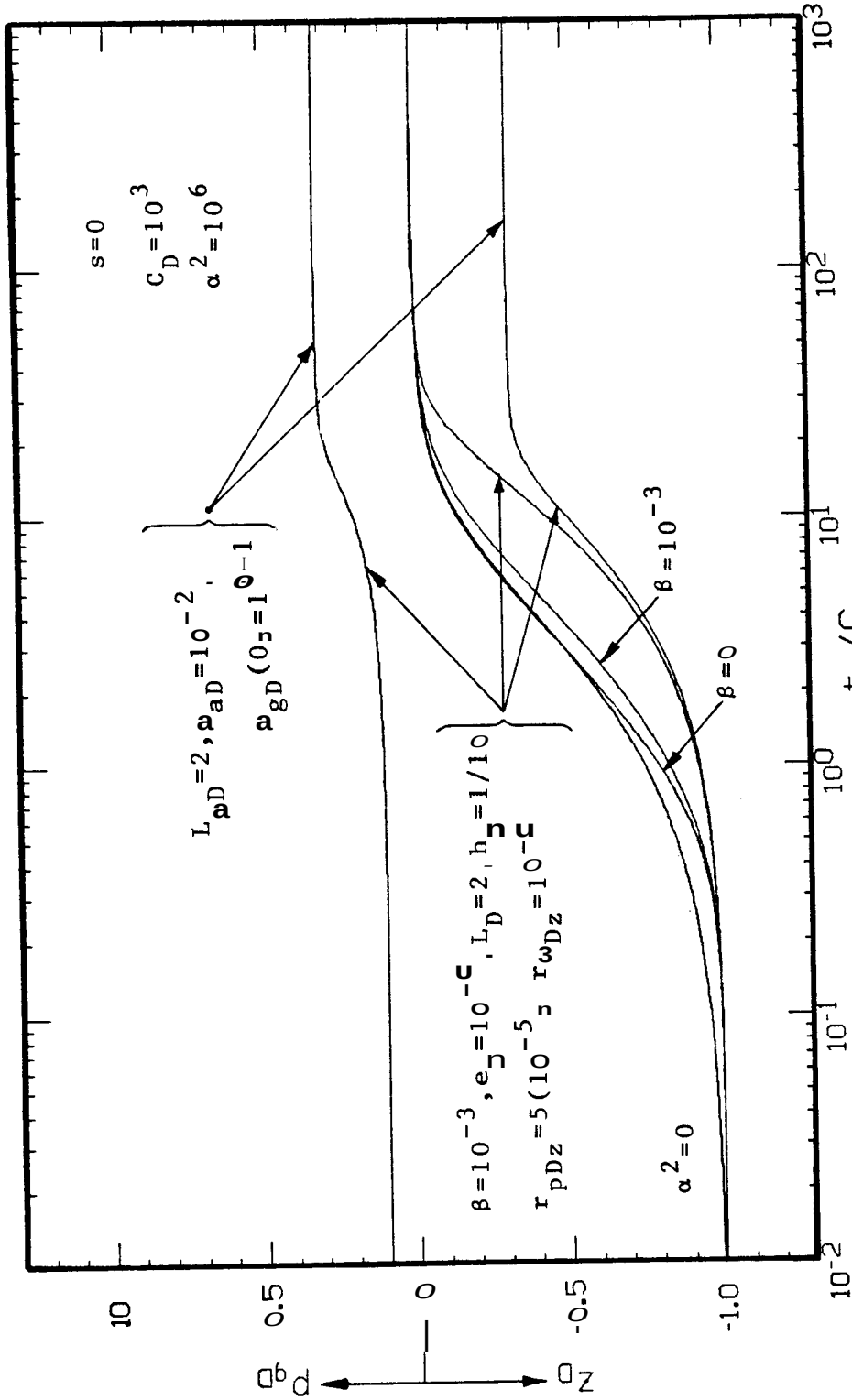

FIG. 6.19.b. SEMI-LOG GRAPH OF CLOSED-CHAMBER TEST SOLUTION FOR P_{gD} VS t_D/C_D IN A SYSTEM WITH s=0 * $C_D=10^3$, $\alpha^2=10^6$, $\beta=10^{-3}$, $e_D=10^{-4}$, $L_D=2$, $h_D=1/10$, $r_{pDz}=5[10^{-}$, $r_{wDz}=10^{-4}$, $L_{pD}=2$, $P_{gD}(0)=1/10$, AND $P_{aD}=10^{-2}$

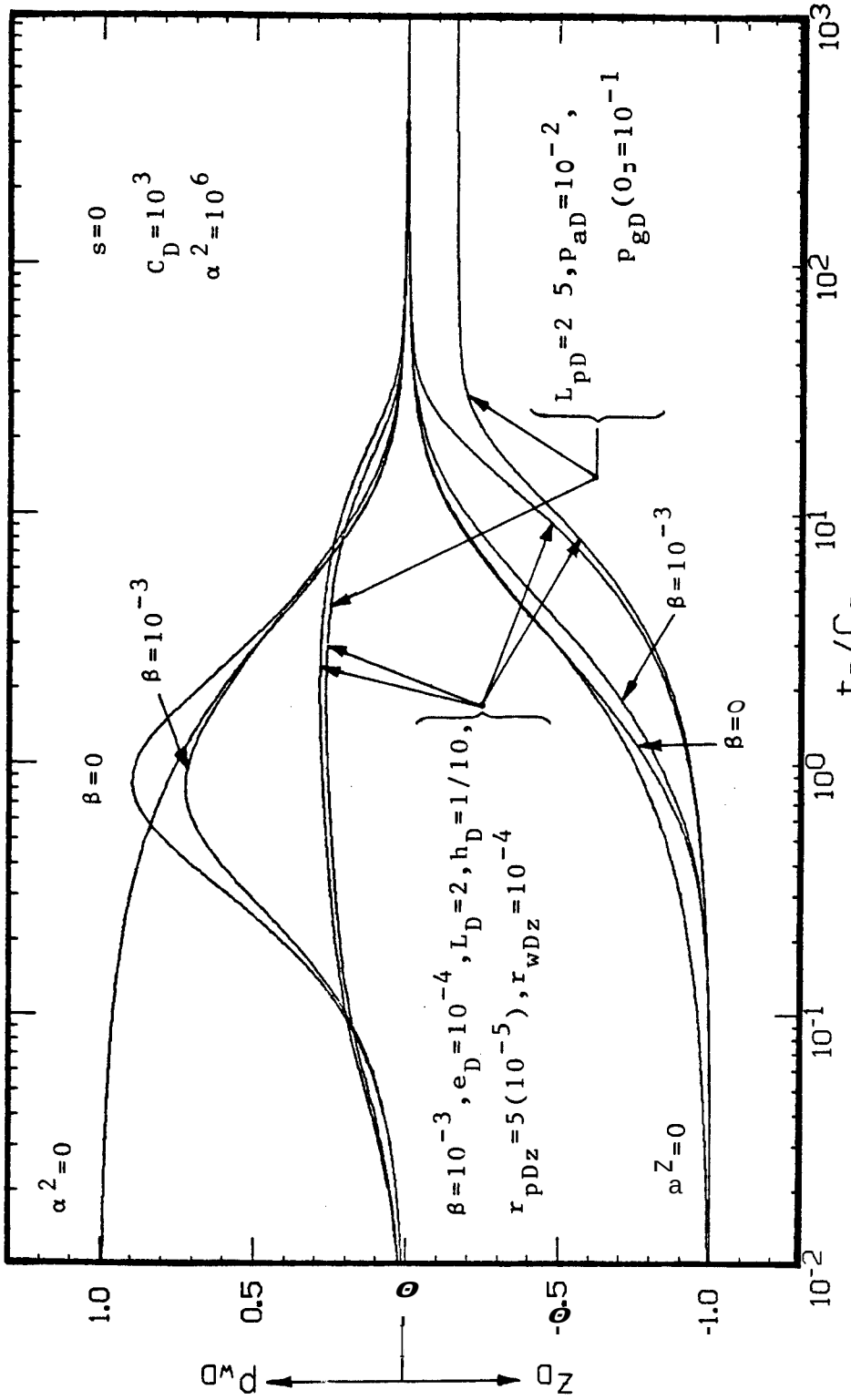

FIG. 6.20.a. SEMI-LOG GRAPH OF CLOSED-CHAMBER TEST SOLUTION FOR p_{wD} VS t_D/C_D IN A SYSTEM WITH $s=0$, $C_D=10^3$, $\alpha^2=10^6$, $\beta=10^{-3}$, $e_D=10^{-4}$, $L_D=2$, $h_D=1/10$, $r_{pDz}=5[10^{-5}]$, $r_{wDz}=10^{-4}$, $L_{pD}=2.5$, $p_{gD}(0)=1/10$, AND $p_{aD}=10^{-2}$

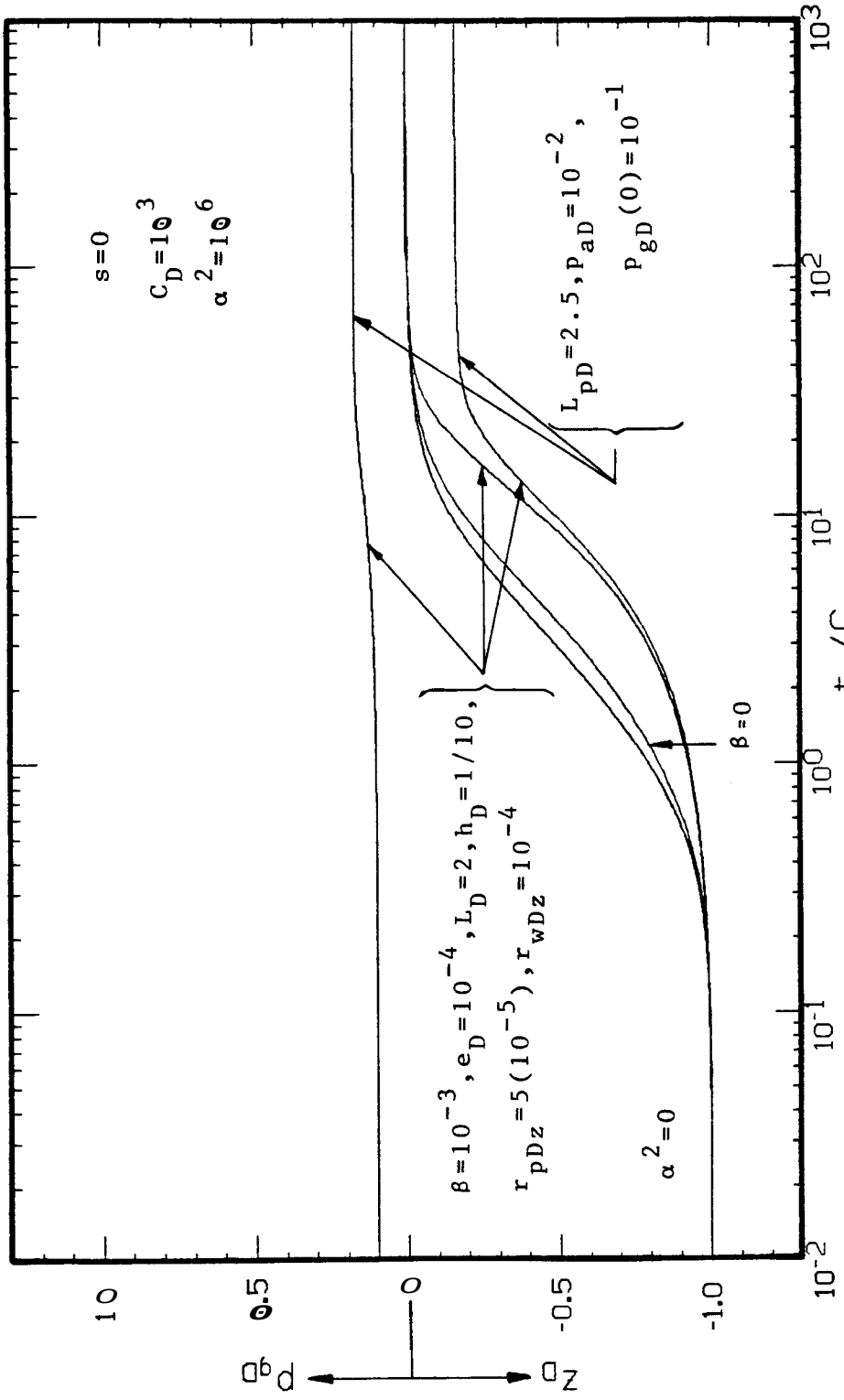

F . 6.20.b. SEMI-LOG GRAPH OF CLOSED-CHAMBER TEST SOLUTION FOR p_{wD} VS t_D/C_D IN A SYSTEM WITH s=0, $C_D=10^3$, $\alpha^2=10^6$, $\beta=10^{-3}$, $e_D=10^{-4}$, $L_D=2$, $h_D=1/10$, $r_{pDz}=5[10^{-5}]$, $r_{wDz}=10^{-4}$, $L_{pD}=2.5$, $p_{gD}(0)=1/10$, AND $p_{aD}=10^{-2}$

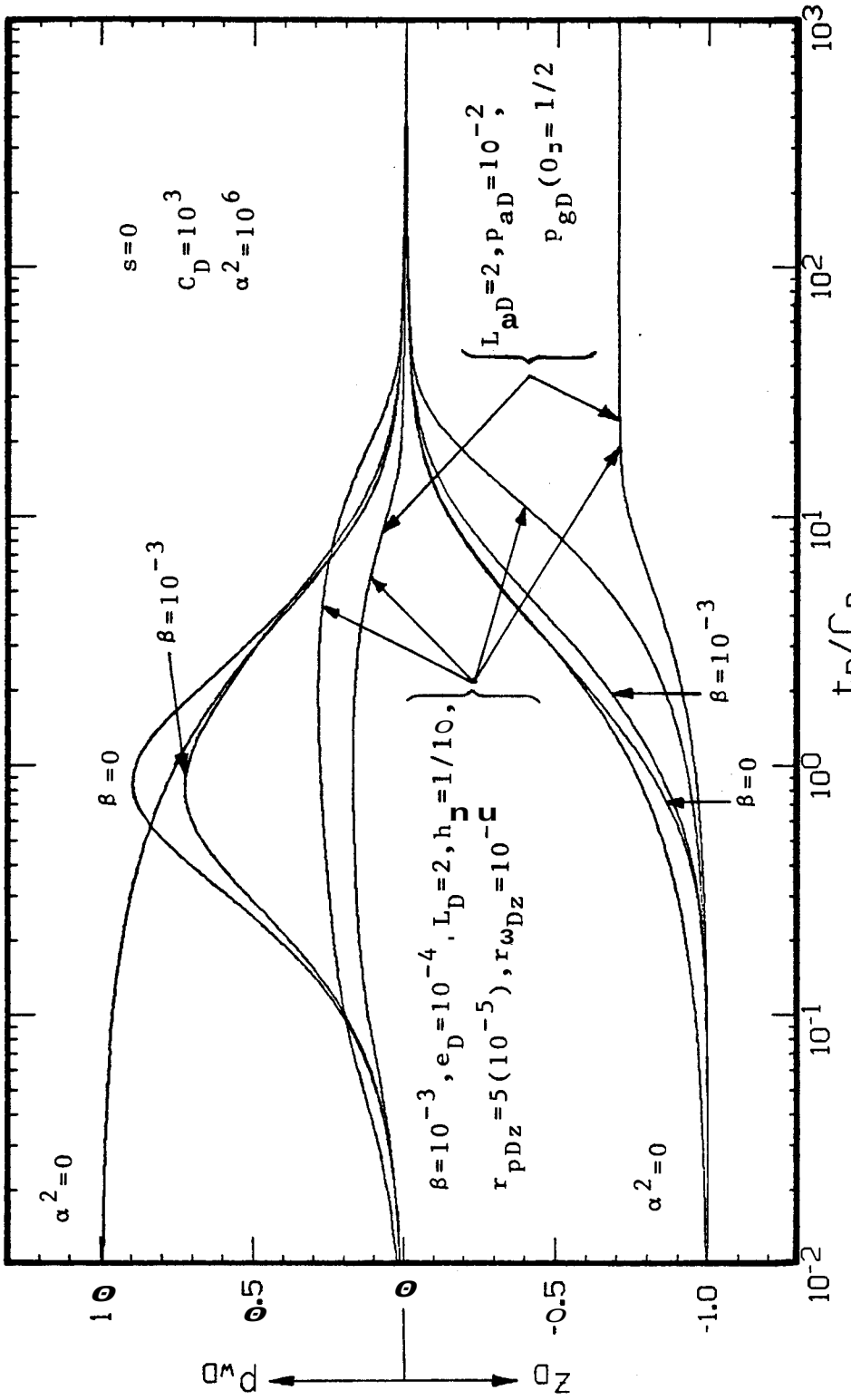

FIG. Ø.21.a. SEMI-LOG GRAPH OF CLOSED-CHAMBER TEST SOLUTION FOR P_{wD} VS t_D/C_D IN A SYSTEM WITH s=0, $C_D=10^3$, $\alpha^2=10^6$, $\beta=10^{-3}$, $e_D=10^{-4}$, $L_D=2$, $h_D=1/10$, $r_{pDz}=5[10^{-5}]$, $r_{wDz}=10^{-4}$, $L_{pD}=2$, $p_{gD}(0)=1/2$, AND $p_{aD}=10^{-2}$

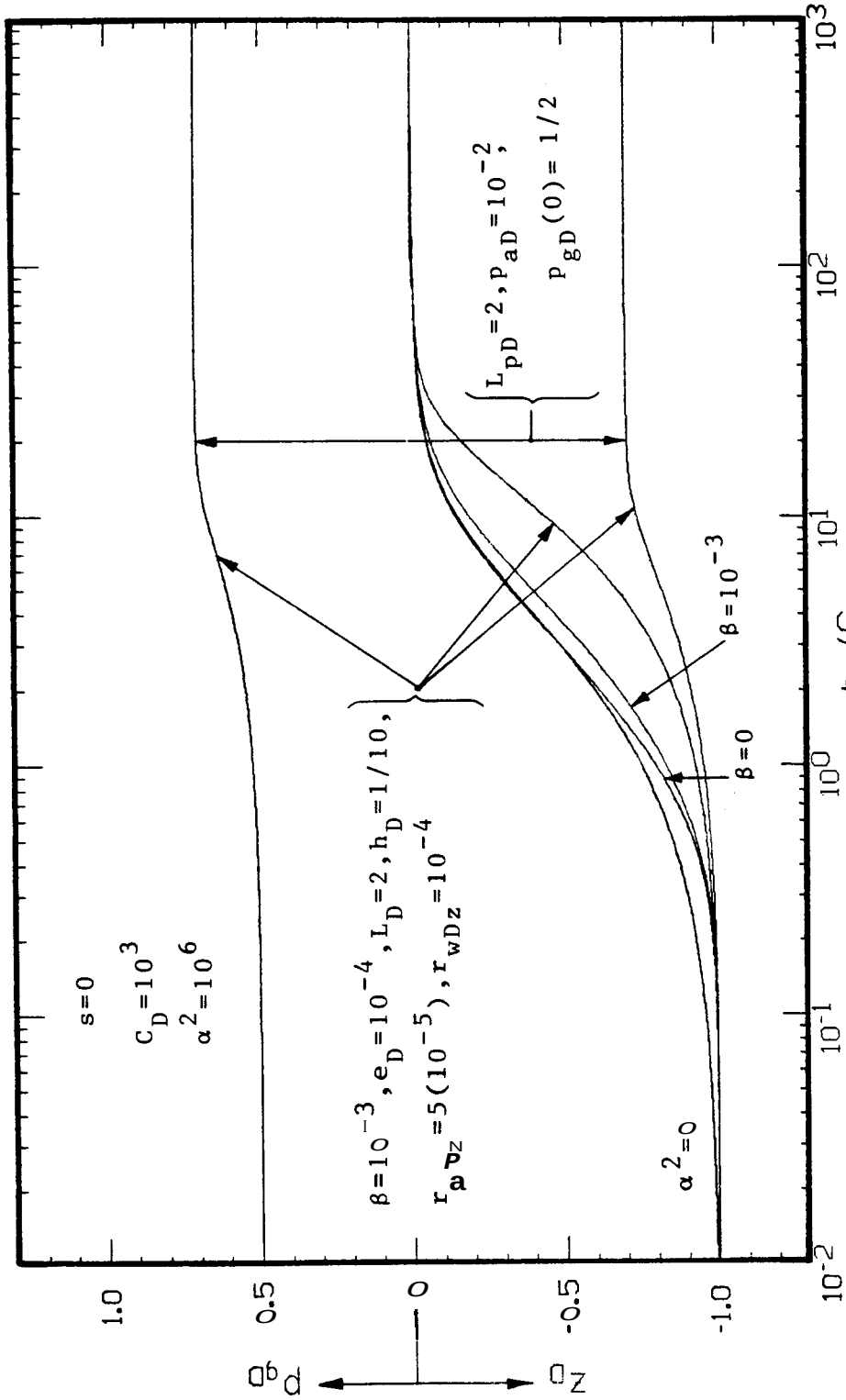

F . 9.21.b. SEMI-LOG GRAPH OF CLOSED-CHAMBER TEST SOLUTION FOR P_{wD} VS t_D/C_D IN A SYSTEM WITH s=0, $C_D=10^3$, $\alpha^2=10^6$, $\beta=10^{-3}$, $e_D=10^{-4}$, $L_D=2$, $h_D=1/10$, $r_{pDz}=5[10^{-5}]$, $r_{wDz}=10^{-4}$, $L_{pD}=2$, $p_{gD}(0)=1/2$, AND $P_{aD}=10^{-2}$

6.7 Closed–Chamber Shut–In Period Solutions

Sometimes, a drillstem test is performed with a valve closed at the surface. This test is equivalent to a closed–chamber test suddenly interrupted by closing the drillstem test valve at the bottom of the wellbore. The computer program presented in Appendix F can be used to obtain solutions for this case by specifying a time or bottomhole pressure at which the well is shut–in.

Figs. 6.22.a and 6.22.b show an example of a closed–chamber test interrupted by a shut–in at $t_D/C_D=10$ for the same set of data as the one used in Fig. 6.19.a. In this case, the liquid level stops moving at $z_D=-0.50$ at the moment at which the drillstem test valve is shut–in.

The relationship between the values of the dimensionless parameters involved in the description of the flow phenomena during a slug test, drillstem test, and closed–chamber test for conditions found in practice is discussed in the following section.

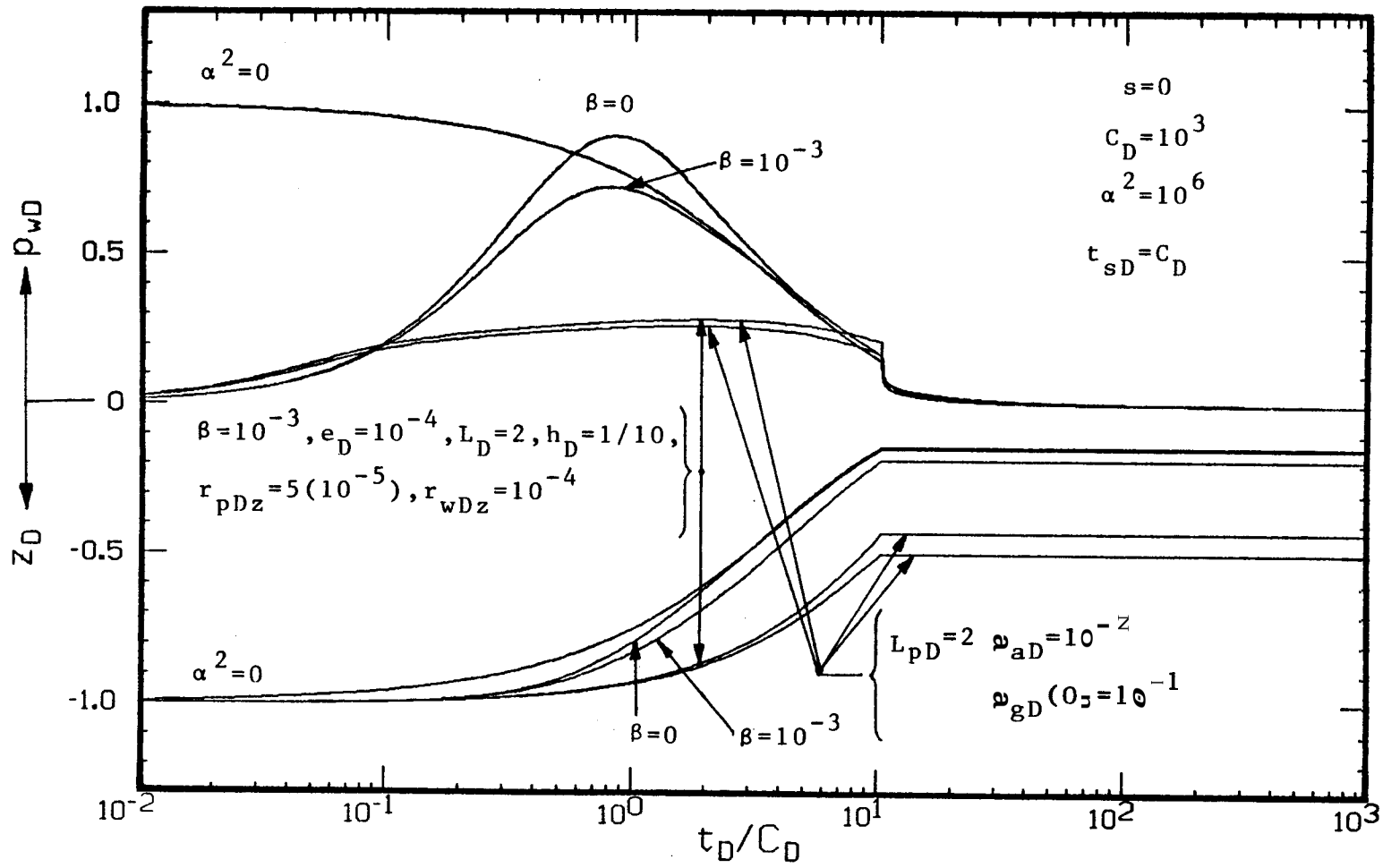

FIG. 6.22.a. SEMI-LOG GRAPH OF THE SOLUTION FOR p_{wD} VS t_D/C_D DURING A FLOW AND SHUT-IN OF A CLOSED-CHAMBER TEST IN A SYSTEM WITH s=0, $C_D=10^3$, $\alpha^2=10^6$, $\beta=10^{-3}$, $e_D=10^{-4}$, $L_D=2$, $h_D=1/10$, $r_{pDz}=5[10^{-5}]$, $r_{wDz}=10^{-4}$, $L_{pD}=2$, $p_{gD}(0)=1/10$, $p_{aD}=10^{-2}$, AND $t_{sD}/C_D=10$

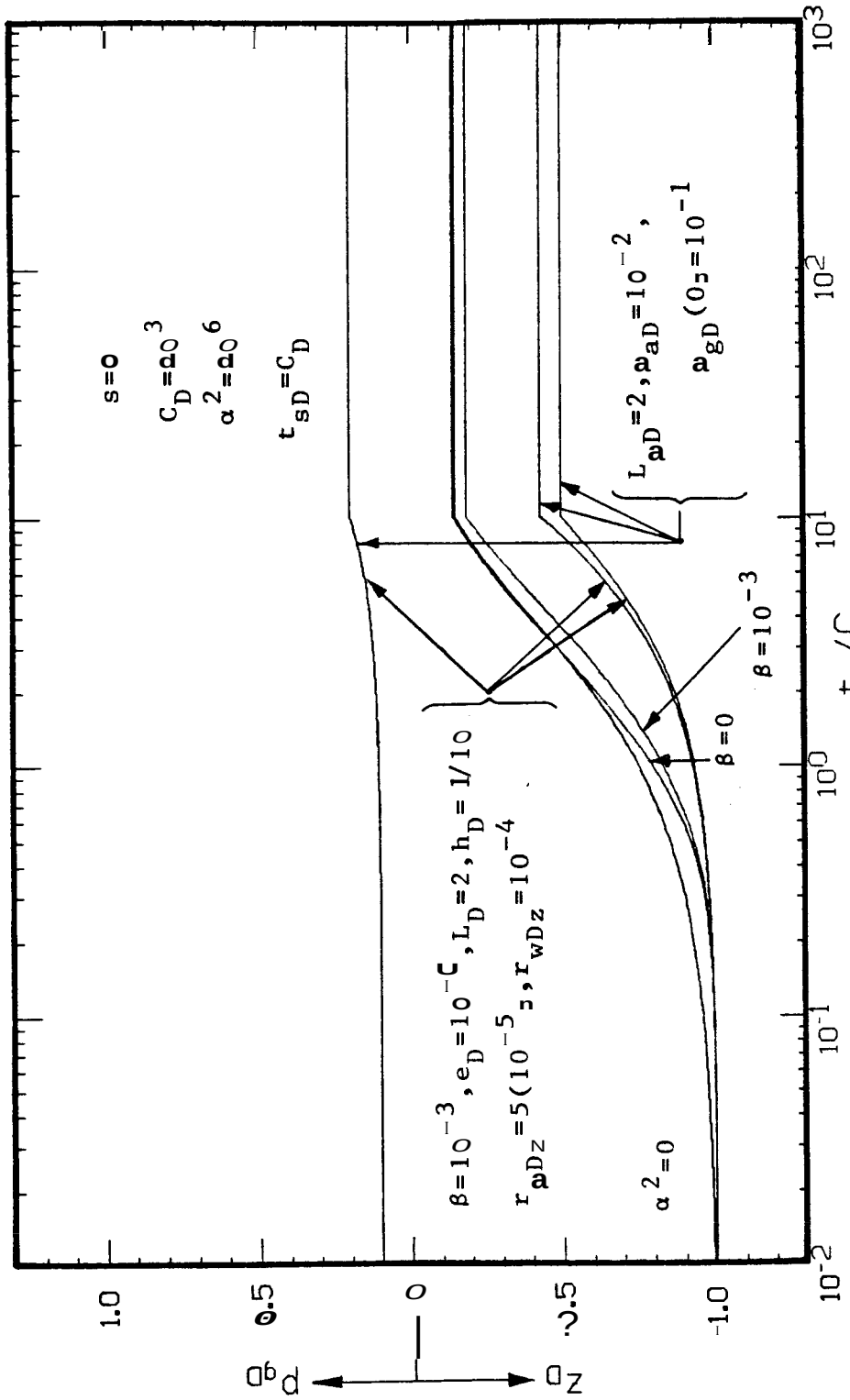

FIG. 6.22.b. SEMI-LOG GRAPH OF THE SOLUTION FOR P_{gD} VS t_D/C_D DURING A FLOW AND SHUT-IN OF A CLOSED-CHAMBER TEST IN A SYSTEM WITH s=0, $C_D=10^3$, $\alpha^2=10^6$, $\beta=10^{-3}$, $e_D=10^{-4}$, $L_D=2$, $h_D=1/10$, $r_{pDz}=5[10^{-5}]$, $r_{wDz}=10^{-4}$, $L_{pD}=2$, $P_{gD}(0)=1/10$, $P_{aD}=10^{-2}$, AND $t_{sD}/C_D=10$

SECTION 7
PRACTICAL CONSIDERATIONS

In order to illustrate examples of the relationship between the values of dimensionless parameters describing wellbore–reservoir system conditions found in practice, slug test and drillstem test field data reported in the literature are reviewed in Section 7.1. Broader limits for the range of values of dimensionless parameters that can be expected in practical applications are generated by defining information for a synthetic reference system, and conducting systematic alterations of that information in Section 7.2.

7.1 Published Field Data

One of the purposes of formulating the mathematical problem describing the flow phenomena during a slug test, drillstem test, or closed–chamber test in terms of dimensionless quantities was to reduce the number of parameters required to define the corresponding solutions. Since a dimensionless parameter is a group of reservoir, fluid, and wellbore characteristics, the effect of a given dimensionless parameter on the solutions obtained in this study represents the combined effect of the system properties included in the definition of that dimensionless parameter.

However, according to the definitions of the dimensionless parameters and variables used in the present study, there are some system properties that appear in two or more of those parameters and variables. For example, k appears in a, B, and t_D, but not in C_D. Therefore, the values of the dimensionless parameters containing one or more system properties in common must be interrelated to correspond to a

system that could be found in practice. Since actual systems can be expected to exhibit values of reservoir, fluid, and wellbore characteristics that vary enormously for different systems, a literature survey was conducted to define ranges of variation for the properties of typical systems found in practical applications of slug tests, drillstem tests, and closed-chamber tests.

Table 7.1 shows information obtained in this literature survey, and includes some parameters not given explicitly in the data but that were estimated from the available description of the corresponding test. As shown in this table, wellbore and pipe radii vary approximately from 0.14 to 0.40 ft, with a weighted average of 0.20 ft, 2.4 in. Omitting the data published by Blankennagel (1968) for injection slug tests conducted to determine rock formations adequate for mining operations below the water table, porosity varies from 0.04 to 0.30, with an average of 0.15, and permeability varies from a few milidarcies to tens of darcies. The largest values of permeability correspond to groundwater aquifers, and values of permeability lower than one hundred millidarcies are usual for commercial oil reservoirs. Rock formation thickness varies from ten to a few hundred feet, with an approximate average of 50 ft. Although total system compressibility can be as low as $2.4(10^{-6})$ psi^{-1} or as high as $2.4(10^{-4})$ psi^{-1}, an average value is $2(10^{-5})$ for oil reservoirs. Liquid viscosity is close to one centipoise in water and in some oil wells. Hot fluids from deep wells show smaller viscosities, but oil produced from shallow formations usually exhibits viscosity reported in multiples of poises. Liquid density is close to that of water, or only as much as 20 % smaller. Reservoir pressures vary from 30 to 4,500 psi. Only a few estimations of skin effect were available in the data reviewed. Also, it was observed that the first flow period of many drillstem tests reported in the literature was performed with no cushion. However, the liquid produced during the first flow period is the cushion for the second flow period, which is normally the longest.

Table 7.2 shows the values of dimensionless parameters C_D, a, and β calculated from the reported data shown in Table 7.1. Values of dimensionless wellbore storage, C_D, vary between $3(10^2)$ to $6(10^2)$ for

TABLE 7.1. PUBLISHED FIELD DATA

AUTHORS		FLUID TYPE	r_p [ft]	r_w [ft]	ϕ [frac.]	k [md]	h [ft]	c_t [psi^{-1}]	μ [cp]	ρ lb/ft^3	p_i [psia]	L [ft]	s
Ferris and Knowles	(1954)	G	0.250	0.250	~0.30	3,300	~200	5(10^{-6})	1.0	62.4	~101	99	~0
Cooper et al.	(1967)	G	0.250	0.250	~0.23	1,850	38	9(10^{-5})	1.0	62.4	~113	178	~0
Blanknagel	(1968)	W	0.250	0.250	~0.25	~1	100	1.0(10^{-6})	1.0	62.4	~1,190	2,662	~0
van der Kamp	(1976)	N	0.167	0.167	~0.30	16,040	36	2.4(10^{-4})	1.0	62.4	32	22	~0
van der Kamp	(1976)	N	0.167	0.167	~0.30	16,550	39	2.2(10^{-4})	1.0	62.4	35	28	~0
van der Kamp	(1976)	W	0.167	0.167	~0.30	15,900	39	2.2(10^{-4})	1.0	62.4	32	15	~0
Dolan, et al.	(1957)	O	0.159	~0.250	0.10	7	20	2.4(10^{-6})	1.0	~50.0	1,815	5,174	+1
Gatlin	(1960)	O	0.159	~0.250	~0.15	22	20	~1.0(10^{-5})	0.4	51.5	4,515	12,573	
Amman	(1960)	O	0.159	0.365	~0.15	13	16	~1.0(10^{-5})	0.6	50.3	1,753	4,968	
Amman	(1960)	O	~0.159	~0.250	~0.15	6	47	~1.0(10^{-5})	0.5	53.0	4,086	11,038	
Maier	(1962)	W	0.159	~0.250	~0.15	11	8	~1.0(10^{-5})	1.0	~50.0	1,806	5,155	
Murphy	(1964)	O	0.159	~0.250	~0.15	36	69	~1.0(10^{-5})	2.4	50.5	1,115	3,102	
Johnston-Miller	(1964)	O	0.159	~0.250	0.10	10	10	8(10^{-6})	1.5	53.0	1,925	5,185	
McAlister, et al	(1965)	O	~0.159	~0.250	~0.10	9	35	1.0(10^{-5})	0.5	50.0	4,019	11,515	
Bredehoeft	(1965)	O	0.39	0.250	~0.15	25	~50	~1.0(10^{-5})	~1.0	~50.0	2,087	5,943	
Brill, et al.	(1969)	O	~0.375	0.750	0.15	5	100	3.0(10^{-6})	0.3	50.0	2,494	7,070	-9
Kohlhaas	(1972)	O	0.159	0.250	0.15	7	9	1.0(10^{-5})	0.4	40.6	2,240	7,888	
Ramey, et al.	(1975)	O	0.188	0.328	0.16	27	14	8.0(10^{-6})	1.0	52.8	3,490	9,471	
Sinha, et al.	(1976)	O	~0.188	0.328	0.15	980	26	1.2(10^{-5})	2.2	53.0	564	1,479	+12
Shimohara and Gray	(1979a)	O	0.39	0.365	0.05	5,320	70	6.0(10^{-6})	156.3	57.7	1,880	4,620	+33

TABLE 7.2. DIMENSIONLESS PARAMETERS FOR PUBLISHED FIELD DATA

AUTHORS		FLUID TYPE	C_D	α	β	$\frac{\alpha}{C_D}$	$\alpha-\beta$	$\frac{C_D}{10}$	$\frac{h}{L}[\frac{r_e}{r_w}]^2$
Harris and Knowles	(1954)	W	$3.8(10^2)$	$4.5(10^2)$	$5.3(10^{-6})$	$1.2(10^0)$	$2.4(10^{-3})$	$3.8(10^1)$	$2.0(10^0)$
Cooper, et al.	(1967)	W	$5.0(10^2)$	$2.2(10^2)$	$1.5(10^{-5})$	$4.4(10^{-1})$	$3.3(10^{-3})$	$5.0(10^1)$	$5.5(10^{-1})$
Blasingame	(1968)	W	$5.8(10^5)$	$5.3(10^2)$	$2.4(10^{-5})$	$9.1(10^{-4})$	$1.3(10^{-2})$	$5.8(10^4)$	$2.1(10^{-2})$
van den Kamp	(1976)	W	$4.5(10^2)$	$4.8(10^2)$	$5.3(10^{-6})$	$1.1(10^0)$	$2.5(10^{-3})$	$4.5(10^1)$	$1.6(10^0)$
van den Kamp	(1976)	W	$4.5(10^2)$	$6.1(10^2)$	$4.7(10^{-6})$	$1.4(10^0)$	$2.9(10^{-3})$	$4.5(10^1)$	$2.3(10^0)$
van den Kamp	(1976)	W	$3.6(10^2)$	$4.3(10^2)$	$4.9(10^{-6})$	$1.2(10^0)$	$2.1(10^{-3})$	$3.6(10^1)$	$3.3(10^0)$
Dolan, et al.	(1957)	O	$1.2(10^5)$	$4.3(10^2)$	$1.2(10^{-4})$	$3.6(10^{-3})$	$5.2(10^{-2})$	$1.2(10^4)$	$9.6(10^{-3})$
Gatlin	(1960)	O	$1.9(10^4)$	$8.5(10^2)$	$3.8(10^{-5})$	$4.5(10^{-2})$	$3.2(10^{-2})$	$1.9(10^3)$	$2.6(10^{-3})$
Ormann	(1960)	O	$1.1(10^4)$	$9.9(10^1)$	$3.2(10^{-4})$	$9.0(10^{-3})$	$3.2(10^{-2})$	$1.1(10^3)$	$6.1(10^{-4})$
Ormamn	(1960)	O	$7.8(10^3)$	$1.4(10^3)$	$2.1(10^{-4})$	$1.8(10^{-1})$	$2.9(10^{-1})$	$7.8(10^2)$	$1.7(10^{-3})$
Maier	(1962)	O	$4.9(10^4)$	$1.1(10^2)$	$5.0(10^{-4})$	$2.2(10^{-3})$	$5.5(10^{-2})$	$4.9(10^3)$	$6.3(10^{-4})$
Murphy	(1964)	O	$5.6(10^3)$	$1.1(10^2)$	$8.6(10^{-4})$	$2.0(10^{-2})$	$9.5(10^{-2})$	$5.9(10^2)$	$9.0(10^{-3})$
Johnston-Macco	(1964)	O	$6.5(10^4)$	$1.2(10^2)$	$6.5(10^{-4})$	$1.8(10^{-3})$	$7.8(10^{-2})$	$6.5(10^3)$	$1.2(10^{-3})$
McAlister, et al	(1965)	O	$1.7(10^4)$	$4.3(10^2)$	$8.5(10^{-5})$	$2.5(10^{-2})$	$3.7(10^{-2})$	$1.4(10^3)$	$5.3(10^{-4})$
Miredehoeft	(1965)	O	$7.8(10^3)$	$2.7(10^2)$	$2.2(10^{-4})$	$3.5(10^{-2})$	$5.9(10^{-2})$	$7.8(10^2)$	$7.0(10^{-5})$
Hill, et al.	(1969)	O	$1.5(10^4)$	$1.8(10^2)$	$1.9(10^{-5})$	$1.2(10^{-2})$	$3.4(10^{-3})$	$1.5(10^3)$	$1.3(10^{-2})$
Kohlhaas	(1972)	O	$3.8(10^4)$	$1.5(10^2)$	$2.1(10^{-4})$	$3.9(10^{-3})$	$3.2(10^{-2})$	$3.8(10^3)$	$4.6(10^{-4})$
Ramey, et al.	(1975)	O	$2.5(10^4)$	$2.5(10^2)$	$2.0(10^{-4})$	$1.0(10^{-2})$	$5.0(10^{-2})$	$2.5(10^3)$	$4.9(10^{-4})$
Samhe, et al.	(1976)	O	$9.5(10^3)$	$1.1(10^3)$	$3.7(10^{-5})$	$1.2(10^{-1})$	$4.1(10^{-2})$	$9.5(10^2)$	$5.8(10^{-3})$
Shinohara and Ramey	(1979.a)	O	$1.1(10^4)$	$7.6(10^2)$	$1.2(10^{-2})$	$6.9(10^{-2})$	$8.6(10^0)$	$1.1(10^3)$	$2.2(10^{-3})$

groundwater wells, and between $5(10^3)$ to 10^5 for oil wells. Values of dimensionless initial deaccelerating factor, a, vary only slightly between 10^2 and 10^3 for both water and oil wells. Values of dimensionless wellbore friction factor, β, are in the order of 10^{-5} for groundwater wells and in the order of 10^{-4} for most of the oil wells with drillstem test data reported in the literature surveyed. The previous values of these dimensionless parameters were used to evaluate the rest of the columns in Table 7.2 and to apply the discriminating criteria proposed in Sections 5 and 6 of the present study.

The column for α/C_D indicates that the value of a is close to the value of C_D for groundwater wells but a is two or three orders of magnitude smaller than C_D for oil wells. According to the criteria developed in Section 5, inertial effects are negligible for:

$$\alpha^2 < a_I^2 = \frac{C_D^2}{10} \quad , \text{for } 0 < s < 5 \qquad \ldots (7.1)$$

which is equal to:

$$\frac{\alpha}{C_D} < \frac{1}{\sqrt{10}} = 0.3162\ldots \quad , \text{for } 0 < s < 5 \qquad \ldots (7.2)$$

Since a skin factor larger than 5 causes an earlier bottomhole pressure response, inertial effects are negligible for the oil wells with drillstem test data shown in Table 7.1. The response of these wells can be expected to lie to the left of the lines for $\alpha^2=C_D^2/10$ in the type curves presented in Figs. 5.7.a - 5.7.k.

Criteria developed in Section 5 for values of $C_D > 103$ indicates that oscillations can be expected for:

$$\alpha^2 > a_o^2 = 20\, C_D^2 \quad , 0 < s < 5 \qquad \ldots (7.3)$$

which is equal to:

$$\frac{a}{C_D} = \sqrt{20} = 4.472\ldots \quad , 0 < s < 5 \qquad \ldots (7.4)$$

A production slug test reported by van der Kamp (1976), and shown as the last set of data for groundwater wells in Tables 7.1 and 7.2, exhibited oscillations although $\alpha/C_D=1.2$. This does not contradict the criterion given by Eq. 7.4 because $C_D=3.6(10^2)$, which is smaller than 10^3.

On the other hand, critically-damped systems correspond to values of a in the range:

$$a_I < \alpha < \alpha_o \qquad \ldots (7.5)$$

Solutions for critically-damped systems only follow the late part of the solutions neglecting inertia that were obtained by Ramey and Agarwal (1972) and correlated in the form of three type curves by Ramey, Agarwal, and Martin (1975). A few lines from those type curves are shown in Figs. 5.4.d - 5.4.f. Shinohara and Ramey (1979.b) included the effect of inertia in the wellbore. Those solutions were reproduced, extended, and correlated in the present study in the form of the type curves shown in Figs. 5.7.a - 5.7.ℓ. An example of the behavior of critically-damped solutions can be observed from the set of lines for $\alpha^2 = C_D^2$ shown in those type curves.

The semi-log type curve in Fig. 5.7.d indicates that for a critically-damped system with a = C_D, the early-time dimensionless bottomhole pressure data points fall above the solution neglecting wellbore inertial effects. Also, such data points will form a steeper line above the solution neglecting inertia. An important observation from Fig. 5.7.d is that the solutions for $\alpha=C_D$ including inertia, and the solutions neglecting inertia merge after p_{wD} is smaller than 0.6, which corresponds to bottomhole pressure recoveries of *40 %* in the range between cushion pressure, p_c, and reservoir pressure, p_i. Since the flow period of many drillstem tests usually shows pressure recoveries smaller than *40 %* before the well is shut-in, type-curve analysis of the flowing bottomhole pressure could be matched with lines for C_De^{2s} much larger than the actual unknown value. This can be an explanation for the large values of C_De^{2s} required to match flowing pressure data from some drillstems tests and liquid level data from some slug tests, for which other sources of information indicate smaller values of C_D and s. Therefore, it is important to estimate the magnitude of the wellbore inertial effects to use the appropriate type curves in the analysis. Also, it is recommended that the value of the dimensionless deaccelerating factor, ***a,*** be calculated after performing an analysis to check the parameters estimation, and repeat the type-curve matching procedure if necessary.

Another source of error in the application of type-curves is the estimation of the cushion pressure, p_c. While the initial reservoir pressure, p_i, can often be obtained from the extrapolation of the pressure buildup curves from the initial or final shut-in periods, hydrostatic cushion pressure, p_c, is usually taken as the lowest pressure recorded immediately after opening the drillstem test valve. Although this can be a valid practice for some systems, wellbore inertial effects can cause an overshoot or an undershoot in bettomhole pressure. For small values of ***a,*** the solutions obtained by Shinohara and Ramey (1979.b) indicate that p_{wD} can become higher than unity, as shown in Figs. 5.5.a - 5.5.e. These conditions cause an overshoot in p_{wD} and correspond to overdamped systems. Values of p_{wD} larger than unity result from bottomhole pressures lower than the hydrostatic

cushion pressure, which can be explained by wellbore inertial effects. Solutions for overdamped systems fall to the left of the set of lines for $\alpha^2 = C_D/10$ shown in the type curves presented in Figs. 5.7.a - 5.7.k. Taking the lowest bottomhole pressure recorded during a flow period as the cushion pressure for an overdamped system results in slightly steeper traces of p_{wD}, which can be matched with type curves for values of $C_D e^{2s}$ larger than the actual values.

On the other hand, results obtained by Shinohara and Ramey (1979.b) also show that some systems will exhibit an undershoot in p_{wD}. In such systems, p_{wD} does not reach the value of unity. That is, the lowest bottomhole pressure recorded during the flow period of a drillstem test is higher than the hydrostatic cushion pressure. As shown in the semi-log type curve presented in Fig. 5.7.d, systems showing an undershoot in p_{wD} have a value of $a > C_D$, and basically correspond to the so called underdamped systems. Taking the lowest bottomhole pressure recorded during a flow period as the cushion pressure for an underdamped system results in slightly flatter traces of p_{wD}, which can be matched with type curves for values of $C_D e^{2s}$ smaller than the actual values.

With respect to frictional wellbore effects, Table 7.2 shows columns with values of $\alpha^2\beta$ and of $C_D/10$, which are useful for applying the following criterion derived in Section 5 to estimate conditions under which laminar frictional wellbore effects are negligible:

$$\alpha^2\beta < \frac{C_D}{10} \qquad \ldots (7.6)$$

A comparison of corresponding values of $a^2\beta$ and $C_D/10$ for each of the tests shown in Table 7.2 indicates that, in general, $a^2\beta$ is from two to four orders of magnitude smaller than $C_D/10$. Therefore, since the criterion given by Eq. 7.6 also applies for common pipe radii and roughnesses, as shown in Section 6, friction losses were negligible during those tests.

Table 7.2 also contains a column showing values of $h/L[r_p/r_w]^2$. Wellbore inertial effects caused by this group of parameters is related to the value of **a** for the corresponding system.

As derived in Section 5, the inertial effects of this group are negligible for:

$$\frac{h}{L}\left[\frac{r_p}{r_w}\right]^2 < \frac{2}{15} = 0.133\ldots \quad \text{, for } a^2 > a_I^2 = \frac{C_D}{10} \qquad \ldots (7.7)$$

As shown in Table 7.2, $h/L[r_p/r_w]^2$ is larger than 0.133 only for some groundwater wells, and is from two to four orders of magnitude smaller for oil wells. These values indicate that the inertial effect of $h/L[r_p/r_w]^2$ is negligible for the oil wells and groundwater wells shown in Table 7.2. However, a small effect can be expected for systems with values of **a** larger than the criterion stated in Eq. 7.7.

As derived in Section 6, inertial and frictional wellbore effects of the cushion size for production slug tests are negligible for:

$$L_D = \frac{L}{-z_0} > 20 \qquad \ldots (7.8)$$

Smaller values of L_T cause a shift of the bottomhole pressure response to earlier times for values of $a^2 < \alpha_I^2 = C_D^2/10$, reducing the effect of inertia. However, for systems with values of $a^2 > \alpha_0^2 = 20C_D^2$, conditions with $L_D < 20$ result in large oscillations due to the cushion size effect. Although not much information is available on the size of the liquid cushion used in the tests reviewed in Tables 7.1, from the corresponding values of a given in Table 7.2, and the description of the drillstem tests, it is estimated that the effect of the cushion size is to reduce the inertial effect in most oil wells. On the other hand, for injection tests with large slugs in groundwater wells, like the ones reported by Ferris and Knowles (1954), and Blankennagel (1968), the effect of the cushion size increases the inertial effects by shifting

the pressure response to later times. However, those investigators measured liquid levels, which are less affected by inertia, as shown in the type curves presented in Fig. 5.7.d.

It is important to emphasize here that slug test and drillstem test field data reported in the literature mainly represent successful applications of the analysis techniques presented or discussed in the corresponding references. This is reflected by the relatively narrow ranges of variation of physical properties with respect to the expected ranges dictated by practical experience. This is specially clear in the case of permeability, k, reservoir thickness, h, and static liquid column length, L. This tendency can be due to one or several of the following reasons:

(1) drillstem testing in prolific and deep reservoirs may have not been required because hydrocarbon manifestations, or mud circulation losses generally indicates the presence of such reservoirs.

(2) Reported field data tend to represent tests for which the flow phenomena can be explained by the theory available at the time of publication.

(3) Unexplained field data is discarded and the test is considered a failure.

(4) Drillstem testing tools and services have been improving gradually, offering more testing options, reliable data, and safety.

(5) Only the pressure buildup data obtained during the shut-in period of a drillstem test has been traditionally considered for analysis and estimation of reservoir properties.

These and other reasons suggest that modern tools and a more general theory should result in a wider range of physical conditions for drillstem testing and analysis. The theory and results presented in this study can be useful in understanding flow phenomena during

drillstem tests in prolific and deep wells like the ones reported by Cinco-Ley, Samaniego, Parra, Dominguez, and Rivera (1983).

The limits of variation of the values of dimensionless parameters that can be expected in practical applications are investigated in the following section.

7.2 Practical Range of Variation for Dimensionless Parameters

The practical range of values for dimensionless parameters is dicussed in this section by defining a reference system and performing separate changes on the properties of the system. This reference system is described by the characteristics shown in Table 7.3. The reference system could represent a system containing heavy oil of low viscosity. Also, the reference system could correspond to a groundwater system with an unusually deep well. Since different variations of the characteristics of the reference system are considered in the following discussion, more practical conditions for oil or for groundwater systems will result as special cases.

According to Eq. 3.1 and the information given in Table 7.3, the length of the static liquid column, L, for the reference system is equal to 10,230 ft. That is, the initial reservoir pressure, pi, can support a liquid column with that length above the top of the formation.

For the practical set of units, used in Tables 7.1 and 7.3, the corresponding units conversion factors required to evaluate dimensionless parameters are given in Table 7.4. The values of the dimensionless parameters describing the reference system, shown in column 2 of Table 7.5, were obtained by using the information given in Table 7.3. A semi-log graph of p_{wD} and z_D vs t_D/C_D for those values of dimensionless parameters is presented in Fig. 7.1. This figure shows that pressure recoveries from cushion pressure, p_c, to initial reservoir pressure, p_i, corresponding to $1-p_{wD}=25$, 50, and 75% occur at $t_D/C_D=1.1$, 3.1, and 7.4, respectively. Cushion pressure can be calculated by

TABLE 7.3. REFERENCE **SYSTEM CHARACTERISTICS**

Reservoir Properties			
Porosity,	ϕ =	0.20	
Permeability,	k =	100	md
Thickness,	h =	150	*ft*
Compressibility,	c_t =	0.00001	psi^{-1}
Initial Reservoir Pressure,	p_i =	*4,480*	psia
Fluid Properties			
Density,	ρ =	62.4	lb_m/ft^3
viscosity,	μ =	1	cp
Wellbore Geometry			
Pipe Radius,	r_p =	0.167	ft
Pipe Relative Roughness,	e_D	0.0001	
Wellbore Radius,	r_w =	0.25	ft
Test Design			
Cushion Length,	L_c =	2,000	ft
General			
Atmospheric Pressure,	p_a =	14.7	psia
Gravity Acceleration,	g =	32.2	ft/s^2

TABLE 7.4. DIMENSIONLESS PARAMETERS IN TERMS OF FIELD UNITS

$$L = 144 \frac{p_i - p_a}{\rho} - \frac{h}{2}$$

$$t_D = \frac{0.000264\ k\ t}{\phi\ \mu\ c_t\ r_w^2}$$

$$C_D = \frac{72\ r_p^2}{9\ e_t\ h\ r_w^2\ \rho}$$

$$\alpha^2 = 1.66(10^{-16})\ L\ \left[\frac{k}{\phi\ \mu\ c_t\ r_w^2}\right]^2$$

$$\frac{\frac{73{,}420}{k}}{\mu_p\ \frac{}{\phi\ \mu\ c_t\ r_w^2}\ r_p^2}$$

$$p_{wD} = p_i - [\ p_c + p_a\ ] \qquad p_D = \frac{p_i - p}{p_i} - [\ p_c + p_a\ ]$$

$$z_D = \frac{z}{-z_0} \qquad L_D = \frac{L}{-z_0} \qquad L_{pD} = \frac{L_p}{-z_0}$$

$$r_{pDz} \quad \frac{r}{-z_0} \qquad r_{wDz} = \frac{r_w}{-z_0}$$

$$r_D = \frac{r}{r_w}$$

TABLE 7.5. DIMENSIONLESS PARAMETERS FOR MODIFICATION OF THE REFERENCE SYSTEM

(1) PARAMETER	(2) REFERENCE SYSTEM	([illegible] SINGLE MOD[illegible]TION	(4[illegible]	(5)	)	([illegible])	(8) REFERENCE SYSTEM WITH ALL MODIFICATIONS
		$p_i^* = p_i/2.5$	$\rho^* = 0.8\rho$	$\mu^* = 10\mu$	$k^* = k/10$	$\phi^* = \phi/2$	
L[ft]	10,[illegible]	[illegible],0[illegible]6	12,8[illegible]6	[illegible]NC[illegible]G[illegible]D	UNCHANGED	[illegible]NCHANG[illegible]D	[illegible],[illegible]2
t/t_D	[illegible] 7[illegible](10^{-6})	UNCHANG[illegible]D	UNCHANGED	4 7[illegible]([illegible]$^{-5}$)	[illegible].7[illegible](1[illegible]$^{-5}$[illegible]	2.37(10^{-6}[illegible]	[illegible].37(1[illegible]$^{-[illegible]}$[illegible]
tC_D/t_D	[illegible].13(10$^{-[illegible]}$)	UNCHANG[illegible]D	1.02(10$^{-[illegible]}$[illegible]	8.13([illegible]$^{-2}$[illegible]	8.13(10^{-2}[illegible]	[illegible]NCHANG[illegible]D	1.05(10$^{[illegible]}$)
C_D	1.[illegible]2(10^{3})	UNCHANG[illegible]D	2 15(1[illegible]^{3})	[illegible]N [illegible]ANG[illegible]D	UNCHANG[illegible]D	[illegible] [illegible]3(1[illegible]^{3}[illegible]	[illegible] [illegible]9(1[illegible]$^{[illegible]}$[illegible]
α^2	1.[illegible]9(1[illegible]^{6}[illegible]	[illegible].29(1[illegible]$^{[illegible]}$)	1.36(1[illegible]^{6}[illegible]	1.09(10$^{[illegible]}$[illegible]	1.09(10$^{[illegible]}$[illegible]	[illegible] 36(1[illegible]^{6}[illegible]	2 15(1[illegible]^{2}[illegible]
β	5 27(10^{-5})	UNCHANG[illegible]D	6.[illegible]9(10^{-5})	5.27(10^{-3}[illegible]	5.[illegible]7(1[illegible]$^{-[illegible]}$[illegible]	[illegible] 6[illegible](1[illegible]$^{-5}$[illegible]	[illegible] 3[illegible](1[illegible]$^{-[illegible]}$)

*modified parameter with respect to the reference system characteristic given in Table 7 3

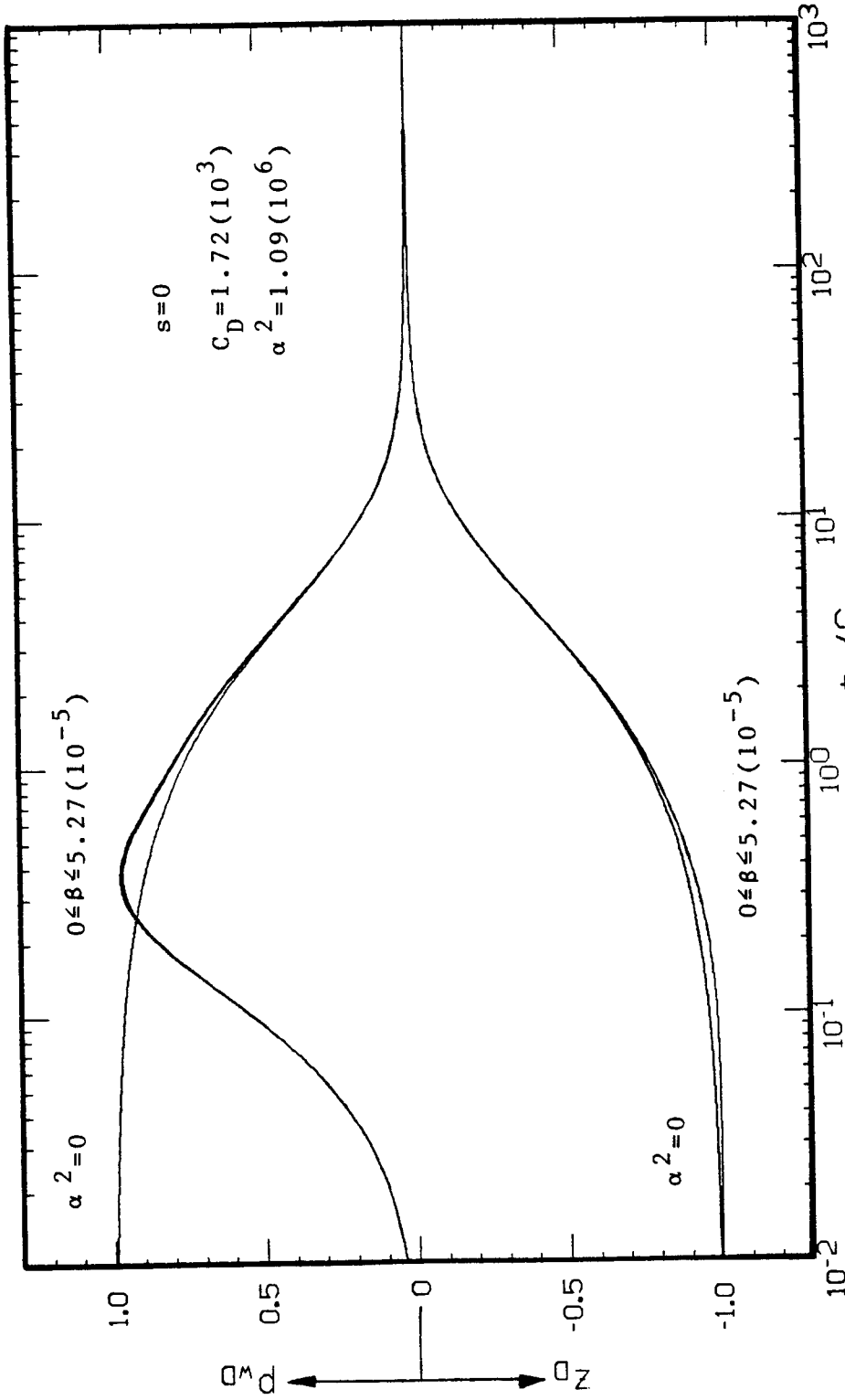

FIG. 7.1. SEMI-LOG GRAPH OF P_{wD} AND z_D vs t_D/C_D FOR THE REFERENCE SYSTEM DESCRIBED IN TABLE 7.3

substituting information given in Table 7.3 into Eq. 3.27, resulting p_c=899 psia. Then, since $t[hr]/t_D=4.74(10^{-6})$ from Table 7.5, bottomhole pressure, p_w, is 895 psia after 0.5 min, 1791 psia after 1.5 min, and 2,686 after 3.6 min.

The magnitude of the wellbore inertial effects can be investigated by evaluating α_I from Eq. 5.30.a and α_O from Eq. 5.31.a. These calculations result in $\alpha_I^2=C_D2/10=2.96(105)$ and $\alpha_O^2=20C_D^2=5.92(107)$. Comparison of these two values with the value of $\alpha^2=1.09(10^6)$, shown in Table 7.5, indicates that the reference system is critically-damped. Moreover, since $a^2\cong C_D^2$ for the refence system, the corresponding behavior of p_{wD} can be approximated from one of the type curves shown in Figs. 5.7.a.-5.7.d. These figures show that p_{wD} increases from 0 to approximately 1 after $t_D/C_D=0.3$ from the start of the test. This behavior corresponds to p_w dropping from p_i=4,480 psia to approximately p_c=899 psia in approximately 9 seconds. This pressure drop would be recorded as an almost vertical line in a regular drillstem test pressure chart.

Figure 5.7.a shows that the behavior of p_{wD} is almost linear for $t_D/C_D<1$, which corresponds to 30 seconds. Fig. 5.7.b shows a slight curvature for the behavior of p_{wD} in the range $0<t_D/C_D<10$, corresponding to times between 0 and 5 minutes. Fig. 5.7.c shows an almost complete pressure recovery for $t_D/C_D=50$, that is, for t=24.5 minutes.

Using values of dimensionless parameters for the reference system given in Table 7.5, $a^2\beta=57.4$. Since this value is smaller than $C_D/10$, frictional wellbore effects are negligible in this case according to Eq. 5.48. Also, according to Eq. 5.53, since $h/L(r_p/r_w)^2=0.00245$ which is smaller than 0.133, the inertial effects of these lengths are also negligible for the reference system.

The magnitude of the effect of the cushion size, L_c=2,000 ft, can be estimated from Fig. 6.7 because for the reference system $L_D=10,230/8,230=1.24\cong 5/4$. This figure shows that this cushion size reduces the effect of wellbore inertial effects because the pressure response shifts to early times. Therefore, pressure recovery data for

$t_D/C_D > 10^{-1}$ for this reference system could be analyzed by using the type curves presented by Ramey, Agarwal, and Martin (1975), Figs. 5.4.d–5.4.f in this study.

Now, in order to evaluate the effect of variations in reservoir or fluid properties on the values of dimensionless parameters, a single reservoir or fluid property of the reference system is altered at a time, as indicated in each column in Table 7.5. Solutions for the resulting modified systems are shown in Fig. 7.2.

The effect of decreasing p_i by a factor of *0.4* is shown in column 3 of Fig. 7.5. Since α^2 is proportional to L, and L is nearly proportional to p_i, a lower p_i results in a lower L and a lower α^2. However, C_D and t_D are not affected by a change in p_i under the implicit assumption that reservoir and fluid properties are independent of pressure. Therefore, inertial wellbore effects decrease as p_i or L decrease.

Column 4 in Fig. 7.5 shows results for a change of liquid density, ρ, from water to light oil. L, t_D/C_D, α^2, and β are slightly larger, indicating that density has only a small effect on the magnitude of the inertial and frictional wellbore effects during a drillstem test.

On the other hand, the effect of liquid viscosity, μ, on the flow phenomena is illustrated by the values in column 5 of Table 7.5. A ten-fold increase in μ results in values of α^2 and β one hundred times smaller than in the reference system. However, t_D is only ten times smaller. Since C_D remains unchanged, an increase in μ causes a delayed pressure response because $t[hr]C_D/t_D$ is larger.

A reduction in reservoir permeability, k, by one order of magnitude results in the values shown in column 6 of Table 7.5. L and C_D remain unchanged, β and t_D decrease by one order of magnitude. However, α^2 decreases by two orders of magnitude. This large reduction of α^2 causes wellbore inertial effects to become less important. Also, this reduction in k shifts the response of p_{wD} towards later times in the same manner as the increase of μ, previously discussed.

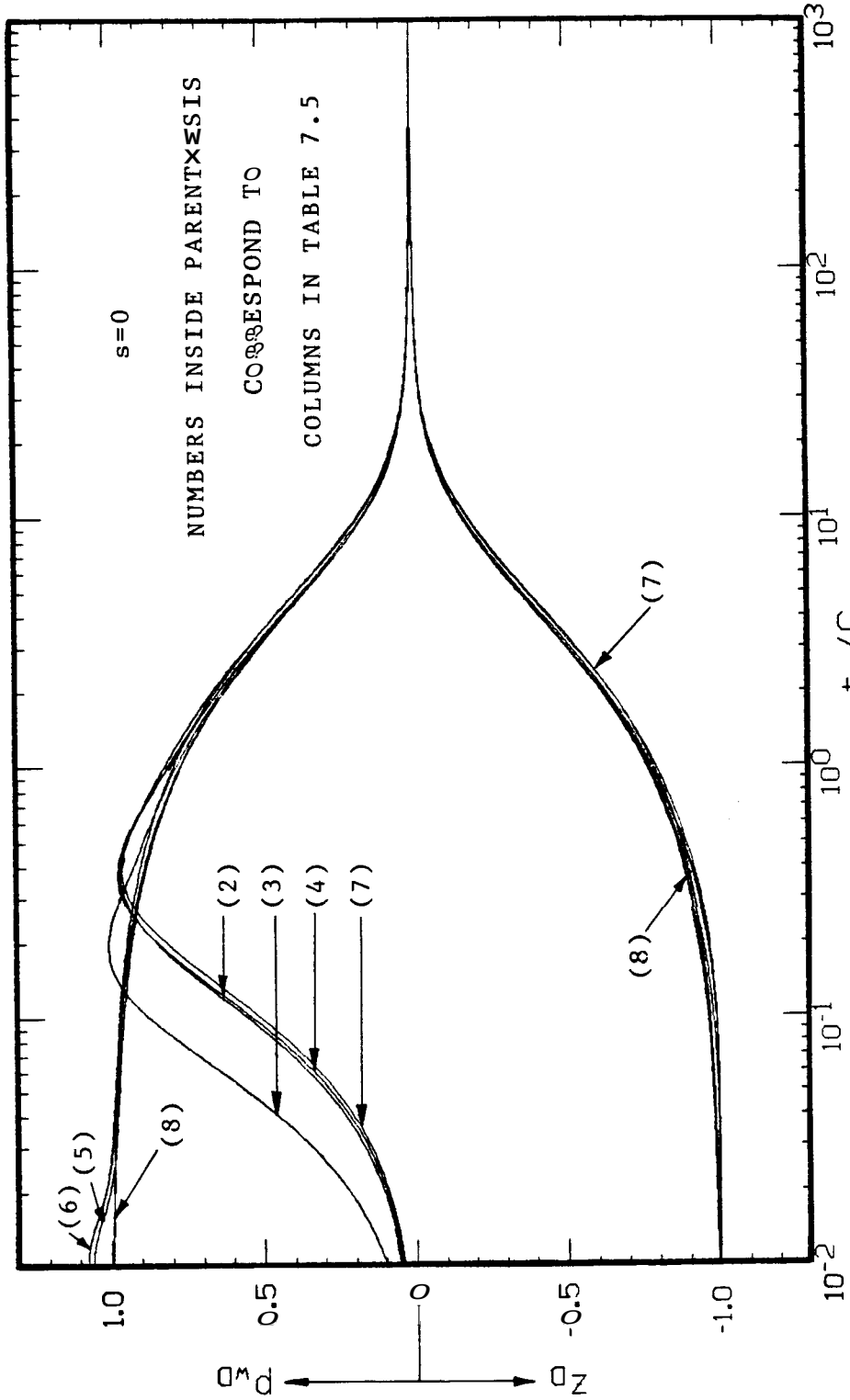

FIG. 7.2. SEMI-LOG GRAPH OF P_{wD} AND z_D vs t_D/C_D FOR THE MODIFICATIONS OF THE REFERENCE SYSTEM DEFINED IN TABLE 7.5

As shown in column 7 of Table 7.5, a 50% reduction in porosity, ϕ, causes a reduction of 50% in β, an increase of 100% in t_D and C_D, and an increase of 400% in a^2. However, L and t_D/C_D remain unchanged. Therefore, the pressure response should be observed in the same period of actual time as for the reference system.

Column 8 in Table 7.5 shows the results for a system with the properties of the reference system, given in Table 7.3, but simultaneously incorporating all the alterations given in columns 3-7 in Table 7.5. As can be observed in Fig. 7.2, wellbore inertial and frictional effects for this modified system are negligible. The pressure response occurs at much later actual times than for the reference system.

This brief discussion of alterations of the properties of a synthetic reference system illustrates the range of variation that can be expected for dimensionless parameters C_D, a, and β in practice, and the relationship between those parameters required to represent a real system.

The main conclusions reached throughout this study are presented in the following section.

SECTION 8
CONCLUSIONS AND RECOMMENDATIONS

Analysis of results presented in this study lead to the following conclusions and recommendations:

(1) A mathematical formulation is proposed to describe the flow phenomena occurring during a slug test, a drillstem test, or a closed-chamber test. This formulation is based on a wellbore momentum balance equation including gravitational, inertial, and frictional effects considered negligible by previous investigators. This wellbore equation is derived by performing momentum balances on two control volumes representing the wellbore.

(2) The wellbore momentum balance equation is coupled with the diffusivity equation by using conditions including skin effect and wellbore storage. Appropriate initial and boundary conditions complete the statement of a general initial value mathematical problem for these types of tests. This problem statement is expressed in terms of dimensionless parameters by defining groups of physical properties that affect the response of a wellbore-reservoir system.

(3) A semi-analytical method based on the Laplace transformation and the Stehfest numerical inversion algorithm is presented to solve slug tests and drillstem tests described by linear mathematical problems.

(4) A numerical method using a finite-difference approximation solved by the Thomas algorithm is derived to reproduce the semi-analytical solutions and to evaluate solutions for slug tests, drillstem tests, and closed-chamber tests described by non-linear mathematical problems.

(5) Both solution methods provide results for the behavior of bottomhole pressure, rate of change of bottomhole pressure, wellbore liquid level, liquid column velocity (flow rate), liquid column acceleration, and reservoir pressure distribution.

(6) Approximate type curves for slug tests in systems with $0 \leq s \leq 5$, including wellbore inertial effects for a small slug size and neglecting frictional effects, are presented in this study. These type curves indicate that inertial effects are negligible in overdamped systems, for which:

$$a^2 < \alpha_I^2 = \frac{C_D^2}{10} \qquad \ldots (8.1)$$

or, in field units:

$$\sqrt{L}\,\frac{\rho}{r_p^2}\,\frac{kh}{\mu} < 1.79(10^9) \qquad \ldots (8.2)$$

Also, these type curves indicate that inertial wellbore effects can cause pressure and liquid level oscillations for underdamped systems, for which:

$$a^2 > \alpha_O^2 = 20\ C_D^2 \qquad \ldots (8.3)$$

or, in field units:

$$\sqrt{L}\,\frac{\rho}{r_p^2}\,\frac{kh}{\mu} > 2.50(10^{10}) \qquad \ldots (8.4)$$

Critically-damped systems correspond to intermediate conditions, for a value of a in the following range:

$$a_I < \alpha < \alpha_O \qquad \ldots (8.5)$$

where α_I and α_O are given in Eqs. 8.1 and 8.3, respectively. Therefore, in field units, critically-damped are defined by the following conditions:

$$1.79(10^9) < \sqrt{L}\,\frac{\rho}{r_p^2}\,\frac{kh}{\mu} < 2.50(10^{10}) \qquad \ldots (8.6)$$

(7) A literature survey reveals that published drillstem test field data mainly correspond to overdamped systems with negligible friction losses. However, the definition of dimensionless deaccelerating factor, a, and practical wellbore-reservoir characteristics suggest that critically-damped systems also occur frequently. Moreover, the shape of the type curves for solutions including inertia indicates that analysis of early-time drillstem test pressure data from critically-damped systems can be erroneously matched with solutions neglecting inertial effects, resulting values of $C_D e^{2s}$ larger than the values corresponding to the correct C_D and s. This can be an explanation of the large values of skin effect, s, obtained from analysis of bottomhole flowing pressure data, as compared to the values of s determined from pressure buildup analysis, for some systems.

(8) The non-linear inertial effects of the cushion size were evaluated using the numerical solution method. These results reproduce the solutions presented by Shinohara and Ramey (1979.b) for systems with:

$$L_D > 20 \qquad (8.7)$$

or, in field units:

$$| z_0 | < \frac{L}{20} \qquad \ldots (8.8)$$

That is, results for cushion sizes corresponding to slug lengths smaller than one twentieth of the static liquid column length are similar. These results also show that the solutions shift to earlier time as the cushion size decreases. This causes a smaller inertial effect for overdamped systems, but a larger inertial effect for underdamped systems. Moreover, these results also show that the effect of the cushion size is small for cushion sizes as small as one twentieth of the static liquid column length. Therefore, the use of a small cushion for overdamped systems improves the applicability of the type curves neglecting inertial and frictional effects proposed by Ramey, Agarwal, and Martin (1975). On the other hand, the use of a small slug (large cushion) in underdamped systems is recommended to obtain a response that can be analyzed by the approximate solution proposed by van der Kamp (1976), or by the solutions presented by Shinohara and Ramey (1979.b). Control of the cushion size also can be exercised to convert a critically-damped system into an overdamped or into an underdamped system by decreasing or increasing the cushion size, respectively.

(9) Laminar friction wellbore effects are evaluated using the semi-analytical solution method, and it is found that these effects are negligible for:

$$\alpha^2 \beta < \frac{C_D}{10} \qquad \ldots (8.9)$$

or, in field units:

$$L \frac{\mu_p}{r_p^4} \frac{kh}{\mu} < 5.89(10^{11}) \quad \ldots (8.10)$$

(10) Results from application of the numerical solution method to systems with common drill pipe sizes indicate that the criterion expressed by Eqs. 8.9 and 8.10 is also applicable for estimating the conditions under which frictional effects for changing flow regimes are negligible for typical testing conditions.

These results do not assume a specific flow regime throughout a test. Calculation of Moody friction factor is performed at each time step by applying standard expressions for laminar, critical, transition, or turbulent flow regimes, according to the value of the Reynolds number for the average velocity during the corresponding time step.

(11) New type curves considering negligible inertial and frictional effects are presented in this study to perform integral bottomhole pressure analysis of the flowing and shut-in periods of a drillstem test, simultaneously. These type curves are obtained by assuming that wellbore storage becomes negligible immediately after the drillstem test valve is shut-in. Therefore, these type curves are applicable to systems with a small volume of liquid inside the wellbore below the drillstem test valve. Validity of this assumption is supported by the similitude between Cartesian representations of these type curves and typical drillstem test pressure traces. These type curves show a linear, or apparently linear, pressure recovery during the flow period, and a discontinuity and subsequent pressure buildup during the shut-in period.

The apparently linear pressure recovery corresponds to the solution presented by Ramey and Agarwal (1972), but is not obvious in the corresponding semi-log and log-log type curves proposed by Ramey, Agarwal, and Martin (1975). Since, inertia and friction during the

flow period are assumed negligible in these solutions, the symmetry between the pressure and liquid level solutions describes an approximate linear bottomhole pressure recovery due to a nearly-constant flow rate at early-times. This is a paradoxical situation, but is commonly observed in typical drillstem test data with short flow periods. Therefore, these solutions suggest that an explanation for this observation is intrinsic in the nature of the flow phenomena occurring at early time during these types of tests.

The proposed type curves also show a sharper discontinuity and a larger initial pressure buildup for a larger value of $C_D e^{2s}$, as can be expected for systems with the same wellbore storage during the flow period, no wellbore storage during the shut-in period, but different values of skin effect.

(12) Finally, the increasing importance of drillstem testing as an early reservoir evaluation and diagnostic tool justifies further research work to improve the understanding of some practical and theoretical aspects of slug test, drillstem test, and closed-chamber test analysis that have been assumed negligible in previous and present studies. The following is a partial list of effects that require additional research:

(a) compressibility of the fluids in the wellbore,
(b) liberation of dissolved-gas,
(c) two-phase vertical flow in the wellbore,
(d) wellbore storage during the shut-in period,
(e) stimulated or fractured well (negative skin effect), and
(f) inertial and frictional effects for drillstem test data analysis in naturally-fractured reservoirs.

NOMENCLATURE

a_i = coefficients below the main diagonal. in a tridiagonal system of equations

A_w = coefficients for the liquid column acceleration term in a wellbore equation

b_i = coefficients on the main diagonal in a tridiagonal system of equations

B_w = coefficients for the liquid column velocity term in a wellbore equation

c_i = coefficients above the main diagonal in a tridiagonal system of equations

c_t = total system compressibility, $[M^{-1}LT2]$

C = wellbore storage constant, Eq. 3.19, $[M-1L4T2]$

C_D = dimensionless wellbore storage constant, Eq. 3.47

$[C_De^{2s}]_m$ = value of C_De^{2s} for type-curve matching

C_w = coefficients for the liquid level term in a wellbore equation

d_i = independent terms in a tridiagonal system of equations

D_w = coefficients for a special term in a wellbore equation

e = 2.71828...

e_D = relative roughness

E_w = coefficients for the bottomhole pressure term in a wellbore equation

f = Moody friction factor (Moody, 1944)

F = force vector, $[MLT^{-2}]$

g = gravity acceleration vector, $[LT^{-2}]$

h = reservoir thickness, [L]

h_D = dimensionless reservoir thickness, Eq. 3.32

J = number of nodes used to represent t'he reservoir, Eq. D.13

k = reservoir permeability, $[L^2]$

L = static wellbore liquid column length, measured from the level of the top of the formation, Eq. 3.1, [L]

L_c = liquid cushion length, measured from the top of the formation, Fig. 3.7, [L]

L_D = dimensionless length L, Eq. 3.31

L_p = pipe length from the wellhead to the top of the formation, Fig. 3.7, [L]

L_{pD} = dimensionless pipe length, Eq. 3.48

L_s = slug length, measured from the static wellbore liquid level, Fig. 3.10, [L]

m = mass, [M]

n_g = number of moles of gas in a closed-chamber, [moles]

N = number of coefficients v_i in Stehfest algorithm, Eq. 4.9

$p(r,t)$ = reservoir pressure at r and t, $[ML^{-1}T^{-2}]$

p_a = atmospheric pressure, $[ML^{-1}T^{-2}]$

p_{aD} = dimensionless atmospheric pressure, Eq. 3.50

p_c = hydrostatic liquid cushion pressure, Eq. 3.27, [M-1T-2]

$p_D(r_D,t_D)$ = dimensionless reservoir pressure at r_D and t_D, Eq. 3.26

p_g = gas pressure on the wellbore liquid level, $[ML^{-1}T^{-2}]$

p_{gD} = dimensionless gas pressure in the chamber, Eq. 3.49

p_i = initial reservoir pressure at the mid-level of the formation, $[ML^{-1}T^{-2}]$

$p_w(t)$ = bottomhole pressure, $[ML^{-1}T^{-2}]$

$p_{wD}(t_D)$ = dimensionless bottomhole pressure, Eq. 3.24

p_{wsD} = value of p_{wD} at which the well is shut-in

$q(t)$ = instantaneous flow rate, (+) for flow from the reservoir into the wellbore, (-) otherwise, Eq. 3.18, $[L^3T^{-1}]$

$q'(t)$ = derivative of $q(t)$ with respect to t, $[L^3T^{-2}]$

r = radial distance, measured from the center of the wellbore, [L]

r_D = dimensionless radial distance r, Eq. 3.29

r_p = wellbore pipe radius, [L]

r_{pDz} = dimensionless wellbore pipe radius with respect to slug size, Eq. 3.33

r_w = wellbore radius, [L]

r_{we} = effective wellbore radius, Eq. 5.24, [L]

r_{wDz} = dimensionless wellbore radius with respect to slug size, Eq. 3.34

R = universal gas constant, Eq. 3.6, $[ML^2T^{-2}mole^{-1}degree^{-1}]$

Re = Reynolds Number, Eq. 5.39

s = skin factor, Eq. 3.21

S = surface area, $[L^2]$

t = time, [T]

t_D = dimensionless time, Eq. 3.30

$[t_D/C_D]_m$ = value of t_D/C_D for type-curve matching

t_m = time for type-curve matching, [T]

t_s = shut-in time after the start of the test, [T]

= dimensionless shut-in time

U = parameter in the Laplace transformation, Eq. B.12

v = fluid velocity, $[LT^{-1}]$

$|v|$ = magnitude of the component of v in the direction normal to S, Eq. 3.3, $[LT^{-1}]$

v_0 = initial liquid column velocity, Eq. 3.11, $[LT^{-1}]$

V = volume, $[L^3]$

V_i = coefficients in Stehfest algorithm, Eq. 4.9

z(t) = vertical coordinate used to describe wellbore liquid level, measured positive upward from L, Fig. 3.10, [L]

z_D = dimensionless liquid level, Eq. 3.23

z_D' = dimensionless liquid column velocity, Eq. 3.35

z_D'' = dimensionless liquid column acceleration, Eq. 3.36

z_0 = initial value of z, [L]

z'(t) = wellbore liquid column velocity, $[LT^{-1}]$

z"(t) = wellbore liquid column acceleration, $[LT^{-2}]$

Z_g = gas deviation factor, Eq. 3.6

a = dimensionless initial deaccelerating factor, Eq. 3.51

β = dimensionless wellbore laminar friction factor, Eq. 5.43

ϕ = reservoir porosity

ε = small number used as a tolerance

μ_p = average fluid viscosity in the wellbore, $[ML^{-1}T^{-1}]$

μ = average fluid viscosity in the reservoir, $[ML^{-1}T^{-1}]$

π = 3.14159...

ρ = average density of the fluid in the wellbore, $[ML^{-3}]$

σ = integration dummy variable

τ = shear stress, $[ML^{-1}T^{-2}]$

Throughout this study, parenthesis () are used to denote the argument of a function. Square brackets [] and braces {} are used to associate and multiply terms. Vertical lines || denote absolute value.

REFERENCES

Abramowitz, M., and Stegun, I. A. (1972) : Handbook of Mathematical Functions with Formulas, Graphs, and Mathematical Tables, U. S. Dept. of Commerce, Applied Mathematics Series 55, p 374-389.

Agarwal, R. G. (1980) : "A New Method to Account for Producing Time Effects When Type Curves Are Used to Analyze Pressure Buildup Data", paper SPE 9289, presented at the 55th Annual Technical Conference and Exhibition of the Soc Pet. Eng. of A. I. M. E., held in Dallas, Tex. (Sept. 22-24) p 1-20.

Agarwal, R. G., Al-Hussainy, R., and Ramey, H. J., Jr. (1970) : "An Investigation of Wellbore Storage and Skin Effect in Unsteady Liquid Flow : I. Analytical Treatment", Soc. Pet. Eng. J. (Sept.) p 279-290.

Alexander, L. G. (1977) : "Theory and Practice of the Closed-Chamber Drillstem Test Method", J. Pet. Tech. (Dec.) p 1539-1544.

Ammann, C. B. (1960) : "Case Histories of Analyses of Characteristics of Reservoir Rocks from Drill-Stem Tests", J. Pet. Tech., (May) p 27-36.

Aziz, K., and Settari, A. (1979) : Petroleum Reservoir Simulation, Applied Science Publishers, Ltd., London.

Barelli, A. (1979) : "Analysis of a Slug Test or Drill Stem Test for Linear Flow", Proc. Fifth Workshop on Geothermal Reservoir Eng., Stanford U., Calif. (Dec. 13-15) p 13-27.

Bird, R. B., Stewart, W. E., and Lightfoot, E. N. (1960) : Transport Phenomena, John Wiley & Sons, Inc., New York, p 208-240.

Blackwell, J. H. (1954) : "A Transient-Flow Method for Determination of Thermal Constants of Insulating Materials in Bulk", J. Applied Physics (Feb.) v 25, n 2, p 137-144.

Blankennagel, R. K. (1968) : "Geophysical Logging and Hydraulic Testing, Pahute Mesa, Nevada Test Site", Ground Water, (July-Aug.) v 6, n 4, p 24-31.

Bouwer, H., and Rice, R. C. (1976) : "A Slug Test for Determining Hydraulic Conductivity of Unconfined Aquifers with Completely or Partially Penetrating Wells", Water Resources Research, v 12, n 3, p 423-428.

Bredehoeft, J. D. (1965) : "The Drill-Stem Test: The Petroleum Industry's Deep-Well Pumping Test", Ground Water, v 3, n 3, p 31-36.

Bredehoeft, J. D. (1967) : "Response of Well-Aquifer Systems to Earth Tides", J. Geophysical Research (Jun. 15) v 72, n 12, p 3075-3087.

Bredehoeft, J. D. (1981) : Personal Communication.

Bredehoeft, J. D., Cooper, H. H, Jr., and Papadopulos, I. S. (1966) : "Inertial and Storage Effects in Well-Aquifer Systems : An Analog Investigation", Water Resources Research, v 2, n 4, p 697-707.

Bredehoeft, J. D., Cooper, H. H., Jr., Papadopulos, I. S., and Bennett, R. R. (1965) : "Seismic Fluctuations in an Open Artesian Water Well", U. S. Geological Survey Research Professional Paper 525-C, p C51-C57.

Brill, J. P., Bourgoyne, A. T., and Dixon, T. N. **(1969)** : "Numerical Simulation of Drill Stem Tests as an Interpretation Technique", J. Pet. Tech. (Nov.) p **1413-1420.**

Brons, F., and Miller, W. C. **(1961)** : "A Simple Method for Correcting Spot Pressure Readings", Trans. A. I. M. E., v **222,** p **803-805.**

Carslaw, H. **S. (1921)** : Introduction to the Mathematical Theory of the Conduction of Heat in Solids, MacMillan and Co., England.

Carslaw, H. S., and Jaeger, J. C. **(1946)** : Conduction of Heat in Solids, First Edition, Oxford Univ. Press, England.

Carslaw, H. S., and Jaeger, J. C. **(1959)** : Conduction of Heat in Solids, Second Edition, Oxford at the Clarendon Press, England.

Cinco-Ley, H., Samaniego, F. V., Parra, J., Dominguez, G. V., and Rivera, J. R., **(1983)** : "Aspectos Practicos del Analisis de Pruebas de Presion en Yacimientos de Alta Permeabilidad - Area de Cantarell", paper presented at the XXI Congreso Nacional de la A. I. P. M., held in Villahermosa, Tab., Mexico (May) p **1-43.**

Cooper, H. H., Jr., Bredehoeft, J. R., Papadopulos, I. S., and Bennett, R. R. **(1965)** : "The Response of Well-Aquifer Systems to Seismic Waves", J. Geophysical Research (Aug. **15)** v **70,** n **16,** p **3915-3926.**

Churchill, R. V. **(1972)** : Operational Mathematics, McGraw-Hill Book Co., New York.

Cooley, R. L., and Cunningham, A. B. **(1979)** : "Consideration of Total Energy Loss in Theory of Flow to Wells", J. Hydrology, v **43,** p **161-184.**

Cooper, H. H., Jr., Bredehoeft, J. D., and Papadopulos, I. **S. (1967)** : "Response **of** a Finite-Diameter Well to an Instantaneous Charge of Water", Water Resources Research, v **3,** n **1,** p **263-269.**

D'arcy, H. (1856) : Les Fontaines Publiques de la Ville de Dijon, Determination des lois d'ecoulement de l'eau a travers le sable, published by Victor Dalmont, France.

Dolan, J. P., Einarsen, C. A., and Hill, G. A. (1957) : "Special Applications of Drill-Stem Test Pressure Data", Trans. A. I. M. E., v 210, p 318-324.

Earlougher, R. C., Jr. (1977) : Advances in Well Test Analysis, Monograph 5 published by the Soc. Pet. Eng. of A. I. M. E., Dallas, Tex.

Earlougher, R. C., Jr., and Kersch, K. M. (1974) : "Analysis of Short-Time Transient Test Data by Type-Curve Matching", J. Pet. Tech. (July) p 793-800.

Ehlig-Economides, C. A., and Ramey, H. J., Jr. (1979) : "Pressure Buildup For Wells Produced at a Constant Pressure", paper SPE 7985, presented at the California Regional Meeting of the Soc. Pet. Eng. of A. I. M. E., held in Ventura, Calif. (April 18-20) p 1-8.

Eskinazi, S. (1962) : Principles of Fluid Mechanics, Allyn and Bacon, Inc., Boston, Mass., p 7-8, 193-196.

Fenske, P. R. (1974) : "Radial Flow with Discharging Well and Observation Well Storage (Abstract)", EOS Trans. Am. Geophysical Union, v 55, n 12, p 1118.

Fenske, P. R. (1977) : "Type Curves for Recovery of a Discharging Well with Storage", J. Hydrology, v 33, p 341-348.

Ferris, J. C., and Knowles, D. B. (1954) : "The Slug Test for Estimating Transmissibility of an Aquifer", U. S. Geological Survey Ground Water Note 26, p 1-7.

Gatlin, C. (1960) : Petroleum Engineering - Drilling and Well Completions, Prentice-Hall, Inc., Englewood Cliffs, N. J., p 253-268.

Gaver, D. F. **(1966)** : "Observing Stochastic Processes and Approximate Transform Inversions", Oper. Res, v **14**, n **3**, p **444-459.**

Gladfelter, R. E., Tracy, G. W., and Wilsey, L. E. **(1955)** : "Selecting Wells Which Will Respond to Production-Stimulation Treatment", Drilling and Production Practices, A. P. I., p **117-129.**

Hawkins, M. F., Jr. **(1956)** : "A Note on Skin Effect", Trans. A. I. M. E., v **207** p **356-357.**

Horner, D. R. **(1951)** : "Pressure Build-Up in Wells", Proc. Third World Pet. Congress, held in The Hague, Sec. 11, **p 503-523.**

Hurst, W. **(1953)** : "Establishment of the Skin Effect and Its Impediment to Fluid Flow Into a Well Bore", Pet. Eng., (Oct.) v **25**, p **B.6-B.16.**

Jaeger, J. C. **(1956)** : "Conduction of Heat in an Infinite Region Bounded Internally by a Circular Cylinder of a Perfect Conductor", Aust. J. Phys., v **9**, n **2**, p **167-179.**

Johnston-Macco **(1964)** : Review of Basic Formation Evaluation, Schlumberger, Houston, Tex., p **1-29.**

Kelvin, W. T., Sir Lord **(1884)** : "Art. LXXII Compendium of the Fourier Mathematics for the Conduction of Heat in Solids, and the Mathematically Allied Physical Subjects of Diffusion of Fluids and Transmission of Electric Signals Through Submarine Cables", Mathematical and Physical Papers, Cambridge Univ. Press, v II, p **41-60.**

Kohlhaas, C. A. **(1972)** : "A Method for Analyzing Pressures Measured During Drillstem Test Flow Periods", J. Pet. Tech. (Oct.) p **1278-1282.**

Lee, J. **(1982)** : Well Testing, Text Book 1 published by the Soc. Pet. Eng. of A. I. M. E., Dallas, Tex.

Maier, L. F. (1962) : "Recent Developments and Field Applications of Drill-Stem Test Interpretation", paper SPE-290, Soc. Pet. Eng. of A. I. M. E., Dallas, Tex.

Matthews, C. S., and Russell, D. G. (1967) : Pressure Buildup and Flow Tests in Wells, Monograph 1 published by the Soc. Pet. Eng. of A. I. M. E., Dallas, Tex.

McAlister, J. A., Nutter, B. P., and Lebourg, M. (1965) : "A New System of Tools for Better Control and Interpretation of Drill-Stem Tests", J. Pet. Tech., (Feb.) p 207-214.

McKinley, M. (1971) : "Wellbore Transmissibility from Afterflow-Dominated Pressure Buildup Data", J. Pet. Tech. (July) p 863-872.

Miller, C. C., Dyes, A. B., and Hutchinson, C. A., Jr. (1950) : "The Estimation of Permeability and Reservoir Pressure from Bottom-Hole Pressure Build-Up Characteristics", Trans. A. I. M. E., v 189, p 91-104.

Moody, L. F. (1944) : "Friction Factors for Pipe Flow", Trans. A. S. M. E. (Nov.) p 671-684.

Moran, J. H., and Finklea, E. E. (1962) : "Analysis of Pressure Buildup Data obtained by the Wireline Formation Tester", J. Pet. Tech. (Aug.) p 899-908.

Murphy, W. C. (1970) : "The Interpretation and Calculation of Formation Characteristics from Formation Test Data", Pamphlet T-101, Halliburton Co., Duncan, Okla., p 1-19.

Muskat, M. (1937) : The Flow of Homogeneous Fluid through Porous Media, McGraw-Hill Book Co., New York.

Ortiz-Ramirez, J. (1981) : Personal Communication.

Papadopulos, I. S., Bredehoeft, J. D., and Cooper, H. H., Jr. (1973) : "On the Analysis of Slug Test Data", Water Resources Research, (Aug.) v 9, n 4, p 1087-1089.

Papadopulos, I. S., and Cooper, H. H., Jr. (1967) : "Drawdown in a Well of Large Diameter", Water Resources Research, v 3, n 1, p 241-244.

Raghavan, R. (1980) : "The Effect of Producing Time on Type Curve Analysis", J. Pet. Tech. (June) p 1053-1064.

Raghavan, R., Reynolds, A. C., and Meng, H. (1982) : "Analysis of Pressure Buildup Data Following a Short Flow Period", J. Pet. Tech. (April) p 904-916.

Ramey, H. J., Jr. (1970) : "Short-Time Well Test Data Interpretation in the Presence of Skin and Wellbore Storage", J. Pet. Tech. (Jan.) p 97-104.

Ramey, H. J., Jr. (1980) : Notes for Course PE 285D, Research Seminar: Programming Hand Calculators, Stanford University.

Ramey, H. J., Jr. (1982) : "Distinguished Author Series : Pressure Transient Testing", J. Pet. Tech. (July) p 1407-1413.

Ramey, H. J., Jr., and Agarwal, R. G. (1972) : "Annulus Unloading Rates as Influenced by Wellbore Storage and Skin Effect", Soc. Pet. Eng. J. (Oct.) p 453-462.

Ramey, H. J., Jr., Agarwal, R. G., and Martin, I. (1975) : "Analysis of Slug Test or DST Flow Period Data", J. Can. Pet. Tech. (July-Sept.) p 37-47.

Shinohara, K. (1980) : A Study of Inertial Effects in the Wellbore in Pressure Transient Well Testing, Ph. D. Dissertation, Stanford University.

Shinohara, K., and Ramey, H. J., Jr. (1979.a) : "Analysis of Slug Test DST Flow Period Data with Critical Flow", paper SPE 7981, presented at the California Regional Meeting of the Soc. Pet. Eng. of A. I. M. E., held in Ventura, Calif. (April 18-20) p 1-8.

Shinohara, K., and Ramey, H. J., Jr. (1979.b) : "Slug Test Data Analysis, Including the Inertia Effect of the Fluid in the Wellbore", paper SPE 8208, presented at the 54th Annual Fall Technical Conference of the Soc. Pet. Eng. of A. I. M. E., held in Las Vegas, Nev. (Sept. 23-26) p 1-13.

Sinha, B. K., Sigmon, J. E., and Montgomery, J. M. (1976) : "Comprehensive Analysis of Drillstem Test Data with the Aid of Type Curves", paper SPE 6054, presented at the 51th Annual Fall Meeting of the Soc. Pet. Eng. of A. I. M. E., held in New Orleans, La. (Oct. 3-6) p 1-24.

Soliman, M. Y. (1981) : "New Techniques for Analysis of Variable Rate or Slug Test", paper SPE 10083, presented at the 56th Annual Fall Technical Conference of the Soc. Pet. Eng. of A. I. M. E., held in San Antonio, Tex. (Oct. 5-7) p 1-10.

Standing, M. B. (1952) : Volumetric and Phase Behavior of Oil Field Hydrocarbon Systems, Reinhold Publishing Corp., New York.

Stehfest, H. (1970) : "Algorithm 368, Numerical Inversion of Laplace Transforms", Communications of the A. C. M., (Jan.) v 13, n 1, p 47-49. Errata in Communications of the A. C. M. (Oct. 1970) v 13, n 10, p 624.

Streeter, V. L., and Wylie, E. B. (1979) : Fluid Mechanics, McGraw-Hill Book Co., New York, p 479-522.

Stright, D. H., Jr. (1979) : "DST Analysis with Pressure Dependent Rock and Fluid Properties", paper SPE 8352, presented at the 54th Annual Fall Technical Conference and Exhibition of the Soc. Pet. Eng. of A. I. M. E., held in Las Vegas, Nev. (Sept. 23-26) p 1-9.

Theis, C. V. (1935) : "The Relationship Between the Lowering of the Piezometric Surface and the Rate and Duration of Discharge of a Well using Ground Water Storage", Trans. A. G. U., v 2, p 519-524.

Uraiet, A. A., and Raghavan, R. (1979) : "Pressure Buildup Analysis for a Well Produced at Constant Bottom-Hole Pressure", paper SPE 7984, presented at the California Regional Meeting of the Soc. Pet. Eng. of A. I. M. E., held in Ventura, Calif. (April 18-20) p 1-6.

van der Kamp, G. (1976) : "Determining Aquifer Transmissivity by Means of Well Response Test: The Underdamped Case", Water Resources Research (Feb.) v 12, n 1, p 71-77.

van Everdingen, A. F. (1953) : "The Skin Effect and Its Influence on the Productive Capacity of a Well", Trans. A. I. M. E., v 198, p 171-176.

van Everdingen, A. F., and Hurst, W. (1949) : "The Application of the Laplace Transformation to Flow Problems", Trans. A. I. M. E., v 186, p 305-324.

van Poollen, H. K., and Weber, J. B. (1970) : "Data Analysis for High Influx Wells", paper SPE 3017, presented at the 45th Annual Fall Meeting of the Soc. Pet. Eng. of A. I. M. E., held in Houston, Tex. (Oct. 4-7) p 1-6.

Wattenbarger, R. A., and Ramey, H. J., Jr. (1970) : "An Investigation of Wellbore Storage and Skin Effect in Unsteady Liquid Flow : 11. Finite Difference Treatment", Soc. Pet. Eng. J. (Sept.) p 291-297.

Wylie, C. R. (1975) : Advanced Engineering Mathematics, McGraw-Hill Book Co., New York.

APPENDIX A
WELLBORE EQUATION DERIVATION

An equation considering gravitational, inertial and frictional wellbore effects is derived in this appendix. A schematic diagram of the reservoir–wellbore system under consideration is shown in Fig. A.1. The wellbore is represented by two static control volumes in this derivation. The volume inside the wellbore pipe from the level of the top of the porous rock formation to the surface is used as an upper control volume. The volume inside the wellbore completion interval in front of the formation is taken as a lower control volume. These two control volumes are coupled through continuity conditions in the wellbore at the level of the top of the formation. This approach was presented by Cooper, et al. (1965). However, the problem considered by those authors justified simplifying assumptions resulting in a special case of the wellbore equation derived in this appendix.

In order to consider gravitational, inertial, and frictional effects in a wellbore equation, a macroscopic momentum balance is performed on each control volume. However, the physical complexity of the flow phenomena in the lower control volume has prevented a rigorous momentum balance for this wellbore section. For practical purposes, the length of the completion interval, h, is small in comparison to the static liquid column length, L, defined in Eq. 3.1. This leads one to consider that inertial and frictional effects in the lower control volume are negligible in comparison to those effects in the upper control volume. Then, a simplified momentum balance for the lower control volume is enough to communicate the upper control volume with the reservoir. This approach includes gravitational effects in the lower control volume.

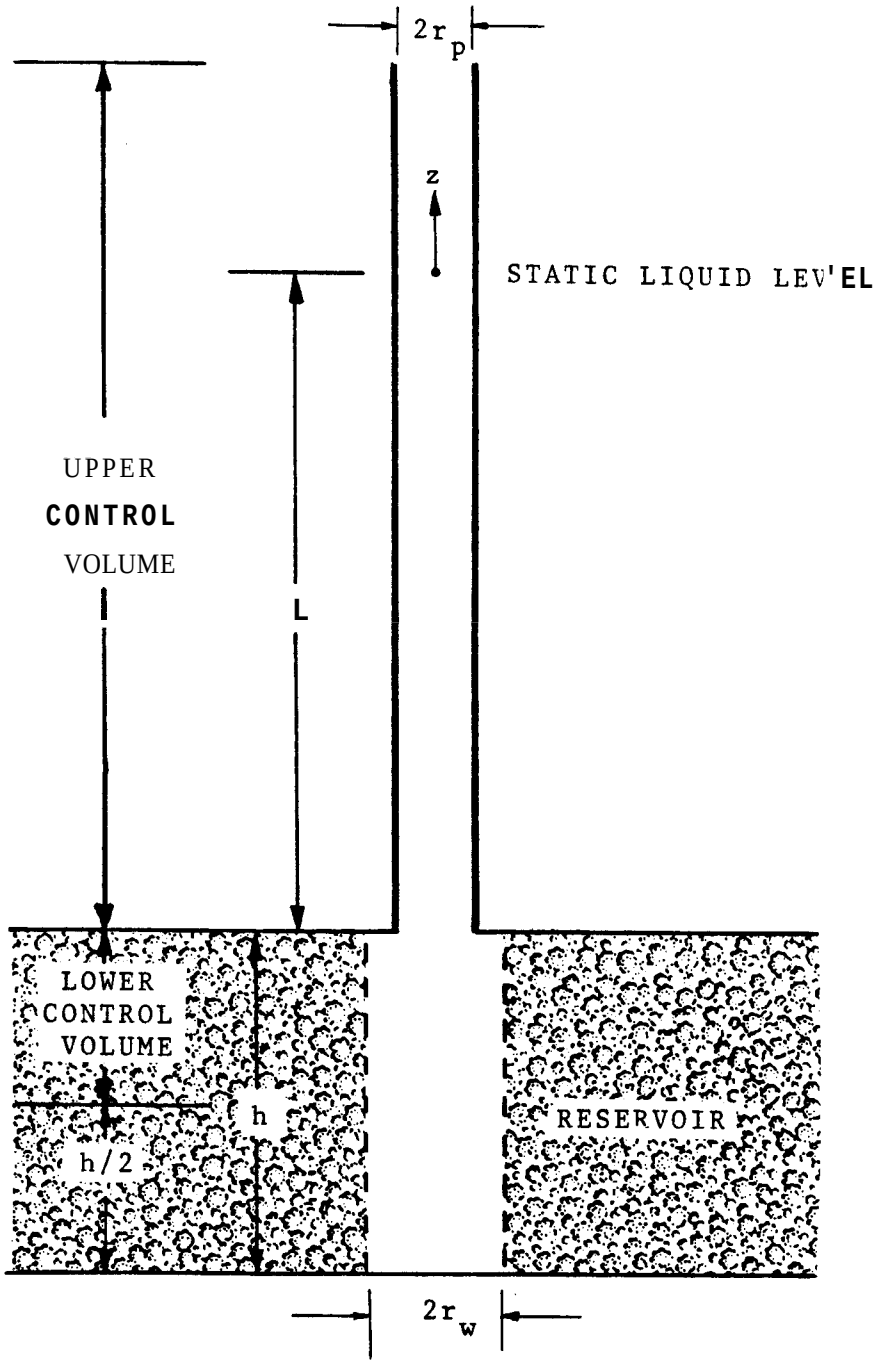

FIG. A.1. SCHEMATIC REPRESENTATION OF A WELLBORE–RESERVOIR SYSTEM SHOWING THE UPPER AND LOWER CONTROL VOLUMES USED TO DERIVE A WELLBORE EQUATION

Momentum Balance for the Upper Control Volume

As described in Section 3.1, Newton's Second Law of Motion applied to a control volume is:

$$\frac{\partial}{\partial t}\int_V \rho\, v\, dV + \int_S \rho\, v\, |\, v\, |\, dS = F \qquad \ldots \text{(A.1)}$$

where:

S = surface area of control volume, $[L^2]$

V = volume of control, $[L^3]$

This integro-differential equation applies at all points inside and on the control volume. A practical approach consists of performing a macroscopic momentum balance, as described by Bird, Stewart, and Lightfoot (1960). In order to apply Eq. A.1 as a macroscopic momentum balance, the following assumptions are adopted:

(a) at fluid entrance and exit of the control volume, time-smoothed fluid velocity v is parallel to conduit walls, and

(b) at fluid entrance and exit of the control volume, fluid density is constant across the conduit cross-section.

Under the above two assumptions, Eq. A.1 can be stated as:

$$\left\{\begin{array}{l}\text{rate of}\\ \text{momentum}\\ \text{accumulation}\end{array}\right\} = \left\{\begin{array}{l}\text{rate of}\\ \text{momentum}\\ \text{influx}\end{array}\right\} - \left\{\begin{array}{l}\text{rate of}\\ \text{momentum}\\ \text{efflux}\end{array}\right\} + \left\{\begin{array}{l}\text{sum of forces}\\ \text{acting on the}\\ \text{control volume}\end{array}\right\} \qquad \ldots \text{(A.2)}$$

and mathematically:

$$\frac{d}{dt}\int_{V(t)} \rho v dV = \rho_1 v_1^2 S_1 - \rho_2 v_2^2 S_2 + p_1 S_1 - p_2 S_2 + m(t)g - F_c \qquad \text{(A.3)}$$

where:

F_c = fluid force on conduit walls, $[MLT^{-2}]$

p_1, p_2 = fluid pressure at control volume entrance and exit, respectively, $[ML^{-1}T^{-2}]$

S_1, S_2 = cross-sectional area of the control volume entrance and exit, respectively, $[L^2]$

v_1^2, v_2^2 = squared time-smoothed entrance and exit velocities averaged over the corresponding cross-section, $[L^2T^{-2}]$

ρ_1, ρ_2 = fluid density at control volume entrance and exit, $[ML^{-3}]$

The left-hand side of Eq. A.3 corresponds to the rate of momentum accumulation in the control volume. The integral must be taken over the total volume of fluid in the control volume at each time of interest. The first two terms on the right-hand side correspond to the rate of momentum influx and efflux by virtue of the bulk fluid motion moving in and out of the control volume, respectively. Note that momentum influx and efflux associated with molecular and turbulent momentum flux at the entrance and exit have been neglected since these contributions are comparatively much smaller. The last four terms on the right-hand side are the forces acting on the fluid in the control volume: (a) pressure forces at the two ends of the control volume, (b) gravity force on the total mass of fluid, and (c) net force, $-F_c$, of the solid surfaces on the fluid, respectively.

Figure A.1 shows a z-coordinate system used to describe the fluid level in the wellbore. This z-coordinate is measured positive upward from a distance L above the level of the top of the formation.

Under the assumption that wellbore pipe radius, r_p, is constant, Eq. A.3 can be applied to the fluid column in the upper control volume at a time t, as follows:

$$\frac{d}{dt}\int_{-L}^{z_p} \rho\, v\, d\sigma = [\,\rho\, v^2\,]_{-L} + [\,\rho\, v^2\,]_{surf} + p_p(-L) - p_g$$

$$- g\int_{-L}^{z_p} \rho\, d\sigma - \frac{2}{r_p}\int_{-L}^{z_p} \tau\, d\sigma \qquad \ldots \text{(A.4)}$$

where:

$p_g(t)$ = gas pressure on the liquid level, $[ML^{-1}T^{-2}]$

$p_p(-L,t)$ = pipe pressure at the level of the top of the formation, $[ML^{-1}T^{-2}]$

$z_p(t)$ = liquid level in the wellbore, [L]

All terms in Eq. A.4 have been divided by the wellbore pipe cross-sectional area πr_p^2. A positive sign represents an upward force and a negative sign represents a downward force. The last term in Eq. A.4 was left as a vector because it corresponds to a force opposite to fluid movement direction. In this last term, the force of the conduit walls on fluid is considered equal to the friction force in an inelastic pipe. Here, τ is the shear stress of the fluid on the conduit walls and depends on the fluid velocity.

For the period of time in which no liquid is produced at the surface, $[pv^2]_{surf} = 0$.

Application of Eq. A.4 requires a mathematical description of the vertical distribution of $\rho(z,t)$ and $v(z,t)$ along $-L \leq z \leq z_p(t)$. However, physical considerations indicate that these distributions are related in turn to unknown liquid level $z(t)$ and unknown pressures $p_p(-L,t) \leq p(z) \leq p_g(t)$. In order to overcome this difficulty, the density of the fluid in the wellbore is assumed to be independent of pressure, i. e., the fluid in the wellbore is incompressible. From the principle of conservation of mass, this assumption implies that the vertical time-smoothed velocity of any layer of fluid in the wellbore pipe must be equal to the velocity of the entire fluid column at a given time, $z_p'(t)$.

Under this assumption, Eq. A.4 simplifies to:

$$\rho \frac{d}{dt} \{ [L + z_p] z'_p \} = P [z'_p 12 + [p_p(-L) - p_g]$$

$$- P g [L + z_p] - \frac{2}{r_p} \int_{-L}^{z} \tau \, d\sigma \qquad \ldots (A.5)$$

Frictional resistance in unsteady flow can be assumed equal to frictional resistance in steady state flow at the same velocity (Streeter and Wylie, 1975). Also, as applied by Cooper, et al. (1965), friction force can be approximated by using the Darcy–Weisbach empirical formula. This formula for head loss due to friction can be written for the upper control volume as follows:

$$h_f = \frac{[L + z_p] f}{4 r_p g} [z'_p]^2 \qquad \ldots (A.6)$$

where:

f = Moody friction factor (Moody, 1944)

Multiplying Eq. A.6 by ρg and substituting the resultant pressure force due to friction on the moving wellbore fluid column into Eq. A.5:

$$\frac{d}{dt} \{ [L + z_p] z'_p \} = [z'_p]^2 + \frac{p_p(-L) - p_g}{\rho} - [L + z_p] g$$

$$- \frac{f}{4 r_p} [L + z] | z'_p | z'_p \qquad \ldots (A.7)$$

The squared velocity in Eq. A.6 has been factored to preserve the sign of velocity, i. e., the direction of the fluid movement, and consider the fact that the friction force is opposite to fluid movement.

Taking the time derivative on the left-hand side of Eq. A.7 and simplifying:

$$[\ L + z_P\ ]\ z_P'' = \frac{P_p(-L) - P_g}{\rho} - [\ L + z_P\ ]\ g$$

$$L + z_-\ ] \text{——} \qquad \text{. . . (A.8)}$$

where:

z_P'' = fluid column acceleration in the pipe, $[LT^{-2}]$

This equation relates, at all times t, pipe gas pressure at the liquid level, $p_g(t)$, pipe pressure at the level of the top of the formation, $p_p(-L,t)$, wellbore fluid level, $z_p(t)$, wellbore fluid velocity, $z_p'(t)$, and wellbore fluid acceleration, $z_p''(t)$.

Momentum Balance for the Lower Control Volume

Fluid flow between the reservoir and the wellbore occurs through the lateral porous walls of the lower control volume as shown in Fig. A.2. The bottom of this control volume is assumed impermeable. A momentum balance on the lower control volume is required to consider the fluid acceleration that takes place along the completion interval as fluid is produced and moves upward in the wellbore.

For the upper control volume, fluid velocity, $z_p'(t)$, and fluid acceleration, $z_p''(t)$, are the same for any fluid layer in the pipe fluid column at a given time. However, fluid velocity and fluid acceleration along the lower control volume vary with fluid layer position and with time. Then, $z_f'(z,t)$ and $z_f''(z,t)$ for $-L-h>z>-L$.

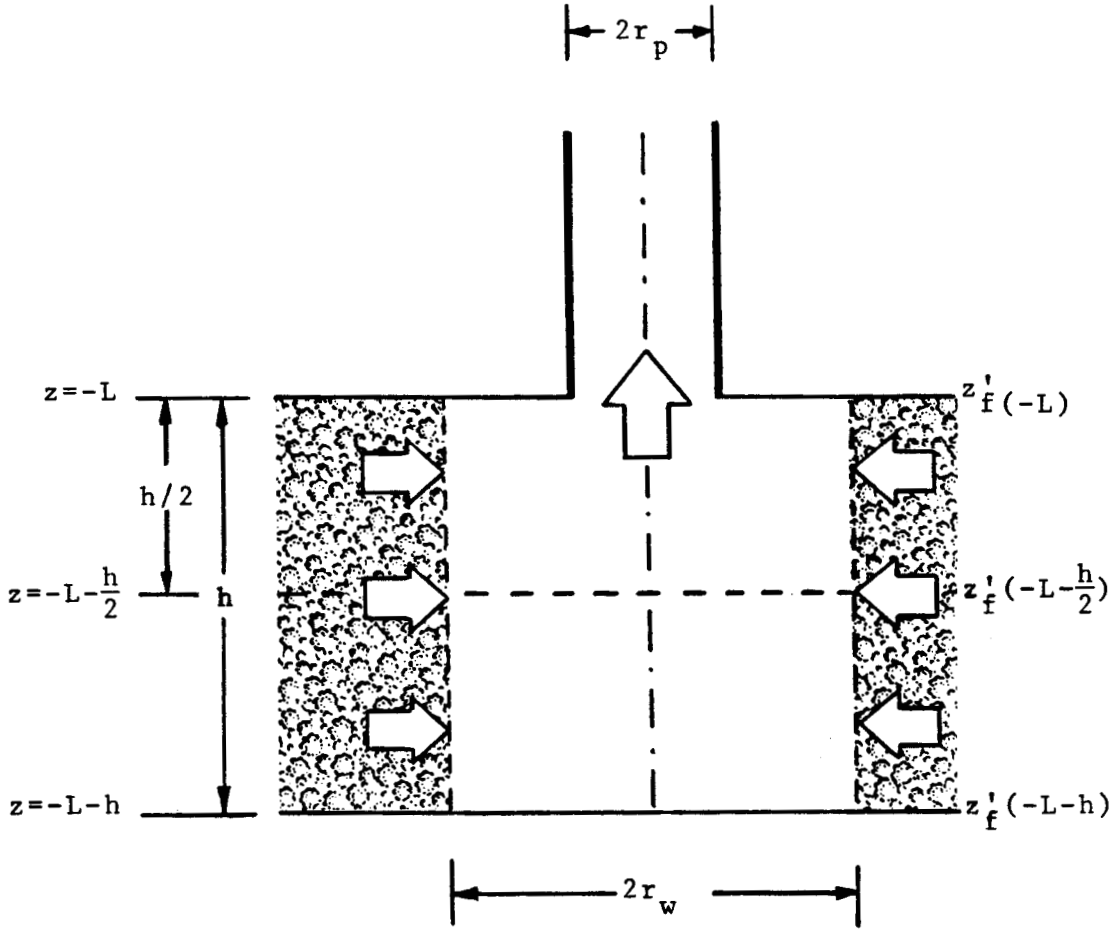

FIG. A.2. SCHEMATIC REPRESENTATION OF THE BOTTOM OF A WELLBORE SHOWING VALUES OF THE PROFILE ASSUMED FOR LIQUID LEVEL VELOCITY

Although inertia of the fluid in the completion interval can cause pressure potential to vary with position along the completion interval (Cooley and Cunningham, 1979), uniform flow from the reservoir into the wellbore along the reservoir thickness is assumed in the present study, as proposed by Cooper, et al. (1965). Under this assumption, the velocity at time t of a fluid layer at depth z, $z_f'(z,t)$, in the completion interval is given by:

$$z_f'(z,t) = \left[1 + \frac{L + z}{h} \right] z_f'(-L,t) \qquad \ldots \text{(A.9)}$$

This equation indicates that, at any time t, fluid velocity increases linearly along the completion interval from $z_f'(-L-h,t)=0$ to a value $z_f'(-L,t)$. This linear increase in velocity implies an instantaneous constant fluid acceleration along the completion interval. Adopting this velocity profile, a transient momentum balance can be performed using only the upper half of the lower control volume.

Applying Eq. A.4 to the upper half of the lower control volume, at time t:

$$\frac{d}{dt} \int_{-L-h/2}^{-L} \rho z_f' d\sigma = \left[\rho z_f' \right]_{-L-h/2}^{2} - \left[\rho z_f' \right]_{-L}^{2} + p_w - p_f(-L)$$

$$- g \int_{-L-h/2}^{-L} \rho d\sigma - \frac{2}{r_p} \int_{-L-h/2}^{-L} \tau d\sigma \qquad \ldots \text{(A.10)}$$

where:

$p_w(t) = p_f(-L-h/2,t)$ = bottomhole wellbore pressure at the mid-level of the formation, $[ML^{-1}T^{-2}]$

All terms in Eq. A.10 have been divided by πr_p^2, where r_p is the pipe radius.

Placing $z_f'(z,t)$ from Eq. A.9 into Eq. A.10 and dividing through by ρ:

$$\frac{d}{dt} \int_{-L-h/2}^{-L} \left[1 + \frac{L + \sigma}{h} \right] z_f'(-L)\, d\sigma = \left[1 + \frac{L - L - h/2}{h} 1^2 \right] \left[z_f'(-L)\, 1^2 \right]$$

$$- \left[1 + \frac{L - L}{h} 1^2 \right] \left[z_f'(-L)\, 1^2 \right]$$

$$+ \frac{p_w - p_f(-L)}{\rho} - g \frac{h}{2} - \int_{-L-h/2}^{-L} \tau\, d\sigma \qquad \ldots \text{(A.11)}$$

Assuming negligible friction losses along the wellbore completion interval, the last term in Eq. A.11 vanishes. Performing the integration and differentiation on the left-hand side and grouping terms:

$$\frac{3}{8} h\, z_f(-L) = -\frac{3}{4} \left[z_f'(-L) \right]^2 + \frac{p_w - p_f(-L)}{\rho} - g \frac{h}{2} \qquad \ldots \text{(A.12)}$$

This equation relates, at all times t, bottomhole pressure at the mid-level of the formation, $p_w(t)$, wellbore pressure at the level of the top of the formation, $p_f(-L,t)$, wellbore fluid velocity at the level of the top of the formation, $z_f'(-L,t)$, and fluid acceleration at the level of the top of the formation, $z_f''(-L,t)$.

Wellbore Momentum Balance Equation

Since there is continuity along the wellbore, the flow rate at the level of the top of the formation must be equal to the flow rate in the pipe, at any time t:

$$\pi r_w^2 z_f'(-L,t) = \pi r_p^2 z_p'(t) \quad \ldots \text{(A.13)}$$

Substituting this equation and its derivative with respect to time into the lower control volume momentum balance Eq. A.12:

$$\frac{3}{8}\left[\frac{r_p}{r_w}\right]^2 z_p'' = -\frac{3}{4}\left[\frac{r_p}{r_w}\right]^4 \left[z_p'\right]^2 + \frac{p_w - p_f(-L)}{\rho} - g\frac{h}{2} \quad \ldots \text{(A.14)}$$

Combining this equation with the upper control volume momentum balance Eq. A.8 through wellbore pressure at the level of the top of the formation, $p_p(-L,t) = p_f(-L,t)$:

$$\left\{ L + z_p + \frac{3}{8} h \left[\frac{r_p}{r_w}\right]^2 \right\} z_p''$$

$$+ \left\{ \left[L + z_p \right] \frac{f}{4} \left| \frac{1}{r_p} z_p' \right| + \frac{3}{4}\left[\frac{r_p}{r_w}\right]^4 z_p' \right\} z_p'$$

$$+ \left\{ L + z_p + \frac{h}{2} \right\} g = \frac{p_w - p_g}{\rho} \quad \ldots \text{(A.15)}$$

Due to the presence of the gas pressure on the wellbore liquid level, p_g, wellbore momentum balance Eq. A.15 applies to slug, drillstem, and closed-chamber tests.

In order to simplify notation, subscript p, which indicates wellbore pipe conditions, is omitted in z_p, z_p', and z_p'' throughout the rest of this study. Therefore, **Eq. A.15** defines a dynamical relationship in the wellbore between gas pressure at the liquid level, $p_g(t)$, bottomhole pressure, $p_w(t)$, liquid level position, $z(t)$, liquid column velocity, $z'(t)$, and liquid column acceleration $z''(t)$.

APPENDIX B
SOLUTION BY LAPLACE TRANSFORMATION

The Laplace transformation is applied to the problem statement given by Eqs. 3.39 - 3.46 in this appendix. For the special cases in which the problem is mathematically linear, the transformed problem can be solved analytically in Laplace space to obtain expressions for $\overline{p_{wD}}(u)$, $\overline{z_D}(u)$, $\overline{p'_{wD}}(u)$, $\overline{z'_D}(u)$, $\overline{z''_D}(u)$, and $\overline{p_D}(r_D,u)$. Symbol u represents the Laplace transformation parameter, and a bar on top of a variable indicates the Laplace transformation of that variable. A numerical Laplace transformation inversion algorithm proposed by Stehfest (1970) is applied in this study to evaluate approximate solutions at specified values of t_D to generate tables and graphs of $p_{wD}(t_D)$, $z_D(t_D)$, $p_{wD}'(t_D)$, $z_D'(t_D)$, $z_D''(t_D)$, and $p_D(r_D,t_D)$.

The initial value mathematical problem describing the flow phenomena during a slug test or a drillstem test stated by Eqs. 3.39 - 3.46 is given as follows, omitting subscript w in coefficients A_w, B_w, C, D, and E_w of the wellbore equation to simplify the notation throughout this appendix:

$$A\, z''_D + B\, z'_D + C\, z_D + D = E\, p_{wD} \quad , 0 < t_D < t_{sD} \qquad \ldots \text{(B.1)}$$

$$\frac{\partial^2 p_D}{\partial r_D^2} + \frac{1}{r_D}\frac{\partial p_D}{\partial r_D} = \frac{\partial p_D}{\partial t_D} \quad , r_D > 1,\ t_D > 0 \qquad \ldots \text{(B.2)}$$

$$z'_D = -\frac{1}{C_D}\left[r_D \frac{\partial p_D}{\partial r_D} \right]_{r_D=1} \quad , t_D > 0 \qquad \ldots \text{(B.3)}$$

$$p_D - s \left[r_D \frac{\partial p_D}{\partial r_D} \right] \Big\}_{r_D=1} \geq 0 \qquad \ldots (B.4)$$

$$\lim_{r_D \to \infty} p_D = 0 \quad , t_D \geq 0 \qquad \ldots (B.5)$$

$$z_D = -1 \quad , t_D = 0 \qquad \ldots (B.6)$$

$$z'_D = 0 \quad , t_D = 0 \qquad \ldots (B.7)$$

$$p_D = 0 \quad , r_D > 1, \; t = 0 \qquad \ldots (B.8)$$

An apostrophe on a variable indicates a derivative with respect to t_D of the variable, and the independent variables are:

$$p_{wD}(t_D) \qquad \ldots (B.9)$$

$$z_D(t_D) \qquad \ldots (B.10)$$

$$p_D(r_D, t_D) \qquad \ldots (B.11)$$

Equations B.1 - B.11 define a linear problem whenever A, B, C, D, E, s, and C_D are constants.

In this case, the problem can be solved by applying the one-dimensional Laplace transformation (Churchill, 1972) given by:

$$\bar{g}(u) = \int_0^\infty e^{-ut_D} g(t_D)\, dt_D \quad , \text{Real}(u) > u_0 \qquad \ldots \text{(B.12)}$$

where $g(t_D)$ is a continuous function for which the integral exists and u_0 is a real constant required for the integral to be convergent.

Applying the Laplace transformation to Eqs. B.1 - B.5:

$$A \left[u^2 \bar{z}_D - u\, z_D(0) - z_D'(0) \right] + B \left[u\, z_D(0) \right] + C \bar{z}_D + \frac{D}{u} = E\, \bar{p}_{wD} \qquad \ldots \text{(B.13)}$$

$$\frac{\partial^2 \bar{p}_D}{\partial r_D^2} + \frac{1}{r_D} \frac{\partial \bar{p}_D}{\partial r_D} = u\, \bar{p}_D + p_D(r_D, 0) \qquad \ldots \text{(B.14)}$$

$$u\, \bar{z}_D - z_D(0) = -\frac{1}{C_r} \left[r_D \frac{\partial \bar{p}_D}{\partial r_D} \right]_{r_D=1} \qquad \ldots \text{(B.15)}$$

$$\bar{p}_{wD} = \left\{ \bar{p}_D - s \left[r_D \frac{\partial p_D}{\partial r_D} \right] \right\}_{r_D=1} \qquad \ldots \text{(B.16)}$$

$$\lim_{r_D \to \infty} \bar{p}_D = 0 \qquad \ldots \text{(B.17)}$$

where $\bar{p}_{wD}(u)$, $\bar{z}_D(u)$, and $\bar{p}_D(r_D, u)$.

Since u is a parameter in the Laplace transformation integral, Eq. B.14 is an ordinary differential equation. Substituting initial condition for p_D given by Eq. B.8 into Eq. B.14:

$$\frac{d^2\overline{p_D}}{dr_D^2} + \frac{1}{r_D}\frac{d\overline{p_D}}{dr_D} - u\,\overline{p_D} = 0 \qquad \ldots \text{(B.18)}$$

This is a modified Bessel equation of zero order (Wylie, 1975) with general solution given by:

$$\overline{p_D} = C_I\, I_0(r_D\sqrt{u}) + C_K\, K_0(r_D\sqrt{u}) \qquad \ldots \text{(B.19)}$$

where C_I and C_K are real constants and I_0 and K_0 are modified Bessel functions of the first kind and second kind, respectively, of order zero.

A graph of $I_0(r_D\sqrt{u})$ and $K_0(r_D\sqrt{u})$ is presented in Fig. B.1. K_0 approaches zero as its argument increases. On the other hand, I_0 tends to infinity as $r_D\sqrt{u}$ increases. Therefore, C_I in Eq. B.19 must be zero to fulfill the reservoir outer boundary condition, Eq. B.17, then:

$$\overline{p_D} = C_K\, K_0(r_D\sqrt{u}) \qquad \ldots \text{(B.20)}$$

Deriving this equation with respect to r_D and according to Bessel functions properties (Abramowitz and Stegun, 1972):

$$\frac{d\overline{p_D}}{dr_D} = -C_K\sqrt{u}\, K_1(r_D\sqrt{u}) \qquad \ldots \text{(B.21)}$$

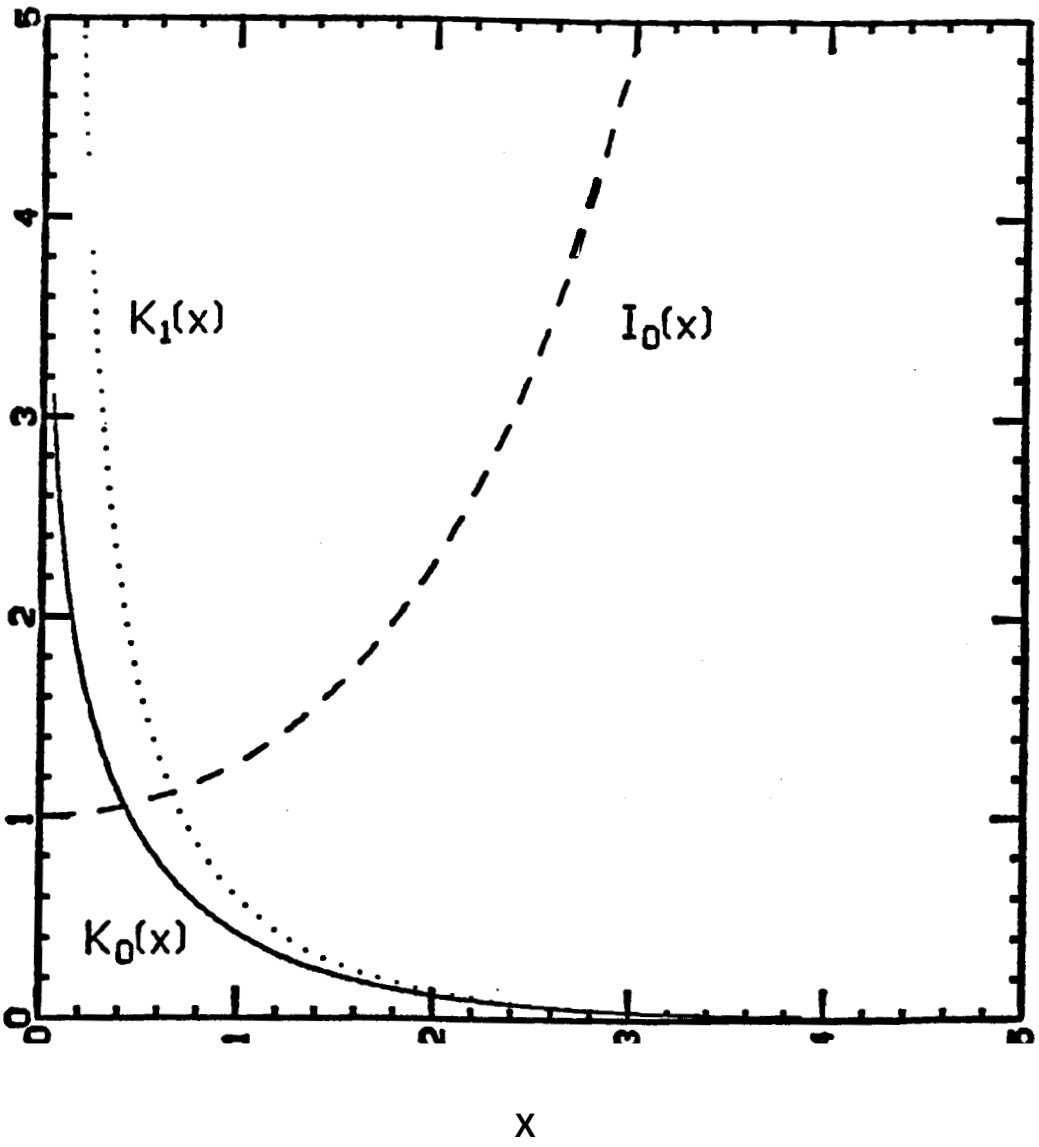

FIG. B.1. GRAPH OF BESSEL FUNCTIONS K_0, I_0, *AND* K_1

where K_1 is the modified Bessel function of the second kind and order unity. A graph of K_1 is also shown in Fig. B.1.

Substituting Eq. B.21 and initial condition for z_D given by Eq. B.6 into Eq. B.15 and solving for C_K:

$$C_K = \frac{C_D [u \overline{z_D} + 1]}{\sqrt{u}\, K_1(\sqrt{u})} \quad \ldots \text{(B.22)}$$

Substituting Eqs. B.20 and B.21 into Eq. B.16:

$$\overline{p_{wD}} = C_K [K_0(\sqrt{u}) + s \sqrt{u}\, K_1(\sqrt{u})] \quad \ldots \text{(B.23)}$$

Substituting C_K from Eq. B.22 into Eq. B.23:

$$\overline{p_{wD}} = \frac{C_D [u \overline{z_D} + 1]}{\sqrt{u}\, K_1(\sqrt{u})} [K_0(\sqrt{u}) + s \sqrt{u}\, K_1(\sqrt{u})] \quad \ldots \text{(B.24)}$$

Substituting initial conditions for z_D and z'_D given by Eqs. B.6 and B.7, respectively, into Eq. B.13 :

$$A [u^2 \overline{z_D} + u] + B [u \overline{z_D} + 1] + C \overline{z_D} + \frac{D}{u} = E \overline{p_{wD}} \quad \ldots \text{(B.25)}$$

Substituting $\overline{p_{wD}}$ from Eq. B.24 into Eq. B.25 and solving for $\overline{z_D}$:

$$\overline{z_D} = -\frac{1}{u} \left\{ \frac{\sqrt{u}K_1(\sqrt{u}) [Au + B + D/u - EC_D s] - EC_D K_0(\sqrt{u})}{\sqrt{u}K_1(\sqrt{u}) [Au + B + C/u - EC_D s] - EC_D K_0(\sqrt{u})} \right\} \quad \ldots \text{(B.26)}$$

This is an explicit expression to evaluate $\overline{z_D}$ and reduces to simpler forms for specific values of A, B, C, D, and E, reproducing special cases available in the literature. An explicit expression for p_{wD} can be obtained by substituting $\overline{z_D}$ from Eq. B.26 into Eq. B.24. Solutions for $\overline{z'_D}$ and $\overline{z''_D}$ can be evaluated by applying the properties of the Laplace transform for derivatives.

Taking the Laplace transformation of z'_D and z''_D:

$$\overline{z'_D} = u\,\overline{z_D} - z_D(0) \qquad \ldots \text{(B.27)}$$

and:

$$\overline{z''_D} = u^2\,\overline{z_D} - u\,z_D(0) - z'_D(0) \qquad \ldots \text{(B.28)}$$

where $\overline{z'_D}(u)$ and $\overline{z''_D}(u)$.

Substituting initial conditions for z_D and z'_D given by Eqs. B.6 and B.7 into Eqs. B.27 and B.28:

$$\overline{z'_D} = u\,\overline{z_D} + 1 \qquad \ldots \text{(B.29)}$$

and:

$$\overline{z''_D} = u^2\,\overline{z_D} + u = u\,\overline{z'_D} \qquad \ldots \text{(B.30)}$$

Similarly, a transformed solution for p_{wD}' is obtatined as follows:

$$\overline{p_{wD}'} = u\,\overline{p_{wD}} - p_{wD}(0) \qquad \ldots \text{(B.31)}$$

where $\overline{p_{wD}'}(u)$.

The value of $p_{wD}(0)$ is implicit in the problem statement. Applying Eqs. B.4 and B.8 at initial conditions, $p_{wD}(0)$ must be zero, and:

$$\overline{p_{wD}'} = u\,\overline{p_{wD}} \qquad \ldots \text{(B.32)}$$

This method of obtaining derivatives of independent variables is restricted by the number of initial conditions in the problem. In other words, additional initial conditions would be required to define transformed solutions for higher order derivatives. By example, for $\overline{p_{wD}''}$:

$$p_{wD}'' = u^2\,p_{wD} - u\,p_{wD}(0) - p_{wD}'(0) \qquad \ldots \text{(B.33)}$$

where $\overline{p_{wD}''}(u)$.

In order to determine $p_{wD}'(0)$, Eq. B.l must be applied at $t_D=0$ and the derivative with respect to t_D taken, resulting in:

$$A\,z_D''' + B\,z_D'' + C\,z_D' = E\,p_{wD}' \;,\; t_D = 0 \qquad \ldots \text{(B.34)}$$

The value of $z_D''(0)$ is implicit in the problem statement for $A \neq 0$. Applying Eqs. B.1 and B.5 at initial conditions:

$$z_D'' = \frac{C - D}{A}, \quad t_D = 0 \qquad \ldots \text{(B.35)}$$

However, a value for $z_D'''(0)$ is still required in Eq. B.34 to define $p_{wD}'(0)$ to be used in Eq. B.33.

Solutions for a slug test or the flow period of a drillstem test can be obtained by numerical Laplace inversion of Eq. B.26 for z_D, Eq. B.24 for p_{wD}, Eq. B.31 for p_{wD}', Eq. B.27 for z_D', Eq. B.28 for z_D'', and Eq. B.20 for $p_D(r_D)$, at desired values of t_D.

Results for p_{wD}', $z_{D'}'$ and z_D'' show that these functions oscillate more rapidly than p_{wD} and z_D. This causes oscillating deviations from smooth trends in the inversion of $\overline{p_{wD}'}$, $\overline{z_{D'}'}$ and $\overline{z_D''}$ using the Stehfest algorithm with Eqs. 3.42 - 3.44.

A more accurate alternative was found in the present study. Consider wellbore Eq. B.1 expressed in the following terms:

$$A \frac{d}{dt_D} \left(\frac{dz_D}{dtD} \right) + B \frac{dz_D}{dt_D} + C\, z_D + D = E\, p_{wD} \qquad \ldots \text{(B.50)}$$

Applying the Laplace transformation to this equation and substituting initial condition for $z_{D'}'$ given by Eq. B.7:

$$A\, u\, \overline{z_D'} + B\, \overline{z_D'} + C\, \overline{zD} + \frac{D}{u} = E\, \overline{p_{wD}} \qquad \ldots \text{(B.51)}$$

Hence, solving for $\overline{z'_D}$:

$$\overline{z'_D} = \frac{-C z_D - \frac{D}{u} + E p_{wD}}{A u + B} \quad , A u + B \neq 0 \qquad \ldots (B.52)$$

Similarly, applying the Laplace transformation on wellbore Eq. B.l:

$$A \overline{z''_D} + B \overline{z'_D} + C \overline{z_D} + \frac{D}{u} = E \overline{p_{wD}} \qquad \ldots (B.53)$$

Solving for $\overline{z''_D}$:

$$\overline{z''_D} = \frac{-B \overline{z'_D} - C \overline{z_D} - \frac{D}{u} + E \overline{p_{wD}}}{A} \quad , A \neq 0 \qquad \ldots (B.54)$$

Equations B.52 and B.54 for inverting $\overline{z'_D}$ and $\overline{z''_D}$, respectively, using the Stehfest algorithm gave smoother results than Eq. B.29 and B.30. The reason for this may be that Eqs. B.52 and B.54 make use of the restrictions imposed by the wellbore Eq. B.1, whereas Eqs. B.29 and B.30, which are direct application of the Laplace transformation properties, involve more critical conditions that cause numerical problems with the Stehfest algorithm.

Still another alternative is available for evaluating z''_D, which is the most rapid oscillatory function in the slug test problem. This alternative consists of calculating z_D'' after inverting z_D, z_D', and p_{wD}. From wellbore Eq. B.l:

$$z''_D = \frac{-B z'_D - C z_D - D + E p_{wD}}{A} \quad , A \neq 0 \qquad \ldots (B.55)$$

Calculation tests for z_D" inverting Eq. B.54 or using Eq. B.55 showed that the inversion of Eq. B.54 gives smoother results for the cases investigated. Application of Eqs. B.52 and B.55 is unrestricted for problems for which $A \neq 0$ and $B \neq 0$. However, these equations can not be utilized for simplified problems with values of $A = 0$ and/or $B = 0$. Eqs. B.29 and B.30 can be used for those simplified problems.

For obtaining the Laplace transformation inversion of $\overline{p_{wD}}$, no alternative to Eq. B.31 is provided by the information defining the problem statement.

The following is a summary of the Laplace transformed solutions obtained in this appendix. These solutions are shown in the form in which they were used to optimize calculations in the computer program presented in Appendix E, which uses the Stehfest numerical Laplace transformation inversion algorithm:

For a given u, let:

$$C_0 = K_0(\sqrt{u}) \qquad \ldots \text{(B.56)}$$

$$C_1 = \sqrt{u}\, K_1(\sqrt{u}) \qquad \ldots \text{(B.57)}$$

From Eq. B.26:

$$\overline{z_D} = -\frac{1}{u}\frac{C_1 \left[A u + B + \frac{D}{u} - E C_D s \right] - E C_D C_0}{C_1 \left[A u + B + \frac{fi}{U} - E C_D s \right] - E C_D C_0} \qquad \ldots \text{(B.58)}$$

From Eq. B.22:

$$C_K = \frac{C_D \left[u \overline{z_D} + 1 \right]}{fi_1} \qquad \ldots \text{(B.59)}$$

From Eq. B.23:

$$\overline{p_{wD}} = C_K \left[C_0 + s\, C_1 \right] \qquad \ldots \text{(B.60)}$$

From Eq. B.32:

$$\overline{p'_{wD}} = u\, \overline{p_{wD}} \qquad \ldots \text{(B.61)}$$

From Eq. B.20, for optionally specified values of r_D:

$$\overline{p_D} = C_K\, K_0(r_D \sqrt{u}) \qquad \ldots \text{(B.62)}$$

From Eq. B.52, for A and/or B ≠ 0:

$$\overline{z'_D} = \frac{-C\,\overline{z_D} - \frac{D}{u} + E\,\overline{p_{wD}}}{A\,u + B} \qquad \ldots \text{(B.63)}$$

or, from Eq. B.29, for A and B = 0:

$$\overline{z'_D} = u\,\overline{z_D} + 1 \qquad \ldots \text{(B.64)}$$

From Eq. B.54, for A ≠ 0:

$$\overline{z''_D} = \frac{-B\,\overline{z'_D} - C\,\overline{z_D} - \frac{D}{u} + E\,\overline{p_{wD}}}{A} \qquad \ldots \text{(B.65)}$$

or, from **Eq. B.30,** for A = 0:

$$\overline{z''_D} = u\,\overline{z'_D} \qquad \text{. . . (B.66)}$$

APPENDIX C
APPLICATION OF THE STEHFEST ALGORITHM

In 1970, Stehfest presented an algorithm for numerical inversion of a known function in Laplace space into unknown functions in real space. If a Laplace transformation $\bar{g}(u)$ is given in the form of an explicit expression in terms of u, the Stehfest algorithm gives an approximate value g_a of the unknown function $g(t)$ at $t=T$, from:

$$g(T) \simeq g_a = \frac{\ln(2)}{T} \sum_{i=1}^{N} V_i \, \bar{g}(U_i) \qquad \ldots (C.1)$$

where:

$$U_i = i \frac{\ln(2)}{T} \qquad \ldots (C.2)$$

and:

$$V_i = (-1)^{(N/2+i)} \sum_{k=[i+1]/2}^{\min(i,N/2)} \frac{k^{N/2}[2k]!}{[N/2-k]![k]![k-1]![i-k]![2k-i]!} \qquad \ldots (C.3)$$

The number N of coefficients V_i required in Eq. C.1 must be even in order to obtain an integer number for N/2 in Eq. C.3. Calculation of coefficients V_i is performed only once for a given N. Another possibility is *to* supply predetermined coefficients V_i from a table (Ramey, 1980).

The Stehfest algorithm improves an approach proposed by Gaver (1966) based on the analogy between the expectation of $g(t)$ with respect to an approximate probability density and the Laplace transformation of $g(t)$:

$$\bar{g}(u) = \int_0^\infty g(t)\, e^{-ut}\, dt \qquad \ldots (C.4)$$

The expectation of a function $g(t)$ with respect to a probability density is given by the integral from zero to infinity of the product of function $g(t)$ and a probability density. Therefore, the expectation of $g(t)$ with respect to probability density $Q_n(a,t)$ is:

$$g_n = \int_0^\infty g(t)\, Q_n(a,t)\, dt \qquad \ldots (C.5)$$

In order to obtain an analogy between Eqs. C.5 and C.4, probability density $Q_n(a,t)$ must have properties equivalent to those of the kernel, e^{-ut}, in the Laplace transformation. With this purpose, Gaver (1966) proposed the following probability density:

$$Q_n(a,t) = a \frac{[2n]!}{n![n-1]!} \left[1 - e^{-at} \right] e^{-nat}, \quad a > 0 \qquad \ldots (C.6)$$

As n tends to infinity, this probability density exhibits properties related to those of the kernel in the Laplace transformation. Therefore, for a value of n=N sufficiently large:

$$\bar{g}(u) = g_N = \lim_{N \to \infty} \int_0^\infty g(t)\, Q_N(a,t)\, dt \qquad \ldots (C.7)$$

This basic review of the approach involved in the Stehfest algorithm indicates that, theoretically, this algorithm could give results as accurate as desired for any function $g(t)$ by increasing N.

However, computational precision limitations in practice can cause significant rounding errors as N increases beyond a particular value. This particular value of N is determined by the nature of the function $g(t)$ and by the number of significant digits used to perform arithmetic operations. Stehfest warned that this algorithm gives the average of a function with a discontinuity at T and that no accurate results are to be expected for rapid oscillating functions at T. A rapid oscillating function is a function with oscillations with wavelength small in comparison to the half-width of the peak which $Q_{N/2}(\ln 2, t)$ has at T.

Application experience of the Stehfest algorithm to a number of pressure transient well test problems has been encouragingly accurate (Ramey, 1982). Several analytical solutions for pressure transient flow problems have been reproduced within 4 and 5 significant digits by using the Stehfest algorithm.

Since oscillating solutions can be expected for slug test problems, understanding the Stehfest algorithm results for simple known oscillating functions is desirable. In this appendix, the Stehfest algorithm is applied to invert the Laplace transformation of $\sin(t_D/C_D)$:

$$\overline{\sin}(u) = \frac{1}{u^2 + 1} \quad \ldots \text{(C.8)}$$

and the Laplace transformation of $\cos(t_D/C_D)$:

$$\overline{\cos}(u) = \frac{u}{u^2 + 1} \quad \ldots \text{(C.9)}$$

Three sightly differents programs were written for inverting each of the transformed functions, given in Eqs. C.8 and C.9, and applying the Stehfest algorithm using three precisions available in an IBM computer: (a) Single Precision with 7 significant digits, (b) Double Precision with 16 significant digits, and (c) Quadruple Precision with 35 significant digits.

Parameter N was increased in several computer runs for each transformed function for each precision.

A common form of presentation of slug test solutions is in semi-log graphs of p_{wD} vs t_D/C_D. Figures C.1 and C.2 show semi-log graphs of the Stehfest algorithm results for $\sin(t_D/C_D)$ and $\cos(t_D/C_D)$, respectively. These applications of the Stehfest algorithm represent oscillatory conditions more severe than the slug test solutions of interest for the present study.

From Fig. C.1, single precision results slightly overshoot the first peak of $\sin(t_D/C_D)$ and converge to zero rapidly. Double precision results reproduce the first peak, overshoot the second peak and converge to zero. Quadruple precision results reproduce the first peak, approximate the second peak, and converge to zero slowly.

From Fig. C.2, single precision results undershoot the first peak of $\cos(t_D/C_D)$ and converge to zero rapidly. Double precision results overshoot the first peak, undershoot the second peak. and converge to zero. Quadruple precision results reproduce the first two peaks, approximate the third peak, and converge to zero slowly.

Two sources of rounding errors exist in practical application of the Stehfest algorithm. Rounding errors occur during calculation of coefficients V_i from Eq. C.3, and during calculation of function approximations from Eq. C.1. In an attempt to reduce rounding errors in the calculation of coefficients V_i, a hybrid approach using quadruple precision in the calculation of N=18 coefficients V_i, and supplying those coefficients to a double-precision program gives the results also shown in Figs. C.1 and C.2.

Since this hybrid approach did not show significant improvement, and no software code was available for Bessel function evaluation with quadruple precision, a compromise between computer time cost and accuracy of results was achieved by using double precision with N=18 to obtain the results presented in this study.

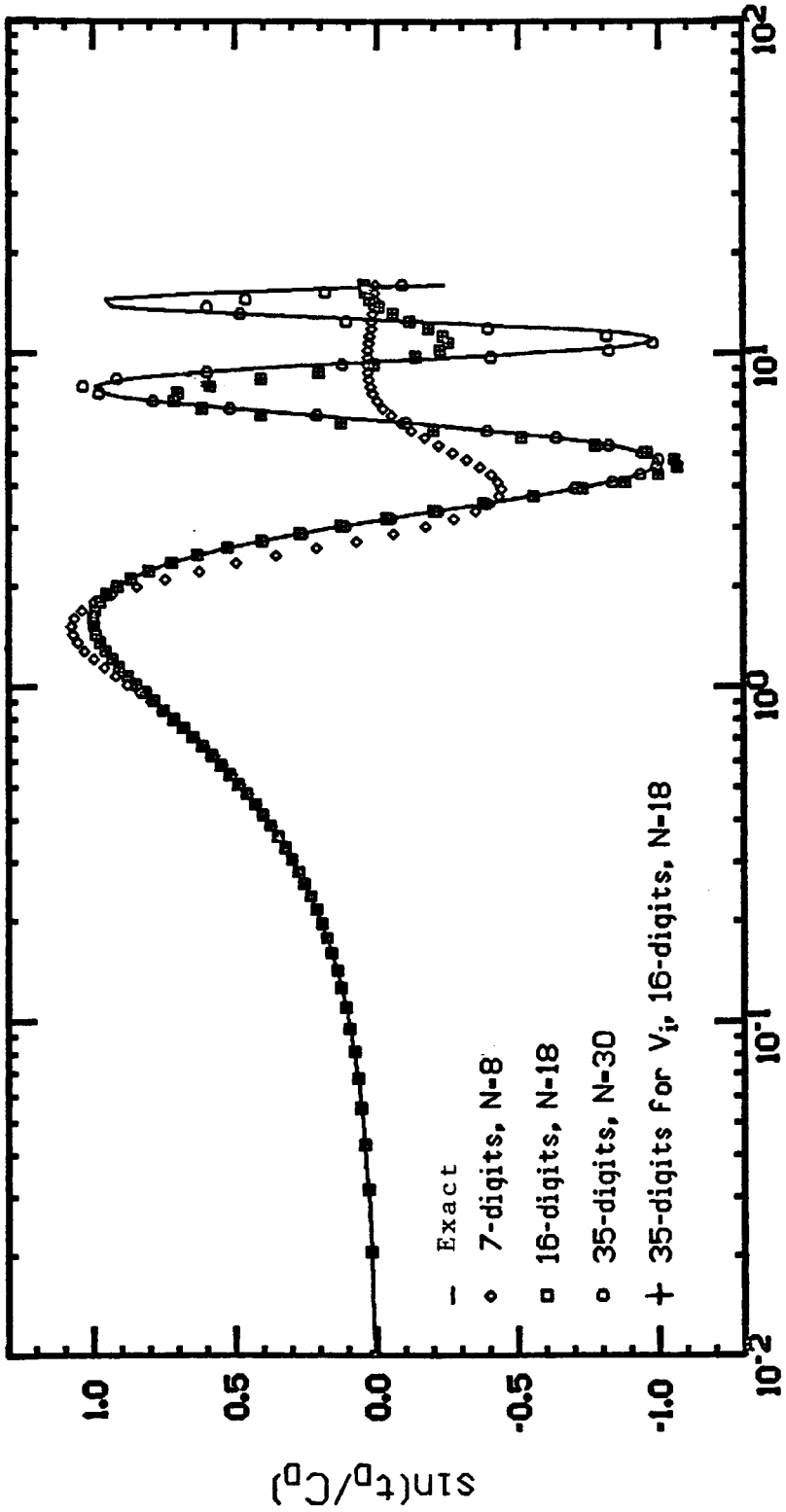

FIG. C.1. RESULTS FROM APPLICATION OF THE STEHFEST ALGORITHM TO INVERT THE LAPLACE TRANSFORMATION OF $\sin(t_D/C_D)$

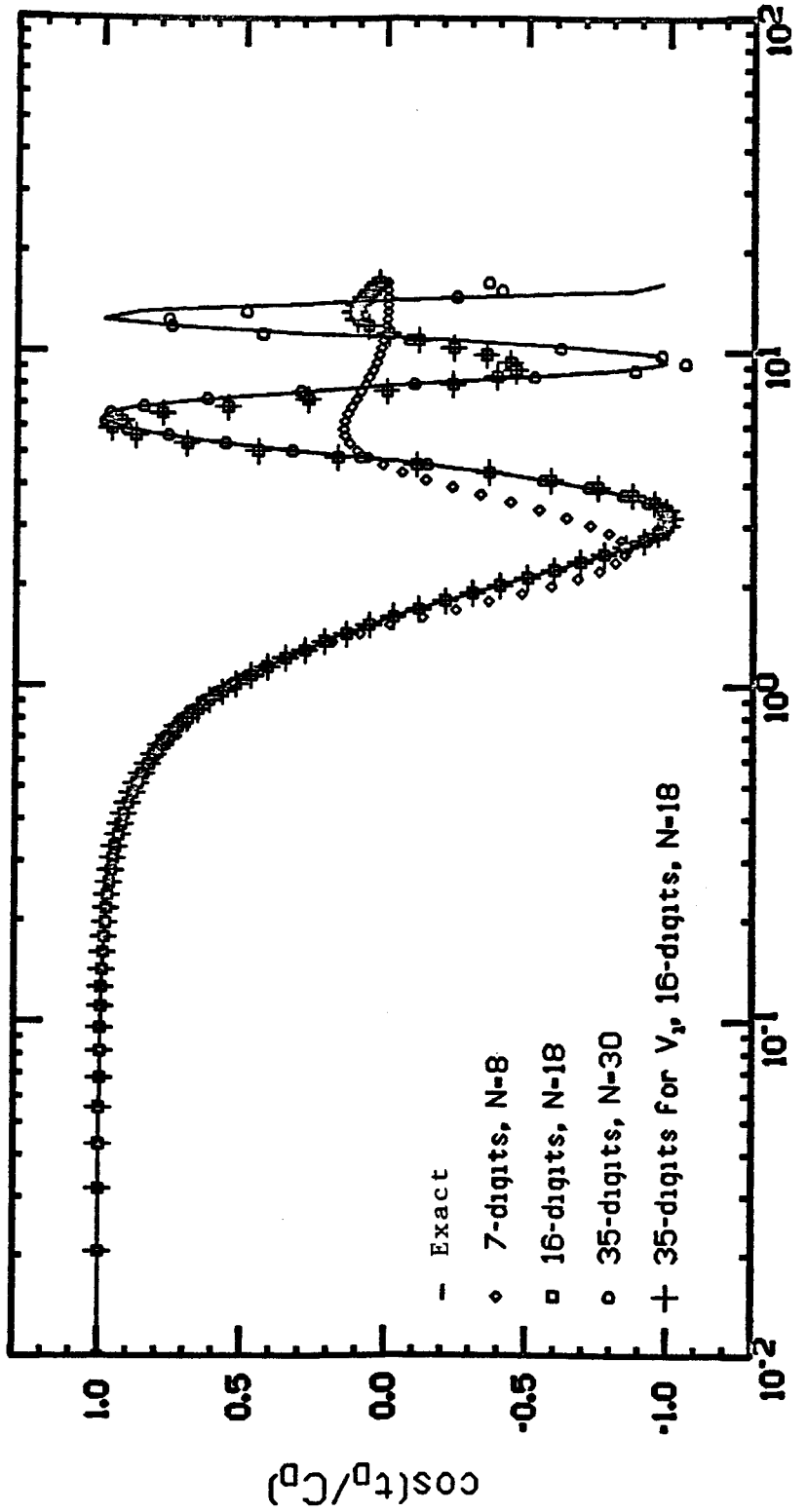

FIG. C.2. RESULTS FROM APPLICATION OF THE STEHFEST ALGORITHM TO INVERT THE LAPLACE TRANSFORMATION OF $\cos(t_D/C_D)$

APPENDIX D
SOLUTION BY FINITE DIFFERENCES

A consistent finite-difference method to solve linear and non-linear slug test, drillstem test, and closed-chamber test problems is derived in this appendix. The mathematical statement of the flow phenomena involved in this type of test, given by Eqs. *3.39* - *3.46*, is approximated by an implicit finite-difference method that is iterative for the case of non-linear problems and has been found to be stable and convergent for the conditions considered in the present study.

D.1 Tridiagonal System of Equations for $s \neq 0$

Any implicit finite-difference approximation requires the solution of systems of simultaneous equations. The approximation presented in this appendix is designed to result in tridiagonal systems of equations that are solved efficiently by a direct elimination method called Thomas algorithm (Aziz and Settari, 1979).

Outer Boundary Reservoir Condition - The outer 'boundary condition for an infinite-acting reservoir, Eq. *3.43*, is:

$$\lim_{r_D \to \infty} p_D(r_D, t_D) = 0, \quad t_D > 0 \qquad \ldots (3.43)$$

Since a finite-difference approximation must have a finite number of unknown variables, this boundary condition has to be replaced by an approximate boundary condition having the same effect for the range of

time of practical interest. By definition, an infinite-acting reservoir outer boundary condition must not affect the pressure in the reservoir or the wellbore appreciably. Therefore, for a sufficiently large radial reservoir, a no-flow condition or a constant-pressure condition at the outer boundary of the reservoir should not cause a different effect on the flow phenomena in the reservoir or the wellbore during times of interest. These two conditions can be stated, respectively, as follows:

$$\left[r_D \frac{\partial p_D}{\partial r_D} \right]_{r_D=r_{De}} = 0 \quad , t_D>0 \qquad \ldots (D.1)$$

and:

$$p_D(r_{De},t_D) = 0 \quad , t_D>0 \qquad \ldots (D.2)$$

Determination of r_{De} to describe a sufficiently large reservoir for the range of times of practical interest can be obtained from the instantaneous line source solution in a manner analogous to the method presented by Lee (1982) to define redius of investigation. The instantaneous line source solution can be expressed in terms of the dimensionless variables used in the present study, as follows:

$$p_D = \frac{1}{2} \frac{C_D}{t_D} e^{-\frac{r_D^2}{4t_D}} \qquad \ldots (D.3)$$

A pressure disturbance in an instantaneous line source well at time zero causes a maximum pressure disturbance at a radius r_D at a time t_D obtained by differentiating Eq. D.3 with respect to time and setting the result equal to zero:

$$\frac{dp_D}{dt_D} = \frac{1}{2}\frac{}{t_D^2} e^{-\frac{r_D^2}{4t_D}} \left[\frac{r_D^2}{4t_D} - 1 \right] = 0 \qquad \ldots \text{(D.4)}$$

This defines the following relationship between r_D and t_D:

$$r_D^2 = 4\, t_D \qquad \ldots \text{(D.5)}$$

The range of times of interest in slug test analysis is given by $10^{-2} < t_D/C_D < 10^3$. Substituting this upper limit, $t_D/C_D = 103$, into Eq. D.5:

$$r_D^2 = 4000\, C_D \qquad \ldots \text{(D.6)}$$

Dimensionless pressure at this radius and time can be calculated from Eq. D.3 by substituting r_D from Eq. D.6 and $t_D = 103 C_D$ with the result that $p_D = 0.00018\ldots$. This value of p_D can be considered negligible and, since the magnitude of the pressure disturbance for a line source well decreases as radius increases, a finite reservoir with the outer radius obtained from Eq. D.6 will exhibit an infinite-acting pressure behavior for the range of times of practical interest for slug test analysis:

$$r_{De} = 2 \left[10^3\, C_D \right]^{\frac{1}{2}} \qquad \ldots \text{(D.7)}$$

This reservoir radius is also appropriate for a damaged well, because pressure drops in the reservoir are smaller for a well with a positive skin factor.

Diffusivity Equation - In order to simplify notation, subscript D indicating a dimensionless variable is omitted throughout the rest of this appendix. Subscript w in the coefficients of wellbore Eq. 3.39 are also omitted hereafter.

The diffusivity equation for radial flow in a reservoir, Eq. 3.40, can be written as follows:

$$\frac{1}{r}\frac{\partial}{\partial r}\left[r \frac{\partial p}{\partial r} \right] = \frac{\partial p}{\partial t} \quad \ldots (3.37)$$

A convenient form of solving this equation is obtained by performing a change of variable from r to the following normalized logarithmic variable x (Aziz and Settari, 1979):

$$x = \frac{1}{m} \ln r \quad \ldots (D.8)$$

where:

$$m = \ln r_e \quad \ldots (D.9)$$

After this change of variable, Eq. 3.40 becomes:

$$\frac{\partial^2 p}{\partial x^2} = m^2 e^{2mx} \frac{\partial p}{\partial t} \quad \ldots (D.10)$$

Applying this equation at point x_j and time t_{k+1} and using implicit finite-difference approximations with three-point central differences in space and two-point backward differences in time:

$$\frac{p_{j+1}^{k+1} - 2p_j^{k+1} + p_{j-1}^{k+1}}{\Delta x^2} = m e^{2 2mx_j} \frac{p_j^{k+1} - p_j^k}{\Delta t_{k+1}} \quad \ldots \text{(D.11)}$$

where:

$$x_j = [\, j - 1 \,] \Delta x \quad , j = 1, 2, 3, \ldots, J \quad \ldots \text{(D.12)}$$

$$\Delta x = \frac{1}{J - 1} \quad \ldots \text{(D.13)}$$

$$\Delta t_{k+1} = t^{k+1} - t^k \quad , k = 1, 2 , \quad \ldots \text{(D.14)}$$

and:

J = number of nodes used to represent the reservoir

This approximation of the diffusivity equation defines a node x_1 at zero and a node x_J at unity. These nodes correspond to the wellbore radius r_w, r_D=1, and to the outer boundary reservoir radius r_e, r_D=r_{De}, respectively, because, from Eqs. D.8 and D.9:

$$r_j = e^{x_j \ln r_e} \quad , j = 1, 2, 3, \ldots, J \quad \ldots \text{(D.15)}$$

Inner nodes (x_j, j = 2, 3, ..., J–1) are equally spaced in x, but correspond to nodes logarithmically spaced in r. This provides high resolution around the wellbore, where pressure gradients are the largest in the reservoir.

In order to reduce round–off errors during the backward substitution required by the Thomas Algorithm, the system of equations is generated from the outer boundary of the reservoir towards the wellbore.

Using index i to denote an equation in the system, the first algebraic equation is obtained by applying Eq. D.11 for i=1 at node j=J+1–i and rearranging:

$$p_{J+1}^{k+1} + \left[-2 - \frac{m^2 \Delta x^2 e^{2mx_J}}{\Delta t_{k+1}} \right] p_J^{k+1} + p_{J-1}^{k+1} = - \frac{m^2 \Delta x^2 e^{2mx_J}}{\Delta t_{k+1}} p_J^k \quad \ldots \text{(D.16)}$$

Since p_{J+1} is outside the reservoir, it can be eliminated by approximating the outer boundary condition of no–flow given by Eq. D.1 using two–point central differences in space at x_J:

$$\frac{p_{J+1}^{k+1} - p_{J-1}^{k+1}}{2\Delta x} = 0 \quad \ldots \text{(D.17)}$$

or:

$$p_{J+1}^{k+1} - p_{J-1}^{k+1} \quad \ldots \text{(D.18)}$$

Then, substituting Eq. D.18 into Eq. D.16 and simplifying:

$$a_1 \, p_{J+1}^{k+1} + b_1 \, p_J^{k+1} + c_1 \, p_{J-1}^{k+1} = d_1 \qquad \ldots \text{(D.19)}$$

where:

$$a_1 = 0 \quad \text{(out of tridiagonal system)} \qquad \ldots \text{(D.19.a)}$$

$$b_1 = -2 - \frac{m \, Ax \, e^{2mx_J}}{\Delta t_{k+1}} \qquad \ldots \text{(D.19.b)}$$

$$c_1 = 2 \qquad \ldots \text{(D.19.c)}$$

$$d_1 = -\frac{m \, Ax \, e^{2mx_J}}{\Delta t_{k+1}} \, p_J^k \qquad \ldots \text{(D.19.d)}$$

Equations for $i=2,3,4,\ldots,J-1$ are determined by applying Eq. D.11 at nodes $j=J+1-i$:

$$a_i \, p_{j+1}^{k+1} + b_i \, p_j^{k+1} + c_i \, p_{j-1}^{k+1} = d_i \quad , \; j = J + 1 - i$$

$$, \; i = 2, 3, \ldots, J-1 \qquad \text{(D.20)}$$

where:

$$a_i = 1 \qquad \ldots \text{(D.20.a)}$$

$$b_i = -2 - \frac{m^2 \Delta x^2 e^{2mx_j}}{\Delta t_{k+1}} \qquad \ldots \text{(D.20.b)}$$

$$c_i = 1 \qquad \ldots \text{(D.20.c)}$$

$$d_i = -\frac{m^2 \Delta x^2 e^{2mx_j}}{\Delta t_{k+1}} p_j^k \qquad \ldots \text{(D.20.d)}$$

Skin Effect Condition - Equation for i=J is obtained by applying the skin effect condition given by Eq. 3.42 at time level k+1:

$$p_w^{k+1} = \left\{ p - s \left[r \frac{\partial p}{\partial r} \right] \right\}_{r=1}^{k+1} \qquad \ldots \text{(D.21)}$$

Performing the change of variable described by Eq. D.8:

$$p_w^{k+1} = \left[p - \frac{s}{m} \frac{\partial p}{\partial x} \right]_{x_1}^{k+1} \qquad \ldots \text{(D.22)}$$

The pressure gradient at the sandface is approximated by using three-point backward differences in space at x_1:

$$\left[\frac{\partial p}{\partial x}\right]_{x_1}^{k+1} = \frac{-p_3^{k+1} + 2\,p_2^{k+1} - 3\,p_1^{k+1}}{2\,\Delta x} \quad \ldots \text{(D.23)}$$

Substituting this approximation into **Eq.** D.22 and rearranging:

$$\left[-\frac{1}{2}\frac{s}{m\Delta x}\right] p_3^{k+1} + \left[2\,\frac{s}{m\Delta x}\right] p_2^{k+1} + \left[-1-\frac{3}{2}\frac{s}{m\Delta x}\right] p_1^{k+1} + p_w^{k+1} = 0 \quad \ldots \text{(D.24)}$$

The **term** with p_3 can be eliminated by applying **Eq.** D.20 at i=J-1, j=2. Multiplying **Eq.** D.20 by s/[2mΔx] and adding the result to **Eq. D.24:**

$$a_J\, p_2^{k+1} + b_J\, p_1^{k+1}\; c_J\, p_w^{k+1} = d_J \quad \ldots \text{(D.25)}$$

where :

$$a_J = \frac{s}{m\Delta x} - \frac{1}{2}\frac{s}{m\Delta x}\,\frac{m^2\,\Delta x^2\, e^{2mx_2}}{\Delta t_{k+1}} \quad \ldots \text{(D.25.a)}$$

$$b_J = -1 - \frac{s}{m\Delta x} \quad \ldots \text{(D.25.b)}$$

$$c_J = 1 \quad \ldots \text{(D.25.c)}$$

$$d_J = \left[-\frac{1}{2}\frac{s}{m\Delta x}\frac{m^2\Delta x^2 e^{2mx_2}}{\Delta t_{k+1}} \right] p_2^k \qquad \ldots \text{(D.25.d)}$$

Wellbore Storage Condition - Equation for i=J+1 is obtained by applying the wellbore storage condition given by Eq. 3.41 at time level k+1:

$$z'_{k+1} = -\frac{1}{C_D}\left[r\frac{\partial p}{\partial r} \right]_{r=1}^{k+1} \qquad \ldots \text{(D.26)}$$

Performing the change of variable described by Eq. D.8:

$$z'_{k+1} = -\frac{1}{mC_D}\left[\frac{\partial p}{\partial X} \right]_{x_1}^{k+1} \qquad \ldots \text{(D.27)}$$

Using three-point backward differences in time at t^{k+1} for unequal time steps to approximate z'_{k+1}:

$$z'_{k+1} \simeq \frac{[\delta^2 - \Delta t_{k+1}^2]\, z^{k+1} - \delta^2 z^k + \Delta t_{k+1}^2 z^{k-1}}{\Delta} \qquad \ldots \text{(D.28)}$$

where:

$$\delta = \Delta t_{k+1} + \Delta t_k \qquad \ldots \text{(D.29)}$$

$$\Delta = \Delta t_{k+1} \left[\Delta t_{k+1} + \Delta t_k \right]^2 - \left[\Delta t_{k+1} + \Delta t_k \right] \Delta t_{k+1}^2 \qquad \ldots \text{(D.30)}$$

Substituting this approximation for z'_{k+1} and the approximation for the pressure gradient at the sandface, given by Eq. D.23, into Eq. D.27 and rearranging terms:

$$p_3^{k+1} - 4\, p_2^{k+1} + 3\, p_1^{k+1} - \frac{2m\Delta x C_D [\delta^2 - \Delta t_{k+1}^2]}{\Delta} z^{k+1} =$$

$$= - \frac{2m\Delta x C \delta^2}{A} z^k + \frac{2m\Delta x C_D \Delta t_{k+1}^2}{A} z^{k-1} \qquad \ldots \text{(D.31)}$$

The term with p_3 and p_2 can be eliminated by multiplying Eq. D.31 by $-s/[2m\Delta x]$ and adding the result to Eq. D.24:

$$a_{J+1}\, p_1^{k+1} + b_{J+1}\, p_w^{k+1} + c_{J+1}\, z^{k+1} = d_{J+1} \qquad \ldots \text{(D.32)}$$

where:

$$a_{J+1} = 1 \qquad \ldots \text{(D.32.a)}$$

$$b_{J+1} = - 1 \qquad \ldots \text{(D.32.b)}$$

$$c_{J+1} = \frac{sC_D[\delta^2 - \Delta t_{k+1}^2]}{A} \quad \ldots (D.32.c)$$

$$J+1 = \frac{sC_D\delta^2}{A} z^k - \frac{sC_D\Delta t_{k+1}^2}{\Delta} z^{k-1} \quad \ldots (D.32.d)$$

Wellbore Equation - The equation for i=J+2 is obtained by applying wellbore Eq. 3.39 at time level k+1, considering that coefficients A, B, C, D, and E are known constants:

$$[\, A z'' + B z' + C z + D = E p_w \,]^{k+1} \quad \ldots (D.33)$$

Using three-point backward differences in time for unequal time steps to approximate z''_{k+1}:

$$z''_{k+1} = \frac{\Delta t_k z^{k+1} - 6 z^k + \Delta t_{k+1} z^{k-1}}{\Delta/2} \quad \ldots (D.34)$$

Substituting this approximation for z''_{k+1} and the approximation for z'_{k+1}, given by Eq. D.28, into Eq. D.33 and rearranging terms:

$$a_{J+2} p_w^{k+1} + b_{J+2} z^{k+1} + c_{J+2} z'_{k+1} = d_{J+2} \quad \ldots (D.35)$$

where :

$$a_{J+2} = E \qquad \ldots \text{(D.35.a)}$$

$$b_{J+2} = -\frac{2\,A\,\Delta t_k}{\Delta} - \frac{B\,[\,\delta^2 - \Delta t_{k+1}^2\,]}{\Delta} - C \qquad \ldots \text{(D.35.b)}$$

$$c_{J+2} = 0 \qquad \ldots \text{(D.35.c)}$$

$$d_{J+2} = \left[-\frac{2A6}{A} - \frac{B\delta^2}{A}\right] z^k + \left[\frac{2A\Delta t_{k+1}}{A} + \frac{B\Delta t_{k+1}^2}{A}\right] z^{k-1} - D \qquad \text{(D. 35. d)}$$

Wellbore Liquid Column Velocity - The equation for i=J+3 is obtained by rearranging the finite differences approximation for z'_{k+1}, given by Eq. D.28:

$$a_{J+3}\, z^{k+1} + b_{J+3}\, z'_{k+1} + c_{J+3}\, z''_{k+1} = d_{J+3} \qquad \ldots \text{(D.36)}$$

where :

$$a_{J+3} = 62 - \Delta t_{k+1}^2 \qquad \ldots \text{(D.36.a)}$$

$$b_{J+3} = - \quad A \qquad \ldots \text{(D.36.b)}$$

$$c_{J+3} = 0 \qquad \ldots \text{(D.36.c)}$$

$$d_{J+3} = \delta^2 \, z^k - \Delta t_{k+1}^2 \, z^{k-1} \qquad \ldots \text{(D.36.d)}$$

Wellbore Liquid Column Acceleration - The equation for i=J+4 is obtained by combining the finite differences approximations for z'_{k+1} and z''_{k+1}, given by Eqs. D.28 and D.34, respectively:

$$a_{J+4} \, z'_{k+1} + b_{J+4} \, z''_{k+1} + c_{J+4} = d_{J+4} \qquad \ldots \text{(D.37)}$$

where :

$$a_{J+4} = - \frac{\Delta t_k \, A}{\delta^2 - \Delta t_{k+1}^2} \qquad \ldots \text{(D.37.a)}$$

$$b_{J+4} = - \frac{A}{2} \qquad \ldots \text{(D.37.b)}$$

$$c_{J+4} = 0 \quad \text{(out of tridiagonal system)} \qquad \ldots \text{(D.37.c)}$$

$$d_{J+4} = \left[\delta - \frac{\Delta t_k \, \delta^2}{\delta^2 - \Delta t^2_{k+1}} \right] z^k + \left[\frac{\Delta t_k \, \Delta t^2_{k+1}}{\delta^2 - \Delta t^2_{k+1}} - \Delta t_{k+1} \right] z^{k-1} \qquad \text{(D.37.d)}$$

This equation for i=J+4 is the last equation in the tridiagonal system of equations for the case with $s \neq 0$. This system is expressed in matrix form in Fig. D.1.

D.2 Tridiagonal System of Equations for s = 0

For the special case with s=0, Eqs. D.25 and D.32 become equal to:

$$p_1^{k+1} - p_w^{k+1} = 0 \qquad \ldots \text{(D.38)}$$

In order to solve this problem, Eq. D.38 is used to eliminate one equation and one unknown, p_w^{k+1}, from the tridiagonal system of equations obtained for the case with $s \neq 0$.

Equation for i=1 is obtained from Eq. D.19.

Equations for i=2,3,...J-1 are obtained from Eq. D.20.

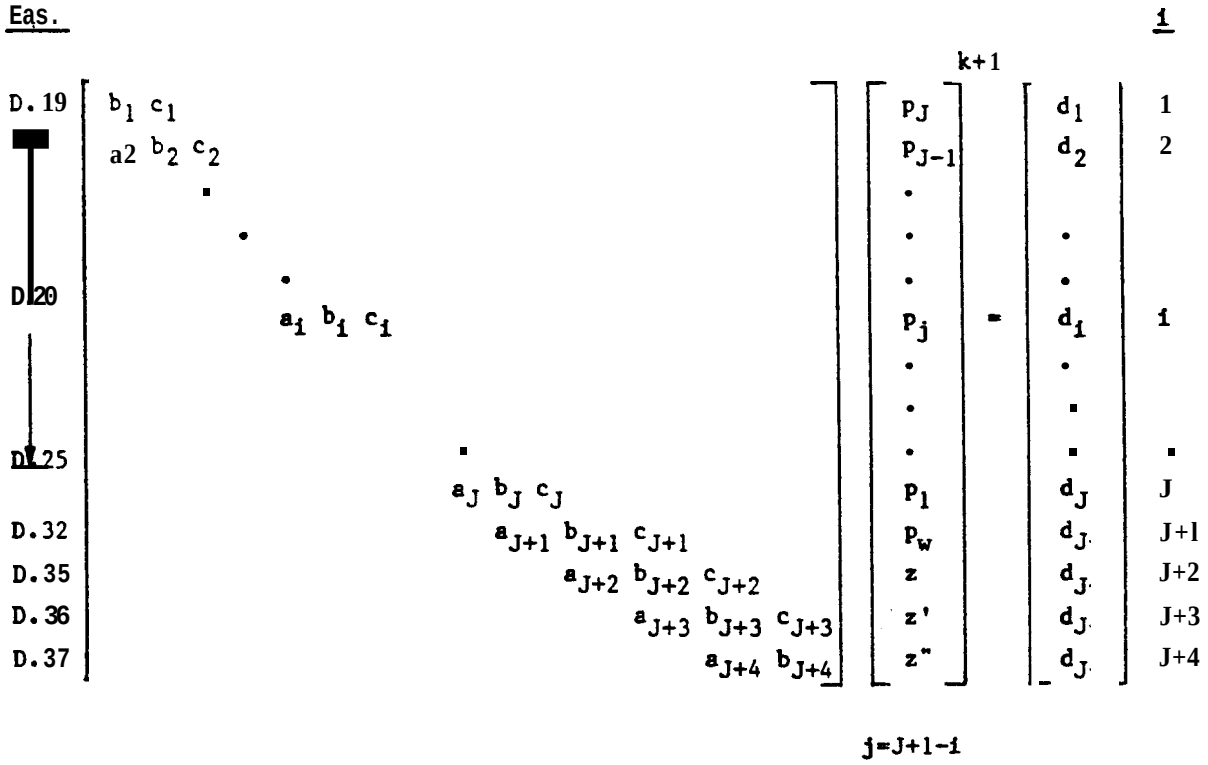

FIG. D.1. TRIDIAGONAL SYSTEM OF EQUATIONS DESCRIBING FLOW PHENOMENA DURING A SLUG TEST, DRILLSTEM TEST, OR CLOSED-CHAMBER TEST FOR A SYSTEM WITH $s \neq 0$.

Wellbore Storage Condition - The equation for i=J is obtained by applying the approximation for wellbore storage condition given by Eq. D.31. The term with p_3 is eliminated by subtracting Eq. D.20 from Eq. D.31, obtaining:

$$a_J\, p_2^{k+1} + b_J\, p_1^{k+1} + c_J\, z^{k+1} = d_J \qquad \ldots \text{(D.39)}$$

where:

$$a_J = -2 + \frac{m^2 A x^2 e^{2mx_2}}{\Delta t_{k+1}} \qquad \ldots \text{(D.39.a)}$$

$$b_J = 2 \qquad \ldots \text{(D.39.b)}$$

$$c_J = -\frac{2\, m\, \Delta x\, C_D \left[\, \delta^2 - \Delta t_{k+1}^2 \,\right]}{A} \qquad \ldots \text{(D.39.c)}$$

$$d_J = \frac{m^2 A x^2 e^{2mx_2}}{\Delta t_{k+1}}\, p_2^k - \frac{2m\Delta x C_D \delta^2}{A}\, z^k + \frac{2m\Delta x C_D \Delta t_{k+1}^2}{A} \qquad \ldots \text{(D.39.d)}$$

Wellbore Equation - The equation for i=J+1 is obtained by substituting Eq. D.38 into Eq. D.35, resulting in:

$$a_{J+1}\, p_1^{k+1} + b_{J+1}\, z^{k+1} + c_{J+1}\, z'_{k+1} = d_{J+1} \qquad \ldots \text{(D.40)}$$

where coefficients a_{J+1}, b_{J+1}, c_{J+1}, and d_{J+1} are equal to the corresponding coefficients in Eq. D.35.

Wellbore Liquid Column Velocity - The equation for i=J+2 is obtained from Eq. D.36:

$$a_{J+2}\, z_{k+1} + b_{J+2}\, z'_{k+1} + c_{J+2}\, z''_{k+1} = d_{J+2} \quad \ldots \text{(D.41)}$$

where coefficients a_{J+2}, b_{J+2}, c_{J+2}, and d_{J+2} are obtained from the corresponding coefficients in Eq. D.36.

Wellbore Liquid Column Acceleration - The equation for i=J+3 is obtained from Eq. D.37:

$$a_{J+3}\, z'_{k+1} + b_{J+3}\, z''_{k+1} + c_{J+3} = d_{J+3} \quad \ldots \text{(D.42)}$$

where coefficients a_{J+3}, b_{J+3}, c_{J+3}, and d_{J+3} are obtained from the corresponding coefficients in Eq. D.37.

Equation for i=J+3 is the last equation for the case with s=0 and the resulting system of equations is expressed in matrix form in Fig. D.2.

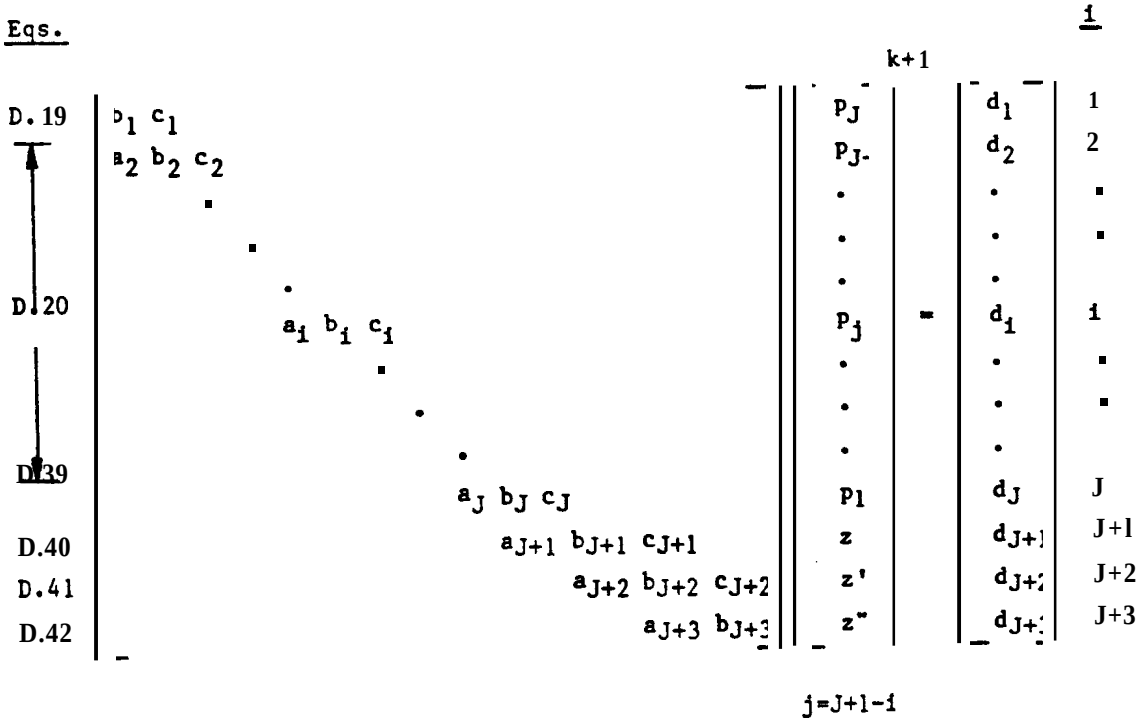

FIG. D.2. TRIDIAGONAL SYSTEM OF EQUATIONS DESCRIBING FLOW PHENOMENA DURING A SLUG TEST, DRILLSTEM TEST, OR CLOSED-CHAMBER TEST FOR A SYSTEM WITH $\varepsilon = 0$

D.3 Iterative Method

In the previous finite-difference approximation, coefficients A, B, C, D, and E of wellbore Eq. 3.39 were considered to be known constants. This is the case for the linear problems solved by the semi-analytical method described in Section 4.1. Since the problem is posed at time level k+1, inspection of the definition of those wellbore coefficients, given by Eqs. 3.39.a - 3.39.e, shows that coefficients A, B, and D are not known constants because z_D^{k+1} and z'_{Dk+1} are involved in Eqs. 3.39.a, 3.39.b, and 3.39.d'.

The oscillatory behavior expected for the solutions for z_D^{k+1} and z'_{Dk+1} prevented the use of an extrapolating algorithm for general application. The successive approximations technique was found to be reliable for the problems solved in the present study. This technique is applied to wellbore Eq. 3.39 as follows:

$$[\ \tilde{A}_w\, z''_D + \tilde{B}_w\, z'_D + C_w\, z_D + \tilde{D}_w = E_w\, p_{wD}\ ]^{k+1} \qquad \ldots \text{(D.43)}$$

where:

$$\tilde{A}_w = \alpha^2 \left\{ \left[1 + \frac{\tilde{z}_D}{L_T} \right] + \frac{3}{8} \frac{h_D}{L_D} \left[\frac{r_{pDz}}{r_{wDz}} \right]^2 \right\} \qquad \ldots \text{(D.43.a)}$$

$$\tilde{B}_w = \alpha^2 \left\{ \left[1 + \frac{\tilde{z}_D}{L_D} \right] \frac{\tilde{f}}{4} \left| \frac{1}{r_{pDz}} \bar{z}'_D \right| + \frac{3}{4} L_D \left[\frac{r_{pDz}}{r_{wDz}} \right]^4 \tilde{z}'_D \right\} \qquad \ldots \text{(D.43.b)}$$

$$C_w = 1 \qquad \ldots \text{(D.43.c)}$$

$$\tilde{D}_w = p_{aD} \left[\frac{L_D - L_{pD} - 1}{L_D - L_{pD} + \tilde{z}_D} \tilde{Z}_g - 1 \right] \qquad \ldots \text{(D.43.d)}$$

$$E_w = -1 \qquad \ldots \text{(D.43.e)}$$

with:

$$\tilde{z}_D = \frac{z_D^{\gamma} + z_D^{\gamma-1}}{2} \qquad \ldots \text{(D.44)}$$

$$\tilde{z}'_D = \frac{z_D'^{\gamma} + z_D'^{\gamma-1}}{2} \qquad \ldots \text{(D.45)}$$

$$\tilde{f} = f(\tilde{Re}) \qquad \ldots \text{(D.46)}$$

$$\tilde{Re} = Re(\tilde{z}'_D) \qquad \ldots \text{(D.47)}$$

$$\tilde{Z}_g = \frac{Z_g^{\gamma} + Z_g^{\gamma-1}}{2} \qquad \ldots \text{(D.48)}$$

where γ indicates iteration level.

This iterative method is stopped when the values of $\tilde{z}_D$ and $\tilde{z}'_D$ are equal to the desired values of z_D^{k+1} and z'_{Dk+1}, within a small tolerance ε_1 and ε_2, respectively. The first estimate of $\tilde{z}_D$ and $\tilde{z}'_D$ to start iteration for a time step k+1 are taken as $\tilde{z}_D = z_D^k$ and $\tilde{z}'_D = z'_{Dk}$.

D.4 No-Flow Wellbore Condition

During a drillstem test or during a closed-chamber test, the well is shut-in by closing the drillstem test valve that is at the bottom of the drill string in the wellbore. This situation is convenient because subsequent wellbore storage effects are only caused by the compressibility of the fluids in the small volume inside the wellbore below the valve. From the moment that the well is shut-in, the wellbore equation, wellbore storage condition and skin effect condition can be replaced by the following boundary condition for no-flow:

$$\left[r \frac{\partial p}{\partial r} \right]_{r_D=1} = 0 \qquad \ldots \text{(D.49)}$$

Performing the change of variable given by Eq. D.8:

$$\left[\frac{\partial p}{\partial x} \right]_{x=0} = 0 \qquad \ldots \text{(D.50)}$$

For the reservoir discretization considered in this appendix, this condition can be replaced by using the following two-point central-difference approximation in space at x_1:

$$\frac{p_0^{k+1} - p_2^{k+1}}{2\,\Delta x} = 0 \qquad \ldots \text{(D.51)}$$

or:

$$p_0^{k+1} = p_2^{k+1} \qquad \ldots \text{(D.52)}$$

Then, substituting this relationship into the diffusivity equation discretization, Eq. D.ll, for i=J at node j=J+l-i:

$$a_J\, p_2^{k+1} + b_J\, p_1^{k+1} + c_J\, p_0^{k+1} = d_J \qquad \ldots \text{(D.53)}$$

where:

$$a_J = 2 \qquad \ldots \text{(D.53.a)}$$

$$b_J = -2 - \frac{m^2\, \Delta x^2\, e^{2mx_1}}{\Delta t_{k+1}} \qquad \ldots \text{(D.53.b)}$$

$$c_J = 0 \text{ (out of the tridiagonal system)} \qquad \ldots \text{(D.53.c)}$$

$$d_J = -\frac{m^2 \Delta x^2 e^{2mx_1}}{\Delta t_{k+1}} p_1^k \quad \ldots (D.53.d)$$

This is the last equation for time steps after the well is shut-in. Since there is no flow from or into the reservoir:

$$p_w^{k+1} = p_1^{k+1} \quad \ldots (D.54)$$

$$z^{k+1} = z^k \quad \ldots (D.55)$$

$$z'_{k+1} = 0 \quad \ldots (D.56)$$

and:

$$z''_{k+1} = 0 \quad \ldots (D.57)$$

Equations for $i=1,2,3,\ldots,J-1$ at nodes $j=J+1-i$ are given by Eqs. D.19 and D.20.

The resulting tridiagonal system of equations is expressed in matrix from in Fig. D.3.

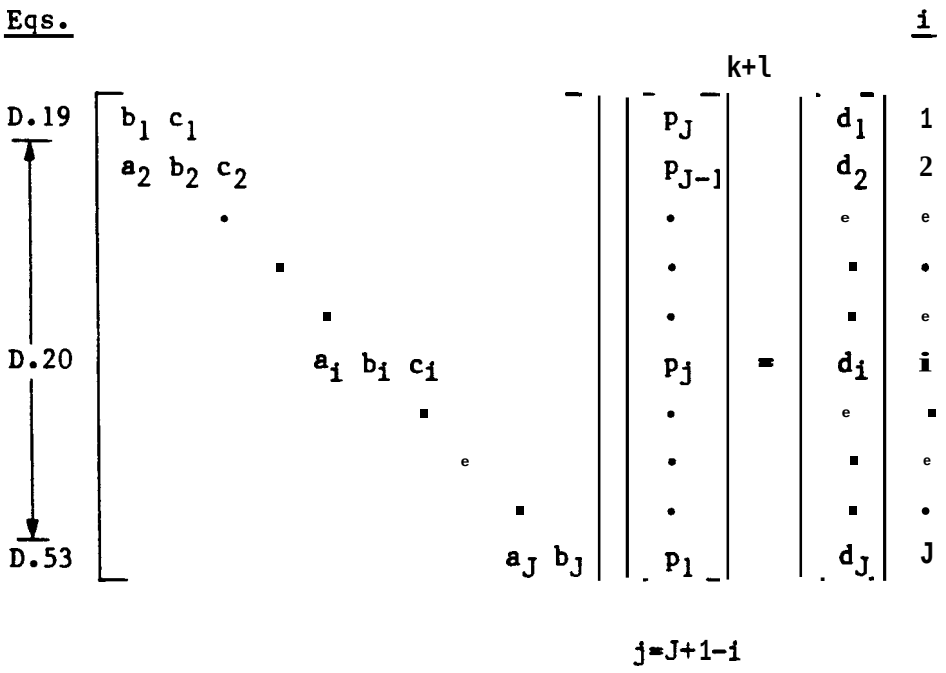

FIG. D.3. TRIDIAGONAL SYSTEM OF EQUATIONS DESCRIBING THE PRESSURE BUILDUP DURING A DRILLSTEM TEST OR CLOSED-CHAMBER TEST

APPENDIX E

COMPUTER PROGRAM FOR SEMI-ANALYTICAL SOLUTIONS

Under a range of practical conditions, the flow phenomena during a slug test or a drillstem test can be described by a linear mathematical problem. The corresponding problem statement consists of Eqs. 3.39 - 3.46, where coefficients A_w and B_w of the wellbore equation are considered to be known constants. A generalized form of the linear problem can be solved by using Laplace transformation and the Stehfest algorithm, as described in Section 4.1. In this appendix, a computer program is presented for performing the corresponding calculations.

This computer program is written in FORTRAN IV language using DOUBLE PRECISION and consists of a main source program, one subroutine, and two external subprograms for evaluating Bessel functions K_0, and K_1. This computer program can be used to generate results for graphs or for tables. Results to be plotted as graphs are regularly distributed in each logarithmic cycle of dimensionless time. This option is used by specifying INT=1 in the data for the program. In this case, values for the final dimensionless time, TDFIN, the duration of the initial dimensionless time step, DTD, and a constant factor to increase the duration of subsequent dimensionless time steps, FAC, must be supplied. Results to be presented in the form of tables are evaluated at ten equal intervals of dimensionless time in each logarithmic cycle. This option is used by specifying INT=0. In this case, values for initial dimensionless time, TDI, and number of logarithmic cycles, NCY, are required. In both cases, the number of coefficients for the Stehfest algorithm is assumed equal to 18, unless an even value different than zero is specified for variable NST in the data.

There are several forms of the wellbore equation resulting in problems of interest. This computer program allows the following four options for the form of the wellbore equation and the information required:

Option 1 (ISLUG=1)

Negligible Inertia and Friction:

$$z_D = - p_{wD} \quad \ldots (5.16)$$

Option 2 (ISLUG=2)

Inertia with Negligible Friction for a Small Slug:

$$\alpha^2 z_D'' + z_D = - p_{wD} \quad \ldots (5.25)$$

Option 3 (ISLUG=3)

Inertia with Laminar Friction for a Small Slug:

$$a^2 z_D'' + \alpha^2 \beta z_D' + z_D = - p_{wD} \quad \ldots (5.42)$$

Option 4 (ISLUG=4)

Inertia with Laminar Friction for a Small Slug and a Large Ratio h/L:

$$a^2 \left\{ 1 + \frac{3}{8} \frac{h_D}{L_D} \left[\frac{r_{pDz}}{r_{wDz}} \right] \right\} z_D'' + \alpha^2 \beta z_D' + z_D = - p_{wD} \quad \ldots (5.47)$$

Several sets of data can be processed in the same run. The program is stopped by specifying ISLUG=0.

Options 1 through 4 for ISLUG require values for s and C_D, plus additional values for the dimensionless parameters considered. ISLUG=2 requires α^2. ISLUG=3 requires α^2 and B. And, ISLUG=4 requires a^2, B, h/L, and r_p/r_w.

All the previous data are supplied using a format of 10X,I10, or 10X,D10.0, according to the type of variable. One or two parameters are required per line of data.

Also, up to 10 values of dimensionless radius, r_D, can be specified to analyze the behavior of the dimensionless pressure distribution, $p_D(r_D)$, in the reservoir.

The results provided by this program are printed in the form of tables with the following columns: (1) t_D/C_D, (2) $t_D/[\alpha^2*C_D]$, (3) p_{wD}, (4) z_D, (5) C_D*p_{wD}', (6) C_D*z_D', (7) $\alpha^2*C_D*z_D'$, (8) $C_D{}^2*z_D''$, (9) $\alpha^2*C_D{}^2*z_D''$, (10) $[1-p_{wD}]$, and (11) $p_D(r_D)$.

This computer program is presented in the following pages of this appendix. A computer program for non-linear problems is presented in Appendix F.

```
C     ***********************************************************************
C
C     DRILLSTEM TEST DATA ANALYSIS CONSIDERING
C     INERTIAL AND FRICTIONAL WELLBORE EFFECTS
C
C     COMPUTER PROGRAM FOR SOLVING LINEAR PROBLEMS
C     BY USING A SEMI-ANALYTICAL SOLUTION METHOD
C
C     PROGRAM FOR DOCTORAL DISSERTATION BY MIGUEL SALDANA
C     ADVISED BY HENRY, J. RAMEY, JR.
C
C     PETROLEUM ENGINEERING DEPARTMENT
C     SCHOOL OF EARTH SCIENCES
C     STANFORD UNIVERSITY
C     NOVEMBER 1983
C
C     ***********************************************************************
C
      IMPLICIT REAL*8 (A-H,O-Z)
      DIMENSION PD(10),RD(10),NPC(10)
C
      DATA NPC/10*10/
      DATA RD(1)/1.D0/,AL2/0.D0/,TDALCD/0.D0/
      DATA MST/100/
C
C     ***********************************************************************
C
C     DATA READING
C
C     ***********************************************************************
C
   20 READ(5,110)ISLUG,INT
      WRITE(6,6001)
      WRITE(6,6020)
      WRITE(6,120)ISLUG
      WRITE(6,125)INT
      IF(ISLUG)30,30,40
   40 IF(INT)30,35,38
   35 READ(5,107)TDI,NCY,NST
      GO TO 39
   38 READ(5,106)TDFIN,DTD,FAC,NST
   39 IF(NST.EQ.0)NST=18
      READ(5,100)S,CD,NRD
      WRITE(6,104)S
      WRITE(6,108)CD
      IF(NRD.GT.1)GO TO 80
      NRD=1
      GO TO 25
   80 READ(5,114)(RD(I),I=1,NRD)
```

```
C
C     ***************************************************************
C
C     CALCULATION OF WELLBORE EQUATION COEFFICIENTS
C
C     ***************************************************************
C
   25 GO TO (1,2,3,4),ISLUG
    1 A= 0.D0
      B= 0.D0
      C= 1.D0
      D= 0.D0
      E=-1.D0
      GO TO 70
    2 READ(5,100)AL2
      WRITE(6,130)AL2
      A= AL2
      B= 0.D0
      C= 1.D0
      D= 0.D0
      E=-1.D0
      GO TO 70
    3 READ(5,100)AL2
      WRITE(6,130)AL2
      READ(5,100)BETA
      WRITE(6,140)BETA
      A= AL2
      B= AL2*BETA
      C= 1.D0
      D= 0.D0
      E=-1.D0
      GO TO 70
    4 READ(5,100)AL2
      WRITE(6,130)AL2
      READ(5,100)BETA
      WRITE(6,140)BETA
      READ(5,100)HL,RPRW
      WRITE(6,180)HL
      WRITE(6,190)RPRW
      A=AL2*(1.D0+3.D0/8.D0*HL*RPRW*RPRW)
      B=AL2*BETA
      C=1.D0
      D=0.D0
      E=-1.D0
      GO TO 70
   70 WRITE(6,150)
      IF(NRD.EQ.1)GO TO 19
      WRITE(6,160)(RD(I),I=1,NRD)
C
   19 TD=0.D0
C
```

```
C
      T=0.D0
      IF(INT)30,55,64
C
C     ***************************************************************
C
C     PRINTING FOR TABLES
C
C     ***************************************************************
C
   55 DO 10 I=1,NCY
      IM1=I-1
      IF(I.NE.1)GO TO 12
      NPI=NPC(I)
      GO TO 13
   12 NPI=NPC(I)-NPC(I)/10
   13 DELTD=10.D0**DFLOAT(I)/NPC(I)*TDI
C
      DO 9 J=1,NPI
      TD=T+DELTD*DFLOAT(J)
C
C     NUMERICAL INVERSION OF LAPLACE-TRANSFORMED SOLUTIONS
C
      CALL DLINV(NST,MST,A,B,C,D,E,S,CD,TD,ISLUG,
     $           ZD,PWD,DPWD,DZD,D2ZD,PD,RD,NRD)
C
C     RESULTS WRITING
C
      TDCD=TD/CD
      ONEMPW=1.D0-PWD
      IF(AL2.NE.0.D0)TDALCD=TD/AL2.CD
      CDDPWD=CD*DPWD
      CDDZD=CD*DZD
      ALCDFD=AL2*CD*DZD
      CDD2ZD=CD*CD*D2ZD
      ALCDSD=AL2*CD*CD*D2ZD
      IF(NRD.EQ.1)GO TO 63
      WRITE(6,170)TDCD,TDALCD,PWD,ZD,CDDPWD,CDDZD,ALCDFD,
     $            CDD2ZD,ALCDSD,ONEMPW
      GO TO 9
   63 WRITE(6,170)TDCD,TDALCD,PWD,ZD,CDDPWD,CDDZD,ALCDFD,
     $            CDD2ZD,ALCDSD,ONEMPW
    9 CONTINUE
C
      T=TD
   10 CONTINUE
C
      GO TO 20
C
```

```
C
C     ***************************************************************
C
C     PRINTING FOR GRAPHS
C
C     ***************************************************************
C
   61, TD=TD+DTD
       IF(TD.GT.TDFIN)GO TO 20
C
C      LAPLACE TRANSFORMATION INVERSION
C
       CALL DLINV(NST,MST,A,B,C,D,E,S,CD,TD,ISLUG,
      $           ZD,PWD,DPWD,DZD,D2ZD,PD,RD,NRD)
C
C      RESULTS
C
       TDCD=TD/CD
       ONEMPW=1.D0-PWD
       IF(AL2.NE.0.D0)TDALCD=TD/A 2/CD
       CDDPWD=CD*DPWD
       CDDZD=CD*DZD
       ALCDFD=AL2*CD*DZD
       CDD2ZD=CD*CD*D2ZD
       ALCDSD=AL2*CD*CD*D2ZD
       IF(NRD.EQ.1)GO TO 163
       WRITE(6,170)TDCD,TDALCD,PWD,ZD,CDDPWD,CDDZD,ALCDFD,
      $            CDD2ZD,ALCDSD,ONEMPW
       GO TO 79
  163 WRITE(6,170)TDCD,TDALCD,PWD,ZD,CDDPWD,CDDZD,ALCDFD,
      $            CDD2ZD,ALCDSD,ONEMPW
   79 DTD=DTD*FAC
       GO TO 64
C
C     FORMATS
C
 6001 FORMAT(1X,'(PROGRAM PHD1C')
 6020 FORMAT(1X,'JOIN 1',/,1X,'SET ORDER X 1.0 DUMMY Y 1.0')
  150 FORMAT(1X,'(  TD/CD    ',1X,' TD/AL2/CD ',1X,'    PWD    ',
      $       1X,'    ZD     ',1X,'  CD*DPWD  ',
      $       1X,'  CD*DZD   ',1X,' AL2*CD*DZD',1X,' CD*CD*D2ZD',
      $       1X,'AL2*C2*D2Z ',1X,'  1 - PWD )')
  100 FORMAT(2(10X,D10.0),10X,I10)
  106 FORMAT(3(10X,D10.0),10X,I10)
  110 FORMAT(2(10X,I10))
  114 FORMAT(8D10.0)
  160 FORMAT(68X,5D11.4)
  170 FORMAT(11(1X,D11.4))
  107 FORMAT(10X,D10.0,2(10X,I10))
  104 FORMAT(1X,'(S    =',D11.4,')')
  108 FORMAT(1X,'(CD   =',D11.4,')')
C
```

```
C
  120 FORMAT(1X,'(ISLUG=',I2    ,')')
  125 FORMAT(1X,'(INT  =',I2    ,')')
  130 FORMAT(1X,'(AL2  =',D11.4,')')
  140 FORMAT(1X,'(BETA =',D11.4,')')
  180 FORMAT(1X,'(H/L  =',D11.4,')')
  190 FORMAT(1X,'(RP/RW=',D11.4,')')
C
   30 STOP
      END
C
C     ****************************************************************
C
C     SUBROUTINE DLINV
C
C     ****************************************************************
C
      SUBROUTINE DLINV(N,M,A,B,C,D,E,S,CD,TD,ISLUG,
     $                 ZD,PWD,DPWD,DZD,D2ZD,PD,RD,NRD)
C
      IMPLICIT REAL*8 (A-H,O-Z)
C
      REAL*8 MMBSK0,MMBSK1
C
      DIMENSION V(30),G(31),PD(1),PN(10),RD(1)
      IF(M.EQ.N)GO TO 4
C
C     ****************************************************************
C
C     CALCULATION OF COEFFICIENTS FOR STEHFEST ALGORITHM
C
C     ****************************************************************
C
      NH=N/2
      NP1=N+1
C
      G(1)=1.D0
      DO 1 I=2,NP1
    1 G(I)=G(I-1)*DFLOAT(I-1)
C
      SN=1.D0
      IE=NH+1
      IH=IE/2
      II=(IE+1)/2
      IF(II.GT.IH)SN=-SN
C
      DO 3 I=1,N
      V(I)=0.D0
      KI=(I+1)/2
      KS=I
      IF(KS.GT.NH)KS=NH
C
```

```
C
      DO 2 K=KI,KS
    2 V(I)=V(I)+DFLOAT(K)**DFLOAT(NH)*G(2*K+1)/
     $           (G(NH-K+1)*G(K+1)*G(K)*G(I-K+1)*G(2*K-I+1))
C
      V(I)=SN*V(I)
      SN=-SN
    3 CONTINUE
C
      M=N
C
C     ***************************************************************
C
C     APPLICATION OF THE STEHFEST ALGORITHM
C
C     ***************************************************************
C
    4 ZD=0.D0
      PWD=0.D0
      DPWD=0.D0
      DZD=0.D0
      D2ZD=0.D0
      DO 8 I=1,NRD
    8 PD(I)=0.D0
C
      AA=DLOG(2.D0)/TD
C
      DO 5 I=1,N
      U=AA*DFLOAT(I)
      SRU=DSQRT(U)
      C0=MMBSK0(1,SRU,IER)
      C1=SRU*MMBSK1(1,SRU,IER)
      ABDE=A*U+B+D/U-E*CD*S
      ABCE=A*U+B+C/U-E*CD*S
      EK0=E*CD*C0
      ZN=-1.D0/U*(C1*ABDE-EK0)/(C1*ABCE-EK0)
      CK=CD*(U*ZN+1.D0)/C1
      PWN=CK*(C0+S*C1)
      DPWN=U*PWN
      DO 7 J=1,NRD
      RSRU=RD(J)*SRU
    7 PN(J)=CK*MMBSK0(1,RSRU,IER)
      ZD=ZD+V(I)*ZN
      PWD=PWD+V(I)*PWN
      DPWD=DPWD+V(I)*DPWN
      DO 9 J=1,NRD
    9 PD(J)=PD(J)+V(I)*PN(J)
      IF(ISLUG-1)31,31,32
   31 DZN=U*ZN+1.D0
      DZD=DZD+V(I)*DZN
      D2ZN=U*DZN
C
```

```
C
      D2ZD=D2ZD+V(I)*D2ZN
      GO TO 5
   32 DZN=(-C*ZN-D/U+E*PWN)/(A*U+B)
      DZD=DZD+V(I)*DZN
      D2ZN=(-B*DZN-C*ZN-D/U+E*PWN)/A
      D2ZD=D2ZD+V(I)*D2ZN
    5 CONTINUE
C
      ZD=AA*ZD
      PWD=AA*PWD
      DPWD=AA*DPWD
      DZD=AA*DZD
      D2ZD=AA*D2ZD
      DO 6 J=1,NRD
    6 PD(J)=AA*PD(J)
C
   69 RETURN
      END
C
C     ***********************************************************************
C
C     END
C
C     ***********************************************************************
C
```

APPENDIX F
COMPUTER PROGRAM FOR NUMERICAL SOLUTIONS

Flow phenomena during a slug test, a drillstem test, or a closed-chamber test can be described by the problem statement given by Eqs. *3.39 - 3.46*, where coefficients A_w, B_w, and D_w of the wellbore equation include independent variable z_D, or/and its time-derivative, z_D'. In this appendix, a computer program, based on the finite-difference approximation derived in Appendix D, is presented to solve a generalized form of this non-linear problem. As described in Section *4.2*, the finite-difference approximation results in tridiagonal systems of simultaneous equations that are solved by using the Thomas algorithm.

For special cases in which wellbore coefficients A_w, B_w, and D_w are constant, the problem is linear and semi-analytical solutions can be obtained as described in Section *4.1*. Those semi-analytical solutions are reproduced by the computer program presented in this appendix. For linear problems, the finite-difference approximation requires the solution of only one tridiagonal system of equations per time step. However, an iterative calculation process is required to solve non-linear problems. As described in Appendix D, this process consists of a successive approximation of coefficients A_w, B_w, and D_w, and requires the solution of a tridiagonal system of equations per iteration.

This computer program is written in FORTRAN IV language using DOUBLE PRECISION and consists of a main source program and one subprogram for evaluating Moody friction factor. In this program, the finite-difference approximation is applied at each time step generated by an algorithm that increases the duration of the time step. Data required for use in this algorithm are: (a) the duration of the initial dimensionless time step, DTD1, (b) a constant factor to increase the duration of subsequent dimensionless time steps, FDTD, and (c) the final dimensionless time, TDF.

This computer program allows the following nine options for the form of the wellbore equation and the information required:

Option 1 (IFIN=1)

Negligible Inertia and Friction:

$$z_D = - p_{wD} \quad \ldots (5.16)$$

Option 2 (IFIN=2)

Inertia with Negligible Friction for a Small Slug:

$$a^2 z_D'' + z_D = - p_{wD} \quad \ldots (5.25)$$

Option 3 (IFIN=3)

Inertia and Laminar Friction for a Small Slug:

$$a^2 z_D'' + \alpha^2 \beta z_D' + z_D = - p_{wD} \quad \ldots (5.42)$$

Option 4 (IFIN=4)

Inertia and Laminar Friction for a Small Slug and a Large Ratio h/L:

$$\alpha^2 \{ 1 + \frac{\hat{}}{8} \frac{D}{L_D} [\frac{p_{Dz}}{r_{wDz}}] \} z_D'' + \alpha^2 \beta z_D' + z_D = - p_{wD} \quad \ldots (5.47)$$

Option 5 (IFIN=5)

Inertia for Large Slug and Negligible Friction:

$$a^2 \left[1 + \frac{\tilde{z}_D}{L_D} \right] z_D'' + z_D = - p_{wD} \qquad \ldots (6.1)$$

Option 6 (IFIN=6)

Inertia and Friction for Small **Slug:**

$$\alpha^2 z_D'' + \alpha^2 \frac{\tilde{f}}{4} \left| \frac{1}{r_{pDz}} \tilde{z}_D' \right| z_D' + z_D = - p_{wI} \qquad \ldots (6.4)$$

Option 7 (IFIN=7)

Inertia for Large Slug and Friction for Small Slug:

$$a^2 \left[1 + \frac{\tilde{z}_D}{L_D} \right] z_D'' + \alpha^2 \frac{\tilde{f}}{4} \left| \frac{1}{r_{pDz}} \tilde{z}_D' \right| z_D' + z_D = - p_{wI} \qquad \ldots (F.1)$$

Option 8 (IFIN=8)

General Slug Test and Drillstem Test Wellbore Equation:

$$a^2 \left[1 + \frac{\tilde{z}_D}{L_D} \right] + \frac{3}{8} \frac{\rho}{\rho} \left[\frac{r_{pDz}}{r_{wDz}} \right]^2 z_D'' +$$

$$a^2 \left[1 + \frac{\tilde{z}_D}{L_D} \right] \frac{\tilde{f}}{4} \left| \frac{1}{r_{pDz}} \tilde{z}_D \right| + \frac{3}{4} \frac{1}{L_D} \left[\frac{r_{pDz}}{r_{wDz}} \right]^4 \tilde{z}_D \quad z_D' +$$

$$z_D = - p_{wD} \qquad \ldots (3.39)$$

Option 9 (IFIN=9)

General Closed-Chamber Test Wellbore Equation:

$$a^2 \left[1 + \frac{\tilde{z}_D}{L_D} \right] + \frac{3}{8} \frac{h_D}{L_D} \left[\frac{r_{pDz}}{r_{wDz}} \right]^2 z''_D +$$

$$a^2 \left[1 + \frac{\tilde{z}_D}{L_D} \right] \frac{\tilde{f}}{4} \left| \frac{1}{r_{pDz}} \tilde{z}'_D \right| + \frac{3}{4} \frac{1}{L_D} \left[\frac{r_{pDz}}{r_{wDz}} \right]^4 \tilde{z}'_D \; z'_D +$$

$$z_D + \frac{L_D - L_{pD} - 1}{L_D - L_{pD} + \tilde{z}_D} p_{gD}(0) - p_{aD} = - p_{wD} \qquad \cdots (3.39)$$

Several sets of data can be processed in the same run. The program is stopped by specifying IFIN=0.

Options 1 through 9 for IFIN require values for s and C_D, plus additional values for the dimensionless parameters considered. IFIN=2 requires α^2. IFIN=3 requires α^2 and β. IFIN=4 requires α^2, β, L_D, h_D, r_{pDz} and r_{wDz}. IFIN=5 requires α^2 and L_D. IFIN=6 requires α^2, β, e_D, and r_{pDz}. IFIN=7 requires a^2, B, e_D, L_D, r_{pDz}. IFIN=8 requires α^2, β, e_D, L_D, h_D, r_{pDz}, r_{wDz}. IFIN=9 requires α^2, β, e_D, L_D, h_D, r_{pDz}, r_{wDz}, L_{pD}, $p_{gD}(0)$, and p_{aD}.

For all the previous options, the wellbore can be shut-in according to values provided for dimensionless shut-in bottomhole pressure, p_{wsD}, or dimensionless flowing time for shut-in, t_{sD}.

All data are supplied using a format of 10X,I10, or 10X,D10.0, according to the type of variable. One or two parameters are required per line of data.

The results provided by this program are printed in the form of tables with the following columns: (1) t_D/C_D, (2) $t_{sD}/\Delta t_D+1$, (3) p_{wD}, (4) z_D, (5) C_D*p_{wD}', (6) C_D*z_D', (7) $C_D{}^2*z_D''$, (8) $[1-p_{wD}]$, (9) p_{gD},

(10) p_{DJ}, (11) Number of Iterations on $\tilde{z}_D$, (12) Number of Iterations on $\tilde{z}'_D$, , (13) Pipe Flow Regime, and (14) Number of Iterations for Transition Flow Regime.

This computer program is presented in the following pages of this appendix.

```
C
C     ****************************************************************
C
C     DRILLSTEM TEST DATA ANALYSIS CONSIDERING
C     INERTIAL AND FRICTIONAL WELLBORE EFFECTS
C
C     COMPUTER PROGRAM FOR SOLVING LINEAR AND NON-LINEAR PROBLEMS
C     BY USING A FINITE-DIFFERENCE APPROXIMATION
C
C     PROGRAM FOR DOCTORAL DISSERTATION BY MIGUEL SALDANA
C     ADVISED BY HENRY, J. RAMEY, JR.
C
C     PETROLEUM ENGINEERING DEPARTMENT
C     SCHOOL OF EARTH SCIENCES
C     STANFORD UNIVERSITY
C     NOVEMBER 1983
C
C     ****************************************************************
C
      IMPLICIT REAL*8 (A-H,O-Z)
      REAL*8 M,LD,LPD
      DIMENSION X(51),PDK(55),A(55),B(55),C(55),D(55),
     $          BT(55),GM(55),XX(55),PDKP1(55)
C
      DATA NX/51/
      DATA IZM/25/,TOLZ/1.D-02/
      DATA IVM/25/,TOLV/1.D-02/
      DATA IFM/25/,TOLF/1.D-02/
C
C     ****************************************************************
C
C     DATA READING
C
C     ****************************************************************
C
   25 READ (5,5001)IFIN
      WRITE(6,6001)
      WRITE(6,6020)
      WRITE(6,6007)IFIN
      IF(IFIN)700,700,5
    5 ISHUT=0
      READ (5,5002)DTD1,FDTD,TDF
      READ (5,5002)TDS,PWSD
      WRITE(6,6017)TDS
      WRITE(6,6018)PWSD
      READ (5,5002)S,CD
      WRITE(6,6002)S
      WRITE(6,6008)CD
C
```

```
C
C     ***************************************************************
C
C     LINEAR WELLBORE EQUATION COEFFICIENTS
C
C     ***************************************************************
C
      GO TO(1001,1002,1003,1004,1005,1006,1007,1008,1009),IFIN
C
 1001 AA=0.D0
      BB=0.D0
      CC=1.D0
      DD=0.D0
      EE=-1.D0
      GO TO 1100
 1002 READ (5,5002)AL2
      WRITE(6,6005)AL2
      AA=AL2
      BB=0.D0
      CC=1.D0
      DD=0.D0
      EE=-1.D0
      GO TO 1100
 1003 READ (5,5002)AL2
      WRITE(6,6005)AL2
      READ (5,5002)BETA
      WRITE(6,6006)BETA
      AA=AL2
      BB=AL2*BETA
      CC=1.D0
      DD=0.D0
      EE=-1.D0
      GO TO 1100
 1004 READ (5,5002)AL2
      WRITE(6,6005)AL2
      READ (5,5002)BETA
      WRITE(6,6006)BETA
      READ (5,5002)LD,HD
      WRITE(6,6009)LD
      WRITE(6,6010)HD
      READ (5,5002)RPDZ,RWDZ
      WRITE(6,6013)RPDZ
      WRITE(6,6011)RWDZ
      AA=AL2*(1.D0+3.D0/8.D0*HD/LD*(RPDZ/RWDZ)**2.D0)
      BB=AL2*BETA
      CC=1.D0
      DD=0.D0
      EE=-1.D0
      GO TO 1100
C
```

```
C
 1005 READ (5,5002)AL2
      WRITE(6,6005)AL2
      READ (5,5002)LD
      WRITE(6,6009)LD
      GO TO 1100
 1006 READ (5,5002)AL2
      WRITE(6,6005)AL2
      READ (5,5002)BETA,ED
      WRITE(6,6006)BETA
      WRITE(6,6014)ED
      READ (5,5002)RPDZ
      WRITE(6,6013)RPDZ
      GO TO 1100
 1007 READ (5,5002)AL2
      WRITE(6,6005)AL2
      READ (5,5002)BETA,ED
      WRITE(6,6006)BETA
      WRITE(6,6014)ED
      READ (5,5002)LD
      WRITE(6,6009)LD
      READ (5,5002)RPDZ
      WRITE(6,6013)RPDZ
      GO TO 1100
 1008 READ (5,5002)AL2
      WRITE(6,6005)AL2
      READ (5,5002)BETA,ED
      WRITE(6,6006)BETA
      WRITE(6,6014)ED
      READ (5,5002)LD,HD
      WRITE(6,6009)LD
      WRITE(6,6010)HD
      READ (5,5002)RPDZ,RWDZ
      WRITE(6,6013)RPDZ
      WRITE(6,6011)RWDZ
      GO TO 1100
 1009 READ (5,5002)AL2
      WRITE(6,6005)AL2
      READ (5,5002)BETA,ED
      WRITE(6,6006)BETA
      WRITE(6,6014)ED
      READ (5,5002)LD,HD
      WRITE(6,6009)LD
      WRITE(6,6010)HD
      READ (5,5002)RPDZ,RWDZ
      WRITE(6,6013)RPDZ
      WRITE(6,6011)RWDZ
      READ (5,5002)LPD,PGID,PAD
      WRITE(6,6015)LPD
      WRITE(6,6019)PGID
      WRITE(6,6016)PAD
      GO TO 1100
C
```

```
C
 1100 WRITE(6,6003)
C
C     ***************************************************************
C
C     CALCULATION OF CONSTANTS
C
C     ***************************************************************
C
      RDE=2.D0*(1.D3*CD)**0.5D0
C
      NXM1=NX-1
      NXP1=NX+1
      NXP2=NX+2
C
      M=DLOG(RDE)
C
      DX=1.D0/(DFLOAT(NX)-1.D0)
C
      DO 100 J=1,NX
      X(J)=DFLOAT(J-1)*DX
  100 CONTINUE
C
      A01=DEXP(2.D0*M)
      A02=M*M*DX*DX
      A03=S/(M*DX)
      A04=M*DX*CD
C
C     INITIALIZATION
C
      DO 200 J=1,NX
      PDK(J)=0.D0
  200 CONTINUE
C
      TDKM1=0.D0
      ZDKM1=-1.D0
      PWDKM1=0.D0
      IF(IFIN.EQ.1)PWDKM1=-ZDKM1
C
      TDK=DTD1
      ZDK=-1.D0
      PWDK=0.D0
      IF(IFIN.EQ.1)PWDK=-ZDK
C
      DZDK=1.D0/CD/CD
      FR=1.D0
C
      ZDM=ZDK
      DZDM=DZDK
C
      DTDK=TDK-TDKM1
C
```

```
C
      TDH=0.D0
      PGD=0.D0
C
C     ******************************************************************
C
C     NON-LINEAR WELLBORE EQUATION COEFFICIENTS
C
C     ******************************************************************
C
  110 IZ=0
      IV=0
      IREG=0
      IF=0
      IF(ISHUT.NE.2)GO TO 111
      DTDK=DTD1/FDTD
      ISHUT=1
C
  111 DTDKP1=DTDK*FDTD
C
      IF(ISHUT.EQ.1)GO TO 2100
C
      GO TO(2001,2002,2003,2004,2005,2006,2007,2008,2009),IFIN
 2001 GO TO 2100
 2002 GO TO 2100
 2003 GO TO 2100
 2004 GO TO 2100
 2005 AA=AL2*(1.D0+ZDM/LD)
      BB=0.D0
      CC=1.D0
      DD=0.D0
      EE=-1.D0
      GO TO 2100
 2006 RE=16.D0/BETA*DABS(DZDM/RPDZ)
      IF=0
      FR=F(RE,ED,FR,IREG,IF,IFM,TOLF)
      AA=AL2
      BB=AL2*FR/4.D0*DABS(DZDM/RPDZ)
      CC=1.D0
      DD=0.D0
      EE=-1.D0
      GO TO 2100
 2007 RE=16.D0/BETA*DABS(DZDM/RPDZ)
      IF=0
      FR=F(RE,ED,FR,IREG,IF,IFM,TOLF)
      AA=AL2*(1.D0+ZDM/LD)
      BB=AL2*FR/4.D0*DABS(DZDM/RPDZ)
      CC=1.D0
      DD=0.D0
      EE=-1.D0
      GO TO 2100
C
```

```
C
 2008 RE=16.D0/BETA*DABS(DZDM/RPDZ)
      IF=0
      FR=F(RE,ED,FR,IREG,IF,IFM,TOLF)
      AA=AL2*(1.D0+ZDM/LD+3.D0/8.D0*HD/LD*(RPDZ/RWDZ)**2.D0)
      BB=AL2*((1.D0+ZDM/LD)*FR/4.D0*DABS(DZDM/RPDZ)+3.D0/4.D0/LD*
     $                DZDM*(RPDZ/RWDZ)**4.D0)
      CC=1.D0
      DD=0.D0
      EE=-1.D0
      GO TO 2100
 2009 RE=16.D0/BETA*DABS(DZDM/RPDZ)
      IF=0
      FR=F(RE,ED,FR,IREG,IF,IFM,TOLF)
      AA=AL2*(1.D0+ZDM/LD+3.D0/8.D0*HD/LD*(RPDZ/RWDZ)**2.D0)
      BB=AL2*((1.D0+ZDM/LD)*FR/4.D0*DABS(DZDM/RPDZ)+3.D0/4.D0/LD*
     $                DZDM*(DZDM/RPDZ)**4.D0)
      CC=1.D0
      PGD=(LD-LPD-1.D0)/(LD-LPD+ZDM)*PGID
      DD=PGD-PAD
      EE=-1.D0
      GO TO 2100
C
 2100 DTKP1C=DTDKP1*DTDKP1
      SDTD=DTDKP1+DTDK
      SDTDC=SDTD*SDTD
      SDMCDC=SDTDC-DTKP1C
      CDTD=DTDKP1*SDTDC-SDTD*DTKP1C
      A05=A02/DTDKP1
      A06=A04/DTDKP1
C
C     ******************************************************************
C
C     DETERMINATION OF THE SYSTEM OF EQUATIONS'
C
C     ******************************************************************
C
      A07=A05*(A01**X(NX))
C
      A(1)=0.D0
      B(1)=-2.D0-A07
      C(1)=2.D0
      D(1)=-A07*PDK(NX)
C
      DO 300 I=2,NXM1
      J=NXP1-I
      A08=A05*(A01**X(J))
C
```

```
C
      A(I)=1.D0
      B(I)=-2.D0-A08
      C(I)=1.D0
      D(I)=-A08*PDK(J)
  300 CONTINUE
C
      NEQ=NX
C
      IF(ISHUT.EQ.0)GO TO 10
C
      A(NEQ)=2.D0
      B(NEQ)=-2.D0-A05
      C(NEQ)=0.D0
      D(NEQ)=-A05*PDK(1)
      GO TO 20
C
   10 A09=A05*(A01**X(2))
C
      IF(S.EQ.0.D0)GO TO 325
      INS=4
C
      A(NEQ)=A03-A03/2.D0*A09
      B(NEQ)=-1.D0-A03
      C(NEQ)=1.D0
      D(NEQ)=-A03/2.D0*A09*PDK(2)
C
      NEQ=NEQ+1
      A(NEQ)=1.D0
      B(NEQ)=-1.D0
      C(NEQ)=S*CD*SDMCDC/CDTD
      D(NEQ)=S*CD*SDTDC/CDTD*ZDK-S*CD*DTKP1C/CDTD*ZDKM1
      GO TO 330
C
  325 INS=3
      A(NEQ)=-2.D0+A09
      B(NEQ)=2.D0
      C(NEQ)=-2.D0*A04*SDMCDC/CDTD
      D(NEQ)=A09*PDK(2)-2.D0*A04*SDTDC/CDTD*ZDK+
     $                   2.D0*A04*DTKP1C/CDTD*ZDKM1
C
  330 NEQ=NEQ+1
      A(NEQ)=EE
      B(NEQ)=-2.D0*AA*DTDK/CDTD-BB*SDMCDC/CDTD-CC
      C(NEQ)=0.D0
      D(NEQ)=(-2.D0*AA*SDTD/CDTD-BB*SDTDC/CDTD)*ZDK+
     $         (2.D0*AA*DTDKP1/CDTD+BB*DTKP1C/CDTD)*ZDKM1+DD
C
```

```
C
      NEQ=NEQ+1
      A(NEQ)=SDMCDC
      B(NEQ)=-CDTD
      C(NEQ)=0.D0
      D(NEQ)=SDTDC*ZDK-DTKP1C*ZDKM1
C
      NEQ=NEQ+1
      A(NEQ)=DTDK*CDTD/SDMCDC
      B(NEQ)=-CDTD/2.D0
      C(NEQ)=0.D0
      D(NEQ)=(SDTD-DTDK*SDTDC/SDMCDC)*ZDK+
     $       (DTDK*DTKP1C/SDMCDC-DTDKP1)*ZDKM1
C
C     ****************************************************************
C
C     SOLUTION OF SYSTEM OF EQUATION BY THOMAS ALGORITHM
C
C     ****************************************************************
C
C     WRITE(6,6100)(A(I),I=1,NEQ)
C     WRITE(6,6100)(B(I),I=1,NEQ)
C     WRITE(6,6100)(C(I),I=1,NEQ)
C     WRITE(6,6100)(D(I),I=1,NEQ)
C6100 FORMAT(12(1X,D10.3))
C
   20 BT(1)=B(1)
      GM(1)=D(1)/BT(1)
      DO 400 I=2,NEQ
      IM1=I-1
      BT(I)=B(I)-A(I)*C(IM1)/BT(IM1)
      GM(I)=(D(I)-A(I)*GM(IM1))/BT(I)
  400 CONTINUE
C
C     WRITE(6,6200)(BT(I),I=1,NEQ)
C     WRITE(6,6200)(GM(I),I=1,NEQ)
C6200 FORMAT(12(1X,D10.3))
C
      XX(NEQ)=GM(NEQ)
      NEQM1=NEQ-1
      DO 500 J=1,NEQM1
      I=NEQ-J
      IP1=I+1
      XXABS=DABS(XX(IP1))
      IF(XXABS.LT.1.D-60)GO TO 350
      XX(I)=GM(I)-C(I)*XX(IP1)/BT(I)
      GO TO 500
  350 XX(I)=0.D0
  500 CONTINUE
C
```

```
C
C     ******************************************************************
C
C     CONVERGENCE TEST
C
C     ******************************************************************
C
      IF(ISHUT.EQ.1)GO TO 3100
C
      GO TO(3001,3002,3003,3004,3005,3006,3007,3008,3009),IFIN
 3001 GO TO 3100
 3002 GO TO 3100
 3003 GO TO 3100
 3004 GO TO 3100
 3005 IF(IZ.GE.IZM)GO TO 3100
      TOL=DABS(TOLZ*XX(NEQ-2))
      DIF=DABS(ZDM)-DABS(XX(NEQ-2))
      IF(DABS(DIF).LE.TOL)GO TO 3100
      ZDM=0.5D0*(ZDM+XX(NEQ-2))
      IZ=IZ+1
      GO TO 2005
 3006 IF(IV.GE.IVM)GO TO 3100
      TOL=DABS(TOLV*XX(NEQ-1))
      DIF=DABS(DZDM)-DABS(XX(NEQ-1))
      IF(DABS(DIF).LE.TOL)GO TO 3100
      DZDM=0.5D0*(DZDM+XX(NEQ-1))
      IV=IV+1
      GO TO 2006
 3007 IF(IZ.GE.IZM)GO TO 3100
      TOL=DABS(TOLZ*XX(NEQ-2))
      DIF=DABS(ZDM)-DABS(XX(NEQ-2))
      IF(DABS(DIF).LE.TOL)GO TO 3100
      ZDM=0.5D0*(ZDM+XX(NEQ-2))
      IZ=IZ+1
      DZDM=0.5D0*(DZDM+XX(NEQ-1))
      IV=IV+1
      GO TO 2007
 3008 IF(IZ.GE.IZM)GO TO 3100
      TOL=DABS(TOLZ*XX(NEQ-2))
      DIF=DABS(ZDM)-DABS(XX(NEQ-2))
      IF(DABS(DIF).LE.TOL)GO TO 3100
      ZDM=0.5D0*(ZDM+XX(NEQ-2))
      IZ=IZ+1
      DZDM=0.5D0*(DZDM+XX(NEQ-1))
      IV=IV+1
      GO TO 2008
 3009 IF(IZ.GE.IZM)GO TO 3100
      TOL=DABS(TOLZ*XX(NEQ-2))
      DIF=DABS(ZDM)-DABS(XX(NEQ-2))
C
```

```
C
      IF(DABS(DIF).LE.TOL)GO TO 3100
      ZDM=0.5D0*(ZDM+XX(NEQ-2))
      IZ=IZ+1
      DZDM=0.5D0*(DZDM+XX(NEQ-1))
      IV=IV+1
      GO TO 2009
C
C     ****************************************************************
C
C     DETERMINATION OF RESULTS
C
C     ****************************************************************
C
 3100 TDKP1=TDK+DTDKP1
      DO 600 I=1,NX
      J=NXP1-I
      PDKP1(J)=XX(I)
  600 CONTINUE
      IF(ISHUT.EQ.0)GO TO 30
      ZDPP=0.D0
      ZDP=0.D0
      ZDKP1=ZDK
      ZDM=ZDK
      PWDKP1=PDKP1(1)
      GO TO 430
   30 ZDPP=XX(NEQ)
      ZDP=XX(NEQ-1)
      ZDKP1=XX(NEQ-2)
      IF(S.EQ.0.D0)GO TO 425
      PWDKP1=XX(NEQ-3)
      GO TO 430
  425 PWDKP1=PDKP1(1)
C
C     ****************************************************************
C
C     RESULTS PRINTING
C
C     ****************************************************************
C
  430 IF(ISHUT.EQ.1)GO TO 40
      IF(TDS.LT.TDKP1)GO TO 38
      IF(PWSD.GT.PWDK)GO TO 40
      IF(PWSD.GE.PWDKP1)GO TO 38
      GO TO 40
   38 ISHUT=2
      TPDT=TDKP1
   40 TDCD=TDKP1/CD
      IF(ISHUT.EQ.0)GO TO 47
      TDH=(TPDT/DTDKP1+1.D0)
   47 PWD=PWDKP1
C
```

```
C
      ONEMPW=1.D0-PWD
      DPWD=(SDMCDC*PWDKP1-SDTDC*PWDK+DTKP1C*PWDKM1)/CDTD
      CDDPWD=CD*DPWD
      ZD=ZDKP1
      CDDZD=CD*ZDP
      CDD2ZD=CD*CD*ZDPP
      WRITE(6,6004)TDCD,TDH,PWD,ZD,CDDPWD,CDDZD,CDD2ZD,ONEMPW,PGD,
     $             PDKP1(NX),IZ,IV,IREG,IF
C
C     ******************************************************************
C
C     RESTORATION
C
C     ******************************************************************
C
      IF(TDKP1.GE.TDF)GO TO 25
C
      TDKM1=TDK
      ZDKM1=ZDK
      PWDKM1=PWDK
C
      TDK=TDKP1
      ZDK=ZDKP1
      PWDK=PWDKP1
      DO 52 I=1,NX
      PDK(I)=PDKP1(I)
   52 CONTINUE
C
      ZDM=ZDKP1
      DZDM=ZDP
      DTDK=DTDKP1
      GO TO 110
C
C     FORMATS
C
 5001 FORMAT(10X,I10)
 5002 FORMAT(3(10X,D10.0))
C
 6001 FORMAT(1X,'(PROGRAM PHD2H)')
 6003 FORMAT( 1X,'( TD/CD     ',1X,' TD+DTD/DTD',1X,'    PWD      ',
     $         1X,'     ZD     ',1X,' CD*DPWD   ',
     $         1X,'  CD*DZD    ',1X,'CD*CD*D2ZD ',1X,'    1-PWD    ',
     $         1X,'     PGD    ',1X,'    PD NX   )')
 6001, FORMAT(10(1X,D11.4),4(1X,I2))
 6002 FORMAT(1X,'(S    =',D11.4,')')
 6005 FORMAT(1X,'(AL2  =',D11.4,')')
 6006 FORMAT(1X,'(BETA =',D11.4,')')
 6007 FORMAT(1X,'(IFIN =',I2   ,')')
 6008 FORMAT(1X,'(CD   =',D11.4,')')
 6009 FORMAT(1X,'(LD   =',D11.4,')')
C
```

```
C
 6010 FORMAT(1X,'(HD   =',D11.4,')')
 6011 FORMAT(1X,'(RWDZ =',D11.4,')')
 6013 FORMAT(1X,'(RPDZ =',D11.4,')')
 6014 FORMAT(1X,'(ED   =',D11.4,')')
 6015 FORMAT(1X,'(LPD  =',D11.4,')')
 6016 FORMAT(1X,'(PAD  =',D11.4,')')
 6017 FORMAT(1X,'(TDS  =',D11.4,')')
 6018 FORMAT(1X,'(PWSD =',D11.4,')')
 6019 FORMAT(1X,'(PGID =',D11.4,')')
 6020 FORMAT(1X,'JOIN 1',/,1X,'SET ORDER X 1.0 DUMMY Y 1.0')
C
C     END
C
  700 STOP
      END
C
C     ******************************************************************
C
C     FUNCTION F
C
C     ******************************************************************
C
      FUNCTION F(RE,ED,FR,IREG,IF,IFM,TOLF)
      IMPLICIT REAL*8 (A-H,O-Z)
C
      IF(RE.GT.0.D0)GO TO 1
      IREG=0
      F=0.D0
      GO TO 5
C
    1 IF(RE.GT.2000.D0)GO TO 2
      IREG=1
      F=64.D0/RE
      GO TO 5
C
    2 IF(RE.GT.4000.D0)GO TO 3
      IREG=2
      F=0.5D0*RE**(-0.3D0)
      GO TO 5
C
    3 SL=(200.D0/ED)**1.16D0
      IF(RE.GT.SL)GO TO 4
      IREG=3
      F1=FR
   55 X=ED+9.34D0/RE/DSQRT(F1)
      F=(1.14D0-2.D0*DLOG10(X))**(-2.D0)
      IF(IF.GE.IFM)GO TO 56
      TOL=DABS(TOLF*F)
      DIF=DABS(F)-DABS(F1)
C
```

```
C
      IF(DABS(DIF).LE.TOL)GO TO 5
      F1=0.5D0*(F+F1)
      IF=IF+1
      GO TO 55
   56 WRITE(6,501)IF
  501 FORMAT(10X,'FRICTION FACTOR ITERATIVE PROCEDURE',
     $' FAILED TO CONVERGE AFTER',2X,I5,' ITERATIONS')
      GO TO 5
C
    4 IREG=4
      F=(1.14D0-2.D0*DLOG10(ED))**(-2.D0)
C
    5 RETURN
      END
C
C     ***********************************************************************
C
C     END
C
C     ***********************************************************************
C
```

* * * * *